Computational Intelligence and Neuroscience

Deep Learning-Enabled Intelligent Control in Assistive Systems

Lead Guest Editor: Gopal Chaudhary
Guest Editors: Bharat Rawal and Smriti Srivastava

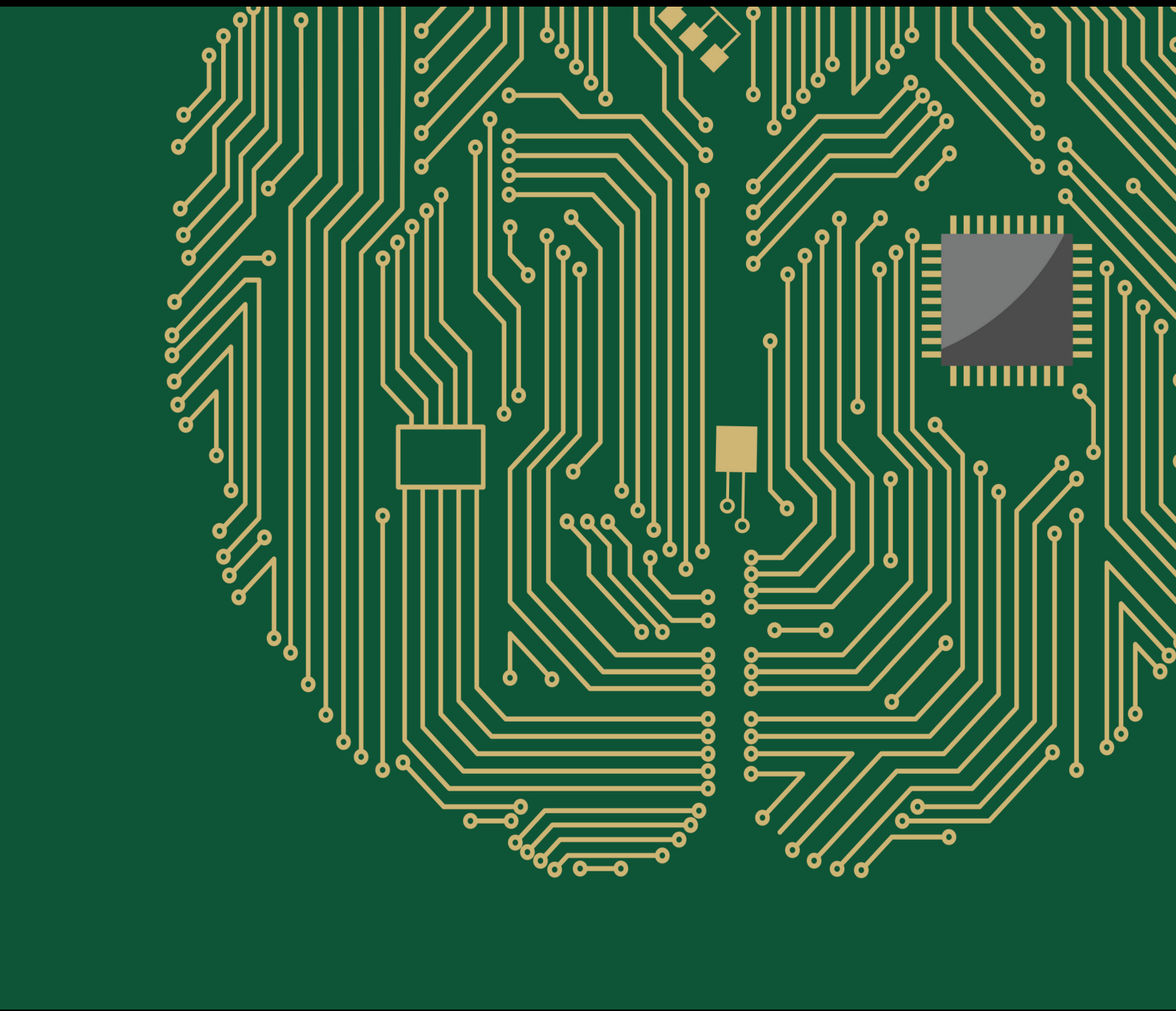

Deep Learning-Enabled Intelligent Control in Assistive Systems

Computational Intelligence and Neuroscience

Deep Learning-Enabled Intelligent Control in Assistive Systems

Lead Guest Editor: Gopal Chaudhary
Guest Editors: Bharat Rawal and Smriti Srivastava

Contents

Contents

Hindawi
Computational Intelligence and Neuroscience
Volume 2023, Article ID 9835129, 1 page
https://doi.org/10.1155/2023/9835129

Retraction

Retracted: Construction Means of Soil Microbial Synusiologic Network Based on ANN

Computational Intelligence and Neuroscience

Received 22 August 2023; Accepted 22 August 2023; Published 23 August 2023

This article has been retracted by Hindawi following an investigation undertaken by the publisher [1]. This investigation has uncovered evidence of one or more of the following indicators of systematic manipulation of the publication process:

(1) Discrepancies in scope
(2) Discrepancies in the description of the research reported
(3) Discrepancies between the availability of data and the research described
(4) Inappropriate citations
(5) Incoherent, meaningless and/or irrelevant content included in the article
(6) Peer-review manipulation

The presence of these indicators undermines our confidence in the integrity of the article's content and we cannot, therefore, vouch for its reliability. Please note that this notice is intended solely to alert readers that the content of this article is unreliable. We have not investigated whether authors were aware of or involved in the systematic manipulation of the publication process.

Wiley and Hindawi regrets that the usual quality checks did not identify these issues before publication and have since put additional measures in place to safeguard research integrity.

We wish to credit our own Research Integrity and Research Publishing teams and anonymous and named external researchers and research integrity experts for contributing to this investigation.

The corresponding author, as the representative of all authors, has been given the opportunity to register their agreement or disagreement to this retraction. We have kept a record of any response received.

References

[1] X. Li, H. Wang, and M. Yuan, "Construction Means of Soil Microbial Synusiologic Network Based on ANN," *Computational Intelligence and Neuroscience*, vol. 2022, Article ID 1708350, 9 pages, 2022.

Hindawi
Computational Intelligence and Neuroscience
Volume 2023, Article ID 9762702, 1 page
https://doi.org/10.1155/2023/9762702

Retraction

Retracted: Innovation and Reform of Ideological and Political Course Mode in Colleges and Universities Based on Big Data Network Platform

Computational Intelligence and Neuroscience

Received 22 August 2023; Accepted 22 August 2023; Published 23 August 2023

This article has been retracted by Hindawi following an investigation undertaken by the publisher [1]. This investigation has uncovered evidence of one or more of the following indicators of systematic manipulation of the publication process:

(1) Discrepancies in scope

(2) Discrepancies in the description of the research reported

(3) Discrepancies between the availability of data and the research described

(4) Inappropriate citations

(5) Incoherent, meaningless and/or irrelevant content included in the article

(6) Peer-review manipulation

The presence of these indicators undermines our confidence in the integrity of the article's content and we cannot, therefore, vouch for its reliability. Please note that this notice is intended solely to alert readers that the content of this article is unreliable. We have not investigated whether authors were aware of or involved in the systematic manipulation of the publication process.

Wiley and Hindawi regrets that the usual quality checks did not identify these issues before publication and have since put additional measures in place to safeguard research integrity.

We wish to credit our own Research Integrity and Research Publishing teams and anonymous and named external researchers and research integrity experts for contributing to this investigation.

The corresponding author, as the representative of all authors, has been given the opportunity to register their agreement or disagreement to this retraction. We have kept a record of any response received.

References

[1] D. Qiu, "Innovation and Reform of Ideological and Political Course Mode in Colleges and Universities Based on Big Data Network Platform," *Computational Intelligence and Neuroscience*, vol. 2022, Article ID 1036168, 9 pages, 2022.

Hindawi
Computational Intelligence and Neuroscience
Volume 2023, Article ID 2911846, 15 pages
https://doi.org/10.1155/2023/2911846

Research Article

High-Precision Positioning Simulation and Experimental Research of Special Operation Vehicles Based on Network RTK

Zhongyi Zhao, Yongzhi Cui, and Shenyu Wang

Faculty of Mechanical Engineering and Automation, Liaoning University of Technology, Jinzhou 121001, Liaoning, China

Correspondence should be addressed to Zhongyi Zhao; jxzhaozy@lnut.edu.cn

Received 7 September 2022; Revised 18 October 2022; Accepted 24 November 2022; Published 2 February 2023

Academic Editor: Gopal Chaudhary

In terms of driverless systems, high-precision positioning technology is one among the critical aspects of driverless cars to achieve driverlessness. This study analyzed the working principles of GNSS (global navigation satellite system) and SINS (strapdown inertial navigation system) and elaborated the principles of the least square method and LAMBDA algorithm in the integer ambiguity resolution. Based on the network RTK positioning technology and the abovementioned theory, the unmanned automatic work vehicle was used as the research object, and the fusion positioning algorithm of the BDS/GPS system and inertial sensor was used to propose a high-precision positioning technology for the unmanned automatic work vehicle. The combined navigation system model was studied and constructed. Relevant verification was carried out through simulation and experiment. The results were as follows: the pitch angle error was less than 0.1°, the roll angle error was less than 0.05°, the speed error was less than 0.2 m/s, and the position error was less than 2.1 m. The outcomes indicate that an integrated navigation and positioning algorithm for driverless vehicles can significantly enhance the localisation accuracy and reliability of navigation. The research results are of engineering value and practical application for the development of unmanned automatic special vehicle positioning systems.

1. Introduction

In the 21st century, the fields such as artificial intelligence, information technology, machinery and electronics, and precision manufacturing have been developed by leaps and bounds. Accordingly, unmanned and automatically operated special vehicles are also used in a wide range of applications, such as industry, agriculture, and fire protection. Since manual operation is not suitable in high-temperature, highly polluting, and high-risk environments, unmanned vehicles are used to replace workers to detect and collect information in harsh and dangerous environments. Furthermore, technologies used in unmanned automatic special vehicles are extensive, including automatic control technology, computer science, and machine vision, which is worthy of studying [1–3].

RTK (real-time kinematic) technology uses GPS carrier phase observations to correct the positioning system, thus carrying out real-time dynamic relative positioning. With the continuous advancement of RTK technology, it has been widely used in transportation, engineering mapping, geological disaster monitoring, and other fields and gradually replaced the traditional navigation and positioning methods [4–6]. Modern society places greater demands on the navigation precision. However, a single navigation technology has difficulty in adapting to the complex working environment. In practical engineering applications, various navigation methods are often combined to complement each other and achieve high-precision positioning [7, 8]. This study focused on the research on high-precision positioning technology of unmanned special operation vehicles by using SINS (strapdown inertial navigation system) and satellite navigation integrated positioning, and relevant tests were carried out.

2. Research on Positioning Theory

2.1. GNSS Differential Observation Equation. In GNSS data processing, the functional relation between the original observation of the receiver and various factors affecting signal propagation is the GNSS observation equation. In

GNSS positioning, satellites constantly broadcast navigation signals, and the receiver calculates the received pseudorange, carrier phase, and Doppler information to achieve navigation and positioning [9]. The pseudorange and carrier phase observations are two primitive observations which have the following observation equations:

$$p_r^s = \rho_r^s + c\left(dt_r - dt^s\right) + T_r^s + I_r^s + \delta_r^s + \varepsilon p_r^s, \tag{1}$$

$$\varphi_r^s = \rho_r^s + c\left(dt_r - dt^s\right) + T_r^s - I_r^s + \lambda N_r^s + \gamma_r^s + \varepsilon\varphi_r^s. \tag{2}$$

In equations (1) and (2), the superscript s denotes the observation satellite, the subscript r denotes the receiver, p and φ denote pseudorange and carrier phase observation, respectively, ρ indicates the actual distance between the satellite and the receiver when the signal is transmitted, c denotes the speed of light in vacuum, dt_r and dt^s d denote the receiver clock error and satellite clock error, respectively, indicating tropospheric error during the propagation of the signal through the atmosphere, I denotes the ionospheric error in the process of signal propagation in the atmosphere, λ denotes the carrier phase wavelength, N denotes the integer ambiguity in weeks, and εp and $\varepsilon\varphi$ denote other errors in pseudorange and carrier phase, respectively (including noise errors).

2.1.1. Double-Difference Observation Model. The principle of double-difference positioning is shown in Figure 1. Double-difference is a method of carrying out the intersatellite difference for another reference satellite [10, 11].

The base station receiver r and the mobile station receiver q perform difference calculation on the same satellite s. The pseudorange and carrier phase observation equations of the base station r are equations (1) and (2), respectively. The pseudorange and carrier phase observation equations for mobile station q are as follows:

$$p_q^s = \rho_q^s + c\left(dt_q - dt^s\right) + T_q^s + I_q^s + \delta_q^s + \varepsilon p_q^s, \tag{3}$$

$$\varphi_q^s = \rho_q^s + c\left(dt_q - dt^s\right) + T_q^s - I_q^s + \lambda N_q^s + \gamma_q^s + \varepsilon\varphi_q^s. \tag{4}$$

The difference between equations (1) and (3) and the difference between equations (2) and (4) can eliminate the satellite clock difference dt_q, thus obtaining a single difference model as follows:

$$\Delta p_{rq}^s = \Delta\rho_{rq}^s + cdt_{rq} + \left(T_r^s - T_q^s\right) + \left(I_r^s - I_q^s\right) + \Delta\delta_{rq}^s + \Delta\varepsilon p_{rq}^s, \tag{5}$$

$$\Delta\varphi_{rq}^s = \Delta\rho_{rq}^s + cdt_{rq} + \left(T_r^s - T_q^s\right) - \left(I_r^s - I_q^s\right) + \lambda\Delta N_{rq}^s + \Delta\gamma_{rq}^s + \Delta\varepsilon\varphi_{rq}^s. \tag{6}$$

In equations (5) and (6), Δ denotes the single difference. With short baselines, the difference between ionospheric and tropospheric delay errors for base stations and mobile stations is small, so the difference between the troposphere and the ionosphere in equations (5) and (6) is regarded as equal to 0, which can be obtained as follows:

$$\Delta p_{rq}^s = \Delta\rho_{rq}^s + cdt_{rq} + \Delta\delta_{rq}^s + \Delta\varepsilon p_{rq}^s, \tag{7}$$

$$\Delta\varphi_{rq}^s = \Delta\rho_{rq}^s + cdt_{rq} + \lambda\Delta N_{rq}^s + \Delta\gamma_{rq}^s + \Delta\varepsilon\varphi_{rq}^s. \tag{8}$$

Assuming that the reference satellite is y, the single difference equation of the base station r and the mobile station q are as follows:

$$\Delta p_{rq}^y = \Delta\rho_{rq}^y + cdt_{rq} + \Delta\delta_{rq}^y + \Delta\varepsilon p_{rq}^y, \tag{9}$$

$$\Delta\varphi_{rq}^y = \Delta\rho_{rq}^y + cdt_{rq} + \lambda\Delta N_{rq}^y + \Delta\gamma_{rq}^y + \Delta\varepsilon\varphi_{rq}^y. \tag{10}$$

By differentiating equations (7) and (9) and equations (8) and (10), the receiver clock difference term is eliminated to obtain the following double-difference observation equation:

$$\begin{aligned}\nabla\Delta p_{rq}^{sy} &= \nabla\Delta\rho_{rq}^{sy} + \nabla\Delta\delta_{rq}^{sy} + \nabla\Delta\varepsilon p_{rq}^{sy},\\ \nabla\Delta\varphi_{rq}^{sy} &= \nabla\Delta\rho_{rq}^{sy} + \lambda\nabla\Delta N_{rq}^{sy} + \nabla\Delta\gamma_{rq}^{sy} + \nabla\Delta\varepsilon\varphi_{rq}^{sy}.\end{aligned} \tag{11}$$

In the above equations, $\nabla\Delta$ denotes the double-difference symbol. The double-difference integer ambiguity retains the integer characteristic and can be effectively separated.

Assuming that there are N available satellites, the number of observation equations for carrier phase and pseudorange is $2(N-1)$, where the unknowns include three direction coordinates of baseline double-difference pseud range and $N-1$ double-difference ambiguity. To solve the float solution of ambiguity, $2(N-1) \geq 3 + (N-1)$ is needed and the solution is $N=4$. Therefore, the simultaneous observation of four visual satellites is the minimum requirement for a single system to realize differential positioning [12, 13].

When four satellites a, b, c, and d are used for calculation, a 6-dimensional equation group can be established by adding pseudorange double-difference observations. Taking the satellite a with large altitude angle as the main satellite, the following results can be obtained:

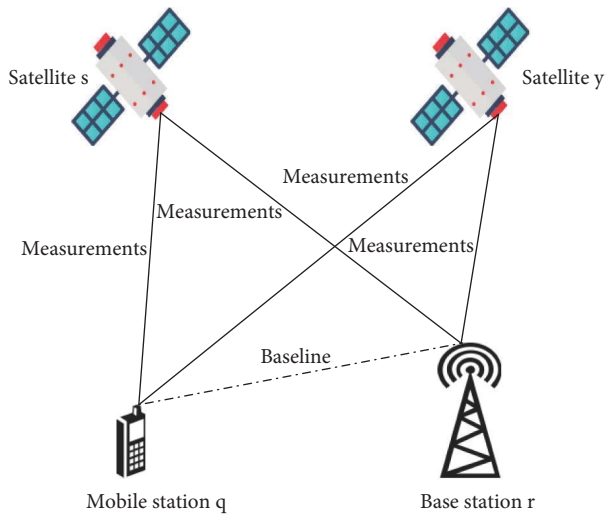

Figure 1: Double-difference observation model.

$$\begin{bmatrix} \lambda * \nabla\Delta\phi_{rq}^{ab} - \nabla\Delta\rho_{rq}^{ab} \\ \lambda * \nabla\Delta\phi_{rq}^{ab} - \nabla\Delta\rho_{rq}^{ab} \\ \lambda * \nabla\Delta\phi_{rq}^{ab} - \nabla\Delta\rho_{rq}^{ab} \\ \nabla\Delta R_{rq}^{ab} - \nabla\Delta\rho_{rq}^{ab} \\ \nabla\Delta R_{rq}^{ac} - \nabla\Delta\rho_{rq}^{ab} \\ \nabla\Delta R_{rq}^{ad} - \nabla\Delta\rho_{rq}^{ab} \end{bmatrix} = \begin{bmatrix} -l_r^{ab} & -m_r^{ab} & -n_r^{ab} & -\lambda & & \\ -l_r^{ac} & -m_r^{ac} & -n_r^{ac} & & -\lambda & \\ -l_r^{ad} & -m_r^{ad} & -n_r^{ad} & & & -\lambda \\ -l_r^{ab} & -m_r^{ab} & -n_r^{ab} & 0 & & \\ -l_r^{ac} & -m_r^{ac} & -n_r^{ac} & & 0 & \\ -l_r^{ad} & -m_r^{ad} & -n_r^{ad} & & & 0 \end{bmatrix} \cdot \begin{bmatrix} \delta X_r \\ \delta Y_r \\ \delta Z_r \\ \nabla\Delta N_{rq}^{ab} \\ \nabla\Delta N_{rq}^{ac} \\ \nabla\Delta N_{rq}^{ad} \end{bmatrix}, \tag{12}$$

where $[l \ m \ n]$ is the unit vector from the satellite to the receiver, $[\delta X \ \delta Y \ \delta Z]$ is the correction number of the receiver's approximate coordinate, and $\nabla\Delta R$ is the double-difference pseudorange observation, and equation (12) is written in the following matrix form:

$$Y = HX. \tag{13}$$

In equation (13), H is the design matrix composed of the unit vector from the receiver to the satellite, X is the baseline vector and ambiguity solution to be solved, and the float solution of ambiguity can be solved by the least square method as follows:

$$\hat{X} = \left(H^T PH\right)^{-1} H^T PY. \tag{14}$$

In equation (14), $\hat{X}$ is the float solution of ambiguity. Let the baseline vector $\hat{m} = [\delta X_r \ \delta Y_r \ \delta Z_r]$ and the double-difference integer ambiguity vector $\hat{n} = \begin{bmatrix} \nabla\Delta N_{rq}^{ab} & \nabla\Delta N_{rq}^{ac} & \nabla\Delta N_{rq}^{ad} \end{bmatrix}$, and the least square result can be expressed as follows:

$$\hat{X} = \begin{bmatrix} \hat{m} \\ \hat{n} \end{bmatrix}, \tag{15}$$

$$Q = \begin{bmatrix} Q_{\hat{m}} & Q_{\hat{m}\hat{n}} \\ Q_{\hat{n}\hat{m}} & Q_{\hat{n}} \end{bmatrix} = \left(H^T PH\right)^{-1}. \tag{16}$$

In equation (16), Q denotes the covariance matrix of vector X, $Q_{\hat{m}}$ denotes the covariance matrix of baseline vector, $Q_{\hat{n}}$ represents the covariance matrix of ambiguity vector, and $Q_{\hat{m}\hat{n}}$ and $Q_{\hat{n}\hat{m}}$ denote the cross-covariance matrix of baseline vector and ambiguity vector, respectively.

2.2. Integer Ambiguity Estimation. Integer ambiguity is crucial to achieve high-precision RTK positioning [14]. At present, there are numerous ambiguity resolution methods, among which the LAMBDA algorithm has a perfect theoretical system, so the LAMBDA algorithm based on the least square estimation algorithm and the residual square of ambiguity is adopted.

The float solution $\hat{X}$ is decomposed into the form of baseline vector and integer ambiguity vector, and the following is obtained:

$$y = M\hat{m} + N\hat{n} + \varepsilon. \tag{17}$$

In equation (18), y is the double-difference observation of pseudorange and carrier phase, $\hat{m}$ is the baseline vector, M is the coefficient matrix of the baseline vector, N is the integer ambiguity coefficient matrix, $\hat{n}$ is double-difference integer ambiguity, and ε is unmodeled error amount. Therefore, the ambiguity solution is transformed into the least square.

$$\min_{\widehat{m}\widehat{n}} \|y - M\widehat{m} - N\widehat{n}\|^2_{Q_y}. \tag{18}$$

In equation (18), Q_y is the covariance matrix of y.

If ambiguity is independent of each other, the covariance matrix of the ambiguity is a diagonal matrix, and the optimal solution can be obtained by the nearest rounding. In general, due to the strong correlation between the ambiguity, the ambiguity covariance matrix is not a diagonal matrix, resulting in a low success rate through the rounding method.

The integer ambiguity float solution $\widehat{X}$ and the covariance matrix Q are obtained through equations (15) and (16), and then, the integer solution $\acute{n}$ of the ambiguity is estimated by using the ambiguity vector float solution $\widehat{n}$ and the covariance matrix $Q_{\widehat{n}}$ to minimize the sum of residual squares of ambiguity, as follows:

$$\min_{n\in Z} (\widehat{n} - n)^T Q_{\widehat{n}}^{-1} (\widehat{n} - n). \tag{19}$$

2.3. Basic Principle of Strapdown Inertial Navigation. Attitude update includes sensing the attitude information of the carrier and converting the measured real-time information to the navigation coordinate system to realize the position and speed update [15, 16].

The solution process is as follows: The initial information of navigation calculation is obtained through initial alignment. Then, the real-time speed, position information, and attitude information of the unmanned vehicle are obtained by calculating the acceleration. SINS is shown in Figure 2.

3. Modeling and Simulation of the Integrated Navigation and Positioning System

3.1. System Modeling

3.1.1. State Equation of Integrated Navigation. When combined navigation uses Kalman filtering for information processing, it is first necessary to establish a state equation that reflects the system state vector dynamic properties. [17, 18].

Generally speaking, the inertial navigation misalignment angle Φ, speed error δv^n, position error δp, random constant drift of gyroscope ε^b, and the random constant bias value of the accelerometer ∇^b are selected in the state equation and are taken as state vectors, and the state equation of the integrated n avigation system is as follows:

$$X(t) = F(t)X(t) + G(t)w^b(t). \tag{20}$$

The state vector of the system state equation is as follows:

$$X(t) = \left[\begin{array}{ccccc} \Phi^T & (\delta v^n)^T & (\delta p)^T & (\varepsilon^b)^T & \left(\nabla^b\right)^T \end{array}\right]^T. \tag{21}$$

The system state transition matrix is as follows:

$$F(t) = \begin{bmatrix} M_{aa} & M_{av} & M_{ap} & -C_b^n & 0_{3\times3} \\ M_{va} & M_{vv} & M_{vp} & 0_{3\times3} & C_b^n \\ 0_{3\times3} & M_{pv} & M_{pp} & 0_{3\times3} & 0_{3\times3} \\ & & 0_{6\times15} & & \end{bmatrix}. \tag{22}$$

Equation (22) is a 15-dimensional system transition matrix. In practical application, the zero drift of gyroscope, accelerometer, and magnetometer varies little with time, so the erasable term in the transition matrix is set as 0. The system noise vector is as follows:

$$w^b(t) = \begin{bmatrix} w_g^b \\ w_a^b \end{bmatrix}. \tag{23}$$

In equation (23), w_g^b denotes the angular velocity measurement noise of the gyroscope and w_a^b denotes the specific force measurement noise of the accelerometer.

3.1.2. Integrated Navigation Measurement Equation. In integrated navigation, the position information and speed information obtained by the MEMS strapdown inertial navigation system are subtracted from the longitude, latitude, and speed information received by the GNSS receiver, and the obtained measurement equation of the speed and position of the unmanned vehicle is as follows:

$$Z(t) = [\,\overline{v}_{INS}^n - \overline{v}_{GNSS}^n \widetilde{p}_{INS} - \widetilde{p}_{GNSS}] = H(t)X(t) + \nu(t), \tag{24}$$

where $\overline{v}_{INS}^n$, $\overline{v}_{GNSS}^n$, $\widetilde{p}_{INS}$, and $\widetilde{p}_{GNSS}$ are the inertial navigation speed, satellite navigation speed, inertial navigation position, and satellite navigation position, respectively.

$$H(t) = [\,0_{6\times3} \;\; I_{6\times6} \;\; 0_{6\times3}\,], \nu(t) = \begin{bmatrix} \nu_v \\ \nu_p \end{bmatrix}. \tag{25}$$

In equation (25), ν_v denotes the speed measurement noise of the satellite receiver and ν_p denotes the position measurement noise of the satellite receiver.

3.1.3. Discretization of Continuous-Time Stochastic Systems. The continuous-time stochastic system given by equation (20) should be discretized. Equations (27)–(29) can be approximated by equivalent discretization of equations (20) and (24).

$X_k = X(t_k)$, $\Gamma_{k-1} = G(t_{k-1})$, $Z_k = Z(t_k)$, and $H_k = H(t_k)$. T_s is the discrete time interval.

$$\Phi_{k/k-1} \approx e^{\int_{t_{k-1}}^{t_k} F(\tau)\mathrm{d}\tau} \approx I + F(t_{k-1})T_s \approx I + \bar{F}(t_k, t_{k-1})T_s, \tag{26}$$

$$Q_{k-1} \approx q(t_{k-1})T_s, \tag{27}$$

$$R_k \approx \frac{r(t_k)}{T_s}. \tag{28}$$

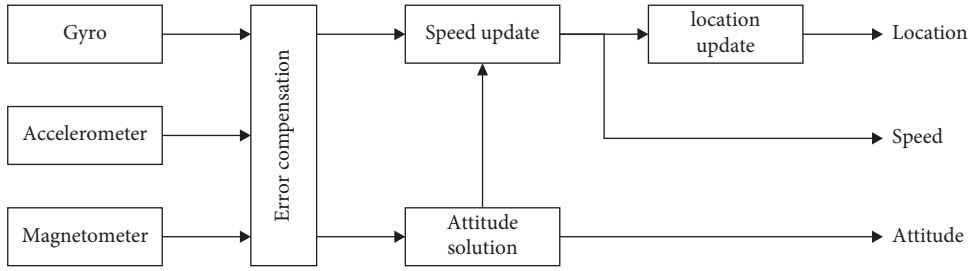

Figure 2: Strapdown inertial navigation system.

In the above equations, $F(t)$ is approximately constant and $F(t_{k-1})T_s$ is a small quantity, that is, $|F(t_{k-1})T_s| \succ\succ F^2(t_{k-1}){T_s}^2$, ignoring the higher-order term of Taylor series expansion.

$\overline{F}(t_k, t_{k-1})$ denotes the mean value of the system matrix in time period $[t_{k-1}, t_k]$.

3.1.4. Integrated Navigation Time Synchronization. In SINS/GNSS integrated navigation, the signal delay of inertial devices is relatively short, while the satellite signal has a relatively long delay from acquisition to positioning solution to transmission to navigation computer, and there is a time asynchrony error between the two.

In SINS/GNSS integrated navigation, the time asynchrony between the receiver and the inertial navigation system is shown in Figure 3. The time lag of inertial navigation and satellite navigation is generally different, and the time asynchrony error is the relative lag of the two systems. Therefore, in the comparison of integrated navigation information, it is necessary to compensate for the time asynchrony error.

The relationship between inertial navigation speed and satellite speed is as follows:

$$v^n_{INS} - v^n_{GNSS} = a^n \delta t. \tag{29}$$

In equation (29), a^n is the average linear acceleration of the unmanned vehicle in the asynchronous time, which can be approximately obtained by differential calculation of the speed of the inertial navigation system in two adjacent times, and the adjacent time is expressed as follows:

$$\begin{aligned} T &= t_m - t_{m-1}, \\ a^n &\approx \frac{v^n_{INS(m)} - v^n_{GNSS(m-1)}}{T}. \end{aligned} \tag{30}$$

In general, it is considered that the value of time asynchrony is relatively fixed.

From equation (29), it can be calculated that the velocity asynchrony error between the satellite and the inertial navigation is as follows:

$$\delta v^n_{\delta t} = v^n_{INS} - v^n_{GNSS} = a^n \delta t. \tag{31}$$

Similarly, the position asynchrony error of the two is as follows:

$$\delta p^n_{\delta t} = p_{INS} - p_{GNSS} = M_{pv} v^n_{INS} \delta t. \tag{32}$$

The actual system is nonlinear, often using EKF (extended Kalman filter). EKF is the Taylor level first, omitting its high-oriented item is approximately linear system, and then Kalman filtering.

3.2. Simulation Analysis. To verify the feasibility of Kalman filter of integrated navigation, the navigation algorithm is compiled by MATLAB for simulation analysis. The simulated motion trajectory parameters of the unmanned vehicle are generated according to the set motion state, and error parameters conforming to the actual application are added on this basis. Finally, the simulated IMU and GNSS data were input into the integrated navigation solution program, thus obtaining the navigation information such as the attitude (heading angle, pitch angle, and roll angle), speed, longitude, and latitude of the unmanned vehicle.

3.2.1. Simulation Device Parameters. The principle of the simulation is shown in Figure 4. Device errors of inertial sensors are added to simulate the pure inertial navigation and SINS/GNSS integrated navigation on the generated data.

The simulation IMU generates the acceleration and angular velocity of the unmanned vehicle, while the three-dimensional velocity of the unmanned vehicle is generated by GNSS. The data update frequency of MEMS is 100 Hz, and the simulation device parameters are shown in Table 1.

The navigation adopts the "east, north, and up" coordinate system, and the initial attitude is 0°, 0°, and 0°. The initial position is longitude 121.07014° E, latitude 41.08478° N, and 50 m high. The initial speed is 0 m/s, the initial velocity error is 0.1 m/s, the initial attitude angle error is 0.03°, 0.01°, and −0.42°, the initial position error is 0 m, and the data output frequency of satellite navigation is 10 Hz.

3.2.2. Simulation Results. Due to the gyroscope drift and random walk of MEMS, its error is very large, and it cannot be used alone for a long time. Therefore, GNSS information is used for integrated navigation, and Kalman filter is used for data fusion to increase the precision and stability of integrated systems. The simulation experiment is designed with a duration of 500 s. The navigation experiment was carried out on the position, attitude angle, and speed under the pure inertial navigation and integrated navigation.

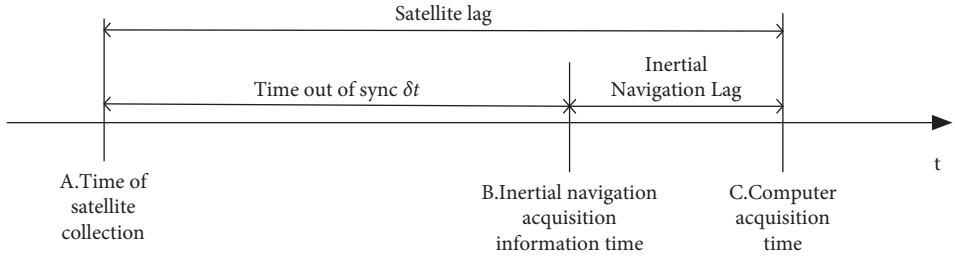

Figure 3: Time asynchrony between receiver and INS.

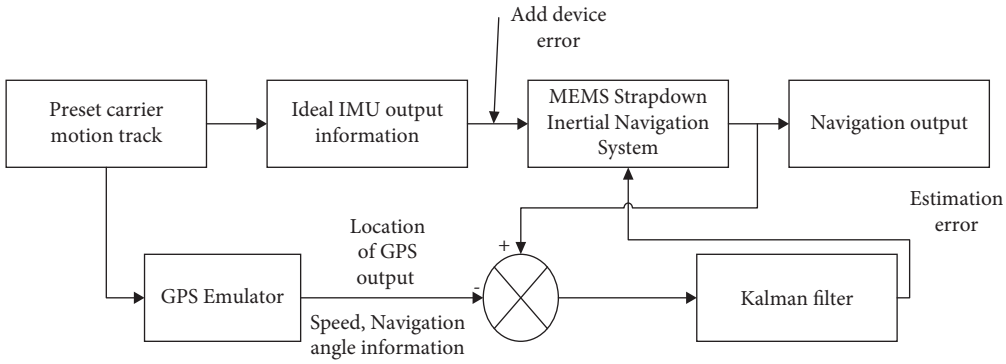

Figure 4: Integrated navigation simulation principle.

Table 1: Simulation device parameters.

Error term	Value	Unit
Angle random walk	0.2	deg/$\sqrt{h}$
Rate random walk	0.02	m/s/$\sqrt{h}$
Gyro static deviation	0.2	deg/s
Static deviation of accelerometer	10	mg

The position and attitude errors of pure inertial navigation are shown in Figures 5 and 6. After 60 s, the position error begins to diverge. After 500 s, the position error can reach −169.1 m, −263.1 m, and −84.67 m. The initial zero bias error of MEMS inertial measurement unit is large, which makes the navigation error result divergent with fast speed. After 500 s of navigation and positioning, the errors of pitch angle, roll angle, and heading angle reach 32.92°, 10.87°, and 32.65°, which cannot meet the navigation accuracy. Therefore, pure inertial navigation cannot be used for positioning alone.

As shown in Figure 7, the position error of integrated navigation fluctuates greatly in the first 50 s, and the longitude and latitude errors fluctuate around 0 in the following 450 s. The position error converges quickly, which shows that the system error of navigation of inertial unit is well suppressed after adding GNSS information. The reason for the fast convergence speed of the longitude and latitude error curves is that while adjusting the parameters of the Kalman filter P, Q, and R matrices, the coefficient of the P matrix is appropriately increased to improve the convergence speed of error curves.

The attitude error of the combined navigation is shown in Figure 8. After using the Kalman filter, the navigation information is corrected by the filtering information, and the attitude error of the combined navigation remains largely fluctuating around 0.

Velocity errors for pure inertial and combined navigation "east, north, and up" directions are shown in Figure 9. If inertial navigation is adopted alone, the velocity errors in the east and north directions fluctuate greatly. When SINS/GNSS integrated navigation is adopted after Kalman filtering, the fluctuation amplitude of velocity errors is significantly reduced and it basically fluctuates around 0.

4. Experimental Study

4.1. Introduction to the Test Platform of Unmanned Vehicles. The external structure of the unmanned special operation vehicle mainly includes 3 Hikvision surveillance cameras, one 5 GHz 433 Mbps outdoor point-to-point network bridge, and two GNSS antennas, as shown in Figure 10. The unmanned special operation vehicle is mainly used for real-time monitoring of the image, sound, air quality, and target temperature, around the observation area. The RTK high-precision BDS/GPS dual-mode positioning and navigation system is used to calibrate the geographic position information and obtain position information of the unmanned vehicle in real time.

4.2. Static Test and Result Analysis. This study used MATLAB to recalculate the saved data of the base station and unmanned vehicle and finally obtained navigation data results. The data update frequency of the GPS system was 10 Hz and that of MEMS was 125 Hz, the observation epoch was 1800 seconds, and the initial position of the unmanned vehicle was latitude 41.08478564° N, longitude 121.0701494° E, and 55.364 m high.

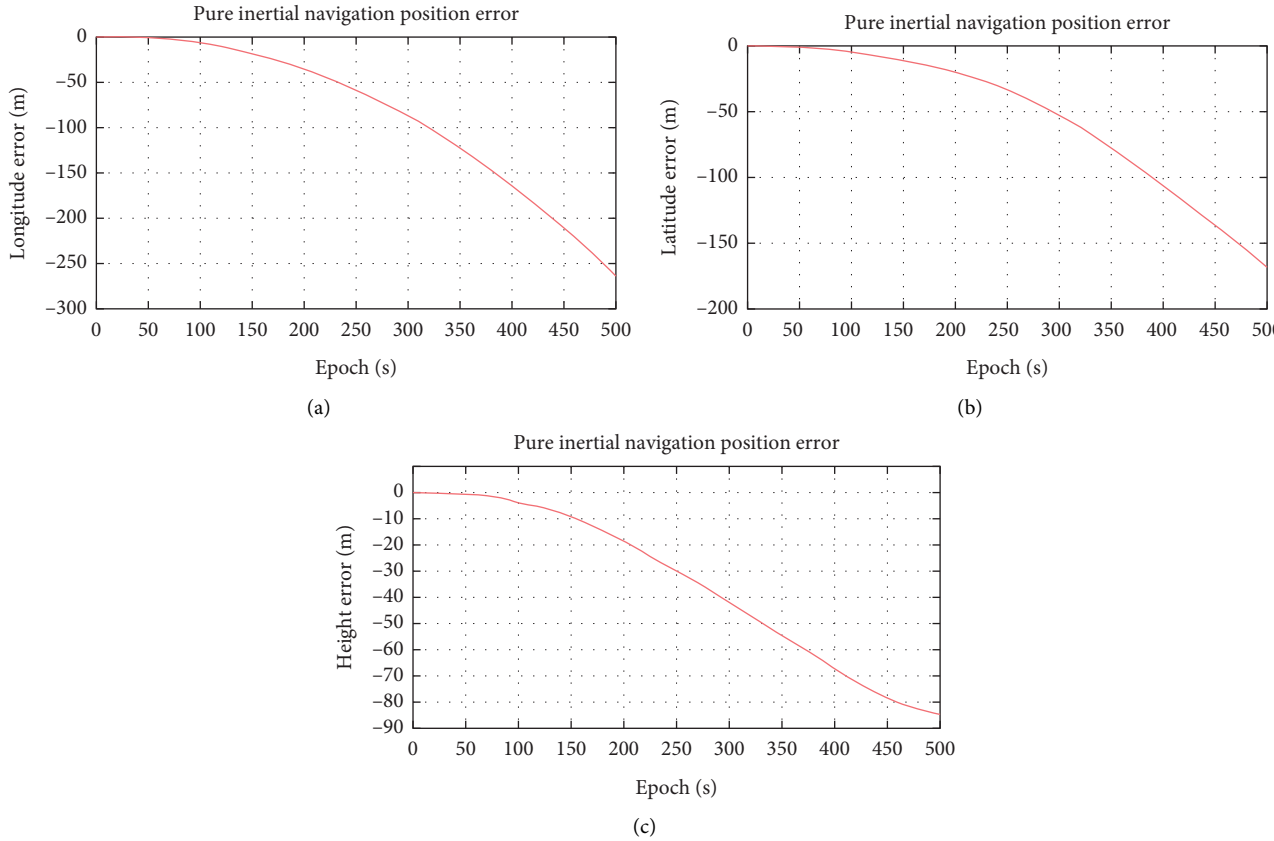

Figure 5: Pure inertial navigation position error. (a) Longitude error. (b) Latitude error. (c) Height error.

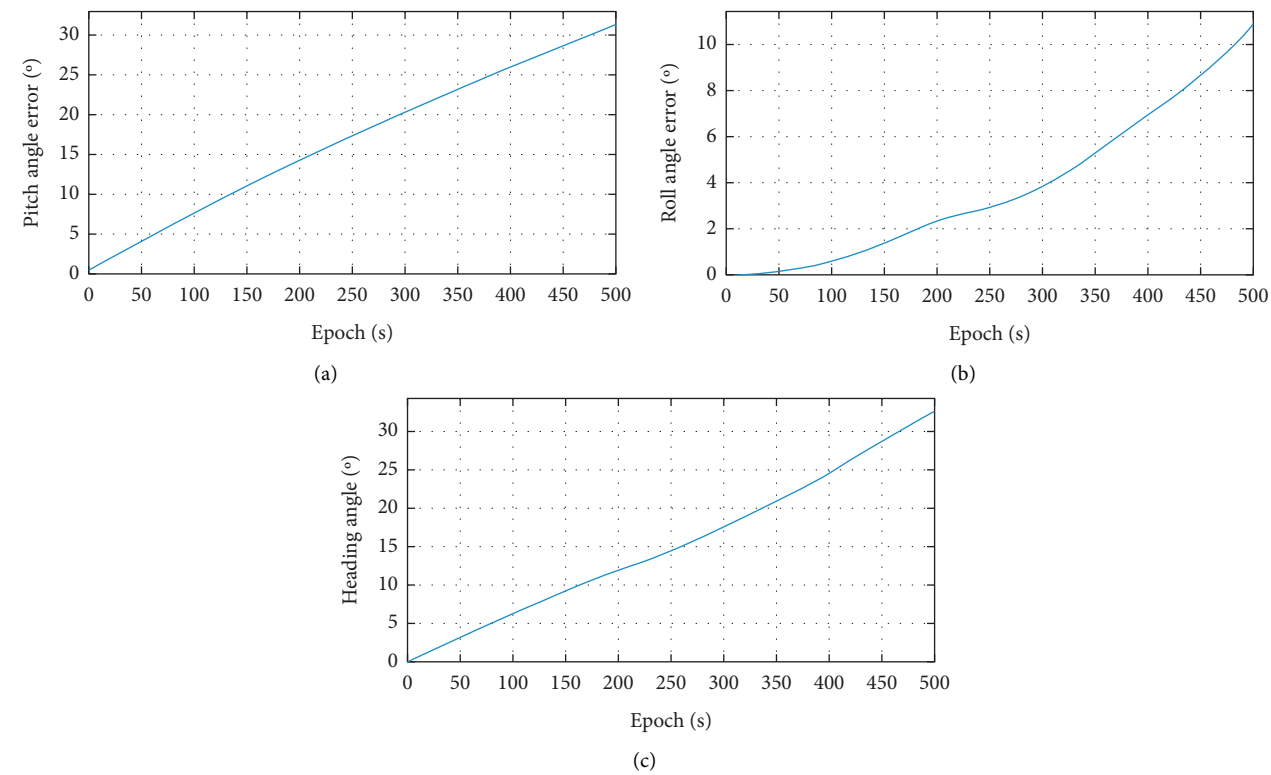

Figure 6: Pure inertial navigation attitude error. (a) Pitch error. (b) Roll angle error. (c) Heading angle error.

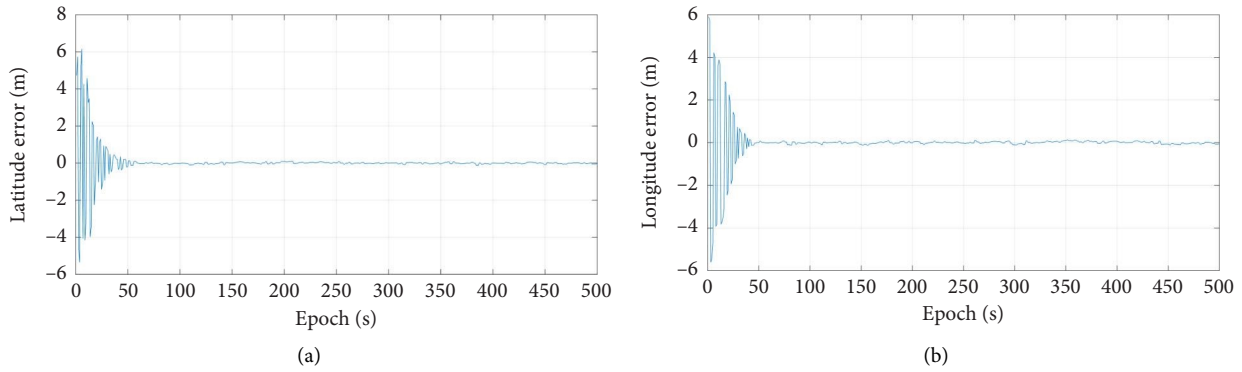

Figure 7: Integrated navigation position error. (a) Latitude error. (b) Longitude error.

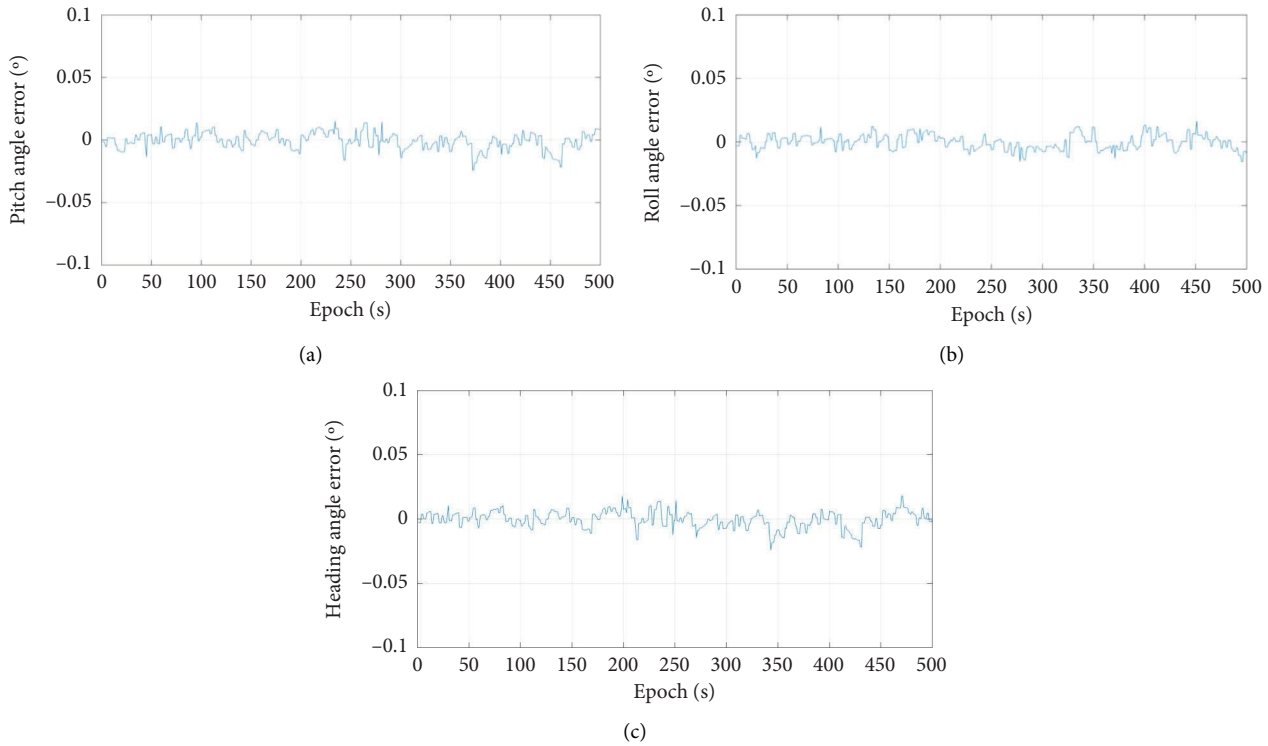

Figure 8: Integrated navigation attitude error. (a) Pitch error. (b) Roll angle error. (c) Heading angle error.

The scatter diagram of longitude and latitude high position obtained by the unmanned vehicle in static state is shown in Figure 11. It can be observed that the static position of the unmanned vehicle is relatively concentrated and the three-dimensional position error is small. The mean value and standard deviation of longitude, latitude, and height were statistically analyzed. The specific information is shown in Table 2.

The number of satellites visible during static testing of unmanned vehicles and base stations is shown in Figure 12. Due to the main reason that the unmanned vehicle is equipped with two GPS antennas, the unmanned vehicle has more visible satellites than the base station in most of the time. In the same time period, if the unmanned vehicle is in a more ideal environment, the number of visible satellites will be more. However, there are more satellites in the base station between 223 and 279 seconds. Especially at the 274th second, the number of visible satellites of the unmanned vehicle is only 11, which may be due to the interference of satellite signals caused by the multipath effect. In the epoch of the static test, the base station has an average of 23.5 (23-24) visible satellites, and the unmanned vehicle has 28, which can meet the basic positioning requirements (the number of visible satellites ≥ 4).

Theoretically, the smaller the HDOP (horizontal dilution of precision), the higher the positioning precision, and its size fluctuates with the number of satellites. The HDOP values of the unmanned vehicle and the base station are shown in Figure 13. HDOP of the unmanned vehicle is smaller than that of the base station. The specific values are

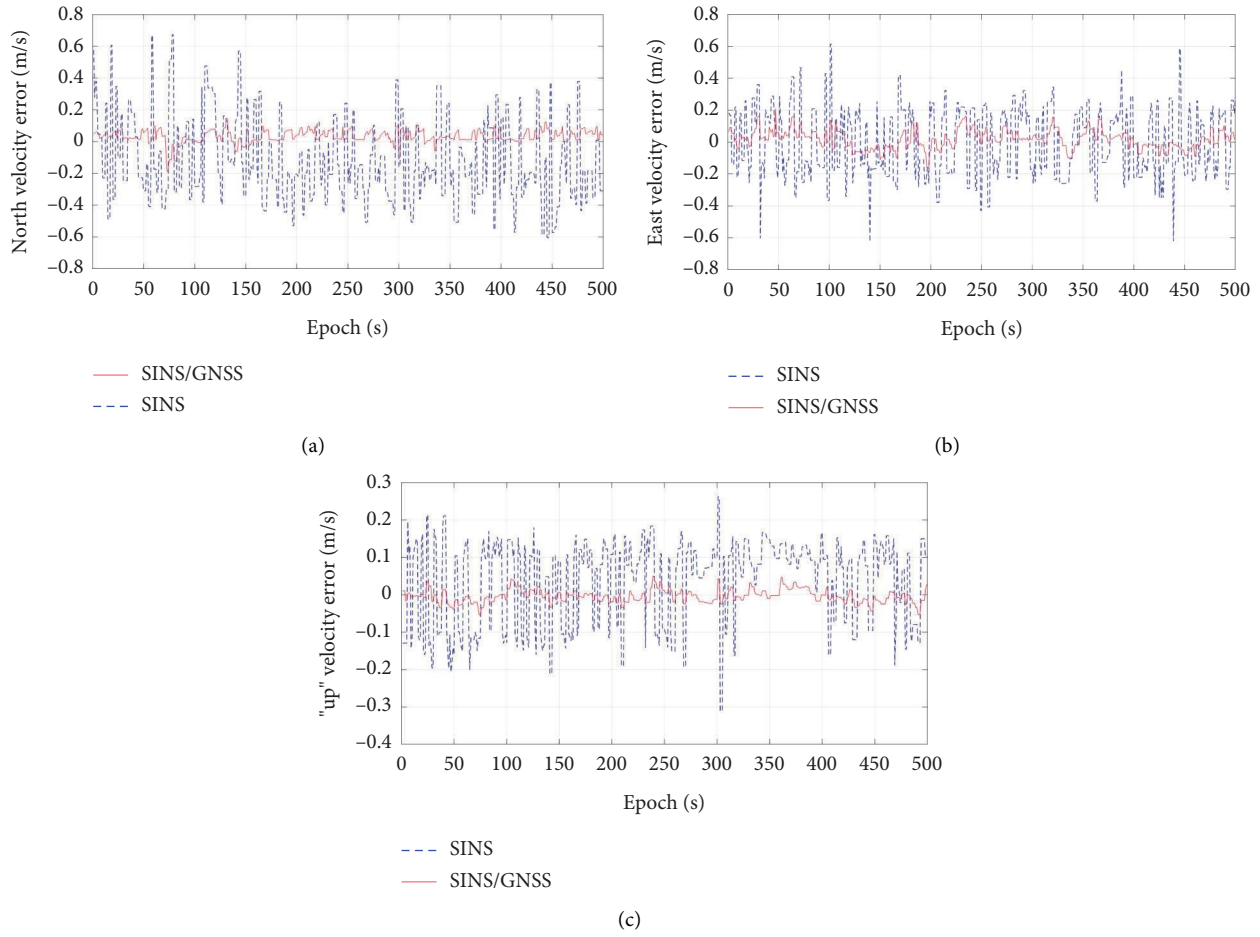

Figure 9: Pure inertial navigation and integrated navigation velocity errors. (a) North velocity error. (b) East velocity error. (c) "Up" velocity error.

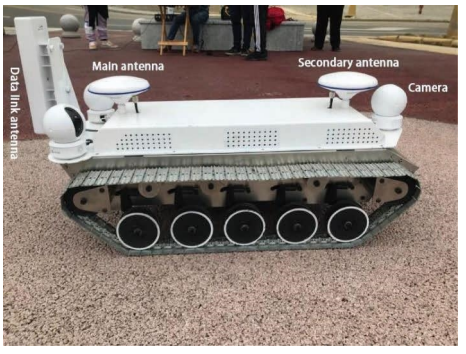

Figure 10: Unmanned vehicle.

as follows: the average HDOP of the unmanned vehicle is 0.55 and the average HDOP of the base station is 0.7.

The attitude angle, eastward speed, and northward speed of static integrated navigation are sorted and counted. The attitude output and speed output of integrated navigation are shown in Figures 14 and 15. The mean value and standard deviation of specific values are shown in Tables 3 and 4.

The pitch angle is stable at −0.0013° and the standard deviation is 0.0021°; the roll angle is stable at 0.0002° and the standard deviation is 0.0074°; and the heading angle is stable at 181.305° and the standard deviation is 0.235°. The standard deviation of pitch angle and roll angle is relatively small, while the course angle has a relatively large standard deviation. The mean and standard deviation of the easting speed and the mean and standard deviation of the northing

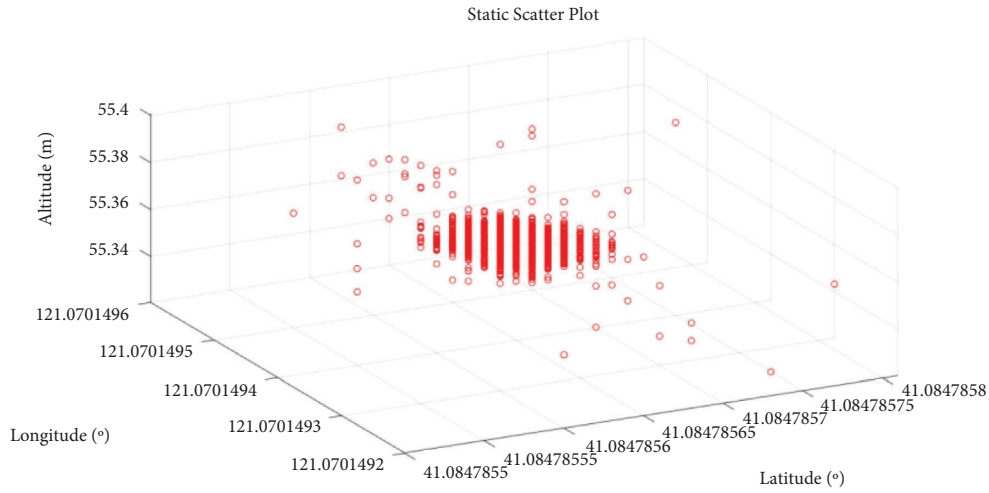

Figure 11: Unmanned vehicle static scatter plot.

Table 2: Static integrated navigation location information statistics.

	Latitude	Longitude	Height
Mean value	41.08478563°	121.0701494°	55.36445 m
Standard deviation (m)	0.0066	0.0034	0.00795

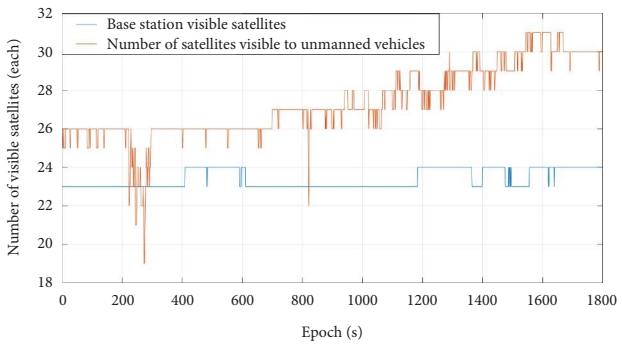

Figure 12: The number of static visible satellites for unmanned vehicles and base stations.

speed are small with little fluctuation, which can meet the needs of high-precision positioning.

4.3. Dynamic Test and Result Analysis. To verify the dynamic stability of the unmanned vehicle, its trajectory on the same rubber track was calibrated to make it move two laps on the set track. The analyzed trajectory is shown in Figures 16 and 17.

The remote controller was used to control the unmanned vehicle to move two laps on the rubber track, and the trajectory obtained on the upper computer is shown in Figures 16(a) and 17(a). The obtained test data are sorted out, and then, the data are processed by MATLAB to convert the obtained motion data into graphic display. The two-dimensional representation of the motion of the unmanned vehicle is shown in Figures 16(b) and 17(b).

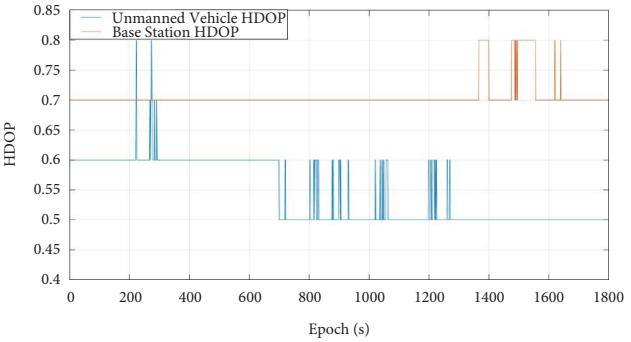

Figure 13: The static HDOP of unmanned vehicle and base station.

As can be seen through the upper computer display of the two movements of the unmanned vehicle and the MATLAB motion trajectory diagram, the satellite receiving state is good during the movement and the trajectory graph formed is clear. Therefore, the first statistical data were selected to analyze the changes of the number of satellites received by the unmanned vehicle, the base station, and the HDOP value. Based on the data collected for the first time, the error between the second data and the first data was observed to analyze the positioning of the unmanned vehicle.

The number of visible satellites of the unmanned vehicle and the base station in the dynamic test is shown in Figure 18 and Table 5. The number of visible satellites of the base station is basically stable at 24 and 25 satellites, while the number of visible satellites of the unmanned vehicle varies greatly, up to 30 and at least 16.

The HDOP of the unmanned vehicle and the base station in the dynamic test is shown in Figure 19. The HDOP value of the base station is 0.7 or 0.8, while the HDOP value of the unmanned vehicle varies greatly, with a maximum of 1.4 and a minimum of 0.5. The mean value and standard deviation are shown in Table 6.

For attitude errors, there are certain errors in about 120 seconds to 180 seconds, 300 seconds to 350 seconds, and

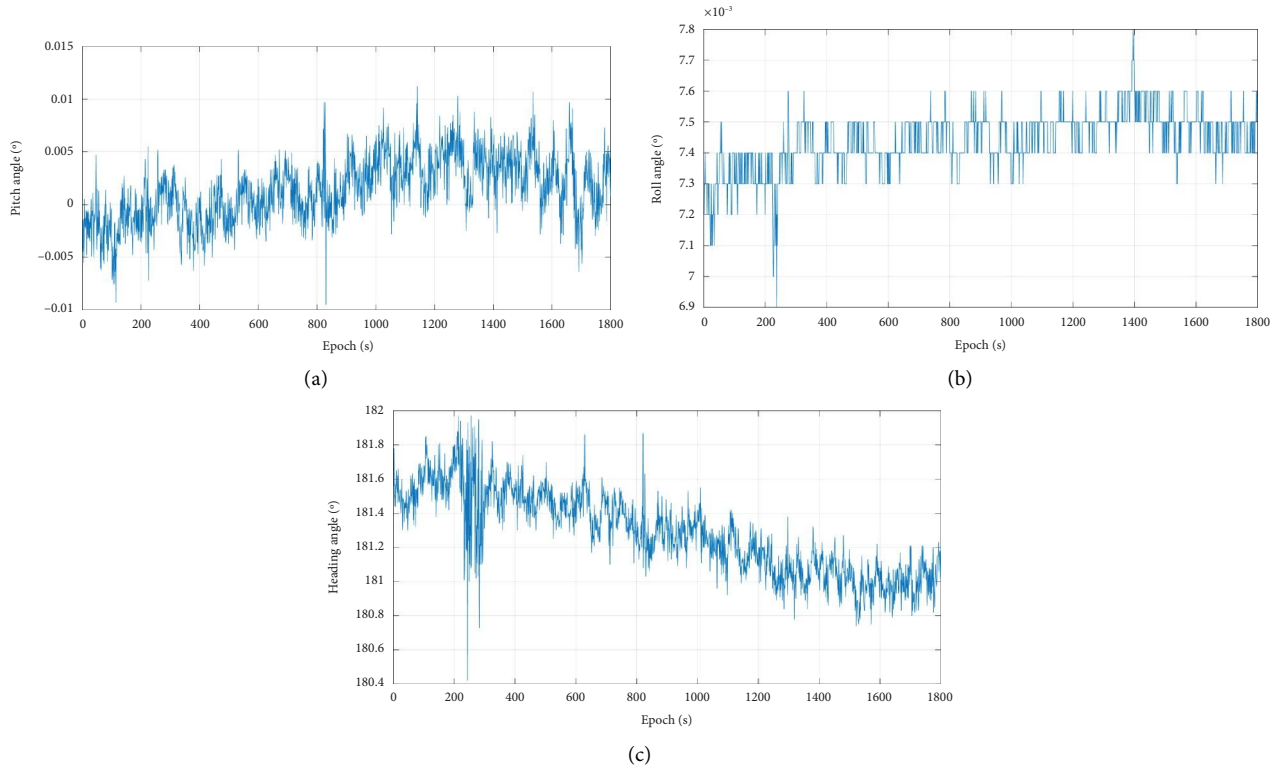

Figure 14: Unmanned vehicle static combined navigation attitude output. (a) Pitch angle. (b) Roll angle. (c) Heading angle.

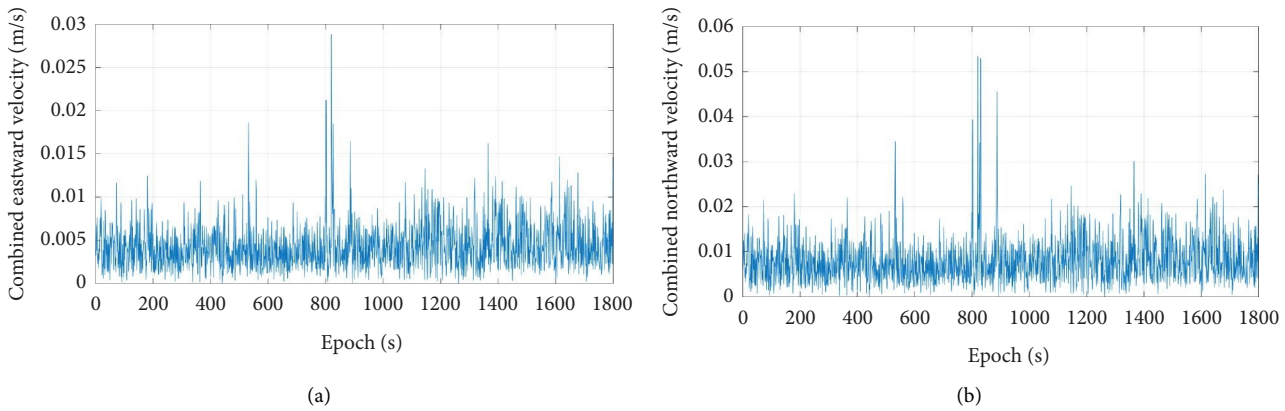

Figure 15: Unmanned vehicle static combined navigation speed output. (a) Combined eastward velocity. (b) Combined northward velocity.

Table 3: Information statistics of static integrated navigation.

	Pitch angle (°)	Roll angle (°)	Heading angle (°)
Mean value	−0.0013	0.0002	181.305
Standard deviation	0.0021	0.0074	0.235

Table 4: Attitude information statistics of static integrated navigation.

	Eastward velocity (m/s)	Northward velocity (m/s)
Mean value	0.00702	0.01425
Standard deviation	0.00377	0.006985

450 seconds to 520 seconds. The pitch angle error is basically −0.1° and 0.1°, the roll angle error is −0.05° and 0.05°, the heading angle error is −0.2°and 0.2°, and only a few epochs reach the end point of the range. The velocity error is also concentrated in the last two time periods of the attitude error. The eastward velocity error is −0.3 m/s and 0.3 m/s, and the northward velocity error is −0.2 m/s and 0.2 m/s, as shown in Figures 20 and 21.

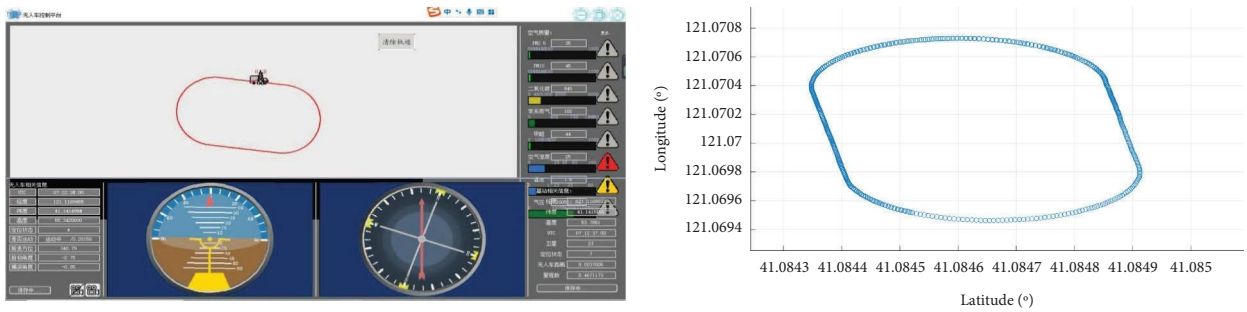

(a) (b)

Figure 16: The first trajectory of the unmanned vehicle. (a) Upper computer display of the first trajectory of the unmanned vehicle. (b) MATLAB display of the first trajectory of the unmanned vehicle.

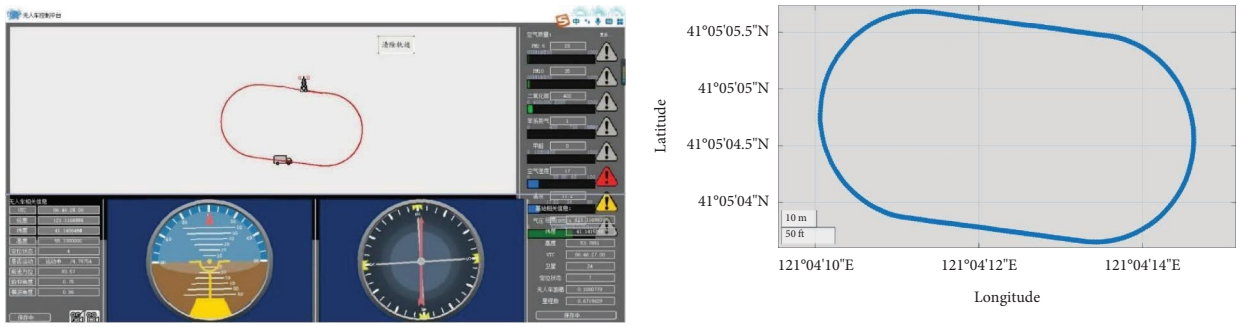

(a) (b)

Figure 17: The second trajectory of the unmanned vehicle. (a) Upper computer display of the second trajectory of the unmanned vehicle. (b) MATLAB display of the second trajectory of the unmanned vehicle.

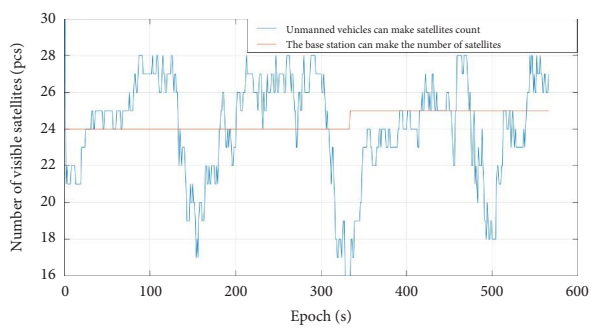

Figure 18: The number of visible satellites in the dynamic test.

Table 5: Visual satellite information statistics.

	Number of visible satellites of the unmanned vehicle	Number of visible satellites of the base station
Mean value	28.5	24.5
Standard deviation	1.5	0.5

The position error of the dynamic integrated navigation of the unmanned vehicle is shown in Figure 22. The error in most time periods is 0, the maximum error in latitude is about 2.1 m, and the maximum error in longitude is about 2.8 m. The main reason for the error is that the unmanned vehicle was disturbed by the surrounding environment during its movement, which affected its positioning precision and stability. The main reasons for the fluctuation of curves in the figure are insufficient

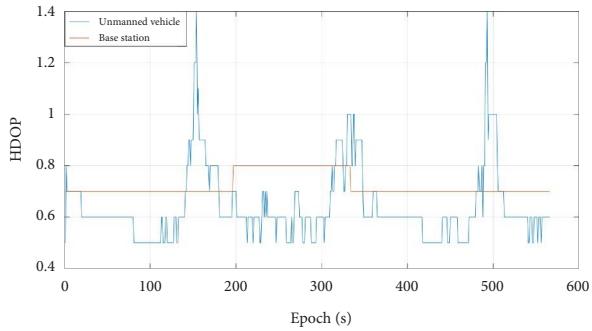

Figure 19: Dynamic test HDOP.

Table 6: HDOP statistics.

	HDOP value of the unmanned vehicle	HDOP value of the base station
Mean value	0.55	0.7
Standard deviation	0.05	0

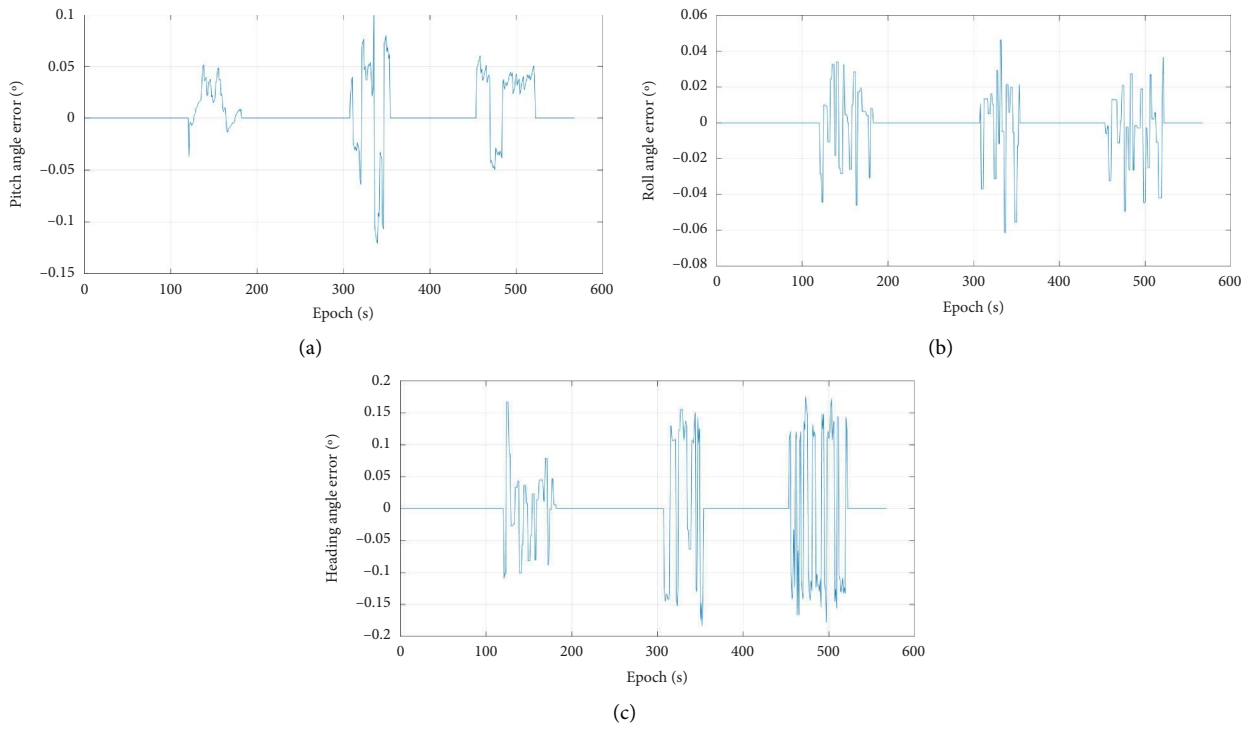

Figure 20: Attitude errors of dynamic integrated navigation. (a) Pitch angle error. (b) Roll angle error. (c) Heading angle error.

compensation of the inertial device and poor stability of the inertial device under dynamic conditions.

The static and dynamic tests of the dual antenna GPS/MEMS integrated navigation system were carried out. The test results showed that if the pure inertial navigation system was used alone for a long time, its error would continue to accumulate with time, which would lead to the failure to complete the high-precision positioning

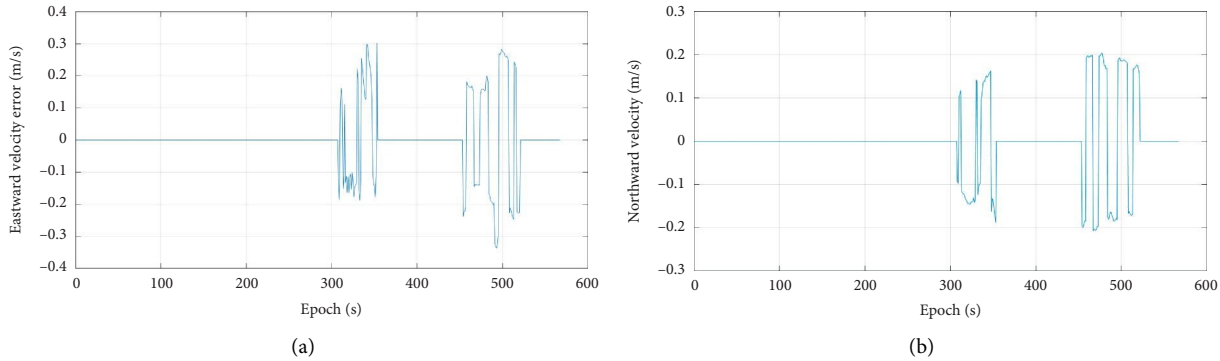

(a) (b)

Figure 21: Velocity errors of dynamic integrated navigation. (a) Eastward velocity error. (b) Northward velocity error.

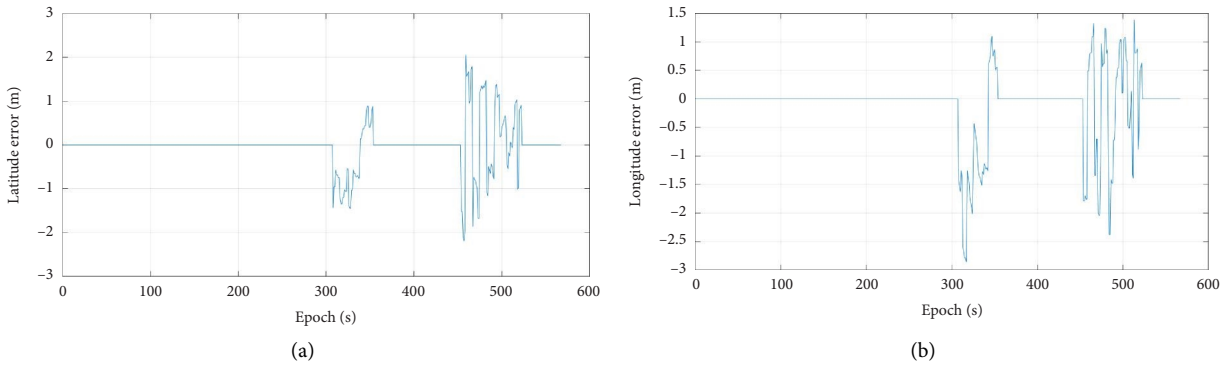

(a) (b)

Figure 22: Position errors of dynamic integrated navigation. (a) Latitude error. (b) Longitude error.

requirements. Therefore, integrated navigation should be used.

Each module of the unmanned vehicle worked well together, the performance was stable, and the positioning module was powerful, which could be applied to the actual situation.

When the unmanned vehicle was in an ideal environment, the satellite signal was better and the number of visible satellites received was relatively large. Using the integrated navigation, the attitude, position, and velocity information of the unmanned vehicle was ideal. When the unmanned vehicle was in a sheltered or complex environment, the error would increase, but it could still maintain a high positioning precision.

5. Conclusions

This study focused on high-precision positioning technology for unmanned autonomous operational special purpose vehicles, leading to the following conclusion.

The combination of innovative attitude sensor and GNSS dual antenna measurement algorithm can greatly enhance the monitoring accuracy of the motion state of unmanned vehicles. Using BDS/GPS for positioning research, the spatial geometry of the satellite is ideal, the number of visual satellites received is relatively large, and the positioning effect is better than that of a single system positioning.

The Kalman filter of integrated navigation and positioning was designed, which can effectively overcome the data divergence of inertial navigation and environmental constraints of satellite navigation and enhance the accuracy and stability of the positioning system. Simulations and experiments have verified that the combined navigation and positioning system can meet the needs of practical applications.

Data Availability

The data used to support the findings of this study are available from the corresponding author upon request.

Conflicts of Interest

The authors declare that they have no conflicts of interest.

References

[1] L. Guo, X. You, Z. Su, J. Zou, and Z. He, "Design and research of navigation and positioning system for unmanned intelligent vehicle[J]," *China Management Informationization*, vol. 22, no. 18, pp. 174–176, 2019.

[2] B. Zheng and X. Xin, "Development demands and research significance of unmanned combat vehicles," *Shandong Industrial Technology*, vol. 37, no. 17, p. 144, 2018.

[3] P. Zhang, *Research on Autonomous Lane Changing Decision-Making and Motion Planning Technology of Unmanned Vehicles Based on Driver Behavior Characteristics*, Jilin University, Changchun China, 2021.

[4] W. Liu and H. Zheng, "Analysis of influence factors of GPS-RTK non-tide sounding precision," *Science Surveying and Mapping*, vol. 40, no. 11, pp. 7–12, 2015.
[5] Y. Xu, *Research on High-Precision Positioning and Navigation System of UAV Based on RTK*, Nanjing University of Aeronautics and Astronautics, Nanjing China, 2018.
[6] L. Meng, *Network RTK Technology Analysis and Applied Research*, Liaoning Technical University, Fuxin China, 2013.
[7] Y. Zhang, X. Miao, D. Cong, R. Wang, and E. Liu, "Comparison of extended kalman filter and particle filter in GNSS/INS integrated navigation," *J], System Simulation Technology*, vol. 16, no. 4, pp. 207–211, 2020.
[8] M. Nie, *Research on Vehicle GPS/SINS Integrated Positioning Technology*, Henan University, Zhengzhou China, 2020.
[9] Y. Wang, *Research on Star Network RTK Key Technology Based on Fixed Virtual Reference Station*, Southeast University, Nanjing China, 2019.
[10] N. Bao, *Research on RTK Positioning Performance of BeiDou Navigation Satellite System*, Civil Aviation University of China, Tianjin China, 2019.
[11] W. Du, C. Yan, W. Xu, and T. Wang, "Algorithm implementation and result analysis of network-RTK based on GPS/BDS," *J], GNSS World of China*, vol. 42, no. 6, pp. 42–47, 2017.
[12] Yi Lai, D. Wang, J. Zhai, and R. Yuan, "Integer ambiguity calculation for real time kinematic positioning [J]," *Modern Navigation*, vol. 5, no. 2, pp. 84–87, 2014.
[13] W. Kan, M. Ahmed, C. Rizos, and J. L. Wang, "Integrity monitoring for horizontal RTK positioning: new weighting model and over bounding CDF in open-sky and suburban scenarios[J]," *Remote Sensing*, vol. 12, no. 7, pp. 1–33, 2020.
[14] S. Yang, *Research on Key Technologies of PPP/INS Integrated System*, Chongqing University, Chongqing China, 2018.
[15] Q. Jia, *Research on GNSS Cycle Slip Detection and Repair Method*, Guilin University of Electronic Technology, Guilin China, 2019.
[16] Hu Jia, *Research on High Precision Integrated Navigation and Positioning Technology Based on GNSS/SINS*, Guilin University of Electronic Technology, Guilin China, 2020.
[17] S. Zhao, *Research on Trajectory Tracking for Autonomous Driving Based on GPS/INS Integrated In-Car Navigation Technology*, Jilin University, Changchun China, 2020.
[18] Y. Chen, *Design and Implementation of GNSS/INS Integrated Navigation System in Embedded System Platform*, Beijing University of Posts and Telecommunications, Beijing China, 2020.

Hindawi
Computational Intelligence and Neuroscience
Volume 2022, Article ID 2586711, 13 pages
https://doi.org/10.1155/2022/2586711

Research Article

Modular Furniture Design by Using Intelligent Platform and Wireless Sensors

Wu Shilin

School of Fine Arts & Design, Guangzhou University, Guangzhou, Guangdong 510006, China

Correspondence should be addressed to Wu Shilin; 20160131@nxmu.edu.cn

Received 9 July 2022; Revised 14 September 2022; Accepted 23 September 2022; Published 23 November 2022

Academic Editor: Gopal Chaudhary

The continuous development of the society has led to the improvement of people's quality of life and consumption level. At the same time, peoples demand for all aspects of production and life is also increasing, thus promoting the emergence and innovation of intelligent household appliances. To manage these devices conveniently and quickly and enrich family life, "smart home" bureau plays a very important role. Smart home, which enters people's family life, uses communication technology, Internet connection technology, automatic fire control technology, network wiring technology, and visual and audio transmission technology to communicate with home. Mobile terminals have been developed, and more and more PC functions have been realized. Based on the hardware platform of the smart home management system, two solutions were put forward. The first solution is combined with the current 5G network, and through it, the user can control the mobile phone and other mobile terminals on the corresponding application operation instructions to create. The second solution is the design of the web server intelligent management system, for relevant information. It is collected into the database of the server, allows remote access to the node and subscriber information related to storage in the database through the Internet, and searches the information to control the home lighting and temperature. This system is designed to imitate the modular scheme, which includes the central control module, sensor data acquisition module, and software module. Finally, on the browser side and the electronic devices of Android operating system, it realizes the wireless control of lighting, air conditioning, washing machine, and other devices, as well as the detection of the home environment.

1. Introduction

Smart home, on the surface, means to make the home smart; in fact, it is to add smart modules in the home to make people's lives more convenient and better. This term has been very popular in China in recent years. In fact, as early as the twentieth century, in 1984, smart buildings were first built and then Western countries started systematic smart home research. With the continuous development of science and technology, the level of fine electronic technology and computer technology has also been promoted to a great extent. People's demand for intelligence in various scenes of work, family, and social life is also becoming higher. The continuous development of the industry has also brought about dual innovation in concept and application. In 1999, the concept of intelligent management of power equipment, such as the Internet of things, was first proposed. This concept and the application have been introduced into the ranks of high-frequency technology. With recent technological developments and breakthroughs, more and more wireless communications, sensor technology, and some smarter sensing technologies have been applied to the Internet of Things. The concept of the Internet of Things has far exceeded current expectations. The smart home system based on the Internet of Things is a technology that integrates electronics, communications, sensors, cloud computing, and other disciplines to improve living standards. With the popularization of Internet of Things technology, various manufacturers have introduced their own smart home systems and adopted a variety of communication methods. The data acquired by the home center controller (coordinator) from each sensor are sent to a mobile terminal,

such as a mobile phone in real-time, via an application on the mobile terminal of the home gateway to take countermeasures and monitor and process at the home.

2. Related Works

At present, the intelligent home network control system has three solutions of PC architecture and MCU architecture embedded architecture. To be able to remotely confirm the working status of each device in the home and perform remote operation, it is hoped that the internal network composed of household devices can be connected to some public communication platforms such as the Internet, GSM/GPRS, 3G mobile network, etc. [1]. Literature introduced the realization of a smart gateway to a smart home system [2]. As the internal network connects home equipment and the external public network, the smart gateway as the core unit of the smart home system is the top priority in the research of smart home. ResidentialGatewayGroup (RG) is the first company that represents the use of the centralized intelligent interface of the home smart gateway. RG connects the home network with the home external network [3]. The home gateway is defined as a simple, standardized, intelligent, and flexible interface device, which can receive information from various external networks and send it to a device on the home network. Cisco Systems defines the home gateway as an intelligent gateway between the network information equipment and the home intelligent broadband access network. Literature Home Gateway enables simultaneous access between "WAN" and "LAN" [4]. This enables the home gateway to be integrated into the "WAN" and "u" (broadband) networks. Literature smart gateways are the physical and logical core of smart home networks. However, it is difficult to unify the current standards of home gateways [5]. Cooperation between smart community developers and property management companies is still difficult to achieve. Many smart home manufacturers have established their own smart gateways. In recent years, China's housing construction industry has developed rapidly. To realize the intelligence of daily life, high-tech electronic information technology has become a top priority. Smart home is a perfect combination of modern high technology, modern architecture, and modern life concepts [6]. Speeding up the development of smart homes will greatly promote the development of science and technology in the country. Literature believes that the smart gateway is the core unit of the smart home system [7]. The successful development of the smart gateway will greatly improve the technical content of the residence. Literature promotes the development of the country's housing construction industry [8]. The research goal of this paper is to design and develop a small smart home control system with perfect functions, low cost, and convenient construction and installation. Based on the iovt2-2530 hardware platform, design, and research, the central control software for the system series information management platform is through the Android platform. The smart home control system can be installed through mobile phones and other terminals to remotely control the home and obtain information about various parts of the house [9]. The terminal can always know the temperature, humidity, power consumption, pressure of the water pipe, and safety information of the house, and the user can control each node through the terminal and take appropriate measures based on the main control information.

3. Optimized Design of Modular Home Based on Artificial Intelligence

3.1. Design Method of Optimized Function. The above content discusses the monitoring functions of smart products. However, the ultimate goal is an independent task. WSN alone is not enough to monitor smart products and control the automatic adjustment of fuzzy PID. On this basis, it is necessary to realize the two main functions of "optimization" and "voluntary" [10]. Optimization is the improvement of intelligent product performance and troubleshooting, such as autonomous operation, including cooperation with other products and systems, self-help enhancement of product performance, self-diagnosis, and self-service of faults. Therefore, in this chapter, we will design intelligent product optimization and autonomous functions and enable algorithms to achieve optimization functions by monitoring data and control functions. The design can be improved by evaluating the maturity of the optimization function through the number of triangular fuzzy. The three functions of fusion rate monitoring, control, and optimization are used to realize the independent function of intelligent products, and after the evaluation of the triangular fuzzy quantity has been mature, the design of the independent function is determined.

Optimization is the third function of smart products. After monitoring data and control functions, ILCS is used to improve the performance of smart products and implement fault diagnosis. The design process of the intelligent product optimization function is shown in the figure. Iterative learning includes non-linear control and control input distortion. If the interference state and the desired trajectory of the output are determined, the trailing desired trajectory will be determined [11]. If the variables of the learning rule of the selection loop PD are mastered, the state variables and output variables will be in a specific time zone, and the iterative learning control algorithm will converge. For optimization features, a number of triangle blurs to assess maturity and improve the design is used. The optimization function of smart products is based on the monitoring function and is realized through multiple iterations of the control algorithm. When smart products are running, performance is not always the best. ILCS seeks appropriate control input and makes the actual performance of smart products closer to the best performance within time, so as to achieve the goal of optimization [12]. The first step is to give the expected track $y_d(t)$ of the smart product, select the initial control input $u_0(t)$ in two steps, namely the initial interference state $w_0(t)$ and the initial interference output v0(t), and confirm the state of the smart phone product x_0 (zero) and initial execution output y_0 (zero) using three inputs

$u_0(t)$, interference state $w_0(t)$, and interference output $v_0(t)$ control program intelligent application products and actual output error $y_0(t)$ $E_0(t) = y_d(t) \sim y_0$ step (t); after iterative learning, the next control input is the fifth step of $u_1(t)$, the output error is ILCS traditional feedback control, and steps 2, 3, and 4 are repeated until you use more information than the system. ILCS uses more information than traditional feedback control systems. ILCS uses the control input of the current operation at the same time. For $u_k(t)$ and the control input $u_k{-}1(t)$ of the last operation, the conventional feedback control system only uses the control input $u_k(t)$ of the current operation. The control input $u_k(t)$ can be calculated offline or online. Similarly, the new control input $u_k + 1(t)$ in the memory will refresh the old control input $u_k(t)$.

$$\begin{aligned} x_k'(t) &= f\left(x_k(t), t\right) + Bu_k(t-\theta) + \omega_k(t), \\ y_k(t) &= Cx_k(t) + v_k(t). \end{aligned} \tag{1}$$

However, $t \in [0,]$, K is the number of repetitions, $\mathrm{UK}(T) \in \mathrm{RP}$, $\mathrm{XK}(T) \in \mathrm{RM}$, and $\mathrm{YK}(T) \in \mathrm{RN}$ are the control input, state, and output of the system, respectively, $\mathrm{wk}(T) \in .\mathrm{RM}$ and $\mathrm{VK}(T) \in \mathrm{RN}$ are state disturbances and output disturbances, respectively. As shown in the figure, when $\mathrm{wk}(T) = 0$ and $\mathrm{VK}(T) = 0$, any bounded expected trajectory YD is assumed to be state XD (T) and initial state XD (0) only from bounded control inputs UD (T) and (T).

$$\begin{aligned} x_d'(t) &= f\left(x_d(t), t\right) + Bu_d(t-\theta), \\ y_d(t) &= Cx_k(t). \end{aligned} \tag{2}$$

Hypothesis 1. there are nonnegative real numbers "1, 2, 3". For any $k > 0$ and $t \in [0, 2]$, it satisfies the nonnegative real numbers "1", "2" and "(0) (0)" ≤ "3" of any $k > 0$ and $t \in [0]$. Suppose 3: for any $x_1(T)$, $x_2(T) \in \mathrm{r\,m}$, the non-linear function $f()$ satisfies the Lipschitz condition.

$$\left\| f\left(x_1(t), t\right) - f\left(x_2(t), t\right) \right\| \le L_f \left\| x_1(t) - x_2(t) \right\|, \tag{3}$$

where L_f is Lipschitz constant. The ILCS of smart products adopts PD-type learning law:

$$u_{k+1}(t) = u_k(t) + \Gamma\left[e_k'(t+\theta) + Le_k(t+\theta)\right],$$

$$\|I - \Gamma CB\| \le p \le 1,$$

$$\begin{aligned} \Delta u_{k+1}(t) &= u_d(t) - u_{k+1}(t) = \Delta u_k(t) - \Gamma\left(e_k'(t+\theta) + Le_k(t+\theta)\right) \\ &= (I - \Gamma CB)\Delta u_k(t) - \Gamma C\left[f\left(x_d(t+\theta) - f\left(x_k(t+\theta)\right)\right)\right] - \Gamma LC\Delta x_k(t+\theta) + \Gamma C\omega_k(t+\theta) + \Gamma(I+L)v_k(t+\theta), \left\|\Delta u_{k+1}(t)\right\|, \\ &\le \|I - \Gamma CB\|\left\|\Delta u_k(t)\right\| + \Gamma\left(L_f I + L\right)C\left\|\Delta x_k(t+\theta)\right\| + \Gamma C\varepsilon_1 + \Gamma(I+L)\varepsilon_2 x_k(t+\theta) \\ &= x_k(0) + \int_{-\theta}^{t-\theta}\left[f\left(x_k(\tau+\theta)\right) + Bu_k(\tau) + \omega_k(\tau+\theta)\right]d\tau, x_d(t+\theta) \\ &= x_d(0) + \int_{-\theta}^{t-\theta}\left[f\left(x_d(\tau+\theta)\right) + Bu_d(\tau)\right]d\tau\Delta x_k(t+\theta) \\ &= \left[x_d(0) - x_k(0)\right] + \int_{-\theta}^{\tau-\theta}\left[f\left(x_d(\tau+\theta)\right) - f\left(x_k(\tau+\theta)\right) + B\Delta u_k(\tau) - \omega_k(\tau+\theta)\right]d\tau, \end{aligned}$$

$$\left\|\Delta u_{k+1}(t)\right\| \le \|I - \Gamma CB\|\left\|\Delta u_k(t)\right\| + \Gamma\left(L_f I + L\right)CB\int_{-\theta}^{\tau-\theta} e^{L_f(t-\tau)}\left\|\Delta u_k(\tau)\right\|d\tau + \Gamma\left[\left(L_f + 1\right)I + L\right]C\varepsilon_1 + \Gamma(I+L)\varepsilon_2 + \Gamma\left(L_f I + L\right)C\varepsilon_3,$$

$$\left\|\Delta u_{k+1}(t)\right\| \le \|I - \Gamma CB\|\left\|\Delta u_k(t)\right\| + \Gamma\left(L_f I + L\right)CB\|h(t)\| + \Gamma\left[\left(L_f + 1\right)I + L\right]C\varepsilon_1 + \Gamma(I+L)\varepsilon_2 + \Gamma\left(L_f I + L\right)C\varepsilon_3,$$

$$\left\|\Delta u_{k+1}(t)\right\|_\lambda \le \|I - \Gamma CB\|\left\|\Delta u_k(t)\right\|_\lambda + \Gamma\left(L_f I + L\right)CB\|h(t)\|_\lambda + \varepsilon\varepsilon = e^{-\lambda(t-\theta)}\left[\Gamma\left[\left(L_f + 1\right)I + L\right]C\varepsilon_1 + \Gamma(I+L)\varepsilon_2 + \Gamma\left(L_f I + L\right)C\varepsilon_3\right],$$

$$\|h(t)\|_\lambda \le \frac{1 - e^{\left(L_f - \lambda\right)T}}{\lambda - L_f}\left\|\Delta u_k(t)\right\|_\lambda,$$

$$\left\|\Delta u_{k+1}(t)\right\|_\lambda \le \left[\|I - \Gamma CB\| + \frac{1 - e^{\left(L_f - \lambda\right)T}}{\lambda - L_f}\Gamma\left(L_f I + L\right)CB\right]\left\|\Delta u_k(t)\right\|_\lambda + \varepsilon,$$

$$\lim_{k\to\infty}\left\|\Delta u_k(t)\right\|_\lambda \le \frac{\varepsilon}{1-\alpha}, \lim_{k\to\infty}\sup_{t\in[0,T]}\left\|\Delta u_k(t)\right\| \le \frac{\varepsilon e^{\lambda t}}{1-\alpha},$$

$$\left\|\Delta x_k(t+\theta)\right\| \le B\int_{-\theta}^{t-\theta} e^{L_f(t-\tau)}\left\|\Delta u_k(\tau)\right\|d\tau + \varepsilon_1 + \varepsilon_3, \left\|\Delta x_k(t+\theta)\right\|_\lambda \le B\|h(t)\|_\lambda + e^{-\lambda(t-\theta)}(\varepsilon_1+\varepsilon_3),$$

$$\left\|\Delta x_k(t+\theta)\right\|_\lambda \le \frac{1-e^{(L_f-\lambda)T}}{\lambda - L_f}B\left\|\Delta u_k(t)\right\|_\lambda + \varepsilon, \lim_{k\to\infty}\left\|\Delta x_k(t+\theta)\right\|_\lambda \le \beta+\varepsilon, \lim_{k\to\infty}\sup_{t\in[0,T]}\left\|\Delta x_k(t)\right\| \le e^{\lambda t}(\beta+\varepsilon),$$

$$\left\|\Delta y_k(t+\theta)\right\| \le C\left\|\Delta x_k(t+\theta)\right\| + \varepsilon_2, \lim_{k\to\infty}\left\|\Delta y_k(t+\theta)\right\|_\lambda \le (\beta+\varepsilon)C + e^{-\lambda(t-\theta)}\varepsilon_2, \lim_{k\to\infty}\sup_{t\in[0,T]}\left\|\Delta y_k(t)\right\| \le e^{\lambda t}(\beta+\varepsilon)C + e^{\lambda\theta}\varepsilon_2. \tag{4}$$

After the optimized function design is determined, its maturity is evaluated to improve the design process. According to the ILCS design of smart products, the evaluation index of the optimization function is summarized as the smart product working model and the degree to which ILCS simulates the actual working conditions of smart products [13]. The operating system of smart products is almost nonlinear, often with time lag, interference, and arbitrary initial states. The closer the working model is to the actual situation, the more reliable the optimization. Orbital optimization algorithm: convergence is a prerequisite for measuring the success of the ILC algorithm. Only when the ILC algorithm converges, the actual output of the smart product can reach the best solution. The best solution is obtained with a certain precision to achieve the goal of optimization. System robustness: tracking system performance under various interferences [14]. When interference exists, the output of the iterative learning controller can converge to the neighborhood of the desired trajectory; after the interference disappears, the actual output of the system converges to the target trajectory. The evaluation criteria are high optimization accuracy, high reliability, and short response time. Similarly, the use of triangular fuzzy numbers to evaluate the maturity of the optimization function and the evaluation process, see the following. When analyzing the evaluation results, the undesirable optimization function design should be improved. To ensure the realization of the improved optimization function, the ticketing cost and customer value must also be considered.

3.2. Design Method of Autonomous Function. Autonomy is the last function of smart products, which is realized by ANFIS and multiagent systems. ANFIS processes information from monitoring, control, and optimization functions, and passes the processed information to multiple ANFIS systems [15]. The multiagent system carries out information distribution, uses knowledge base and Q-learning algorithm for decision-making analysis, and realizes autonomous functions. The fuzzy number of triangles evaluates the maturity of autonomous functions and improves the design of autonomous functions. The information from the monitoring, control, and optimization functions needs to be processed first. This is a process of multiple inputs and outputs.

$$\begin{aligned} R &= A\times B\times C\to D \\ &= \{[A_1\times B_1\times C_1\to D_1], [A_2\times B_2\times C_2\to D_2], \ldots, [A_m\times B_m\times C_m\to D_m]\}. \end{aligned} \tag{5}$$

Here, according to the formula, a is monitoring information, b is control information, and c is optimization information. The rule base contains m rules, and each rule exists in the form of multiple inputs and a single output. Since the m rules are independent of each other, the MIMO process can be decomposed into m MIMO processes. The design process of autonomous functions of smart products is shown in Figure 1.

Taking into account the advantages of autonomous learning of neural networks and fuzzy inference of fuzzy systems, ANFIS uses the back propagation algorithm or a hybrid algorithm of the back propagation algorithm and least square method to learn input and output data pairs, and obtain fuzzy membership functions and fuzzy rules independently so that the constructed fuzzy inference system (such as the Takagi-Sugeno model) can better simulate the actual input-output relationship. The learning process calculates the error between the actual output value and the target value and adjusts the system parameters through error back propagation until the system error is met. Therefore, ANFIS is used to solve the multiinput problem of autonomous functions (as shown in Figure 2).

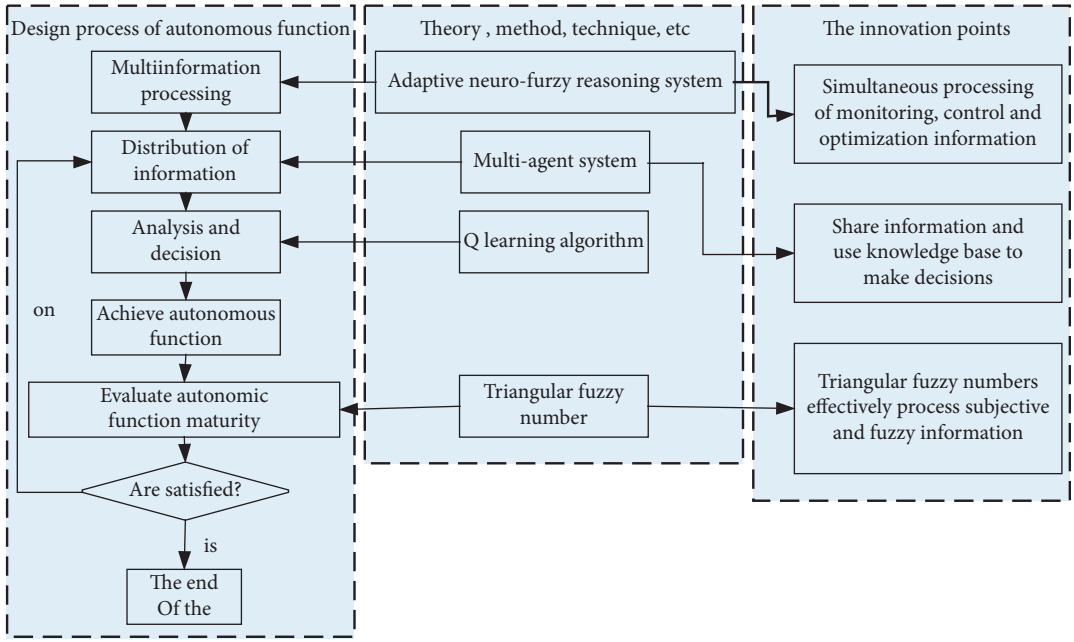

Figure 1: Design process of autonomous functions of smart products.

In the first layer, the input information blurs the output function of node i, shown as follows:

$$O_i^1 = \mu_{A_i}(x), O_i^1 = \mu_{B_i}(y), O_i^1 = \mu_{C_i}(z). \tag{6}$$

Here, x y and z are input monitoring control and optimization information, A_i, B_i, and C_i are fuzzy sets of monitoring control and optimization, and 1 is the member shiv function value of A_i, B_i, and C_i. In other words, the order in which x, y, and z belong to A_i, B_i, and C_i is a subordinate function, and this order is usually chosen so that the maximum value of the Gaussian or Bell function is 1 and the minimum value is 0. Take "Smart Scanning Robot" as an example. In the second layer, the input signal multiplication method multiplies the input signal to calculate the reliability of the rule.

$$\begin{aligned} \omega_i &= \mu_{A_i}(x) \times \mu_{B_i}(y) \times \mu_{C_i}(z), \\ \varpi_i &= \frac{\omega_i}{\sum_{i=1}^{m} \omega_i}, \\ O_i^4 &= \varpi_i f_i = \varpi_i \left(p_i x + q_i y + t_i z + r_i\right), \\ O^5 &= \sum_{i=1}^{m} \varpi_i f_i = \frac{\sum_{i=1}^{m} \omega_i f_i}{\sum_{i=1}^{m} \omega_i}. \end{aligned} \tag{7}$$

3.3. Design Principles of Modular Furniture. The powerful functions and important advantages of modular furniture are obvious to everyone, but its design is not a direct and rough decomposition and functional transplantation of traditional furniture. Not all types of modular furniture are suitable for small- and medium-sized comprehensive bookstores. Modular furniture has many models and there are countless variations. When designing, there are actually rules to follow for basic modules and combinations that seem to have no rules.

The golden ratio, ergonomics, etc. may also affect the spiritual needs of users and the creation of the space atmosphere. However, with the diversification of small and medium-scale integrated bookstore space development, the design standard is not just the comfort of modular furniture. The seemingly applicable standards require flexibility to make each piece of furniture more scientific and reasonable within its own functional scope. For example, when considering the width of a standing reading shelf, the baffle is placed at a lateral distance of 45°, which not only ensures comfort but also emphasizes space saving; for example, compared with the table in the restaurant area, the reading table is slightly smaller than the standard value Wider, you can put more books, use distance to hinder communication, you can better create a quiet reading and self-thinking environment. The desktop size of the dining area should be narrow and standard to shorten the distance. This is the scientific, reasonable, and flexible design principle of as many "ergonomics" as possible for the so-called multifunctional area.

If you compare modular furniture to "mosaic," it may be the most appropriate. Each basic element has its own characteristics, single but abstract. However, when several elements are continuously combined, people will gradually realize its overall meaning. Therefore, the design of modular furniture for bookstores must consider the independence of the individual and follow the principle of the overall application. In general, the following points should be considered for overall applicability: (1) "multiple births" effect. Since the uniform appearance is the most direct and complete, the color, material, and contour type of the module combination must be consistent. It is recommended

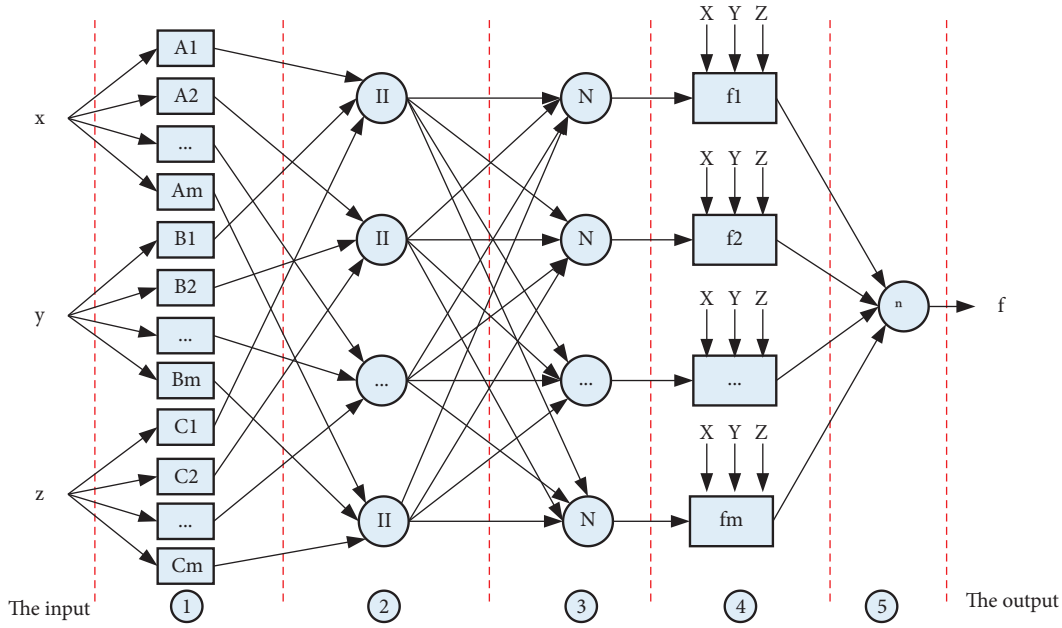

Figure 2: ANFIS structure of smart products.

to keep the same state after free change and reversal; (2) the versatility and interchangeability of the module. When the combination of modules does not have a fixed pattern or any module can be replaced, it fully reflects the overall combination's adaptability to location and individual, so a universal connection method must be used in the design; (3) the continuity of module combination. The most amazing performance of modular furniture is whether there is any mutual generation. To better adapt to spaces of different sizes, it must have a certain continuity to have an overall concept.

Even small- and medium-sized bookstores, there is not very few furniture in the space. In addition to later consumption and maintenance, it is not advisable to pay attention to one thing and lose the other. We must follow the design principles of saving and material recycling. To achieve high output and low consumption, we can start from two aspects: high output of furniture manufacturing and low consumption of furniture use. The intervention of modular design means mass production, and its versatility also minimizes maintenance and replacement costs. In the design process, the module design is tried to be made close to the raw material itself to reduce the difficulty of the manufacturing process. In manufacturing engineering, a reasonable selection of materials is made. Only economy and materials can form a smooth circulation system, and spiritual culture can be better inherited.

The original intention of modular furniture is to provide people with more comfortable and humanized services rather than turning a beautiful and comfortable space into a Torah. IKEA modular furniture has always been loved by people all over the world, but no matter how affordable and applicable, due to uneven stress, it results in the death of children and people are far away from it. In particular, small- and medium-sized comprehensive bookstores have the characteristics of publicity and openness. In the face of a variety of audiences, we should pay attention to prevention, especially the protruding or sharp outline of the surface of furniture products; there are unfixed and falling modules in the furniture system; the furniture is folded because the mechanical performance of the products is not up to standard or the bearing capacity is overloaded or the manufacturing materials produce harmful substances. In a word, no matter how easy the shape and function of furniture are to change, there is no doubt that the principle of safety design is strictly followed.

Furniture and people have a close "skin blind date" relationship. Good furniture can not only bring people a comfortable feeling but also protect or improve the physiological function of the human body in the long-term process and ensure the emotional health of users. This good effect is reflected in the scale and shape of the furniture, which is based on the design principles of ergonomics. According to the size and range of activities of age and gender and the use of different furniture functions and other needs, the size of the furniture itself has to be restricted and the distance between furniture and furniture has to be standardized to ensure the needs of the different number of users. As modular furniture is made of splicing modules, according to the size of the overall furniture, different users have different functions for furniture size.

4. Modular Furniture System Design Based on Wireless Sensors

4.1. System Design Overview. The smart home wireless control system is mainly based on the smart home system software iotv2 CC2530 hardware system and can control the home equipment of a single user. The system consists of a central server, a smart phone, and a personal computer with

a wireless sensor network for centralized management and control of the entire building. All the information collected by the sensor nodes is stored in the real-time server database. Android phones, PDAs, and tablets are gateways, and the server transmits the server through the gateway through the Ethernet on the network (4 G/3 G/Internet/GPRS, etc.) through the CC2530 system. To realize the remote control function of home equipment, the system eliminates the complexity of hardware controller design, does not need to destroy the room layout, does not need to buy new electrical appliances, is simple to install, and saves user costs. The system can not only connect lighting equipment and general equipment, it can also be connected to other equipment, adapt to the needs of new smart life, and has a high degree of scalability. The overall design of the smart home system is shown in Figure 3.

The central server is the main controller of the entire smart home system, controlling all home appliances, including televisions and lighting equipment. The control commands of lighting appliances, infrared household appliances, and various sensors are stored here. Through the alternate interface of the control center, the temperature sensor is equipped with sensors of the intelligent control system, which realizes the convenience of household equipment. The sensors in the system include temperature sensors, smoke sensors, and light intensity sensors. These sensors are connected to the subcontroller (2.4 G module) through a specific circuit module according to their working characteristics. The system collects and analyzes the operating status information of the equipment in real-time. If an abnormality occurs, the status information and abnormal analysis result will be sent to the control center and an alarm will be issued with a "beep". In this way, the user can know what happened in a short time and react first. The design of the smart home system is divided into two parts: software design and hardware selection. The software mainly includes the design of Android applications, the design of the control system under the Bash architecture, and the communication protocol between wireless sensor nodes, that is, the 2.4 G module design.

4.2. System Hardware Selection. Smart home 2.4 G wireless control system uses tiiotv2-2530 hardware platform, a smart gateway, and some subnodes can be configured with three detailed node modules, power module board sensor control module, and a wireless node module. There are mainly three wireless node modules. Module configuration, high-frequency carrier microcontroller wireless communication module, and 2.4 g frequency antenna power module board: power transmission to the system, connection between wireless node module and sensor control module, main power mode can drive battery power or reserve power external DC power supply interface. Sensing and control module: users can also expand their sensor and controller units through the bus. The whole module is a 5VDC power input, built-in DC/DC chip. The input 5VDC power requires 3.3 V and the maximum output current is 200 mA. The single-chip solution used in this system is used in the 2530 system planning stage by extracting the chip signal at the module level and + manual reset chip and reliable phase reset is performed. The 2-wire debugging interface (hardware option operation) is started through the dedicated 5-pin FPC socket. To convert it to a standard debugging plug, an additional expansion board is required. The wireless node module uses two side-by-side 20-pin sockets to send and receive signals. Pin socket 1 pin definition is as shown in Table 1. Pin socket 2 pin definition is as shown in Table 2.

All sensors and controller modules operate uniformly under the control of the 2530 module and have the same control interface, including control signals and physical dimensions. The sensor module uses two rows of 20-pin sockets supported by the power board to communicate with the wireless node module, which is controlled by the wireless node module. The module types supported by the system are introduced as shown in Table 3.

The chip uses EEPROM to complete the ID design and storage of all modules, the interface is IIC, the module characteristic attribute is 2 bytes, the address is 0 and 1, the first byte is used to describe the working mode and attributes, and the second byte is used to describe specific equipment. After he code 2530 is turned on, the current valid ID code of the sensor module or controller module is read from the EEPROM, and the subsequent boot process is determined according to the ID code, mainly the configuration of the IO port and the functional module. The front-end hardware part is composed of cameras and video compression chips. The camera uses a JVCCCD camera, and this design uses a CDD camera. The video compression chip is designed based on TI's DaVincTM series of high-resolution processors tms320dm365. The processor continues the DaVincTM series DM355 processor architecture and integrates the H.264 high-resolution codec processor MJCP, which supports the ARM926EJ-S core and the H.264/MPEG-4 high-resolution video codec together. The data are collected by the camera and controlled by functions such as ARM926EJ-S, H.264 encoding, dual-stream control, and data storage. Finally, it is output through the digital RGB/YUV interface.

4.3. Software System Design. The smart home control system uses two software architectures: B/S and C/S. The browser client can access the remote server through wired or wireless Internet (hammer mode), and the Android client application can access the remote server wirelessly. B/S (Browser/Server) is a software architecture improved and developed under the C/S mode. Users mainly implement related functions through the browser and the server is mainly used to implement the logic of things. Compared with the traditional C/S model, the B/S-based software structure not only reduces the load on the client but also reduces the difficulty of future use and maintenance and reduces the cost of use. There are many ways to use the B/S architecture to access the remote database (LAN/WAN/Internet). The advantages of B/S architecture, especially the emergence of cross-platform languages (JAVA), emphasize the advantages of B/S architecture. The system can implement the control system of the text more quickly and

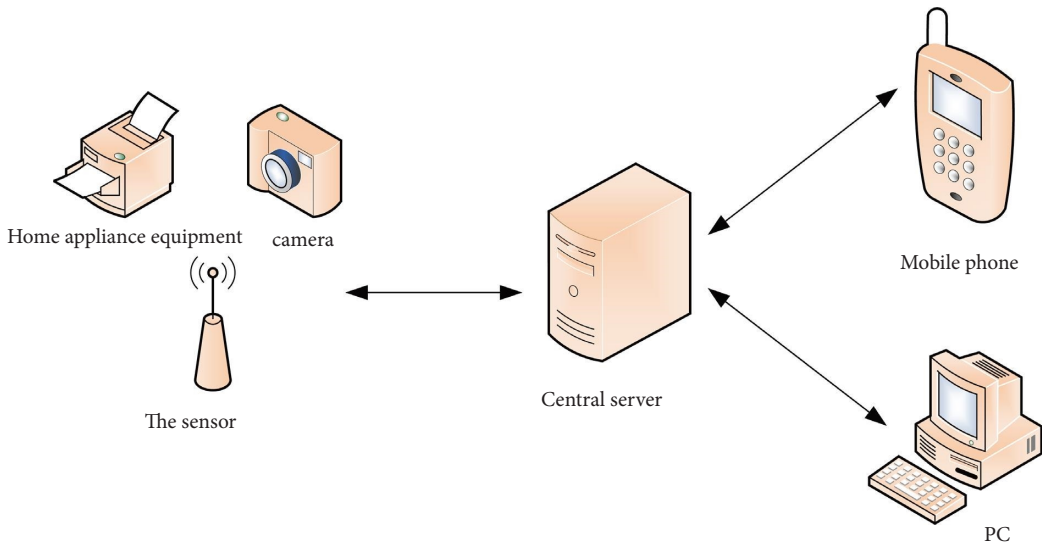

Figure 3: Smart home overall design structure.

effectively. The central control module is wirelessly connected to the indoor subnodes to realize the orderly exchange and management of home appliance data. The data retrieval server is the core of the entire control system, the central node of information management, and the bridge between the client and the management device. The client manages all the data received from the client's control room in an upward and downward manner and the control and management of all the corresponding equipment received by the client up and down realize that the remote server is actually optimized management software. Display the operating status and parameters of on-site electrical equipment and remotely control the equipment. The system architecture is shown in Figure 4.

The Android-based control system uses a simple Android interactive graphical interface. Not only is it easy to use, but it is also highly convenient and can be operated anytime, anywhere. The system includes six detailed modules: scene, monitoring, function, area, and system. The functions of the program mainly include high-sensitivity signal monitoring, electrical equipment switch control, infrared human body monitoring, emergency alarms, etc. It is very convenient for abandoned children, the elderly, and company employees.

4.4. System Implementation Based on Wireless Sensors. To make the smart home control system run stably, it is necessary to design the system according to the SimpliciTI protocol to make it suitable for the home environment. Table 4 shows the detailed description of each data in the frame format.

The specific architecture of the intelligent system is shown in Figure 5. The presentation layer can express the content after transcoding, which is the interactive page presented to users by the system at last. This layer is divided into two modules: the view layer and the control layer. The former is used to display the interface for users to operate, while the latter is used to verify, store, and control the page skipping of data submitted by users. For users, the presentation layer is a mini program running on the browser. In fact, the network socket video frequency monitoring function was also implemented in this way. Control layer: as the core layer of the system, the control layer plays the most important role and the largest task, including providing external services such as video server, web server, and peripheral control program. Data layer: a large amount of information generated during the whole system operation is saved in the call through this layer. The main data saved and called are XML files of tables in database and file system. Figure 6 shows the system structure.

A device refers to one that communicates with an external device in accordance with a prescribed protocol. The interface includes serial ports, Ethernet, USB, etc., but the final connection to the Internet of Things service is Ethernet. If the device is a non-Ethernet interface, the corresponding adapter must be converted to a network interface. For example, in a wireless sensor network application, the coordinator is the device. But the output is serial data, which needs to be connected to the Internet of Things service through a "serial network port" converter. The communication between the device and the Internet of Things service must be in accordance with the prescribed protocol and process. The device communication process is divided into two stages. The first step is to communicate with the intermediate service. The device mainly establishes a connection with the intermediate service to complete the initialization of the device type identification and certain communication parameters. After the first stage is completed it enters the second stage. The second phase requires the cooperation of high-level applications. If the upper-layer application is also connected to the service, the device starts to communicate with the upper-layer application through the service. At this time, the role played by the service is data forwarding. The communication between the upper-level application and the device without processing data is coordinated.

Table 1: Pin socket 1 pin definition.

Serial number	Name	Type	Detailed description
1	VCC	PWR	3.3 V power input pin
2	VCC	PWR	3.3 V power input pin
3	BDECT	I	Use type detection input, power board = L; smart motherboard = H
4	RSV2	P	Reserved pins, do not connect
5	RS V0	P	Reserved pins, interconnected with corresponding positions on the sensor board
6	RSVI	P	Reserved pins, interconnected with corresponding positions on the sensor board
7	JTAG_VCC	PWR	JTAG debug interface power pin
8	JTDO	0	JTAG debugging interface TCK. pin (2530 chip P2_l pin)
9	JTCK	I	JTAG debug interface TCK pin (P2_2 pin of 2530 chip)
10	JTMS	I	JTAG debug interface TMS pin
11	JTDI	0	JTAG debug interface TDL pin
12	JTRST	I	JTAG debug interface JTRST pin
13	GND	PWR	GND pin of 3.3 V power supply
14	GND	PWR	GND pin of 3.3 V power supply
15	LCD_AO	0	AO control bit of LCD controller
16	LCD_SCL	0	SCL control bit of LCD controller
17	LCD_SDA	IO	SDA control bit of LCD controller
18	LCD-CS	0	CS control bit of LCD controller
19	LCD_RESET	0	RESET control bit of LCD controller
20	RESET	I	Module overall reset control signal input, low effective

Table 2: Pin socket 2 pin definition.

Serial number	Name	Type	Detailed description
1	VCC	PWR	5 V power input pin
2	VCC	PWR	5 V power input pin
3	ADIN0	ADINO	Analog input pin, AD acquisition input 0
4	ADIN1	ADIN1	Analog input pin, AD acquisition input 0
5	GND	GND	GND pin of 5 V power supply
6	GND	GND	GND pin of 5 V power supply
7	ESCL	0	SCL pin of expansion device IIC bus
8	ESDA	IO	The SDA pin of the expansion device IIC bus
9	ETXD	0	TXD pin of UART, TTL level
10	ETXD	I	RXD pin of UART, TTL level
11	EGPI00	IO	External logic input pins, used as networking control buttons when the system is started
12	EGPI01	IO	External logic input pins, used as networking control buttons when the system is started
13	GND	PWD	GND pin of 5 V power supply
14	GND	PWD	GND pin of 5 V power supply
15	EG POO	0	External logic control output pin, programmable control
16	INT	I	External logic control output pin, programmable control
17	EREQ	0	Peripheral function request handshake request signal output
18	EACK	I	Peripheral function request handshake response signal input
19	RSV5	P	Reserved pins, do not connect
20	RESET	I	Module overall control signal input, low effective

5. Analysis of the Modular Furniture Design Strategy

5.1. The Design Method of Modular Furniture. Compared with ordinary traditional furniture, the characteristics of modular furniture are eye-catching. Regardless of form or function, modular furniture has broken through traditional boundaries, giving furniture more meaning. This means that the design of modular furniture is also different from traditional furniture, and not only the overall combination form must be considered, but also the establishment of single units. In addition, the specific environment of the small and medium comprehensive bookstore also has a certain impact on its design techniques. The form and function of modular furniture are closely related with the combination of modules. It is precisely because of the diversity of combinations that modular furniture can be "variety." (1) As the name implies, the package layout and combination design select the module with the largest volume as the outer frame, and other modules can be classified into the largest module according to the order of size. This design method can make the furniture module an individual, meet the needs of multiple people at the same time, and free up more space for use without the need to combine or accept. Due to the characteristics of module combination and splitting, it can be based on the acceptance object. The appropriate module

Table 3: Module function introduction.

Serial number	Name	Function introduction
1	Current sensor	The measurement range is 0.5 A ~ 2 A, the resolution is 0.01 A, at least the ad of lobit is used.
2	Temperature and humidity sensor	The temperature measurement range is −20°C ~ i30c, and the measurement accuracy is 0.1°C; the humidity measurement range is 0–100%, and the accuracy is 0.1%.
3	Illumination sensor	It is realized by one channel ad, and the measurement range is. The resolution is 101x.
4	Infrared control output	Using serial port + CPU scheme, three groups of IR are output.
5	Relay control	Using IIC extended GPIO chip, 4 groups of relays, normally open/normally closed, can be configured arbitrarily.

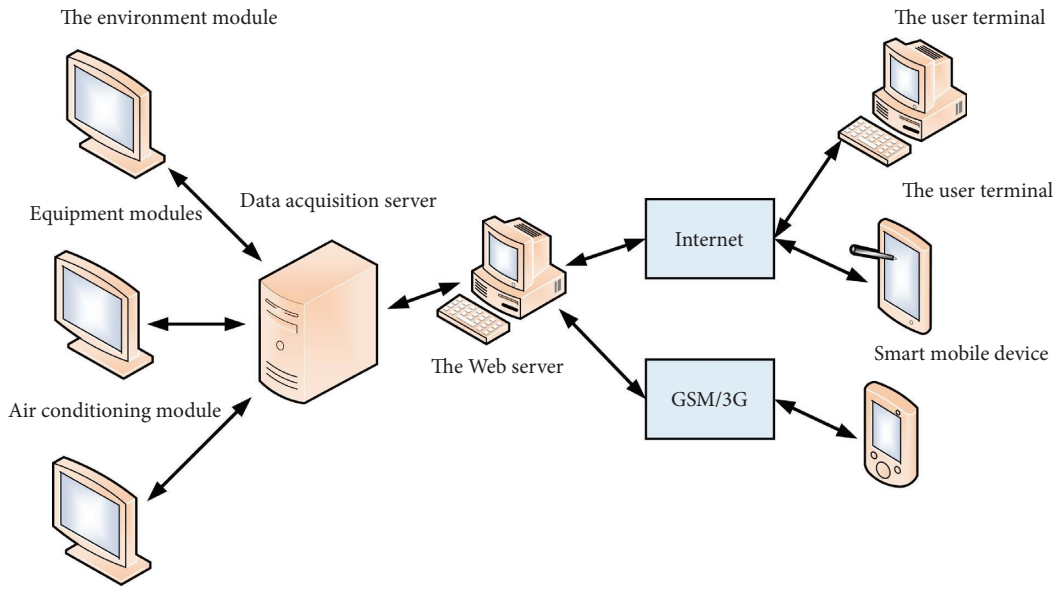

Figure 4: System architecture.

Table 4: Detailed description of each data in the frame format.

Name	Length (bit)	Value	Description
Message type	8	01	Electrical control (control center one electrical equipment module)
		02	Temperature and humidity control (control center a temperature and humidity module)
		03	Temperature collection (temperature control module-control center)
		04	Infrared learning (an infrared control module in the control center)
		05	Infrared transmission (infrared centralized module one control center)
		06	Infrared control (an infrared control module in the control center)
Destination address	8	0–255	The address of the device receiving the control command
Source address	8	0–255	The address of the device sending the data
Data length	8	0	No data
		1–255	Actual number length
Valid data	n		The actual data

for the size is chosen and the internal space is effectively used. (2) Stackable type is also called building block type. Like building blocks, modules are furniture stacked according to the needs of users. To improve the safety of the furniture, some stackable furniture modules will adopt a fixed connection structure to ensure that the furniture will not collapse under the action of external forces. This design method is simple and convenient to operate, can quickly and effectively decompose scattered furniture into parts, and clean and organize the environmental space. (3) The method of assembly design is similar to the method of building blocks, but the modules are fixed to each other through connectors such as screws and bolts or the grooves and structures of the modules themselves. By connecting components and connecting structures to assemble modules, various shapes of furniture can be made, which are very flexible. (4) The splicing type divides the modular furniture into the furniture type with connecting pieces and plates as

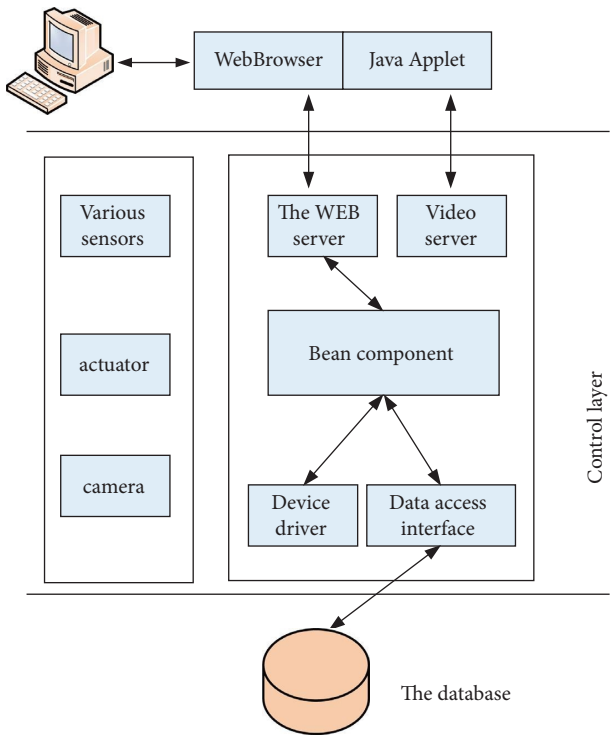

Figure 5: The architecture of the system.

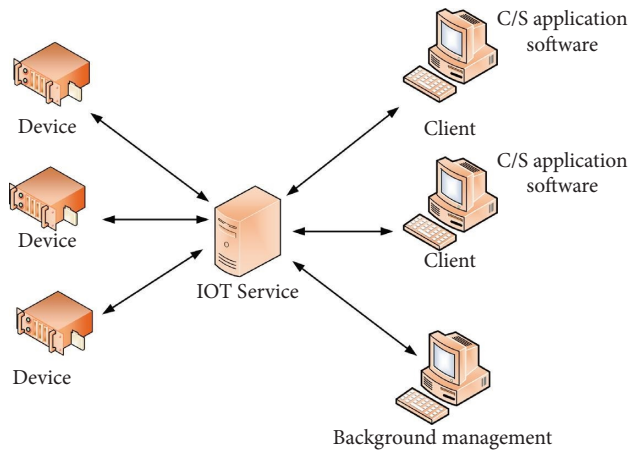

Figure 6: System structure.

the assembly parts, namely the panel furniture, which is the most widely used and most complete type of modular furniture. Various styles of furniture can be combined according to the size of the board and the shape of the connecting piece.

The main market competitiveness of modular furniture is its versatility. However, as one of the important decorations of bookstores, the "look" of furniture cannot be ignored. In addition to considering the powerful functions of the module combination, the design must also follow the rules of formal beauty, such as the color, material, and shape of the furniture. This combination of art and function makes modular furniture one of the characteristics of bookstores and can attract customers who experience consumption. The design method of integrating art into functions is not only oriented to a single module but also simulates the combined overall furniture, ensuring that no matter how the user is reorganized consistently, the bookstore environment can bring in people a sense of fun.

Furniture design in bookstores affects creativity in many ways. In the method of integrating the experience into bookstores, modular furniture plays an important role. (1) The overall design of furniture is one of the elements that change the atmosphere of the space. The so-called "successful furniture, failed furniture", if the design of furniture only pays attention to the form and function of the individual, and does not pay attention to the overall coordination of the space, it will be exactly. On the contrary, it will deteriorate the atmosphere of the space and even hinder the use of certain functions. (2) As a furniture system, modular furniture should not only protect the independence of each module but also consider the integrity of the combination; as a space element, modular furniture should not only provide comprehensive functions but also pay attention to the overall coordination of the space. Only by focusing on the overall development of each link can a good experience space environment be created. (3) Interesting furniture design text has the magical power to make people feel on the scene, while modular furniture can truly make people live in the world of children.

5.2. Development Trend of Modular Furniture. Modular furniture has gradually entered people's daily lives. With the increasing demand for cosmic experience and the popularization of technological intelligence, the design of modular furniture has become more humane, and the scope of application will also expand. With continuous maturation and development of the society and economy, people's needs are increasing day by day, and the optimization and progress in the design and application of modular furniture are constantly promoted. Designers must always pay attention to the development of science and technology and the changes in human needs. The modularization of modular furniture is more reasonable, the function is more complete, the shape is more changeable, and the connection method is more scientific. Therefore, some bold predictions can be made.

The main contents are as follows: (1) in the progress and development process of modern artificial intelligence in the continuous acceleration and in the application of modular furniture, artificial intelligence terminal system has become an indispensable part. In the future, the embedding and development of artificial intelligence devices have emerged in the production and research and development process of furniture, which can not only provide the basic efficiency of furniture but also enhance the interaction between people and furniture to provide personalized services for people's emotional and psychological needs. In addition, artificial intelligence transplantation can provide uninterrupted humanized services, save human resources, and conform to the design principles of sustainable development. (2) With

the development of modular automation, self-transforming DIY models are not limited to material changes that directly contact the human body and the manufacturing process, not just artificial parts. According to the combination of mobile terminal and furniture, the components of modular furniture in the future may apply the principle of automation. Through the intelligent design of computer calculation, the automatic module components are automatically deformed to form new furniture. (3) The reproducible mass production of modular furniture for parametric production development is its biggest feature. The premise of this mass production is that this series of modules can be well applied to different collars and have a high degree of matching with other parts. Therefore, calculating the relevant matching value of the module components is an important link that needs to be considered in the design process and requires a lot of time and effort. Relevant data from the parameter library are collected, the computer terminal is used to analyze the relationship between various data, the combination rule is found, and these parameters are used to configure the intelligent module. To improve the comfort of modular furniture, we provide scientific and reasonable division and combination of furniture modules. I think that with the continuous advancement of science and technology, people have put forward more advanced design concepts and design methods, and the development potential of modular furniture will also be greater. Big digging has the characteristics of fast production speed, large output, and multiple functions, and has good applications in the space environment of the data age.

6. Conclusion

Based on people's actual life needs, this paper designs an intelligent system with Android system as the server, which can run indoors and interact with people. According to the previous research results of this system, the relevant literature is analyzed and sorted out as well as the special research and the development status and future development trend of the internal software of smart phones are deeply discussed. Android's smartphone interior management system designed a plan. Finally, the software design of the Android client is completed under the Eclipse development tool. The smart home control system designed in this paper supports data monitoring, processing, storage, and other functions of the home environment. Module functions include electrical equipment control, high-sensitivity signal monitoring, remote intelligent anti-theft system, etc., which fully meet the needs of most families. This framework is based on customer needs and aims to monitor, control, optimize smart products and realize autonomous functions. The content of the framework includes the determination and analysis of requirements based on the maximization of customer value, the conversion of customer requirements into technical attributes, the design of optimization and independent functions, and the design process and key technologies that support the realization of the content of the framework.

Data Availability

The data used to support the findings of this study are available from the author upon request.

Conflicts of Interest

The author declares no conflicts of interest.

Acknowledgments

This paper was supported by Guangzhou Social Sciences Planning Project 2019: Research on Green Furniture Design of Public Rental House Based on the Concept of Ecological City (2019GZGJ244).

References

[1] M. Khan, B. N. Silva, and K. Han, "Internet of things based energy aware smart home control system," *IEEE Access*, vol. 4, pp. 7556–7566, 2016.

[2] M. A. E. L. Mowad, A. Fathy, and A. Hafez, "Smart home automated control system using android application and microcontroller," *International Journal of Scientific Engineering and Research*, vol. 5, no. 5, pp. 935–939, 2014.

[3] J. Han, J. D. Jeong, I. Lee, and S. H. Kim, "Low-cost monitoring of photovoltaic systems at panel level in residential homes based on power line communication," *IEEE Transactions on Consumer Electronics*, vol. 63, no. 4, pp. 435–441, 2017.

[4] P. Wang, F. Ye, and X. Chen, "A smart home gateway platform for data collection and awareness," *IEEE Communications Magazine*, vol. 56, no. 9, pp. 87–93, 2018.

[5] S. R. Moosavi, T. N. Gia, A. M. Rahmani et al., "SEA: a secure and efficient authentication and authorization architecture for IoT-based healthcare using smart gateways," *Procedia Computer Science*, vol. 52, pp. 452–459, 2015.

[6] B. L. Risteska Stojkoska and K. V. Trivodaliev, "A review of Internet of Things for smart home: challenges and solutions," *Journal of Cleaner Production*, vol. 140, pp. 1454–1464, 2017.

[7] K. Kotis and A. Katasonov, "Semantic interoperability on the internet of things: the semantic smart gateway framework," *International Journal of Distributed Systems and Technologies*, vol. 4, no. 3, pp. 47–69, 2013.

[8] Y. Zhang, T. Qu, O. K. Ho, and G. Q. Huang, "Agent-based smart gateway for RFID-enabled real-time wireless manufacturing," *International Journal of Production Research*, vol. 49, no. 5, pp. 1337–1352, 2011.

[9] R. J. Robles and T. H. Kim, "Applications, systems and methods in smart home technology: a," *Int, " Journal of Advanced Science And Technology*, vol. 15, pp. 37–48, 2010.

[10] O. Taiwo and A. E. Ezugwu, "Smart healthcare support for remote patient monitoring during covid-19 quarantine," *Informatics in Medicine Unlocked*, vol. 20, Article ID 100428, 2020.

[11] F. Cui, H. Hu, and Y. Xie, "An intelligent optimization method of E-commerce product marketing," *Neural Computing & Applications*, vol. 33, no. 9, pp. 4097–4110, 2021.

[12] K. Juelke and C. Romagnani, "Differentiation of human innate lymphoid cells (ILCs)," *Current Opinion in Immunology*, vol. 38, pp. 75–85, 2016.

[13] A. Rao, O. Strauss, E. Kokkinou et al., "Cytokines regulate the antigen-presenting characteristics of human circulating and tissue-resident intestinal ILCs," *Nature Communications*, vol. 11, no. 1, pp. 2049–2115, 2020.

[14] M. J. Mens, F. Klijn, K. M. de Bruijn, and E. van Beek, "The meaning of system robustness for flood risk management," *Environmental Science & Policy*, vol. 14, no. 8, pp. 1121–1131, 2011.

[15] M. Rezakazemi, A. Dashti, M. Asghari, and S. Shirazian, "H2-selective mixed matrix membranes modeling using ANFIS, PSO-ANFIS, GA-ANFIS," *International Journal of Hydrogen Energy*, vol. 42, no. 22, pp. 15211–15225, 2017.

Hindawi
Computational Intelligence and Neuroscience
Volume 2022, Article ID 9467623, 10 pages
https://doi.org/10.1155/2022/9467623

Research Article

Financial Data Mining Model Based on K-Truss Community Query Model and Artificial Intelligence

Zhuhua Han,[1,2] **Feng Li**,[2,3] **and Gong Wang**[2,3]

[1]*School of Bid Data Science, Hebei Finance University, Baoding, Hebei 710051, China*
[2]*Applied Technology Research and Development Center Wisdom, Hebei University, Baoding, Hebei 710051, China*
[3]*School of Computer and Information Engineering, Hebei Finance University, Baoding, Hebei 710051, China*

Correspondence should be addressed to Zhuhua Han; 1733271191@xzyz.edu.cn

Received 30 July 2022; Revised 14 September 2022; Accepted 28 September 2022; Published 11 October 2022

Academic Editor: Gopal Chaudhary

With the continuous development of Internet technology and related industries, emerging technologies such as big data and cloud computing have gradually integrated into and influenced social life. Emerging technologies have, to a large extent, revolutionized people's way of production and life and provided a lot of convenience for people's life. With the popularity of these technologies, information and data have also begun to explode. When we usually use an image storage system to process this information, we all know that an image contains countless pixels, and these pixels are interconnected to form the entire image. In real life, communities are like these pixels. On the Internet, communities are composed of interconnected parts. Nowadays, in various fields such as image modeling, we still have some problems, such as the problem of recognition rate, and we also found many problems when studying the community structure, which attracts more and more researchers, but the research on community query problems started late and the development is still relatively slow, so designing an excellent community query algorithm is a problem we urgently need to solve. With this goal, and based on previous research results, we have conducted in-depth discussions on community query algorithms, and hope that our research results can be applied to real life.

1. Introduction

Since the advent of the Internet in the early 1970s, a series of emerging science and technology, such as big data and cloud computing, has emerged [1]. These technologies have greatly improved people's quality of life and facilitated people's life and production work. With the popularity of these technologies, information and data have also begun to explode. When we usually use an image storage system to process this information, we all know that an image contains countless pixels, and these pixels are interconnected to form the entire image [2]. Nowadays, researchers have made in-depth discussions and research on the problems found in the community. The problems of community surveys are part of the problems found in the community [3]. The research on this problem is late and has a long process. Based on the results of previous research, the researchers designed a variety of community structures in order to extract the characteristics of the community and other data and information. Among them, the most widely used is the K-truss system, which mainly detects the relationship between pixels through a triangle formed by pixels in the image and designs an excellent community structure based on the detection results [4]. This article is mainly aimed at the K-truss system and uses algorithms to design a data model. For the smooth progress of the research, we decided to use a directed power graph for analysis [5].

2. Related Work

Literature pointed out that the network signal has a very important influence on the entire research process [6]. In the K-core system, we found that the signal in the network is very stable. Only the pixels of the image will affect the recognition rate of dense subimages. Therefore, in this way, we can choose a dense subgraph with firm edges and then

use the number of triangles in the K-truss system to observe the firmness. Literature shows that the signal stability in the network can be obtained by the number of triangles, so we can know that the system needs to be connected to a stable signal to design a good data model in order to improve the efficiency of the entire experimental process [7]. The literature describes the method of using functions to design the K-truss system, and the method is also introduced into the MapReduce system [5]. The literature improved the method, increased the calculation efficiency, and reduced the amount of calculation. On this basis, it explained a way to deal with large graphs. Some researchers have proposed some more excellent algorithms to improve the efficiency of processing large images, such as K truss [8]. But at the same time, the problems and disadvantages of this system are also revealed in the actual application scenarios. Literature pointed out that some scholars introduced a heuristic algorithm OLAK to make up for the shortcomings of the system. This problem needs to fix b key points outside the K core (not deleted because of the degree), so that k in the original graph core becomes the largest [9]. The literature also explained the solutions to these problems and also raised some other problems, such as in the network operation, users will affect the transmission of signals and information in the network [10]. In general, in a community structure, the fewer the users, the sparser the relationship, and the more stable the signal. But if some important users go offline or the relationship between important users breaks, it will cause damage to the community structure. For example, some Zhihu users will leave Zhihu because their questions are not answered satisfactorily [11]. This may also cause other users to leave. This will break the social structure, which will also affect other different social networks [12]. Therefore, the research on the key points of the network is particularly important, which is also conducive to our maintenance of the entire social network and social structure. This problem is extended to the K-truss version in the reference [13]. It is mentioned that in a complex network structure, the actions between users will also have a huge impact on the stability of the network. Often the more users in a social network, the closer the relationship between users, the more active the social network, and the higher the stability [14]. In the network, the departure of some key users, or the break of the relationship between some key users, will have a greater impact on the structure of the entire social network, and even "collapse" the network structure.

3. Research on K-Truss Community Query Model

3.1. K-Truss Community Query Model Design. In the previous research process, we used the K-core system to standardize the pixels in the image and stipulate that the size of each pixel must be greater than the k value, but the edges are not standardized. In this section, we mainly use the K-truss system and regulate the length of the sides, stipulating that the sides in the K-truss system should form $k-2$ triangles. In the actual process, we found that the K-truss system is similar to the K-core system, but the effect is better than that of the K-core system, and the results are more accurate.

We assume that there is an edge set B and use Tk (B, G) to represent the K-truss system after the edge set B is extracted. Because the set B of edges is extracted, which reduces the length of other edges or even cannot meet the requirements of K truss, we make these edges a subset of the set B. The relationship between the two is shown in the following equation:

$$F_i\left(B, T_k(G)\right) = E_{T_k(G)} - E_{T_k(B,G)} \cup B. \tag{1}$$

From this, we can lead to the problem of the maximum value in the K-truss system. In the weighted directed graph G, we need to extract the edges of the network to form a set B, and the edges in the K-truss system after obtaining B are reduced, so we get the largest subset of B.

Figure 1 shows the process of obtaining the minimum value in the K-truss system. There is an online social platform whose users are an element of the platform, and there is an edge between every two users. At this time, the number of common concerns of the two users will reflect the familiarity of the relationship between the two. In the hypothesis process, we simulated 15 social platforms. In the K-truss system, assuming that the number of common attention of two users is greater than $k-2$, it can indicate that the relationship between the two is not harmonious, and the number of corresponding edges will be reduced, so this will also affect the relationship with other users and even affect the entire platform. We use red, blue, and black to mark the different sides. The blue side is 5, the black side is 4, and the red side is 3.

3.2. Experimental Environment Design. We will explain the experimental process in detail, analyze the information base used and collected, evaluate the results, and compare the computational efficiency of various algorithms and functions to prove the accuracy of the results. The following processor is used in our experimental equipment: Intel Corei6-2450M with a memory of 9 GB. The design data model is designed using computers and monitors, and we use the cloud data platform to write algorithms. In this process, we use the B language.

In the research process, several algorithms are used for constructing community structure: (1) BFS Steiner tree algorithm based on social network elements, (2) Steiner tree algorithm on edges described in this article, (3) BulkDelete algorithm for collecting elements and samples, and (4) BulkDelete++ algorithm used by other researchers. In order to prove the accuracy of the results, we will compare the algorithms according to certain standards.

This article collects key data and information in the following 5 information databases to ensure the smoothness of the research. These information databases are Facebook, Amazon, Twitter, YouTube, and LiveJournal. These 5 information databases are processed through the right to have pictures. Table 1lists the characteristics of the database, including |V| refers to the total number of users, |E| refers to the number of elements, $d_{max}$is the meaning of on3dmax

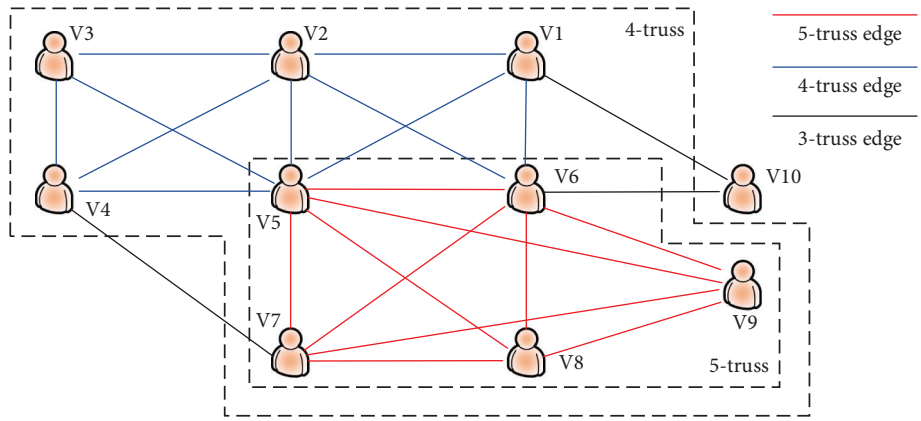

Figure 1: Example of K-truss minimization problem.

side length, and I (Ø) refers to all pixels in the truss is refers to the pictures.

Information database Twitter is a social network platform developed in the United States. This information database is obtained by collecting the information of Twitter users. This platform is composed of users and their relationships. The elements represent different users and the edges represent the relationship between the two. From the chart, we can see that the size of the element points in the Twitter information database exceeds 1085, and the k value in the K-truss system exceeds 89. This shows that the relationship between users is sticky and the social network is relatively mature and stable. Amazon is an online shopping platform developed in the United States. This information database is obtained through data released by Amazon. The element represents the product, and the edge represents that the product was purchased by two people. Facebook is a social networking platform developed in the United States. This information database is obtained from users and published data on Facebook. Elements represent users, and edges represent mutual friends between users. YouTube is the largest video platform in the United States. On the YouTube platform, users can follow each other in groups. The elements in the information database represent users, and the edges represent common concerns among users. LiveJournal is also an online social platform. Similar to Weibo, multiple users can form a circle of friends, which becomes an online community. The elements in the figure represent users, and the edges represent the stickiness of users in the online community.

In terms of the accuracy of the evaluation results, the evaluation index items in this study are mainly divided into two parts. The first is to judge the effect of the algorithm used in this study. By comparing the value of the original K-truss system calculated by the two algorithms, it is found that the BFS algorithm has a better performance, which proves that the algorithm used in this study has a better effect than the point-based algorithm in the original algorithm. The larger the value of k, the higher the accuracy of the proposed algorithm. The smaller the value of k, the lower the accuracy of the algorithm results. In order to make the comparison result more objective, we need to use the controlled variable

Table 1: Real dataset statistics.

Dataset	(V)	(E)	dmax	i (Ø)
Facebook	4 K	88 K	1045	80
Amazon	335 K	926 K	549	7
DBLP	317 K	1 M	342	86
YouTube	1.1 M	3 M	28754	19
LiveJournal	4 M	35 M	14815	253

method, which is to measure the time from the beginning to the end of the Steiner tree algorithm and fix the same calculation time. The calculated subgraph $G0$ uses the same parameters, but the final result of the K-truss system subgraph $G0$ is different, so we do not collect the data. Even if the key data are collected, we cannot calculate the time fixed in the same range.

The second is to compare the results of the initial BulkDelete algorithm with the improved BulkDelete++ algorithm in this article. We will compare the number of elements in the two algorithms to prove that the improved algorithm is more accurate and efficient. The two algorithms will delete the same subgraph $G0$. Table 2 lists in detail several evaluation indicators and the number of element points in the η value information database, and we fixed the value of γ as 4, and Q as the number of edges. In this part, we also apply the method of controlling variables, and mainly to analyze the samples in the collection, we start with a collection of 2 samples and randomly select the following samples. In order to make the experimental process more objective, we will perform the above process 150 times to calculate the final evaluation criteria for the mean.

3.3. Experimental Results and Analysis. In order to further prove the accuracy of the UP-Edge algorithm results, we also compared the subsets generated by different algorithms. Because some algorithms are very complex and computationally intensive, they may become more and more complex as the b set increases. Therefore, we chose two sets with fewer elements to compare the number of subsets of different algorithms. From the above figure, we can see that the number of subsets generated by the UP-Edge algorithm is similar to the number of subsets generated by the accurate

Table 2: Experimental parameters.

Parameter	Description
γ	The penalty coefficient in the truss distance formula
Q	Query node collection
η	Threshold to control the size of the expanded subgraph

algorithm, and there is basically no difference. However, the number of subsets generated by the UP-Edge algorithm is less than the number of subsets generated by the complexity algorithm. In these information databases, we have also compared the number of subsets generated by heuristic algorithms and complexity algorithms. It can be clearly seen from Figure 2 that in these selected databases, the number of generated subsets generated by the UP-Edge algorithm is less than the number of subsets generated by the complexity algorithm.

Figure 3 shows the validity experiment, in order to prove the accuracy of the UP-Edge algorithm calculation results in different situations, and we have studied the UP-Edge algorithm and the complexity algorithm on two information databases, using different variables. In the study of variable b, we set k as 30 and b from 1 to 9. In the study of variable k, we set b as 6 and k from 21 to 30. From the figure, we can clearly see that when the value of b is fixed, the number of subsets of the two algorithms is proportional to the value of k. The smaller the value of k, the smaller the number of subsets. This also proves the properties mentioned in the above content and the function $f = |\mathrm{Ft}\ (B,\ \mathrm{Tk}\ (G))|$ is a linear function. When more edges are deleted, the number of subsets will also increase. However, in these two information bases, the UP-Edge algorithm produces more subsets than the complexity algorithm, and the k value has a great influence on the generation of subsets, but it is not linear. The experimental results show that the calculation results of the UP-Edge algorithm are more accurate and efficient.

We also compared the difference between K core and K truss for selecting dense subgraphs. We compared the parameters of the two systems in the above five information databases. Before that, the specific calculation method is as follows:

$$C(G) = \frac{3 \times \mathrm{numberoftrianglesinG}}{\sum_{v \in V_G} \begin{pmatrix} \deg(v) \\ 2 \end{pmatrix}}. \tag{2}$$

In order to make the comparison result more objective and credible, we have selected different elements in each image. In the K-core system, we selected 40% of the elements, and in the K-truss system, we selected the trussness of the edges and 40% of the elements. We compare the parameters of the dense submap formed by these elements. After comparison, we can see that the parameters of the dense submap selected in the truss system are all lower than those in the core system, which indicates that the result error of the truss system is smaller and easy to calculate. Moreover, the calculation complexity of the K-truss system is lower than that of the K-core system, so at the same time, the calculation speed of the K-truss system is faster.

Then, the computational and operational efficiency of the UP-Edge algorithm should be evaluated. By comparing the computation time of UP-Edge algorithm, complexity algorithm, and heuristic algorithm in the same information base and the same coefficients, that is, when the coefficients of other variables are the same, the computation time of UP-Edge algorithm, complexity algorithm, and heuristic algorithm is compared. In these information databases, we set fixed parameters to ensure the objectivity of the experimental results and measured the calculation time of the three algorithms. The results show that the calculation time of the UP-Edge algorithm on all information databases is less than that of the other two algorithms, especially in the Facebook and Twitter information databases. This algorithm is 10 times faster than the complexity algorithm. Figure 4 shows the high-efficiency experiment (change k).

In order to further prove the great advantages of UP-Edge, we chose two other information repositories, namely, YouTube and Amazon. We set the same parameters in these two databases for experimentation and comparison. In order to obtain the relationship between the value of k and the calculation efficiency of the algorithm, we set $b = 6$ in the Amazon information database and take values from 20 to 35 for k. In the YouTube database, we set $b = 4$ and k from 5 to 10. The figure shows the calculation time of the three algorithms under different k values. From these two datasets, we can see that the higher the value of k, the shorter the computation time of the algorithm. The lower the value of k, the longer the computation time. Since the number of edges in Tk (G) increases only if k decreases, so does the number of corresponding elements. Through these experiments, we found that the UP-Edge algorithm is optimal, with small error and high computational efficiency.

4. Design and Application of Financial Data Mining Model Based on Artificial Intelligence

4.1. Establishment of Data Mining Model. In this section, we will analyze the financial data processing system in the securities industry. In this system, we build a financial data estimation system on the basis of an improved genetic neural network system and also use a classification algorithm to collect key characteristics between different stocks to build a reasonable data model. The specific structure is shown in Figure 5.

In the information we collect, we refer to the data published by the global financial center or company, namely, the opening price, the high price, the low price, and the closing price. The collected data cannot be used directly, because the amount is too large and the types are too many to reduce the efficiency of the subsequent process, because we need to process, classify, and process the collected data, which can reduce the amount of calculation in the subsequent calculation process and improve efficiency.

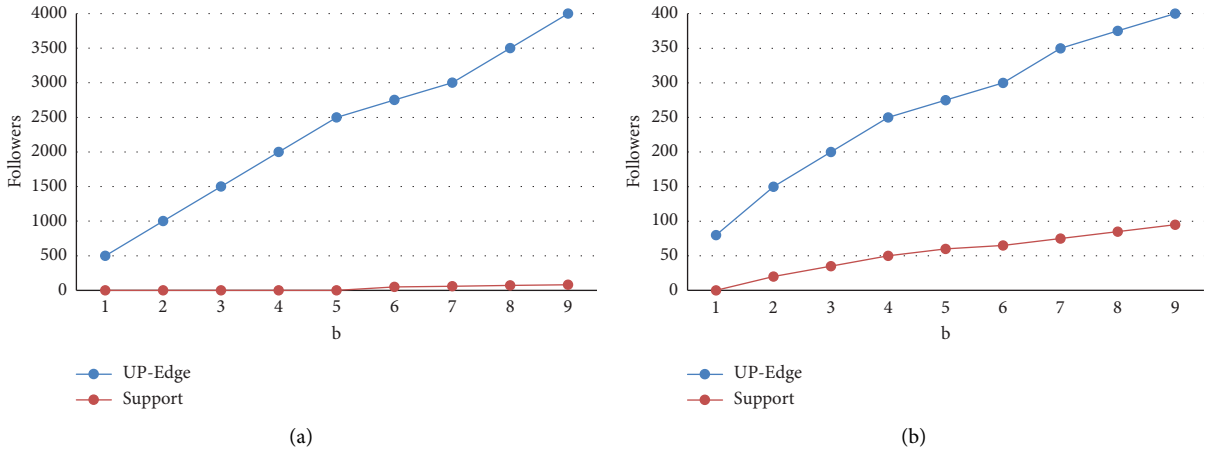

Figure 2: Validity experiment (change b). (a) Live journal (vary b). (b) Live journal (vary b).

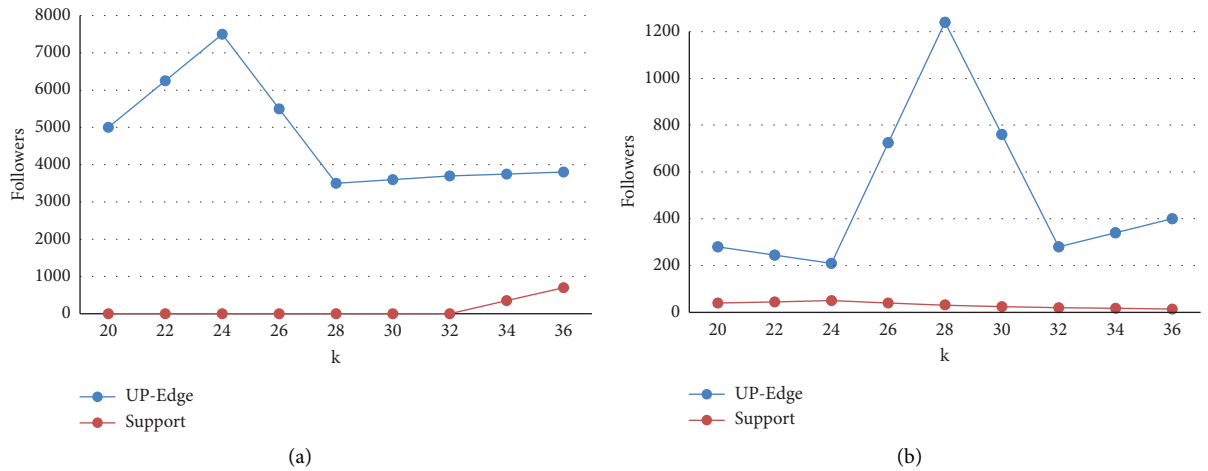

Figure 3: Validity experiment (change k). (a) Live journal (vary k). (b) Live journal (vary k).

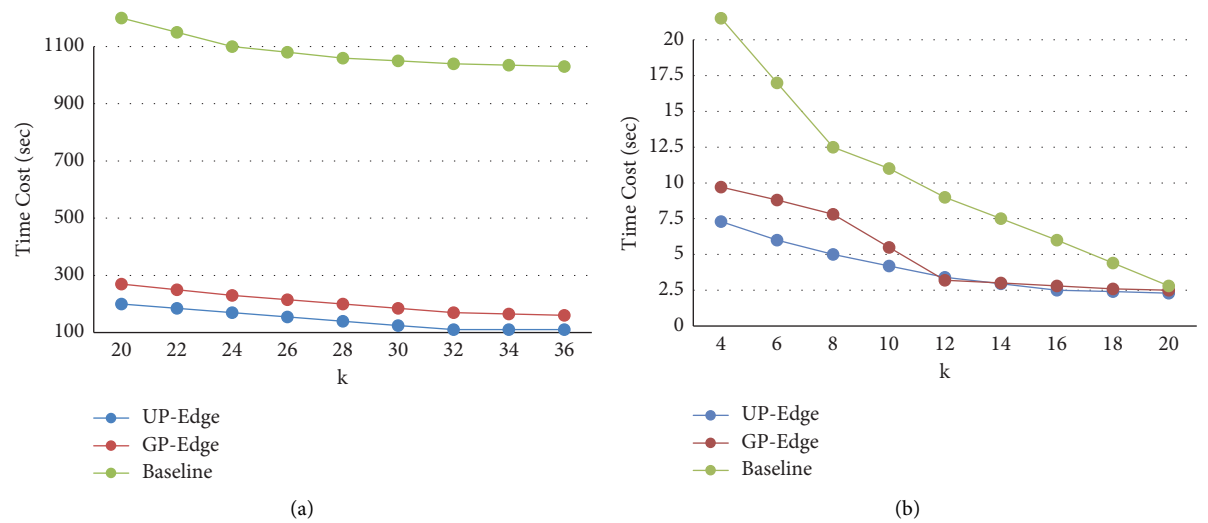

Figure 4: High-efficiency experiment (change k). (a) Live journal (vary k). (b) Live journal (vary k).

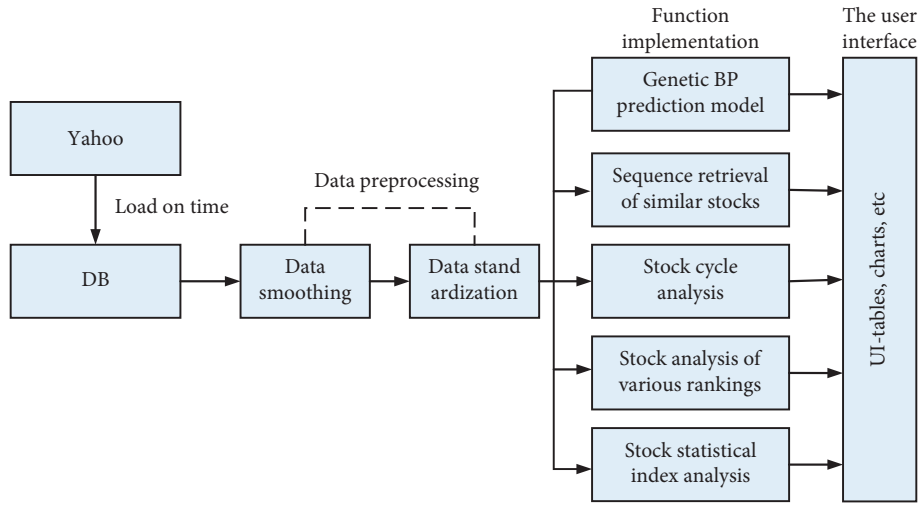

Figure 5: System model framework.

(1) *Smoothing*. We first need to smooth the data. It is expressed as follows:

$$\widehat{y}_i = \frac{\sum_{i=1}^{n} K_k(i-t)y_i}{\sum_{i=1}^{n} K_h(i-t)}. \tag{3}$$

Among them, the heuristic function is as follows:

$$K_h(x) = \frac{1}{h\sqrt{2\pi}} e^{s^2/2k^2}. \tag{4}$$

(2) *Standardization*. In the previous research, we used the sigmoid function to analyze the neural network, but this function can only identify data in the binary system, so we need to express these data in the binary system. Nowadays, many researchers have explained different functions. Through research, we have found a function with a better effect. The specific formula is as follows:

$$\begin{aligned}\overline{x}_{i-1} &= \frac{0.1-0.9}{\min(X_i)-\max(X_t)} x_{i-1} \\ &\quad + \frac{0.9\min(X_i)-0.1\max(X_t)}{\min(X_i)-\max(X_t)}.\end{aligned} \tag{5}$$

After the data are expressed in the binary system, the calculation is performed, and the calculated result needs to be analyzed in the decimal system, so we need a second conversion.

During the research process, we performed operations such as calculating the average, shifting the average, and formulating evaluation standards. In the financial data analysis system, investors need to consult various information and data about stocks, including closing prices, opening prices, highest prices, and turnover. Therefore, we entered the following information into the system and processed it:

(1) *Basic Information*. Opening price, closing price, highest price, lowest price, transaction amount, drop rate, etc.

(2) *Change Information*. Weekly change, monthly change, quarterly change, annual change, etc.

4.2. System Development and Design. This system uses a three-tier architecture model, which is now the most commonly used model, mainly composed of three parts: information layer, processing layer, and display layer. The information layer is mainly used to collect different data and information and transcode them so that they can be transmitted to other platforms. This layer is to provide device support through computers, databases, and cloud platforms. The processing layer is the transitional part between the information and the display layer. It is mainly used to process information and classify and integrate data according to the parameters set by the experimenter. After processing according to certain rules, these data are then transmitted to other devices and the display layer. The display layer is mainly supported by the display as a device, and users can check and obtain information on this layer.

In this process, we mainly use Python to complete the design of the entire algorithm and use Microsoft Visual Studio 2006 to provide equipment support. This computer is fully functional and complete, runs fast, can process a variety of data at the same time, and has a large memory, these calculation results can be stored, real-time data transmission can also be realized, and the data can be transmitted to other platforms. In the research process, we can know that the database and information library play a great role in the experiment. In order to keep the data complete and long-term, we chose Microsoft's Microsoft SQL Service 2006 system, which has a large memory and can also interact with multiple devices that are connected. After that, we used PowerDesignerl0 to construct models and systems. This device can complete the construction of multiple models with high efficiency and low cost.

4.3. Similar Stock Retrieval Model. We have explained the relevant data model and database in detail. In this section, we analyze the stock characteristics and the market. We will use

the data system to process and integrate the stocks, then collect the characteristics of the stocks, and then use the classified. The method ranks the stocks, and we also evaluate the authenticity of these data through corresponding standards to ensure the smooth progress of the following process.

First, we need to analyze the Euclidean distance. The principle is to extract variables at different times as an element in the Euclid chart, then estimate the distance between these variables according to the distance between the elements in the Euclid icon, and use these distances as a fixed standard, and the specific formula is as follows:

$$D(X,Y) = \sum_{i=1}^{n} (X_i - Y_i)^2. \tag{6}$$

Other scholars have also proposed another method, the principle of which is to use a linear regression function to estimate an approximate value, correspond the initial value to the parameters in the function, calculate the Euclidean distance, then use the initial time series as a set, classify the elements in this set, and get a subset:

$$f(t,w) = w_0 + w_1 t + w_2 t^2 + \cdots + w_{p-1} t^{p-1}. \tag{7}$$

We divide the set into seven subsets, which include k elements. If an element in this set belongs to an unknown pattern, then this element is the key point of this pattern. When the coefficient $f > 0$, the element is the key point of mode P. The necessary and insufficient conditions for $£ \in x$ not to belong to the unknown mode are as follows:

$$d(x\prime, x) < \frac{\zeta}{2}. \tag{8}$$

From the perspective of big data, the sequence set is composed of randomly selected variables, so it is also a set of known and unknown elements. Known elements are composed of basic information of data, unknown elements are composed of random samples, and different data models are also included. Because linear parameters are unknown elements of the sequence set, some scholars use ACF to calculate the similarity value of the sequence set. He first collected 25 elements in the sequence set, matched these elements with ACF values one to one, and then processed and classified these data and information. The calculation formula is as follows:

$$r_k = \frac{\sum_{i=1}^{n-k} (y_i - \overline{y}_i)(y_{i+k} - \overline{y}_{i+k})}{\sqrt{\sum_{i=1}^{n-k} (y_i - \overline{y}_i)^2 \sum_{i=1}^{n-k} (y_{i+k} - \overline{y}_{i+k})^2}}. \tag{9}$$

Among them,

$$r\overline{y}_t = \frac{1}{n-k} \sum_{t=1}^{n-k} y_t, \overline{y}_{t+k} = \frac{1}{n-k} \sum_{t=1}^{n-k} y_{t+k}. \tag{10}$$

It is connected with other data systems and has corresponding values. Therefore, we can see that it is also a linear function:

$$x_t = a_1 x_{t-1} + a_2 x_{t-2} + \cdots + a_p x_{t-p} + \varepsilon_t. \tag{11}$$

The coefficients in the PR data system can be judged from the following formula:

$$c_n = \begin{cases} -\alpha_1, & \text{if } n = 1 \\ -\alpha_n - \sum_{m=1}^{p} \left(1 - \frac{m}{n}\right) \alpha_m c_{n-m}, & \text{if } 1 < n \le p, \\ -\sum_{m=1}^{p} \left(1 - \frac{m}{n}\right) \alpha_m c_{n-m}, & \text{if } p < n. \end{cases} \tag{12}$$

The collected coefficients basically meet the requirements of the sequence collection, so it is sufficient to collect the coefficients of the previous part. These coefficients are relatively stable and will not change with changes in experimental data. Among them, the Euclidean distance can be used to evaluate the similarity between sequence sets, which can simplify the calculation process and improve the calculation efficiency. It is very suitable for processing complex data of different types.

The FCM algorithm is used to classify and integrate data, and its main principle is to select a subset of $X \times Y$ fuzzy. Fuzzy relations need to be converted into binary, and the specific process is as follows:

$$\begin{aligned} R\colon X \times Y &\longrightarrow [0,1], \\ (x,y) &\mapsto R(x,y). \end{aligned} \tag{13}$$

The principle of FCM is mainly to correspond the minimum value of the linear function L to the set X to obtain an approximate value and then perform data classification. The calculation formula of the linear function is as follows:

$$\text{Minimize} J_m(X\colon U,V) = \sum_{i=1}^{c} \sum_{j=1}^{n} \left(u_{ij}\right)^m \left\| x_j - v_i \right\|^2. \tag{14}$$

Later, we discussed the results of the previous formula by classification:

$$u_{ij}\begin{cases}\left[\sum_{r=1}^{c}\left(\frac{\left\|x_j-v_i^0\right\|}{\left\|x_j-v_r^0\right\|}\right)^{\frac{2}{m-1}}\right]^{-1}, & \text{if}\left\|x_j-v_i^0\right\|>0\,(1\le j\le n, 1\le i\le c),\\ 1, & \text{if}\left\|x_j-v_i^0\right\|=0,\\ 0, & 0\text{if}\exists r, r\ne i, \left\|x_j-v_i^0\right\|=0',\end{cases} \tag{15}$$

$$v_i=\frac{\sum_{j=1}^{n}\left(u_{ij}\right)^m x_j}{\sum_{j=1}^{n}\left(u_{ij}\right)^m}, 1\le i\le c.$$

Considering the aforementioned AR algorithm, we can formulate a series of standards to evaluate the parameters, and the process is as follows:

$$V_{\text{xie}}(U,V,c)=\frac{\sum_{k=1}^{n}\sum_{i=1}^{c}u_{ki}^m\left\|v_i-x_h\right\|^2}{n\times\min_{i\ne j}\left\|v_i-x_j\right\|^2}. \tag{16}$$

The V value is the ratio of the calculation time of the function to the size of the dataset, and the U value can measure the number of samples in the set. The algorithm of V value proposed by S. H. Kwon is as follows:

$$V_{\text{hren}}(U,V,c)=\frac{\sum_{i=1}^{c}\sum_{j=1}^{n}u_{ki}^m\left\|v_j-x_i\right\|^2+1/c\sum_{i=1}^{c}\left\|v_i-\right\|^2}{\min_{i\ne j}\left\|v_i-x_j\right\|^2}. \tag{17}$$

This function improves calculation efficiency. When the value of C becomes smaller, it will be farther and farther away from the value of n, and the final result will be greater than 0. At this time, there will be an error in the result. So, S. H. Kwon proposed the concept of a penalty function to reduce the error and improve the accuracy of the result. At the same time, H. Sun-S. and Q. Jiang also proposed the algorithm of V value:

$$V_{\text{WSJ}}(U,V,c)=\text{Scat}(c)+\frac{\text{Sep}(c)}{\text{Sep}(C_{\max})}. \tag{18}$$

Among them,

$$\begin{aligned}\text{Scat}(c)&=\frac{1/c\sum_{j==1}^{c}\left\|\sigma(v_i)\right\|}{\left\|\sigma(X)\right\|},\\ \text{Sep}(c)&=\frac{D_{\max}^2}{D_{\min}^2}\sum_{i=1}^{c}\left(\sum_{j=1}^{c}\left\|v_i-v_j\right\|^2\right)^{-1}.\end{aligned} \tag{19}$$

Scat (c) represents the accuracy of the result, and its principle is to reduce the error of the result. Later, Dae Won Kim also proposed the calculation method of V value:

$$V_{OS}(c,U)=\frac{\text{Overlap}^N(c,U)}{\text{Sep}^N(c,U)} \tag{20}$$

Among them,

$$\begin{aligned}\text{Overlap}^N(c,U)&=\frac{\text{Overlap}(c,U)}{\text{Overlap}_{\max}},\\ \text{Overlap}(c,U)&=\frac{1}{c(c-1)}\sum_{p=1}^{c-1}\sum_{q=p+1}^{c}\times\left[\sum_{n}\sum_{j=1}^{n}\delta\left(x_j,u:\right)\omega\left(x_j\right)\right]\\ \delta\left(x_j,u:\overline{F}_p,\overline{F}_q\right)&=\begin{cases}\omega\left(x_j\right),\text{if}\left(\mu_{\overline{F}_p}\left(x_j\right)\ge u\right)\text{an d}\left(\mu_{\overline{F}_q}\left(x_j\right)<u\right),\\ 0.0,\text{otherwise},\end{cases}\\ \text{Sep}^{\text{N}}(c,U)&=\frac{\text{Sep}(c,U)}{\text{Sep}_{\max}},\\ \text{Sep}(c,U)&=1-\min_{p\ne q}\left[\max_{x\in X}\min\left(\mu_{\overline{F}_p}(x),\mu_{\overline{F}_q}(x)\right)\right].\end{aligned} \tag{21}$$

After many experiments, we found that some of the algorithm results have errors, or the original data has been destroyed, so we have improved them, and we will introduce them in detail later.

Nowadays, many standards are related to "compactness" and "separation." Compactness refers to the situation where data are very tightly distributed, and separation refers to the situation where data distribution is very sparse. Effectiveness is to find the maximum compactness and minimum separation. In the process of research, we found that the previous effectiveness index has some drawbacks, and we have improved it. The calculation formula is as follows:

$$\sigma\left(x_j,u,C_p,C_q\right)=\begin{cases}\varepsilon_1^{1/m}0.65<u'\le 1.0,\\ \varepsilon_1^{1/m}0.55\le u'\le 0.65,\\ \varepsilon_1^{1/m}0.50\le u'<0.55.\end{cases} \tag{22}$$

At this time, we use the linear regression function to calculate the C value, which has a great influence on the final

result. When the c value is obtained, the following calculations are performed:

$$\begin{aligned}\mathrm{Sup}(U,V,c)\prime &= \frac{2}{c(c-1)}\sum_{p=1}^{c-1}\sum_{q=p-1}^{c}\lambda\left(u,C_p,C_q\right),\\ &= \frac{2}{c(c-1)}\sum_{p=1}^{c-1}\sum_{q=p-1}^{c}\sum_{i=1}^{n}\sigma\left(x_i,u,C_p,C_q\right).\end{aligned} \tag{23}$$

Then, we proceed to the following process:

$$\mathrm{Sup}(U,V,c) = \frac{\mathrm{Sup}(U,V,c)\prime}{\max\limits_{e}\mathrm{Sup}(U,V,c)\prime}. \tag{24}$$

4.4. System Function Design and Realization. The composition and structure of the system are explained in detail, including some data processing modules. The module structure of the system is mainly composed of data processing and prediction, access analysis, classification, and integration. The first is data processing and prediction. In this module, the main functions are data collection and processing. First, we must collect the data released by the financial center, update the data in real time every day, classify and integrate the data, and put them into different sets in order. We design a system with two independent modules, which is a kind of intelligent system for stock prediction based on the genetic BP neural network model. The system modules are the initial genetic BP data prediction system and the improved genetic BP data prediction system. By comparing the results of the two prediction systems, the superiority of the improved system can be confirmed. In the reference analysis module, we use ACF to collect the characteristics of stocks. Later, in similar data, we will enter these data and do not consider the time factor, which greatly improves efficiency. Below, we will conduct experiments on the KDJ and RSI indicators. The first is the KDJ indicator. The steps involved in the calculation process are as follows:

(1) First, we calculate the RSV value in a period, and here, we calculated it in nine days:

$$n\mathrm{HRSV} = \left(C_m - L_m\right) + \left(H_n - L_n\right) \times 100. \tag{25}$$

The symbols in the formula and their meanings are as follows: Cn represents the opening price on day n and L_n represents the highest price on day N. After calculating the RSV value, the value shows that the fluctuation is between 1 and 150.

(2) Then, we calculate the K and D values as follows:

K value of the day = 1/3 × RSV of the day + 2/3 × K value of the day before

D value of the current day = 1/3 × K value of the current day + 2/3 × D value of the previous day

(3) Then, we calculate the J value, $J = 3D - 2K$.

After calculating the RSI indicator, it is also necessary to choose the period. We have selected the three periods of 5, 10, and 15 days. The value of the RSI indicator fluctuates from 0–150. If it exceeds 75, it is a strong market, and if it does not exceed 50, it is a weak market.

Table 3: X30 (class 3) experimental results.

Index	V_{xte}	V_{baid}	V_{kwon}	V_{HR}	V_{vmj}	V_{OB}	V_{xij}
Result	3	10	2	3	3	3	3

Table 4: IRIS (class 3) experimental results.

Index	V_{xte}	V_{baid}	V_{kwon}	V_{HR}	V_{vmj}	V_{OB}	V_{xij}
Result	2	10	2	2	3	2	3

Table 5: Dataset three (6 categories) test results.

Index	V_{xte}	V_{baid}	V_{kwon}	V_{HR}	V_{vmj}	V_{OB}	V_{xij}
Result	6	10	6	3	6	6–10	6

Table 6: Experimental results of dataset 4.

Index	V_{xte}	V_{baid}	V_{kwon}	V_{HR}	V_{vmj}	V_{OB}	V_{xij}
Result	4	10	6	4	5	4	5

4.5. Experiment and Result Analysis. After that, we conducted a lot of experiments. In the experiment, we set $m = 2$, Cmin = 2, and Cmax = 10. The specific operation process is as follows:

First, we must test the sample set. The sample set consists of 35 variables. We divide it into 3 categories for comparison experiments. The results are listed in Table 3.

Then, we tested the second set of sample set IRIS and also divided the samples into 3 categories for controlled variable tests. The results are listed in Table 4.

After that, we will test the third sample set, which includes 6 types of two-dimensional data. Through the linear regression function, we can see the results, as listed in Table 5.

Finally, we conduct experiments on the fourth sample set, and the results are shown in Table 6.

Through these experiments, we can see that the improved indicators make up for the previous deficiencies, improve efficiency, and reduce costs and errors.

5. Conclusion

Since the emergence of the Internet in the middle and late 20th century, emerging technologies such as big data and cloud computing have also emerged. These technologies, to a great extent, have revolutionized people's way of production and life, not only accelerating the efficiency of production, but also facilitating people's life. The proliferation of technology has also led to an exponential explosion of information and data. Especially in recent years, with the rapid development of emerging technologies, especially the remarkable development of the Internet and the spread and

rise of network social platforms, many researchers begin to pay attention to the related research in this field. In this case, we chose two subgraph systems, namely, K-core system and K-truss system, and compared the effects of the two systems. Based on the K-core and K-truss systems, we found two problems, namely, the K-core maximization problem and the K-truss minimization problem. We collect the edges in the social network structure by solving these two problems. Because this problem is too complicated and takes a long time, we have chosen a heuristic algorithm to solve this problem in order to simplify the calculation process and improve calculation efficiency. We also designed related models to optimize the structure of the social network platform, hoping that our research results can solve real-life problems.

Data Availability

The data used to support the findings of this study can be obtained from the corresponding author upon request.

Conflicts of Interest

The authors declare that they have no conflicts of interest.

Acknowledgments

This work was supported by the Youth Fund of Science and Technology Research Project of Hebei University, China (Grant no. QN2019186), Applied Technology Research and Development Center Wisdom in Hebei University, China (Grant no. XGZJ2021013C), and Baoding Science and Technology Plan Project: Research on Fuzzy Comprehensive Evaluation of Baoding New Energy Industry Competitiveness (Grant no. 2011ZG011).

References

[1] C. Yang, Q. Huang, Z. Li, K. Liu, and F. Hu, "Big Data and cloud computing: innovation opportunities and challenges," *International Journal of Digital Earth*, vol. 10, no. 1, pp. 13–53, 2017.

[2] H. S. Li, Z. Qingxin, S. Lan, C. Y. Shen, R. Zhou, and J. Mo, "Image storage, retrieval, compression and segmentation in a quantum system," *Quantum Information Processing*, vol. 12, no. 6, pp. 2269–2290, 2013.

[3] A. F. Jorm, S. J. Bourchier, S. Cvetkovski, and G. Stewart, "Mental health of Indigenous Australians: a review of findings from community surveys," *Medical Journal of Australia*, vol. 196, no. 2, pp. 118–121, 2012.

[4] Z. Zheng, F. Ye, R. H. Li, G. Ling, and T. Jin, "Finding weighted k-truss communities in large networks," *Information Sciences*, vol. 417, pp. 344–360, 2017.

[5] M. Alemi and H. Haghighi, "KTMiner: distributed k-truss detection in big graphs," *Information Systems*, vol. 83, pp. 195–216, 2019.

[6] A. Hajbabaie and R. F. Benekohal, "A program for simultaneous network signal timing optimization and traffic assignment," *IEEE Transactions on Intelligent Transportation Systems*, vol. 16, no. 5, pp. 2573–2586, 2015.

[7] D. K. Dheer, S. Doolla, S. Bandyopadhyay, and J. M. Guerrero, "Effect of placement of droop based generators in distribution network on small signal stability margin and network loss," *International Journal of Electrical Power & Energy Systems*, vol. 88, pp. 108–118, 2017.

[8] Z. Yang, X. Li, X. Zhang, W. Luo, and K. Li, "K-truss community most favorites query based on top-t," *World Wide Web*, vol. 25, no. 2, pp. 949–969, 2022.

[9] C. Chu and J. K. Aggarwal, "The integration of image segmentation maps using region and edge information," *IEEE Transactions on Pattern Analysis and Machine Intelligence*, vol. 15, no. 12, pp. 1241–1252, 1993.

[10] M. Z. Win, W. Dai, Y. Shen, G. Chrisikos, and H. Vincent Poor, "Network operation strategies for efficient localization and navigation," *Proceedings of the IEEE*, vol. 106, no. 7, pp. 1224–1254, 2018.

[11] T. S. Ustun and Y. Aoto, "Analysis of smart inverter's impact on the distribution network operation," *IEEE Access*, vol. 7, pp. 9790–9804, 2019.

[12] T. A. Snijders, "Statistical models for social networks," *Annual Review of Sociology*, vol. 37, no. 1, pp. 131–153, 2011.

[13] C. Durugbo, W. Hutabarat, A. Tiwari, and J. R. Alcock, "Modelling collaboration using complex networks," *Information Sciences*, vol. 181, no. 15, pp. 3143–3161, 2011.

[14] M. O. Jackson, "An overview of social networks and economic applications," *Handbook of social economics*, vol. 1, pp. 511–585, 2011.

Hindawi
Computational Intelligence and Neuroscience
Volume 2022, Article ID 3029039, 10 pages
https://doi.org/10.1155/2022/3029039

Research Article

Emergency Information Communication Structure by Using Multimodel Fusion and Artificial Intelligence Algorithm

Liping Lei

School of Political Science and Public Administration, East China University of Political Science and Law, Shanghai 201620, China

Correspondence should be addressed to Liping Lei; 1601407130@zjbti.net.cn

Received 30 July 2022; Revised 14 September 2022; Accepted 20 September 2022; Published 10 October 2022

Academic Editor: Gopal Chaudhary

With the development of The Times, social events are increasing, and emergency management has gradually become the main helper to solve the crisis in the public domain. By observing the current situation of many countries and regions, we can find that various types of public crises often occur in many countries and regions in the world, which have severely affected people's daily life, lives, and property. Through long-term research and analysis, it can be known that the emergency management mechanism currently established in China has certain shortcomings. The communication problem of emergency information is likely to cause the emergency work to not proceed smoothly. In addition, problems in the communication channels of emergency information are likely to cause problems in the cooperation of various departments when people carry out emergency management work, and the efficiency of the government in dealing with problems will also be reduced in real scenarios. In order to improve the efficiency of emergency information management, this paper aims at the various problems existing and facing in the construction of emergency management system. On this basis, the integration of various relevant emergency information management plan models is analyzed and sorted out, and based on the research and integration of the development of artificial intelligence algorithms. The main research results of emergency information management at home and abroad are comprehensively studied and evaluated. Finally, a QG algorithm based on more model fusion is developed. In the process of analysis, this article uses artificial intelligence algorithms to build a prediction model of multiple modes and collects the data needed to build the model by random extraction. Through the analysis of different data sets, it is used as the basic training data for prediction. Through comprehensive analysis, the model constructed in this paper can promote the sharing of emergency information among departments to a certain extent.

1. Introduction

In order to improve the efficiency of problem handling as much as possible, it is necessary to enhance the effectiveness and immediacy of information communication between various government departments, whether in the beginning or the follow-up process of public crisis handling. In the process of carrying out emergency management, emergency information is the carrier of key signals transmitted by various departments, and it can also explain the connections between various subjects in public crises [1]. Improving the efficiency of communication of emergency information can promote the resolution of public crises to a certain extent. Under the current development background, various countries and regions are getting closer and closer, and many issues are related to the interests of multiple subjects [2]. Public crisis events have gradually shown new characteristics, which require all departments to do a good job of information and communication work. When dealing with emergencies, problems in the communication channels of emergency information are likely to lead to problems in the cooperation of various departments when people carry out emergency management work [3]. In reality, the efficiency of the government in handling problems will also be reduced. In actual scenarios, the transmission and sharing of information is an important way to determine whether public crisis events can be resolved quickly. Government departments must not only use professional measures to increase the speed of information transmission but also establish a crisis event alert system [4].

Due to technical difficulties, the data transmission speed and sharing function of existing information and communication systems are limited to some extent [5]. In view of the current problems, in the future of the development of information and communication system, we can rely on new technology and new theoretical knowledge to improve and optimize the development and construction of the existing information and communication management system. In order to solve the above problems and improve the efficiency of early warning and emergency information management, this paper conducts a multimodel fusion study. Combined with the development of artificial intelligence algorithms, this paper comprehensively analyzes the main achievements of emergency information management research at home and abroad and finally proposes a QG algorithm based on the multifusion model [6]. In the process of analysis, this article uses artificial intelligence algorithms to build a prediction model of multiple modes and collects the data needed to build the model by random extraction. The collected data can be used as the training data for the prediction model [7]. Ensure the scientific of the analysis results. After overall analysis, the model constructed in this article can promote the sharing of emergency information among various departments to a certain extent. Through the experimental analysis shows that through this article builds a fusion model of multiple factors, and through the use of an artificial intelligence algorithm, which is combined with the actual scene, the application of information transfer and sending and receiving efficiency and accuracy can be a certain level, to improve the communication efficiency of government departments and social crisis event comprehensive public relations capacity.

2. Related Work

Literature introduced the specific situation of emergency management to people, expounded on the concept and types of emergency management, and also analyzed the importance of information management to emergency management [8]. In the process of analysis, the article also introduced the grid theory, and the technology introduced by the theory can improve the effect of information integration to a certain extent and can realize information sharing and efficient dissemination between various departments. The literature also analyzes the information transmission and sharing in crisis management, the integration of various models, the development of artificial intelligence algorithms, and the main research results of emergency information management at the present stage [9]. Finally, an algorithm using multiple model fusion is proposed to improve the management efficiency of emergency information. Literature analyzes a variety of factors that affect information transmission and uses the knowledge and technology of grid theory to study the methods of information transmission and communication [10]. The article believes that the knowledge and technology of grid theory can improve the crisis. The efficiency of information management in management has confirmed the feasibility of this method based on specific analysis [11]. Literature introduced the details of information management, analyzed the development of information management and existing problems, and studied the methods of information sharing [12]. This paper conducts a series of analyses on the internal structure, operation means, and corresponding procedures of the information management system and finds that there are still a series of problems in the current system, such as uncoordinated and unbalanced communication, insufficient transparency of external information disclosure, and no connection between various communication channels [13]. Literature uses existing theories and technologies to build an information communication model. This model is mainly supported by the technology used in gridding theory [14]. In the process of research, the article also tested and analyzed the role of this model in government crisis management. Literature analyzes the practical application of gridding theory and believes that various government departments can use the advantages of gridding to realize remote office work and establish virtual information communication organizations in various regions, which can promote the improvement of information communication efficiency [15]. Help all departments and regions realize the sharing of information resources.

This article uses the knowledge of grid theory and related technologies to optimize the distribution of information communication channels and establishes a grid information-sharing system through integration. The integrated system has functions such as digital transmission, voice calls, and video chats [16]. The system can also back up various types of data at any time, realizing information sharing among different levels, different departments, and different regions. In this paper, an artificial intelligence algorithm is used to construct a fusion model of various modes in the analysis process. Under the realistic situation that the original organizational structure of the organization is controlled as much as possible without changing, the information communication channels are broadened and enriched, the level of information management is improved to a certain extent, and the quality of information management is guaranteed [17–19].

3. Multimodel Fusion and Artificial Intelligence Algorithm

3.1. Multimodel Fusion

3.1.1. Sequence-to-Sequence Generative QG Model. The construction of the QG model needs to rely on the generation of the sequence. In the process of building the model, the encoder must be used to calculate the expression of the result. After the calculation is calculated, the decoder is used to sort the answer vector, so that a complete question can be generated. Let's introduce the detailed situation.

The purpose of using the encoder is to turn question-and-answer sentences with inconsistent lengths into fixed-length vectors. This type of vector is continuous, and different neural networks can be used to achieve the purpose of the encoder. The decoder will predict the problem output by the system based on the content of the sequence, which can be expressed as a mathematical formula:

$$p(q|a) = \prod_{t=1}^{|q|} p(q_t|q < t, a). \tag{1}$$

This article uses an attention-based structure, which can calculate the probability of each word in the answer sentence. The calculation formula is as follows:

$$p(q_t|q < t, a) = f_{dec}(q_{t-1}, s_t, c_t). \tag{2}$$

When encoding, the attention system will set a different probability or weight for each hidden state in each time step. The specific calculation formula is as follows:

$$c_t = \sum_{i=1}^{|a|} \alpha < i, i > h_i. \tag{3}$$

During the running of the model, the model will record the appearance of each word in different sentences, and the model will not reuse words that have already appeared. The specific calculation formula is as follows:

$$\alpha < t, i > = \frac{\exp\left[z\left(s_t, h_i, \sum_{j=1}^{N} \alpha < t-1, j > h_j\right)\right]}{\sum_{i'=1}^{N} \exp\left[z\left(s_t, h_{i'}, \sum_{j=1}^{N} \alpha < t-1, j > h_j\right)\right]}. \tag{4}$$

In the QG model, each component can solve the differential function, so all the parameters in the model can be learned using the backpropagation algorithm. The specific formula of the algorithm is as follows:

$$l_{qg}(q, a) = -\sum_{t=1}^{|q|} \log\left[p(y_t|y < t, a)\right]. \tag{5}$$

In the process of building the model, using the grid beam search algorithm can expand the search range of the traditional beam algorithm and can calculate all the words before decoding. The algorithm can calculate the language sentences of all models. The detailed calculation formula is as follows:

$$p(y|X) = \coprod_t p(y_t|X; \{y_0 \ldots y_{t-1}\}). \tag{6}$$

3.1.2. Evaluation Index. In the process of analyzing the question types, the QGSTEC2010 assessment meeting was used in this study. The assessors can divide the test questions and sentences into five parts for scoring. The details of the scoring of the first part are shown in the following Table 1.

In the evaluation process, the question sentence needs to be converted into the corresponding query sentence, so that the system can match the corresponding data, and the output result is the answer to the question, so that it can also judge whether the type of the question is correct. The details are shown in the following Table 2.

In the process of evaluation, it is also necessary to judge whether the syntax of the question sentence is correct.

The fourth part of the assessment is the clarity of the question statement. The details are shown in the following Table 3.

Table 1: QGSTEC2010 one of the evaluation standards: whether the question is related.

1	The generation question is completely related
2	The generation problem is basically related
3	The generation problem is basically irrelevant
4	The generation problem is completely irrelevant

Table 2: One of QGSTEC2010 evaluation standards: is the question type correct?

Sort	Description
1	The generated problem is of a given type
2	The generation problem is not a given type

In order to improve the efficiency of emergency information management, this paper analyzes various fused emergency information management scheme models on the basis of relevant problems existing in the current construction of emergency management system. Based on the research on the development of artificial intelligence algorithm, this paper refers to the main achievements of emergency information management research. Finally, a QG algorithm based on more model fusion is developed. The specific flow of the algorithm is shown in Figure 1.

In the process of designing the model, this article mainly uses the problem clustering algorithm, which can select the common problems needed to build the model from many problems. The specific calculation formula is as follows:

$$\mathrm{Im}pts(q_t^m) = \sum_{q_k \in q_c} \delta(q_t^m, q_k) \cdot \left|q_t^m\right|. \tag{7}$$

The calculation formula for the elements of the model input layer is as follows:

$$Att_{i,j} = \cos ine\left(v_i^s, v_j^{q_p}\right). \tag{8}$$

In the above formula,

$$\begin{aligned} v_k^s &= \max_{1 < l < \left|q_p\right|} \left\{Att_{k,l}\right\}, \\ v_k^{q_p} &= \max_{1 < l < |s|} \left\{Att_{l,k}\right\}. \end{aligned} \tag{9}$$

Next, the attention distribution needs to be generated on each attention vector. The specific calculation formula is as follows:

$$\begin{aligned} D_k^s &= \frac{e^{v_k^s}}{\sum_{l=1}^{|s|} e^{v_l^s}}, \\ D_k^{s_y} &= \frac{e^{v_k^{q_p}}}{\sum_{l=1}^{\left|q_p\right|} e^{v_l^{q_p}}}. \end{aligned} \tag{10}$$

After the convolution layer and pooling layer are processed in sequence, the data will be classified and packaged and transferred to the output layer. This is the expression form of the vector that requires the activation function to be calculated. The calculation formula is as follows:

Table 3: One of QGSTEC2010 evaluation standards: is the problem clear?

Sort	Description	For example
1	More information is needed to clarify the meaning of the problem	Who was nominated in 1997?
2	When there is no context, the answer is ambiguous	Who was nominated?

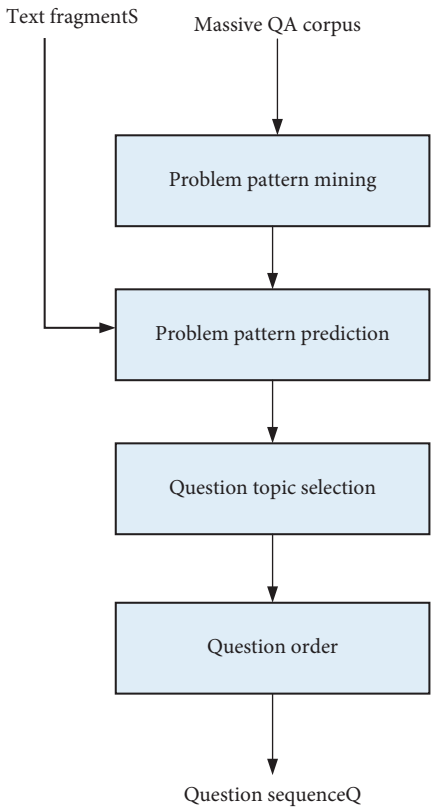

Figure 1: QG model framework based on problem model prediction.

$$y(s) = \tanh\left(W_s \cdot l_p^s\right). \tag{11}$$

During the operation of the convolutional layer, the composition of the data is mainly obtained by convolution calculation on the feature map and convolution kernel output by the previous layer, and the convolution kernel can be obtained through system learning. In the calculation process, different convolution kernels will produce different feature maps. The specific calculation formula is as follows:

$$L = \max\{0, M - \cos ine(y(s). \tag{12}$$

The encoder will read the fragments of the input layer, and the decoder will predict the output word sequence based on the read results. The specific calculation company is as follows:

$$q_p = \left(q_{p1}, q_{p2}, \ldots, q_{p|q_p|}\right). \tag{13}$$

In the following calculations, professional analysis tools are used to extract the candidate results of the question. If the candidate results can be extracted, the formula can be used to determine the degree of matching between the answer and the question. The specific formula is as follows:

$$s\left(q_t, q_p\right) = \frac{1}{N} \cdot \sum_k \#\left(q_p^{t_k}\right) \cdot dist\left(v_{q_i}, v_{q_p^{lk}}\right). \tag{14}$$

If the placeholder in the formula below represents the word in the question, then this article can choose the word in the formula as the topic of the question. The specific conditions that the formula meets are as follows:

$$w_j = \arg\max_{w_j \in S} \alpha_{ij} = \arg\max_{w_j \in S} \frac{\exp\left(e_{ij}\right)}{\sum_{k=1}^{|S|} \exp\left(e_{ik}\right)}. \tag{15}$$

The features required in the above formula can be combined using a linear model. The specific formula is as follows:

$$p(q|s) = \sum \lambda_i \cdot h_i\left(q, s, q_p, q_t\right). \tag{16}$$

3.2. Artificial Intelligence Algorithm. The convolutional nerve is composed of a convolutional layer and a pooling layer. The two layers will alternately appear in the system as the operating cycle of the system changes. After many iterations, the system will change the pixel size of the last layer of pooling layer. It is expressed in the form of a vector, and the result is transmitted to the artificial neural network, so that the final result can be obtained. The operation process of the convolutional layer in the convolutional neural network is mainly to borrow a filter that can be used for data training to process the convolution input image and add a bias cylinder, so that the convolutional layer can be obtained. The operating process of the pooling layer is to calculate the maximum or average value of a part of pixels at intervals of a certain distance and use the calculated values to draw a feature map. Both the convolution process and the pooling process can use the activation function to activate the relevant calculation process according to the speed of the network convergence when running, so that people can extract complete image information. The specific structure of the network is shown in Figure 2.

Stacked sparse self-encoding neural network consists of two parts. The main function of the autoencoder is to extract the features contained in the image. The encoder of the neural network is composed of many sparse encoders, which can improve the accuracy of feature extraction sex. In addition, the Softmax classifier is also an important part of the neural network. The classifier can classify the extracted image features and improve the work efficiency of people analyzing image features.

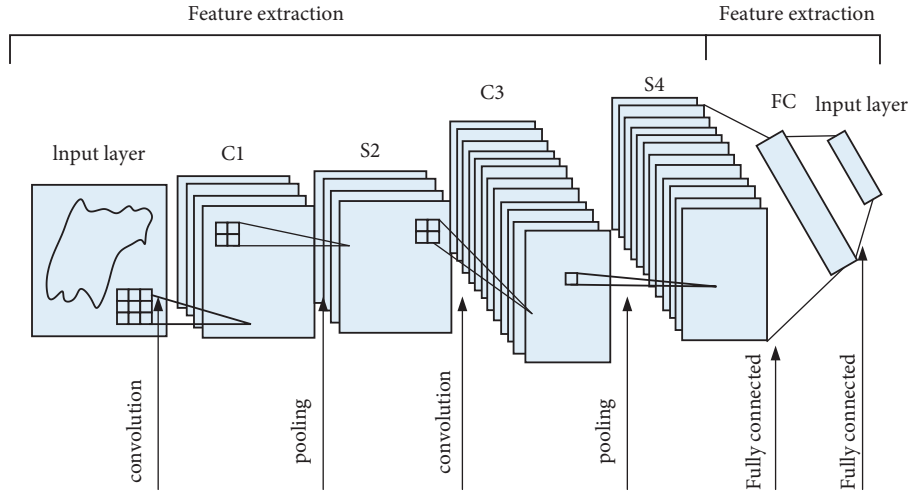

Figure 2: CNN network structure diagram.

3.2.1. Stacked Sparse Autoencoder. The autoencoder can use unsupervised learning for grid training, encode the data input to the system, restructure the data structure, and reduce the error of the restructured data, so that the characteristics of the input data in the hidden layer and the detailed structure can be obtained, as shown in Figure 3.

The hidden layer extracted by the self-encoder cannot express the data of the input layer very well. Therefore, Shausen and other related personnel have proposed a theory of sparse coding. Through the research and analysis of the brain's unsupervised learning process, they learned that the human body uses the neurons in the human body to learn external things. In fact, most of the application elements are not in the working state, some are not involved in the work, and only a small part of the neurons are activated after being stimulated, which means that the response of the neurons is incomplete. Because of this, the human brain has a better effect on learning all kinds of data information. This ability is also suitable for the autoencoders we mentioned above. With incomplete restrictions, the sparse encoder can be used for features. The sparse expression plays a good role in learning, so that the relevant information we extract is easy to distinguish. The limitation of incompleteness means that when the value of the output function of the neuron is close to 1 without limitation, the output is activated. When infinitely close to 0, the output is inhibited. In many cases, where the output is inhibited, it can be called as sparsity limitation. The specific calculation formula is as follows:

$$\widehat{\rho}_j = \frac{1}{m}\sum_{i=1}^{m}\left[a_j\left(x^i\right)\right]. \tag{17}$$

During the operation of the network, the output of neurons will be suppressed, so the sparse activation parameters need to be used to improve the output performance of neurons, which can be expressed as

$$KL\left(\rho\|\widehat{\rho}_j\right) = \rho\log\frac{\rho}{\widehat{\rho}_j} + (1-\rho)\log\frac{1-\rho}{1-\widehat{\rho}_j}. \tag{18}$$

The loss function can be used to measure how the model processes the data. The specific formula is as follows:

$$J(W,b) = \frac{1}{m}\sum_{i=1}^{m}\frac{1}{2}\left\|h_{W,b}\left(x^i\right) - x^i\right\|^2. \tag{19}$$

After adding the penalty factor to the model, the loss function of the encoder can be expressed as

$$J_{sparse}(W,b) = J(W,b) + \beta\sum_{j=1}^{s}KL\left(\rho\|\widehat{\rho}_j\right). \tag{20}$$

In shallow networks, sparse autoencoders can extract features that have large differences. Combining multiple sparse autoencoders to form a large encoder can improve the learning effect of deep networks. In the process of model operation, the structure of the encoder is more complicated, and the gradient disappears, which is not conducive to the training of the data, so it is necessary to adopt an unsupervised layer-by-layer greedy training method, so that the structure of the network can be optimized, thereby improving the model. The performance of the encoder is shown in Figure 4.

3.2.2. Softmax Classifier. The Softmax classifier can classify the extracted image features and improve people's work efficiency in analyzing image features. When classifying, you need to use the hypothesis function to determine the characteristics of the problem. The specific formula is as follows:

$$h_\theta[x(i)] = \begin{bmatrix} p(y(i)) = 1 \mid x(i);\theta) \\ p(y(i)) = 2 \mid x(i);\theta) \\ \vdots \\ p(y(i)) = k \mid x(i);\theta) \end{bmatrix}. \tag{21}$$

The loss function of the classifier can be determined using the maximum entropy model, which can be expressed as

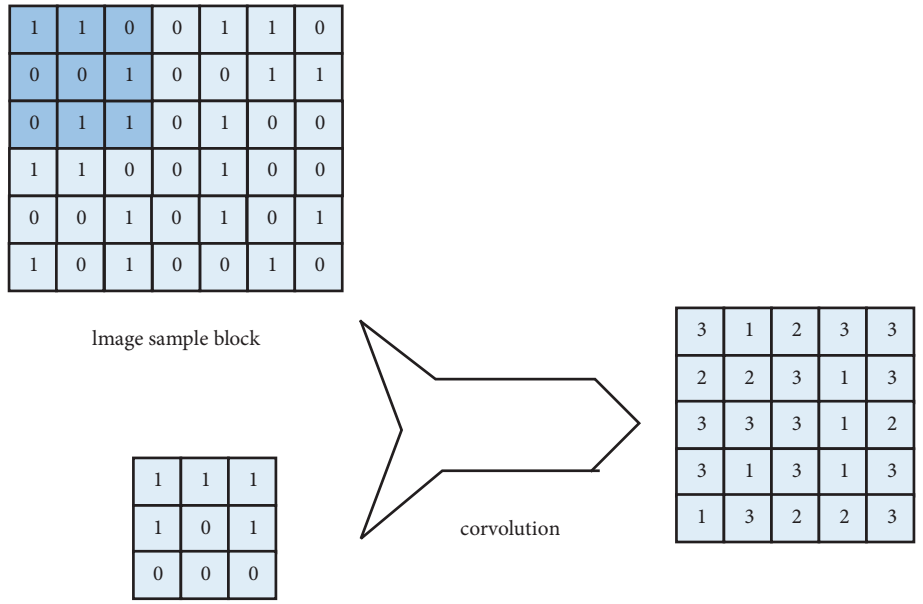

Figure 3: Autoencoder structure.

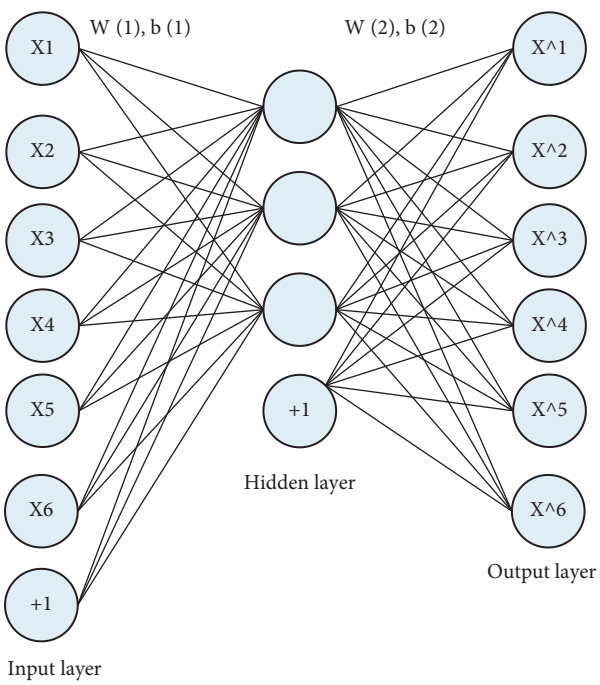

Figure 4: Stacked sparse autoencoder structure.

$$J(\theta) = -\frac{1}{m}\left[\sum_{i=1}^{m}\sum_{j=1}^{k} 1\left\{y(i) = j\log\frac{e^{\theta_j^T x(i)}}{\sum_{i=1}^{k} e^{\theta_i^T x(i)}}\right\}\right]. \quad (22)$$

In the process of data training, if the fit between the data is poor, the parameter value of the penalty function will be too large, so weights need to be used to reduce the attenuation term. At this time, the loss function can become as follows:

$$J(\theta) = -\frac{1}{m}\left[\sum_{i=1}^{m}\sum_{j=1}^{k} 1\left\{y(i) = j\log\frac{e^{\theta_j^T x(i)}}{\sum_{i=1}^{k} e^{\theta_i^T x(i)}}\right\}\right] + \frac{\lambda}{2}\sum_{i=1}^{k}\sum_{j=0}^{n}\theta_{ij}^2. \quad (23)$$

4. Research on Emergency Information Communication Structure

4.1. Analysis of the Status Quo of Emergency Information Communication Channels. The main objects of government emergency information communication are mostly related departments responsible for public crisis emergency management tasks. Many crisis-related data are reserved. They are important departments for the transmission and transmission of relevant emergency information. In China, the communication and exchange of this type of information generally include the following types of institutions and related personnel:

(1) In China, the highest administrative leading agency for emergency management of public crises that occur suddenly is the State Council. As the highest authority, it is also the leading agency. Many affairs are discussed by its Standing Committee and presided over the work. When necessary, the relevant working groups will also be designated to guide the relevant work behaviors of other relevant agencies.

(2) Main work departments. They are mainly responsible for synthesizing the relevant regulations of the government during the emergency period and then carrying out relevant coordination work. The relevant agencies responsible for these affairs are mainly the emergency offices under the State Council Office,

which is an important organization that can link related affairs together.

(3) Subordinate offices. Most of these institutions are responsible for dealing with relevant emergency affairs, but when dealing with these affairs, they need to carry out reasonable analysis and processing of relevant types of affairs in accordance with relevant legal regulations and their own rights. Similarly, the drafting and implementation of relevant measures are also included, and the relevant matters decided by the Party Central Committee of the State Council are implemented and carried out to the end.

(4) Local institutions. This part of the agency is the secondary management agency responsible for handling the emergency management of public crises that occur suddenly. They are lower than the related agencies mentioned above and are mainly responsible for handling the relevant areas within their jurisdiction.

(5) Specially dispatched expert groups and technical teams. Relevant responsible agencies generally will vigorously recruit relevant talents to form what we call the government's advisory team and will also invite and dispatch relevant experts to join relevant organizations when relevant work is needed. This is what the government faces. Put forward some valuable opinions on related issues. The government very much hopes and welcomes these professionals to actively participate in related work. In fact, when dealing with related practical issues, communication is essential, and information is needed at any time. In addition to the related institutions we have introduced above, there are many other exchanges that can be regarded as the whole of emergency information communication. These include many small temporary emergency command agencies, relevant departments such as the information early warning center, as well as some related personnel such as commanders, information officers, leaders of small teams, and related organizations, as well as some organizations with a wider range of handling such as the public and relevant media. In a state of public crisis, everyone may unwittingly become the main body of information communication. Every word spoken is a message. It may become people's concern and cause very serious consequences to other personnel. It is precisely because the scope of the subject is very wide that it should be more recognized and valued for the importance of information exchange.

The determination of the government's emergency information communication process determines the government's ability and efficiency to handle public crisis events. When a public crisis event occurs, the government should reasonably arrange the order of information transmission according to the needs of the work. In the process of the Chinese government's handling of crisis events, the information communication process follows certain institutional requirements. The specific process can be divided into three steps. The details are as follows:

(1) After a crisis event occurs, government departments need to report the information collected in the previous period. Once each department discovers a crisis event, it needs to report specific information to the relevant management department within four hours. In the process of handling the incident, each part also needs to report the progress of the processing in time.

(2) Government departments should make preliminary responses according to the severity of crisis events. If some crisis events have a large and severe impact, each department should use their powers to initiate emergency plans and then discuss specific solutions.

(3) Publicize the detailed information of the crisis event to the public, and determine the accuracy of the information before the information is released to avoid the public misunderstanding of the information. Although government departments are required to publish relevant information in a timely manner, in actual life, the government has some omissions in this aspect of work. After a crisis occurs, government departments should not only make preparations for crisis management but also verify the reliability of information through the differences and correlations of various release channels on the basis of verifying the reliable source of information, so as to ensure the authenticity of the source and content of information to the greatest extent. The specific process of government emergency information communication is shown in Figure 5.

4.2. Basic Model Analysis of Emergency Information Communication Channels. When constructing an information communication channel model, it is necessary to synthesize and analyze the communication channels of all information in public crisis events in various fields of society. The information communication channel is the sum of these communication channels. Government departments need to rely on information communication channels to mobilize the masses in society to cope with crisis events. This requires the government to understand the psychology and needs of the public, so as to promote the distribution and use of human resources and government funds. In the process of information transmission, multiple communication channels can improve the efficiency of information use. If information transmission and communication are not timely, it will be difficult for government departments to deal with crisis events in a short time, which is not good for the normal operation of society. From all perspectives of social development, Chinese researchers have conducted effective research on the expansion of government emergency information communication channels.

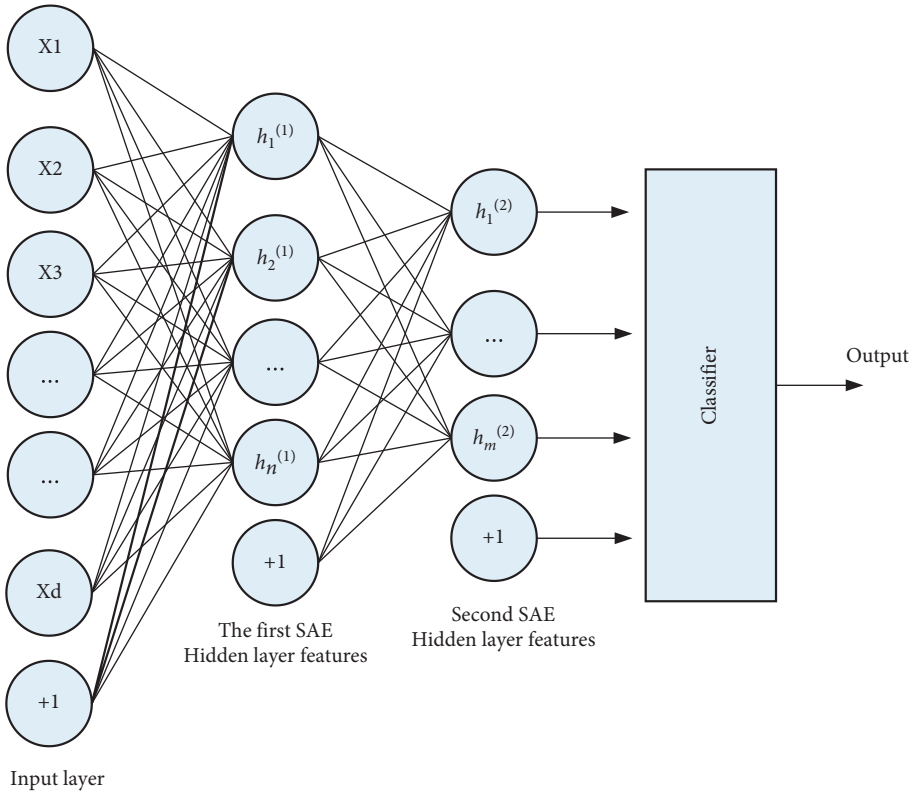

Figure 5: Routine general government emergency information communication process.

4.2.1. Triangular Interactive Communication Model. This model is one of the most used models for the early handling of crisis events. This model can establish connections between government departments, the public, and the media and promote the exchange and dissemination of information among various local subjects. The social public part of the model mainly refers to the social groups that are affected when a public crisis event occurs. The government department should promptly inform this group of the progress of the crisis in the process of handling the crisis event. In addition, civil servants are a part of the groups affected by crisis events who shoulder more social responsibilities. This part of personnel should consciously fulfill their responsibility for social development.

4.2.2. Regular Government Information Communication Model. The model is mainly aimed at the public and various government departments. The model designs different connections for each communication subject. Each subject can realize horizontal, vertical, and diagonal communication. Different communication methods can be connected through chains. The establishment of this model fully takes into account the government's need to deal with crisis events, and the established contacts can allow the government to communicate and exchange information with the outside world in a timely manner. In the process of government work, communication between various departments is indispensable, and government agencies and the outside public are also indispensable. Although the model has established multiple communication channels between the government and the public, the model has not tested specific performance in the actual scenarios of crisis events, which is likely to cause errors in fieldwork.

4.3. Model Construction of Grid Emergency Information Communication Channels. In the process of establishing grid-based information communication channels, a separate organization should be established to manage grid-based information communication channels. This organization should be composed of systematic organizational departments. Although it is a department under government management, the daily work of the organization is independent. In the process of forming the system, the supervisory center will match the supervisors according to the grid units that have been divided, so that the supervisory efficiency of the relevant areas can be guaranteed, and the supervisory axis can be formed in this way. The command center and various work departments will deal with the information of the crisis together, thus forming the axis of execution. In the grid-based communication channel, the district-level platform has two command centers, which can refine the crisis events in the city. When managing urban objects, things in the city can be materialized, and urban public facilities, road traffic, environmental protection work, emergency resource allocation, and various other types of urban things can be uniformly managed at the same time.

In the work process of the government, each divided area should carry out corresponding activities according to the

requirements of the work, and the supervision and implementation of each part should cooperate with each other. When the command center and the control center release and inspect the work of each department, they should let the monitoring axis cooperate with the specific work of the axis. The two centers should always issue reasonable tasks to each area and supervise each area to perform tasks. Through specific practice, we can know that all parts of the system are connected to a certain degree, which can ensure that there will be no omissions in the process of information communication, and each part of the system can check the content of the information. Once a crisis event occurs, each part information will be released to the center of the system, so that the efficiency of government departments in handling crisis events can be improved.

5. Conclusion

In the development of recent years, many countries and regions in the world often have various types of public crises, which have severely affected people's daily life, lives, and property. Through long-term research and analysis, it can be known that the emergency management mechanism currently established in China has certain shortcomings. The communication problem of emergency information is likely to cause the emergency work to not proceed smoothly. In addition, problems in the communication channels of emergency information are likely to cause problems in the cooperation of various departments when people carry out emergency management work, and the efficiency of the government in dealing with problems will also be reduced in real scenarios. In the process of analyzing related issues, this article elaborates on the concept of information communication channels, the concept of emergency management, the principles of information communication, and the characteristics of information sharing. The article believes that the knowledge and technology can provide a good help for the communication and sharing of information. When dealing with emergencies, problems in the communication channels of emergency information are likely to lead to problems in the cooperation of various departments when people carry out emergency management work. In reality, the efficiency of the government in handling problems will also be reduced. In actual scenarios, the transmission and sharing of information is an important way to determine whether public crisis events can be resolved quickly. Government departments must not only use professional measures to increase the speed of information transmission but also establish a crisis event alert system based on the characteristics of the information. This ensures that the crisis management department can grasp the detailed incident information in a timely manner, and ensure that the public can understand the specific situation of incident handling. This article also analyzes the problems that Chinese government departments have in the process of handling public crises and provides a reasonable plan for information communication and sharing between various departments and subjects. In the future development process, an emergency information management system based on multimodel fusion and artificial intelligence algorithms will provide more convenience to the work of government departments.

Data Availability

The data used to support the findings of this study are available from the corresponding author upon request.

Conflicts of Interest

The author(s) declare that they have no conflicts of interest.

Acknowledgments

This research has been financed by the East China University of Political Science and Law Research Project in 2018: The Mechanism of Communication Barriers in Emergency Organizations (18HZK015).

References

[1] J. Kim, J. Bae, and M. Hastak, "Emergency information diffusion on online social media during storm Cindy in U.S," *International Journal of Information Management*, vol. 40, pp. 153–165, 2018.

[2] S. Garg, J. Aryal, H. Wang, T. Shah, G. Kecskemeti, and R. Ranjan, "Cloud computing based bushfire prediction for cyber-physical emergency applications," *Future Generation Computer Systems*, vol. 79, pp. 354–363, 2018.

[3] J. Blackburn, K. Ousey, and E. Goodwin, "Information and communication in the emergency department," *International emergency nursing*, vol. 42, pp. 30–35, 2019.

[4] B. Kang and H. Choo, "A deep-learning-based emergency alert system," *ICT express*, vol. 2, no. 2, pp. 67–70, 2016.

[5] P. Blasco, D. Gunduz, and M. Dohler, "A learning theoretic approach to energy harvesting communication system optimization," *IEEE Transactions on Wireless Communications*, vol. 12, no. 4, pp. 1872–1882, 2013.

[6] Z. Liu, E. Blasch, Z. Xue, and W. ZhaoLaganiereWu, "Objective assessment of multiresolution image fusion algorithms for context enhancement in night vision: a comparative study," *IEEE Transactions on Pattern Analysis and Machine Intelligence*, vol. 34, no. 1, pp. 94–109, 2012.

[7] R. B. Vallee, R. J. McKenney, and K. M. Ori-McKenney, "Multiple modes of cytoplasmic dynein regulation," *Nature Cell Biology*, vol. 14, no. 3, pp. 224–230, 2012.

[8] A. Boin, "Organising for effective emergency management: lessons from Research1," *Australian Journal of Public Administration*, vol. 69, no. 4, pp. 357–371, 2010.

[9] Y. Cao, Q. Li, J. Chen, and L. GuoMiaoYangChenLiLi, "Hospital emergency management plan during the COVID-19 e," *Academic Emergency Medicine*, vol. 27, no. 4, pp. 309–311, 2020.

[10] Z. Zhou, X. Bai, Z. H. Li, X. Jing, Z.-J. Li, and H.-L. Li, "Novel fault diagnosis approach of smart transmission grid based on knowledge grid technology," *Proceedings of the CSEE*, vol. 30, no. 4, pp. 8–15, 2010.

[11] F. Tao, L. Zhang, and A. Y. C. Nee, "A review of the application of grid technology in manufacturing," *International Journal of Production Research*, vol. 49, no. 13, pp. 4119–4155, 2011.

[12] H. Liang, A. K. Tamang, W. Zhuang, and X. S. Shen, "Stochastic information management in smart grid," *IEEE Communications Surveys & Tutorials*, vol. 16, no. 3, pp. 1746–1770, 2014.

[13] Y. Chu, "Construction of student personal information management system relying on computer," *Journal of Physics: Conference Series*, vol. 1915, no. 4, Article ID 042080, 2021.

[14] G. F. Gui-Fang Shao, F. Fan Yang, and Q. Qian Zhang, "Using the maximum between-class variance for automatic gridding of cDNA microarray images," *IEEE/ACM Transactions on Computational Biology and Bioinformatics*, vol. 10, no. 1, pp. 181–192, 2013.

[15] C. Chang and C. D. Sarris, "A spatially filtered finite-difference time-domain scheme with controllable stability beyond the CFL limit: theory and applications," *IEEE Transactions on Microwave Theory and Techniques*, vol. 61, no. 1, pp. 351–359, 2013.

[16] S. Hiller, "The impact of information technology and online library resources on research, teaching and library use at the University of Washington," *Performance Measurement and Metrics*, vol. 3, no. 3, pp. 134–139, 2002.

[17] G. A. M. Meiring and H. C. Myburgh, "A review of intelligent driving style analysis systems and related artificial intelligence algorithms," *Sensors*, vol. 15, no. 12, pp. 30653–30682, 2015.

[18] D. W. Kim, H. Y. Jang, K. W. Kim, and S. H. ShinPark, "Design characteristics of studies reporting the performance of artificial intelligence algorithms for diagnostic analysis of medical images: results from recently published papers," *Korean Journal of Radiology*, vol. 20, no. 3, pp. 405–410, 2019.

[19] M. A. Talib, S. Majzoub, Q. Nasir, and D. Jamal, "A systematic literature review on hardware implementation of artificial intelligence algorithms," *The Journal of Supercomputing*, vol. 77, no. 2, pp. 1897–1938, 2021.

Hindawi
Computational Intelligence and Neuroscience
Volume 2022, Article ID 7238789, 10 pages
https://doi.org/10.1155/2022/7238789

Research Article

Prediction Model and Data Simulation of Sports Performance Based on the Artificial Intelligence Algorithm

Guang Lu

School of Sports and Physical Education, Shandong Sport University, Rizhao 276826, Shandong, China

Correspondence should be addressed to Guang Lu; luguang@sdpei.edu.cn

Received 19 July 2022; Revised 21 September 2022; Accepted 26 September 2022; Published 7 October 2022

Academic Editor: Gopal Chaudhary

There is still a certain deviation between the current artificial intelligence technology and the traditional learning mode, which makes it unable to be effectively applied in teaching and learning. Therefore, an effective method needs to be proposed to use functions to predict data. Function calculation can not only solve the complex problems of data calculation process but also make the data evenly distributed to take full advantage of the capabilities of each system. In this experiment, we mainly use the control function. After substituting the data into the control function, the function will automatically classify the data. In this paper, according to the actual situation of physical education in colleges and universities, from the two aspects of artificial intelligence and comprehensive learning algorithm, to build a system which can collect and analyze the past achievements of college students' physical education performance simulation can effectively help the design of physical education curriculum. According to the distribution of experimental data, a specific conclusion can be drawn; that is, the test model we choose can calculate and measure the physical fitness level of students, but there are big differences. In contrast, our experimental method using the ensemble computing model can not only predict and analyze the physical fitness level of college students but also reduce errors and shorten the time required for the experiment.

1. Introduction

The integrated-learning model refers to combining multiple systems so that they can serve the learning mechanism together. By combining the advantages of many learning systems, a more optimized learning method can be obtained so that the model can promote the development of students [1]. In terms of analyzing data, the new model is significantly better than the previous model. This report is based on the integration model and proposes a relatively novel classification method in the ADA system. The specific experimental steps are as follows: The first step is to extract samples. We first select n items related to the integrated system in the database. Then substitute the data into the FAD system to start the functions in each system [2]. The second step uses the classification mechanism in different systems to divide the selected data into several categories and save them in the hardware. This can avoid the information interference that is encountered during transmission, resulting in data loss, but in this way, the calculation steps of the computer will increase, and the calculation difficulty of the system will increase. Finally, we substitute the data divided into several categories into the ADA system to get more detailed results after the division [3]. Through specific experiments, we can know that the integrated model has many advantages and can improve the shortcomings of the previous model so that the student's sports performance data can be more accurate and more practical suggestions can be obtained. People's material level is getting higher and higher, which makes people's demand for the quality of life also increasing, but with the emergence of smart devices such as mobile phones, people often spend a lot of time on entertainment ignoring the development of their own physical health. Nowadays, few people take physical exercises. We focus on the physical activities of college students. Through the collection and analysis of college students' physical education courses, which enable students to enjoy physical activities, we understand that physical test results are also an important

resource for studying the development of students' physical fitness [4].

To make the experiment successful, you need to focus on the problem of aggregation. The aggregation mode is different from the data collection and classification mode [5]. It integrates the data with the same characteristics, and then the characteristics of the data are significantly different. This process is automated and does not require the supervision and assistance of any equipment. The final classification result is composed of many connected sets. When we analyze the collection data, because each category does not have its own fixed name, we need to code according to the characteristics of the collection and then arrange them in order. When encoding, we can use the MAC system, which is the fastest and most concise algorithm [6]. This report focuses on the application of artificial intelligence in integrated algorithm systems. The physical performance of college students will be different due to different ages, genders, and physical conditions. They are unstable, but the types of differences are more stable and typical. Therefore, we combine theory with neuroscience to design a collection of students, which is a new way of testing performance in sports. The first step is to design a new model that is generally suitable for the analysis of college students' sports performance, then fix the initial data and the maximum calculated value in the model to minimize the error, and finally analyze the experimental results based on the calculated data.

2. Related Works

Literature believes that we should focus on the design of the new model [7]. Only when the model is designed accurately can the final sports test results be accurate. Therefore, researchers have put forward many questions about the completeness and accuracy of the experiment. There are many ways to answer the questions. One of the methods is a diversified experimental model, but because the model is greatly affected by function calculations, the data output is relatively unstable, so it is impossible to accurately predict sports performance. Literature proposes a method for predicting the physical fitness of students through a neural network scientific system [8]. This method is not affected by the function model and can be well combined with linear systems. However, the system is only partially effective in the category but not strong in analyzing the overall results. Literature proposes to predict students' sports performance through a linear network system, which can improve the predictive ability of some functions, but linear network systems are often affected by signals and have high environmental requirements, so there are also shortcomings [9]. The conclusion of the literature is that when we use this model for data analysis room, we need to combine these functions and then perform data calculations, so as to avoid the problems of traditional models and make the effect of processing data more obvious [10]. Literature believes that if we only analyze from the overall point of view, data deviation is easy to occur, so the data classification obtained has problems, and the system can easily delete positive data as irrelevant data if the test result is wrong [11]. Literature found that today's model establishment can already deal with the above-mentioned problems, and the performance of the system is relatively good, mainly to solve the problems of inaccurate data classification and unbalanced time distribution [12]. However, for more complex situations, it is necessary to change the overall experimental method. While updating the system, the selection of hardware equipment must also be changed to a certain extent. This method should be the most optimized method at present. Literature compares the traditional experimental model with the newly designed experimental model and improves the shortcomings of the traditional experimental model so that the data can be distributed in various systems in a more balanced manner [13]. The optimized new experimental model has a high use value and experimental value. Literature believes that in order to make the experiment more complete, it is necessary to divide the entire system into different parts first and then perform a final analysis according to the classification results so that not only can the functions of each system be fully utilized but also deleting duplicate data has made us a major improvement in the balanced distribution of data [14].

3. Integrate the Learning Algorithm and Artificial Intelligence Algorithm Prediction Model Establishment

3.1. Integrated Learning Algorithm. Nowadays, people have introduced artificial intelligence technology in many fields, which allows people to use new methods to learn and make learning more profound. This is also an important area of research by many scholars. Function calculations can not only solve the complex problems of data calculation process but also make data evenly distributed and make full use of the functions of each system. In this experiment, we mainly use the control function. After substituting the data into the control function, the function will automatically classify the data. We can know that if the result of the data output is closer to the result we initially predicted, it means that the experimental model is relatively successful. After getting improved, it can be applied to specific experiments, and the system consumes less energy. However, if the data we get is far from the data predicted at the beginning, it means that some functions of this mode have problems. It is difficult for us to classify and analyze the input data through this mode. Therefore, we cannot use this mode for experiments. When we process image information, we can know that different images have different resolutions and sizes. If we do not process the original image and convert the image into data, the system will recognize that there is a great difficulty because the memory occupied by the image is much larger than the number, so the system can only calculate from the overall angle when identifying, and there is no way to analyze it in detail, and some images will still be unrecognizable. The loss function mainly solves the situation that the amount of data is too large and the data are more complex, so the loss function has more advantages than the control function in calculation, and the loss function can also

Table 1: Experimental data set description.

Numbering	Data set	Total number of samples	Number of attributes	Less effective	Multi-like wood	Imbalance rate
1	Ionosphere	351	34	126	225	1.78
2	Letter	20000	16	789	19211	24.35
3	Abln	731	8	42	689	16.40
4	Haber survival	306	3	81	225	2.78
5	Yst	471	8	18	429	10.21
6	Specific heart	157	44	15	142	9.47
7	Wnr	186	13	48	138	2.87
8	Gls	182	9	38	144	3.79
9	Eli	336	7	20	316	15.80
10	Breast	699	9	241	458	1.90

solve the problem of the image occupying too much memory, making the data classification more detailed At the same time, we can also add a new loss function as an aid, which can speed up the experiment. The specific function formula is as follows:

$$CE(p_i) = -\alpha_t \log(p_i). \tag{1}$$

Although the method of cross calculation can temporarily calculate the general results of the data, it ignores many small but very critical issues. In the calculation process, the cross calculation is easy to be confused by the data with decimal points, and data errors occur. There is no way to introduce this kind of calculation method with large error into the experiment. Therefore, in order to make the cross calculation method more accurate, we upgrade the system to make the function calculation dominant. The cross calculation is in the function formula based on the data analysis, and we also introduce new factors so that the two complement each other and can better solve the computational problems. The specific principles are as follows:

$$\begin{aligned} FL(p_i) &= -(1-p_i)^{\gamma} \log(p_i), \\ FL(p_i) &= -\alpha(1-p_i)^{\gamma} \log(p_i). \end{aligned} \tag{2}$$

In the process of function calculation, the greater the influence of the initial data on the cross calculation, the greater the error index. On the contrary, the smaller the influence of the initial data on the cross calculation, the smaller the error index, which means the higher the accuracy.

In order to make the data classification of the experiment more reasonable, we conducted data sample experiments on different types of data sets. We analyzed the characteristics of the data with less data in the set and then added the data to those with similar characteristics according to the characteristics. In the collection, this can reduce the amount of data calculation and the type of analysis. At the same time, we have to upgrade the system so that the new system can adapt to the new classification set, then draw conclusions through calculations, and then compare the latest conclusions with the most original data. From the results, we can know that when the classification group decreases, the accuracy of sample analysis increases, and the difficulties encountered in the experiment process are relatively reduced. The latest sample analysis formula is as follows:

$$D_{i+1}(x) = \frac{D_i(x) e^{-\alpha_i f(x) h_i(z)}}{Z_i}. \tag{3}$$

We combine the function calculation and the updated system to get a simpler calculation method as follows:

$$D_{i+1}(x) = \frac{D_i(x) e^{-\alpha_i f(x) h_i(z) f\left(1-p_i\right)^2}}{Z_i}. \tag{4}$$

The next step is to design a specific experimental step. We selected a number of experimental sets as the initial data and import these data into the UCI system for calculation. The purpose of this experimental step is to verify the experimental data and obtain more accurate results. The following specifically explains the main characteristics of each data set after the calculation is completed under the UCI system, such as the size, quantity, and name of the data. Experimental data set description is as shown in Table 1.

Through the specific analysis of the characteristics in the table, we can know that the characteristics of each data set are different, and the gap between the data sets is large, and the feedback information is also different, but the characteristics in each data set are representative. There is no duplication, and different problems in different situations are analyzed. Next, we analyzed the two columns of data specifically, namely the collection with less data and the collection with more data. We can clearly see that the collection with less data has more detailed features and is easier to process but the data are more. The features obtained from multiple sets are more general , which is more troublesome to deal with, and further analysis is needed. The unbalance rate of experimental data are as shown in Figure 1.

This article used several methods to analyze the experimental results. We used the ADA system to further verify the experimental results and then compare the latest results with the previous results to find out the rules and conclusions. In the ADA system, we did not focus on the average distribution of data but adopted more traditional calculation methods, combining experimental data with SMO calculation methods and analyzing each data set as a whole. Ignore the smaller data, and the data after the decimal point can be temporarily deleted to make the data more tidy. We can also use the RUS calculation method, which is to randomly combine the data, which will not only make the

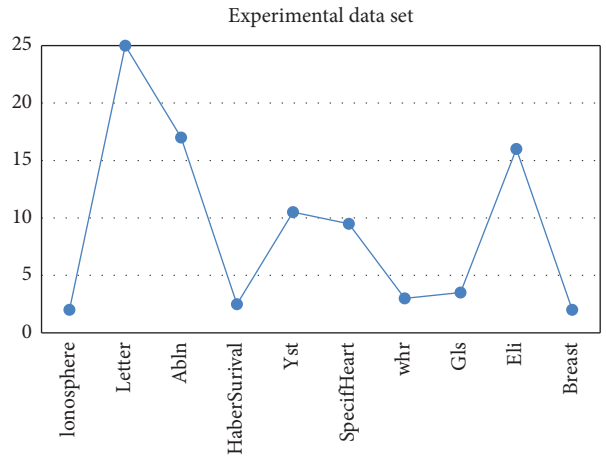

Figure 1: Unbalance rate of experimental data.

experimental data more extensive but also make the system functions better. The following table compares the centralized calculation methods. Comparison of accuracy values of the four algorithms is as shown in Table 2.

From the above table, we can know that the ADA calculation method has a higher accuracy rate and stands out in the analysis of several sets of data, and the error of the ADA calculation method is very small, and data errors or data loss are rarely seen. Therefore, in the experiment, our first recommended calculation method is the ADA calculation mode. At the same time, we have also introduced several other calculation methods to find out whether there is a better calculation mode through comparison. The specific analysis and comparison data are shown in the following table. Through a lot of analysis, we can know that the accuracy of the calculation method of RADA surpasses the ordinary ADA calculation method, becoming the best classification method for this experiment and has the highest accuracy. However, the SUI system did not combine the original data with the new conclusions in the calculation, so the accuracy of the experimental results of the system is the worst. Comparison of the recall value of the four algorithms is as shown in Table 3, Comparison of the four algorithms is as shown in Table 4.

According to the data shown in the above table, we can know that the main experimental methods are selected from the ADA calculation method, SMO calculation method, RUS calculation method, and RADA calculation method. The specific meaning value after calculation is given in the above table. Through the data, we can know that the RADA calculation method has the highest meaning value after several sets of experiments, so we can draw a more accurate conclusion: the function of the RADA system is the best, and the calculation method under this system is the simplest, and the accuracy of the experimental results is also the highest. On this basis, we analyzed the ADA calculation method, SMO calculation method, and RUS calculation method to know the ADA calculation. Although the practicability of the method is not as good as the RADA calculation method, the function is still relatively complete, and it can also be applied to the field of sports performance prediction after improvement. However, the performance of the SMO calculation method is relatively poor because the calculation method does not combine the original data with the new conclusions. Comparison of the average classification performance of the four algorithms is as shown in Table 5.

3.2. Establishment of a Sports Performance Prediction Model. If we want to solve some unexplainable and uncertain problems, we must use the gray forecasting model because the model can analyze smaller data based on big data, such as how to solve the number after the decimal point. In many cases, this technology has become the focus of scholars' research, and various functions are constantly being improved and gradually applied to various fields. The prediction model, as the name implies, is to predict the data. When we make data predictions, we must pay attention to not input the data into the model at one time but divide the data into different categories and then substitute them into the model, and note that the number of data in each group should not be too much; otherwise, the experimental results will be wrong. Using the gray prediction model can not only consolidate the experimental results of the above analysis but also reduce the fluctuation range of the experimental data results and determine the results to be within an easier-to-analyze range and then arrange the data according to different characteristics. The principle is as follows:

$$X^{(1)}(i) = \sum_{k=1}^{i} X^{(0)}(i). \tag{5}$$

According to the arrangement order, the formula can be obtained as follows:

$$\frac{dX^{(1)}}{dt} + aX^{(1)} = u. \tag{6}$$

The specific prediction model formula is

$$\widehat{X}^{(1)}(k+1) = \left[\widehat{X}^{(0)}(0) - \frac{u}{\widehat{a}}\right]e^{-\widehat{a}k} + \frac{\widehat{u}}{\widehat{a}}. \tag{7}$$

The GM (1, 1) model can predict nonlinear models with uncertainties in a small sample condition, which is in line with the problem of predicting college students' sports performance. However, the GM (1, 1) model has high prediction errors when there are abnormal data in the system, and it is difficult to meet the actual demand.

Neural network science refers to a science that combines specific scientific theories with the human nervous system. On this basis, we design a new model. Through the connections and interconnections between different neurons, we get specific function formula. The experimental process of this model is relatively simple, mainly including input system and output system. It can not only analyze and integrate the experimental data but also compare and predict the results of the data. Typical BP neural network is as shown in Figure 2.

The neural network algorithm system can be divided into two modes: forward transmission and reverse transmission. The specific steps are as follows: The first step is to pass the

Table 2: Comparison of accuracy values of the four algorithms.

Numbering	Data set	AdaBoost	SMO-boost	RUS-boost	R-AdaBoosi
1	Ionosphere	0.82	0.86	0.88	0.89
2	Letter	0.54	0.50	0.67	0.73
3	Abln	0.66	0.62	0.76	0.85
4	Haber survival	0.68	0.65	0.73	0.76
5	Yst	0.91	0.93	0.92	0.95
6	Specific heart	0.92	0.94	0.95	0.94
7	Wnr	0.74	0.7S	0.82	0.85
8	Gls	0.76	0.75	0.78	0.78
9	Eli	0.62	0.64	0.73	0.79
10	Breast	0.83	0.82	0.85	0.87

Table 3: Comparison of the recall value of the four algorithms.

Numbering	Data set	AdaBoost	SMO-boost	RUS-boost	R-AdaBoost
1	Ionosphere	0.81	0.80	0.81	0.87
2	Letter	0.60	0.62	0.69	0.70
3	Abln	0.65	0.64	0.69	0.72
4	Haber survival	0.62	0.61	0.65	0.69
5	Yst	0.77	0.82	0.85	0.89
6	Specific heart	0.63	0.65	0.72	0.71
7	Wnr	0.54	0.62	0.61	0.68
8	Gls	0.57	0.61	0.63	0.67
9	Eli	0.79	0–81	0.83	0.89
10	Breast	0.69	0.74	0.78	0.76

Table 4: Comparison of the four algorithms.

Numbering	Data set	Ada -boost	SMO-boost	RUS-boost	R-Adaboost
1	Ionosphere	0.85	0.84	0.87	0.91
2	Letter	0.66	0.64	0.75	0.74
3	Abln	0.62	0.61	0.71	0.75
4	Haber survival	0.85	0.93	0.88	0.94
5	Yst	0.94	0.96	0.93	0.96
6	Specific heart	0,75	0.79	0.83	0.87
7	Wnr	0.73	0.85	0.89	0.88
8	Gls	0.86	0.87	0.86	0.91
9	Eli	0.69	0.75	0.76	0.81
10	Breast	0.83	0.85	0.84	0.89

Table 5: Comparison of the average classification performance of the four algorithms.

	AdaBoost	SMO-boost	RUS-boost	R-AdaBoost
AvgPrccision	0.748	0.749	0.809	0.841
AvgRccall	0.667	0.692	0.726	0.758
AvgG-mean	0.778	0.809	0.832	0.866

data into the system through the input system for analysis, then pass the screening layer to the more disturbing data Delete, then connect neurons with the same characteristics, then use the output system to output the conclusions of these connected neurons, and then analyze and compare the new experimental results with the initially predicted experimental results. This experimental method is forward transmission; on the contrary, if we first transfer data from the output system and then get the latest result through the input system, this method is the reverse transmission mode. The specific output formula is as follows:

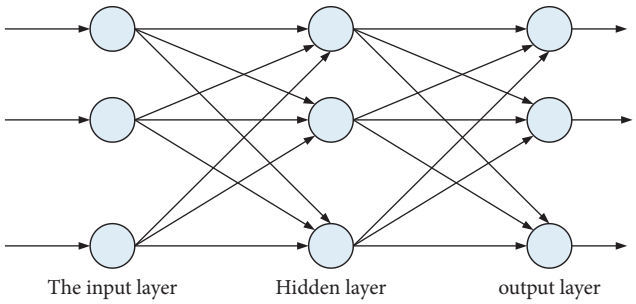

Figure 2: Typical BP neural network.

$$y_i = \phi_n\left(\sum_{k=1}^{r} w_{ik}x_k + \theta_i\right). \tag{8}$$

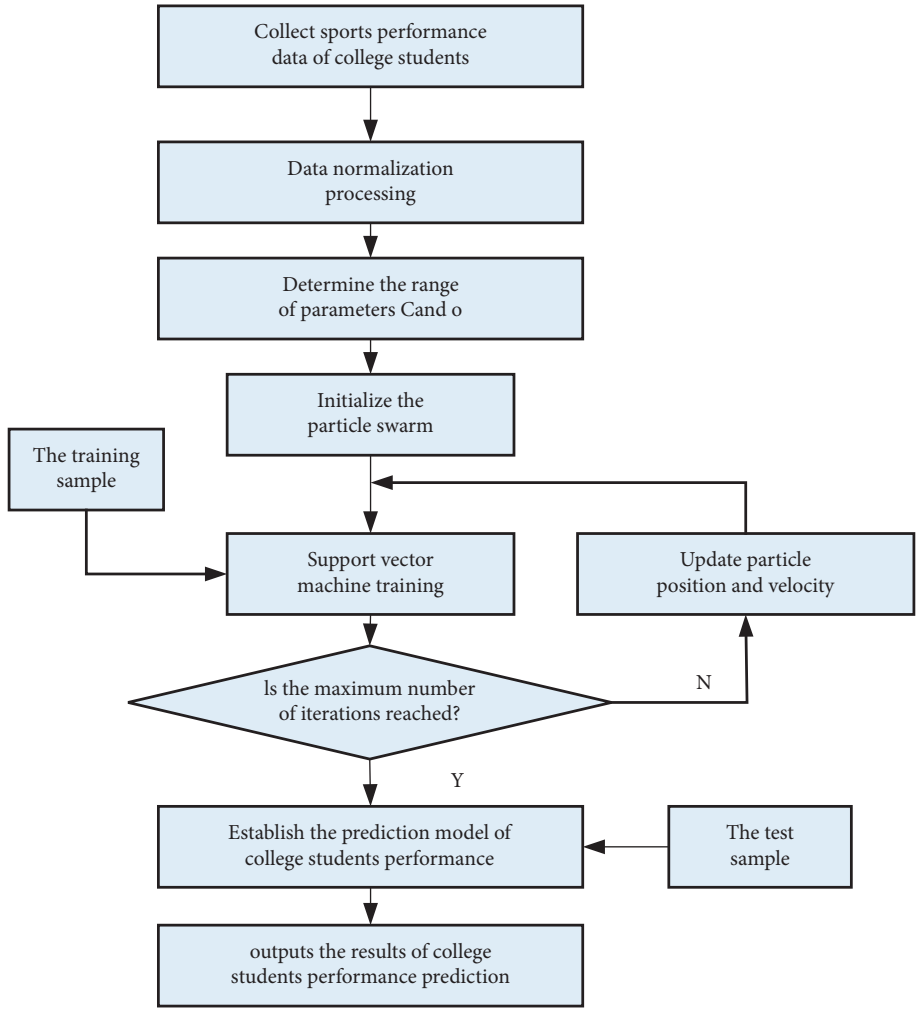

Figure 3: Work flow of predictive model of university students' sports performance.

For the data output in the input system, we can express it as

$$z_j = \phi_m\left(\sum_{i=1}^{n} w_{ji} y_i + \theta_j\right). \tag{9}$$

For the data output in the output system, we can express it as

$$e_j = \frac{1}{2}\left(d_j - z_j\right)^2. \tag{10}$$

The adjusted mode for each system is

$$\begin{aligned} \delta_{ji} &= \frac{\partial e_j}{\partial z_j} = \left(d_j - z_j\right)\phi\prime_m(\bullet), \\ \Delta w_{ji} &= -\eta\frac{\partial e_j}{\partial w_{ji}} = \eta\delta_{ji} y_i. \end{aligned} \tag{11}$$

The specific analysis method of the filter layer is

$$\begin{aligned} \delta_{ik} &= \frac{\partial e_{ji}}{\partial y_i} = \left(d_{ji} - y_i\right)\phi\prime_n(\bullet), \\ \Delta w_{ik} &= -\eta\frac{\partial e_{ji}}{\partial w_{ik}} = \eta\delta_{ik} x_k. \end{aligned} \tag{12}$$

The advantage of the neural network system is obvious; that is, it can be well combined with other models. We can combine the neural network algorithm system with the linear calculation method to get a better performance the experimental model, but in the neural network algorithm system, there are also many problems; that is, we have to choose the input data because the system has higher requirements for data. Once the initial data are wrong, then the data brought into the model must also be wrong, which will affect the analysis of part of the data. At the same time, when using neural network algorithm systems in practice, we often encounter problems such as complicated experiment process, long experiment time, and high energy consumption. This tells us that we only use neural network algorithms. The method of the system is not feasible because the shortcomings of the system are too obvious, so in order to be able to make the experimental results more accurate, we need to combine the above-mentioned models, so as to benefit the sports performance model establishment and assessment of students' physical fitness.

The application of artificial intelligence in neural network science obviously has great advantages, which is beyond ordinary technology because artificial intelligence is more flexible in operation, requires less data conditions, and

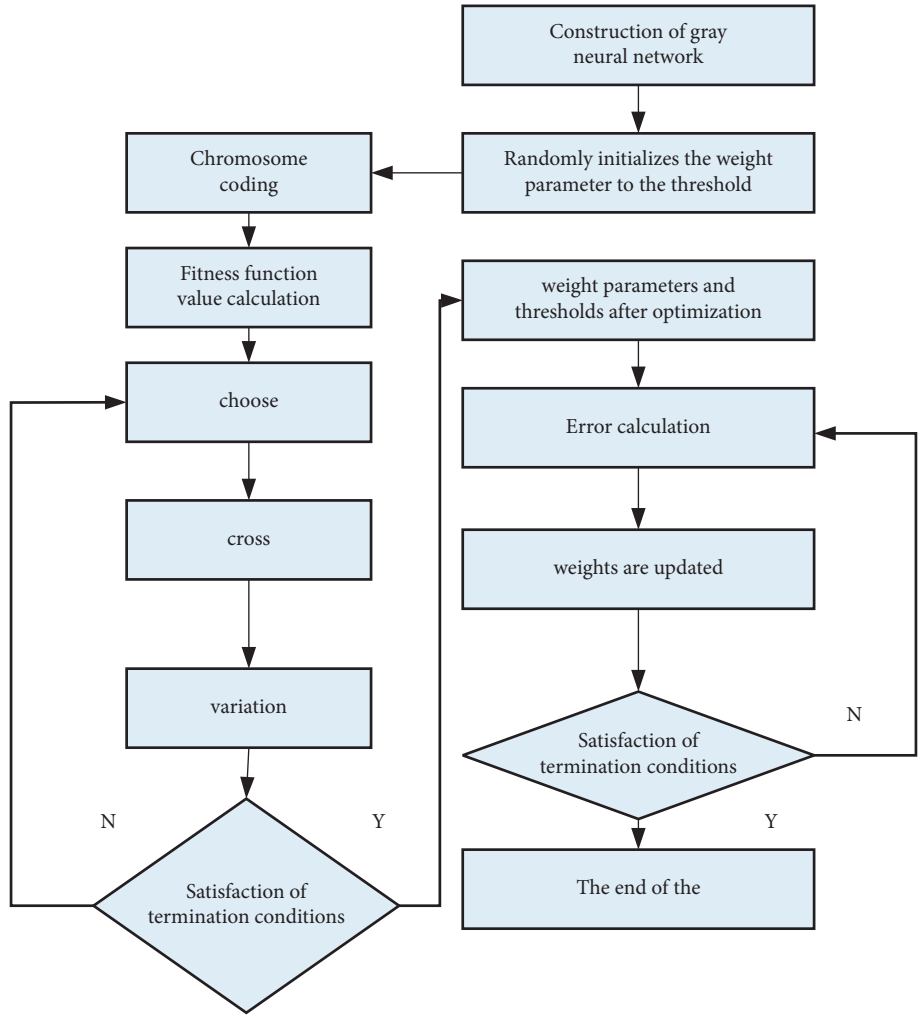

Figure 4: Integrated-learning algorithm model based on genetic algorithm optimization.

has no serious shortcomings. Therefore, this model is the best way to analyze the physical fitness of students. We used a linear model to design a new model.

In the following formula, the main variables are W and B. If we want to get a more complete experiment, we must focus on the values of W and B, so the formula we got is as follows:

$$\min \frac{1}{2}\|w\|^2 + C\frac{1}{k}\sum_{i=1}^{n}\varepsilon\left(f\left(x_i\right)-y_i\right),$$

$$s.t.\varepsilon\left(f\left(x_i\right)-y_i\right)=\begin{cases}\left|\left(f\left(x_i\right)-y_i\right)\right|-\varepsilon, \left|w\cdot\varphi\left(x\right)+b-y_i\right|\geq\varepsilon\\ 0, \left|w\cdot\varphi\left(x\right)+b-y_i\right|<\varepsilon\end{cases}. \tag{13}$$

In order to reduce the experimental error, we change the formula to

$$\begin{aligned}\min_{a^{(*)}\propto R^{if}}&\frac{1}{2}\sum_{i,j=1}^{n}\left(a_i^*-a_i\right)\left(a_j^*-a_j\right)k\left(x_i,x_j\right)\\ &+\varepsilon\sum_{i,j=1}^{n}\left(a_i^*+a_i\right)-\sum_{i,j=1}^{n}y_i\left(a_i^*-a_i\right).\end{aligned} \tag{14}$$

The function of the variable can be described as

$$k\left(x_i,x_j\right)=\exp\left(-\frac{\left\|x_i-x_j\right\|^2}{2\sigma^2}\right). \tag{15}$$

The most suitable model for the particle swarm algorithm is the pbest algorithm. We can analyze the particle performance by

$$\text{fitness}=\frac{1}{2N}\sum_{i=1}^{N}\sum_{j=1}^{D}\left(y_{ij}-t_{ij}\right)^2. \tag{16}$$

The update method of the speed and position of the particles when they change is

$$\begin{aligned}v_{id}^{k+1}&=\varpi v_{id}^{k}+c_1\text{Ran d}\left(p_{id}-x_{id}^{k}\right)+c_2\text{Ran d}\left(p_{\text{ghest}}^{k}-x_{id}^{k}\right)\\ x_{id}^{k+1}&=x_{id}^{k}+v_{id}^{k}\end{aligned} \tag{17}$$

(1) The exercise data of students in a specific physical activity are then screened. The specific experimental steps are as follows:

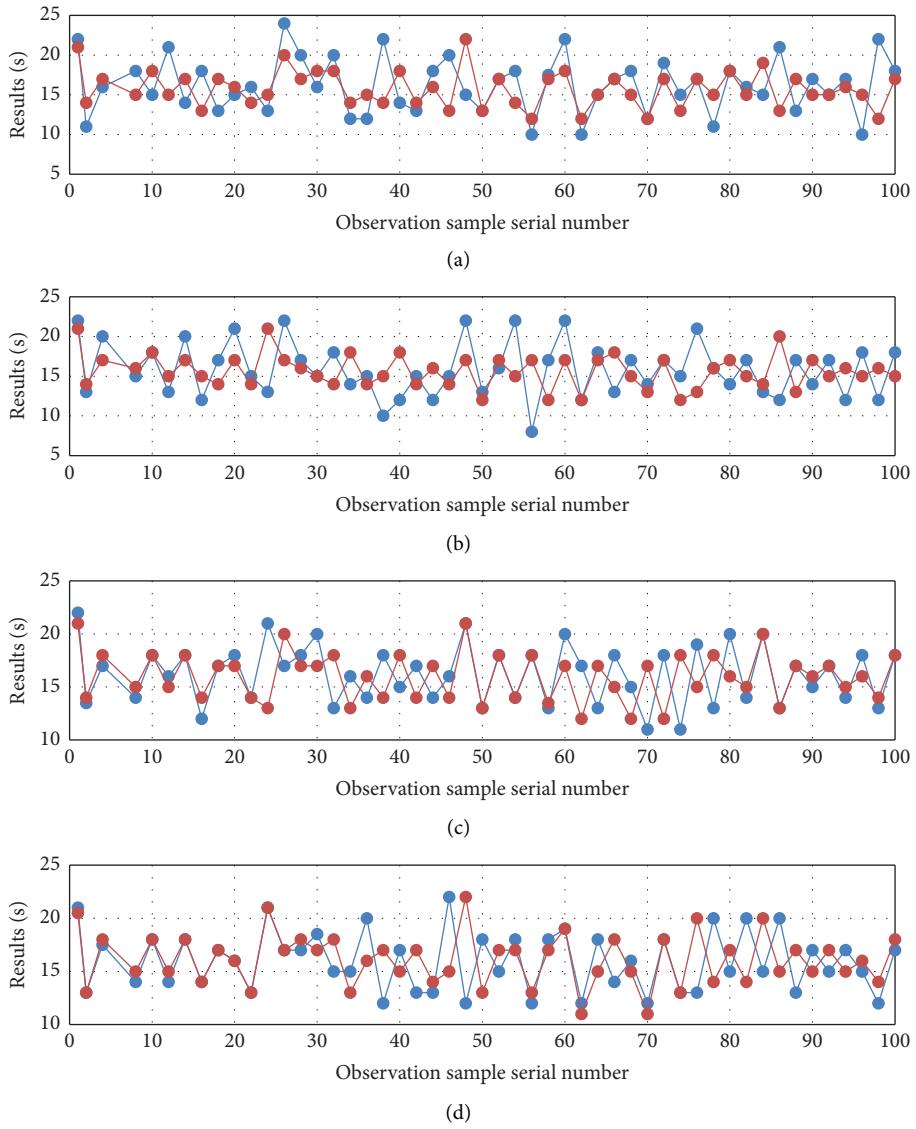

Figure 5: Prediction results: (a) prediction result of GM (1, 1), (b) BPNN prediction results, (c) GM-BPNN prediction results, and (d) prediction results of GA-GM-BPNN.

$$x_i' = \frac{x_i - x_{\min}}{x_{\max} - x_{\min}}. \tag{18}$$

(2) Input data into different models to get specific output data.

(3) The neural network system, integrated calculation method, and other modes are combined to compare the obtained results with the original data and draw conclusions.

(4) Establish a sports performance prediction model suitable for college students.

(5) Substituting the physical test scores of college students of different ages and genders into the model, and the conclusion is drawn after analysis.

The specific model operation process is as shown in Figure 3.

4. Results and Analysis of Sports Performance Prediction Model

4.1. Genetic Algorithm Prediction Model Optimization. The advantage of the neural network system is obvious; that is, it can be well combined with other models. We can combine the neural network algorithm system with the linear calculation method to get a better performance experimental model, but in the neural network algorithm system, there are also many problems; that is, we have to choose the input data because the system has higher requirements for data. Once the initial data is wrong, then the data brought into the model must also be wrong, which will affect the analysis of part of the data and even the output of the final result. Therefore, in order to make the prediction of student sports performance more accurate, we introduced the concept of weight to make the model test faster, and the experimental results are more

Table 6: Table of error statistics of four prediction models.

Predictive model	RMSE	MAPE/%
GMO	0.149	11.43
BPN	0.208	14.91
GM-BPN	0.085	4.59
GA-GM-BPN	0.031	2.71

accurate. The integrated learning algorithm model based on genetic algorithm optimization is as shown in Figure 4.

When we substitute each data into the neural network algorithm system and integrated calculation mode, the specific function formula obtained is.

$$f_D = \frac{1}{\sum_{j=1}^{n}\left(d_j - z_j\right)}. \tag{19}$$

4.2. Results and Analysis of Sports Performance Prediction. In order to prove that the newly designed predictive model is effective in analyzing the physical fitness of college students and the experimental results are correct, we concretely apply this model to a certain college and use the experimental results of the school students as a sample to test. In this test, we collected the number of sit-ups of 1,000 students. The specific data collection results are shown in the figure below. First of all, we selected 700 students as the main survey objects to obtain the exercise model of these 700 students, then tested the performance of the remaining 300 students, and then collected the data of the students with better physical fitness and poorer physical fitness data.

We selected 700 out of 1,000 experimental samples as the real experimental data, and based on the neural network algorithm system, linear calculation model, integrated calculation model, and other models, we analyzed the sports performance of the remaining 300 students. The specific experimental results are as shown in Figure 5.

According to the above data distribution, a specific conclusion can be drawn; that is, the test model we have selected can calculate and measure the physical fitness level of students if there is a big difference among them. As shown in the figure above, there are obvious signs of errors in the experimental results of the linear system model and the neural network algorithm system, but the experimental data results have more errors after comparison, so we cannot get them based on these two models and the level of physical fitness of the student. In contrast, we used the experimental method of ensemble computing model not only to predict and analyze the physical fitness level of college students but also to reduce errors and shorten the time required for the experiment. Error statistics of four prediction models are as shown in Table 6.

5. Conclusion

Nowadays, few people take physical exercises. In order to change this situation, we will focus on the physical activities of college students. Through the collection and analysis of college students' physical education courses, we understand that they enable students to enjoy physical activities, so how to turn these good wishes into reality has become a key research object of society and the government. Finally, the researchers decided to design a new sports performance analysis model to carry out specific experiments; in the era of rapid development of science and technology and very advanced network technology, it is not out of reach to combine the sports performance test model with artificial intelligence technology. Therefore, in order to improve the physical fitness of students, we decided to design a new model. Data collection and analysis of the students' physical education results and then the main reasons for the declining enthusiasm and physical fitness of modern college students are obtained. At the same time, this article also compared the traditional model with the newly designed model, pointed out the shortcomings of the traditional model and ideas on how to improve the method. We mainly used the integrated learning method to combine the theory with the machine to successfully establish the model and then apply this model to a university for testing. The ensemble learning model is a topic that researchers are very interested in. It has a great research and experimental value. This learning model has a huge impact on data analysis. More and more people are studying this field, and the future development prospects are good.

Data Availability

The data used to support the findings of this study are available from the corresponding author upon request.

Conflicts of Interest

The author declares that there are no conflicts of interest.

Acknowledgments

This work in this article was supported by Shandong Sport University.

References

[1] T. Baranova, L. Khalyapina, A. Kobicheva, and E. Tokareva, "Evaluation of students' engagement in integrated learning model in a blended environment," *Education Sciences*, vol. 9, no. 2, p. 138, 2019.

[2] Z. Xiao, L. Zhu, F. Dongyu, and D. Zhang, "Performance optimization of distributed database aggregation computing," *Journal of Computer Applications*, vol. 37, no. 5, pp. 1251–1256, 2017.

[3] N. Fazriyah, Y. Supriyati, and W. Rahayu, "The effect of integrated learning model and critical thinking skill of science learning outcomes," *Journal of Physics: Conference Series*, vol. 812, no. 1, Article ID 012014, 2017.

[4] A. E. Staiano and S. L. Calvert, "Exergames for physical education courses: physical, social, and cognitive benefits," *Child development perspectives*, vol. 5, no. 2, pp. 93–98, 2011.

[5] J. Conlisk, "An aggregate model of technical change," *Quarterly Journal of Economics*, vol. 104, no. 4, pp. 787–821, 1989.

[6] S. Jin and P. Hrnjak, "Refrigerant and lubricant distribution in MAC system," *SAE International Journal of Passenger Cars-Mechanical Systems*, vol. 6, no. 2, pp. 1013–1020, 2013.

[7] A. S. Welch, A. Hulley, C. Ferguson, and M. R. Beauchamp, "Affective responses of inactive women to a maximal incremental exercise test: a test of the dual-mode model," *Psychology of Sport and Exercise*, vol. 8, no. 4, pp. 401–423, 2007.

[8] C. Sdangare and S. S Apte, "Improved study of heart disease prediction system using data mining classification techniques," *International Journal of Computer Application*, vol. 47, no. 10, pp. 44–48, 2012.

[9] Z. Haiyun and X. Yizhe, "Sports performance prediction model based on integrated learning algorithm and cloud computing Hadoop platform," *Microprocessors and Microsystems*, vol. 79, Article ID 103322, 2020.

[10] P. Zhu and F. Sun, "Sports athletes' performance prediction model based on machine learning algorithm," in *Proceedings of the International Conference on Applications and Techniques in Cyber Security and Intelligence*, pp. 498–505, Springer, Cham, July 2019.

[11] F. Zhang, "Research on improving prediction accuracy of sports performance by using glowworm algorithm to optimize neural network," *International Journal of Information and Education Technology*, vol. 9, no. 4, pp. 302–305, 2019.

[12] D. Kabakchieva, "Student performance prediction by using data mining classification algorithms," *International journal of computer science and management research*, vol. 1, no. 4, pp. 686–690, 2012.

[13] H. Altabrawee, O. A. J. Ali, and S. Q. Ajmi, "Predicting students' performance using machine learning techniques," *JOURNAL OF UNIVERSITY OF BABYLON for pure and applied sciences*, vol. 27, no. 1, pp. 194–205, 2019.

[14] Z. Yangsheng, "An AI based design of student performance prediction and evaluation system in college physical education," *Journal of Intelligent and Fuzzy Systems*, vol. 40, no. 2, pp. 3271–3279, 2021.

Hindawi
Computational Intelligence and Neuroscience
Volume 2022, Article ID 3112092, 10 pages
https://doi.org/10.1155/2022/3112092

Research Article

Design of Political Online Teaching Based on Artificial Speech Recognition and Deep Learning

Xiajin Chen

Yiwu Industrial & Commercial College, Yiwu, Zhejiang 322000, China

Correspondence should be addressed to Xiajin Chen; cxj1986@ywicc.edu.cn

Received 18 July 2022; Revised 18 September 2022; Accepted 26 September 2022; Published 6 October 2022

Academic Editor: Gopal Chaudhary

With the emergence of the information age, computers have entered the homes of ordinary people and have become essential daily appliances for people. The integration of people and computers has become more popular and in-depth. Based on this situation, how to make computers and humans communicate intelligently and make human-computer interaction more convenient and practical is the main issue of scientific research and discussion on computers. Language recognition is widely used in industry, the economy, commerce, tourism, style, and sports. The BP neural network based on deep learning has supercomputing functions and is very suitable for speech recognition, which promotes the promotion and application of speech recognition technology in many fields. Different types of applications and diverse scenarios enable users to experience different personal experiences. This paper examines the use of application software for ideological and political theory courses in colleges and universities and the application of application software for ideological and political theory courses in colleges and universities in the management of ideological and political theory courses. Analyzed the use of apps in the management of ideological and political theory courses in colleges and universities, analyzed the possibilities and challenges that this brought to the management of ideological and political theory courses in colleges and universities based on the app, and put forward the necessary countermeasures. Including the development and design of ideological and political theory applications, combining deep learning and CTC algorithms to build acoustic models, using server-client interaction, designing an ideological and political theory course app based on speech recognition and deep learning, and forming an offline speech recognition system software platform, the app provides a certain reference for improving the skills of teaching managers.

1. Introduction

With the development of Internet technology and the unremitting efforts of manufacturers of mobile devices in various countries in the world, wireless mobile terminal devices have become very popular in people's daily work, production, and lives [1]. With the drastic reduction of communication costs, the rapid increase of network speeds, and the full coverage of wireless networks, all these increasingly perfect conditions have accelerated the rapid promotion and popularization of mobile terminals such as smartphones and tablet computers [2]. The proportion of Internet equipment used by everyone has been rapidly increasing and has gradually become the most important mobile terminal equipment used by people, gradually replacing the use of computers and notebooks in people's lives [3]. Therefore, it is no exaggeration to say that smartphones have been closely linked with our work, production, and life and have become an indispensable item in our daily work and life, and even an essential thing in our daily lives. In the current period, with the deepening of research, the exploration of the teaching and management of ideological and political theory courses has gradually deepened. Various applications in smartphones are very convenient and simple, with high efficiency and low cost. They can fully meet the requirements of students to learn anytime, anywhere, and are favored by students [4]. This is the development trend of learning methods in the future. At this stage, the number of mobile Internet users in my country is very large. Due to the rapid improvement of the

educational information industry and the strong growth of user demand, apps as an application are indispensable in education and teaching [5]. It can not only promote the integration of educational theory and information technology but also strengthen the dissemination of educational ideas and scientific theories.

With the emergence of the information age, computers have entered the homes of ordinary people and have become essential daily appliances for people. The integration of people and computers has become more popular and in-depth [6]. Based on this situation, how to make computers and humans communicate intelligently and make human-computer interaction more convenient and practical is the main issue of scientific research and discussion on computers. Language recognition is widely used in industry, economy, commerce, tourism, style, and sports [7]. The BP neural network based on deep learning has super-computing functions and is very suitable for speech recognition, which promotes the promotion and application of speech recognition technology in many fields. After the emergence of new media, while breaking with the original advantages of the old media, the content and methods of teaching and management of ideological and political theory courses have been updated, which stimulated students' interest in learning, creativity, and teachers' enthusiasm [8]Better management efficiency provides new methods for ideological and political theory education. However, the application of apps is extremely rich and complex, which not only provides new methods for ideological and political education management but also brings great challenges [9]. The requirements for teachers and students are higher, and its freedom, diversity, and rapid dissemination also pose challenges and puts forward higher requirements for teachers' abilities. Therefore, the need to combine some modern computer science and technology has become the focus of this article.

2. Related Work

For a long time, speech recognition has mainly focused on speech machines and natural language processing, as well as the sound signal itself. People obtain a lot of outside information through human-computer interaction. About 76% of people's daily communication is conducted through speech. Automatic language recognition technology is also called speech recognition technology, which is the technology responsible for converting speech into text [10]. This includes technology and knowledge of multiple disciplines. Automatic speech recognition technology performs speech recognition in human-computer interaction. Automatic speech recognition technology is committed to completing the smooth communication between humans and machines. The world's first speech recognition system was first researched and developed by American scientists. At first, it could only recognize simple numbers, but it provided new ideas for the development and research of automatic speech recognition technology. Compared with the original text interaction method, the method of human-computer interaction using speech recognition technology is more suitable for people's habit of communicating through language [11]. In addition, voice interaction will be smoother, more efficient, and have fewer errors. Voice recognition technology is mainly used in voice management systems, intelligent dialogue inquiry systems, dictation, transcription systems, and situational dialogue systems. In the beginning, researchers used pattern engineering methods to build a speech recognition system, but the results were minimal.

After the emergence of deep learning, speech recognition technology has gradually reached a modern level on a large scale [12]. This research study uses a deep neural network, and the research proves that, compared with previous research results, the recognition error rate has been significantly reduced by 40%. The literature records a deep-faith network that pre-trains deep neural networks layer by layer through a limited Boltzmann machine, which greatly reduces the difficulty of deep neural networks and significantly improves the modeling level of neural networks. The study of neural networks has triggered a wave of deep learning. In depth neural network and hidden Markov mixture model, depth neural network is used to replace Gaussian mixture model, and speech signal model is established. Great progress has been made in speech recognition effect. The reference records a sequence discrimination technique that makes deep neural network training directly determine the level of recognition frequency, greatly reducing the huge error in recognition and becoming a standard part of subsequent deep neural network training. Literature established a highly consistent speech-recognition neural network [13]. The literature accurately simulates the correlation between the different dimensions of the speech frequency spectrum function, shows a high level of anti-noise, and greatly improves the noise reduction ability of the deep neural network. Researchers used long-term and short-term memory models in speech recognition. People use long-term historical framework information to make more precise decisions and achieve better results than prospective neural networks. Researchers used short-term classification termination technology in speech recognition, which severely weakened the role of HMM (a technology that has been used for nearly half a century) and significantly improved the performance of continuous numbering and other items [14]. A codec-based speech recognition scheme is used. The input of this end-to-end model is the speech spectrum function, and the output is direct words. The original acoustic model and language model are interwoven into a deep neural network for common modeling, almost completely destroying the traditional speech recognition framework.

Digital recognition technology is one of the key technologies for mobile application development. The term "mobile learning" refers to a type of learning that can be performed at any time and any place using mobile computer equipment. Mobile computer equipment used for mobile learning requires a certain ability to display learning content and provide teachers with communication between students [15]. Technical features of the new system include intelligence and digitization, digital transformation and coding, and new functions beyond the media. The literature explains

the important role of mobile media devices. From the birth of human beings to the birth of mobile phones, these two functions have been separated [16]. The development of science and technology has merged these two mutually independent parts. The record pointed out that the emergence and use of the Internet has improved the level of cultural thought and educational technology, and the idea of educational management has been added to cultural and technical learning to guide and inspire students. Media literacy education is no longer a violation of students. The education of media experience is no longer regarded as a means of discrimination or an observation of ideology, and pointed out that the future of media education will be different [17]. It has the characteristics of socialization. It can improve its own quality through traditional school education. Participate in media life to achieve social media education and improve students' social participation. The positive and negative effects of the Internet era on college education are used as a basis to study on how to improve and perfect college ideological and political theory education to cope with the changes of the times.

3. Research on Speech Recognition Control System Based on Deep Learning

3.1. Deep Learning Model and Algorithm Application. The original neural network is a decision model, and the deep-faith network is a hybrid model, which combines a generative model and a decision model, as shown in Figure 1. Therefore, the network can realize the common probability arrangement of observation data and tags, which is convenient for estimating the former probability and the latter probability. In the deep trust network model, the middle hidden layer is mainly composed of limited Boltzmann machines.

The neurons in the speech recognition system present a Gaussian distribution, so neuron V is a hidden neuron h. Under this condition, the energy function is

$$E(v,h\mid\theta)=\sum_{i=1}^{n}\frac{(v_i-a_i)^2}{2\sigma_i^2}-\sum_{j=1}^{m}b_jh_j-\sum_{i=1}^{n}\sum_{j=1}^{m}\frac{v_i}{\sigma_i}W_{ij}h_j. \tag{1}$$

In the energy function, the conditional probability that can be achieved is

$$\begin{aligned}P(v_i=1\mid h)&=N\left(a_i+\sum_i W_{ij}h_j,\sigma_i^2\right),\\ P\left(h_j=1\mid v\right)&=S\left(b_j+\sum_j\frac{v_i}{\sigma}W_{ij}\right).\end{aligned} \tag{2}$$

In order for the contrast divergence algorithm to be quickly applied, the input data of visual data is usually normalized into multiple islands with an average value of 0 and a variance of 1. The energy function and conditional probability are changed to

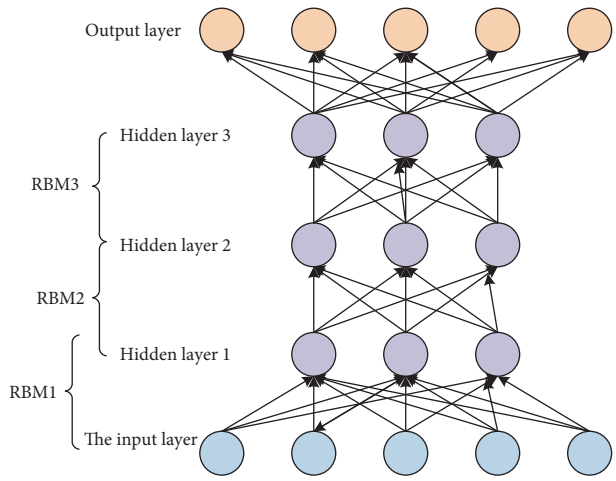

Figure 1: Deep belief network structure model.

$$E(v,h\mid\theta)=\sum_{i=1}^{n}\frac{(v_i-a_i)^2}{2\sigma_i^2}-\sum_{j=1}^{m}b_jh_j-\sum_{i=1}^{n}\sum_{j=1}^{m}\frac{v_i}{\sigma_i}W_{ij}h_jv_i,$$

%

$$P\left(h_j=1\mid v\right)=S\left(b_j+\sum_j W_{ij}\right). \tag{3}$$

In the actual situation, the main considerations are the operating environment of the management system and the network environment. This requires that the extracted function value must have good robustness, and tries to obtain the absorbed sound in different situations and environments corresponding to the function value. It is necessary to improve the original auto-encoder structure and add noise to generate noise reduction codes, as shown in Figure 2.

This will create a new hidden layer code for input data and information. When decoding, the decoder can estimate the initial information that has been interfered from the information without noise interference, and send most of the initial information to reduce the impact of these noises. After multiple in-depth training, the function value improves the robustness.

For noise reduction coding calculation, the general algorithm is: consider the initial input data x, add noise to the input data, and obtain new input data. When coding, the characteristic formula obtained is

$$h=f(\tilde{x})=s_f(w\tilde{x}+p). \tag{4}$$

The output obtained during decoding is

$$y=g(h)=s_g(\tilde{x}h+q). \tag{5}$$

The final loss function of Ender is

$$J_{\mathrm{DAE}}(\theta)=\sum_{x\in s}L(x,g(f(\tilde{x}))). \tag{6}$$

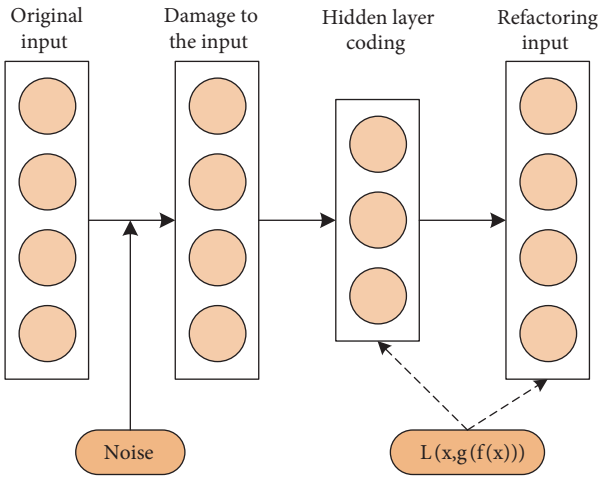

Figure 2: Noise reduction encoder algorithm structure.

3.2. Construction and Training of Acoustic Model Based on Deep Learning. When the spectrogram function is decomposed, the Fourier transform is only performed on each frame signal within a short time after the frame is divided, and the spectrum is obtained through the window. Then square the modulus spectrum to get the energy spectrum, and then take the logarithm to get the logarithmic energy spectrum of each frame. The logarithmic conversion makes the low-amplitude component higher than the high-amplitude component, so you can see the signal period hidden in the low-amplitude noise. Finally, the logarithmic spectrum calculated for each frame is rotated and decomposed in time to obtain the final characteristic sequence spectrum. Figure 3 is a calculation diagram of the parameters of the spectrogram function.

In the Fourier transformation, the transformation of a nonperiodic continuous time signal $x(t)$ is

$$X(\omega) = \int_0^{\infty} x(t) e^{-j\omega t} dt. \tag{7}$$

Given a discrete signal of finite length $x(n)$, $n = 0,1, \ldots, n-1$, the discrete Fourier transform is

$$X(k) = \sum_{n=0}^{N-1} x(n) W_N^{kn}, K = 0, 1N-1, W_N = e^{-j2\pi/N}. \tag{8}$$

In the basic acoustic model of this article, the middle layer 3 adopts the pool layer module. Each convolutional pool layer module is two layers with a folding layer + 1 layer pool layer. The fully connected layer adopts two hidden layers, and the number of modules constructed is 1,425, and the size of the rear probability matrix of 200×1425 is transmitted via Softmax. The specific structural parameters are shown in Table 1.

3.3. Optimized Design of Deep Learning Speech Enhancement Baseline System. The deep neural network has strong nonlinear adaptability and can obtain the nonlinear mapping relationship between noisy speech and speech. The deep

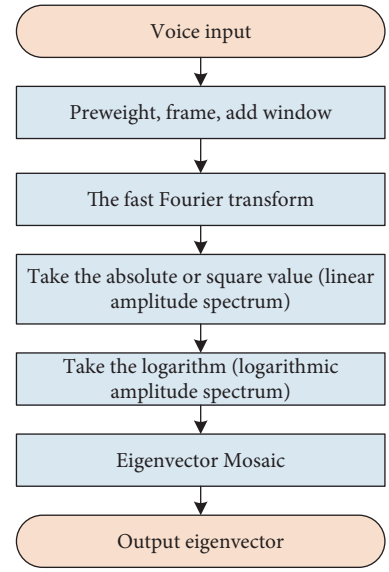

Figure 3: Feature extraction flowchart of spectrogram.

neural network improvement algorithm includes two processes. The specific process is shown in Figure 4.

Before subjective evaluation, testers must first understand the scoring criteria and then give them more audit training so that the testers can evaluate the sound quality more accurately. Subjective and objective scoring uses the average sentence core scale method. The MOS score is mainly divided into five levels to evaluate the quality of the sound. The score reflects the process of voice quality. See Table 2 for details.

The normalization method in this article is BN. It can converge quickly and improve the versatility of the network. Because the use of BN may interfere with the test and training data, the batch test data is different, which helps to improve the accuracy of the model. BN needs to learn these parameters when normalizing the γ and β parameters, and transform and construct the normalized data to break the learned function distribution. Assuming that the input of the small batch data is B and the parameters to be learned are γ, β, then the calculation of BN is: the average calculation formula:

$$\mu_B = \frac{1}{m} \sum_{i=1}^{m} x_i. \tag{9}$$

Variance calculation formula:

$$\sigma_B^2 = \frac{1}{m} \sum_{i=1}^{m} (x_i - \mu_B)^2. \tag{10}$$

Standardized calculation formula:

$$\hat{x}_i = \frac{x_i - \mu_B}{\sqrt{\sigma_B^2 + \epsilon}}. \tag{11}$$

Modification formula:

$$y_i = \gamma \hat{x}_i + \beta \equiv BN_{\gamma\beta}(x_i). \tag{12}$$

Table 1: CTC-CNN baseline acoustic model parameters.

Network layer	Parameter
InputLyer	300 dimensional harmony
conv2d_Lyer1	33 convolution channels, convolution kernel 4×4, step size 3×3, activation function
conv2d_Lyer2	33 convolution channels, convolution kernel 4×4, step size 3×3, activation function
max-poolng2d	Maximum pooling 3×3
conv2d_Lyer3	65 convolution channels, convolution kernel 4×4, step size 3×3, activation function
conv2d_Lyer4	65 convolution channels, convolution kernel 4×4, step size 3×3, activation function
max-poolng2d	Maximum pooling 3×3
conv2d_Lyer5	129 convolution channels, convolution kernel 4×4, step size 3×3, activation function
conv2d_Lyer6	129 convolution channels, convolution kernel 4×4, step size 3×3, activation function
max-poolng2d	Maximum pooling 3×3
Reshap	Feature map transformation output 300×3300
FC_Lyer1	Number of neurons 129, activation function
FC_Lyer2	The number of neurons is 1425, the activation function
Softmx	Activation output matrix, the dimension is 300×1425
CTC	Probability matrix, the length of the sonogram, the length of the label sequence

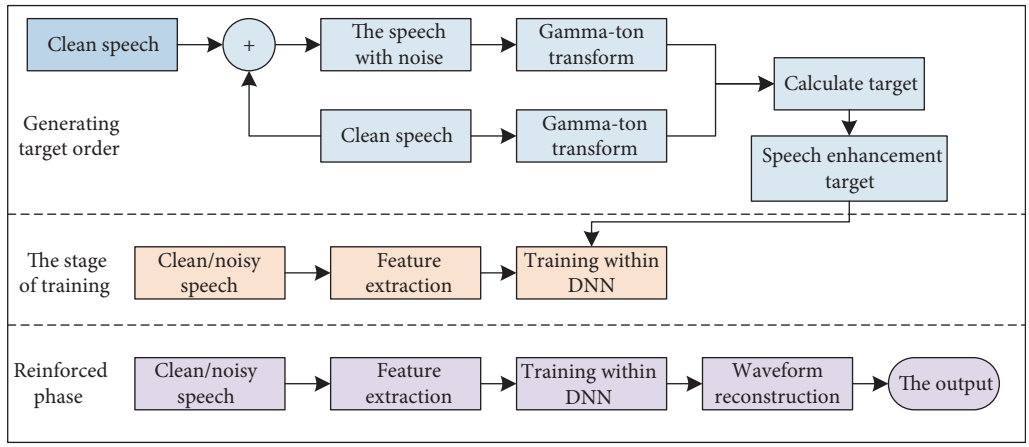

Figure 4: The general flow chart of the deep neural network speech enhancement method.

Table 2: MOS scoring and related application description.

MOS score	Quality level	Distortion level
5	Great	Not aware
4	Better	Slightly aware
3	General	Aware, but lighter
2	Poor	Clearly aware
1	Difference	Very obvious

The entrance of the previous layer is directly transmitted to the next layer. The expression output from each remaining module is

$$H(x) = F(x) + x. \tag{13}$$

3.4. Experimental Results and Analysis. As the speed and volume of the training set body change, the signal length of the training body changes accordingly. The method described in this paper is applied to the regeneration of the adjusted GMM-HMM system of the velocity distortion data and the adjusted GMM-HMM system of the volume adjustment data, for DFSMN acoustic model training based on the speech enhancement data. First, the experiment researched the influence of the speed distortion-based speech data amplification method on the acoustic DFSMN model recognition. The experimental conditions and results are shown in Table 3:

Secondly, the experiment researched the effect of speech enhancement data on DFSMN acoustic model recognition; see Table 4 for details.

Based on the abovementioned experimental results, the discriminant training method based on the sMBR criterion, the treble adaptive method based on the discriminant vector function, and the voice data amplification method based on speed distortion are further combined. The experimental results of these three methods are shown in Table 5.

A speech recognition system using DFSMN and TDNN acoustic models can recognize and transcribe experimental datasets without manual annotations. Among them, DFSMN chose the best model so far, and its vocabulary on the test set is 20.34%. The word error rate on the TDNN test set is 29.88%, so the DFSMN recognition result is regarded as a text label, and the word error rate of each voice recognition result in the dataset is calculated and determined by TDNN, as shown in Table 6.

Table 6 shows that the distribution of word error rate in each time interval is more balanced. Because of the insertion problem in speech recognition, the vocabulary error rate of a

Table 3: Comparison of experimental results based on velocity disturbance.

Model	WER (%)	SER (%}
Baselne	25.95	78.73
SP09	22.68	68.08
SP11	22.81	68.32
SPe-BAND	22.58	67.98
SP09 + SP11	21.49	67.65
SP-RAND2	21.73	67.74

Table 4: Comparison of experimental results based on volume gain adjustment.

Model	WER (%)	SER (%)
baselne	25.95	78.73
VL05	22.85	68.58
VL15	22.83	68.53
VLe-RAND	22.88	68.64
VL05 + VL15	23.98	69.75
VL-RAND2	22.94	68.94

Table 5: Comparison of the results of the fusion of the three optimization methods.

Model	WER (%)	SER (%}
baselne	25.95	78.73
i-vctor + sMBR	23.18	69.13
SP09 + SP11	21.49	67.65
i-vector + sMBR + SP09+SP11	20.34	63.88

Table 6: Recognition result distribution statistics.

WER (%) interval	Duration (hours)	Proportion (%)
0–10	21.4	10.66
10–20	20.2	10.06
20–30	21.7	10.81
30–40	24.6	12.26
40–50	26.3	13.11
50–60	18.5	9.21
60–70	17.6	8.76
70–80	16.8	8.36
80–90	14.5	7.21
90–100	11.3	5.61
≥100	8.2	4.06

single voice may exceed 100%. Therefore, we selected audio tapes with vocabulary frequencies of 0–10%, 10%–20%, and 20%–30% as the extended dataset, used the recognition results of these audio tapes on DFSMN as text annotations, and added them to the existing speech training package, as shown in Table 7.

3.5. Fine-Tuning and Optimization of Deep Learning Speech System. When the RBM model is completed, a classifier is added on top of the pattern classification. Compared with logistic regression, only two types of nonlinear classification can be performed. The Softmax method is used to extend logistic regression to complete multiple classifications. They

Table 7: Automatically annotated speech data augmentation experiment.

Model	WER (%)	SER (%}
Baselne	25.95	78.73
DFSMN (0–10)	21.88	66.68
DFSMN (10–20)	22.17	67.89
DFSMN (20–30)	23.96	70.45

are mutually exclusive, that is, two classifications cannot be occupied by a sample at the same time to meet the experimental requirements. The specific method is given below.

In order to minimize the difference between the actual output and the expected output of the model, the fault uses cross-human correction.

$$H(r,S) = -\sum_{i}^{d} \left(r_i \log S_i + (1-r_i)\log\left(1-S_i\right)\right). \tag{14}$$

Train network parameters i by minimizing failures.

$$\theta^* = \operatorname{argmin}_{\theta} H(r,S). \tag{15}$$

Finally find the child thread:

$$\frac{\partial H(r,S)}{\partial \theta} = -\sum_{i=1}^{d} \left(r_i, S_i\right) \frac{\partial g_i}{\partial \theta}. \tag{16}$$

The partial derivatives of W and b are

$$\begin{aligned} \frac{\partial H(r,S)}{\partial W} &= (S-r)^T X, \\ \frac{\partial H(r,S)}{\partial b} &= S - r. \end{aligned} \tag{17}$$

The process of using the gradient reduction method to update the weights is

$$\begin{aligned} W' &= W - \eta\left((S-r)^T X + \lambda W\right), \\ b' &= b - \eta(S - r + \lambda b). \end{aligned} \tag{18}$$

Taking the time-distorted Mel cepstral coefficient and the first-order differential mixing parameter of Mel cepstral coefficient as input data, one can construct classification in the output for identification. If the amount of sample data is small and the number of hidden layers is large, the experimental effect is better, but the relative time spent increases sharply. The experiment process improves the network model according to the set rules and improves the learning efficiency of the model. RBM reconstruction performance is show in Figure 5.

4. Research on App Design and Communication in Political Education

4.1. Design Principles and Structure Analysis of the Ideological and Political Education App

4.1.1. The Principle of Scalability. With the rapid development of Internet technology and the advancement of society, students' requirements for learning platforms will also change accordingly. Therefore, when developing and

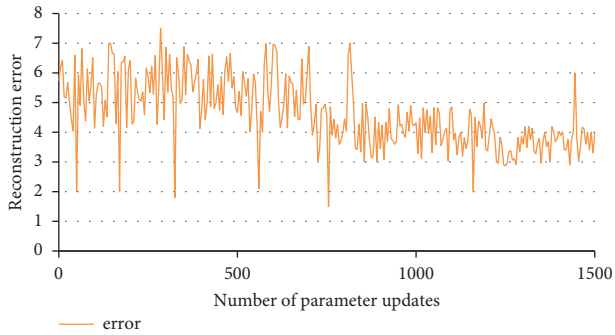

Figure 5: RBM reconstruction performance.

designing a platform, not only must it meet the requirements of primary school students, but it must also leave opportunities for future development and improvement. This leaves room for development in subsequent content and function expansion.

4.1.2. Principle of Feasibility. This principle needs to fundamentally complete the research and development of the main functions under the actual conditions of the current software and hardware and the operation of student mobile terminals.

4.1.3. Safety Principles. First, when developing the platform, it is necessary to fully consider the information security situation, suspend user permissions, and protect user privacy and platform security. Second, the platform should try to avoid abusing users, and the interface should be concise and clear to reduce the number of abused users; the information prompt function of the operation should be set so that the user clearly knows the result of this operation.

4.1.4. Principle of Good Interactivity. Good interactivity is very important for the development and design of this application. In this process, the student must be the center. First of all, we must meet the needs of students. We must use the simplest and most practical learning results to achieve the most optimized goal.

The ideological and political education app combines the characteristics of the mobile learning environment, the design concept, and development principles of the app and is a new device for carrying out ideological and political education activities and a new way of mobile learning. The details are shown in Figure 6.

4.2. Database Design of Ideological and Political Education App. Table 8 is a detailed description of various learning resource modules.

Sound performance, complete functions, and fast operation are closely related to the database. Therefore, comprehensive consideration must be given to database design. Through the analysis of the application of the ideological and political education app, this article points out that the units of the database design mainly include elementary school students, news information, topic discussions, etc.

4.2.1. User Information Table. The structure of the specific user information table is shown in Table 9.

4.2.2. News Information Table. The detailed content of the specific news information table is shown in Table 10.

4.3. Performance Test and Guarantee Design of Ideological and Political Education App. When the network is transplanted to the last layer, the neural network compares the predicted situation with the actual situation and calculates the deviation inside. This calculation function is also called the loss function. The commonly used loss function is the cross entropy loss function, and the calculation formula is

$$J(W, b, a, y) = -y \cdot \ln a - (1 - y) \cdot \ln (1 - a). \tag{19}$$

The concept of the gradient formed by the jth neuron in the lth layer is

$$\delta_j^l = \frac{\partial C}{\partial Z_j^l} = \frac{\partial C}{\partial a_j^l} \cdot \frac{\partial a_j^l}{\partial Z_j^l}. \tag{20}$$

C is the value of the loss function to calculate the deviation of the last layer of the neural network

$$\delta^l = \frac{\partial C}{\partial a^l} \bullet \frac{\partial a^l}{\partial Z^l}. \tag{21}$$

Then continue to calculate the deviation of the previous layer

$$\delta^l = \left(\left(w^{l+1}\right)^T \delta^{l+1}\right) \bullet f'\left(z^l\right). \tag{22}$$

And the slope of the previous layer

$$\begin{aligned} \frac{\partial c}{\partial w_{jk}^l} &= a_k^{l-1} \delta_j^l, \\ \frac{\partial c}{\partial b_j^l} &= \delta_j^l. \end{aligned} \tag{23}$$

Assuming that the learning speed is set, the learning speed must be multiplied by the weight w and the deviation b of the variable update. Using the software testing method, package the application in the form of an apk and install it on a suitable machine, and test the main functions of the application, as shown in Table 11.

4.4. Analysis of App Communication Strategies in Ideological and Political Education. Usually, people generally pay attention to the information they are interested in. Therefore, we must first take the ideological and political training app as the focus of party building and focus on the timely change and system optimization of the app's content. Therefore, when disseminating and promoting ideological and political

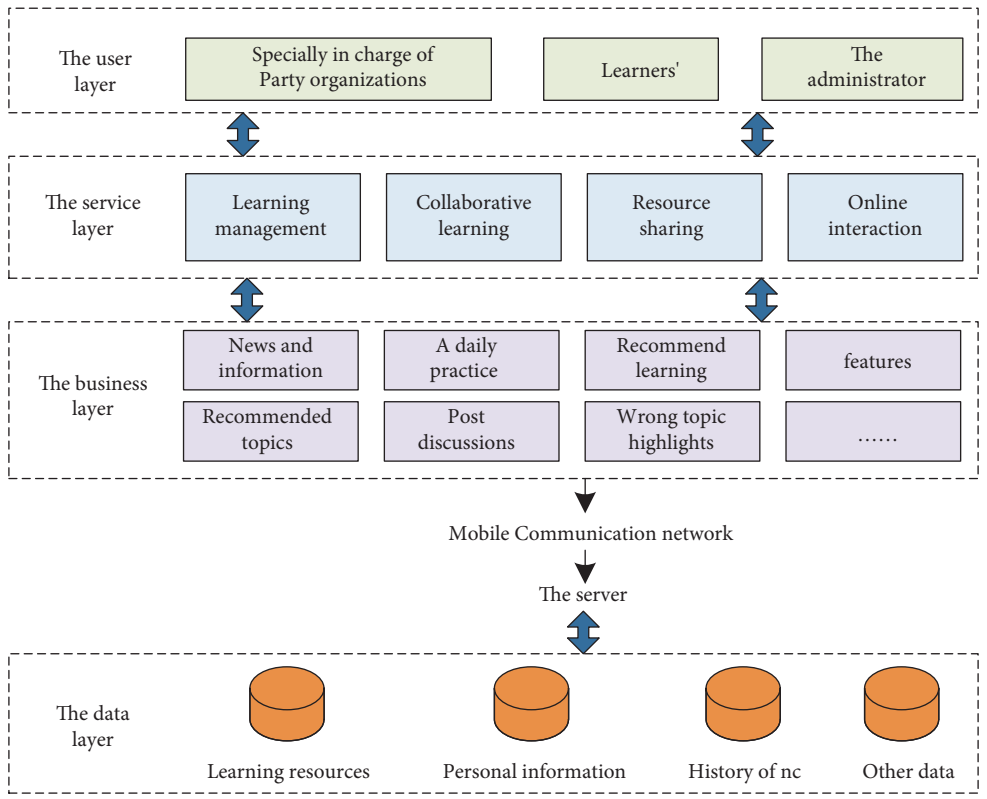

Figure 6: App overall architecture.

Table 8: Organization and classification design of learning resources.

Learning capital	Functional module	Text, pictures, charts	Features
Study plan	Study plan	Text, image, audio and video, etc	Understanding the learning plan
Learning resource library	Daily practice News report Study item Column content	Text, image, page	Provide various forms of learning content to promote students' independent learning
Learning activity library	Activity theme Main content Start a discussion	Text, page	Provide topic discussions to help students work together to solve problems
Learning evaluation library	Daily practice Quiz	Text, page, monitoring	Assess student learning effectiveness
Learning monitoring library	Practice daily monitoring of learning Self-monitoring Student monitoring	Text, image, table	Monitor student learning

education apps, we should focus on the needs of the public, pay attention to customer feedback, choose effective content from the platform, and promote interactive circular information. The application of ideological and political education is very important for the rapid dissemination of information. In the Internet era, the public has access to a huge amount of information, and attention has become less important in the media. The speed and area of information transmission will have the greatest effect on the success or failure of evaluation and management.

Although the content of the ideological and political education application is different from other applications that people know, it is also a mobile terminal application that should pay great attention to user experience, system innovation, and optimization of functions and uses. Because the application is suitable for mobile terminal devices, the environment used by the application is mainly a mobile environment. Therefore, the convenience of product operation and user comfort have become the main criteria for evaluating the experience of application users. Therefore, the

Table 9: User information form.

Field content	Type of data	Content description
Id	inte(10)	Self-growing primary key
Usrname	varehr(100)	User name
Pasword	varchr(32)	User password
Headmg	varchr(255)	User image
Sex	inte(1)	Gender
Stats	tinynt(1)	User status
reg_tme	inte(10)	Log in time
last_logn_time	inte(10)	Log in time
last_logn_ip	varchr(15)	Login address
Tokn	varchr(100)	Instruction board
Token tme	inte(11)	Expire date
study_pan	varchr(255)	Study plan
Phon	varchr(20)	Contact number
Long _tme	inte(10)	Cumulative study time

Table 10: News information sheet.

Field content	Type of data	Allow to be empty	Content description
Id	inte(11)	Not allowed	Increase primary key
User_id	inte(11)	Allow	User address
News_id	inte(11)	Allow	News category address
Title	varehr(255)	Allow	Topic
Url	varchr(100)	Allow	Connection
Status	varchr(255)	Allow	Subscribe

Table 11: Login registered test case table.

Use case number	Side trial example	Expected results	Test result
1	Click client	The login interface appears	Accord with
2	Enter the registration page	Jump to the registration interface	Accord with
3	Enter the phone number to get the verification code	Sending text verify code	Accord with
4	Write verification code	Enter the verification code correctly and jump to the registration interface	Accord with
5	Supplement information and submit	Successful registration appears, enter the main interface	Accord with
6	Enter the system again	Go directly to the main interface	Accord with
7	Click the back button	Back to the previous level	Accord with

primary goal of optimizing the process of ideological and political education app user experience is to be direct, simple, fast, comfortable, and easy to understand and give people a user-friendly and easy-to-use experience.

5. Conclusion

Different types of applications and diverse scenarios enable users to experience different personal experiences. This paper examines the use of application software for ideological and political theory courses in colleges and universities and the application of application software for ideological courses and analyzes the use of apps in the management of ideological and political theory courses in colleges and universities. Including the development and design of ideological and political theory applications, combining deep learning and CTC algorithms to build acoustic models, using server-client interaction, designing an ideological and political theory course app based on speech recognition and deep learning, and forming an offline speech recognition system software platform, the app provides a certain reference for improving the skills of teaching managers.

Data Availability

The data used to support the findings of this study are available from the corresponding author upon request.

Conflicts of Interest

The author(s) declare(s) that they have no conflicts of interest.

Acknowledgments

This paper was supported by Yiwu Industrial & Commercial College: Research on the application of 5G network and artificial intelligence in ideological and political education in colleges and universitie, ZD2021GJ38802.

References

[1] M. Liu, K. Yang, N. Zhao, Y. Chen, H. Song, and F. Gong, "Intelligent signal classification in industrial distributed wireless sensor networks based industrial internet of things," *IEEE Transactions on Industrial Informatics*, vol. 17, no. 7, pp. 4946–4956, 2021.

[2] T. Yan, D. Chu, D. Ganesan, A. Kansal, and J. Liu, "Fast app launching for mobile devices using predictive user context," in *Proceedings of the 10th international conference on Mobile systems, applications, and services*, pp. 113–126, Windermere, UK, June 2012.

[3] C. L. Ventola, "Mobile devices and apps for health care professionals: uses and benefits," *P and T: A Peer-Reviewed Journal for Formulary Management*, vol. 39, no. 5, pp. 356–364, 2014.

[4] W. Journell, "Teaching politics in secondary education: analyzing instructional methods from the 2008 Presidential Election," *The Social Studies*, vol. 102, no. 6, pp. 231–241, 2011.

[5] T. M. Philip and A. Garcia, "Schooling mobile phones: assumptions about proximal benefits, the challenges of shifting meanings, and the politics of teaching," *Educational Policy*, vol. 29, no. 4, pp. 676–707, 2015.

[6] C. Chen, R. Jafari, and N. Kehtarnavaz, "A survey of depth and inertial sensor fusion for human action recognition," *Multimedia Tools and Applications*, vol. 76, no. 3, pp. 4405–4425, 2017.

[7] H. Liu, R. Jia, X. Zhou, and L. Fu, "Virtual assembly of man-machine interactive mechanical seed-metering device based on matter-element identification," *Transactions of the Chinese Society of Agricultural Engineering*, vol. 32, no. 1, pp. 38–45, 2016.

[8] G. Wei and Y. Jin, "Human resource management model based on three-layer BP neural network and machine learning," *Journal of Intelligent and Fuzzy Systems*, vol. 40, no. 2, pp. 2289–2300, 2021.

[9] Y. Xia, "Big data based research on the management system framework of ideological and political education in colleges and universities," *Journal of Intelligent and Fuzzy Systems*, vol. 40, no. 2, pp. 3777–3786, 2021.

[10] M. Johnson, S. Lapkin, V. Long et al., "A systematic review of speech recognition technology in health care," *BMC Medical Informatics and Decision Making*, vol. 14, no. 1, pp. 94–14, 2014.

[11] M. Benzeghiba, R. De Mori, O. Deroo et al., "Automatic speech recognition and speech variability: a review," *Speech Communication*, vol. 49, no. 10-11, pp. 763–786, 2007.

[12] Z. Zhang, J. Geiger, J. Pohjalainen, A. E. D. Mousa, W. Jin, and B. Schuller, "Deep learning for environmentally robust speech recognition: an overview of recent developments," *ACM Transactions on Intelligent Systems and Technology (TIST)*, vol. 9, no. 5, pp. 1–28, 2018.

[13] G. E. Dahl, D. Yu, L. Deng, and A. Acero, "Context-dependent pre-trained deep neural networks for large-vocabulary speech recognition," *IEEE Transactions on Audio Speech and Language Processing*, vol. 20, no. 1, pp. 30–42, 2012.

[14] A. B. Nassif, I. Shahin, I. Attili, M. Azzeh, and K. Shaalan, "Speech recognition using deep neural networks: a systematic review," *IEEE Access*, vol. 7, pp. 19143–19165, 2019.

[15] H. Crompton and D. Burke, "The use of mobile learning in higher education: a systematic review," *Computers & Education*, vol. 123, pp. 53–64, 2018.

[16] R. Wang, M. Li, L. Peng, Y. Hu, M. M. Hassan, and A. Alelaiwi, "Cognitive multi-agent empowering mobile edge computing for resource caching and collaboration," *Future Generation Computer Systems*, vol. 102, pp. 66–74, 2020.

[17] M. Al-Emran, H. M. Elsherif, and K. Shaalan, "Investigating attitudes towards the use of mobile learning in higher education," *Computers in Human Behavior*, vol. 56, pp. 93–102, 2016.

Hindawi
Computational Intelligence and Neuroscience
Volume 2022, Article ID 5634385, 11 pages
https://doi.org/10.1155/2022/5634385

Research Article

Research on Information Leakage Tracking Algorithms in Online Social Networks

Junli Xiong[1] **and Huayi Huang**[2]

[1]*Computer Engineering Technical College (Artificial Intelligence College), GuangDong Polytechnic of Science and Technology, ZhuHai 519090, China*
[2]*School of Computer Science, South China Normal University, GuangZhou 510000, China*

Correspondence should be addressed to Junli Xiong; 2007045@muc.edu.cn

Received 6 July 2022; Revised 29 August 2022; Accepted 5 September 2022; Published 4 October 2022

Academic Editor: Gopal Chaudhary

An online social network is a platform where people can communicate with friends, share information, speed up business development, and improve teamwork. A large amount of user privacy information existing in real social networks is leaked from person to person, and this issue has hardly been studied. With the rapid expansion of the network, the issue of privacy protection has received increasing attention. So far, many privacy protection methods including differential protection algorithms, encryption algorithms, access control strategies, and anonymization have been researched and applied. Information leakage means that the information shared by the user is disseminated or downloaded by his friends without the user's consent, and the transmission of private information will not be recorded. In order to track and find out the ways and methods of information leakage, this article adopts an unusual method, namely, the probability judgment based on trust. By screening the similarities between users, past information exchanges, and the topology of social networks, a trust model is established to evaluate and estimate the degree of trust between users. According to the rating information privacy of friends' trust, an information dissemination system is established, which can be applied to online social networking platforms to reduce the risk of information leakage, thereby ensuring the security of users' private information. At the same time, this paper expands the transmission system model without user authorization and proposes a fingerprint-based deterministic leak tracking algorithm.

1. Introduction

At present, the registration of various software requires the entry of personal information, including private information such as identity information, social relations, and financial transaction information, and the purpose of submitting user-related data information is to confirm the authenticity of their identity information, for example, the current implementation The real-name system is to ensure that users experience it personally, and each step is operated by themselves [1, 2]. And it is precisely this kind of operation that was originally believed to be safe to leak users' information, making the interests of online social network users unable to be protected, as if they may be stolen at any time, and it is urgent to use technological means to protect their interests [3]. However, the research focus of traditional social networks is to protect big data from infringement, and common information leakage methods are not mentioned. Often such violations of privacy cannot be confirmed on social media, and it is difficult to find the source of information leakage [4]. For example, if an individual leaks a secret to another individual and this secret subsequently appears on other platforms, then the culprit of the leaked information is obvious and beyond doubt. But, if multiple people know this secret at the same time, things will become very complicated [5]. Assuming that everyone gets the exact same data at the same time and one of them secretly leaked the secret, it is mathematically impossible to determine whether a person is guilty or not. Therefore, it can be considered that when some people have all the data, but others do not, then the security of the information can be improved by encrypting the data [6]. When many customers

purchase digital rights, data providers provide customers with keys so that they can unlock the encrypted data. However, it is generally believed that the encryption method cannot solve the fundamental problem because it cannot prevent the authorization to view the message while sending it out, and it is impossible to view the downloading of the information and the purpose of the information. This way of disseminating and disclosing information is also impossible to trace the source. We call it unauthorized verbal errors [7]. It is this kind of human-to-human verbal error that has brought unimaginable problems to our research on information leakage algorithms. Therefore, on social networking platforms, the relevant laws used by users should be clarified, that is, no one can spread the information of others by any means for any reason without the permission of others [8].

2. Related Work

Literature proposed a space-based text fingerprinting algorithm, which uses the word spacing of text lines to watermark text documents [9]. The coding technology adjusts the word spacing in the text document so that the average spacing between the lines shows the characteristics of the sine wave, so as to complete the sine wave coding of the information. The watermark is embedded in the horizontal and vertical directions, which has the effect of anti-interference [10]. In addition, the presence or absence of the original image does not affect the recovery of information. Literature analyzes the collusion resistance of the system to the average collusion attack, obtains performance indicators expressed in false negative probability and false positive probability, and derives the upper and lower limits of the maximum number of confluences that can meet the requirements. It is also proved that the detectors used are robust to collusion attacks of different performance [11]. Literature unknowingly inserts it into the low-frequency component of the data by spread spectrum, constructing the watermark into an independent uniform Gaussian random vector and Gaussian flux [12]. Estun introduced a two-layer codeword structure in the code domain to resist high-probability colluders. Literature proposed some digital fingerprint encoding methods for social networks, including tree structure and neighbor hashing. The literature concluded that "out-of-quantity" employees usually have a higher level of the trust relationship and the trust level of members will increase [13]. This paper proposes a trust model based on the degree of trust between online social network users. Existing trust research focuses on strange users, and the premise is that the trust of neighbor users is known. In most social network platforms, the degree of understanding between people is very low. Only through text communication to understand each other, it is impossible to fully understand each other's personality, which leads to mutual understanding of each other on social network platforms [14]. The degree of trust is greatly reduced, so in order to complete this known premise, it is necessary to evaluate the trust between adjacent users. The calculation of user familiarity not only considers the historical interaction frequency between users but also considers the number of mutual friends and the number of public communities. In the system model used this time, there are not only the data related to the network structure but also the user's past communication information on the social network platform. The system model can achieve the diversification of the use of dimensions and also ensure the comprehensiveness and accuracy of evaluation results [15], but the system model of this information leakage algorithm research is not particularly comprehensive, and the degree of research is also limited, so we need a method that enables us to use the existing data and understanding of the network structure to help us. The trust model is quantified, and the influence of the two factors is increased so that the system model can be improved.

3. Related Theoretical Foundations of Privacy Protection Algorithms in Social Networks

3.1. Social Network Model. Social networks are actually composed of two important parameters: nodes (user attributes) and their links (user interaction history). The content of the link is defined by the node according to its theme, interest, and so on (e.g., trade financing, relatives and friends, hobbies, business trade). Figure 1 is a diagram of common social network topology. The social network itself has many characteristics. F is the collection of nodes in the social network, and the fifth is the collection of all social relations. In social networking platforms, a small number of users have more adjacent nodes, which are called central nodes. This node and a large number of nodes around it form a star network structure, as shown in Figure 1.

Online social networks are not only an opportunity but also some risks, such as the theft of users' identity information such as photos or users' messages. For solving these problems, relevant personnel have conducted relevant research and developed corresponding tools to help users better prevent privacy leakage. However, these suggestions still lack a conceptual model, which was first proposed by Aclice et al. The core is equivalent to a framework that weighs more on the privacy risks of social network users. The framework controls the mechanism from the structural attributes and outlines of the social graph to access the relationship. The most typical method is to establish a simulated trust mechanism. Through data information such as user credibility and user interaction, a dynamic trust model is established to protect user privacy and help users make decisions. This paper proposes a hybrid trust model to describe how two users trust each other. This model not only considers the direct and indirect trust between two users but also considers group trust. Trusted groups describe how users are trusted by other users in the group.

(1) The public neighbor node index is defined by the following formula:

$$\mathrm{CN}\left(u_i, u_j\right) = \left|C\left(u_i\right) \cap C\left(u_j\right)\right|. \quad (1)$$

This is the most obvious measure of trust between nodes. The more common the neighbor nodes, the

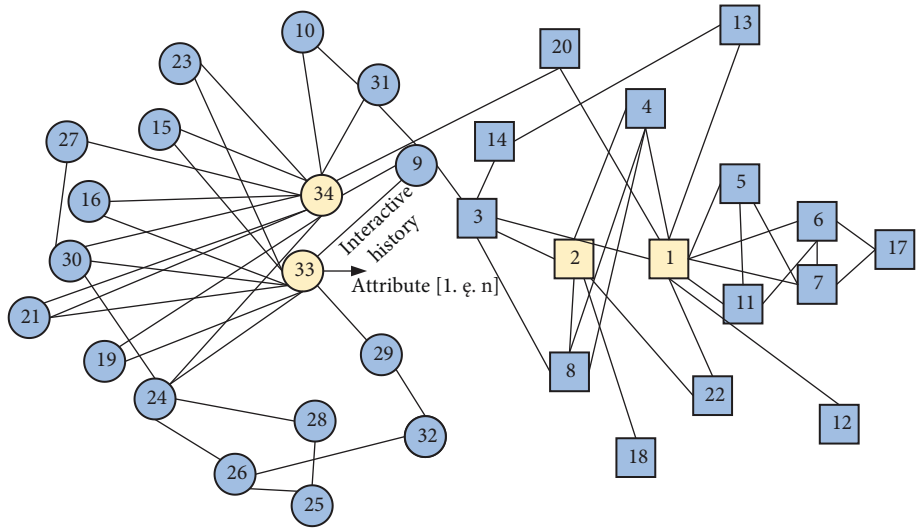

Figure 1: Social network model.

higher the similarity between the two. Simply put, the more tolerant two people meet each other in social situations, the more likely they are to become friends.

(2) Jaccard index is defined by the following formula:

$$\text{Jaccar d}\left(u_i, u_j\right) = \frac{\left|C\left(u_i\right) \cap C\left(u_j\right)\right|}{\left|C\left(u_i\right) \cup C\left(u_j\right)\right|}. \tag{2}$$

In fact, this is a way to correct the calculation of the common neighbor node index, and it is one of the factors that affect the trust value between nodes. Because in some cases, the number of public neighbors may not match the trust value between nodes.

(3) Salton index is defined by the following formula:

$$\text{Salton}\left(u_i, u_j\right) = \frac{\left|C\left(u_i\right) \cap C\left(u_j\right)\right|}{\sqrt{N\left(u_i\right) \times N\left(u_j\right)}}. \tag{3}$$

In summary, the three calculation methods described above are suitable for a wide range, but in addition to using the method based on the network structure to assume the trust between users, the historical interaction between users and the similarity of user attributes should also be considered.

3.2. Hash Mapping Algorithm. Recently, research on hashing in the fields of object retrieval, image matching, and automatic learning has attracted people's attention. Indyk et al. first studied and established the metric hash paradigm based on random projection of cosine similarity. It projects large-size data into a binary hash code and quantifies it. Hash mapping modes can be divided into two categories: independent data and dependent data.

(1) Locally sensitive hash (LSH): The basic principle of the LSH algorithm is to map similar objects (rather than distant objects) to the same storage space with high probability through a series of hash functions. Let S be the domain of all objects and D be the distance function between all objects.

$$\begin{aligned} &\text{if } D(q, p) \le r, \Pr\left[h(q) = h(p)\right] \ge p_1, \\ &\text{if} D(q, p) \ge cr, \Pr\left[h(q) = h(p)\right] \le p_2. \end{aligned} \tag{4}$$

Adjust the parameters to $c > 1$ and $p1 > p2$ and apply LSH to approximate the nearest neighbor search. In this regard, a type of LSH family based on hash criteria is proposed, which is defined as follows:

$$h_{a,b}(v) = \left|\frac{(a * v + b)}{W}\right|. \tag{5}$$

(2) SPH algorithm: in order to solve the random limitation of the LSH method, a machine algorithm with higher coding efficiency is used for calculation. Among them, SPH is considered to be a more effective solution, which handles the training process of the hash code of the sample data and the training process of the hash function of the data separately. We denote the incidence matrix.

$$W(i, j) = \text{rxp}\left(\frac{-\left\|x_i - x_j\right\|^2}{\epsilon^2}\right). \tag{6}$$

For in-sample data, in order to ensure that similar items can be assigned to similar code words and there are enough code words, the mapping matrix R of Z must meet the following conditions:

$$\min_Y: \ tr\left(Y^T L Y\right) s.t. \ y_i \in \{-1, 1\}^k; Y^T 1 = 0; Y^T Y = 1. \tag{7}$$

It is not difficult to see that the above formula is an NP-hard problem, but the vector with the smallest

feature value is selected from L, and then these feature vectors are set aside to obtain a compromise solution, and finally, a binary code is obtained. For out-of-sample data, under the assumption that the data are uniformly distributed, a closed solution can be effectively extended to out-of-sample expansion. The specific operation method is as follows: select the PCA analysis method to find the main characteristics of X and use the rectangle approximate calculation along the PCA direction. The threshold value of the analysis characteristic function is reduced to zero, and the binary code is obtained. However, in the real world, it is difficult for X to meet the assumption of uniform data distribution, so the SPH method is not practical.

$$W(i,j) = \begin{cases} \dfrac{x_i^T x_j}{\|x_i\|} \cdot \|x_j\|, & \text{if } x_i \in N_k(x_j) \text{ or } x_j \in N_k(x_i), \\ 0, & \text{otherwise.} \end{cases} \tag{8}$$

(3) STH algorithm: simply put, the principles of generating hash codes are the same for the two algorithms. In this method, a linear support vector machine (LSVM) is introduced to predict the hash code of out-of-sample data.

$$\min_{w,\xi_i \geq 0}: \ \frac{1}{2}W^T W + \frac{C}{n}\sum_{i=0}^{n} \xi_i \ s.t: \ y_i^{(p)} w^T x_i \geq 1 - \xi_i. \tag{9}$$

Compared with SPH, the expansion of out-of-sample data in STH can ignore the assumption of uniform data distribution. However, the STH algorithm still has two important shortcomings. One is that the two-stage training method does not have the performance of the trial function when performing hash code training, resulting in poor generalization ability. Furthermore, the time cost of SVM-based classifiers in training hash codes bit by bit is immeasurable. Although the SVM classifier can be offline, it is not suitable for high-dimensional large-scale social networks.

(4) LPP algorithm: partially preserved projection: After the original data in the space is dimensionally reduced by the LPP algorithm, the relative change between the data points in the sample is not significant. At the same time, in this algorithm, after assigning an appropriate amount of weighted data points, the difference between most sample points can be enhanced, and feature matching has become more accurate and convenient. LPP is actually a linear transformation. At the same time, suppose the data set $X = [x1, x2, \ldots, xn]$, the purpose is to find a changeable matrix V and map the d-dimensional original data space to the m-dimensional data space. $Y = [y1, y2, \ldots, yn]$, where $y_i = V_{xi}$ represents the data point corresponding to the low-dimensional mapping of xi. The optimized objective function is as follows:

$$\sum_{i,j}(y_i - y_j)^2 W_{ij}, \tag{10}$$

where W is the adjacency matrix, which belongs to the category of a sparse matrix, and its weight can be defined in the following two ways:

(1) Thermonuclear definition

$$W_{ij} = \begin{cases} e^{-\left(\|x_i - x_j\|^2/t\right)}, & \text{if } x_j \in N(x_i), \\ 0, & \text{otherwise,} \end{cases} \tag{11}$$

where N(xi) represents the vectors of all neighbors.

(2) Simplified definition:

If the vector between xi and xj, it is Wij = 1; otherwise, it is Wij = 0. Among them, Wij is set to 1 so that the similarity of the original data in the mapped hash code is close. Assuming that V is a set of transformation vectors, the objective function is simplified to

$$\begin{aligned} \sum_{i,j}(y_i - y_j)^2 W_{ij} &= \sum_{i,j}\left(v^T x_i - v^T x_j\right)^2 W_{ij} \\ &= 2\sum_i v^T x_i D_{ii} x_i^T v - \sum_{ij} v^T x_i W_{ij} x_i^T v \\ &= 2v^T X(D - W)X^T v \\ &= 2v^T XLX^T v, \end{aligned} \tag{12}$$

where D is the diagonal matrix and L is the Laplacian matrix, $L = \mathrm{D} - \mathrm{W}$. The larger the Di, the more important the corresponding Yi, so add a restriction.

$$Y^T \mathrm{DY} = 1 \Rightarrow v^T \mathrm{XD} X^T v = 1. \tag{13}$$

Minimizing the objective function can be expressed as follows:

$$\begin{aligned} &\arg_{v^T XDX^T \min_{v=1}} v^T XLX^T v, \\ &XLX^T v = \lambda XDX^T v. \end{aligned} \tag{14}$$

4. Probabilistic Leaker Judgment Scheme Based on the Trust Model

4.1. Trust Model in Social Networks. Trust is subjective, transferable, and asymmetric. It can be understood as "a person's subjective expectation of another person in the future," which promotes the exchange of information between social network users. Therefore, in the relevant content, the degree of trust between nodes is regarded as one of the important factors of whether they will spread messages between them. The credibility is based on the user's past credibility performance. Therefore, in this section, we will focus on the calculation of trust between neighboring users.

Many users are unwilling to publicly judge the trust level of neighbor users in social networks. In most platforms, the relationship between two points is two-way and can only be

established after confirmation by both parties, such as Facebook and WeChat. But, in other platforms, the node relationship is not bidirectional, and only part can be changed under the premise of mutual attention. Regardless of whether or not, the trust between them is directional but asymmetric. Secondly, the relevant definition and calculation formula of the trust model are proposed. Finally, we will show how to build a trusting social network.

4.1.1. Related Definitions

Definition 1. User similarity: It describes the similarity of attributes and interests among users.

Many studies have proposed similar concepts to express the similarity between objects. The similarity between user Xi and user xj is represented by Sim(Xi, xj).

Definition 2. User interaction: It depicts information that two adjacent users have exchanged before.

The historical interaction information between users has an important influence on the degree of trust between users, such as the frequency of interaction, the number of interactions, and so on. The trust score of interaction between users is expressed as Int(Xi, xj).

Definition 3. Network structure: important structure information between social node pairs. Depicts the influence of the topology map on the trust degree, and the trust value calculated by the social network structure is expressed as NS(ui, uj).

4.1.2. Trust Calculation Model. The trust between all adjacent users is initially equal, and the trust value we evaluate is represented by any two directly connected users in an asymmetric social network T(ui, uj). The comprehensive trust value uj of the user interface is based on the similarity between users. The calculation formula of T(UI, uj) is as follows:

$$T(u_i,u_j)=\alpha\cdot \mathrm{Sim}(u_i,u_j)+\beta\cdot \mathrm{Int}(u_i,u_j)+\gamma\cdot \mathrm{NS}(u_i,u_j), \tag{15}$$

where the values of T(ui, uj), Sim(ui, uj), Int(ui, uj), and NS(ui, uj) are all in the range of 0 to 1.0 means that user ui does not trust user uj at all, that is to say, T(ui, uj) = 1 means full trust, and the larger the value, the higher the trust. The adjustment of the value of α, β, and γ will make the trust model to be optimized along a specific dimension. The attributes in the social network determine the distribution of the specified weight.

We choose factors that have a great influence on the application, not all factors. Next, we will describe the calculation of three important factors affecting trust, in order:

(1) Similarity calculation: The similarity between users in the model includes interest similarity, as well as similarity of different attributes, such as gender, age, educational background, and social background. It is easier to trust each other with similar attributes than without similar attributes. The same is true for similar collaborative filtering algorithms. The calculation formula for the similarity between users is as follows:

$$\mathrm{Sim}(u_i,u_j)=w_1 f\left(A_{u_i1},A_{u_j1}\right)+w_2 f\left(A_{u_i2},A_{u_j2}\right)+\cdots+wnf\left(A_{u_in},A_{u_jn}\right), \tag{16}$$

where n is the number of attributes available in the network and wk is the weight of the similarity between the attributes of user ui and the attributes of user uj, and the value range is 0 to 1. The larger the value, the greater the similarity of the attribute.

The last three formulas in Table 1 are used to calculate the similarity of multivalued attributes. Table 1 lists the user attribute information obtained by using the appropriate similarity calculation formula. Single-valued attributes are calculated by simple comparison and interval ratio.

(2) User interaction computing: a basic feature in social networks. The more interaction between users, the higher the degree of trust between them, and they will think each other is more trustworthy.

$$\mathrm{Int}(u_i,u_j)=\frac{\left|A(u_i,u_j)\right|}{\sum_{u_j\in N}A(u_i,u_j)}, \tag{17}$$

where A (ui, uj) represents the total number of interactions between user ui and user uj, and N is the user's neighbor set. The essence of formula (20) is the ratio of the number of interactions between user ui and user uj to the total number of interactions of user ui.

(3) Social network structure. The structure of a social network can be expressed as N(G, E), where G represents the set of user nodes and E represents the edge of the relationship between users.

$$\mathrm{NS}(u_i,u_j)=\frac{\left(\left|\Gamma(u_i)\cap\Gamma(u_j)\right|\right)+\left(\left|C(u_i)\cap C(u_j)\right|\right)}{\left(\left|\Gamma(u_i)\cup\Gamma(u_j)\right|\right)+\left(\left|C(u_i)\cup C(u_j)\right|\right)}. \tag{18}$$

Calculate the trust between users based on the social network structure, by calculating the mutual friends between users, the user's entry degree (the number of edges pointing to the user), and the exit degree (the number of edges pointing to other nodes). The more mutual friends a user has, the more likely they are to trust each other. The rule of "a common friend is equal to a common neighbor" is also applicable to social networks. After the area is divided, the more common communities owned by users, the higher the degree of understanding. The relationship structure between users is constantly changing with the dynamic network. The interaction history and hobbies between adjacent users are

Table 1: Similarity calculation method.

Calculation	Formula	Description
Simple comparison	S(ui, uj) = 1, if x = y 0, if x≠	x and *y* are the attributes of user ui and uj, respectively
Interval ratio	S(ui, uj) = 1-|x-y|/N	N can be max(|x-y) or manually set
Jaccard coefficient	$J(ui, uj) = \|A(ui) \cap A(uj)\| / \|A(ui) \cup A(uj)\|$	A(ui) and A(uj) are the attribute sets of user ui and uj, respectively
Cosine similarity	$Cos(ui, uj) = \|V(ui) \cap U(uj)\| / \|\|V(ui)\|\|\|V(uj)\|\|$	The vectors V(ui) and V(uj) are the attributes of user ui and uj, respectively
Pearson coefficient	$P(ui,uj) = \sum_{k=1}^{n} (xk - \overline{x})(yk - \overline{y}) / \sqrt{\sum_{k=1}^{n} (xk - \overline{x}) \sum_{k=1}^{n} (yk - \overline{y})}$	xk and yk represent different attributes of user ui and uj, respectively

also constantly changing, so the trust model should be updated regularly.

The trust calculation scheme proposed above is a basic algorithm that can be adjusted to optimize the results of any given network. In fact, because trust is a relatively vague concept, it will be implemented in different ways in the network environment and community environment, so it is unreasonable to apply a set of strict algorithms to all networks. When implementing the algorithm in the network, we should understand the basic characteristics of the network and the acquired data resource information, so as to adjust the implementation of the parameters accordingly. In the following content, we can use the trust value and user credibility to determine the probability of a certain user in a network leakage event.

In fields such as e-commerce, it is often necessary to rate interactions to quantify the credibility of Facebook users. The reputation value in the model of this article is an important factor that affects users' unauthorized communication. In addition, there are more complex evaluation systems. Therefore, we formally give a conceptual definition of reputation.

$$\mathrm{Rp}(u_i) = \frac{1}{n} \sum_{u_j \in N(u_i)} T(u_j, u_i), \tag{19}$$

where N(ui) represents the neighbor set of user ui, and n is the number of users in the N(ui) set.

4.2. The Leaker's Judgment Plan. There are edges between two nodes. The definition of social network topology indicates that they have interacted before and have a higher probability of interaction in the future. In addition, user credibility is also an important factor that affects whether users are willing to disclose information. The publisher-centered information dissemination probability model is based on the weighted trust and reputation social network topology between the trust attributes and the node reputation attributes and calculates the probability of illegal information dissemination for each recipient.

As shown in Figure 2, the user publishes a piece of digital media to the recipient. When digital media is found on the public platform, the user hopes to find the person responsible for the leak. The method proposed in this chapter is to calculate the probability of a user being a recipient of disclosure based on the social attributes in the social network. Figure 2 defines a G-weighted social network topology (the total number of nodes is W). We choose a path of no more than three hops under two factors: first, in reality, more than three hops are less spread; second, the number of users leads to an explosive increase in the computational complexity of each hop.

Build a smaller network topology, including necessary nodes, and reduce the time complexity of path search. Figure 3 is the initial structure of the social network. Figure 4 is a common topology of a small social network. As shown in Figure 4, the first-level nodes are the direct friends of user *D*; the second-level nodes are the friends of user D's direct friends; and so on. As shown in Figure 4, we have established node *D* of the nearest neighbor extension GD. The *D* node can be a user group or user solves U. By three-hop nearest neighbor set intersection extension user set *R* and three-hop nearest neighbor set extension for user U, we can get the network topology of all nodes and can spread information, which we call *G*.

After obtaining the social network topology G' for the search of information propagation paths, we use the DFS method of depth-first search to obtain all paths between two nodes that are less than three hops. Assume that nodes B, K, P, *Q*, and V belong to the receiver user set RI, node N is the message publisher, and node *D* is the unauthorized information receiver U. Then we found all the paths from the user setting RI to unauthorized user U, as shown in Table 2. At this point, we have all possible paths within three hops from the receiving user set Ri to the unauthorized user U (i.e., all message propagation paths). Table 2 just shows a simple idealized example, illustrating that the topology of a real social network is very complicated.

The edge weight W(ni,nj) in the topological graph of Figure 4 represents the probability of the user spreading information. The factors that affect the probability of information dissemination include the degree of trust among users and the credibility of the information. The credibility of information is essentially an important criterion for reflecting whether users will spread information about others without authorization. If there is a directed edge between two nodes, the edge weight W(Ni, Nj) can be calculated by the following formula (similarly, W(Ni, Nj) can be calculated):

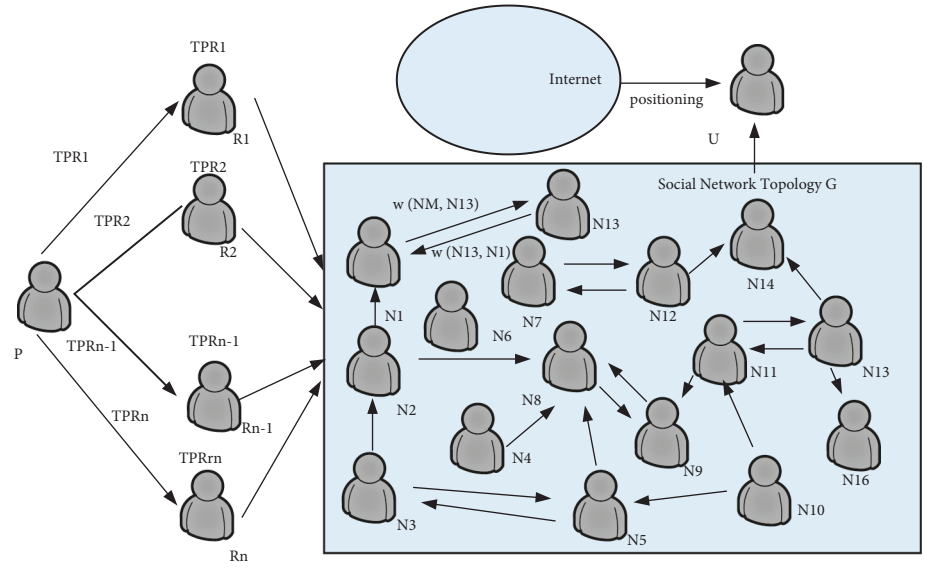

Figure 2: Information disclosure model weighted by trust and honor.

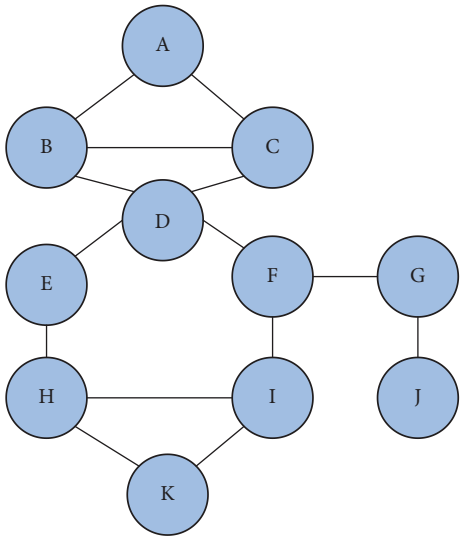

Figure 3: Initial structure of the social network.

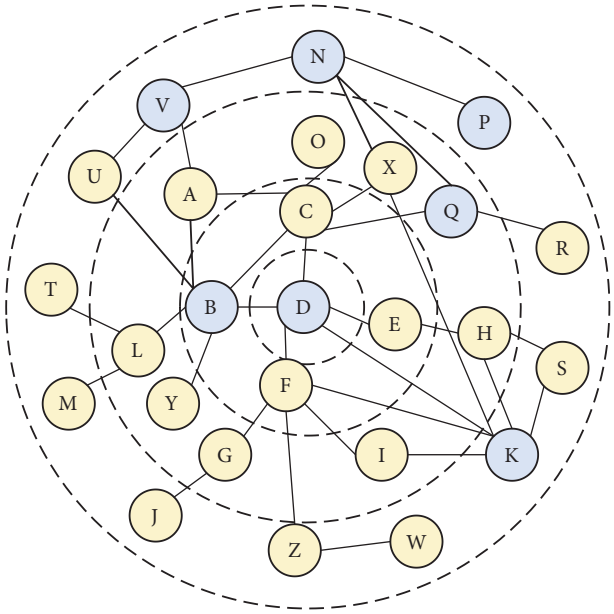

Figure 4: Layered network topology diagram.

$$W(N_i, N_j) = \begin{cases} \dfrac{T(N_i, N_j)}{Rp(N_i)}, \text{if } T(N_i, N_j) < Rp(N_i), \\ T(N_i, N_j), \text{if } T(N_i, N_j) \geq Rp(N_i). \end{cases} \quad (20)$$

When we find a copy of the leaked information, we can directly lock the uploader A of the copy. Transform the problem. In particular, if A is a user in the RI, the leaker can be directly identified. When A is not a member of RI, we perform the following steps to identify the leaker. First, we traverse the social network topology G′=(N′, E′) to find all the paths of the target user u; these paths do not include any other users in the receiver set except Ri.

$$W_j(R_i, U) = \begin{cases} W(R_i, N_x) \times W(N_x, N_y) \times W(N_y, U) \text{if length}(l_{ij}) == 3, \\ W(R_i, N_k) \times W(N_k, U) \text{if length}(l_{ij}) == 2\,(3-7), \\ W(R_i, U) \text{if length}(l_{ij}) == 1. \end{cases} \quad (21)$$

Table 2: Summary of paths within three hops.

	Path 1	Path 2	Path 3	Path 4
Node B	B—D	B—C—D	B—A—C—D	No
Node K	K—D	K—F—D	K—I—F—D	K—H—E—D
Node P	No	No	No	No
Node Q	Q—C—D	Q—C—B—D	No	No
Node V	V—u—B—D	V—A—B—D	V—A—C—D	No

Table 3: The accuracy and time cost of the algorithm for judging the probability of leakage.

Node pair	1	2	3	4	5	6	7	8	9	10
Accuracy	100%	100%	100%	100%	100%	100%	100%	100%	100%	100%
Time overhead (ms)	20,993	37,012	76,505	41,345	10,965	19,688	20,675	11,587	50,049	26,673

By comparing the values of all paths Wj(Rj, U) from Ri to the target user U, the path with the largest weight is found and defined as the weight from the user Ri to the target user U, namely

$$W(R_i, U) = \mathrm{MAX}\{W_j(R_i, U) \mid j \in N*\}. \tag{22}$$

Before judging, we should determine which paths are reasonable, so we define a threshold M that is the average of all information propagation paths. When a certain information propagation path is greater than M, it indicates that the path is reasonable, so

$$W*[R_i, U] = \begin{cases} W(R_i, U), & \text{if } W(R_i, U) \geq M, \\ 0, & \text{if } W(R_i, U) < M. \end{cases} \tag{23}$$

After all the propagation paths are obtained, the probability of a certain user's leakage is obtained by

$$\Pr*(R_i, U) = \frac{W*(R_i, U)}{\sum_{i \in [1,n]} (R_i, U)}, \tag{24}$$

where Pr∗(Ri,U) is the probability of user Ri leaking information.

The judgment algorithm is realized by MATLAB programming. In order to verify the accuracy of the algorithm, we chose the Facebook data set downloaded from the Snap website. The data set contains a total of 4,034 nodes and 88,434 edges. In order to verify the accuracy of the leakage probability judgment algorithm, we can only manually calculate the path between nodes that are less than or equal to two hops. By comparing the leakage probability judgment algorithm to calculate the result of user leakage probability and the result of statistical user manual leakage probability, the accuracy of the algorithm is obtained. At the same time, we calculated the time cost of the leak probability judgment algorithm within 3 hops of 10 pairs of nodes, as shown in Table 3. It can be seen from the table that the accuracy of the user leakage probability algorithm can reach 100%, and the time cost is within an acceptable range.

5. Deterministic Leaker Tracking Scheme Based on Digital Fingerprints

5.1. System Model. Digital fingerprints can effectively solve the increasingly concerned digital copyright issue. Therefore, the research on digital fingerprints is of great significance. At present, there are two main research directions for digital fingerprints: one is the information (such as text) itself, which uses algorithmic information to get a fingerprint. When it is found that the fingerprint generated by a suspicious leak is the same as the suspicious version, then a similar method is used to judge whether there is plagiarism between documents. The other is to obtain a digital fingerprint through the field of digital copyright and incorporate it into digital media technology to track leakers. The fingerprint here is a non-specific fingerprint, which is a binary sequence added in the form of a digital watermark. Every digital media purchased by consumers has a unique digital fingerprint. When piracy occurs, it can be traced back to the source of the leak accurately. Compared with traditional digital fingerprints, the differences between digital fingerprints in social networks are as follows.

Traditional digital fingerprint coding can even be applied to more than one million users, but it is ahead of the user level of social platforms. Therefore, the existing digital fingerprint coding cannot provide the uniqueness of fingerprint codes for such a large number of user networks. The fingerprint identification system not only embeds fingerprints into multimedia content but also has a series of codes and corresponding tracking algorithms for identity traitors. The basic system model of the digital fingerprint tracking scheme is shown in Figure 5. The publisher sends the information Z to each recipient, which includes many versions of different types of information. If illegally copied information is detected, the leaker can be identified by the difference in fingerprints. Input a code word w' and output at least one leaker, so traditional digital fingerprint coding is not suitable for digital fingerprint coding in social networks.

5.2. Digital Fingerprint Detection and Simulation Results and Analysis. Hash BF digital fingerprint coding scheme still has a challenging and urgent problem: the large-scale fingerprint set makes fingerprint detection and tracking very difficult or even impossible. However, it is still an arduous task to distinguish the distance between fingerprints of all users using the traditional linear search method. The digital fingerprint code word proposed in this paper is a binary sequence. Compared with the traditional high-dimensional data search, the efficiency is extremely low, and the efficiency

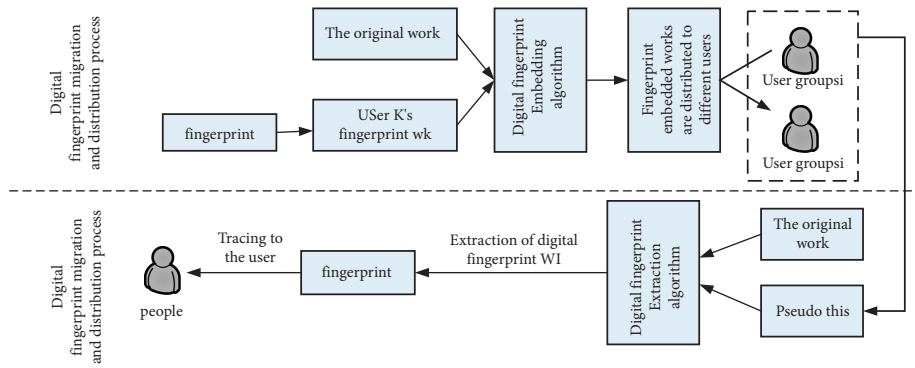

Figure 5: Digital fingerprint scheme system model.

Table 4: Digital fingerprint index table.

Hash code (ordered)	Random sequence code	User ID
0x2DF3C9EA	0xAFB68CD7	94. vv
0x2DF3C9EA	OxFB6EE3D7	Kk. 66
0x2DF3C9EB	0xAD68CD7F	Hk. . . . . .ki
0xFFE2A97 C	0xAFB64CD7	54. . . . . .gr
0xFFE2A97D	OxBF6E8AD7	Rt. 6g

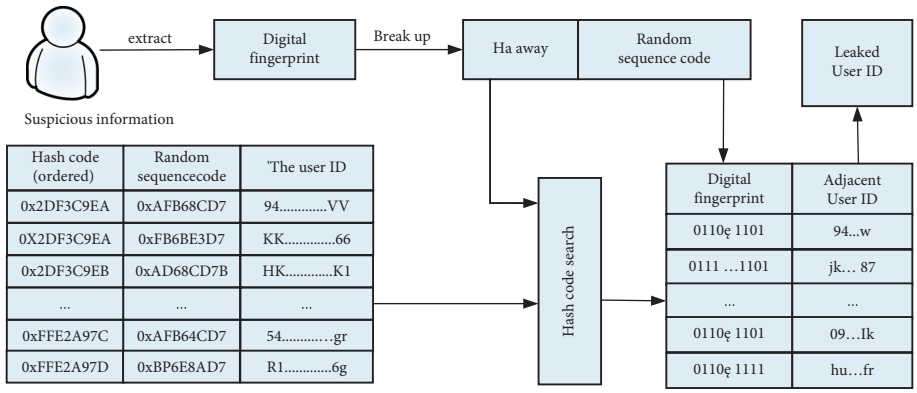

Figure 6: Information leakage tracking flowchart.

and accuracy are further improved. We build an index table based on the user's digital fingerprint and user ID. The format of the index table is shown in Table 4, where the hash codes are sorted. For the hash code sorting index table, dichotomy can be used to quickly find the nearest neighbor set of the target user's hash code. We can appropriately expand the search range and search the user ID and complete fingerprint sequence in the obtained nearest neighbors.

Search the binary index table to find the closest hash code and extract the corresponding fingerprint and user identifier. The specific process is to compare each user's fingerprint with the nearest target fingerprint. The user with the smallest distance is considered to be the culprit. Convert table content into image content; the image is shown in Figure 6:.

(1) In order to verify the feasibility and performance of the Hash BF fingerprint allocation algorithm, we downloaded three sets of social media data from the Stanford University SNAP1 website for simulation experiments, namely Facebook, Twitter, and Google+. The content of the data set is formatted as a TXT file, which contains the nodes in the social network and the edges between nodes. The former is not directed, and the latter two are directed. The specific data set size is shown in Table 5.

(2) In order to verify the performance of the GLPP algorithm in maintaining the structural characteristics of the social network, a twofold cross-validation method is used for experiments.

(3) We use DCT intermediate frequency digital algorithm and its corresponding Filipe extraction algorithm to verify the accuracy of the Hash BF algorithm in actual fingerprint scenes and conduct diving and fingerprint code extraction experiments. After extracting the fingerprint from the suspicious copy, the fingerprint is divided into two parts: hash

Table 5: Social network data set attributes.

Data set	Number of nodes	Number of edges	Do you want to report back?	Number of communities
Facebook	4,039	88,234	No	10
Twitter	81,306	1,768,149	Yes	1,000
Google+	107,614	13,673,453	Yes	133

code and binary random sequence code. Then we compare the distance between Hamming and the user's hash code to find all the neighbors closest to the whistleblower. The calculation methods of accuracy and recall are as follows:

$$\begin{cases} \text{precision} = TP(TP + FP), \\ \text{recall} = TP(TP + FN). \end{cases} \tag{25}$$

So far, we have only maintained the nearest neighbor performance of our algorithm under different d values. In order to show the performance advantages of our algorithm over other classic algorithms, we also selected the Twitter data set in the experiment and set the d value to 0.

Traditional privacy research has not kept pace with the times. The scheme introduced in this article first searches the nearest neighbor set and then searches the nearest neighbor set according to the binary random sequence code. The specific process is to compare each user's fingerprint with the Hamming distance of the target fingerprint in the nearest neighbor set. The user with the smallest Hamming distance is judged as a leaker. In our Google+ social network collection, we randomly select from 10,000 to 100,000 nodes for the experiment, where we selected 10 times the threshold, Hamming distance d=3, and hash code and binary random sequence code length of 64 bits.

6. Conclusion

In online social networks, the traditional research on privacy protection is mainly to prevent information from being intercepted by intruders during transmission. This can be achieved by implementing multiple encryption methods. Probabilistic judgment based on trust is the most commonly used privacy protection method for information leakage. With the continuous development of the Internet age, the speed of information dissemination has also increased, and many people have applied anonymization and differential algorithms to protect their privacy. However, few people study or write articles on common leakage methods. Perhaps it is too common. Most people do not have the confidence to find a way to crack or prevent information leakage. In the real world, if a publisher publishes digital content on a certain platform, then the user who receives the content may be one person or multiple people because, once the information is disclosed, it is equivalent to being placed. In the eyes of many people in society, everyone can see, so the data cannot be protected. Once users publish digital content (assuming that private information is not invaded by intruders), if unauthorized information is detected to be spread, the source of the leakage must be traced. So far, many privacy protection methods including differential protection algorithms, encryption algorithms, access control strategies, and anonymization have been researched and applied. This article also introduces the trust degree model and the encryption protection of private information, hash mapping, and digital fingerprint algorithms and uses the several methods mentioned in the former, and constructs a weighted social network topology based on trust on the premise of several methods mentioned previously. The shortest path algorithm is backed by the calculation probability, and an information release system for user security classification and information sensitivity classification has been established. With an attitude that can reduce the risk of information leakage and maintain the security of private information, a comprehensive system has been developed and improved; thereby, it can effectively reduce the risk of user information being leaked. While ensuring that user information is not leaked, it can also ensure the normal operation of the online social system so that the interests of online social users are protected. The system solves the urgent need for online social network users and platforms, also blocks the illegal path of bad elements, and promotes the operation and development of the network social system on a normal track.

Data Availability

The data used to support the findings of this study are available from the corresponding author upon request.

Conflicts of Interest

The authors declare that they have no conflicts of interest.

Acknowledgments

This work was supported by the "Double High Plan" construction project of Guang Dong Polytechnic of Science and Technology's Software Technology Specialty Group, the construction project of the national vocational education teaching innovation team, and the school-level scientific research project (No.: xjjs202004).

References

[1] Z. Qu, P. He, and L. Hou, "Studies on internet real-name system and network action surveillance system," *International Conference on E-Health Networking Digital Ecosystems and Technologies*, vol. 1, pp. 469–472, 2010.

[2] K. Shang and G. U. O. Qing, "Analysis of the real-name system of express delivery in China," *Studies in Sociology of Science*, vol. 7, no. 5, pp. 21–25, 2016.

[3] K. Buhmann, "Business and human rights: analysing discursive articulation of stakeholder interests to explain the consensus-based construction of the'Protect, respect, remedy UN framework," *International Law Research*, vol. 1, no. 1, p. 88, 2012.

[4] K. Martin, "The penalty for privacy violations: how privacy violations impact trust online," *Journal of Business Research*, vol. 82, pp. 103–116, 2018.

[5] N. Kökciyan and P. Yolum, "PriGuard: a semantic approach to detect privacy violations in online social networks," *IEEE Transactions on Knowledge and Data Engineering*, vol. 28, no. 10, pp. 2724–2737, 2016.

[6] O. M. Awad Al-Hazaimeh, "A new approach for complex encrypting and decrypting data," *International journal of Computer Networks & Communications*, vol. 5, no. 2, pp. 95–103, 2013.

[7] E. Hillin and R. W. Hicks, "Medication errors from an emergency room setting: safety solutions for nurses," *Critical Care Nursing Clinics of North America*, vol. 22, no. 2, pp. 191–196, 2010.

[8] E. C. Tandoc and J. C. B. Lee, "When viruses and misinformation spread: how young Singaporeans navigated uncertainty in the early stages of the COVID-19 outbreak," *New Media & Society*, vol. 24, no. 3, pp. 778–796, 2022.

[9] A. Amir, A. Apostolico, G. M. Landau, and G. Satta, "Efficient text fingerprinting via Parikh mapping," *Journal of Discrete Algorithms*, vol. 1, no. 5-6, pp. 409–421, 2003.

[10] C. Y. Chan, H. I. Yu, W. K. Hon, and B. F Wang, "Faster query algorithms for the text fingerprinting problem," *Information and Computation*, vol. 209, no. 7, pp. 1057–1069, 2011.

[11] M. Rezvani, A. Ignjatovic, E. Bertino, and B. F. Jha, "Secure data aggregation technique for wireless sensor networks in the presence of collusion attacks," *IEEE Transactions on Dependable and Secure Computing*, vol. 12, no. 1, pp. 98–110, 2015.

[12] E. Yen and L. H. Lin, "Rubik's cube watermark technology for grayscale images," *Expert Systems with Applications*, vol. 37, no. 6, pp. 4033–4039, 2010.

[13] S. K. Rajput and O. Matoba, "Optical multimodal biometric encryption that uses digital holography," *Journal of Optics*, vol. 22, no. 11, Article ID 115703, 2020.

[14] N. F. Kolan, N. Jailani, M. Abu Bakar, and R. Latih, "Trust model based on Islamic business ethics and social network analysis," *International Journal of Advanced Science, Engineering and Information Technology*, vol. 8, no. 6, pp. 2323–2331, 2018.

[15] Q. He, X. Wang, F. Mao et al., "CAOM: a community-based approach to tackle opinion maximization for social networks," *Information Sciences*, vol. 513, pp. 252–269, 2020.

Hindawi
Computational Intelligence and Neuroscience
Volume 2022, Article ID 7423411, 12 pages
https://doi.org/10.1155/2022/7423411

Research Article

Cloud Computing Image Processing Application in Athlete Training High-Resolution Image Detection

Hongtao Li

Physical Education College of Xiangnan University, Chenzhou, Hunan 423000, China

Correspondence should be addressed to Hongtao Li; chenli@xnu.edu.cn

Received 8 July 2022; Revised 12 September 2022; Accepted 19 September 2022; Published 3 October 2022

Academic Editor: Gopal Chaudhary

The rapid development of Internet of things mobile application technology and artificial intelligence technology has given birth to a lot of services that can meet the needs of modern life, such as augmented reality technology, face recognition services, and language recognition and translation, which are often applied to various fields, and some other aspects of information communication and processing services. It has been used on various mobile phone, computer, or tablet user clients. Terminal equipment is subject to the ultralow latency and low energy consumption requirements of the above-mentioned applications. Therefore, the gap between resource-demanding application services and resource-limited mobile devices will bring great problems to the current and future development of IoT mobile applications. Based on the local image features of depth images, this paper designs an image detection method for athletes' motion posture. First, according to the characteristics of the local image, the depth image of the athlete obtained through Kinect is converted into bone point data. Next, a 3-stage exploration algorithm is used to perform block matching calculations on the athlete's bone point image to predict the athlete's movement posture. At the same time, using the characteristics of the Euclidean distance of the bone point image, the movement behavior is recognized. According to the experimental results, for some external environmental factors, such as sun illumination and other factors, the image detection method designed in this paper can effectively avoid their interference and influence and show the movement posture of athletes, showing excellent accuracy and robustness in predicting the movement posture of athletes and action recognition. This method can simplify a series of calibration tasks in the initial stage of 3D video surveillance and infer the posture of the observation target and recognize it in real time. The one that has good application values has specific reference values for the same job.

1. Introduction

The proposal of mobile cloud computing (MCC) provides new solutions to application requirements [1]. MCC uses the wireless network to offload the application tasks of the mobile terminal to the cloud with stronger computing power for execution, which can solve the problem of insufficient terminal computing power and reduce terminal energy consumption [2]. The cloud server position relative to the location of the user terminal, compared with the traditional server further, rather than the location of the user key network is usually far away, so if we want to realize the customer terminal and exchange data with the cloud server, data transmission can take place not only in the process of extension of time but also in the process of data exchange and resource transmission [3] with the increase of energy consumption. Moreover, for many specific applications, such as voice recognition and intelligent environment control, a long time delay will damage the user experience and affect the performance of related applications.

In order to solve the above shortcomings of mobile cloud computing, the European Telecommunications Standards Institute proposed a new type of computing and storage service technology called mobile edge computing (MEC). As a core technology of 5G, MEC can more effectively address users' needs for specific application services, such as high computing power, storage, reliability, and mobility and low latency, by deploying servers at edge locations closer to users, such as nearby gateways and base stations [4]. The MEC network is used to migrate the computing tasks of

geographically dispersed users from mobile terminal devices to resource-rich MEC servers, thereby speeding up the execution of tasks. However, due to the limitation of the communication capacity of the mobile edge computing network and computing resources and the storage capacity of the MEC server, if too many computing tasks are offloaded at the edge, the limited computing resources will bring huge burden to the MEC servers and the user expansion of network transmission and edge computing services expansion of edge computing services [5]. The athlete's motion posture tracking estimation and action recognition method based on the local image features of the athlete's bone points can effectively represent the athlete's motion posture [6]. If the 3D depth video capture technology is used in the experiment to capture the athletes' motion data, the depth image of the movement can be obtained, and the influence of the external environment and other lighting on the experimental results can be avoided to a certain extent so that the accuracy of athletes' motion image detection can be achieved, and more accurate and effective recognition effect can be obtained [7].

2. Related Work

Kuang et al. studied the problem of multiuser computing offloading in a dynamic environment. Taking into account the channel interference problem when multiple IoT devices offload computing tasks through the wireless channel at the same time, this research formulates the user's computing offloading decision problem as an evolutionary game model and designs an evolutionary game algorithm based on reinforcement learning used to solve the user's unloading decision [8]. Yuan et al. studied the problem of computing offloading based on the vehicle edge computing network. Considering that the vehicle needs to determine its task offloading strategy in real time in a dynamic network environment, this research proposes a multiuser noncooperative computing offloading game to adjust the task offload probability of each vehicle in the vehicle edge computing network and consider the vehicle at the same time, , while taking into account the distance from the vehicle to the edge computing access point. Furthermore, the research constructed a distributed optimal response algorithm based on the computational unloading game model to maximize the utility of each vehicle [9]. Chen et al. constructed the user unloading problem under the three-tier architecture suitable for mobile and computing scenarios and proposed a distributed balanced computing algorithm to determine the user's computing task unloading decision [10]. Lin et al. studied the problem of multiuser computing offloading of mobile cloud computing in a dynamic environment [11]. Taking into account the problems in the user's free calculation process, it is finally determined that the user's personal privacy rights are settled. Zhang et al. proposed the joint offloading optimization problem of mobile edge computing and cloud computing and designed offloading scheduling and load balancing schemes based on game theory. However, this survey only models and optimizes users' offloading decisions under a hierarchical framework. Edge/cloud computing and communication resource allocation have not yet been optimized [12]. The above-mentioned related studies have given some solutions to the user task offloading decision-making problem, but these studies mainly focus on the user's offloading decision-making problem, ignoring the limited communication and computing resource allocation of the system during the offloading process [13]. In view of the problems in the above research, Yousafzai et al. studied the problem of computing offloading of multiple channels and multiple users under the wireless channel interference environment based on mobile edge-cloud computing, and we jointly studied the problem of computing cloud resource allocation [14]. In order to minimize the energy consumption of users' mobile devices in mobile edge computing systems, Ren et al. proposed a universally available corresponding optimization strategy, which can be applied in computing offloading calculation, resource allocation, and subcarrier allocation [15]. The limited score algorithm has been modified to find the best global solution. The literature proposed a scheme of partial offloading and resource allocation of common user computing tasks, in order to minimize the latency caused by all executions; the required energy consumption, partial offloading, and resource allocation constraints are also investigated. In order to minimize energy consumption and delay, Larson et al. proposed a three-step algorithm: jointly optimizing the offloading decision, calculating user tasks, and allocating communication resources, consisting of semideterministic relaxation, alternate optimization, and continuous adjustment, generated by performing tasks for all users [16]. In this paper, the cost and operation delay of user computing offloading for mobile edge computing are analyzed in depth. In order to reduce the cost of mobile device system and the delay caused by execution as much as possible, this study proposes a multifunctional computing offloading and resource allocation algorithm to jointly optimize the offloading determination and resource allocation of edge users [17]. Reference is oriented to the computing tasks of fog nodes in the industrial Internet of things scenario, with the goal of minimizing energy consumption of fog nodes, so an energy-saving computing offloading scheme is proposed, with comprehensive consideration of fog node energy consumption, local computing, transmission status, and energy consumption in the waiting state [18]. Aiming at the problem of minimizing energy consumption, the research proposed an accelerated gradient algorithm that can quickly find the optimal task offload ratio, thereby improving the convergence speed of the traditional method. This paper designs an algorithm framework that can realize energy-saving offloading. This framework is based on mobile edge computing, which can not only optimize wireless communication resources but also improve the performance of computing resources to a large extent. In addition, in order to reduce the energy consumption of the user system as far as possible, based on the greedy algorithm with the Gini coefficient as a variable, the use of computing resources and operation speed are improved, and an intelligent algorithm system is developed that can greatly reduce the energy consumption of the user when using the client without increasing other

consumption. At the same time, this paper also studies the MEC energy-saving calculation program based on a 5G heterogeneous network and its corresponding offloading mechanism. The energy consumption of the system is controlled by jointly optimizing the task unloading program and the wireless resource allocation structure. The 5G network has a unique structural feature; its multiple access can meet the new information transmission form, and combined with the unique nature of this network structure and based on the study of the relevant network transmission structure, this paper designs an energy-saving algorithm, namely, energy-efficient computing and offloading (EECO) algorithm. The literature studied the problem of joint user offloading decision-making and resource optimization at the edge or near-end cloud and proposed a heuristic offloading decision algorithm to improve the utility of the system. However, the above research only considers that user tasks are only offloaded to the edge or the cloud and does not consider the strategy of how users perform offloading and the optimization of resources in the environment of edge-cloud joint computing.

3. Research on Cloud Collaborative Multiuser Computing Task Migration

3.1. Local Calculation. This article defines the set of the number of users covered by MeNB as $U = \{1,2,...,U\}$, where uU represents a certain user in the user set. Each user can choose one of the following task execution modes: local computing, which uses local terminal equipment to process tasks; edge computing, in which after offloading tasks to MeNB through the cellular network the tasks will be processed by the edge computing server; and cloud computing, in which tasks are offloaded to MeNB through the cellular network first and then forwarded to the remote cloud server through the core network. In addition, this paper also defines the decision variables for task offloading.

When the user chooses to offload the task to the edge and the cloud, the total time to complete the task includes (1) the time $t_u^{up(e)}$ required for the user to upload the computing task to MeNB, (2) the execution time $t_u^{exe(e)}$ of the user task in MEC, and (3) the time to transmit the result of task completion from MEC to the user equipment. It is assumed that tasks can be unloaded and uploaded to the cloud for a series of uninstallation operations. The time required to upload tasks to the total server is the total time consumed by the whole task process from the start to the end. Considering the downlink transmission, overall, the output of the task is very small compared to the input size of the task.

The speed is much higher than the uplink speed, so this article ignores the time for the task to be transmitted from the cloud to MEC and the time for MEC to be transmitted to the user equipment. This article considers that the user network is a multiuser orthogonal frequency division multiple access system when uploading. Each channel in the system is orthogonal, so the interference in the cell can be ignored. Define B as the uplink bandwidth of the wireless link of the system, then the available uplink bandwidth $W = B/N$ for each user, where N is the number of users in the cell. Thus, the uplink transmission rate of task T_u for user u is

$$R_u(p_u) = Wlb\left(1 + \frac{p_u h_u}{\sigma_0^2}\right), \tag{1}$$

where p_u represents the transmit power when the input of the upload task of user u is d_u, which is a positive number and does not exceed the maximum allowed value P_u, namely, $0 < p_u \le P_u$; h_u represents the cellular uplink channel gain between user u and the base station; and σ_0^2 represents the transmission background noise power. According to formula (1), the uplink transmission time $t_u^{up(e)}$ for the user u to unload the task T_u to MeNB is

$$t_u^{up(e)} = \frac{d_u}{R_u}. \tag{2}$$

Next, it is necessary to calculate the program runtime spent by user U to perform the uninstall task in MEC. This article represents the highest degree limit of computing resources for MEC servers, that is, the number of CPU cycles available in all edge servers. For all end users who issue requests and need to unload tasks and transfer them to the MEC server for computing, they can obtain the computing resources of the MEC server to run the resources in the cloud and share them with the uninstaller. fe^u is defined as the size of the computing resource allocated to the user u offloaded to the edge through the MEC server and must be greater than 0, that is, $fe^u > 0$. However, the computing resources of MEC server are not unlimited, but the highest limit of computing. Therefore, when the actual unloading of resources occurs, the constraints need to be met. When the system is uninstalling, it cannot complete all tasks, and there is always a certain limit., that is, the upper limit of computing resources of the cloud server that needs to be lower than that of the MEC server, which can be expressed as follows:

$$\sum_{u \in u_e} f_u^e \le f^e. \tag{3}$$

According to the calculation resource size f_u^e allocated by the MEC server, it can be concluded that the calculation time $t_u^{exe(e)}$ of task T_u on the MEC server is

$$t_u^{exe(e)} = \frac{C_u}{f_u^e}. \tag{4}$$

According to formulae (3) and (4), it can be concluded that when the user transmit power p_u is given, the total delay for the user to select the edge computing mode to perform task offloading is

$$t^e_{u=t_u^{up(e)}+t_u^{exe(e)}}. \tag{5}$$

The energy consumption E_u^e generated by the user through the margin calculation mode is

$$E_u^e = p_u \frac{d_u}{R_u}. \tag{6}$$

3.2. Cloud Computing. When the user selects the cloud computing mode to perform task offloading, it is assumed that the size of computing resources allocated by the cloud to the offloading task is f_u^c. Although the cloud has very rich computing resources, because the number of task requests that require remote cloud computing is very large, the cloud will allocate fixed and limited computing resources to each user. This article assumes that f_u^c is fixed and is equal to the maximum value of computing resources that the cloud can allocate to users. Therefore, similar to formula (6), the computing time $t_u^{exe(c)}$ of the user task in the cloud can be obtained as

$$t_u^{exe(c)} = \frac{C_u}{f_u^c}. \tag{7}$$

Considering that the execution of user tasks in the cloud needs to be transmitted to the remote cloud server through the core network, it can be concluded that the total upload delay of task uninstallation when the cloud execution mode is selected is

$$\begin{aligned} t_u^{up(c)} &= t_u^{up(e)} + t_u^{up(ec)} \\ &= \frac{d_u}{R_u} + \frac{d_u}{R_u^c}, \end{aligned} \tag{8}$$

where $t_u^{up(e)}$ is the time for the task to be offloaded from the user equipment to MeNB, $t_u^{up(ec)}$ is the time for the task to be transmitted from MeNB to the cloud, and $t_u^{up(ec)}$ is the transmission rate allocated by the core network to the user u. Considering that the total transmission bandwidth of the core network is limited, R_u^c satisfies the constraints shown in the following:

$$\sum_{u \in u_c} R_u^c \le R^c. \tag{9}$$

According to formulae (8) and (9), it can be concluded that the total delay for users to choose the cloud computing mode to perform task offloading is

$$t_u^c = t_u^{up(c)} + t_u^{exe(c)}. \tag{10}$$

Since the user only consumes energy when uploading tasks to MeNB, the energy consumption generated by the user through the cloud computing mode is

$$\begin{aligned} E_u^c &= E_u^e \\ &= p_u \frac{d_u}{R_u}. \end{aligned} \tag{11}$$

3.3. System Utility Maximization Problem Based on Edge-Cloud Joint Computing. Under the edge-cloud joint computing framework, the user's QoE is mainly reflected by the delay and energy consumption in completing tasks. Based on the above content, the uninstallation model and user preferences can be calculated in each mode. This article defines the uninstallation utility function using u as

$$\begin{aligned} V_u = {} & x_{u,1}\left(\beta_u^t \frac{t_u^l - t_u^e}{t_u^l} + \beta_u^e \frac{E_u^l - E_u^e}{E_u^l}\right) \\ & + x_{u,2}\left(\beta_u^e \frac{t_u^l - t_u^{ce}}{t_u^l} + \beta_u^e \frac{E_u^l - E_u^c}{E_u^l}\right), \end{aligned} \tag{12}$$

where β_u^t and β_u^e, respectively, represent the user's preference weight for the time delay and energy consumption to complete the task and β_u^e, $\beta_u^t \in [0,1]$, $\beta_u^e + \beta_u^t = 1$. For example, when the user u's device battery can be used for a short period of time, the user will prefer to increase the value of β_u^e to save power at the expense of time delay. Based on the above-mentioned unloading utility function of user u, this paper defines the system utility function as $V = \sum_{u=1}^{U} V_u$.

The above-mentioned system utility function model involves the allocation of communication resources, edge server computing resources, and cloud transmission resources. It not only considers the utility of users but also pays attention to the resource allocation of resource providers. Therefore, this paper expresses the system utility maximization problem based on edge-cloud joint computing as

$$\begin{aligned} & \max_{f,x,p,R} V = \sum_{u=1}^{U} V_u \\ & s.t.C1:\ x_{u,j} = \{0,1\}, u \in U, j \in \{1,2\}, \\ & C2:\ 0 < p_u \le P_u, \forall_u \in U, \\ & C3:\ \sum_{u \in U_e} f_u^e \le f^e, \\ & C4:\ f_u^e > 0, \forall_u \in U_e, \\ & C5:\ \sum_{u \in U_c} R_u^c \le R^c, \\ & C6:\ R_u^c > 0, \forall_u \in U_c. \end{aligned} \tag{13}$$

By optimizing the offloading decision X, and optimizing the communication resources and computing resources at the same time, the synergistic effect of the two can be achieved, and the peak value problem of the above system utility can be solved. Since the unloading decision x is a 0-1 integer vector and f, p, and R are continuous vectors, the optimization problem of formula (14) is an MINLP. Considering the expression structure of the optimization problem, when the value of the unloading decision x is given, the original optimization problem with higher complexity

can be decomposed into the main problem with lower complexity and a series of subproblems. Therefore, the problem shown in formula (13) can be transformed into

$$\max_{x} \max_{R,f,p} \sum_{u\in U_e\cup U_c} V_u s.t.\, C1 \sim C6. \tag{14}$$

Since the constraints $C1$ of unloading decision and $C2$–$C6$ of resource allocation policy are separable, the optimization problem shown in formula (14) can be decomposed into the main problem and subproblem, as shown in the following formulae, respectively:

$$\max_{x} V^* \quad s.t. C1, \tag{15}$$

$$V^* = \max_{R,f,p} \sum_{u\in U_e\cup U_c} V_u s.t.\, C2 \sim C6. \tag{16}$$

Decomposing the optimization problem of formula (14) into the optimization problems of formulae (15) and (16) does not change its optimal solution. Next, this article will give the optimization problems of formulae (15) and (16), respectively, and finally solve the problem of formula (17).

3.4. Joint Optimization of the Edge-Cloud Resource Method. According to the form of formula (13), when the unloading decision x is given, the optimization problem of formula (17) can be transformed into

$$\max_{R,f,p} V(x,p,f,R) = \max_{R,f,p} \sum_{u\in U_e\cup U_c} \left(\beta_u^t + \beta_u^e\right) - I(x,p,f,R), \tag{17}$$

where $I(x,p,f,R)$ is

$$I(x,p,f,R) = \sum_{u\in U_e} \left(\beta_u^t \frac{t_u^e}{t_u^l} + \beta_u^e \frac{E_u^e}{E_u^l}\right) + \sum_{u\in U_e} \left(\beta_u^t \frac{t_u^c}{t_u^l} + \beta_u^e \frac{E_u^c}{E_u^l}\right). \tag{18}$$

When the unloading decision x is given, $\sum_{u\in U_e\cup U_c}(\beta_u^t + \beta_u^e)$ is a constant, so formula (18) can be transformed into an $I(x,p,f,R)$ minimization problem, namely,

$$\min_{p,f,R} I(x,p,f,R) s.t. \quad C2 \sim C6. \tag{19}$$

According to formulae (1)~(19), we can get

$$I(x,p,f,R) = \sum_{u\in U_e\cup U_c} \frac{\varnothing_u + \varphi_u p_u}{lb(1+p_u\gamma_u)} + \sum_{u\in U_e} \frac{\beta_u^t f_u^l}{f_u^e} + \sum_{u\in U_c} \frac{\beta_u^t f_u^l}{f_u^c} + \sum_{u\in U_c} \frac{\beta_u^t d_u f_u^l}{c_u R_u^c}, \tag{20}$$

where $\varnothing_u = \beta_u^t d_u / t_u^l W$, $\varphi_u = \beta_u^t d_u / E_u^l W$, and $\gamma_u = h_u/\sigma_0$.

According to the form of formula (20), it can be found that when the uninstallation strategy x is given, the third term on the right side of the equal sign in formula (20) is a constant.

3.5. Analysis of Simulation Results. The P_u^l corresponding to the computing power of the user equipment selected in this paper is {0.5 W, 0.75 W, 0.9 W}. If the user's maximum transmission power $P_u = 100$ mW, the total uplink transmission rate from MeNB to the cloud is $R^c = 100$Mbit/s. Other relevant simulation parameter settings are shown in Table 1.

Under the same parameter settings, this section chooses to compare the system utility performance of the user offloading strategy based on the edge-cloud joint computing solution proposed in this paper with the following solutions:

(1) Local computing: all users use local computing to complete tasks.

(2) Total offloading strategy of joint resource optimization based on edge computing: all users offload tasks to the edge for execution and adopt an optimized resource allocation plan.

(3) Total offloading strategy of joint resource optimization based on cloud computing: all users offload tasks to the cloud for execution and adopt an optimized resource allocation plan.

Without loss of generality, the simulation results are the results of each simulation experiment repeated 1,000 times and averaged.

The system utility value of each program will change with the change of the number of users, and the trend of each program is shown in Figure 1. The overall observation and analysis of Figure 1 shows that the system utility value of the solution designed in this paper has made great progress and is relatively stable when compared with that of other similar schemes under various states with the increase of the number of users. Except for the local calculation scheme, when the number of users is at a low level, the relationship between the system utility value of the other three schemes and the number of users is in direct proportion, and the system utility value of the solution in this paper is better than that of the other two schemes. The graph shows that the system utility value of the local calculation scheme is always 0. And when the number of users is once more than a given

Table 1: Simulation parameter settings.

Parameter name	Value
System bandwidth B (MHz)	20
Path loss model	128.1 + 37.5lg10(d)
Background noise σ_0^2 (dBM)	100
Standard deviation of lognormal shadow fading (dB)	10
Edge computing resources f^e (GHz)	20
Computing resources allocated to users in the cloud f_u^c (GHz)	5

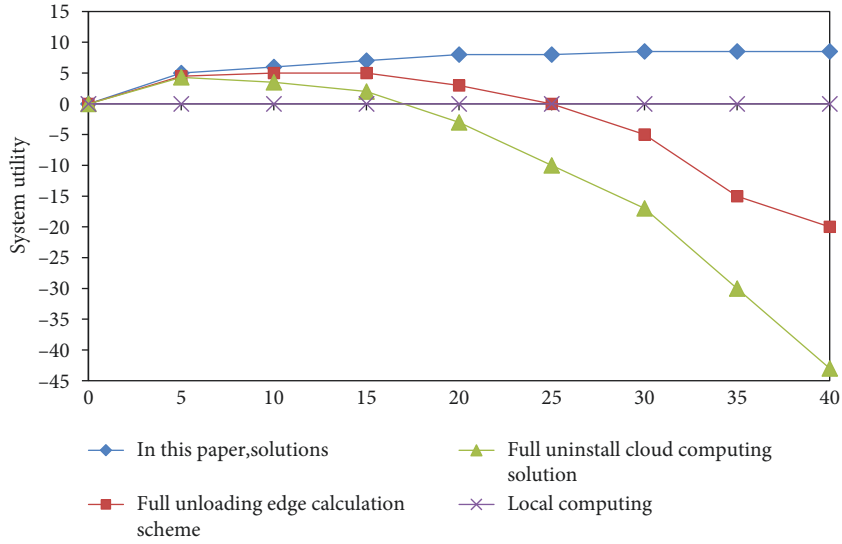

Figure 1: System utility of each scheme under different total numbers of users.

value, the system running will reach a peak, the increase of users in the cloud computing scheme of the system is inversely proportional to the utility value roughly, which already cannot satisfy the user's demand to uninstall the program, and the utility value of the other two calculation schemes is lower than that of the local calculation scheme and decreases with the increase of the number of users, so there is an inverse relationship. Compared with that of the local calculation scheme, the system utility value of the solution in this paper is always at a higher stable level in the process of increasing the number of users. This is because when the number of offloaded users is too large, the limited uplink communication resources and edge computing resources cannot provide richer resource requirements for each demanding user, resulting in higher computing time and transmission delay. Users sending and executing tasks in a fully uninstalled manner will cause all users to compete for limited resources. When there are too many unloaded users, the computing resources allocated to users by edge nodes under the edge computing solution will be lower than the local computing resources, and the low uplink communication resources of users under the cloud computing solution will cause the transmission delay of task offloading to be too high. In turn, the system utility of the above two schemes is reduced or even lower than the utility of local computing. With the increase of users, the user uninstallation strategy selection algorithm under this scheme can still maintain a high and stable system utility value. This is because the solution can reasonably plan the mode selection of task offloading for users, thereby ensuring the maximum utilization of limited computing and communication resources.

In this paper, the actual scenario of face recognition application of this system is selected, and the system utility performance of the proposed solution is used to conduct experiments and evaluations on index changes. Firstly, in order to complete the task, the total amount of computing resources required by the cloud is Cu = 1000 Mcycle. In addition, when data are input, their size is du = 420 KB, and the experimental results are shown in Figure 2.

From the observation and analysis of Figure 2, it can be concluded that the system utility value of the proposed solution performs significantly better than the numerical display of the other two solutions in the specific application task of face recognition, and it always maintains a certain level of efficiency. In addition, with the increase of the number of users, the system utility value of the other two schemes will decrease by different magnitudes after reaching a certain threshold upper limit, while the system utility of the solution proposed in this paper can still maintain a high and stable running state. The solution in this paper combines all available computing and communication resources on the edge, cloud, and local sides to maintain a stable and dominant system utility when the number of users increases.

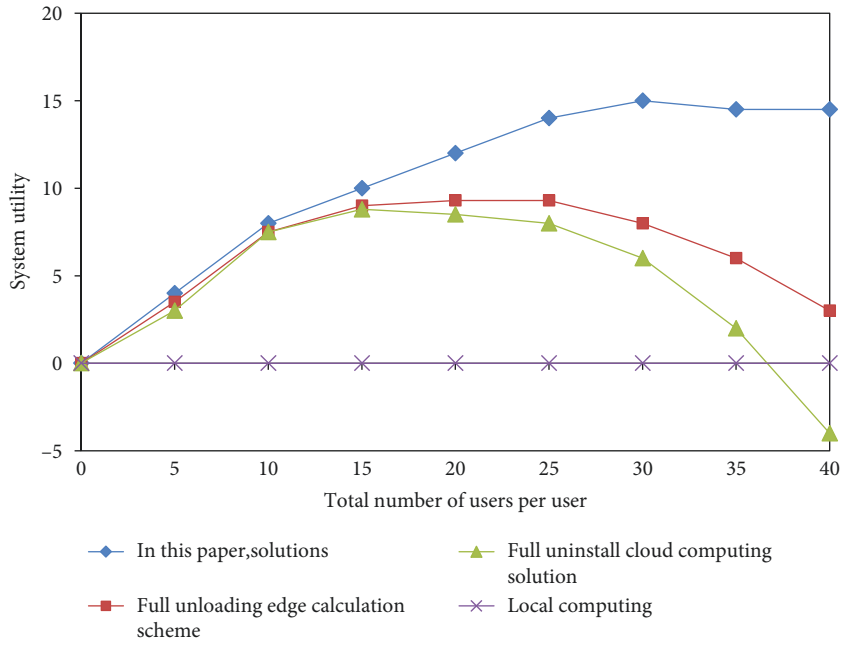

Figure 2: System utility of each scheme under the condition of different total users under specific tasks.

4. Application of High-Resolution Image Detection for Athlete Training Based on Visual Images

4.1. Athlete Motion Posture Tracking Estimation and Recognition Method Based on Visual Images. Now, methods for obtaining 3D depth images of athletes can be divided into two categories: methods based on athlete boundary objects and methods based on depth cameras. The former requires multiple testing devices and sensors on the observation object. Although the boundary-based identification method has high sensitivity and accuracy, it is not suitable for general research because of its high cost and very complex operation. With the improvement of the technical level, the depth camera-based modeling method is developing very rapidly. In the aspect of 3D depth image acquisition, it has been gradually applied as the main method.

In this paper, a 3-stage exploration algorithm TSS based on the block matching method is used to track and estimate the motion pose of the target. The block matching method is a motion estimation algorithm based on local image features. Set the target macroblock in the observation image, find the best motion direction of the target macroblock between adjacent image frames, calculate the motion displacement vector, and perform motion estimation of the observation target. The schematic diagram of the block matching method is shown in Figure 3.

High precision and high speed are the basis for real-time tracking and estimation of athletes' motion posture in the athlete's motion posture detection method. Based on the local image characteristics of the target, the three-step search algorithm finds the smallest absolute value difference between macroblocks according to the search range from large to small patterns.

The block matching algorithm of the three-step search algorithm applies the minimum average absolute value difference method for calculation, and the calculation method is shown as

$$\mathrm{MAD}\left(d_x, d_y\right) = \frac{1}{MN} \sum_{(x_1, y_1) \in B} \left| f_k(x_1, y_1) - f_{k-1}\left(x_1 + d_x, y_1 + d_y\right) \right|. \tag{21}$$

In the aspect of the action recognition of athletes, this paper mainly designs an action recognition method based on the local image features of the athlete's skeleton. Figure 4 is a 3D coordinate diagram of the athlete's bone points obtained by the Kinect depth camera. After observing the target extinction, the local coordinates of the athlete's bone point data and altitude will change.

After obtaining the performance characteristics of the athlete's sports behavior, this paper uses the Euclidean distance to calculate the displacement D. The athlete's bone point image does not need to consider the three-dimensional coordinates of the camera to detect the local characteristics of the adjacent time, the image bone point, and the z-coordinate target distance. The calculation formula of displacement D is shown as

$$D = \sqrt{\left(x_i - y_i\right)^2 + \left(x_j - y_j\right)^2}, \tag{22}$$

which represents the relative change of the local features of the athlete in the skeleton point image to identify the athlete's movement. According to experience, a threshold value is set for the local characteristic changes of the bone points of the destrength attack action, and D is obtained, which is

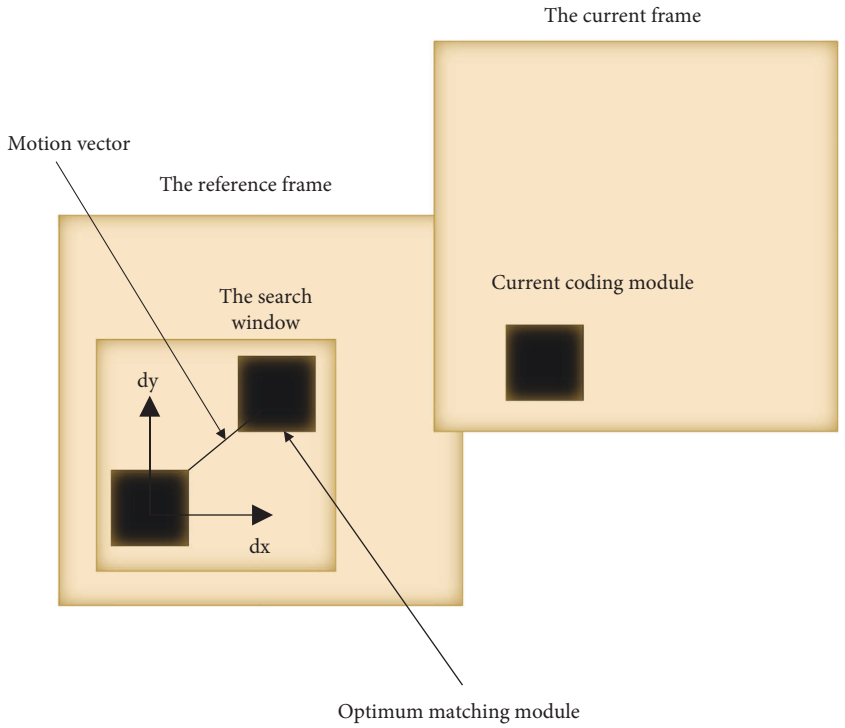

Figure 3: Schematic diagram of the block matching method.

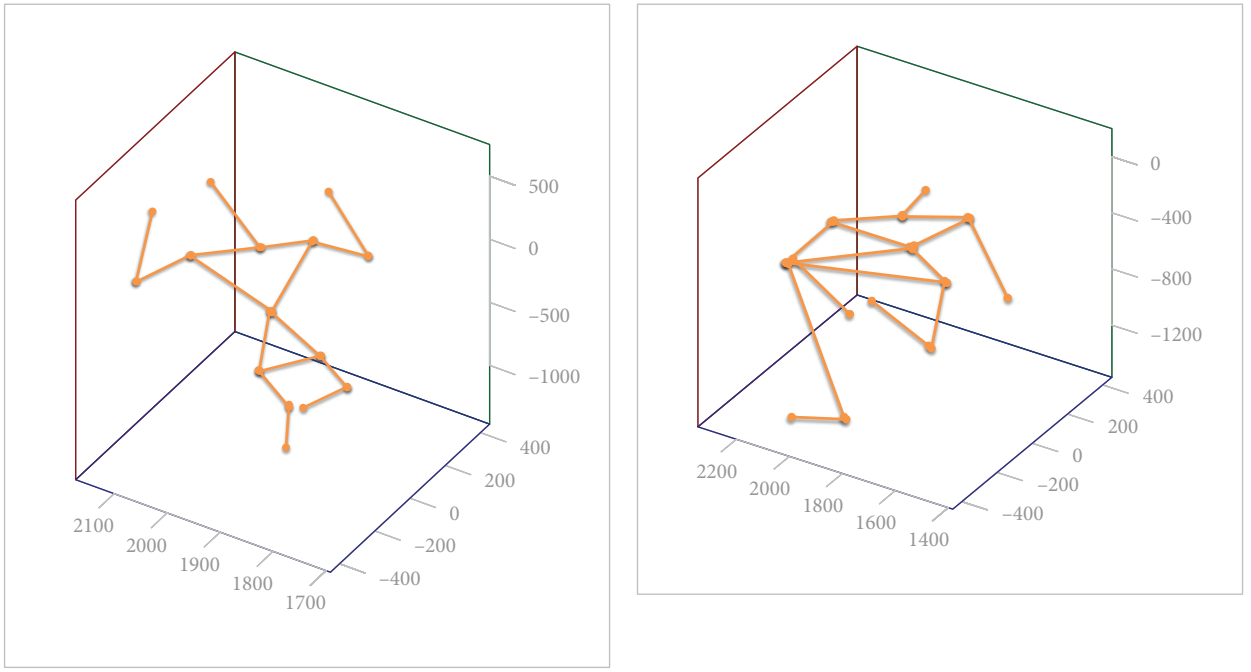

(a) (b)

Figure 4: Example diagram of the athlete's 3D skeleton point posture. (a) Sample image of standard posture. (b) Image action in the process of motion.

compared with the threshold value. When D is greater than the set threshold, it is decided to act as a destrength attack. Otherwise, it is judged that the operation is normal. The example diagram of the athlete's 3D skeleton point posture is shown in Figure 4.

4.2. High-Resolution Image Detection Algorithm. The KSVD algorithm is a powerful tool for sparse scoring. D_x represents dictionary-based information. KSVD can be used in combination with various tracking algorithms. The following formula is used to express the objective function of solving the coefficient:

$$\min_x \|x\|_0 s.t. y = Dx, \quad \min_x \|x\|_0 s.t. \|y - Dx\| \le \varepsilon. \tag{23}$$

In the face of high-resolution SAR images, the detailed information of the SAR image will increase significantly, and the complexity of the object will also increase. At the same time, high-resolution SAR images will also lose the general SAR image texture function. In the same area, the distribution parameters are also different (because of the large amount of gradient information, the traditional resolution SAR image information does not exist, but the high-resolution SAR image information obviously exists), but they are used to create more refined and clear partitions. All these models can only describe areas with a few simple targets and terrain types. In other words, statistical models have "regional characteristics." In a large-area scene, because the target and terrain are complex, it is not practical to use only a statistical model containing a few parameters to describe the entire image. However, if there are too many parameters, the application may have problems. If we want to train a dictionary for these broad characteristics, the dimension of the dictionary will inevitably become excessive. Moreover, due to insufficient data, the number of features is far greater than the amount of data available for training, so overmatching will inevitably occur.

In order to solve the above problems, we propose a hierarchical dictionary learning method to solve the problem of too high dimensionality of the dictionary when simulating high-resolution SAR images. This algorithm will solve the self-learning dictionary problem in high-resolution SAR image detection. However, due to the large geographical features of the ultrahigh resolution SAR image, the dimensionality of the dictionary is very high, and there are some cases that cannot be tolerated and cannot solve the problem. In this paper, we introduce a hierarchical algorithm, namely, the grammar in a hierarchical structure. According to the size of the target vehicle, high-resolution SAR images are regional characteristics. In this article, in SAR images, since the average vehicle target resolution is above 1000 pixels (0.3 meters), the target and shape will be considered. Shadows themselves also have certain distribution characteristics. Like the idea of classification, they are formed between specific information structures. The distribution characteristics and structure information are used to detect targets and complete incomplete targets.

The basic principle of the hierarchical dictionary learning method is to make dictionaries of each category (target, grass, runway, building, tree, etc.) of different SAR images (the same category of different SAR images also has obvious differences). Moreover, the dimension of the dictionary may reach thousands of dimensions (or 10,000 dimensions). But at the same time, because different SAR images are used as different areas of the dictionary on specific characteristics, and one of the most obvious differences in darkness requires different SAR images, different images can be used to construct the dictionary part of the grayscale average mark and the background area. The calculation ofgray-level average value starts from the image with too many possibilities. The simple distribution parameters obtained from the training image are shown in Table 2.

After constructing the dictionary, the problem to be faced is how to quickly find α and λ in $\Omega_\vee = \Omega\lambda^T$ and $y = \Omega_\vee\alpha$ as features. The solution to this can be transformed into the following equation:

$$\alpha = \arg\min_y \left\|\Omega_\wedge y\right\|_0 = \arg\min_y \left\|\Omega\lambda^T y\right\|_0, \tag{24}$$

where Ω is a dictionary and α is the coefficient of x in the dictionary. The objective function form of the basis tracking (BP) algorithm is

$$\min \|\alpha\|_1 s.t. A = \Omega\alpha. \tag{25}$$

This algorithm is relatively simple and is not common in practical applications, but it is a very basic method. Understanding this algorithm will help deepen the understanding of subsequent algorithms.

As one of the classic methods of analyzing signal decomposition, the match pursuit (MP) algorithm is widely used, and the effect is remarkable. The purpose is to use a complete dictionary to disassemble the sample, and the expression after decomposition is required to be as correct as possible. Assuming that the sample signal f represented belongs to the Hilbert space, f is expressed as the weighted sum of several elements selected in the dictionary D:

$$f(x) = \sum_i a_i g_i(x), i = 1, 2, \ldots, N. \tag{26}$$

If a dictionary is given, the MP algorithm first uses the inner product of the largest original signal correlation (the largest) as the gesture of $f(x)$ to select, then selects the similarity of the two signals as the corresponding weight, and then selects the larger signal. Combine the $f(x)$ of the above tuple until the inner product of the elements and the selected signal better fit the edge of $f(x)$. The steps of the MP algorithm are shown in Table 3.

The MP algorithm is often used in the fields of signal coding, image coding, video coding, etc., to obtain better tracking results. This algorithm has some limitations, such as high computational complexity and low ease of use in applications that require real-time tracking.

The orthogonal matching pursuit (OMP) algorithm is based on the extension of MP algorithm. The objective function of this algorithm can be roughly expressed by

$$\min\|f - \Omega\alpha\|_F^2 s.t. \|\alpha\|_0 \ll N. \tag{27}$$

4.3. Athlete Training High-Resolution Image Detection Results and Analysis. Using the initialization conditions proposed in this paper, the orthogonal matching tracking algorithm is

Table 2: Initialization of model parameters.

Distribution image	Gaussian distribution		Generalized gamma distribution			Fourth-order polynomial distribution
	μ	δ	α	δ	λ	
Background	69.12	1205.53	0.1260	$2.09E-7$	28.89	$-5.88E-9$ $4.15E-6$ $-6.24E-3$ $7.06E-2$ $-1.98E-4$
Background	58.05	1055.82	0.1338	$1.04E-10$	36.48	$-8.11E-11$ $4.77E-8$ $-9.13E-6$ $5.65E-4$ $7.56E-4$
Dark scene	20.20	122.41	0.1280	$1.08E-11$	36.48	$1.16E-12$ $-9.10E-9$ $4.39E-6$ $-6.80E-4$ 0.0323
Building	151.87	5210.61	0.3560	0.0852	14.00	$7.69E-11$ $-3.42E-8$ $4.54E-6$ $-1.62E-4$ 0.0026
Shadow	14.39	99.12	0.1671	$2.19E-8$	28.98	$1.07E-10$ $-6.93E-8$ $1.58E-5$ -0.0015 0.0467
Shadow	13.35	42.62	0.2248	$8.90E-6$	23.97	$1.16E-10$ $-7.46E-8$ $1.68E-5$ -0.0016 0.0483
Aims	183.49	5967.72	0.5564	4.84	7.41	$1.68E-10$ $-7.52E-8$ $1.05E-5$ $-4.85E-4$ 0.0064
Min	13.35	42.62	0.1280	$1.08E-11$	7.41	$1.07E-10$ $-7.52E-8$ $-7.64E-6$ -0.0016 $-2.63E-4$
Max	183.49	5967.72	0.5564	4.84	36.48	$1.16E-12$ $4.77E-8$ $1.68E-5$ $5.65E-4$ 0.0483

Table 3: MP algorithm description.

Enter	To be represented signal $f(x)$, dictionary D
Output	Tracking results, representing the yuan and its corresponding coefficients $a_i g_i(x)$
Algorithm initialization	$R_1 = f(x)$
Cycle strategy	$g_i(x) \in Ds.t. \max\{\lvert\langle f(x), g_i(x)\rangle\rvert\}$ $a_i = \lvert\langle f(x), g_i(x)\rangle\rvert R_{i+1} = R_i - a_i g_i(x)$
Termination condition	$\lVert R_i\rVert <$ Threshol d

Table 4: Fit test.

Distribution/estimation map/assessment		GRD		Gaussian		Method of this paper
		MoM	MoLC	MoM	MoLC	Dictionary
Figure a	KL	0.8101	0.7244	1.0758	0.9125	0.0214
	KS	0.1012	0.3034	0.1419	0.1716	0.0145
	MSE	$2.6e-4$	$2.2e-4$	$7.7e-3$	$4.5e-4$	$1.7e-9$
Figure b	KL	0.2318	0.4517	0.9578	1.2651	0.0145
	KS	0.0988	0.817	0.1099	0.0977	0.0020
	MSE	$4.3e-3$	$2.2e-2$	$3.8e-3$	$5.5e-2$	$1.4e-9$
Figure c	KL	0.4007	0.1917	0.2381	0.3219	0.0098
	KS	0.1372	0.2418	0.6099	0.4917	0.0124
	MSE	$9.8e-7$	$2.2e-6$	$5.8e-7$	$2.2e-6$	$7.9e-10$
Figure d	KL	0.8198	0.2789	0.2237	0.5941	0.0914
	KS	1.0911	1.3412	1.0901	0,9879	0.0038
	MSE	$5.7e-4$	$3.2e-4$	$5.1e-5$	$9.7e-6$	$3.7e-8$
Figure e	KL	1.1098	1.0091	0.9178	0.9914	0.0099
	KS	0.7816	0.4648	0.7816	0.8817	0.0014
	MSE	$1.4e-5$	$4.7e-6$	$8.9e-6$	$2.6e-5$	$5.4e-10$
Figure f	KL	0.1498	0.1147	0.4512	0.3645	0.0012
	KS	0.1278	0.2918	0.7828	0.6514	0.0009
	MSE	$5.4e-10$	$5.4e-10$	$5.4e-10$	$5.4e-10$	$4.4e-10$

used to obtain the characteristic parameter vector of the data, as shown in Table 4.

Through the above test, it is obvious that the tracking algorithm using the overmatching dictionary proposed in this paper can better adapt to the data model. By using this method, the obtained coefficient vector can be used as the feature of subsequent classification and detection steps, and good results can be obtained after testing. In the dictionary tracking process, spactive is used to express features. In other words, there are few elements other than zero in the coefficient vector obtained by tracking. Therefore, the classification and detection process will not cause a lot of time loss. On the contrary, the tracking process does not require a lot of mathematical optimization, so the calculation time can be further reduced.

A three-step search algorithm is used to calculate the displacement vector of the bone point image. After error correction, as shown in Figure 5, the displacement vector diagram of the bone point image of the athlete's movement posture can be obtained. The experimental results show that the robustness of the three-step search algorithm is good. The lighting and the athlete's movement track and direction can be obtained from the displacement vector to estimate the athlete's movement behavior.

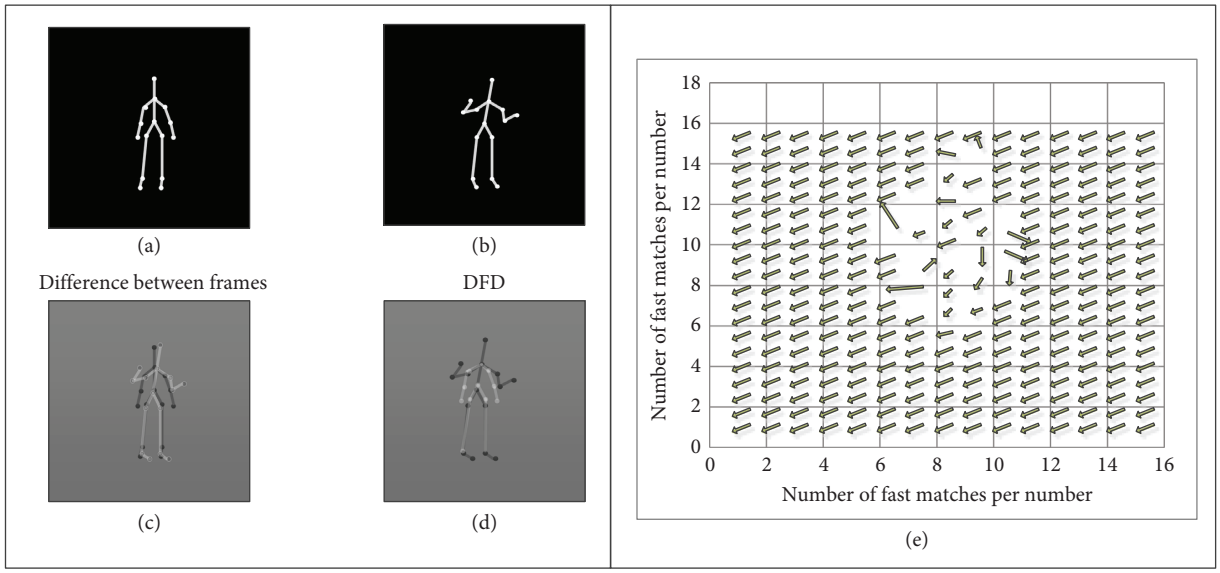

Figure 5: Motion estimation experiment results under sufficient light conditions. (a) Interframe difference of the first frame; (b) DFD value of the second frame; (c) Image difference between the two frames; (d) Difference between the displacement frames; (e) Fast matching of each digit in the second frame image vector.

5. Conclusion

In the detection of sports postures of athletes, because two-dimensional video images cannot overcome the influence of the lighting environment, a real-time image detection method of sports postures of athletes based on the local image features of depth images is proposed. First, a 3D depth image is obtained based on the scene depth camera, and the depth image is converted into an image of the athlete's bone point. In order to achieve the purpose of estimating the movement posture of athletes, it is necessary to calculate the displacement vector of the local features of the bone point image and use the three-step search algorithm to calculate the specific movement direction of athletes. In addition, it is necessary to calculate the Euclidean distance change of the local features of the bone point image and identify the movement behavior of athletes. Through the analysis of the experimental data results, it can be concluded that the method in this paper can accurately detect and obtain the athletes' movement posture and effectively avoid the influence caused by external factors such as light, showing great positive significance for the accuracy of the tracking estimation of athletes' movement posture and athletes' action recognition and simplifying a series of calibration tasks for observed targets. It is the initial stage of the video surveillance process to achieve the effect of real-time surveillance. Athlete posture detection is the basis of athlete tracking estimation and motion recognition, which is widely used in video surveillance technology. It has very important application value in motion recognition monitoring, social network security, social and family monitoring, etc. This dynamic image recognition method based on local image features can help to solve the problem of randomness and nonrigidity of athletes' movement and has certain effectiveness in the expression of athletes' movement behavior. Currently, local image feature detection methods based on two-dimensional images cannot overcome the effects of changes in the lighting environment and cannot detect observation objects in real time. The detection method based on the local image features of the 3D depth image can flexibly measure the three-dimensional information of the target under various conditions and effectively overcome the influence of the light environment. In addition, there is no need to set the calibration object of the observation object, and the posture estimation and action recognition of the object are performed in real time.

Data Availability

The data used to support the findings of this study are available from the author upon request.

Conflicts of Interest

The author declares that there are no conflicts of interest.

Acknowledgments

This work was supported by Xiangnan University.

References

[1] D. Huang, "Mobile cloud computing," *IEEE COMSOC Multimedia Communications Technical Committee (MMTC) E-Letter*, vol. 6, no. 10, pp. 27–31, 2011.

[2] A. u. R. Khan, M. Othman, S. A. Madani, and S. U. Khan, "A survey of mobile cloud computing application models," *IEEE communications surveys & tutorials*, vol. 16, no. 1, pp. 393–413, 2014.

[3] M. Sookhak, H. Talebian, E. Ahmed, A. Gani, and M. K. Khan, "A review on remote data auditing in single cloud server: taxonomy and open issues," *Journal of Network and Computer Applications*, vol. 43, pp. 121–141, 2014.

[4] Y. Mao, C. You, J. Zhang, K. Huang, and K. B. Letaief, "A survey on mobile edge computing: the communication perspective," *IEEE communications surveys & tutorials*, vol. 19, no. 4, pp. 2322–2358, 2017.

[5] N. Abbas, Y. Zhang, A. Taherkordi, and T. Skeie, "Mobile edge computing: a survey," *IEEE Internet of Things Journal*, vol. 5, no. 1, pp. 450–465, 2018.

[6] A. K. Cole, M. L. McGrath, S. E. Harrington, D. A. Padua, T. J. Rucinski, and W. E. Prentice, "Scapular bracing and alteration of posture and muscle activity in overhead athletes with poor posture," *Journal of Athletic Training*, vol. 48, no. 1, pp. 12–24, 2013.

[7] P. Merkle, K. Müller, and T. Wiegand, "3D video: acquisition, coding, and display," *IEEE Transactions on Consumer Electronics*, vol. 56, no. 2, pp. 946–950, 2010.

[8] L. Kuang, T. Gong, S. OuYang, H. Gao, and S. Deng, "Offloading decision methods for multiple users with structured tasks in edge computing for smart cities," *Future Generation Computer Systems*, vol. 105, pp. 717–729, 2020.

[9] X. Yuan, Z. Xie, and X. Tan, "Computation offloading in UAV-enabled edge computing: a stackelberg game approach," *Sensors*, vol. 22, no. 10, p. 3854, 2022.

[10] X. Chen, L. Jiao, W. Li, and X. Fu, "Efficient multi-user computation offloading for mobile-edge cloud computing," *IEEE/ACM Transactions on Networking*, vol. 24, no. 5, pp. 2795–2808, 2016.

[11] L. Lin, X. Liao, H. Jin, and P. Li, "Computation offloading toward edge computing," *Proceedings of the IEEE*, vol. 107, no. 8, pp. 1584–1607, 2019.

[12] H. Zhang, Y. Xiao, S. Bu, D. Niyato, F. R. Yu, and Z. Han, "Computing resource allocation in three-tier IoT fog networks: a joint optimization approach combining Stackelberg game and matching," *IEEE Internet of Things Journal*, vol. 4, no. 5, pp. 1204–1215, 2017.

[13] Z. Cao, J. Lin, and C. Wan, "Optimal cloud computing resource allocation for demand side management in smart grid," *IEEE Transactions on Smart Grid*, vol. 8, no. 4, pp. 1943–1955, 2016.

[14] A. Yousafzai, A. Gani, R. M. Noor et al., "Cloud resource allocation schemes: review, taxonomy, and opportunities," *Knowledge and Information Systems*, vol. 50, no. 2, pp. 347–381, 2017.

[15] W. Ren, Y. Sun, H. Luo, and M. Guizani, "A novel control plane optimization strategy for important nodes in SDN-IoT networks," *IEEE Internet of Things Journal*, vol. 6, no. 2, pp. 3558–3571, 2019.

[16] A. M. Larson, A. M. Fung, and F. C. Fang, "Evaluation of tcdB real-time PCR in a three-step diagnostic algorithm for detection of toxigenic Clostridium difficile," *Journal of Clinical Microbiology*, vol. 48, no. 1, pp. 124–130, 2010.

[17] H. Huang and Y. Li, "Virtual network resource allocation algorithm based on high reliability and intelligent offloading strategy under 5G network slicing," *International Conference on Automation Control Algorithm, and Intelligent Bionics (ACAIB 2022)*, vol. 12253, pp. 361–366, 2022.

[18] H. C. Ke, H. Wang, H. W. Zhao, and W. J. Sun, "Deep reinforcement learning-based computation offloading and resource allocation in security-aware mobile edge computing," *Wireless Networks*, vol. 27, no. 5, pp. 3357–3373, 2021.

Hindawi
Computational Intelligence and Neuroscience
Volume 2023, Article ID 9835129, 1 page
https://doi.org/10.1155/2023/9835129

Retraction

Retracted: Construction Means of Soil Microbial Synusiologic Network Based on ANN

Computational Intelligence and Neuroscience

Received 22 August 2023; Accepted 22 August 2023; Published 23 August 2023

This article has been retracted by Hindawi following an investigation undertaken by the publisher [1]. This investigation has uncovered evidence of one or more of the following indicators of systematic manipulation of the publication process:

(1) Discrepancies in scope
(2) Discrepancies in the description of the research reported
(3) Discrepancies between the availability of data and the research described
(4) Inappropriate citations
(5) Incoherent, meaningless and/or irrelevant content included in the article
(6) Peer-review manipulation

The presence of these indicators undermines our confidence in the integrity of the article's content and we cannot, therefore, vouch for its reliability. Please note that this notice is intended solely to alert readers that the content of this article is unreliable. We have not investigated whether authors were aware of or involved in the systematic manipulation of the publication process.

Wiley and Hindawi regrets that the usual quality checks did not identify these issues before publication and have since put additional measures in place to safeguard research integrity.

We wish to credit our own Research Integrity and Research Publishing teams and anonymous and named external researchers and research integrity experts for contributing to this investigation.

The corresponding author, as the representative of all authors, has been given the opportunity to register their agreement or disagreement to this retraction. We have kept a record of any response received.

References

[1] X. Li, H. Wang, and M. Yuan, "Construction Means of Soil Microbial Synusiologic Network Based on ANN," *Computational Intelligence and Neuroscience*, vol. 2022, Article ID 1708350, 9 pages, 2022.

Hindawi
Computational Intelligence and Neuroscience
Volume 2022, Article ID 1708350, 9 pages
https://doi.org/10.1155/2022/1708350

Research Article

Construction Means of Soil Microbial Synusiologic Network Based on ANN

Xia Li,[1,2] **Huixian Wang**,[2] **and Miaoxin Yuan**[3]

[1]*College of Mechanical and Vehicle Engineering, Taiyuan University of Technology, Taiyuan, Shanxi 030024, China*
[2]*Shanxi Academy of Agricultural Science, Shanxi Agricultural University, Taiyuan, Shanxi 030031, China*
[3]*China Energy Conservation DADI (Hangzhou) Environment Remediation Co Ltd, Hangzhou, Zhejiang 310020, China*

Correspondence should be addressed to Xia Li; 19403628@masu.edu.cn

Received 13 June 2022; Accepted 2 August 2022; Published 3 October 2022

Academic Editor: Gopal Chaudhary

With the construction of synusiologic civilization and synusiologic environmental protection entering a new era driven by data, the breadth and depth of application of the DM technique in the domain of synusiologic environmental protection are constantly strengthened. If reasonable planning is not carried out in the process of social construction, it will cause unpredictable damage to the synusiologic environment. However, traditional synusiologic planning means too much human interference, and there are still some shortcomings in accuracy and operability, which means they cannot guide synusiologic construction well. In order to analyze the contribution of the soil nutrient data to soil fertility and dig out the knowledge describing soil fertility, this paper studies the construction means of soil microbial synusiologic network by ANN. By simulating the learning, memorizing, and processing problems of human brain neurons, the artificial network establishes a parallel distributed processing system computing DMG model with a large number of connections, which can quickly acquire knowledge from the outside world and store and process it and respond to the changes in the external environment in time. According to the research in this paper, the network performance of this algorithm is 18% better than that of the traditional algorithm, and it is suitable to be widely put into practice.

1. Introduction

With the rapid improvement of social eco, the intensity of land use in China is increasing year by year, and the soil pollution caused by it is becoming more and more prominent and serious [1]. Land is the source of the basic means of subsistence for human beings. The advancement of message technique, in the complex production system in agricultural production makes the soil fertility level highly uncertain, which has a great impact on the growth of crops [2]. The DM technique is a process of classifying and extracting massive data, discovering the interrelations among them, and generating new rules [3]. The purpose of the DM technique is to analyze the relationship between data from multiple dimensions, search for the message hidden in the data, provide decision support for scientific research, and promote the transformation of production and lifestyle. In order to understand the overall situation of soil pollution and remediation, study the mutual influence of various factors in the domain of soil remediation [4]. At the same time, synusiologic civilization construction and synusiologic environmental protection have entered a new era driven by data [5]. The data collected in the work of resolutely fighting the battle against pollution, continuously improving the quality of the synusiologic environment, and constantly meeting the people's growing beautiful synusiologic environment are often incomplete, unclear, large, and random, so they cannot be separated from the support of the DM technique [6]. The concept of a synusiologic network in ecology has a long history and was put forward in 1859. Nowadays, synusiologic network, as a branch of ecology, mainly studies the complex structure and interaction among species, explores the temporal and spatial variation laws, clarifies the internal structure of complex systems, analyzes the specificity of different ecosystems, and then discusses the ways and strategies to keep the sustainability of natural

systems [7]. At present, the city is in a period of rapid improvement and construction. However, in the process of urban improvement and construction, the problem of urban construction's consumption and destruction of synusiologic background has become more and more serious, and the fragmentation of a large number of agricultural and forestry green spaces has greatly affected the urban natural synusiologic landscape [8]. Since the 1990s, the concept of synusiologic network has been studied and applied by many disciplines, such as ecology, geography, and planning, and the knowledge of synusiologic network in various disciplines has been continuously integrated, which has enriched the connotation of synusiologic network and made the expression of form and structure more and more clearly visible [9]. In the process of urban improvement and people's daily life, the existence of green space has important value and significance. It can optimize the spatial pattern of cities, support the improvement and construction of cities, improve the synusiologic environment of cities, provide a good living environment for human beings, etc., so it is very important for the planning and construction of urban green space [10]. The technical level has always restricted the improvement of land use, and the industrial revolution has promoted the application of nature protection and synusiologic network thought in the planning domain [11]. From the end of the 19th century to the beginning of the 20th century, natural landscapes began to become the content of urban planning. The second industrial revolution transformed cities and villages, and seminatural areas began to be transformed into agricultural land and expanded continuously. Since the end of the 20th century, the establishment of national parks and nature reserves has become the main way to slow down the extinction of species and the decline of natural ecosystems [12]. In the process of urbanization, the construction of a synusiologic civilization cannot be ignored. The function of the synusiologic environment plays a vital role in the improvement of urban and rural areas, including protecting biodiversity, reducing pollution and noise generated in the process of urban improvement, reducing the urban heat island effect, and other functions.

The innovation of this paper lies in the following:

(1) The ANN is introduced. This is the algorithm of this paper, so it is necessary to discuss it. ANN is a computing model of a parallel distributed processing system, which is established by simulating the learning, memory, and problem solving functions of human brain neurons. It can quickly acquire knowledge from the outside world and store and process it and respond to the changes in the external environment in time.

(2) The application of ANN to a synusiologic network is introduced. This is a discussion around the theme of this article. It is feasible to apply synusiologic ANN to the evaluation or identification of synusiologic environmental quality. At the same time, because of its excellent properties, such as self-organization, self-adaptation, self-learning, and fault tolerance, and its complex parallel distributed processing ability, it can accurately evaluate the synusiologic environment quality from the specific learning samples.

(3) The model construction is discussed. Let readers have a certain understanding of this principle. Ecological environmental quality evaluation is essentially a pattern recognition problem, that is, the actual monitoring results of the synusiologic environmental quality evaluation index system are compared with the array of corresponding synusiologic environmental quality evaluation standard values, and the synusiologic environmental quality grade corresponding to the standard value array closest to the array of monitoring values is the recognition result of the BP ANN model, that is, the synusiologic environmental quality evaluation result of the corresponding area.

This paper is divided into five parts: The first part is the background and brief introduction of this paper; the second part is related research and the introduction of this paper. The third part is at the means adopted and the discussion of this research. The fourth part, which is the core of this paper, is the construction of relevant theories and models. The fifth part is the conclusion.

2. Related Work

Li established a two-level BP network model for urban comprehensive environmental quality evaluation, in which the first-level evaluation established BP network models for three subsystems atmosphere, surface water, and noise and evaluated the atmospheric environmental quality, surface water environmental quality, and acoustic environmental quality [13]. Wu suggested that qualitative research be adopted. By studying the public perception of the Chicago River synusiologic corridor, it was found that six elements of the green space synusiologic network, nature, art, cleanliness, safety, improvement power, and proximity, have a direct influence on the public perception of the green space synusiologic network [14]. Schütz suggested that landscape ecology is a new branch that extends from ecology, taking the landscape as the object and applying synusiologic principles to study the spatial structure, function, and dynamic changes of the landscape in a large enough area [15]. Taghizadeh-Mehrjardi suggested quantitative research and found that the vegetation types and the degree of protection on both sides of the river bank have a great influence on public perception [16]. Xie suggested that the BP network should be used for comprehensive evaluation of urban environmental quality, and the nonlinear relationship between the urban environment and its influencing factors was established to evaluate the grade of urban environmental quality [17]. Mandakovic suggested that 433 typical cases of greenbelt synusiologic networks in Northern Ireland, Scotland, England, and Wales should be investigated by a questionnaire, which aimed at the definition, current situation, and a local greenbelt synusiologic network project, etc., so as to determine the public's understanding of

greenbelt synusiologic networks [18]. Yu suggested that the atmospheric environmental quality evaluation model based on the BP network should be established, and the model should be used for atmospheric environmental quality evaluation, and the evaluation results were compared with those of fuzzy mathematics evaluation means, which showed that BP ANN was universal, reasonable, and practical [19]. She suggested that, based on regional land cover, synusiologic evaluation, wildlife protection, and other objectives, corridors and networks should be regarded as the framework of the green space synusiologic network for overall planning, and important patches should be selected as synusiologic nodes through node weight analysis, and seven different network schemes should be formed after synusiologic corridors are connected, then the network structure index of each scheme should be calculated, and finally the best scheme can be obtained by analyzing and comparing them [20]. Li suggested using the BP network model to evaluate the atmospheric environmental quality of a city and compared the evaluation results of this means with fuzzy decision, grey clustering, and comprehensive evaluation means, which proved the superiority of the BP network model in atmospheric environmental quality evaluation [21]. Zhang suggested that the landscape structure index should be applied to the evaluation of urban green space synusiologic network, and the corridor index, patch index, and matrix index should be used to optimize it through comprehensive analysis [22]. It is suggested that the BP network should be applied to lake water quality classification, and the water quality index data of 25 lakes in China should be used as training samples. Zhang established a water quality classification model and used the model to classify the water quality of 6 lakes [23, 24].

The rapid improvement of China's cities has led to the continuous expansion of construction land, which has led to the increasingly broken landscape blocks of urban green space, which has a negative impact on the synusiologic function of the whole city. The synusiologic function of urban green space is closely related to the urban landscape, and the construction of landscape pattern is crucial to urban synusiologic construction. It is very important to establish an ecosystem simulation and prediction model, but it is often difficult. It is of great significance to study the construction means of soil microbial synusiologic network based on ANN in this paper.

3. ANN

3.1. Overview of ANN. With the improvement of science and technique, computers have been widely used for their powerful computing power and message processing power. However, in terms of perception, pattern recognition, and decision-making problems, the processing ability of computers is not as good as that of people. DM is the process of extracting hidden, unknown but potentially useful messages and knowledge from a large number of incomplete, noisy, fuzzy and random practical application databases. In today's message age, people are eager for ever-changing messages. At present, in the transaction records and financial statements in various enterprises and commercial domains and the data collected in scientific research domains (for example, meteorological images returned by meteorological satellites), the data scale is often tens of megabytes, or even hundreds of gigabytes. The DM technique based on the neural network is to explicitly express the knowledge implied in the neural network in an easy-to-understand way. People began to study the organizational structure and operation mechanism of the human brain, hoping to find a new means of message display, storage, and processing by imitating the human brain and design a brand-new processing structure model, which prompted the birth of the artificial neural network (ANN) research algorithm. The structure of the BP neural network is shown in Figure 1.

The BP neural network result algorithm is as follows:

The network has I nodes in the input layer, J nodes in the hidden layer, and K nodes in the output layer. Let $x_p = (x_{p1}, x_{p2}, \ldots, x_{pI})$ represent the network input, and $O_p = (o_{p1}, o_{p2}, \ldots, o_{\mathrm{pk}})'$ and $T_p = (t_{p1}, \ldots, t_{\mathrm{pk}})'$ represent the actual output and expected output of the network, respectively, where $p = 1, 2, \ldots, P$ and the number of samples is P. $(o_{p1}', o_{p2}', \ldots, o_{pJ}')$ denotes the output of hidden layer nodes, w_{ij}' denotes the weights of the $i\,(i = 1, 2, \ldots, I)$th input layer node to the $j\,(j = 1, 2, \ldots, J)$th hidden layer node, and w_{jk} denotes the weights of the jth hidden layer node to the $k\,(k = 1, 2, \ldots, K)$th output layer node.

The excitation function of the network is $f(x) = 1/1 + e^{-x}$, then for the pnd sample, there are the following:

The output of the hidden layer of the network is

$$o_{\mathrm{pj}}' = f\left(\mathrm{net}_{\mathrm{pj}}\right) = f\left(\sum_{i=1}^{I} w_{\mathrm{ij}}' x_{\mathrm{pi}}\right), j = 1, 2, \ldots, J. \quad (1)$$

The output of the output layer of the network is

$$o_{\mathrm{pk}} = f\left(\mathrm{net}_{\mathrm{pk}}\right) = f\left(\sum_{j=1}^{J} w_{\mathrm{jk}} o_{\mathrm{pj}}'\right), k = 1, 2, \ldots, K. \quad (2)$$

So far, BP network has completed the approximate mapping of I-dimensional space vector to K-dimensional space.

Using the square error function, the error of the pth sample is

$$E_p = \frac{1}{2} \sum_{k=1}^{K} \left(t_{\mathrm{pk}} - o_{\mathrm{pk}}\right)^2, p = 1, 2. \ldots, P. \quad (3)$$

For P samples, the global error is

$$E = \frac{1}{2} \sum_{p=1}^{P} \sum_{k=1}^{K} \left(t_{\mathrm{pk}} - o_{\mathrm{pk}}\right)^2 = \sum_{p=1}^{P} E_p. \quad (4)$$

Synonyms similar to DM include data fusion, data analysis, and decision support. From this definition, we can realize that the following data must be true, abundant, and noisy discoveries, which are knowledge discoveries that users are interested in. Knowledge should be acceptable, understandable, and applicable, which does not require the

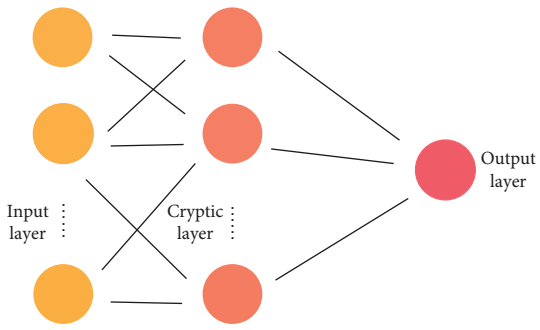

Figure 1: BP neural network structure.

discovery of universal knowledge but only supports specific discovery problems. Modern computer and database techniques can already support the storage and quick retrieval of such a database. This means that we have the ability to transform such "data floods" into "orderly" but "mountain-like" data sets. The DM technique of neural network integrates parallel intuition and serial logic and seeks an unknown message by learning the known message. It is suitable for nonlinear data and noisy data, especially when fuzzy, imprecise, and incomplete knowledge (data) is the feature, or there is no clear mathematical algorithm to analyze the data, it can achieve the effect that traditional symbolic learning means cannot achieve. ANN is a computing model of a parallel distributed processing system, which is established by simulating the learning, memory, and problem-solving functions of human brain neurons. It can quickly acquire knowledge from the outside world, store and process it, and respond to the changes in the external environment in time.

In a broad sense, data and messages are also forms of knowledge, but people regard concepts, rules, patterns, rules, and constraints as knowledge and data as the source of knowledge. Original data can be structured data such as relational databases, semi-structured data such as text, images, or even heterogeneous data distributed on the network. However, in the face of "mountain-like" data collection, the traditional data analysis means are difficult to cope with in terms of time and space, and people cannot understand and effectively use such data. With the continuous improvement of various computer management message systems and message technologies, more and more data is being collected into databases at an unprecedented speed. However, due to the huge and complex amount of data and the lack of effective data analysis tools, only a small amount of data will be used, and more will become "data garbage". With the improvement of ANN research, people's theoretical research on neural networks mainly focuses on using the research results of neural basic theory to explore neural network models with more perfect functions and superior performance by mathematical means.

Many people regard DM as knowledge discovery in a database. The means of knowledge discovery can be mathematical, nonmathematical, deductive, or inductive. The discovered knowledge can be used for message management, query optimization, decision-making knowledge, and process control, etc., and can also be used for the maintenance of data itself. For the current general database management system, all it can do is to make some simple queries and report statistics, which cannot keep up with the needs of the times. Faced with such a huge database, people are more eager to process and analyze these data at a higher level in order to get the general characteristics of the data and forecast the improvement trend. An ANN is a nonlinear dynamic system composed of a large number of parallel distributed processing units. It is very suitable for dealing with nonlinear and noisy data, especially those problems which are characterized by fuzzy, incomplete, and imprecise knowledge or data. These are the problems that DM tools have to face and try to solve.

3.2. ANN for Synusiologic Network. The ecosystem is a very complex big system. Whether it is a global ecosystem or a small regional ecosystem such as a watershed or a small reservoir (lake), its complexity is not only manifested in the structure of the ecosystem but also in the influencing factors of the ecosystem. Therefore, it is generally difficult to establish a more accurate mathematical model. However, due to the need for research, sometimes we have to overcome this difficulty and try to establish a reliable and easy-to-use quantitative model. The ecological environmental quality evaluation is one of the important means of synusiologic environmental management. Through environmental quality evaluation, the synusiologic environmental quality of a certain area can be scientifically evaluated, and a scientific basis can be provided for synusiologic environmental management, synusiologic environmental engineering, formulation of synusiologic environmental standards, synusiologic environmental planning, and synusiologic environmental construction.

A comprehensive evaluation of synusiologic environmental quality is based on the regional synusiologic environmental investigation, aiming at the characteristics of the eco-environment in this region, selecting certain evaluation indexes to evaluate by mathematical means, so as to identify the synusiologic environmental quality status and existing problems of different evaluation units and put forward countermeasures for comprehensive treatment. The ecological environmental quality evaluation is an identification process of comprehensively comparing the monitoring data of each index of the evaluated object with all levels of standards to see which level is closest to it. Many people have studied the identification and evaluation of synusiologic environmental quality. It is feasible to apply synusiologic ANN to the evaluation or identification of synusiologic environmental quality. At the same time, because of its excellent properties, such as self-organization, self-adaptation, self-learning, and fault tolerance, and its complex parallel distributed processing ability, it can accurately evaluate the synusiologic environment quality from the specific learning samples.

The traditional synusiologic environment monitoring means are to set up a monitoring system covering the whole area, which mainly uses artificial ground observation,

measurement, positioning monitoring, and laboratory analysis to obtain various statistical indicators and comprehensively evaluates the regional synusiologic environment. With the improvement of satellite remote sensing and the characteristics that remote sensing images can quickly provide synusiologic environment messages, the synusiologic environment remote sensing monitoring means have been widely used, from a single factor investigation and monitoring of a synusiologic environment to a comprehensive evaluation supported by multiple data. ANN is widely connected by a large number of simple neurons. It relies on computers to acquire superb computing power, and through the complex network system that simulates the thinking mode of the human brain, it makes use of accumulated knowledge to acquire recognition and association abilities similar to those of human beings.

Because of the complexity of the relationship between input and output in the ecosystem, it is generally reluctant to establish a simple mathematical model. The nonlinear relationship between synusiologic environmental quality and synusiologic environmental index requires the synusiologic environmental quality extraction model to have the function of nonlinear function fitting. The ANN means can handle the nonlinear relationship among variables well, solve the above problems in synusiologic environment quality message extraction, and provide a new technical means for regional synusiologic environment classification message extraction based on remote sensing. The ANN means have made some progress in regional synusiologic environment classification and are an important application of neural network pattern recognition. ANN has been widely used in the domains of system identification and pattern recognition and has made some progress. The ecological environmental quality evaluation is essentially a pattern recognition process, so it is feasible to apply ANN to a synusiologic environmental quality evaluation or recognition. At the same time, because it has excellent properties such as self-organization, self-adaptation, self-learning, and fault tolerance, as well as complex parallel distributed processing ability, it can obtain the weights based on objective data from specific learning samples, and evaluate the synusiologic environment quality more accurately.

4. Soil Microbial Synusiologic Network and Its Construction

4.1. Soil Microbial Synusiologic Network. A soil ecosystem is a whole composed of the interaction between organisms and the nonchemical environment in the soil through energy conversion and material circulation. The soil ecosystem includes soil minerals, soil organic matter, soil organisms, soil water, and soil air, among which soil microorganisms are the main components of the soil ecosystem. Traditional analysis of microbial community diversity and structure in soil ecosystems is mostly to isolate and culture microorganisms, and then analyze them through general biochemical traits or specific phenotypes, which are limited to isolating microorganisms from the solid culture medium. With the research on the in-situ living state of microorganisms in the soil, it is increasingly found that it is difficult to comprehensively evaluate the diversity of microbial communities by conventional isolation and culture means.

As an important part of the ecosystem, soil microbes play an important role in energy flow, material circulation, soil formation, and maturation, and are one of the sensitive indicators to reflect the changes in the soil ecosystem. Their quantity, population, and composition are important parameters to evaluate soil environmental quality. Soil microorganisms include prokaryotic microorganisms and eukaryotic microorganisms, among which prokaryotic micro-organisms include archaea, bacteria, actinomycetes, cyanobacteria, and myxobacteria, while eukaryotic microorganisms include fungi, algae, and lichens. These microorganisms are the main promoters of nutrient cycling in soil and play a very important role in the soil ecosystem.

Microorganisms in the soil rarely exist alone, but always have more populations gather together. They are mutual environments, influence each other, depend on each other, and repel each other. The knowledge of these interaction laws is soil microbial morphology. Microbial diversity refers to the changes in living organisms at the genetic, species, and ecosystem levels. It represents the stability of the microbial community and also reflects the influence of soil synusiologic mechanism and soil stress on the community. The study of soil microorganisms plays a positive role in understanding the functions of various biological systems. With the improvement of the subject, the research means of microbiology are constantly improved and improved, and new means are constantly emerging.

4.2. Construction of Soil Microbial Synusiologic Network. Since the 1920s, the synusiologic function of green space has been paid attention to, which has gradually changed the research of green space from extensive to detailed, from qualitative description to quantitative research. Landscape ecology enables people to know the landscape of green space scientifically, especially through the analysis and research of synusiologic elements structure of green space on a landscape scale has outstanding advantages. Land synusiologic suitability evaluation is based on synusiologic environmental sensitivity evaluation. Ecological sensitivity refers to the sensitivity of the ecosystem to human activities, which is used to reflect the possibility of synusiologic imbalance and synusiologic environmental problems. Ecological environmental quality evaluation is essentially a pattern recognition problem, that is, the actual monitoring results of the synusiologic environmental quality evaluation index system are compared with the array of corresponding synusiologic environmental quality evaluation standard values, and the synusiologic environmental quality grade corresponding to the standard value array closest to the array of monitoring values is the recognition result of the BP ANN model, that is, the synusiologic environment quality evaluation result of the corresponding area. The synusiologic environmental grade diagram is shown in Figure 2.

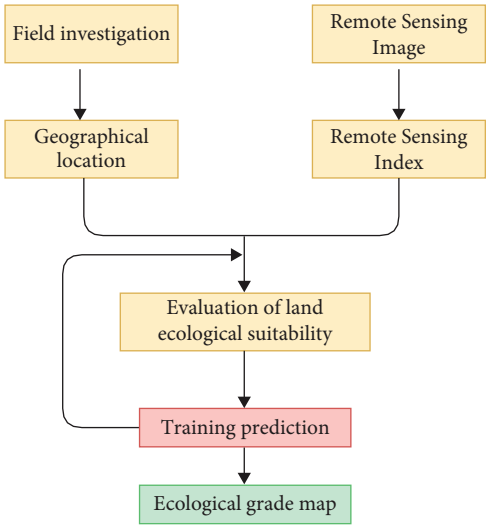

Figure 2: Ecological environment level map.

The synusiologic environment is a huge, complex, and changeable system, which is not only influenced by various factors of the wetland ecosystem itself but also affected by various factors in the basin. Therefore, when quantitatively evaluating the quality of its synusiologic environment, it is difficult to realize if all the factors involved are listed as evaluation indexes at present, mainly because some factors are difficult to obtain or cannot be quantified. Precipitation temperature and its distribution, vegetation improvement and its community structure, basic topographic features, and spatial pattern, etc. directly affect the stability and natural balance ability of the regional environment and are the basic elements that constitute the synusiologic environment. Appropriate water and heat are the basic conditions for the survival and reproduction of all living things and affect the regional synusiologic environment. Generally speaking, the modules of the network have more biological significance than the whole network. First of all, each OTU in the module can determine its chemical characteristics according to its respective generic or species names. Then, according to the relationship between the characteristics of each OTU, the function of a module can be determined. Landscape pattern analysis is of great significance in green space planning, and the deep cognition of green space on the site is the foundation of scientific green space planning. The analysis of urban synusiologic landscape patterns is the basis of the implementation, management, and planning of green space synusiologic networks.

This paper selects the following indicators to analyze the landscape pattern of green space in the study area:

The number of patches (NP), NP refers to the total number of patches included in a certain patch type or the total number of patches in the whole landscape. The number of patches can reflect both landscape heterogeneity and landscape fragmentation. The calculation principle is

$$\mathrm{NP} = N, \tag{5}$$

where N represents the total number of patches.

Percent of Landscape (PLAND) refers to the percentage of a landscape block type in the total landscape area. The calculation principle is

$$\mathrm{PLAND} = \frac{\sum_{j=1}^{n} a_{\mathrm{ij}}}{A} \times 100. \tag{6}$$

Among them, i represents the type of patches, j represents the number of patches, a_{ij} is the area of landscape patches, and A is the area of all patches in the landscape. The value range of PLAND is from 0 to 100. When the value of PLAND is equal to 100, there is only one patch type in the landscape. When PLAND approaches 0, this type is particularly rare in the landscape. PLAND is an important index to select the dominant landscape types in the landscape, which can reflect the biodiversity and dominant species in the landscape.

Class area (CA) represents the total area of each landscape type. The calculation principle is

$$\mathrm{CA} = \sum_{j=1}^{n} a_{\mathrm{ij}}\left(\frac{1}{10000}\right). \tag{7}$$

Among them, CA is the total area of a certain type of patch in the landscape, a_{ij} represents the area of patch m^2, taking A as the unit, 555 as the total area of landscape patches, taking hm^2 as the unit, and n as the number of all patches in the landscape.

Patch density (PD), the calculation principle is

$$\mathrm{PD} = \frac{N}{A}. \tag{8}$$

Among them, N is the total number of a certain type of patches in the landscape, and A is the total area of a certain type of patches in the landscape. The larger the value, the wider the distribution of this type of patches in the landscape.

The maximum patch index is (LPI), which indicates the degree of influence of different types of landscapes on the whole landscape. The calculation principle is shown in the following formula:

$$\mathrm{LPI} = \frac{\mathrm{Max}\left(a_1 \ldots a_n\right)}{A}(100). \tag{9}$$

The patch index reflects the impact of human activities on landscape pattern and the calculation principle is

$$\mathrm{LSI} = \frac{0.25E}{\sqrt{A}}. \tag{10}$$

Among them, E is the perimeter of all patches in the landscape and A is the area of all patches in the landscape. The more irregular the patch shapes in the landscape, the greater the value of LSI.

The landscape aggregation index is (AI), and the calculation principle is

$$\mathrm{AI} = \left[\sum_{i=1}^{m}\left(\frac{g_{\mathrm{ii}}}{\max - g_{\mathrm{ii}}}\right)P_i\right] \times 100. \tag{11}$$

Among them, g_{ii} is the number of patches of the same type that are connected between i types of patches in the

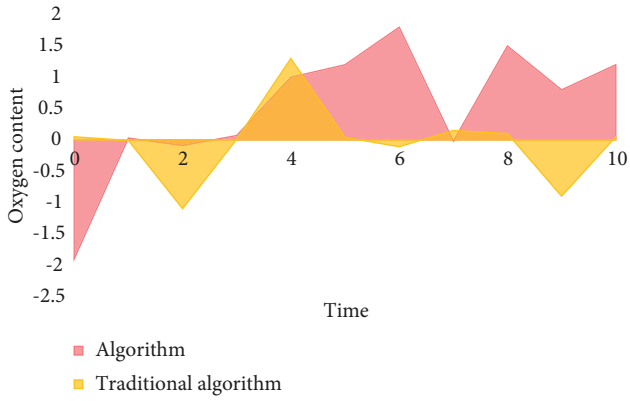

Figure 3: Oxygen content in physical process.

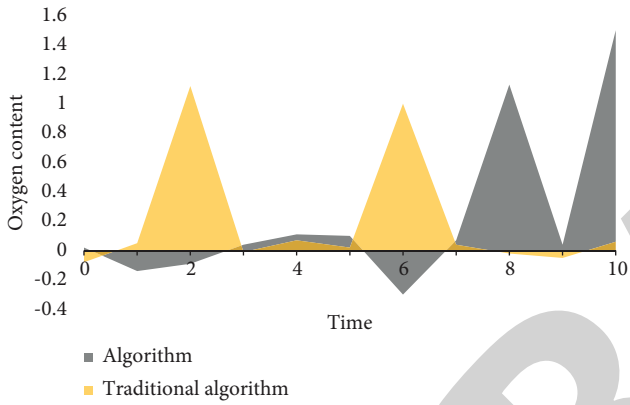

Figure 4: Oxygen content in synusiologic process.

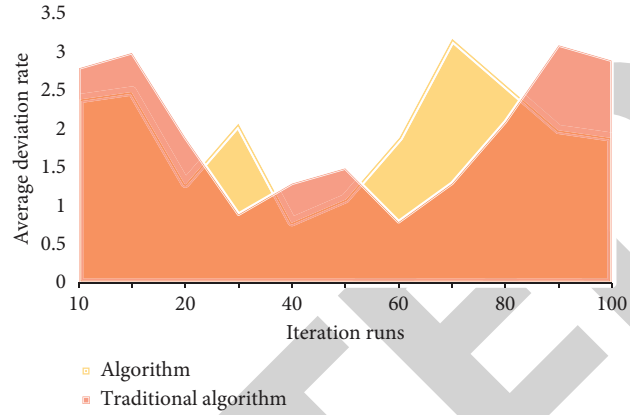

Figure 5: Average deviation rate.

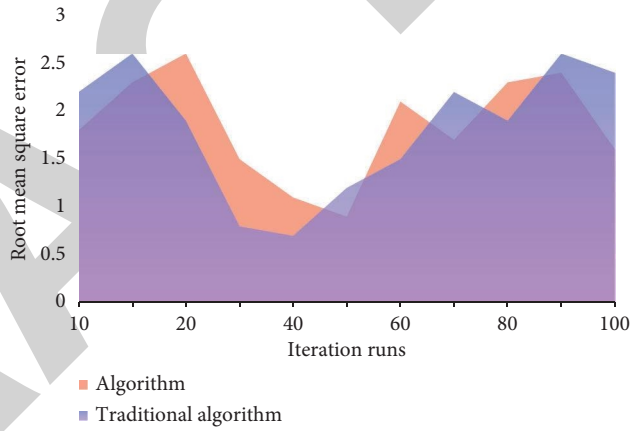

Figure 6: RMS error situation.

landscape, max is the maximum number of patches of the same type that are connected between i types of patches, and P_i is the ratio of the number of patches of the type i to the total number of landscape patches. The larger the value of AI, it means that this type is about aggregated this landscape.

Eco-sensitivity evaluation is the evaluation of the possibility, scope, and degree of regional synusiologic environmental problems. According to the spatial difference of synusiologic environmental sensitivity, the study area can be divided into an extremely sensitive area, a highly sensitive area, a moderately sensitive area, a slightly sensitive area, and an insensitive area. The stronger the sensitivity of the regional synusiologic environment, the higher the level of land synusiologic suitable use type, and the more restrictions on its improvement and utilization. Training samples are also called expert samples, that is, the "teacher value" of the BP network model, which is usually a matrix composed of several groups of "input-output pairs". With the improvement of computer techniques, graph theory has been widely used in almost all domains and has achieved unprecedented improvement. Graph theory is a branch of mathematics, taking graphs as the research object. Among them, a graph is a graph composed of a number of given points and lines connecting two points. This graph is usually used to describe a certain relationship between some things. Points represent things, and lines show that corresponding things have this relationship. In the past, the research on the BP ANN model of environmental quality evaluation usually used the national environmental quality standard as the training sample, but for the evaluation of the synusiologic environmental quality of small towns, if the national synusiologic environmental quality standard was used as the training sample, then the synusiologic environmental quality of administrative villages in the small town might be concentrated on one or two levels. As shown in Figures 3–6, this algorithm is superior to the traditional algorithm. With the increase in training times of the improved neural network, the error rate gradually decreases and the prediction accuracy gradually improves.

The algorithm of the BP model learning process consists of two parts: forward propagation and backward propagation. Its basic idea is: in the forward propagation process, the input sample is processed by the hidden layer unit from the input layer and transmitted to the output layer; If the output layer cannot get the expected output vector when using the existing network connection weights and thresholds in the forward propagation, that is, the error function value is large, it will be transferred to the backward propagation. Modern scientific theories and viewpoints such as system mathematics, fuzzy theory, and grey theory hold that numerous

Table 1: Changes of K value.

	0	10	20	30	40	50	60	70	80	90	100
Algorithm	2.7	2.5	1.8	2	0.8	1.4	1.5	2.3	2.1	2.8	3.2
Traditional algorithm	2.2	1.7	2.1	1.5	2.1	2.0	2.5	1.9	1.6	2.1	2.3

Table 2: Network training results.

	0	5	10	15	20	25	30	35	40	45	50
Algorithm	3.1	1.4	1.5	2.6	2.5	2.3	1.2	2.2	2.9	3.2	3.5
Traditional algorithm	1.8	2.2	1.2	3.1	2.4	3.3	2.8	1.5	1.9	2.3	1.7

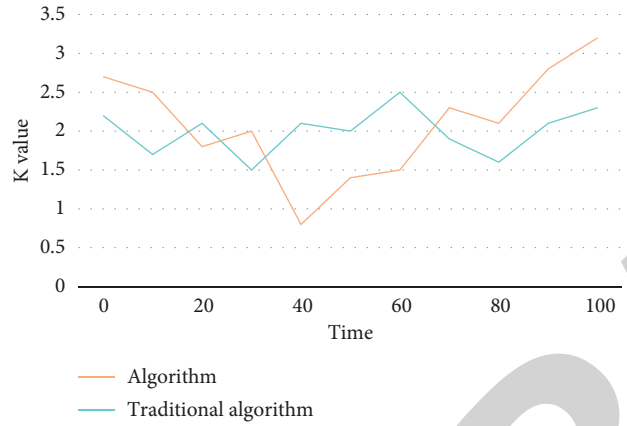

Figure 7: Change of k value.

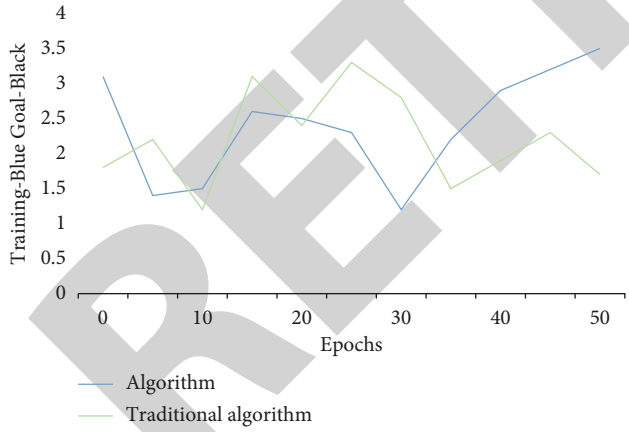

Figure 8: Network training results.

and complex influencing factors in the ecosystem have different influences on the synusiologic environment. There are not only primary and secondary points but also some factors that can be ignored. As shown in Tables 1 and 2 and Figures 7 and 8, the network performance of this algorithm is 18% better than that of the traditional algorithm, and the network has reached a certain synusiologic level, which can provide a buffer for the random shock caused by the rigid interaction mode at the customer level.

As a matter of fact, any system containing a certain binary relationship can be simulated by graphs. Whether two points in a graph are connected or not is our main object of investigation. Because this is closely related to what we are concerned about the internal specific relationship between two objects, the straightness of the connecting line in a graph is not the key point of concern. Therefore, the above elements are ignored, and the concept of graphs is produced by mathematical abstraction. Many factors are interrelated and mutually mapped. One factor can be mapped to another factor, and even many factors can be mapped. Therefore, selecting the main, easily accessible, quantitative, and other factors that can be mapped as much as possible as the evaluation index is enough to obtain the evaluation results that are more in line with the actual synusiologic environment quality.

5. Conclusions

Around the world, people pay more and more attention to the quality of human settlements. In order to avoid the conflict between land use and nature protection, the construction of a green space synusiologic network, as a new means of green space planning, is helpful to make strategic decisions on existing expenditures (such as land protection and utilization) and future benefits (such as natural resources and quality of life). The system has different characteristics, so its evaluation index system is also different. When applying a neural network to synusiologic environment quality evaluation, for a complex synusiologic environment or ecosystem with many evaluation indexes, the number of hidden nodes or hidden layers of the network can be appropriately increased to improve the learning ability and training effect of the neural network. ANN is a mature modeling means with many advantages. It has specific applications in many aspects, especially in complex large systems like ecosystems. According to the research in this paper, the network performance of this algorithm is 18% better than that of the traditional algorithm, and it is suitable to be widely put into practice.

Data Availability

The figures and tables used to support the findings of this study are included in the article.

Hindawi
Computational Intelligence and Neuroscience
Volume 2022, Article ID 1126785, 12 pages
https://doi.org/10.1155/2022/1126785

Research Article

Design of Flute Music Remote Teaching System Based on Multi-Pass Scheduling Optimization

Zhao Jing

North University of China, Taiyuan, Shanxi 030051, China

Correspondence should be addressed to Zhao Jing; 181960142@stu.lixin.edu.cn

Received 10 July 2022; Accepted 16 September 2022; Published 29 September 2022

Academic Editor: Gopal Chaudhary

With the gradual development of the Internet industry, every aspect of people's life has been affected by the Internet, playing increasingly irreplaceable functions in people's entertainment, office, and other aspects. Judging from the current development situation, the old Internet digital teaching system has many problems, such as low artificial intelligence, weak information processing ability, and lack of effective learning ability. This paper designs the flute music remote teaching system, which can realize remote music teaching and provide help in providing real-time music teaching. The music learning system includes the user's access records, the user's operation and the completion of the test data, the discussion and communication of online participation, the user's interests, specialties and operation methods, learning progress and scoring, and so on. In addition, it explores and explains all the key steps required by the current distance education model and invents a sample of the distance education model. On this basis, Internet algorithm programs will be used for all key processing functions of the system. The use of Internet algorithm programs is interactive and automated, which greatly enhances the role of the education system. This article first discusses the unique teaching and automated teaching mode of the system, which lays the cornerstone for further reforms in this field in the future.

1. Introduction

Due to the advent of the digital age of the Internet, a variety of Internet digital algorithm programs continue to appear. The digitalization of the Internet has brought great convenience to people in communication, entertainment, information sharing, entertainment, online shopping, and many other aspects [1]. Manager algorithm program is the field of artificial intelligence algorithm program development. The software invented as algorithm program has a certain degree of intelligence, can help people make decisions, and can independently complete certain commands such as human behavior [2]. Moreover, it has certain self-improvement skills and can reason and predict things in development [3]. With the continuous maturity of algorithm programs, the use of various fields is also increasing. In today's distance education mode, the application of algorithm programs to realize the ancient and tedious Internet digital education has become an epoch-making role in the development of distance education systems in the current era [4]. The long history of flute art began in distant European lands and has been introduced to China for nearly 150 years. In the past 100 years, Chinese flute art has undergone rapid development. The reason for the popularity of flute art at present is firstly inseparable from its beautiful tunes [5]. The treble part is subtle and elegant, the mid-range part is solid and mellow, and the bass part is thick and deep. After listening, the audience stays and does not want to leave. Then, the flute looks good and is easy to store [6]. Finally, with the exchange and penetration of various countries and fields, the Chinese people have improved their understanding of symphony, accepting and loving the "big band." Of course, the flute is loved by the public and is the most important classical instrument of the Symphony Wood Orchestra [7].

2. Related Work

The continuous development of digital technology and the continuous improvement of network technology have brought many cases to people's life. In addition to the initial communication, the current Internet technology has also

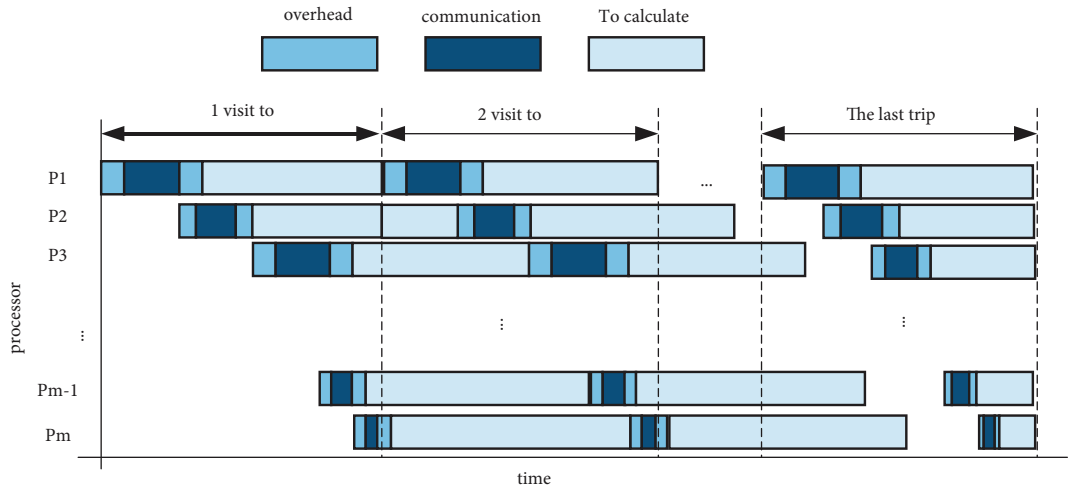

Figure 1: Multi-pass scheduling in blocking mode.

played its role in many aspects of people's shopping and entertainment [8]. Moreover, the rich resources of the digitalization of the Internet provide people engaged in research and learning with important the supporting role [9]. Under the strategic idea of rejuvenating the country through science and education, online teaching in some relatively remote areas is an effective means. Literature pointed out that with the generalization of Internet digitalization and the maturity of algorithm programs, the current era of distance learning algorithm programs has become an irresistible development trend in the teaching field. This also puts forward high requirements for cultural training places such as universities, time, and crowd education mode [10]. There are many constraints for learners, and it is difficult to adapt to people's needs for knowledge. The continuous development of Internet technology has brought some development opportunities to traditional education and teaching, and online teaching has gradually developed. In the literature, distance learning tasks are used to transform the existing learning environment into the Internet, and uses new algorithms and new data sequences to ensure that distance education achieves better results than the old learning model [11, 12]. It is worth mentioning that the innovation of algorithm programs must express the scientific development concept of "people-oriented," and the modern distance teaching model must be able to achieve "humanization" before it can develop into a truly humanized application mode [13]. The literature points out that with the wide use of algorithm programs in daily life, the introduction of algorithm programs into distance learning mode and the establishment of an automated Internet digital learning environment are becoming the mainstream trend of the future distance education system [14, 15].

2.1. Multi-Pass Scheduling Model and Algorithm Research of Separable Tasks

2.1.1. Periodic Multi-Pass Scheduling Optimization Model for Separable Tasks with Given Scheduling Order. As shown in Figure 1, the layering of the Internet in the routing architecture determines that the mobile port of the Internet can also have a two-layer topology. One of them is the high-level self-determination management level department. They are considered the "real" topology, that is, the domain link rotation between the node in its own management department and the self-management department is constructed by domain links, and the other A topological structure is a low-level rotation level.

In general, in order to make the running algorithm time and the time of communicating information of one of the target machines the same as other machines, we have obtained the number of requirements of each machine from this. Therefore, you can get

$$\begin{aligned}\alpha_1 V(z_1+w_1)+o_1+s_1 &= \alpha_2 V(z_2+w_2)+o_2+s_2\\ &= \cdots\\ &= \alpha_m V(z_m+w_m)+o_m+s_m,\end{aligned} \tag{1}$$

$$\alpha_2 = \frac{\alpha_1 V(z_1+w_1)+o_1+s_1-o_2-s_2}{V(z_2+w_2)}. \tag{2}$$

It is known that

$$\alpha_1+\alpha_2+\cdots+\alpha_m = 1. \tag{3}$$

From (2) and (3), we can get

$$\begin{aligned}\alpha_1 &+ \frac{\alpha_1 V(z_1+w_1)+o_1+s_1-o_2-s_2}{V(z_2+w_2)}\\ &+ \frac{\alpha_1 V(z_1+w_1)+o_1+s_1-o_3-s_3}{V(z_3+w_3)}\\ &+\cdots+\frac{\alpha_1 V(z_1+w_1)+o_1+s_1-o_m-s_m}{V(z_m+w_m)} = 1.\end{aligned} \tag{4}$$

For the convenience of the following discussion, define the following two new variables:

$$\begin{cases} \Delta_i = \dfrac{z_1 + w_1}{z_i + w_i}, \\ \Phi_i = \dfrac{o_1 + s_1 - o_i - s_i}{z_i + w_i}. \end{cases} \tag{5}$$

Substituting (5) into simplified form:

$$\alpha_1 \left(1 + \sum_{i=2}^{m} \Delta_i \right) + \frac{1}{V} \sum_{i=2}^{m} \Phi_i = 1. \tag{6}$$

As a result, the optimal solution of the internal scheduling arrangement allocation plan can be obtained as shown in the following formula:

$$\begin{cases} \alpha_1 = \dfrac{1 - (1/V) \sum_{i=2}^{m} \Phi_i}{1 + \sum_{i=2}^{m} \Delta_i}, \\ \alpha_i = \alpha_1 \Delta_i + \dfrac{1}{V} \Phi_i, i = 1, 2, \ldots m. \end{cases} \tag{7}$$

Existing research indicates that in the final scheduling process, all slave processors must complete the algorithm formula together, so that it minimizes the total completion time of the task. Figure 1 shows a situation in which all processors in the system studied in this article complete job scheduling at one time, which allows the machine to have time to complete the job of the last trip of each slave processor, as shown in formulas (8) and (9).

$$T(\beta_1) = o_1 + z_1 \beta_1 V + s_1 + w_1 \beta_1 V, \tag{8}$$

$$T(\beta_i) = \sum_{j=1}^{i-1} \left(o_j + z_j \beta_j V \right) + o_i + z_i \beta_i V + s_i + w_i \beta_i V. \tag{9}$$

For all processors, the total completion time of the task is the same, namely,

$$T(\beta_m) = T(\beta_{m+1}). \tag{10}$$

Therefore,

$$s_i + w_i \beta_i V = o_{i+1} + z_{i+1} \beta_{i+1} V + s_{i+1} + w_{i+1} \beta_{i+1} V, \tag{11}$$

$$\beta_{i+1} = \frac{s_i - (s_{i+1} + o_{i+1})}{V(w_{i+1} + z_{i+1})} + \frac{w_i}{w_{i+1} + z_{i+1}} \beta_i. \tag{12}$$

For the sake of simplicity, two new variables are defined below:

$$\begin{cases} \delta_{i+1} = \dfrac{s_i - (s_{i+1} + o_{i+1})}{w_{i+1} + z_{i+1}}, \\ \varepsilon_{i+1} = \dfrac{w_i}{w_{i+1} + z_{i+1}}. \end{cases} \tag{13}$$

(11) can be simplified to

$$\beta_{i+1} = \frac{1}{V} \delta_{i+1} + \varepsilon_{i+1} \beta_i. \tag{14}$$

Let us set it up:

$$\delta_i \geq 0. \tag{15}$$

If the workload of calculation is very heavy, let all those who can work participate in the calculation operation; then, the assumption is correct, and if β_i is negative, then Pi does not participate in the calculation. So, to sum up, (13) can be changed to

$$\begin{cases} E_i = \prod_{j=2}^{i} \varepsilon_j, \\ \Gamma_i = \sum_{j=2}^{i} \left(\delta_j \prod_{k=j+1}^{i} \varepsilon_k \right). \end{cases} \tag{16}$$

Because

$$\sum_{i=1}^{m} \beta_i = 1. \tag{17}$$

then

$$\begin{cases} \beta_1 = \dfrac{1 - 1V \sum_{i=2}^{m} \Gamma_i}{1 + \sum_{i=2}^{m} E_i}, \\ \beta_2 = E_i \beta_1 + \dfrac{1}{V} \Gamma_i i = 2, \ldots, m. \end{cases} \tag{18}$$

After formula (18), in systems with different structures, it is easy to obtain the number of tasks assigned to each slave processor in the final adjustment process, where the cost of starting information transmission and the starting cost of algorithm operation should be considered.

Assuming that the number of slave processors participating in the algorithm operation is m and the number of reserved strokes is $n + 1$, then a separable task optimization scheduling model can be obtained. The following is a description of the sample.

$$\min_{n,m} T(W) = \min \left[n(\alpha_1 V(z_1 + w_1) + o_1 + s_1) + \beta V(z_1 + w_1) + o_1 + s_1 \right],$$

subjecte d to

$$\begin{cases} \alpha_i > 0, i \in \{1, 2, \ldots, m\}, \\ \sum_{i=1}^{m} \alpha_i = 1, \\ \beta_i > 0, i \in \{1, 2, \ldots, m\}, \\ \sum_{i=1}^{m} \beta_i = 1. \end{cases} \tag{19}$$

2.2. Verification of Inspection Results for a Given Scheduling Sequence. In the problem of enhanced knowledge, the terminal artificially implanted in the intelligent program usually does not know the model of the environment and can only update itself by constant trial and error. The traditional enhanced knowledge algorithm often has unstable results in the complex MDP environment. There is no guarantee that it will

Table 1: Experimental parameters.

P	o	s	z	w
P_1	4.11	1.59	0.44	6.82
P_2	10.23	2.98	0.67	1223
P_3	17.04	4.28	0.95	18.48
P_4	11.58	3.12	0.76	13.84
P_5	6.29	1.91	0.59	8.90
P_6	11.67	3.56	0.78	13.53
P_7	17.25	5.47	0.96	19.04
P_8	9.43	3.74	0.53	27.05
P_9	1.43	1.99	0.16	8.06
P_{10}	4.32	2.13	0.42	9.96
P_{11}	7.50	2.57	0.64	11.90
P_{12}	5.38	2.43	0.44	12.42
P_{13}	3.37	2.45	0.25	13.80
P_{14}	2.98	3.06	0.24	14.84
P_{15}	2.28	3.60	0.23	15.64
P_{16}	6.56	2.43	0.52	10.62
P_{17}	10.78	1.22	0.82	5.78
P_{18}	10.34	2.51	0.78	8.74
P_{19}	11.90	3.88	0.83	11.92
P_{20}	10.08	2.70	0.72	8.84
P_{21}	8.13	1.52	0.63	5.62
P_{22}	5.32	3.28	0.81	10.28
P_{23}	2.50	5.06	0.18	16.12
P_{24}	1.86	3.98	0.16	12.03
P_{25}	1.69	2.92	0.14	9.36
P_{26}	5.42	2.78	0.46	9.47
P_{27}	8.02	2.60	0.79	9.68
P_{28}	3.78	3.52	0.44	11.19
P_{29}	2.57	4.26	0.19	13.48
P_{30}	6.38	3.78	0.37	15.39

converge to the optimal strategy every time. There are many reasons for this result. For example, the surrounding environment is too chaotic. The terminal artificially implanted in the intelligent program cannot fully judge the surrounding situation. The algorithm of the artificially implanted intelligent program terminal itself is flawed, and the environment estimation is inaccurate, resulting in errors and instability. Since the sample algorithm discussed in this chapter is for the samples proposed in the material, there are many articles in the master's thesis of Xidian University in Wanfang's library. This experiment will be studied, and a new algorithm will be proposed as a comparison algorithm, to compare it with the FPMISA proposed in this experiment. The main reason for random variance is the use of algorithms with random equations, such as ϵ-greedy algorithm, when updating the value equation. The classical reinforcement knowledge algorithm Sarsa and Q-learning algorithm both use the ϵ-greedy algorithm in the action strategy, but in the update strategy, the greedy algorithm used by Q-learning and the ϵ-greedy algorithm used by Sarsa are updated by changing the ϵ-greedy selection. It becomes the expectation equation, which effectively reduces the random variance of the original Sarsa at the cost of increasing the complexity of the algorithm. The number of processor parameters is shown in Table 1.

In the literature, a kind of command algorithm that can be allocated in a heterogeneous distributed system is proposed to find multiple positive solutions. In the following experiments, the algorithm proposed in this section will be used in the range of 50,000 to 40,000 tasks. FPMISA and Amin's method are performed under the same scheduling order. Schedule and compare results. The two scheduling sequences used in the experiment are represented by IZ in the order of increasing information transmission rate and IW in the order of increasing algorithm running rate. It can be seen from Table 2 that under a large amount of tasks, whether it is scheduling using sequential IZ or IW, the proposed algorithm has the following two characteristics: first, it uses more processors, and second it uses less scheduling. In terms of the number of passes, it can be seen that the algorithms proposed in this article have achieved relatively good scheduling results. For the experimental results, the analysis is as follows. The algorithm proposed in this article gives priority to using more processors under the premise of producing feasible solutions, which can make better and more full use of the system's algorithm operation resources and improve the concurrency of the system. At the same time, the running program of this article can solve the most suitable number of scheduling trips. While reducing the idle time between processors, it will not introduce too many scheduling trips, thus avoiding excessive startup overhead. In summary, the new algorithm proposed in this article can solve better scheduling results more efficiently. Table 2 shows the task completion time comparison test.

2.3. Dividable Task Regularity Multiple Scheduling Model of Optimal Scheduling Order. Same as the explanation in the previous section, it derives a new regular multi-pass scheduling model for separable tasks to solve the optimal scheduling sequence.

As shown in Figure 2, in each internal scheduling, in order to make a slave processor such as P complete its current algorithm, the central processing system can give it the next instruction that needs to be operated. Therefore, for all processing, we strive to make the information transmission and algorithm time of each processor the same for each internal scheduling. In short, we have determined the number of instructions for each processor so that the information transmission and algorithm running time of each processor is equal to the information transmission and algorithm running time of all other processors. From this, we can get

$$\begin{aligned} &\alpha_{\sigma_1} V\left(z_{\sigma_1} + w_{\sigma_1}\right) + o_{\sigma_1} + s_{\sigma_1} \\ &= \alpha_{\sigma_2} V\left(z_{\sigma_2} + w_{\sigma_2}\right) + o_{\sigma_2} + s_{\sigma_2} \\ &= \ldots \\ &= \alpha_{\sigma_m} V\left(z_{\sigma_m} + w_{\sigma_m}\right) + o_{\sigma_m} + s_{\sigma_m}. \end{aligned} \tag{20}$$

$$\alpha_{\sigma_2} = \frac{\alpha_{\sigma_1} V\left(z_{\sigma_1} + w_{\sigma_1}\right) + o_{\sigma_1} + s_{\sigma_1} - o_{\sigma_2} - s_{\sigma_2}}{V\left(z_{\sigma_2} + w_{\sigma_2}\right)}, \tag{21}$$

Table 2: Task completion time comparison test.

Algorithm	Task volume	Scheduling sequence	$m+1$	m	Complete time
Amin's method FPMISA	50000	LZ	3	21	30136
		LW	89	12	37346
		LZ	3	30	23098
		LW	42	30	19912
Amin's method FPMISA	100000	LZ	7	22	54900
		LW	123	13	69650
		LZ	6	30	42218
		LW	60	30	39338
Amin's method FPMISA	150000	LZ	10	22	80938
		LW	1487	14	98388
		LZ	9	30	61339
		LW	73	30	53636
Amin's method FPMISA	200000	LZ	12	23	103279
		LW	170	14	130899
		LZ	12	30	80459
		LW	84	30	77994
Amin's method FPMISA	250000	LZ	17	23	128413
		LW	190	14	163379
		LZ	15	30	995800
		LW	94	30	97276
Amin's method FPMISA	300000	LZ	21	23	153418
		LW	208	14	195873
		LZ	18	30	118700
		LW	103	30	116540
Amin's method FPMISA	350000	LZ	25	23	178445
		LW	222	15	217231
		LZ	21	30	137821
		LW	112	30	135790
Amin's method FPMISA	400000	LZ	28	22	203557
		LW	238	15	248088
		LZ	25	30	156815
		LW	119	30	155029

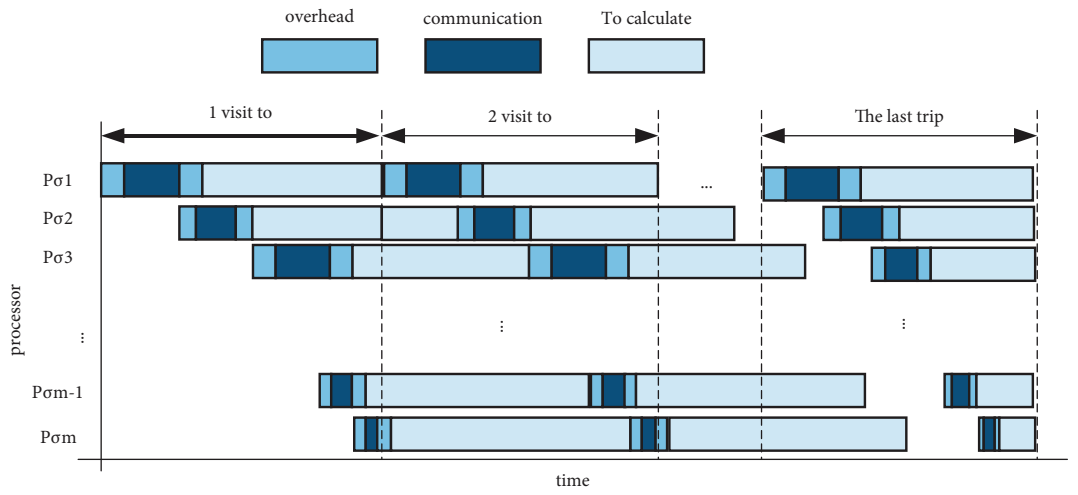

Figure 2: Multiple scheduling with obstructive mode considering scheduling order.

$$\alpha_{\sigma_1} + \alpha_{\sigma_2} + \cdots + \alpha_{\sigma_m} = 1. \tag{22}$$

From (21) and (22), we can get

$$\begin{aligned} &\alpha_{\sigma_1} + \frac{\alpha_{\sigma_1} V\left(z_{\sigma_1} + w_{\sigma_1}\right) + o_{\sigma_1} + s_{\sigma_1} - o_{\sigma_2} - s_{\sigma_2}}{V\left(z_{\sigma_2} + w_{\sigma_2}\right)} \\ &+ \frac{\alpha_{\sigma_1} V\left(z_{\sigma_1} + w_{\sigma_1}\right) + o_{\sigma_1} + s_{\sigma_1} - o_{\sigma_3} - s_{\sigma_3}}{V\left(z_{\sigma_3} + w_{\sigma_3}\right)}, \\ &+ \cdots \\ &+ \frac{\alpha_{\sigma_1} V\left(z_{\sigma_1} + w_{\sigma_1}\right) + o_{\sigma_1} + s_{\sigma_1} - o_{\sigma_m} - s_{\sigma_m}}{V\left(z_{\sigma_m} + w_{\sigma_m}\right)} = 1. \end{aligned} \tag{23, 24}$$

For the convenience of the following discussion, define the following two new variables:

$$\begin{cases} \Delta_{\sigma_i} = \dfrac{z_{\sigma_1} + w_{\sigma_1}}{z_{\sigma_i} + w_{\sigma_i}}, \\ \Phi_{\sigma_i} = \dfrac{o_{\sigma_1} + s_{\sigma_1} - o_{\sigma_i} - s_{\sigma_i}}{z_{\sigma_i} + w_{\sigma_i}}. \end{cases} \tag{25}$$

Substituting (22) into simplified form:

$$\alpha_{\sigma_i}\left(1 + \sum_{i=2}^{m} \Delta_{\sigma_i}\right) + \frac{1}{V}\sum_{i=2}^{m} \Phi_{\sigma_i} = 1. \tag{26}$$

The results show that the compact solution of the internal scheduling task allocation strategy can be obtained as

$$\begin{cases} \alpha_{\sigma_i} = \dfrac{1 - (1/V)\sum_{i=2}^{m} \Phi_{\sigma_i}}{1 + \sum_{i=2}^{m} \Delta_{\sigma_i}}, \\ \alpha_{\sigma_i} = \alpha_{\sigma_1}\Delta_{\sigma_i} + \dfrac{1}{V}\Phi_{\sigma_i}, i = 1, 2, \ldots m. \end{cases} \tag{27}$$

Research shows that when scheduling, the proposed algorithm has the following two characteristics: first, it uses more processors, and second, it uses less scheduling. It can be seen that the algorithms proposed in this article have achieved relatively better scheduling results. For the experimental results, the analysis is as follows. The algorithm proposed in this article will give priority to using more processors on the premise that it produces feasible solutions, which can make better use of the system's algorithm running resources and improve the concurrency of the system. Therefore, the task completion time of the last pass of any processor can be obtained, as shown below.

$$\begin{aligned} T\left(\beta_{\sigma_i}\right) &= o_{\sigma_i} + z_{\sigma_i}\beta_{\sigma_i} V + s_{\sigma_i} + w_{\sigma_i}\beta_{\sigma_i} V, \\ T\left(\beta_{\sigma_i}\right) &= \sum_{j=1}^{i-1}\left(o_j + z_{\sigma_j}\beta_{\sigma_j} V\right) + o_{\sigma_i} + z_{\sigma_i}\beta_{\sigma_i} V + s_{\sigma_i} + w_{\sigma_i}\beta_{\sigma_i} V. \end{aligned} \tag{28}$$

It can be known that for each processor, the time to complete the task is always the same, which is

$$T\left(\beta_{\sigma_m}\right) = T\left(\beta_{\sigma_{m+1}}\right). \tag{29}$$

So, we have

$$s_{\sigma_i} + w_{\sigma_i}\beta_{\sigma_i} V = o_{\sigma_{i+1}} + z_{\sigma_{i+1}}\beta_{\sigma_{i+1}} V + s_{\sigma_{i+1}} + w_{\sigma_{i+1}}\beta_{\sigma_{i+1}} V, \tag{30}$$

$$\beta_{\sigma_{i+1}} = \frac{s_{\sigma_i} - \left(s_{\sigma_{i+1}} + o_{\sigma_{i+1}}\right)}{V\left(w_{\sigma_{i+1}} + z_{\sigma_{i+1}}\right)} + \frac{w_{\sigma_i}}{w_{\sigma_{i+1}} + z_{\sigma_{i+1}}}\beta_{\sigma_i}. \tag{31}$$

For the convenience of discussion, two new variables are defined below:

$$\begin{cases} \delta_{\sigma_{i+1}} = \dfrac{s_{\sigma_i} - \left(s_{\sigma_{i+1}} + o_{\sigma_{i+1}}\right)}{w_{\sigma_{i+1}} + z_{\sigma_{i+1}}}, \\ \varepsilon_{\sigma_{i+1}} = \dfrac{w_{\sigma_i}}{w_{\sigma_{i+1}} + z_{\sigma_{i+1}}}. \end{cases} \tag{32}$$

(31) can be simplified to

$$\beta_{\sigma_{i+1}} = \frac{1}{V}\delta_{\sigma_{i+1}} + \varepsilon_{\sigma_{i+1}}\beta_{\sigma_i}. \tag{33}$$

In which

$$\delta_{\sigma_i} \geq 0. \tag{34}$$

When there are many targets, let all processors join the operation; then, this conjecture can be established, and if β_{σ_i} is negative, it is equivalent to P_{σ_i} not participating in scheduling. After running with the program algorithm, (34) can be transformed into

$$\begin{cases} E_{\sigma_i} = \prod_{j=2}^{i} \varepsilon_{\sigma_j}, \\ \Gamma_{\sigma_i} = \sum_{j=2}^{i}\left(\delta_{\sigma_j}\prod_{k=j+1}^{i} \varepsilon_{\sigma_k}\right). \end{cases} \tag{35}$$

Because

$$\sum_{i=1}^{m}\beta_{\sigma_i} = 1, \tag{36}$$

then

$$\begin{cases} \beta_{\sigma_1} = \dfrac{1 - 1V\sum_{i=2}^{m}\Gamma_{\sigma_i}}{1 + \sum_{i=2}^{m} E_{\sigma_i}}, \\ \beta_{\sigma_2} = E_{\sigma_i}\beta_{\sigma_1} + \dfrac{1}{V}\Gamma_{\sigma_i} i = 2, \ldots, m. \end{cases} \tag{37}$$

From the calculation of (35), considering the influence of the initial cost of information transmission and the initial cost of running algorithms in a heterogeneous system, the workload allocated to each slave processor in the last scheduling can be easily obtained.

It is conjectured that the number of subordinate processors participating in the algorithm operation is m and the number of scheduling passes is n 1, where n is the number of structural scheduling, so that a scheduling sample with separable tasks can be constructed. The situation of the model is as follows:

$$\min_{n,m} T(W) = \min \left[n\left(\alpha_{\sigma_1} V\left(z_{\sigma_1} + w_{\sigma_1}\right) + o_{\sigma_1} + s_{\sigma_1}\right) + \beta V\left(z_{\sigma_1} + w_{\sigma_1}\right) + o_{\sigma_1} + s_{\sigma_1}\right],$$

subjecte d to

$$\begin{cases} \alpha_{\sigma_i} > 0, i \in \{1, 2, \ldots, m\}, \\ \sum_{i=1}^{m} \alpha_{\sigma_i} = 1, \\ \beta_{\sigma_i} > 0, i \in \{1, 2, \ldots, m\}, \\ \sum_{i=1}^{m} \beta_{\sigma_i} = 1. \end{cases} \tag{38}$$

2.4. Analysis of the Experimental Results of the Optimal Scheduling Sequence. This section will explain a brand-new scheduling order of multiple scheduling samples of regular assignment tasks. In reinforcement learning, the variance of the estimated value is also an important factor affecting its stability. Even if the expected value of the estimated value is relatively accurate, if the variance is too high, severe swings in the estimated value will make the strategy swing with it and ultimately lead to unstable results. Also, for the model manufacturing, a new comprehensive improved genetic algorithm is proposed for calculation.

The relevant parameter indicators of the machine in this experiment are as follows. In the experiment, the algorithm FPMISA and Amin's method proposed in this section will be used in the range of 50,000 to 40,000 tasks to perform scheduling and compare the results in the same scheduling order. The two scheduling sequences used in the experiment are represented by IZ in the order of increasing information transmission rate and IW in the order of increasing algorithm running rate. Under a larger task load, whether it is to use sequential IZ or IW for scheduling, the proposed algorithm has the following two characteristics: first, it uses more processors, and second, it uses fewer scheduling passes. The algorithms proposed in this article have achieved relatively good scheduling results. For the experimental results, the analysis is as follows. The algorithm proposed in this article gives priority to using more processors under the premise of producing feasible solutions, which can make better and more full use of the system's algorithm operation resources and improve the concurrency of the system. Table 3 shows the experimental parameters.

The relevant letter settings below are expressed in the experiment on genetic algorithms as follows: the total sample size PopSize 100, the interleaving probability $p_c = 0.6$, the change probability $p_m = 0.02$, the maximum number of replacements is 2000 generations, and the number of high-level individuals is 5.

In the literature, the scheduling order proposed by Hsu is $z_i/(z_i + w_i)$, which is a gradually increasing order; the set is m, $n + 1$ and the total completion time is under the range of 50,000 to 400,000 in total. Table 4 shows the task completion time comparison experiment.

Table 3: Experimental parameters.

P	o	s	z	w
P_1	4.11	1.59	0.44	6.82
P_2	10.23	2.98	0.67	12.23
P_3	17.04	4.28	0.95	18.48
P_4	11.58	3.12	0.76	13.84
P_5	6.29	1.91	0.59	8.90
P_6	11.67	3.56	0.78	13.53
P_7	17.25	5.47	0.96	19.04
P_8	9.43	3.74	0.53	27.05
P_9	1.43	1.99	0.16	8.06
P_{10}	4.32	2.13	0.42	9.96
P_{11}	7.50	2.57	0.64	11.90
P_{12}	5.38	2.43	0.44	12.42
P_{13}	3.37	2.45	0.25	13.80
P_{14}	2.98	3.06	0.24	14.84
P_{15}	2.28	3.60	0.23	15.64
P_{16}	6.56	2.43	0.52	10.62
P_{17}	10.78	1.22	0.82	5.78
P_{18}	10.34	2.51	0.78	8.74
P_{19}	11.90	3.88	0.83	11.92
P_{20}	10.08	2.70	0.72	8.84
P_{21}	8.13	1.52	0.63	5.62
P_{22}	5.32	3.28	0.81	10.28
P_{23}	2.50	5.06	0.18	16.12
P_{24}	1.86	3.98	0.16	12.03
P_{25}	1.69	2.92	0.14	9.36
P_{26}	5.42	2.78	0.46	9.47
P_{27}	8.02	2.60	0.79	9.68
P_{28}	3.78	3.52	0.44	11.19
P_{29}	2.57	4.26	0.19	13.48
P_{30}	6.38	3.78	0.57	15.39

The experimental results in Table 5 show the optimal scheduling order obtained by the algorithm of this article under different tasks. It can be seen from the table that with the difference in the amount of tasks, the optimal scheduling order obtained by the solution has also changed. On the other hand, it shows that there is no fixed scheduling order that can achieve the best under different tasks. Optimal scheduling results demonstrated that the scheduling sequence has an important impact on the task scheduling results.

3. Design and Application of Flute Music Remote Teaching System for Artificial Intelligence

3.1. System Structure Design. For a relatively complete teaching system with distance education mode functions, the following main supporting functional sections are included, such as online learning section, online course preparation module, homework module, examination module, question and answer module, information discussion module, and information processing module. As shown in Figure 3, these functional modules are independent of each other and communicate through the system. Through the interconnection between the data, the data can be systematized and an effective support can be constructed.

Each distance teaching platform in our country is in its own line, with different positioning and different teaching content. For Internet teaching, self-acquisition of knowledge

Table 4: Task completion time comparison experiment.

Algorithm	Task volume	$n+1$	m	Complete time
IZ	50000	3	21	30186
IW		89	12	37346
Hsu		37	22	29554
GA		33	30	19725
IZ	100000	7	22	54900
IW		123	13	69650
Hsu		56	23	55404
GA		48	30	39097
IZ	150000	10	22	80985
IW		147	14	98388
Hsu		63	24	79507
GA		57	30	58370
IZ	200000	14	23	103279
IW		170	14	130899
Hsu		72	24	105806
GA		66	30	77630
IZ	250000	17	23	128413
IW		190	14	163379
Hsu		81	24	132091
GA		74	30	96870
IZ	300000	21	23	153418
IW		208	14	195837
Hsu		89	24	158362
GA		81	30	116095
IZ	350000	25	23	178445
IW		222	15	217231
Hsu		96	24	184622
GA		87	30	135310
IZ	400000	28	23	203557
IW		238	15	248088
Hsu		103	24	210876
GA		93	30	154519

Table 5: The optimal scheduling sequence under different target quantities.

Task volume	Scheduling sequence
50000	23, 9, 25, 24, 29, 1, 13, 14, 15, 10, 28, 12, 26, 16, 8, 30, 11, 2, 5, 4, 20, 6, 18, 27, 22, 19, 21, 17, 3, 7
100000	25, 9, 24, 1, 15, 21, 23, 29, 14, 13, 10, 28, 12, 26, 16, 8, 30, 5, 11, 2, 20, 4, 6, 18, 27, 22, 19, 17, 3, 7
150000	24, 9, 25, 29, 15, 23, 1, 13, 14, 10, 28, 12, 26, 16, 8, 30, 11.5, 2, 4, 20, 6, 18, 27, 22, 19, 21, 17, 3, 7
200000	24, 9, 25, 29, 14, 23, 1, 13, 15, 10, 28, 12, 26, 16, 30, 5, 8, 11, 2, 20, 4, 6, 18, 27, 22, 19, 21, 17, 3, 7
250000	23, 9, 25, 24, 29, 15.1, 14, 13, 10, 12, 28, 26, 30, 16, 8, 5, 11, 2, 20, 4, 6, 27, 18, 22, 21, 17, 19, 7, 3
300000	23, 9, 25, 24, 29, 14, 1, 15, 13, 10, 28, 12, 26, 16, 8, 30, 5, 11, 2, 20, 4.18, 6, 27, 22, 21, 17, 19, 3, 7
350000	23, 9, 25, 24, 29, 15, 1, 14, 13, 10, 28, 12, 26, 16, 8, 30, 5, 11, 2, 20, 4, 18, 6, 27, 22, 21, 17, 19, 3, 7
400000	24, 9, 25, 29, 13, 15, 23, 1, 14, 10, 28, 12, 26, 16, 8, 30, 5, 11, 2, 20, 4, 18, 6, 27, 22, 21, 19, 17, 3, 7

is the core. Therefore, in the process of teaching, teachers should conduct individual students' autonomous learning awareness. Strengthen it to form the habit and ability of independent learning. At the same time, we should also advocate the integration of "teaching" and "learning," provide timely test feedback to students, consider students, and conduct one-to-one instructional learning for them. These suggestions are for data system reasoning. Both have great reference value. This information includes the user's visit records, the completion of user operations and test data, the discussion and exchange of online participation, the user's interests and specialties and operation methods, learning progress and scoring, and so on. Most of the system is divided into a number of different areas for identification, and these areas will deal with the various scenes encountered in teaching. According to the division of these functional sections, we can create the level of help to solve the problem and build by these to help users complete the required tasks. Each functional module has mutual dependence, which can be solved through agent interaction and cooperation. Through the above analysis and explanation, we have established many samples of modern distance education systems to solve the above difficulties. Its schematic diagram is shown in Figure 4.

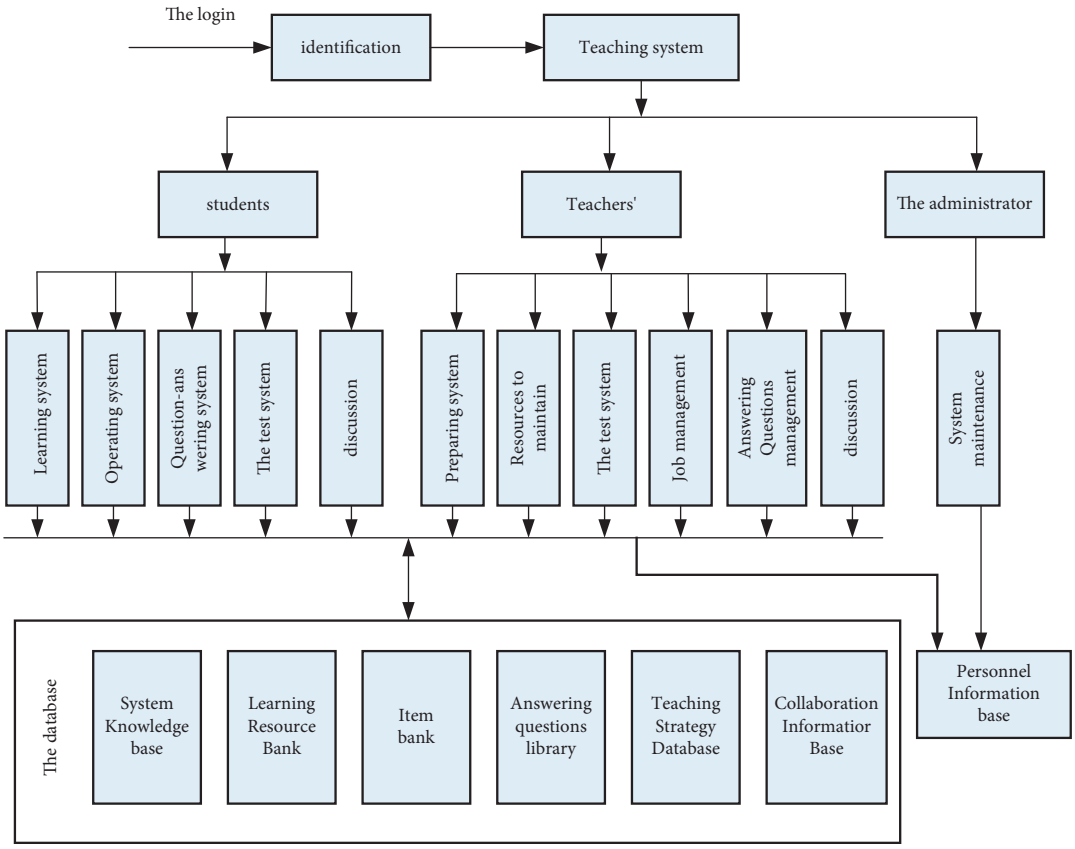

Figure 3: Function diagram of distance teaching system.

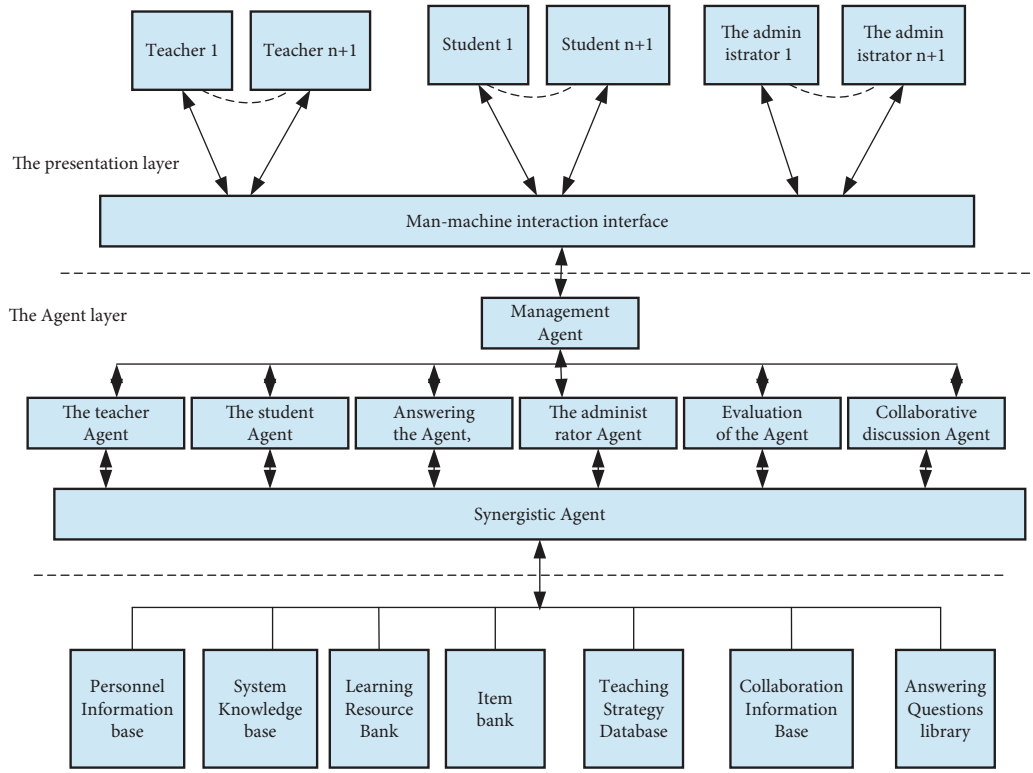

Figure 4: Targeted distance teaching system model.

From the above schematic diagram, it can be found that the entire teaching system is divided into three levels in a logical sense:

(1) Basic database layer: the database system that stores all the data in the system.

(2) Management agent: it is used to help various learning, which contains 8 components, namely, agent student, agent, evaluation agent, agent Q&A, management teacher agent, administrator agent, collaborative discussion agent, and collaborative agent.

(3) Interface presentation layer: it is the interface between the user and the system, including the interactive man-machine interface. It mainly provides assistance to three types of users: instructors, researchers, and managers.

3.2. Construction of Each Agent in the System. The construction of agent is the most time-consuming and most difficult work in the entire system. If you start research and construction directly at the bottom, it takes too much time and energy, and it is not easy to put more energy into the realization of functions and ideas. Therefore, building a mature service sector is the most effective and wise choice, and the platform can also quickly build multiple sectors. The platform invented a simple configuration method, so users do not need to pay attention to the transmission of basic information and structure. Since it is developed for the platform, the interface is also very easy to use.

This information includes the user's visit records, the completion of user operations and test data, the discussion and exchange of online participation, the user's interests and specialties and operation methods, learning progress and scoring, and so on. Moreover, they are clearly stratified samples. These factors allow users to carry out relevant research according to their different needs and different levels. Because the level of agent intelligence of this platform is not perfect, it is necessary to rely on the methods created by the developers to achieve its intelligence requirements. Most of the system is divided into a number of different areas for identification, and these areas will deal with the various scenes encountered in teaching. According to the division of these functional sections, we can create the level of help to solve the problem and build by these to help users complete the required tasks. Each functional module has mutual dependence, which can be solved through agent interaction and cooperation. Through the above analysis and explanation, we have established many samples of modern distance education systems to solve the above difficulties. The ability to create an agent construction model efficiently and quickly puts forward higher requirements on the inventors, which can only be achieved in thought with extra effort and time.

The management agent in the system is used to help various learning, which contains 8 components, namely, student agent, agent, evaluation agent, agent Q&A, management teacher agent, administrator agent, collaborative discussion agent, and collaborative agent. The KQML language is used to transfer information between agents, so as to exchange information to complete tasks. The way to help learners complete the research tasks is to complete the task by sharing tasks. The specific levels between the agents are shown in Figure 5.

3.3. System Development and Testing. At present, many applications of Internet digitization are aimed at the system development tool B/S browser server mode. The model mentioned in this article is also aimed at the B/S model, which uses the JPS algorithm program to express the development platform of the application system and uses this as an innovative development tool for the database. Students choose the courses they need to study according to the study plan to start learning. When a student enters the system, the algorithm program will automatically create a personalized code corresponding to the student. At the same time, the program can also track whether the student has reached the teaching standard. The homework in the course is a way for students to practice the learning outcomes in class and deepen their understanding of the learning outcomes. After completing a specific knowledge point, it is necessary to repeatedly consolidate the foundation. Students only need to click the "class practice" button, and the database will call the exercises of the relevant task points in the practice library. When the student completes the question and clicks the "Submit Assignment" button, the system will submit the data and compare the provided test with the correct answer to score, and the score of the question made by the student is displayed to the student. For the wrong question, the system gives correct answers for students' reference. When the students get low scores in the practice of a certain knowledge point, the system will automatically process the data, and the user will not provide the answering process to the related questions, so that the students can learn again.

The system will store the learning situation of each student in a database of individual student information and use it as a sample to guide future students. As a complete education model, the test system is an essential part. Testing is the most direct and effective way to test students' learning effects. The test link can enable teachers to have a clear understanding of students' knowledge acquisition and can comprehensively evaluate students through their learning achievements and daily performance. At the same time, it also gives the next learning strategy according to the student's learning effect, extracts the reasonable results, finds some related problems, and puts the information in the hands of the students. If you cannot find any useful knowledge or your students have objections to the answers found, ask the teacher a question, and the system will reflect the answer to the students. When the student closes the program and clicks the "Logout" button after completing the current study task, it may also interrupt the research process

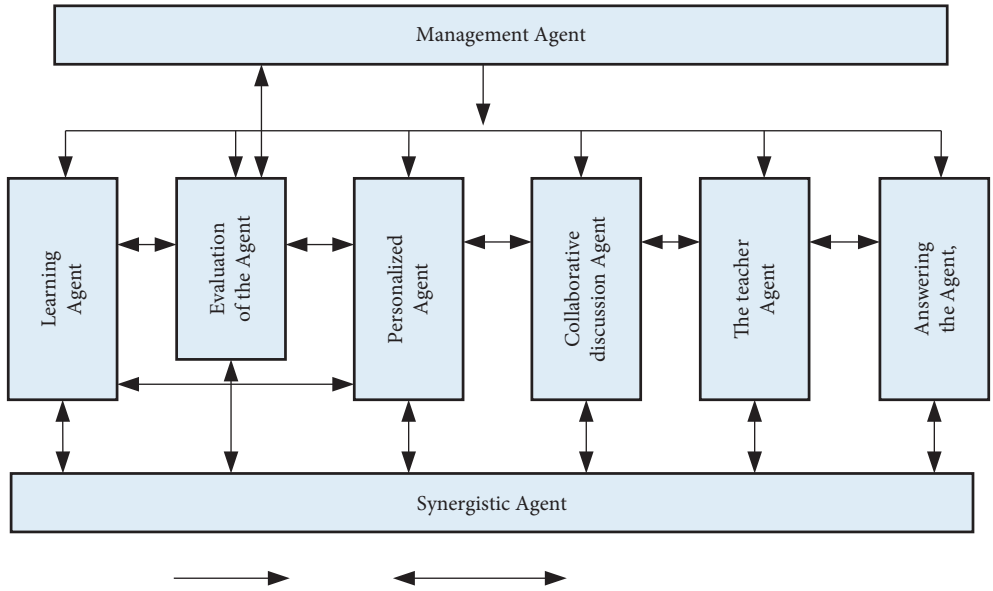

Figure 5: Agent relationship diagram.

due to abnormalities and unexpected circumstances, and it will also save the information recorded by the student to its database. At the same time, it manages the abnormal state of students to repair and open resources.

3.4. Suggestions for Flute Music Teaching and Development. If you want to endure for a long time and pass on an art form from generation to generation, it must show its artistic value, and it must be handed down to pass it on. The same is true for flute art. Ever since the flute was invented in the West, classic achievements have been made. The Internet in the 21st century has brought many opportunities for development, and the Internet has brought another "spring" to flute art. Therefore, adding new technology to the existing flute music algorithm program is another opportunity to reform the flute art. Teenagers are the infinite motive force for social development. Therefore, it is necessary to do a good job in enlightening children's flute education to lay a solid foundation for training specialized flute talents in the future. The author believes that forming a school band is a very good idea. Children must establish a sense of cooperation with others in the band, learn from each other, and develop in a common environment. Modern children's flute enlightenment education is different from previous education. The former flute classroom model was a 1:1 classroom with a teacher and a student, but now it is a group classroom model where a group of 3 to 5 people study and research together. The hot topic of discussion is whether to practice together or compete together. This way of competing with each other will cultivate children's enthusiasm. Today's society is no longer a society that advocates individual efforts but is a win-win society. Therefore, the ideological enlightenment education of juvenile flute must keep up with the development and progress of society.

In the long-distance flute teaching in our country, the relatively backward technical equipment in our country is the evaluation system and monitoring. These two factors are the main culprits for students' inability to learn musical instruments efficiently. Through the establishment of a certain foundation of constant supervision and network problem diagnosis and through tests, mock examinations, and issuance of certificates, domestic students can easily learn through distance education. There are many ways of supervision, which can be divided into final evaluation and self-scoring. There are many types of detection methods, using the positioning system to track and store learners' learning information. In the remote communication, the acceptance of students' activities or learning results is of great help to students, which is more effective than one-to-one effects. Although everyone's understanding and level of music are different, flute happens to be an art form that has no hard indicators to evaluate its quality. In the class mode of music schools at home and abroad, a large number of large-scale lectures are used and the commonality of flute is discussed together, while the short-term courses focus on the execution of algorithm programs. This can not only effectively enhance students' cognition of their own performance level but also broaden students' understanding and ideas.

4. Conclusion

The development of Internet technology has brought convenience to people's life, so the traditional teaching methods are bound to produce some changes. Intellectuals must first have certain "information processing ability" and "novel creative ability." However, the current old Internet digital teaching model has many problems, such as low intelligence, weak interaction, lack of effective learning guidance mechanism, lack of effective evaluation mechanism, and so on, which makes it difficult to satisfy people's needs in Internet digital teaching. There is need for knowledge. This article is aimed at the problems encountered by the old Internet digital education, such as the low level of artificial

intelligence, the lack of information processing ability, the lack of effective learning ability, the lack of mature self-improvement ability, and so on. The thirst for knowledge can hardly be satisfied by the current Internet digital teaching. We propose a new algorithm program in the field of reasonable allocation of artificial intelligence: the invention of the agent algorithm program is an Internet digital teaching system for algorithm programs. This article has carried out a comprehensive and systematic explanation and analysis of the agent algorithm program. In addition, it explores and explains all the key steps required by the current distance education model and invents a sample of the distance education model. This article preliminarily summarizes the automatic teaching and personalized education functions of this model, laying the foundation for future development and exploration in this field.

Data Availability

The data used to support the findings of this study are available from the corresponding author upon request.

Conflicts of Interest

The author declares that there are no conflicts of interest.

Acknowledgments

This study was supported by North University of China.

References

[1] S. Ren, Y. Hao, L. Xu, H. Wu, and N. Ba, "Digitalization and energy: how does internet development affect China's energy consumption?" *Energy Economics*, vol. 98, Article ID 105220, 2021.

[2] D. Toratani, "Application of merging optimization to an arrival manager algorithm considering trajectory-based operations," *Transportation Research Part C: Emerging Technologies*, vol. 109, pp. 40–59, 2019.

[3] C. D. Montano, "Android sms and file manager encrypted application using aes-vigenere and aes/ecb/pkcs5/padding a hybrid encryption algorithm," *South Asian Journal of Engineering and Technology*, vol. 12, no. 1, pp. 55–59, 2022.

[4] X. Wang, H. He, F. Sun, and J. Zhang, "Application study on the dynamic programming algorithm for energy management of plug-in hybrid electric vehicles," *Energies*, vol. 8, no. 4, pp. 3225–3244, 2015.

[5] A. Karpyak, "Flute art in the light of the historical significance of methodological schools and directions in music education: the past and present," *Journal of History Culture and Art Research*, vol. 9, no. 1, pp. 286–294, 2020.

[6] R. Rust, J. Kumbani, N. Rusch, and S. Wurz, "Flute playing in the rock art of the Klein Karoo and Cederberg, South Africa-a potential link to ancient sound," *Rock Art Research: The Journal of the Australian Rock Art Research Association (AURA)*, vol. 39, no. 1, pp. 104–113, 2022.

[7] Z. Ju, Z. Deng, X. Xue, and A. Liu, "Soundscape composition analysis combined with acoustics and musicology: a case study on the music piece of Daybreaking," *INTER-NOISE and NOISE-CON Congress and Conference Proceedings*, vol. 263, no. 6, pp. 810–816, 2021.

[8] S. Gavrila Gavrila and A. de Lucas Ancillo, "COVID-19 as an entrepreneurship, innovation, digitization and digitalization accelerator: Spanish Internet domains registration analysis," *British Food Journal*, vol. 123, no. 10, pp. 3358–3390, 2021.

[9] A. Sestino, M. I. Prete, L. Piper, and G. Guido, "Internet of Things and Big Data as enablers for business digitalization strategies," *Technovation*, vol. 98, Article ID 102173, 2020.

[10] S. V. Shokaliuk, Y. Y. Bohunenko, I. V. Lovianova, and M. P. Shyshkina, "Technologies of distance learning for programming basics on the principles of integrated development of key competences," *CTE Workshop Proceedings*, vol. 7, pp. 548–562, 2020.

[11] R. Fojtík, "Problems of distance education," *International Journal of Information and Communication Technology Education*, vol. 7, no. 1, pp. 14–23, 2018.

[12] E. Murphy and M. A. Rodríguez-Manzanares, "Rapport in distance education," *International Review of Research in Open and Distance Learning*, vol. 13, no. 1, pp. 167–190, 2012.

[13] D. Zhang, "Study on the teaching model based on multimedia and network environment," *International Education Studies*, vol. 3, no. 1, pp. 161–164, 2010.

[14] Y. Zhang, L. Zhou, X. Liu et al., "The effectiveness of the problem-based learning teaching model for use in introductory Chinese undergraduate medical courses: a systematic review and meta-analysis," *PLoS One*, vol. 10, no. 3, Article ID e0120884, 2015.

[15] X. H. Wang, J. P. Wang, F. J. Wen, J. Wang, and J. Tao, "Exploration and practice of blended teaching model based flipped classroom and SPOC in higher university," *Journal of Education and Practice*, vol. 7, no. 10, pp. 99–104, 2016.

Hindawi
Computational Intelligence and Neuroscience
Volume 2022, Article ID 5066004, 9 pages
https://doi.org/10.1155/2022/5066004

Research Article

Design of the Artificial Intelligence Vocal System for Music Education by Using Speech Recognition Simulation

Junqing Bai

Shanxi Vocational University of Engineering Science and Technology, Jinzhong, Shanxi 030619, China

Correspondence should be addressed to Junqing Bai; 20060032@nxmu.edu.cn

Received 7 July 2022; Revised 12 September 2022; Accepted 16 September 2022; Published 27 September 2022

Academic Editor: Gopal Chaudhary

At present, computer technology is not limited to the network but to many aspects of spread out, including artificial intelligence technology, signal processing technology, speech recognition technology, and so on which have been better developed, and music teaching has also obtained certain achievements. If the detected speech data have no other clutter in the speech, then the endpoint detection can achieve ideal results. The music education system includes the development of four dimensions: WEB terminal, mobile terminal, web interface, and database. Using the powerful functions of computers, such as computing functions and processing functions, combined with advanced intelligent technology and related equipment, the intelligent learning model based on computer technology is established. It can be applied in college teaching, combined with the actual needs of current college music teaching, corresponding to the curriculum and teaching plan issued by the school, combined with the design of online learning system and reasonable use of computer technology to build a vocal music education system. The intelligent system can improve the requirements of vocal music education management level, teaching organization ability, and teaching platform operation ability.

1. Introduction

The realization of everything is a process of unifying the theoretical foundation and practical activities, as is the music education system. At present, since the ITS system does not have its complete theoretical foundation, it will bring a series of development problems to the vocal music system [1]. In this article, we mainly discuss the study of music education system from three major aspects: the development process of music education, the comparison of cross-regional development, the goals, and tasks of music education, and the vocal music system developed according to the characteristics of music education [2]. Among them, for the music education system, in the research of this article, we mainly use J2EE technology, UML modeling, JAVA language, and web programming technology based on the current music teaching needs, combined with music theory preparation to carry out relevant practices of music education activities [3]. The music education system with J2EE technology as the core includes the design and configuration of system management skills, the design and configuration of music resource management skills, and the design and configuration of music course management skills [4]. The realization of speech recognition function is the result of the unification of acoustics, computer science, artificial intelligence, and other technologies [5]. At present, speech recognition technology still has a lot of room for improvement. For example, in real life, when we communicate with others, because of the flexibility of language and the language rules established by the society, we can flexibly pause and delete according to our own expression needs, but when we communicate with machines, if it is for a single word or more words, then we must pause when necessary; otherwise, the machine will fail to recognize errors [6]. At present, the development of the Linux operating system is unstoppable, and the development of graphical user interfaces under its system has become a hot topic at the moment [7]. The graphical user interface is based on the processing of various icons, using the powerful functions of the computer, such as calculation functions and processing functions, , combined

with advanced intelligent technology, related equipment, etc., to put the operator and the machine in the same high level and to achieve the purpose of coordination and cooperation between the two so as to bring users a simple and clear experience in the operation process [8]. The graphical user interface requires it to have the basic functions of small footprint, high performance, and high security. It can be seen that the graphical user interface has a high position in the software system. Of course, due to the lack of its own hardware, its changes cannot be controlled.

2. Related Work

Literature shows that the design principle of modern embedded system is a series of work carried out on the basis of mutual cooperation between software and hardware [9]. For example, the powerful data processing capability of embedded system is embedded in the microprocessor and digital signal, realized on the basis of mutual cooperation of processors. The design of the traditional embedded system really separates the two. First, the two parts of software and hardware are correspondingly processed, and then the hardware part is processed first, and the software performs corresponding operations afterwards. To some extent, compared with modern embedded systems, the operation process of traditional embedded systems is extremely complex and time-consuming. Literature shows that XML—a metadata language can be described in a unified and convenient way, and the result can be structured data, and the system can perform related operations on data across multiple platforms. The final result is more meaningful [10]. XML is not just a service for certain programs, and it has all versatility. The program is easy to execute and can be changed according to user needs. It is proposed in the literature that communication between people and computers can be realized by simulating the dialogue between people [11]. This is a case of applying speech recognition technology to the field of communication and bionics for the benefit of society. For example, for people with physical disabilities, when they are inconvenient to operate with their hands, the emergence of voice recognition can completely get rid of the operation of computer hardware. When this operation is applied to the factory floor, it can be operated manually [12]. Significantly reducing labor costs will help companies realize industrial transfer; in addition, language recognition technology can convert speech into words and words into sounds, which greatly facilitates our lives. According to the literature, from the most fundamental structure, artificial neural network is a learning and training method that simulates neural complexity [13], and the exploration of artificial neural network is completed through continuous deep learning to deal with the complex relationship of the data, so as to carry out mathematical modeling algorithms. Literature shows that the research on neural networks dates back to 2006 [14]. At that time, some people tried to explore with traditional training algorithms, but the results were not successful. The literature shows that most of the students majoring in music in colleges and universities in our country are students whose main major is vocal music learning. To sum up, vocal music education in colleges and universities needs a high level of teaching [15]. However, from the current teaching situation, we can see that music education in colleges and universities still has a lot of negligence: backward teaching materials, aging teaching equipment, one-sided teaching management, unscientific teaching arrangements, and teaching methods that are difficult to stimulate students' interest in learning. These are the legacy of the old teaching. We are also facing another problem of lack of teachers. In the field of vocal music education and teaching, we urgently need to improve. The literature shows that the subject of music is different from the education and teaching of other cultural courses [16]. It has its own unique needs for teachers' teaching level and teaching equipment. In accordance with the current development needs, many schools have optimized vocal music education, adjusting teaching plans, teaching equipment, teaching programs, and other aspects.

3. Research on Language System

3.1. Basics of Speech Recognition. Next, based on the embedded language system, a comprehensive analysis of the linear model of its speech signal and important technologies in language recognition technology will be carried out. Voice signal is defined from the human physiological level, and when a person is making a sound, the airflow causes an impact on the vocal tract, making the person's vocal cords to vibrate, and then the airflow can flow out of the oral cavity or nasal cavity according to the characteristics of the pronunciation. The model is built based on the appearance of the voice signal. Because of the one-way nature of the path, the model also presents this linear pattern. The path is generated for it, as shown in Figure 1:

We can introduce them one by one as follows:

(1) The study of the excitation model points out that when people make different sounds, the excitation generated by the speech signal is also different. When g_1 and g_2 are both close to 1, then

$$E(z) = \frac{A_v}{1 - z^{-1}}. \tag{1}$$

A_v represents energy which is represented as

$$U(z) = G(z)E(z) = \frac{A_v}{1 - z^{-1}} \times \frac{1}{\left(1 - g_1 z^{-1}\right)\left(1 - g_2 z^{-1}\right)}. \tag{2}$$

(2) When the pronunciation is different, the vocal tract changes differently. There are two main changes: when the vowel sounds, the oral environment is relatively stable. When consonants are pronounced, high-pressure waves appear in the vocal tract. We usually use formant models to indicate these changes. The resonance peak can be represented by

$$V(z) = \frac{1}{\sum_{i=0}^{p} a_i z^{-i}}. \tag{3}$$

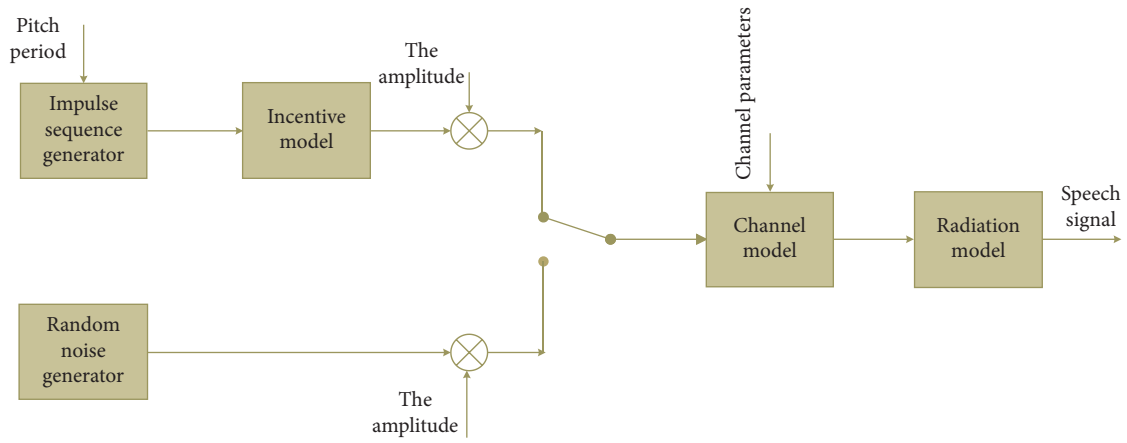

Figure 1: The relationship between the speech signal models.

(3) The voice signal is essentially a sound pressure wave. In the process of voice signal generation, it will have a specific speed through the vocal cords. These two inverse factors are called radiation impedance. It represents the interaction between the lips. Formula (4) is the relationship between the lip area and the head when the speech signal is generated:

$$z_L(\Omega) = \frac{j\Omega L_r R_r}{R_r + j\Omega L_r}. \tag{4}$$

The radiation model is given as

$$R(z) = 1 - \left(rz^{-1}\right). \tag{5}$$

Among them, $r \sim 1$.

In summary, the linear model of the speech signal can be inspired by the three examples cited above:

$$H(z) = U(z)V(z)R. \tag{6}$$

Because most of the initial speech is an original signal, we cannot directly get the information we need, so it needs to be preprocessed. Figure 2 shows the preprocessing steps.

Next, we explain the pretreatment process in detail.

When we store sound information in the computer, we need to perform voice signal ⟶ digital signal, as shown in Figure 3:

Analog audio⟶digitalization can be shown as

$$x(n) = x_n(n - T). \tag{7}$$

In this formula, T is voice sampling period; electrical signal ⟶ binary code.

The power spectrum of the speech signal is not completely invariant, and it has an inverse correlation with energy. The higher the energy, the smaller the value. Therefore, most of the energy is concentrated in the low frequency part of the signal, but this phenomenon can easily cause the high-frequency part of the signal to be unrecognizable, so our solution is to use pre-emphasis to process the sampled and quantized voice signal. This can raise the high-frequency part of the signal and break the energy tilt phenomenon. The same conditions can be used to solve the frequency of the signal:

$$H(z) = 1 - uz^{-1}. \tag{8}$$

The voice signal, taking humans as an example, is a signal that changes all the time and does not have stability, but its changes are small in a very short period of time. So we can regard it as a steady-state signal in some processing. But in the case of extremely short signal, if there is a transition between two adjacent syllables or between the first letter and the last, the sound will change between two adjacent tracks. In this case, its characteristic parameters may vary greatly. Like the pre-emphasis above, we need to place the voice signal in the same part for processing, and the method used is frame processing. In the framing operation, $x(n) \times w(n)$, and then the derived results are weighted. The following formula (9) is the windowed voice signal which is given as

$$y(n) = \sum_{-\infty}^{+\infty} x(m)w(-n). \tag{9}$$

Speech analysis usually uses three types of window function, such as Hamming window, Hanning window and rectangular window

Figure 4 shows the amplitude frequency response of the window function, a represents the attenuation of the first lobe, and B represents the width of the main lobe. Then compare the characteristics of the window function. Table 1 shows the characteristic parameters:

3.2. Endpoint Detection. It can be seen from the table that closing A at the first side line of the window function is the largest. This shows that the leakage of the spectrum is much smaller than the other two, and the characteristics of passing through the blocking will be better. The system uses the clear function to identify the smoothing requirements of the signal. The frame length reported here is 256, and the frame shift is 80.

In a complete language, the starting point and focus of the language also need to be tested, which uses a program called endpoint detection.

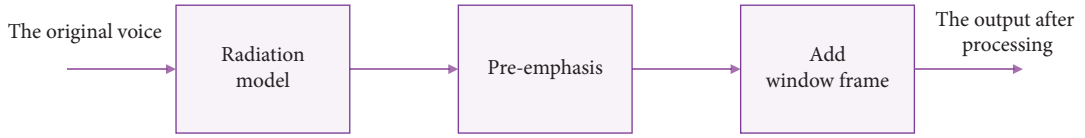

Figure 2: Pretreatment process.

Figure 3: Analog-to-digital conversion process.

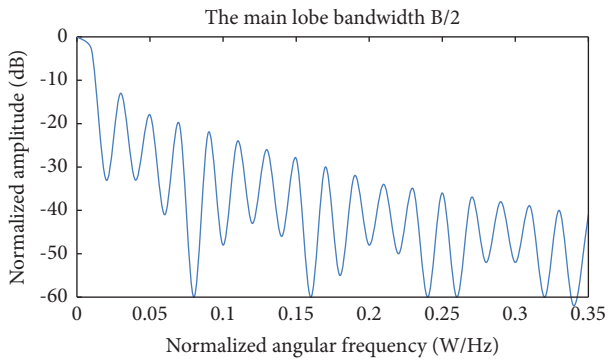

Figure 4: Amplitude frequency response of the window function.

Table 1: First side lobe attenuation A and main lobe width B.

	Rectangular window	Hanning window	Hamming window
B	0.89 Δw	1.44Δw	1.30Δw
A/dB	13	32	43

(1) Combined with the above, in the voice data, the i-th frame data is $y_i(n)$, and $y_i(n)$ needs to meet:

$$y_i(n) = w(n) * x((i-1) * \text{frameinc} + n), \quad 1 \le n \le L, 1 \le i \ge f_n. \tag{10}$$

The short-term energy of the i-th frame is

$$E_i = \sum_{n=0}^{L-1} y_i^2(n), 1 \le i \le n. \tag{11}$$

The following formula (12) is the average amplitude of speech:

$$M(i) = \sum_{n=0}^{L-1} y_i(n). \tag{12}$$

(2) After the speech recognition technology is recognized, data ⟶ digital signal. It can be seen that after recognition, the speech signal has a sign change. The total number of these sign changes is called the short-term average zero-crossing rate. It is calculated as

$$zcr(i) = \frac{1}{2}\sum_{n=0}^{L-1}\left|\text{sgn}[y_i(n) - \text{sgn}[y_i(n-1)]]\right|, 1 \le i \le f_n. \tag{13}$$

In the following formula sgn is a symbolic function:

$$\text{sgn}[x] = \begin{cases} 1, & x \ge 0, \\ -1, & -1, x < 0. \end{cases} \tag{14}$$

In the process of detecting voice endpoints, it is likely that the detection is not accurate enough. Therefore, we will introduce a new language endpoint detection method, that is, the first proposed two-layer critical price method. This method uses short-term average English based on exchange rate and short-term energy, and the principle is that Chinese finals contain vowels and have high energy, which will have higher frequencies depending on the pronunciation and will have a higher short-term repetition rate according to different letters, which can be distinguished according to two characteristics such as the uppercase letters of the sound and the last Chinese syllable. The two-layer critical value method is shown in Figure 5, which is embodied on the basis of the second judgment method.

In Figure 6, the start and end points of the speech are marked as A and F, respectively. The endpoint detection procedure are as follows: (1) the pre- and window setting of the voice signal; (2) the voice after the stage will calculate the ratio of the short-term average energy and the short-term average zero transition; (3) finally, the critical price comparison and endpoints analysis; and (4) perform the original terminal monitor for the sound signal. The endpoint detection results are shown in Figure 6.

Noise will have a certain degree of influence on speech detection. If the detected voice data have no other messy sounds in the voice, then the endpoint detection can achieve the desired result. If the speech is superimposed with some messy sounds, that is, noise, then its recognition will be hindered to a certain extent.

Comparing the figure above, it can be clearly seen that there is a big difference in the short-term average zero-crossing rate between the two. This also shows that the voice signal under the influence of noise is affected as a result and even caused an error in the detection structure:

$$y(n) = \text{med}(x(n-L), x(n-L+1), \ldots, x(n), \ldots, x(n+L)). \tag{15}$$

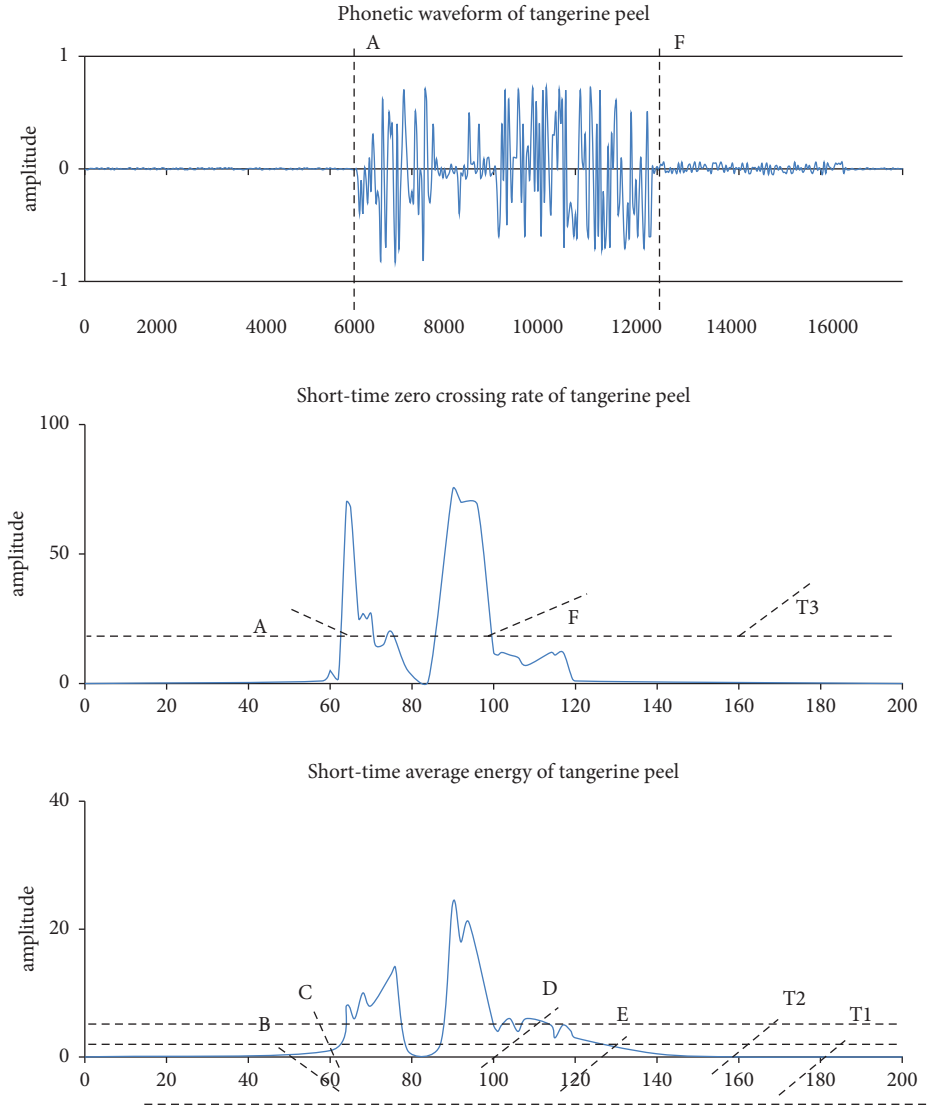

Figure 5: Schematic diagram of the two-level judgment method.

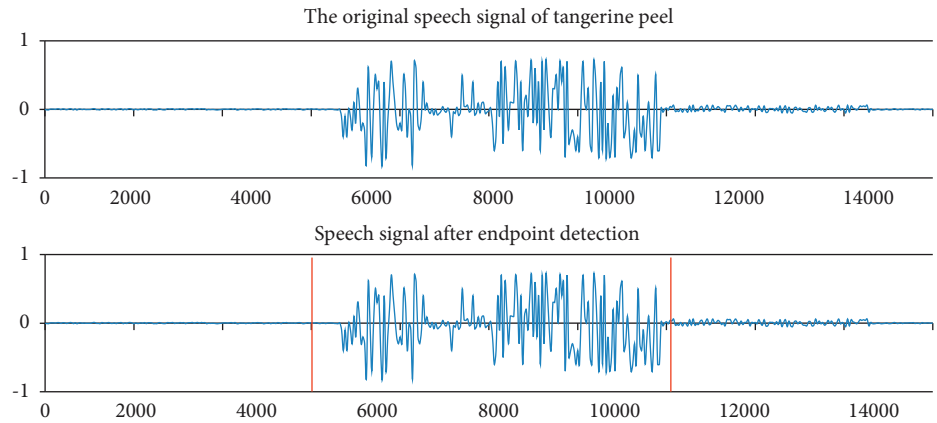

Figure 6: "Tangerine peel" endpoint detection results.

Formula (15) can self-clear some speech endpoints that have no effect, leaving only the effective endpoints, and after they are cleared, the existence value of the sound paragraphs without energy fluctuations will not have a major impact. Of course, in actual applications, we will make changes in a certain link according to actual needs. For example, in some special cases, we need to change the maximum value of dual-threshold endpoint detection to make it meet our needs.

The energy min is

$$amp0 = 1.2 * \text{mean}(\text{amp1}). \tag{16}$$

Energy max = min × 1.5, and the threshold of zero-crossing rate is

$$zcr1 = 0.8 * \text{mean}(\text{zcr1}). \tag{17}$$

Because our research was conducted in a laboratory environment, it is inevitable that our voice collection will have noise superimposition, which will cause the relative value of noise to be higher. In order to solve this problem, in the collected voice samples, Gaussian white noise is added, and the next experiment will continue to use the original speech as the research object.

Because of the complexity of the speech signal, we are prone to ambiguities in the research process. At this time, we often use a large number of parameters to explain, but when the parameters reach a certain number, we may violate the essence of the research. On the contrary, it will cause another complicated situation. Therefore, using the least parameters to describe the most comprehensive experimental results is an important aspect of our speech signal research. When solving this problem, we have used the time domain, and its description of the experimental results is pass, but it still does not get rid of the phenomenon of disordered parameters. So based on this phenomenon, we later discovered a new method; that is, in speech recognition, different speech generation models are described separately to avoid the mixing of the two, that is, to separate the speech signal. The method is to conduct research on the basis of the nature of the speech signal, which effectively circumvents many complicated analyses and makes the feature parameters come out.

Linear predictive analysis is mainly used in voice recognition, speech synthesis, and speech analysis technology used in coding. The basic principle of linear predictive analysis is that because the collection of various speech signals is in the same space, they will be similar to a certain extent. Therefore, in order to avoid the interference of results caused by this phenomenon, we can pay attention to some samples before sampling, or we can repeat the test and analyze the results of multiple tests. It is also possible to use the LPCC analysis method for processing. The calculation step of this method is

$$H(z) = \frac{1}{A(z)} = \frac{1}{1 - \sum_{j=1}^{p} a_j z^{-j}}. \tag{18}$$

Cepstrum $h\prime(n)$ can be given as

$$\ln H(z) = \sum_{n=1}^{\infty} h\prime(n) z^{-n}. \tag{19}$$

Formula (18) when combined with formula (19), we can get

$$\frac{\partial}{\partial z^{-1}} \ln \frac{1}{1 - \sum_{k=1}^{p} a_k z^{-k}} = \frac{\partial}{\partial z^{-1}} \sum_{n=1}^{\infty} h\prime(n) z^{-n}, \tag{20}$$

which is,

$$\sum_{n=1}^{\infty} h\prime(n) z^{-n} = \frac{\sum_{k=1}^{p} a_k z^{-k+1}}{1 - \sum_{k=1}^{p} a_k z^{-k}}. \tag{21}$$

So we have

$$1 - \sum_{k=1}^{p} a_k z^{-k} \sum_{n=1}^{\infty} n h\prime(n) z^{-n+1} = \sum_{k=1}^{p} k a_k z^{-k+1}. \tag{22}$$

According to formula (22), the relationship between $h\prime(n)$ and a_k can be obtained as

$$\begin{cases} h\prime(0) = 0, \\ h\prime(1) = a_1, \\ h\prime(n) = a_n + \sum_{k=1}^{n-1} \left(1 - \frac{k}{n}\right) a_k h\prime(n-k), 1 \le n \le p, \\ h\prime(n) = \sum_{n=1}^{p} \left(1 - \frac{k}{n}\right) a_k h\prime(n-k), n > p. \end{cases} \tag{23}$$

In view of the complex parameter problems in the above table, we then introduce the Mel cepstrum coefficient MFCC, which is our most commonly used parameter in the current speech recognition system. It is mainly based on the model development process that people obtain speech signals in the process of hearing and has strong characteristics of identifying noise and speech.

3.3. Research on Embedded Systems. XML is a conversion medium for data conversion of language signals. It can realize the mutual conversion of language signals and language data under certain standards. Of course, it can also be used to leap across different platforms instead of constrained by one platform. XML is a universal standard. It is the same as the above. It is not only applicable to one mode but can also achieve leapfrogging under different platforms, avoiding the complexity caused by situational constraints.

It can be said that this module is another important part of the system, but it is no longer a purely technical limitation, and it includes a part of the embodiment of personal will. In this module, it mainly refers to the assembly of the user interface and the customization of its style. Therefore, affected by the designer and related research and development institutions, it will have some corporate colors and personal will. Its form is flexible, and it is no longer purely due to technical factors which are limited. Combined with the user interface customization module introduced above, for the

assembly of the user interface, we only need to follow the respective group interface, and then connect with the corresponding user interface system.

3.4. Test for the Speech Recognition System. The software environment of the experiment is the Microsoft Visual C++ development environment under the windows operating system. This speech recognition system uses 10 Chinese words as commands. Table 2 shows the no feedback speech recognition system recognition, and Table 3 shows the unmonitored VGC method recognition.

It can be seen from the above table that it has a good ability to respond when facing changes in the voice signal and can be adjusted appropriately according to the changes in the speaker, the environment, and certain objective conditions. So we can say that this detection method can be quantitatively copied in its own program, and the effect of batch learning is amazing. Table 4 shows the monitoring of the results of VGC method recognition, and Table 5 shows the unmonitored TWA method recognition results.

4. Design and Research on the Artificial Intelligence Vocal Education System

4.1. Artificial Intelligence. From the above table, we can clearly see that the work learning efficiency of artificial intelligence is several to several tens of times than that of human work and learning. In the field where artificial systems have been used on a large scale, artificial intelligence systems already have the corresponding operating principles and have data processing imported into their instruction programs, so they only need to be able to work with power guarantees, and as long as there is no electricity limitation, it can continue to go on. At the same time, it has an obvious advantage. It does not have human consciousness, the quality of the working environment, the level of salary, and the good relationship between staff members. Bad things will not cause them to oppose and protest, and for certain areas that humans cannot reach, they can also replace humans in work. At the same time, to a large extent, there will be no uneven work results. Therefore, the emergence of artificial intelligence has begun to gradually replace people's positions in certain fields, which will bring greater changes to today's job changes. Of course, on the positive side, using artificial intelligence systems to replace humans will greatly reduce corporate expenditures, improve corporate economic efficiency, promote industrial transfer, and promote economic development.

The three parts of the model, view, and controller can be integrated and named as the MVC mode. This mode is usually used for software design, system development, and module repair, and it has a variety of styles in it. By design, the operator can use this ready-made service to carry out related operations, which greatly reduces the manual operation time. At present, the music education system we mainly use is WEB programming technology, which is the current mainstream development technology. It includes the development of four dimensions: WEB, mobile, web interface, and database.

Table 2: No feedback speech recognition system recognition results.

Tesp speech	(Each one has 50 test samples)									
	1	2	3	4	5	6	7	8	9	10
No.1	47	0	0	0	0	0	0	0	0	0
No.2	0	48	0	0	0	0	0	0	0	0
No.3	0	0	34	0	0	0	0	0	0	0
No.4	0	0	0	30	0	0	0	0	0	0
No.5	0	0	0	0	44	0	0	0	0	0
No.6	0	0	0	0	0	38	0	0	0	0
No.7	0	0	0	0	0	0	48	0	0	0
No.8	0	0	0	0	0	0	0	45	0	0
No.9	0	0	0	0	0	0	0	0	47	0
No.10	0	0	0	0	0	0	0	0	0	46

Table 3: Unmonitored VGC method recognition results.

Tesp speech	(Each one has 50 test samples)									
	1	2	3	4	5	6	7	8	9	10
No.1	50	0	0	0	0	0	0	0	0	0
No.2	0	48	0	0	0	0	0	0	0	0
No.3	0	0	45	0	0	0	0	0	0	0
No.4	0	0	0	43	0	0	0	0	0	0
No.5	0	0	0	0	42	0	0	0	0	0
No.6	0	0	0	0	0	47	0	0	0	0
No.7	0	0	0	0	0	0	47	0	0	0
No.8	0	0	0	0	0	0	0	48	0	0
No.9	0	0	0	0	0	0	0	0	48	0
No.10	0	0	0	0	0	0	0	0	0	48
	N	N	N	N	N	N	N	N	N	N

Table 4: Monitoring the results of VGC method recognition.

Tesp speech	(Each one has 50 test samples)									
	1	2	3	4	5	6	7	8	9	10
No.1	50	0	0	0	0	0	0	0	0	0
No.2	0	48	0	0	0	0	0	0	0	0
No.3	0	0	49	0	0	0	0	0	0	0
No.4	0	0	0	49	0	0	0	0	0	0
No.5	0	0	0	0	45	0	0	0	0	0
No.6	0	0	0	0	0	47	0	0	0	0
No.7	0	0	0	0	0	0	48	0	0	0
No.8	0	0	0	0	0	0	0	49	0	0
No.9	0	0	0	0	0	0	0	0	48	0
No.10	0	0	0	0	0	0	0	0	0	48
	N	N	N	N	N	N	N	N	N	N

IThis study is mainly based on J2EE technology and uses SQLServer2012 as the database development tool in the development of the database. At present, based on the actual situation, we mainly have two common online communication modes as follows:

(1) *An online communication method similar to QQ and WeChat.* When we need to talk to someone, we can find the other person's dialog box on the relevant interface, and then have a one-to-one private chat. Of course, we can also open multiple dialog boxes at the same time and then communicate with multiple

Table 5: Unmonitored TWA method recognition results.

Tesp speech	(Each one has 50 test samples)									
	1	2	3	4	5	6	7	8	9	10
No.1	47	0	4	31	0	0	0	0	0	0
No.2	0	48	0	0	0	0	3	0	0	0
No.3	0	0	1	0	31	0	0	0	0	0
No.4	0	0	20	43	0	0	0	0	0	0
No.5	0	0	1	0	47	0	0	3	0	0
No.6	0	0	0	0	0	8	3	40	0	0
No.7	0	0	0	10	0	1	40	0	0	0
No.8	0	0	0	0	0	0	0	48	0	51
No.9	2	0	0	0	0	0	0	0	49	0
No.10	0	0	38	0	0	0	13	0	0	0
	N	N	N	N	N	N	N	N	N	N

people in real time. When the user is temporarily offline, the pop-up interface will show the other party's situation. Once the other party is online, the dialog box in the information list will automatically sound a reminder.

(2) *Another online communication is very similar to the forum mode*. We can open the corresponding interface to see others' answers under different types of questions. At the same time, we can also express our own opinions and put forward the problems that we urgently need to solve. We can also have online discussions with many users in the forum, and everyone can express their views, and finally everyone unanimously chooses the answer that best fits the topic.

4.2. Status Quo and Development of Vocal Music Teaching. The current university vocal music education curriculum system has many problems that are not adapted to the development of the times. Teaching materials are outdated, teaching equipment is aging, teaching management is one-sided, teaching arrangements are not scientific, and teaching methods are difficult to stimulate students' interest in learning. These are the legacy of old-fashioned teaching. At the moment, we are also facing another problem of lack of teachers.

The suggestion on how Chinese universities should improve the quality of vocal music classes is reform the traditional one-to-one courses and introduce small class teaching and group teaching methods, then students can help each other in the classroom, learn from each other, encourage each other, and influence each other. When encountering problems, analyze, review, and solve problems together, improve students' ability to analyze and solve problems, and cultivate students' ability to create music. Students are required to boldly express their opinions on the choice of vocal music works. In order to protect students' personalities and form a good teacher-student relationship, a relaxed educational environment should be established to stimulate students' love for music and art, and for students' future teaching work to provide models. In the vocal music classes of various schools, we must be brave to innovate, train students with solid professional qualities, and boldly reform the vocal music teaching model. Through teaching, students are exposed to a large number of works, and let them form their own vocal works of different styles. Experience the emotional elements and aesthetics contained in various vocal music works and explore the aesthetic value of vocal music. Students must not only be limited to simple learning in the learning process but also master the basic singing skills and also broaden students' horizons and enhance their perception and expression ability by focusing on acquiring and expressing the content of the song.

4.3. Design and Research of the Vocal Music Education System. Java not only provides a framework but also roughly agrees on the overall architecture of web applications. Moreover, a series of specifications have been made for this requirement, which is J2EE. The specification only provides the overall structure, process, and API, and the user implements these specifications. For example, Tomcat implements Web Container and its API. So to sum up, J2EE is a series of specifications related to web development on the Java platform. Companies such as Sun/Oracle/IBM/Red Hat provide the implementation of J2EE specifications. We generally use one or the other when we use Java for web development and multiple implementations. Correspondingly, our own code also follows the J2EE specification.

UML is an acronym for Unified Modeling Language called Standard Modeling Language. UML is a visual modeling language for software-intensive systems, often expressed in graphical form. Specifically, a typical UML diagram includes several blocks or block diagrams, connecting lines, and text representing additional information of the model of these elements. The main method of UML is not software design but software requirements analysis. UML can help analyze and execute software requirements and software design work. When using UML to analyze the software requirements, the learning threshold will be greatly reduced, and the grammatical complexity will also be reduced.

5. Conclusion

Speech recognition has been actively developed as a new method of human-computer interaction. This article introduces the operation process of each system function. The main functions of the system include system management function, music education management function, music course management function, and online communication function. The courses of ordinary colleges and universities are not rich, and the division is not detailed, and the curriculum setting is relatively scattered, unsupervised, and lacks a complete academic system, and there is no overall plan, so the range of choices for students is small. The existing music teaching programs in colleges and universities can no longer meet the new curriculum requirements, and there are still many problems, and it is difficult for students to learn to meet the requirements of the development of the times. For nonmusic major students, their

music teaching is more of a formality that students cannot really learn more music knowledge. The teaching content combines general knowledge of music and singing ability. But the songs are arbitrarily selected, and it also contains songs by many singers and excellent folk songs. However, from the perspective of humanities and culture, there are few vocal works with broad meaning, ideology, artistry, and greater training value. Therefore, this aspect needs to be further optimized. At the same time, university vocal music teachers should also respond to this. Continuous optimization is needed, so we have to pay more efforts for the dissemination of music art.

Data Availability

The data used to support the findings of this study are available from the corresponding author upon request.

Conflicts of Interest

The author declares that there are no conflicts of interest regarding the article.

Acknowledgments

This work in this article was supported by Shanxi Vocational University of Engineering Science and Technology.

References

[1] J. Sun, "Research on resource allocation of vocal music teaching system based on mobile edge computing," *Computer Communications*, vol. 160, pp. 342–350, 2020.

[2] E. Georgii-Hemming and M. Westvall, "Music education–a personal matter? Examining the current discourses of music education in Sweden," *British Journal of Music Education*, vol. 27, no. 1, pp. 21–33, 2010.

[3] V. L. Bond, "Culturally responsive education in music education: a literature review," *Contributions to Music Education*, vol. 42, pp. 153–180, 2017.

[4] A. A. Kallio and M. Heimonen, "A toothless tiger? Capabilities for indigenous self-determination in and through Finland's extracurricular music education system," *Music Education Research*, vol. 21, no. 2, pp. 150–160, 2019.

[5] T. Y. Ahn and S. M. Lee, "User experience of a mobile speaking application with automatic speech recognition for EFL learning," *British Journal of Educational Technology*, vol. 47, no. 4, pp. 778–786, 2016.

[6] T. Neher, T. Lunner, K. Hopkins, and B. C. J. Moore, "Binaural temporal fine structure sensitivity, cognitive function, and spatial speech recognition of hearing-impaired listeners," *Journal of the Acoustical Society of America*, vol. 131, no. 4, pp. 2561–2564, 2012.

[7] G. Xiao, Z. Zheng, and H. Wang, "Evolution of Linux operating system network," *Physica A: Statistical Mechanics and Its Applications*, vol. 466, pp. 249–258, 2017.

[8] B. Xu and Z. Yang, "PAMLX: a graphical user interface for PAML," *Molecular Biology and Evolution*, vol. 30, no. 12, pp. 2723-2724, 2013.

[9] J. Cheng, "Evaluation of physical education teaching based on web embedded system and virtual reality," *Microprocessors and Microsystems*, vol. 83, Article ID 103980, 2021.

[10] T. M. Adams, "Coding with XML for efficiencies in cataloging and metadata," *Journal of Electronic Resources Librarianship*, vol. 31, no. 1, pp. 49-50, 2019.

[11] M. Johnson, S. Lapkin, V. Long et al., "A systematic review of speech recognition technology in health care," *BMC Medical Informatics and Decision Making*, vol. 14, no. 1, pp. 94–14, 2014.

[12] A. K. Elimat and A. F. AbuSeileek, "Automatic speech recognition technology as an effective means for teaching pronunciation," *The JALT CALL Journal*, vol. 10, no. 1, pp. 21–47, 2014.

[13] Y. LeCun, Y. Bengio, and G. Hinton, "Deep learning," *Nature*, vol. 521, no. 7553, pp. 436–444, 2015.

[14] M. Tkáč and R. Verner, "Artificial neural networks in business: two decades of research," *Applied Soft Computing*, vol. 38, pp. 788–804, 2016.

[15] R. Hu, "Research on music teaching system based on virtual reality technology," *Journal of Suzhou University of Science and Technology (Natural Science Edition)*, vol. 36, no. 1, pp. 80–84, 2019.

[16] P. Archie, E. Bruera, and L. Cohen, "Music-based interventions in palliative cancer care: a review of quantitative studies and neurobiological literature," *Supportive Care in Cancer*, vol. 21, no. 9, pp. 2609–2624, 2013.

Hindawi
Computational Intelligence and Neuroscience
Volume 2022, Article ID 3849610, 10 pages
https://doi.org/10.1155/2022/3849610

Research Article

Application of Human-Computer Interaction System in Regional Tourism Competitiveness Analysis under IoT Background

Zhenli Jia,[1] **Jing Zhang**,[2] **and Zhongquan Cui**[2]

[1]*Faculty of Business, Yuxi Normal University, Yuxi 653100, China*
[2]*Faculty of Business, City University of Macau, Macau 999078, China*

Correspondence should be addressed to Zhongquan Cui; 2007037@muc.edu.cn

Received 3 August 2022; Revised 2 September 2022; Accepted 6 September 2022; Published 22 September 2022

Academic Editor: Gopal Chaudhary

With the continuous development of Internet of Things technology, this technology is not limited to the laboratory but is more and more applied in the process of commercialization. Large-scale machine communication is one of the three most important scenarios for 5G applications. Its features include larger uplink access, smaller data packets, higher device energy consumption requirements, lower device transmission speed, higher latency, and bursty communication. With the development of the Internet of Things in the 5G era, interpersonal interaction experience has been further optimized and welcomed by the market and adopt Qt/embedded multilayer menu design mode to improve our computer system interaction to facilitate the operation and Maintenance system. The software function of the human-computer interaction system has reached the expected result. By constructing the application of a human-computer interaction system in the analysis of regional tourism competitiveness, we analyze the temporal and spatial changes of tourism competitiveness in four major economic regions in China and combine multiple linear regression and geographic detector models to analyze China's tourism competitiveness. On this basis, we propose to further enhance the tourism competitiveness of areas with weak tourism development infrastructure and encourage potential tourism development areas to complement each other with high-quality resources between regions.

1. Introduction

The development of the Internet of Things has promoted the progress of all aspects of the city, from the big smart city to the small smart home, all continue to develop [1]. In this process of development, there are various demands, so the network must be connected quickly with the actual scenes of different fields, so as to promote the optimization and development of all aspects and achieve the goal of multiaspect connection [2]. In general, 5G provides a good network infrastructure and technical support for Internet applications, as well as communication between people and communication between people (MTC), which allows the network to be more extensively used in the industry [3]. Because we are in such a big era, we use the Windows CE platform of SQLite database to develop a human-computer interaction system and establish a reasonable local storage structure [4]. Compared with the old version of the database system, the SQLite database is usually smaller, portable, easy to use, and has more complete functions to complete data management tasks and perform fast and effective search queries to meet the visual human-machine interface (HMI) system [5]. The product's requirements for database management will further create huge value. Because the menu components, graphic icons, and language information of the oscilloscope interactive interface maintain the same height, the same size, and the unified sequence, the oscilloscope has attracted the attention of many manufacturers, and it is this factor that speeds up the oscilloscope's man-machine Development and design of interactive systems. Through the interactive experience provided by the computer interactive system, oscilloscope manufacturers can attract more social users, further increase the loyalty of oscilloscope users, and significantly increase the value of oscilloscope products [6]. The competition in the regional tourism industry has become increasingly fierce as the people's material needs

continue to increase [7]. It is also because of this factor that the tourism industry is at the forefront of the development of the national economy, and it has also stimulated the strategic position of the tourism industry in China [8]. With the support of local governments, competition in the region is becoming increasingly fierce. Cities, autonomous regions, and municipalities have placed tourism development in an important strategic position, making regional tourism a key industry and core industry.

2. Related works

Some research uses Qt/Embedded multi-layer menu setting mode to improve the human-computer interaction of the system and makes it easier for employees to operate and maintain the system [9]. Because the SQLite database file is small, it can save space. The software functions of the human-computer interaction system can achieve the predetermined design goals [10]. Some research through the research and development of various products, related tourism service departments, administrative departments, and local tourism companies in the region to improve the infrastructure, so that the region can meet the needs of tourists [11]. In turn, economic and social benefits can be obtained. Some research under the background of the increasing influence of information on tourism competition has conducted research on the query behavior of tourism information, established a theoretical research model, and provided information basis for tourists [12]. And it can be used to query usage methods and influencing factors. Some research based on the Qt platform centered on the oscilloscope human-computer interaction interface, systematically designed the oscilloscope human-computer interaction, and designed a custom font library that satisfies the interface display requirements to achieve mutual response [13]. Some research shows a reliable transmission method based on NOMA without the need for distributed scheduling. Since the random access mechanism of non-distributed transmission eliminates the risk of instability, we first studied the stability of the distributed free reservation access system based on the Foster–Lyapunov standard fast retransmission mechanism and then provided a stable noncooperative system to Control the probability of distributed transmission [14].

3. Human-Computer Interaction System Design for 5g Internet of Things

3.1. 5G Internet of Things Dispatch-free NOMA Model Design. NOMA technology increases the power resources of the power domain. Therefore, the machine uses CO (connection option) instead of blocking the source at regular intervals to display the connection source. The number of connection options at any given time in the OMA system can only be controlled by the number of available low access points, which is determined by the number of connection options. Due to the limited resources of the OMA system, the available connection options are not sufficient for large-scale transmission whenever there is available space, as shown in

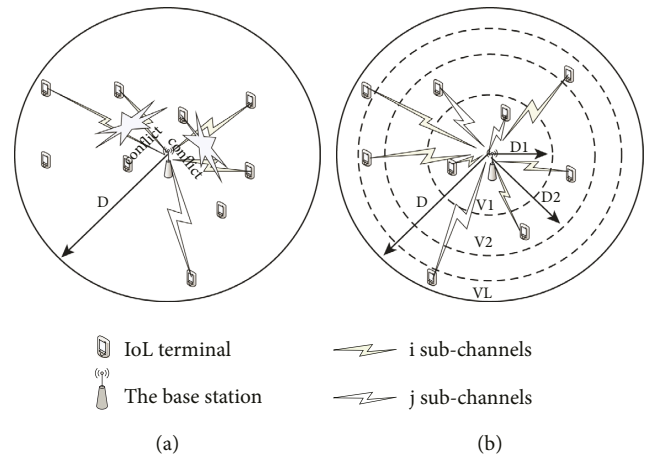

Figure 1: Represents the schematic diagram of unplanned transmission.

Figure 1(a). At the same time, in the case of the uplink transmission of the communication channel of the base station, considerable competition occurs at the receiving end. The schematic diagram of the distributed hierarchical NOMA strategy is shown in Figure 1(b).

First, set the received power level and the corresponding received power in advance. For example, there are L predetermined target received powers within the range of the base station, and the received power V is very large, from large to small to $>.,>...>v$. If the SNR of the receiving end must be at least T, and the decoding order of the receiving end depends on the magnitude of the received power, it includes the interference of the same frequency of the L signal and the "interference" of the noise and are

$$V_1 = \begin{cases} \sum_{k=1+1}^{L} v_k, & l = 1, \ldots, L-1, \\ 0, & l = L. \end{cases} \tag{1}$$

We can obtain $v = T(T+1)$ based on $v = F(\mathrm{V}+1)v = T(T+1)$. The received power with the smallest received power difference can also be obtained, which helps increase the value of L. In practical application scenarios, it can be considered that the farther away from the base station, the greater the signal fading caused by large-scale fading. At this time, in order to reduce the transmission power of device_uplink communication, according to the distance from the base station, the entire cell is divided into L circular areas called L layers. Taking into account the uniform distribution of equipment, the standard for dividing layers is divided according to the area of the following areas, namely,

$$D_l = \begin{cases} D\sqrt{\dfrac{l}{L}}, & l = 1, \ldots, L, \\ 0, & l = 0. \end{cases} \tag{2}$$

According to the distance from short distance to long distance, the estimated reach power of each device layer is v. Devices on the same layer have the same functions. In this way, the equipment far away from the base station can be reduced to make the power reach the expected level, and the

transmission power of the equipment of the entire system can be reduced. As shown in Figure 1(b), in this mechanism, the cell is divided into L concentric circles, and IoT devices in different source areas have different target uplink received powers. Since the gain of other channels is considered, the more the outer loop, the smaller the target received power. The regional MTCD will determine its transmission capacity by enabling location-based segmentation and CSI. For example, for a specific MTCDk, if it is far away from the base station, the device belongs to the set $K = \{k \setminus D. < D \le D\}$, and V represents the standard power received. Since each MTCD has CSI information about the channel, i g.i- = ...M. Therefore, the transmission capacity can be calculated by calculating $P = v$,/maxg.k ∈ K.

Using this method, the cell is divided into L layers, each layer of equipment can use the resources of all channels at the same time, while the distributed layer NOMA can double the resources. The purpose is to increase the probability of successful random access and reduce signaling overhead by using unscheduled transmission to avoid the four-way handshake process of accessing resources (random access process adopted in cellular networks such as LTE).

According to the set difference rule, if there are M active users whose $M \le L$, the NOMA power level is set to be higher. If other power levels are selected, the M signal can be successfully decoded, and the receiving end is SIC to eliminate the same channel interference. However, due to the interaction with the decoding of another layer, the value of L cannot be too large. By selecting $M \le L$ and other powers, the base station can successfully decode all signals of M users. Conversely, if each user selects the same power, the signal cannot be decoded.

If M is greater than 1, the average MTCD transmission power in the system provided by NOMA can be expressed as follows:

$$\begin{aligned} \mathrm{E}[P_k] &\le \frac{\min\{2\ln\ 2, M/M-1\}}{L} \sum_{l=1}^{l} \frac{v_i}{A_l} \\ &= \frac{\min\{2\ln\ 2, M/M-1\}}{L} \sum_{l=1}^{L} \frac{\Gamma(\Gamma+1)^{L-1}}{A_0 (D\sqrt{l/L})^{-\beta}}. \end{aligned} \tag{3}$$

Here, β represents the road loss index, and Ao represents the constant relative antenna gain.

3.2. Design and Analysis of Distributed Hierarchical Scheduling-Free NOMA Architecture. When MTCD selects this time slot for uplink transmission, it depends on the location, mainly based on the distance d from the base station. The target MTCD is at the location level 1 of the base station through d, the information of each MTCD channel and the information gain of the subchannel to which it belongs. According to the principle of the lowest transmission power, the power of the transmission slot is calculated as follows:

$$P_k = \frac{v_l}{\max g_{i.k}}. \tag{4}$$

Here, P is the transmission power used by MTCD, and v is the power previously received by the target at the site level.

The uplink transmission uses a nonorthogonal multiplexing connection method, and the scheduling-free random access technology based on the distributed layer NOMA uses resources nonorthogonally through the signals of multiple devices on the power domain NOMA. The same frequency at the same time. It can be seen from Figure 2.

The detailed steps of the framework design are as follows:

(1) Access is granted in the time slot of the cell, and each MTCD transmits its signal on the subchannel selected based on the independently calculated transmit power.

(2) After the MTCD is successfully sent if the MTCD receives a DLACK signal indicating successful reception within a certain period of time, the communication is successful. Otherwise, MTCD will return to the next free time and try to connect. If the MTCD data burst is small, the signaling process of the connection-oriented method and the proposed hybrid transmission method is shown in Figure 2. For small data packets that are usually tens of bytes on the Internet of Things, the connection-oriented method will generate a large amount of signaling overhead of up to 220 bytes, and the proposed hybrid transmission method has multiple broadcast signaling overheads. Can reduce the use of bytes.

There is no separate event for power conflicts at each power level in NOMA. That is to say, if the power reaches the maximum and suddenly occurs at the power level I, it will not affect −1 level signals, even if there are a large number of levels of signals colliding, it cannot be against the power level $l+$. The signal is decoded.

In the designated distributed layer unlicensed NOMA framework, in view of the competition of C MTCD and M subchannels, the connection probability PCon of the first layer is expressed as follows:

$$P_l^{(im)} = \left(1 - \frac{1}{M}\right)^{(l-1}\left(1 + \frac{C}{M-1}\right)^{l-1}. \tag{5}$$

Since the target of MTCD under the K constraint is V, it is first determined at the end of the receiving end, so it has nothing to do with signals of other powers, so

$$p_{c,m,1}^{smcc} = p_{c,m,1}^{\mathrm{sel}}. \tag{6}$$

The successful transmission of the MTCD signal belonging to the set Kz is not only related to the unique selection of the specific subchannel m in the hierarchical structure but also related to the MTCD selection subchannel of the set Kr. For m, the signals on this channel will not conflict. And, so

$$p_{c.m.2}^{sncc} = p_{c.m.2}^{sncc}\left\{\sum_{c=1}^{c} p_{c.m.1}^{sncc} + p_{m.l}^{\mathrm{nosel}}\right\}. \tag{7}$$

Obtained from formula (7),

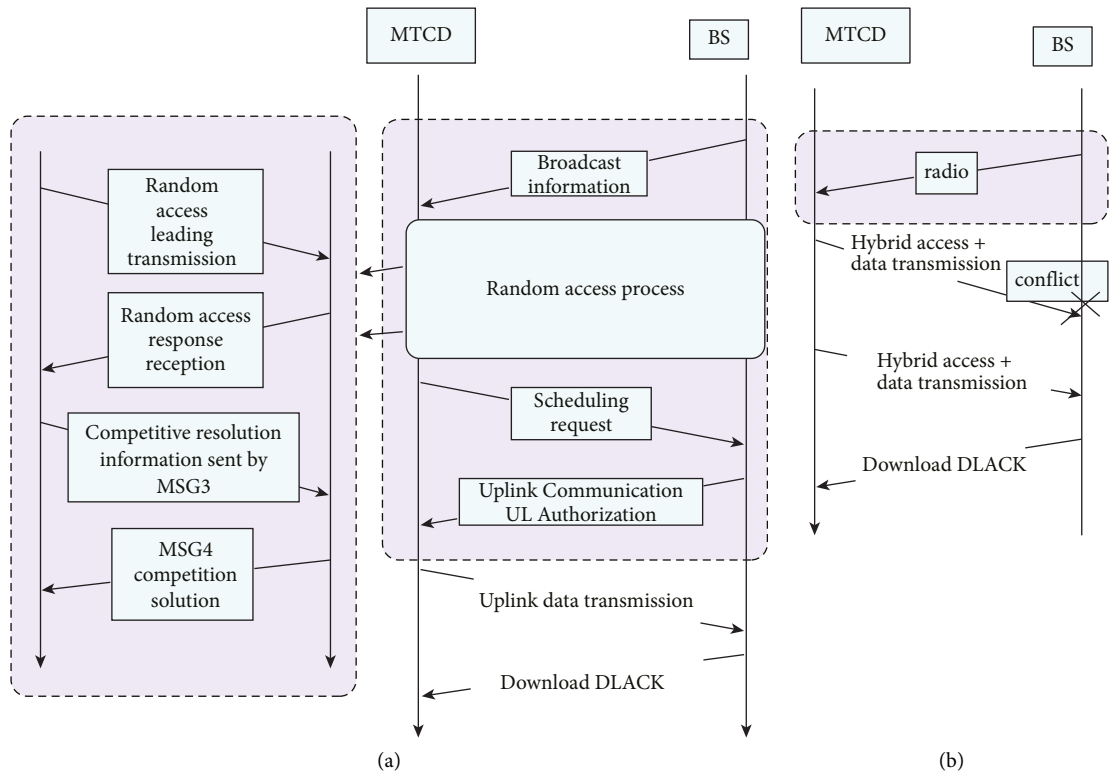

Figure 2: (a) Connection-oriented communication (b) Comparison of hybrid access and data transmission.

$$\sum_{c=1}^{C} p_{c,m.1}^{smc} + p_{m.1}^{n_{0,c/}} = \frac{p_{c.m.2}^{sicc}}{p_{c,m.2}^{se'}}. \tag{8}$$

For any MTCD belonging to set K, we can obtain the following equation:

$$\begin{aligned} p_{c.m.3}^{sncc} &= p_{c.m.3}^{sel}\left\{\sum_{c=1}^{c} p_{c.m.2}^{sncc} + p_{m.2}^{nosel}\left\{\sum_{c=1}^{c} p_{c.m.1}^{sncc} + pp_{m.1}^{\text{nosel}}\right\}\right\} \\ &= p_{c.m.3}^{sel}\left\{\sum_{c=1}^{c} p_{c.m.2}^{sncc} + p_{m.2}^{\text{nosel}}\left\{\frac{p_{c.m.2}^{sncc}}{p_{c.m.2}^{sel}}\right\}\right\} \\ &= p_{c.m.3}^{sel} p_{c.m.2}^{sncc}\left(C + \frac{p_{m.2}^{\text{nosel}}}{p_{c.m.2}^{\text{sel}}}\right). \end{aligned} \tag{9}$$

The following rules can be found:

$$p_{c,m,l}^{\text{succ}} = p_{c,m,l}^{\text{sel}} p_{c,m,l-1}^{\text{succ}}\left(C + \frac{p_{m.l-1}^{\text{nosel}}}{p_{c,m,l-1}^{\text{sel}}}\right), l = 2, 3, \ldots, L. \tag{10}$$

Figure 3 shows the numerical value and simulation result of the connection throughput of each layer of MTCD in the formula. The greater the number of MTCDs, the lower the probability of successful connection in a single time slot that matches the actual situation. Therefore, the above-mentioned link output can accurately reflect system performance and can be used as a measure of system performance.

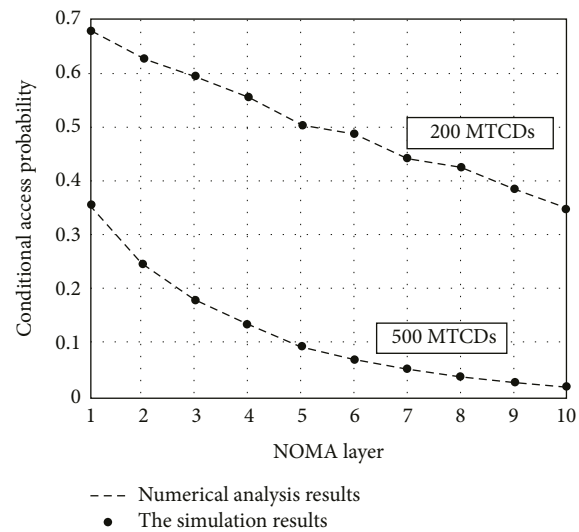

Figure 3: Numerical results for different presets.

3.3. Principle of Power Layer Algorithm Selection and Joint Access Control □. Through pa = $p(E + \text{AB})\cdot$pstcc, where p(s/ki) = ($\sum(j = 1)$l psπc‘)/L, psucc’ is successfully transmitted by

the MTCD of the first layer Probability. Therefore, the average transmission time of the MTCD of the system can be expressed as follows:

$$\begin{aligned} D_{\text{the}} &= T_P \cdot T_{\text{are}} \\ &= \frac{T_P}{P_a}. \end{aligned} \tag{11}$$

At present, we need to start from two aspects: firstly, to maximize the throughput of the connection, and secondly, to optimize the power limit and delay during transmission.

$$\begin{aligned} \max T^{\text{Con}} &= \sum_{l=1}^{L} T_l^{Cm} \\ \text{s.t. } C1&: L \in \mathrm{L_T} = \{1.2 \ldots . L_{\max}\} \\ C2&: D_{\text{ave}} \le D_{rc}. \end{aligned} \tag{12}$$

Among them, $C1$ and $C2$ in turn indicate that the most common constraints allowed are transmission power and average transmission delay. Lr represents the NOMA power level setting below the average transmission power limit.

Choose $L = \mathrm{Lmx}$ because the connection throughput TCon is an increasing characteristic of the NOMA power level L. P: A group that meets the average delay requirement. P can be obtained from the following formula:

$$\mathrm{P} = \left\{ p_E \mid \begin{array}{c} \dfrac{T_p}{p_a} \le D_{\text{req}} \\ \\ 0 < p_E \le 1 \end{array} \right\}, \tag{13}$$

where $p_a = p_{E:}/L_{\max} \sum_{l=1}^{L} (1 - 1/M)^{(Q \cdot p_E / l_{\max}) l-1} (1 + Q \cdot p_E / L_{\max} / M - 1)^{|-1}$. Therefore, the optimal p is

$$p_E^* = \arg \max_{p_E \in \mathbb{P}} T^{\text{Cnn}}. \tag{14}$$

If P is an empty set, it means that there is no optimal solution to the optimization problem even under the constraints of the maximum allowable power level and the optimal transmission control parameters. In the case that the quantity is still insufficient, P is determined as follows:

$$p_E^* = \arg \max_{0 < p_k \le 1} T^{\text{Con}}. \tag{15}$$

3.4. Human-Computer Interaction Graphical Interface Function Realization. Qt combines the functions of the digital classroom with various functions, such as buttons, input dialogs, and transfer bars. This window is an example of the QWidget class or subclass. All user window classes inherit from the QWidget class. The oldstyle relationship of the QWidget class is shown in Figure 4.

A form usually contains multiple subforms, which appear in the client area of the parent form. There are no restrictions on Qt windows. This window has top-level forms or sub-forms of other forms. When the parent form is hidden or deleted, these tasks also apply to the child form. The size and position of each part placed on the form must be appropriate.

These classes are usually used to improve the interaction with people and computers. The inheritance relationship of the design manager class is shown in Figure 5.

4. Evolution and Influencing Factors of Regional Tourism Competitiveness

4.1. Research Methods of Regional Tourism Competitiveness. In this study, the evolving law of China's domestic competitiveness differences and investigating the main factors affecting the competitiveness of the tourism industry are mainly entropy methods, and the coefficient of variation method is multivariate linear, including regression analysis, regional analysis, and detection. Maker and other models. Using the coefficient of variation method of the entropy method, this paper analyzes the temporal and spatial changes of the tourism competitiveness of China's four main economic regions and combines multiple linear regression analysis methods and geographic detector models to analyze the competitiveness of China's major economic regions.

The entropy method is used to determine the degree of dispersion of indicators. The calculation method and formula are as follows:

$$r'_{ij} = \frac{\max\left(r_{ij}\right) - r_{ij}}{\max\left(r_{ij}\right) - \min\left(r_{ij}\right)}. \tag{16}$$

Set $b_{ij} = 1 + \hat{r_{ij}}'$ to make lnf_{ij} meaningful. The entropy value of each index is calculated. H_{ij} is the entropy value of the i indicator:

$$H_i = -k \sum_{j=1}^{n} f_{ij} \times \ln f_{ij}. \tag{17}$$

Here, $f_{ij} = b_{ij} / \sum_{j=1}^{n} b_{ij}, k = 1/\ln n$(Assume $f_{ij} = 0$, In $f_{ij} = 0$). Determination of the weight of indicator i:

$$W_i = \frac{1 - H_i}{m - \sum_{i=1}^{m} H_i}. \tag{18}$$

The coefficient of variation method is used as an indicator to show the relative differences between data. This study introduces the coefficient of variation method to study the evolution of regional competitiveness differences in China. Calculated as follows:

$$\delta = \sqrt{\frac{\sum_{i=1}^{n} \left(Y_i - \overline{Y}\right)}{n}}, CV = \frac{1}{\overline{Y}} \sqrt{\frac{\sum_{i=1}^{n} \left(Y_i - \overline{Y}\right)}{(n-1)}}. \tag{19}$$

Here, δ represents the standard deviation of the data, CV represents the coefficient of variation, Y; represents the data value of the i region, and Y represents the average value of the entire region.

An important tool for detecting changes in impact is geographic recognition methods. The principle of special calculation is as follows:

$$q = 1 - \frac{1}{n\delta^2} \sum_{a=1}^{m} n_a \delta^2. \tag{20}$$

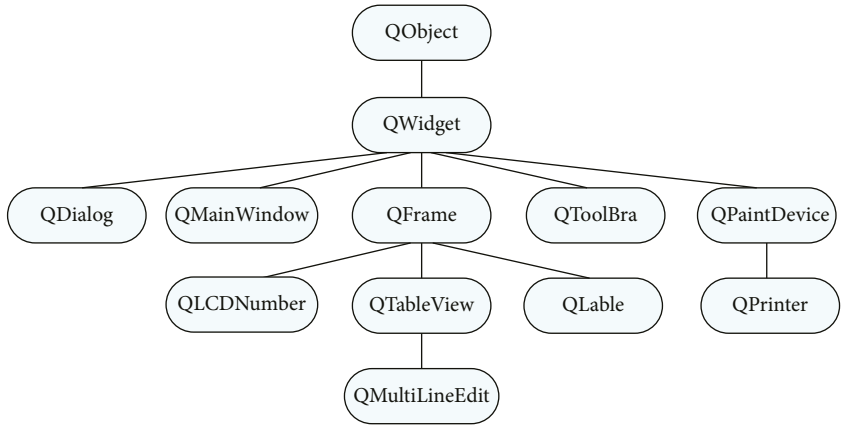

Figure 4: The inheritance relationship of the QWidget class.

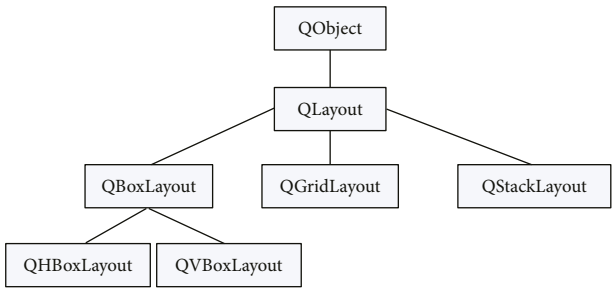

Figure 5: Layout manager class inheritance diagram.

Here, the value of q varies between 0–1. The closer the value of q is to zero, the weaker the influence of the influencing factor. The closer the value of q is to 1, the stronger the influence of the influencing factor.

4.2. Indicator Selection and Data Processing. The collected data is first sorted by year, and the 20 index data contained in the measurement layer of Table 1 are dimensionless and adjusted to eliminate size changes, and the index data becomes a constant value between the merge gaps.

Use the scale conversion method to perform standardization, the formula is

$$y_i = \frac{x_i}{\max(x_i)}. \tag{21}$$

Here, Y_i: the balance value of the indicator; x_i: the original data of the indicator; the maximum value (x_i): the maximum value of the indicator. Model index system of regional tourism competitiveness development level is shown in Table 1.

According to the entropy method of determining the weight formula:

$$r'ij = \frac{\max(r_{ij}) - r_{ij}}{\max(r_{ij}) - \min(r_{ij})}. \tag{22}$$

Set $b_{ij} = 1 + r_{ij}^{\hat{}\prime}$ to make $1nf_{ij}$ meaningful, and then calculate the entropy value of each index.

H_i is the entropy value of the i indicator:

$$H_i = -k\sum_{j=1}^{n} f_{ij} \times \ln f_{ij},$$
$$f_{ij} = \frac{b_{ij}}{\sum_{j=1}^{n} b_{ij}}, k = \frac{1}{\ln n}. \tag{23}$$

Here, (assuming $f_{ij} = 0$, $\mathrm{In}f_{ij} = 0$), then the weight of index i is obtained:

$$W_i = \frac{1 - H_i}{m - \sum_{i=1}^{m} H_i}. \tag{24}$$

$W = w1\ w2\ w3...]T$, W is the required eigenvector.

4.3. Analysis of China's Regional Tourism Competitiveness. According to the coefficient of variation method, the coefficient of variation of the internal tourism competitiveness of the four major economies in the east, central, west, and northeast was calculated and displayed in a line chart, as shown in Figure 6. The overall difference in China's tourism competitiveness is relatively large, and the overall trend is to increase first and then decrease the fluctuation range. The regional differences between the central, western and northeastern regions are shrinking, and the differences in tourism competitiveness in the eastern region have mainly increased from 2008 to 2010.

The difference in the competitiveness of the tourism industry in the eastern region shows a trend of shrinking and increasing. The difference in tourism competitiveness varies from small to large. The maximum coefficient of variation in 2000 was 0.5244, and the minimum coefficient of variation in 2010 was 0.3641. The difference in tourism competitiveness in the central region showed a trend of increasing and then decreasing. When there was a big change in 2005, the difference in tourism competitiveness in the central region was the largest, and then gradually decreased. The value of the coefficient of variation in 2005 was 0.7495, and the minimum value in 2015 was 0.2513. The difference in the competitiveness of tourism in the western region was between 2000 and 2015. This difference first narrowed and then tended to increase. The difference in tourism competitiveness within the region has hardly changed, and the regional

Table 1: Model index system of regional tourism competitiveness development level.

Target layer	Criterion layer	Measures layer
The development level of regional tourism competitiveness	Supply competitiveness	The total turnover of tourism in ten thousand yuan) (X1)
		Passenger turnover (100 million person-kilometers) (X2)
		Average length of stay (days) (X3)
		Total number of tourists received (10,000 person-times) (X4)
		Cost per person per day (USD per person day) (X5)
	Guaranteed competitiveness	Number of 5A-level scenic spots (a) (X6)
		Total number of travel agencies (number) (X7)
		Average room occupancy rate (%) (X8)
		Number of civilian passenger vehicles (units) (X9)
		Number of star-rated hotels (units) (X10)
		Number of beds in health institutions (units) (X11)
		Highway network density (km/km2) (X12)
		Number of employees in travel agency (person) (X13)
		Number of employees in star-rated hotels (persons) (X14)
		Number of colleges and universities (offices) (X15)
	Economic competitiveness	Local fiscal revenue (ten thousand yuan) (X16)
		Operating income of travel agencies (thousand yuan) (X17).
		Per capita disposable income of urban residents (yuan) (X18)
		Per capita disposable income of rural residents (yuan) (X19)
		Hotel operating income (thousand yuan) (X20)

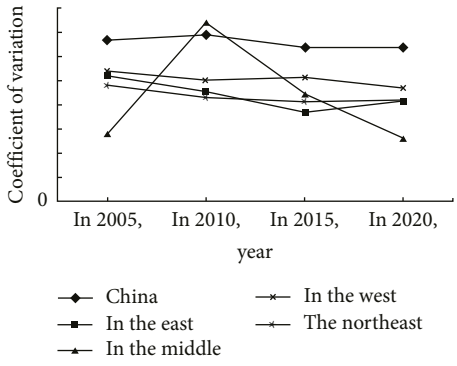

Figure 6: Examines the differences in the level of tourism competition in the four economic zones.

difference is small every year. The maximum value of the coefficient of variation in 2000 was 0.5234, and the minimum value in 2015 was 0.5525. The difference in the competitiveness of the tourism industry in the Northeast region has generally shown a downward trend, and the difference in the competitiveness of the tourism industry in the region has changed significantly, with slight changes in 2015. The coefficient reached its maximum value of 0.4846 in 2000 and its minimum value of 0.4191 in 2005.

Multiply the weights obtained in Table 1 by the standardized index and add them to get the tourism competitiveness level score of each local government department, as shown in Table 2.

The region with the highest tourism competitiveness is in the east. The tourism competitiveness of the central region is lower than that of the east, and the tourism competitiveness of the northeast and western regions is not ideal.

4.4. Identification of the Dominant Factors in the Evolution of Regional Tourism Competitiveness Differences. Compared with 2010, the 19 factors affecting the competitiveness of the region have been reduced to 12.5 A-level scenic spots; passenger attrition rate, total tourism income, average staying time, per capita daily consumption, the number of beds in medical institutions, and the number of hotel employees do not have an important impact. These include local fiscal revenue, hotel operating profit, total number of tourists, number of travel agencies, total tourism revenue, and disposable income of residents. The impact on the competitiveness of the region is weak. Per capita disposable income, higher education institutions, road network density, passenger turnover, and the increase in the number of private cars and star-rated hotels in the region have affected tourism competitiveness as shown in Table 3.

According to the analysis of the variance table of the model used in 2000, 2005, 2010, and 2015, see Table 4.

Perform the F test of the regression model and check the confidence level $\alpha = 0.05$ and the F distribution table, you can see that $F0.05(20,10) = 2.774\, F > 1970 > 2.774$. In the table, the annual regression model is selected as the model with the highest F value in the stepwise regression. Since 1970, the F values of the four selected models have shown

Table 2: Scores of tourism competitiveness in different years in different regions.

Situation in each region		2000 tourism competitiveness level score	2005 Tourism Competitiveness Level Score	2010 tourism competitiveness level score	2015 tourism competitiveness level score
East area	Shandong	0.216	0.275	0.378	0.256
	Jiangsu	0.271	0.362	0.462	0.302
Central region	Shaanxi	0.096	0.112	0.162	0.116
	Shanxi	0.066	0.113	0.141	0.095
Western region	Inner Mongolia	0.054	0.066	0.113	0.085
	Qinghai	0.146	0.165	0.048	0.183
North-east area	Heilongjiang	0.092	0.103	0.126	0.073
	Jilin	0.066	0.112	0.105	0.075

Table 3: Table of stepwise regression coefficients in 2015.

	Unbalance factor B	Standard error	Standard coefficient	T	SIG	Poor statistical report capacity	VIF
(Constant)	0.002	0.005		0.235	0.816		
Restaurant operating income (thousand yuan)	0.112	0.004	0.236	12.423	0.000	0.042	19.162
Total number of tourists received (10,000 person-times)	0.364	0.003	0.632	124.351	0.000	0.861	1.152
Number of employees in travel agency (person)	0.063	0.006	0.151	7.198	0.000	0.053	18.577
Highway network density (km/km2)	0.025	0.003	0.061	6.872	0.000	0.269	3.832
Local fiscal revenue (ten thousand yuan)	0.155	0.002	0.265	50.710	0.000	0.898	1.113
Total turnover of tourism (ten thousand yuan)	0.057	0.004	0.184	14.864	0.000	0.165	5.77
Number of colleges and universities (offices)	0.028	0.005	0.068	5.304	0.000	0.148	6.753
Per capita disposable income of residents (yuan)	0.031	0.004	0.036	4.883	0.000	0.284	3.323
Number of vehicles owned by civilian passengers (units)	0.0364	0.004	0.087	9.341	0.000	0.237	3.920
Per capita disposable income of urban residents (yuan)	0.030	0.004	0.047	7.842	0.000	0.689	1.452
Passenger turnover (100 million person-kilometers)	0.032	0.004	0.046	5.657	0.000	0.241	4.232
Number of star-rated hotels (units)	0.015	0.004	0.035	3.334	0.004	0.224	4.457

Table 4: Variance table.

Model	Sum of square	df	Mean square	F	Sig.
2000 regression model	0.244	10	0.024	1970.915	0.000n
2005 regression model	0.449	19	0.024	4215326.708	0.000u
2010 regression model	0.577	19	0.03	8879209.509	0.000u
2015 regression model	0.311	12	0.026	3402.186	0.000n

that they have a regression effect on the four cursor models. The evolution of China's regional competitiveness differences and its influencing factors.

After that, in 2000, 2005, and 2010, the 2015 20 index data were applied to the geographic detector model. The analysis and TT calculation results are shown in Table 5. Number of institutions of higher learning, per capita disposable income in rural areas, operating income of travel agencies, travel agencies, passenger transfers, number of private cars, total number of tourists, and fiscal revenues in the region. The result of the geo-detector analysis is that we can see six factors, such as passenger conversion, total number of tourists, private cars, travel agencies, local fiscal revenues, and travel agencies. Operating income helps improve the competitiveness of the Chinese region, and its influence is greater.

The comprehensive regression analysis based on the cross-priority index selection principle and the calculation result of the geographic detector will determine the total number of tourists, private cars, travel agencies, and local fiscal revenue. Four indicators that affect China's competitiveness in the region dominate.

Table 5: The q value of each indicator in the four years.

Index	2000	2005	2010	2015
Total tourism revenue (ten thousand yuan)	0.35	0.38	0.45	0.43
Passenger turnover (100 million person-kilometers)	0.52	0.49	0.47	0.51
Average length of stay (days)	0.19	0.23	0.27	0.29
Total number of tourists received (10,000 person-times)	0.61	0.51	0.60	0.67
Average daily cost per person (USD/person Yao)	0.29	0.32	0.37	0.34
Number of 5A-level scenic spots	0.36	0.41	0.49	0.43
Total number of travel agencies (a)	0.39	0.41	0.53	0.45
Average room occupancy rate (%)	0.25	0.23	0.37	0.31
Number of vehicles owned by civilian passengers (units)	0.56	0.57	0.64	0.35
Number of star-rated hotels (units)	0.32	0.35	0.51	0.49
Number of beds in health institutions (units)	0.37	0.31	0.28	0.32
Highway network density (km/km^2)	0.35	0.31	0.28	0.34
Number of employees in travel agency (person)	0.47	0.49	0.43	0.51
Number of employees in star-rated hotels (persons)	0.27	0.35	0.41	0.39
Number of colleges and universities (offices)	0.39	0.37	0.41	0.38
Local fiscal revenue (ten thousand yuan)	0.57	0.61	0.68	0.63
Total turnover of travel agency (thousand yuan)	0.41	0.57	0.60	0.54
Per capita disposable income of urban residents (yuan)	0.36	0.34	0.32	0.35
Per capita income of rural residents (yuan) (X19)	0.38	0.47	0.42	0.40
Hotel operating income (thousand yuan)	0.19	0.21	0.23	0.26

4.5. Suggestions for the Development of Regional Types of Tourism Competitiveness. According to the main characteristics of China's regional tourism competitiveness, four regional development proposals will be put forward with reference to the national tourism development policy and research results related to regional tourism development. Tourists are often attracted by novelties when traveling, and often have travel motives, but the homogeneity of tourism products and the high-speed and transparent information distribution between regions are very serious. The development of tourism resources with regional characteristics is of great significance to improving regional competitiveness. Secondly, we need to reveal the more in-depth local culture and tourism resources. With the improvement of people's living standards, the trend of tourism development is to dig deeper into local culture and transform it into iconic tourism products.

Actively promote tourism, social services, and infrastructure construction in the area. In addition, the existing highway toll stations, bus terminals, railway stations, etc., will be upgraded to facilitate traffic inside and outside the area. Further enhance the tourism competitiveness of areas with weak tourism development infrastructure, grasp the main limiting factors of weak tourism development zones, and encourage potential tourism development zones and high-quality resources between regions. The development of the spatial structure of the tourism industry and the improvement of regional competitiveness are constantly developing in the direction of higher quality. At the same time, areas with low tourism competitiveness are improving their competitiveness, actively expanding investment in the tourism industry, introducing investment companies and attracting high-quality tourism talents, cultivating tourism companies, and introducing unique tourism development models and development methods.

5. Conclusion

Based on the commercial characteristics of small packet bursts and the stability of random competition in the Internet of Things communications, this paper provides a stable transmission method based on NOMA, which does not require distributed scheduling. According to the Foster–Lyapunov level, we quickly used a series of methods to study the robustness of the nondistributed scheduling system to provide reliable noncooperative distributed transmission probability control. When designing the human-computer communication system, Qt oscilloscope firstly described the development history and status quo of internal human-computer communication, and combined with the oscilloscope's requirements for the human-computer interaction system, it analyzed the entire framework of the oscilloscope and human-computer interaction system and analyzed and analyzed one by one. Realize the entire design of the human-computer interaction system.

Data Availability

The data used to support the findings of this study are available from the corresponding author upon request.

Conflicts of Interest

The authors declare that they have no conflicts of interest.

Acknowledgments

This work in this article was supported by City University of Macau.

References

[1] R. Petrolo, V. Loscrì, and N. Mitton, "Towards a smart city based on cloud of things, a survey on the smart city vision and paradigms," *Transactions on Emerging Telecommunications Technologies*, vol. 28, no. 1, Article ID e2931, 2017.

[2] L. D. Xu, W. He, and S. Li, "Internet of things in industries: a survey," *IEEE Transactions on Industrial Informatics*, vol. 10, no. 4, pp. 2233–2243, 2014.

[3] L. Chettri and R. Bera, "A comprehensive survey on Internet of Things (IoT) toward 5G wireless systems," *IEEE Internet of Things Journal*, vol. 7, no. 1, pp. 16–32, 2020.

[4] J. Mi and Y. Takahashi, "Whole-body joint angle estimation for real-time humanoid robot imitation based on Gaussian process dynamical model and particle filter," *Applied Sciences*, vol. 10, no. 1, p. 5, 2019.

[5] R. Prasad and V. Rohokale, *Internet of Things (IoT) and Machine to Machine (M2M) Communication*, pp. 125–141, Springer Series in Wireless Technology, Berlin, Germany, 2019.

[6] K. K. Du, Z. L. Wang, and M. Hong, "Human machine interactive system on smart home of IoT," *The Journal of China Universities of Posts and Telecommunications*, vol. 20, pp. 96–99, 2013.

[7] M. Petrova, N. Dekhtyar, O. Klok, and O. Loseva, "Regional tourism infrastructure development in the state strategies," *Problems and Perspectives in Management*, vol. 16, no. 4, pp. 259–274, 2018.

[8] Y. Zuo, H. Chen, J. Pan, Y. Si, R. Law, and M. Zhang, "Spatial distribution pattern and influencing factors of sports tourism resources in China," *ISPRS International Journal of Geo-Information*, vol. 10, no. 7, p. 428, 2021.

[9] S. Jeon, J. Bang, K. Byun, and S. Lee, "A recovery method of deleted record for SQLite database," *Personal and Ubiquitous Computing*, vol. 16, no. 6, pp. 707–715, 2012.

[10] J. M. Carroll, "Human–computer interaction: psychology as a science of design," *International Journal of Human-Computer Studies*, vol. 46, no. 4, pp. 501–522, 1997.

[11] C. P. Barros and F. P. Alves, "Productivity in the tourism industry," *International Advances in Economic Research*, vol. 10, no. 3, pp. 215–225, 2004.

[12] M. Fetscherin and R.-M. Stephano, "The medical tourism index: scale development and validation," *Tourism Management*, vol. 52, pp. 539–556, 2016.

[13] J. O. Wobbrock and J. A. Kientz, "Research contributions in human-computer interaction," *Interactions*, vol. 23, no. 3, pp. 38–44, 2016.

[14] W. Ahn and R. Y. Kim, "Distributed triggered access for BSM dissemination in 802.11bd V2V networks," *Applied Sciences*, vol. 10, no. 1, p. 311, 2019.

Hindawi
Computational Intelligence and Neuroscience
Volume 2022, Article ID 9592376, 9 pages
https://doi.org/10.1155/2022/9592376

Research Article

Design of Urban Garden Landscape Visualization System Based on GIS and Remote Sensing Technology

Wenpeng Zhang [1,2]

[1]*School of Financial Technology, Shanghai Lixin University of Accounting and Finance, Shanghai 201209, China*
[2]*University Kuala Lumpur Business School, University Kuala Lumpur, Wisma Yayasan, Selangor 50300, Kuala Lumpur, Malaysia*

Correspondence should be addressed to Wenpeng Zhang; 1732261190@xzyz.edu.cn

Received 10 July 2022; Revised 3 September 2022; Accepted 6 September 2022; Published 22 September 2022

Academic Editor: Gopal Chaudhary

Urban green ecological space is an important manifestation of the environmental characteristics of a green city. The research results show that the urban green ecological space has obvious cooling and humidity effects, which are very important for reducing the urban heat island effect. Remote sensing technology describes the slow-release effects of urban green parks in different seasons from the two perspectives of thermal slow-release intensity and thermal slow-release distance. In this paper, UAV remote sensing is used to extract the internal and external factors of the urban green environment characteristics and to identify the main factors that affect the slow-release heat effect and seasonal changes of the urban green environment. In addition, it analyzes the factors that affect the urban environmental temperature within the environmental temperature slow-release range of urban green space, establishes a model to predict the environmental temperature within the thermal slow-release range outside the park, and realizes the largest thermal slow release in the urban greening ecological space. These are new technologies created in the context of digitization, which include image understanding and synthesis, which involve the use of computer graphics and image processing technology to convert data into graphics or images displayed on the screen to achieve an interactive process.

1. Introduction

This article mainly studies the visualization of urban landscape. The main research object is the shape of urban landscape groups or individuals. Then, using the rapid development of virtual reality technology in recent years, the growth process of the landscape of the research object in the three-dimensional space is produced on the computer. Urban landscape visualization has become the main focus of this article. Landscape visualization refers to the use of virtual reality technology to reproduce the growth process of the landscape in a three-dimensional space on the computer to study the shape and structure of the landscape [1]. Visualization is mainly through observation and measurement, using computer software to set the landscape growth parameters, and then adjusting based on experience to obtain the ideal landscape effect [2]. In the later work, it is also necessary to change the texture and color of the landscape organs through the graphics library to make the modeling of landscape growth clearer. In the urban garden landscape, three-dimensional modeling and visualization have achieved concrete results, mainly including landscape matrix and landscape model [3]. However, the effectiveness in landscape design is now expressed in a two-dimensional, qualitative, and static form. This article uses landscape visualization in landscape design for the first time to create a dynamic display landscape in a time-based design. The landscape performance achieves a four-dimensional effect [4]. The design is also more intuitive, rich, and practical. Most software currently used in garden design cannot show landscape visualization. After screening, this article chose the GreenLab visualization software provided by the Institute of Automation to visualize a single landscape [5]. If you want to realize the application of landscape visualization in garden design, first of all, you must have a powerful database. In the next stage, combined with the garden design made

during the internship, landscape visualization is introduced into the static 3D landscape, creating new garden landscape efficiency and making the garden landscape effect more dynamic, flexible, and creative [6]. Then, combined with remote sensing technology to analyze the characteristics of the green city environment, it is concluded that the heat release effect of the urban green ecological space has seasonal changes [7]. In summer and winter, the average temperature in a certain park is lower than the temperature outside the park. As the distance from the park boundary increases, the temperature also rises, which also proves that the green air of the city affects the city's heat-releasing effect [8]. The average temperature in the park at night in winter is higher than the surrounding environment of the city, reflecting the "warm island effect" of the city's green environment. From summer to winter, the average slow heat release (CEI) intensity of the park decreased from 3.63°C to 2.02°C, and the average slow heat release (SCE) distance decreased from 246 m to 172 m.

2. Materials and Methods

2.1. Theoretical Basis. The sequence of data processing is radiometric calibration, atmospheric correction, geometric correction, and ortho correction. This article mainly studies radiation calibration and atmospheric correction. Geometric correction can ensure that the quality of satellite images is consistent with their original position on the Earth's surface. In this study, the metadata provided by Landsat 8 imagery were used for correction. In addition, the purpose of radiometric correction is to provide data with pixel values related to surface backscatter. The radiometric data are calibrated for backscatter coefficients, atmospheric correction is performed to improve data quality, and FLAASH (fast line of sight) is used to perform hypercube spectral analysis. FLAASH can analyze a wide range of visible light, multispectral and hyperspectral. Use remote sensing image processing tools to combine panchromatic bands to achieve higher spatial resolution (region extraction accuracy will be comparable to that of multispectral bands, and there is no need for later merging).

Affected by objective factors limited by the satellite direction and altitude, the image obtained by the sensor will cause geometric distortion, which must be corrected using the proposed correction model; geometric correction includes the following concepts:

Geocoding: rectify the image to a single standard coordinate system.

Geotagging: use multiple checkpoints to correct the geographic coordinates of the image.

Image registration: an image (reference image) in an area is calibrated with another image.

The general steps for correcting the geometric accuracy of an image are as follows. This is the most important step for correcting the geometry. Checkpoints can be selected from the topographic map as a reference, can also be obtained from a field survey, or can be obtained from a calibration image. The selected control points have the following characteristics: remote sensing data have obvious characteristics, such as reservoirs, construction land, rivers, and so on; the ground objects of the control points will not change with time.

2.2. Research Methods. In this study, Thermochron iButtons sensors are used to collect temperature and humidity inside and outside the urban green environment.

Mean square error:

$$\mathrm{RMSE} = \sqrt{\frac{\sum_{i=1}^{n}\left(x_{1,t} - x_{2,t}\right)^2}{n}}. \tag{1}$$

$X_{1,t}$ and $X_{2,t}$ represent the measurement data of iButtons and weather station, respectively. Correlation analysis:

$$r = \frac{\sum(X_i - \overline{X})(Y_i - \overline{Y})}{\sqrt{\sum(X_i - \overline{X})^2 \sum(Y_i - \overline{Y})^2}}. \tag{2}$$

X_i and Y_i represent the observed values of iButtons and weather stations, respectively, while $\overline{X}$ and Y represent the average values of iButtons and weather station sample values, respectively. Significant difference test:

$$t = \frac{\overline{X_1} - \overline{X_2}}{\sqrt{\left((n_1 - 1)S_1^2 + (n_2 - 1)S_2^2/(n_1 + n_2 - 2)\right)(1/n_1 + 1/n_2)}}. \tag{3}$$

S_1^2 and S_2^2 are the variances of the measured data of iButtons and the weather station, n_1 and n_2 are the sample sizes, and $\overline{X_1}$ and $\overline{X_2}$ represent the average values, respectively. Thermal release strength:

$$\mathrm{CEI} = \frac{2b^3 + \left(2b^2 - 6ac\right) * \sqrt{b^2 - 3ac} - 9abc}{27a^2}. \tag{4}$$

CEI is the thermal sustained release strength of the study area. Thermal release impact distance:

$$\mathrm{SCE} = \frac{-b - \sqrt{b^2 - 3ac}}{3a}. \tag{5}$$

SCE is the thermal slow-release influence distance in the study area; a, b, and c are the coefficients of the cubic term, quadratic term, and first term in the cubic polynomial, respectively.

3. Results

3.1. Environmental Temperature Characteristics of Green Cities. Figure 1 shows the temperature change characteristics of five planting surfaces in a park, including forests, shrubs, grasslands, ponds, and hard surfaces in summer. It can be seen from the figure that the daily temperature characteristics of the five underlying surfaces in summer are in an inverted U-shaped distribution, with obvious troughs (05:00) and peaks (14:00). After sunrise (6 o'clock in the morning), the average temperature of the five surfaces of forests, shrubs, grasses, ponds, and hard surfaces will increase over time. From 12:00 to 14:00 in the afternoon, the temperature of the underlying surface is the highest.

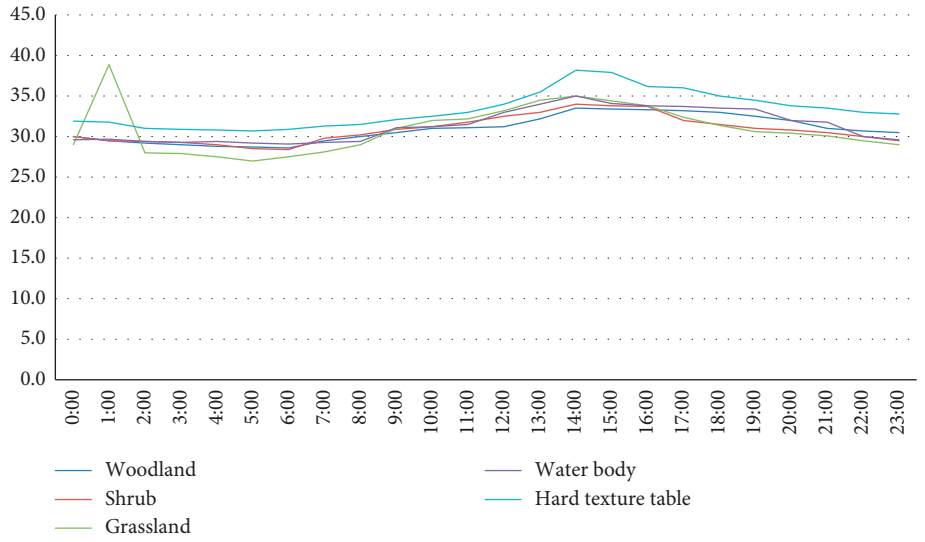

Figure 1: Diurnal changes in air temperature of five underlying surfaces in summer.

Table 1: The temperature difference of five underlying surfaces in summer (Student's t-test test results).

Underlying surface type	Woodland	Shrub	Grassland	Water body	Hard ground
Woodland	—	0.197	0.87	0.018	0.001
Shrub	0.197	—	0.205	0.012	0.001
Grassland	0.87	0.205	—	0.015	0.001
Water body	0.018	0.012	0.015	—	0.001
Hard texture table	0.001	0.001	0.001	0.001	—

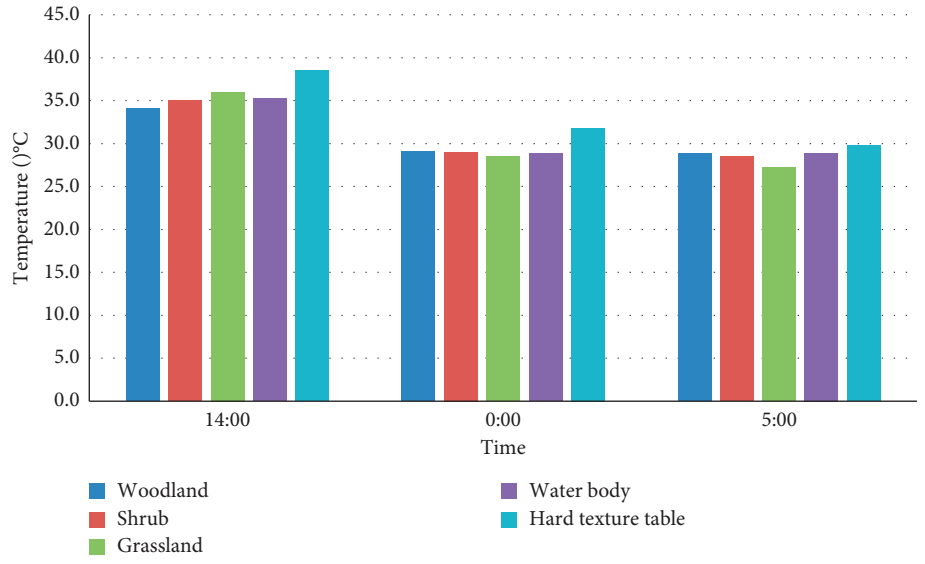

Figure 2: The air temperature difference of the underlying surface during the three periods of noon, midnight, and sunrise in summer.

From the temperature difference of the following surface types, Table 1 shows the result of Student's t-test on the temperature of the five main surfaces in summer. The results show that there is a difference in the average summer temperature between the hard ground, the water bod,y and the other three planting surface($P < 0.05$).

For this, this study compares the temperature difference between the five main surfaces of a park during the afternoon (14:00), midnight (00:00), and sunrise (05:00) (Figure 2).

Figure 3 shows the daily temperature changes of the five underlying surfaces in the winter park. It can be seen from

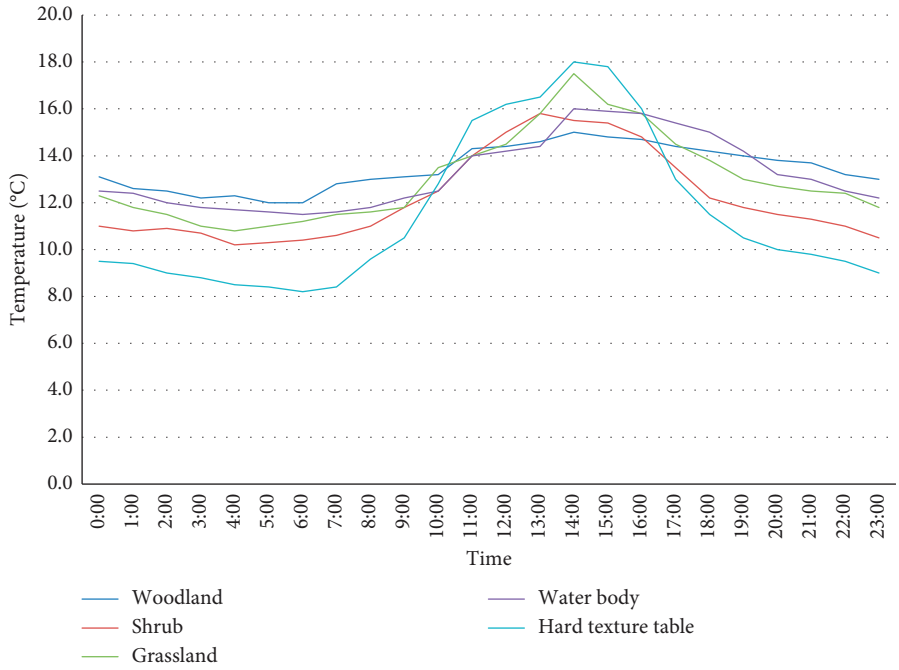

Figure 3: Diurnal changes in air temperature of five underlying surfaces in winter.

Table 2: Student's *t*-test test results of the temperature difference of five underlying surfaces in winter.

Underlying surface type	Woodland	Shrub	Grassland	Water body	Hard texture table
Woodland	—	0.001	0.137	0.116	0.003
Shrub	0.001	—	0.001	0.001	0.016
Grassland	0.137	0.205	—	0.015	0.001
Water body	0.116	0.001	0.385	—	0.002
Hard texture table	0.003	0.016	0.001	0.002	—

the figure that the diurnal variation characteristics of the five surfaces in winter are in an inverted U-shaped distribution, but the degree of line oscillation is not as strong as in summer, and there is only an obvious peak in winter (14:00).

Table 2 shows Student's *t*-test test results of five underlying surface temperatures in winter. From the temperature difference of the underlying surface types, the average temperature of the five underlying surfaces (woodland, shrubs, grassland, water body, and hard surface) in winter all have certain differences ($P < 0.05$). Among them, the *P*values between vegetation (woodland and shrubs, shrubs, and grassland) are all less than 0.05, which indicates that there is a big difference in temperature between woodland and shrubs, shrubs and grassland in winter.

This study compares the temperature difference between five underlying surfaces during the day (14:00), midnight (00:00), and before sunrise (05:00).

3.2. Environmental Comfort Characteristics of Green Cities. Environmental comfort is a manifestation of emotional well-being, and it is the satisfaction of psychological and physical problems to the environment. With the gradual increase in the intensity of urban tropical islands, it will have different levels of impact on the living environment of urban people. A large number of studies have confirmed that urban green spaces have the effects of cooling and humidification. The comfort of green cities is also judged by two aspects, such as climate and environment, which can directly affect human senses, and can also directly complete perceptual evaluation by senses. The temperature of the urban environment is discussed above. This section analyzes the impact of different summer trees on environmental comfort under natural conditions. This paper selects forests, shrubs, and grasslands to study, calculates the individual comfort levels of different types of underground and outdoor areas in the park, and compares them, and improves the difference of human comfort through different environmental planning.

Table 3 calculates the discomfort index of different types of underlying surfaces at different times in summer. It can be seen from the table that the average discomfort rate of forests, shrubs, and grassland is less than 27, and only a few people have discomfort. This is the best place for activities. The daily average values of discomfort index of control points and hard surfaces are both greater than 28.

The thermal comfort improvement degree (HCI) of various underlying surface types in a park in summer is calculated. The picture shows that different time periods and different types of surfaces have different degrees of improvement in water body comfort. In summer, the comfort

Table 3: Discomfort levels of five underlying surfaces and control points at different moments.

Time	0:00	2:00	4:00	6:00	8:00	10:00	12:00	14:00	16:00	18:00	20:00	22:00	Daily average
Woodland	26.26	25.67	25.06	24.83	27.08	28.38	28.96	29.19	29.16	28.41	28.19	27.32	27.37
Shrub	27.09	26.33	25.53	25.25	26.78	28.46	29.28	30.14	30.61	29.39	28.76	28.07	27.97
Grassland	26.08	25.48	25.23	24.68	26.12	29.01	30.86	31.17	30.88	29.57	28.78	27.52	27.94
Water body	26.98	26.78	26.68	27.24	27.45	29.43	30.45	30.85	30.27	29.47	28.28	26.63	28.37
Hard texture table	27.81	27.75	27.48	28.06	28.82	30.76	31.74	33.04	31.96	30.88	29.95	29.04	29.77
Control point	28.82	29.08	28.97	30.46	30.76	31.55	32.69	33.54	31.74	30.74	30.68	29.88	30.74

Table 4: Correlation between air temperature, discomfort index, and structural characteristics in summer and winter.

Factor	Underlying surface type	Structural feature factor		
		Area	Three-dimensional green quantity (3D-GQ)	Sky visibility factor (SVF)
Air temperature (summer)	Woodland	−0.412	−0.77	0.526
	Shrub	−0.376	−0.577	0.758
	Grassland	−0.234	−0.385	0.792
	Hard texture table	0.396	—	0.718
Discomfort index (summer)	Woodland	−0.523	−0.828	0.642
	Shrub	−0.446	−0.494	0.744
	Grassland	−0.28	−0.366	0.89
	Hard texture table	0.242	—	0.922
Air temperature (winter)	Woodland	−0.365	−0.378	0.473
	Shrub	−0.266	−0.462	0.514
	Grassland	−0.136	−0.214	0.411
	Hard texture table	0.359	—	0.569

improvement (HCI) of forests, shrubs, and water bodies is the most important one. The improvement of thermal comfort is 2.68–4.35, and the average improvement is 2.68.

Table 4 shows the relationship between the temperature, discomfort index, and structural characteristics of each surface that exist in summer and winter. It can be seen from the table that vegetation temperature (forest, shrubs, and grassland) is negatively correlated with area and three-dimensional green number and positively correlated with sky visibility coefficient ($P < 0.05$), while hard surface temperature and sky visibility coefficient are also positively correlated ($P < 0.05$).

3.3. Visualization Process of Urban Garden Landscape. Three-dimensional visualization is a tool used to display and explain the characteristics of soil geological phenomena and is widely used in geological and physical research. 3D visualization is different from various modeling technologies. It uses a form of expression that uses model data to visualize and understand things. Three-dimensional visualization technology can model the mechanical production process, reveal the reliability of data, and find the need to solve current problems. Technical support for analytical modeling and decision making bridges communication and collaboration between various disciplines. The realization of 3D visualization is mainly divided into two categories: construction model and texture display.

Three-dimensional visualization, or three-dimensional cartography, is a major function of geographic information systems. The research field of three-dimensional imaging is in the environment of three-dimensional space, which contains a wide variety of shapes, complexities and varieties, and spaces of different sizes. The visualization process of three-dimensional spatial data is shown in Figure 4.

Generated Data. This is a combination of three-dimensional objects in space using abstract data and images to perform visual effects on them. For example, field data collection uses digital altitude models for aerial photography. Digital elevation models are created by inserting and fitting polynomials to multiple discrete elevation points.

Simplification and Data Processing. Achieving 3D visualization requires the maximum possible accuracy and precision of the model while ensuring system speed and visualization effects and configuring appropriate system software and hardware to respond to the real situation of large 3D spatial data, such as LOD or detailed model level.

Drawing. In order to better improve the performance of real 3D objects in the 2D plane, it is necessary to convert various data and visually mapped object data into graphics that can be viewed on a computer. Calculate the color of each pixel on the video screen, and the color value of each pixel can be displayed on the screen.

3.4. Construction of Urban Garden Landscape Visualization System. The overall design of the 3D visual city system in a certain area adopts the traditional structure of CIS, that is, the client structure. This structure can use the hardware advantages of both parties to provide sufficient complete client and server tasks, thereby reducing development costs

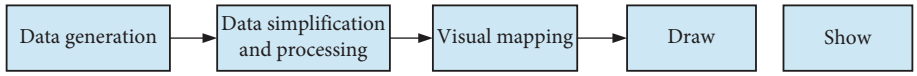

Figure 4: 3D spatial data visualization process.

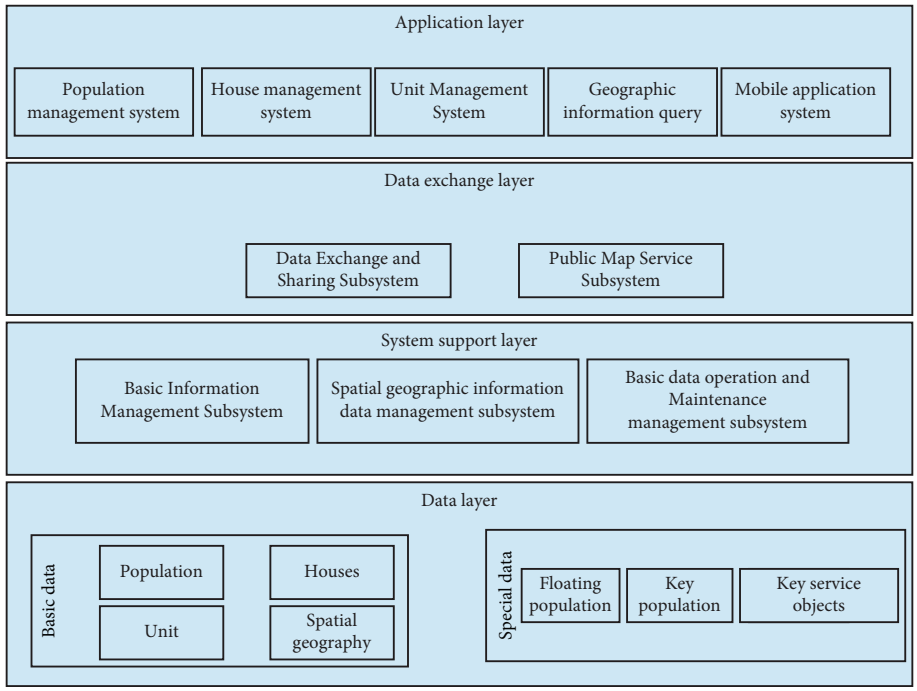

Figure 5: The overall frame structure of the system.

and improving operational efficiency. Considering a large amount of data processing and system integration, the organization of three-dimensional scenes, and a large amount of data release, the advantage is to avoid direct contact between customers and data, which affects system performance. The system is shown in Figure 5.

Skylin TerraSuit generally includes three product types: TerraBuilder, TerraExplorer Pro, and TerraGate. The three types of products are integrated to manage different geospatial data and quickly distribute them to users in the office, at home, or on-site. The 3D modeling of modern organization and urban data management methods usually uses two methods: file format and object-oriented relational spatial database. Traditional geometry and texture data storage libraries are stored separately, forcing a large amount of spatial information and related columns to generate redundant information of index relations, which is not conducive to data management, maintenance, and update. The object-oriented relational spatial database management method uses aggregate data and related texture data, stored in a spatial model, and each three-dimensional information is regarded as an entity with the same spatial information and attributes. This not only simplifies data query and retrieval but also improves the security of database management and retrieval of historical data. The data management model of this project uses the corresponding tools on the ArcGIS platform to convert 3ds into multibatch data types and connects to the Oracle database through the ArcSDE spatial data engine to realize data addition, deletion, and modification operations, and finally realizes the management and maintenance of the 3D database. ArcSDE can capture, retrieve, update, and manage large amounts of data, which can improve system operating efficiency and manage model data more effectively.

An important data framework for 3D terrain visualization includes 3D terrain data. This is a model of the terrain surface, created by technologies such as terrain modeling and texture mapping. It does not include landscape models and 2D vector data. As the basis for creating 3D scenes, they only need to use Skyline TerraBuilder to combine digital high-resolution model data and image texture data with remote sensing processing.

System implementation is the process of transforming the design results into a real controllable system, that is, transforming the logical model and physical model of the design phase into practical applications, and it is necessary to use a programming language to build a system that people can use. First, the program is developed using one or more programming languages, and then the program is tested and debugged. The development and realization of the 3D visualization system has the characteristics of a wide variety of data, a large amount of data, and real-time display requirements. Therefore, there are specific requirements for the software and hardware environment and operating mode of the development and operation of the system.

The first is the preparatory work, including data collection, plan formulation, staffing, and project allocation. Then, arrange for staff to collect textures on site. The photographer must sort the data on the same day and send it back to the office team for texture processing. Secondly, according to the data obtained, 3D models are made using 3ds Max, and the 3D models required by the urban area are made. Using preprocessed data and texture data collection, 3D modeling is performed on a 1 : 500 topographic map according to the outline of the building, and the texture data processed at the same time are applied to the map to export the built-in 3D model.

4. Discussion

4.1. Analysis of Environmental Characteristics of Green Cities. This paper analyzes the thermal environment characteristics of five major garden surface types. Studies have shown that the surface temperature of different city parks is different in summer and winter. The five surfaces have different air temperatures, and the daily temperature fluctuation characteristics are in an inverted U-shaped distribution [9]. The fluctuation range in summer is definitely stronger than that in winter, and the intensity of fluctuation during the day is stronger than that at night. In summer and winter, when the surrounding temperature rises, the temperature of each underlying surface rises. At 14:00 in the afternoon, the daily average temperature of each surface was the highest; after that, the temperature of the underlying surface dropped slightly. As for the first time the sun comes out (5 o'clock in the morning), the temperature of each surface is the lowest in the day. In the temperature difference of the underlying surface, the temperature difference of the five underlying surfaces in summer is inversely proportional to the temperature difference in winter, and the temperature difference in summer is definitely greater than that in winter. In summer, the temperature difference between the five most obvious surfaces—up to 4.2°C, and the lowest temperature at midnight in summer—is only 2.7°C. Different from summer, the minimum temperature difference between the underlying surface in winter is 2.7°C, and at night, the temperature difference on the underlying surface increases with the passage of time.

In summer, the diurnal variation characteristics of the thermal slow-release intensity (CEI) of the five underlying surfaces generally present a "U-shaped distribution," with an obvious peak (05:00) and a trough (14:00). During the summer day, the woodland, shrubs, and water bodies in the park have a certain degree of heat release strength, and the temperature of the grass and hard surface is higher than the temperature of the external reference point of the park, which becomes the heat source inside the park. In summer, this paper calculates the diurnal variation characteristics of the discomfort index from the external control points of the park and the underlying surface of the five parks [10, 11]. It can be seen that the discomfort index of the five underlying surfaces in the park increased first and then decreased, showing a single-peak curve, reaching a peak in the summer afternoon; therefore, the discomfort of the human body gradually decreases, and the discomfort is the lowest when the sun rises. Compared with the external control point of the park, vegetation such as forests, shrubs, and ponds can effectively improve the thermal comfort of the human body. The improvement rate of human comfort is 2.68–4.37, with an average of 2.67. Although the improvement of the ranch during the high temperature (12:00~14:00) period is limited, the ranch still has a better chance to improve the thermal comfort in other periods. For cities with high temperature and high humidity in summer, it is recommended to increase the underlying surface area of forests, shrubs, and ponds to reduce the harmful effects of high temperature.

4.2. Requirements and Principles of Urban Garden Landscape Visualization System Construction. In combination with the wide spread of regional improvement and innovative social governance, and in accordance with the requirements of collective integration and effective management, people should formulate and improve the concept, and strengthen and create innovative social government information systems in advanced urban areas at home and abroad. People promise to create a comprehensive, multifunctional, and specific regional urban landscape visualization system based on practical work, according to the requirements of "internal managers," with electronic maps as operators and 3D geographic information technology as support. This can directly and clearly reflect the relationship between regional population, buildings, units, events, organizations, and spatial geography, and understand the relationship between population, housing, and units [12]. It also has the functions of searching and locating subject databases, statistical analysis and providing relevant service management solutions [12]. It also has functions such as searching and locating the subject database, statistical analysis and providing related service management solutions.

Demand analysis is the analysis of the needs of users who use the system. Developers should strive to ensure that the developed system can meet the needs of users. With the help of demand analysis, developers can determine in advance the type of data required by the system, plan how to manage the system database, develop functional modules, and so on [13]. The 3D visualization system in this area is based on the city's remote sensing images, 2D data, and 3D model data. People use GIS technology, combined with computer graphics, 3D visualization, database technology, etc., through the creation of accurate 3D building models and virtual reality technology, to achieve interactive 2D and 3D geographic information query, 3D data roaming, information retrieval and other basic functions, to achieve 3D spatial analysis and mobile terminal management. People combine the Internet and mobile communication network to build urban information service system [14]. The specific performance is as follows:

(1) Complete basic data informatization construction.
Based on housing, the system establishes three major databases of population, housing, and units and forms direct links with information such as roads,

communities, networks, buildings, units, floors, and households. The combination of spatial geographic information realizes functions such as population information query, housing information query, unit information query, accurate population address positioning, and regional demographic analysis.

(2) 3D model effect display with artistic characteristics.

The system uses standardized, advanced programming and real-time rendering technology to create a three-dimensional display of lifelike urban effects. Displaying and exploring three-dimensional information intuitively and quickly determines people's views on the stage.

(3) Efficient operation and management of massive data.

The two-dimensional vector data and city model data contained in the system have a large amount of data. Professional technical means must be used to quickly view the massive modeling data.

(4) Wide range of practical applications, convenient for the management of various departments.

Provide authoritative, fresh, comprehensive, and efficient geographic information services in accordance with the requirements of "one stop." In accordance with relevant technical standards and specifications, with the "command platform" as the main body, it provides convenient and efficient system services for decision-making departments to use, which is convenient for all departments.

(5) Develop a mobile terminal management system to ensure the authenticity of information.

In the mobile PDA of the smart terminal, create basic data entry functions, modify query functions, and support comprehensive statistical analysis of some data, so that community or field staff can enter the population, housing, and unit data into the space for query and modification. It can classify events and components in time and upload them to district, road, and community management platforms from different perspectives.

4.3. Analysis of the Importance of Urban Garden Landscape Visualization. The current garden environment is highly valued. In real estate transactions, people do not usually buy houses in this way. The ecological landscape of the community is gradually becoming the main factor that forces people to buy houses [15]. When people buy a house, they also need to look at a good ecological environment. Therefore, the community not only needs a good living environment and beautification but also hopes that the place of residence has a fresh and lively atmosphere.

Community greening is the main component of the community environment. Generally speaking, this applies to the management of residential buildings, public buildings, and greening outside the residential area, garden buildings and garden sketches, or roads within the residential area, or land for leisure and entertainment provided for residents. The green area is more in line with the lives of residents and better serves residents. Public green space is a good place for residents to carry out daily outdoor activities; green space creates necessary ventilation and lighting, and the visual space between residential buildings is usually green. This can effectively improve the ecological environment of the residential area; thanks to landscaping and construction cooperation, the open space of the residential area has undergone many changes, forming a pleasant and typical residential area landscape environment.

The most important point of beautifying the community is the coordination with the environment, not just the requirement for the amount of greenery. This kind of coordination is not only something that some grasses, flowers, trees, and shrubs can do, but also a higher level of greening should be achieved by improving the quality of indoor greening. The greening of high-quality houses emphasizes the relationship between the park landscape and life and culture. Under the premise of the combination of garden landscape, architecture, garden waterscape, paving, garden trails, etc., make full use and protection of natural resources to create a cultural landscape and a lofty ecological living environment.

Environmental Protection Function. Since the main element of the residential landscape is the landscape, landscaping can not only reduce dust, purify the air, absorb sound, and protect the environment but also help improve the climate of the residential area, effectively absorb the heat of the sun, adjust the temperature accordingly, and reduce the wind speed at the same time. In addition, when there is no wind in summer, there is a certain temperature difference between the indoor and outdoor environments of the living space, which can increase the air exchange and the formation of wind.

Aesthetic Function. Colorful green communities, seasonal urban landscapes, some decorative buildings, and various landscape decorations not only enhance the appearance of the home environment and residential area, but also make the residential community more lively and interesting.

5. Conclusion

The thermal slow-release effect of urban green space is the result of the comprehensive effects of different underlying surfaces on the environmental green space. The area ratio and spatial structure characteristics of different underlying surface types have an important impact on the environmental thermal slow release, and the greening effect and human comfort also have significant influence. This paper then conducts research on landscape visualization, showing the growth process of using virtual reality technology in landscape visualization space. Visualization is mainly through observation and measurement; visualization software adjusts landscape growth parameters and then adjusts based on experience to achieve the expected landscape growth effect. In the later work, it is also necessary to change the texture and color of the landscape organs through the

graphics library to make the modeling of landscape growth clearer. Then, this paper realizes the three-dimensional visualization design of the urban landscape in the research area based on specific research projects. Combining theory with practice, it studies the three-dimensional terrain dataset and three-dimensional model data in depth and summarizes the construction requirements and principles of the urban garden landscape visualization system based on the actual needs of the project. Finally, a three-dimensional visualization system was established on the Skyline platform combined with the database and ArcGIS Engine.

Data Availability

The data used to support the findings of this study are available from the corresponding author upon request.

Conflicts of Interest

The author declares that there are no conflicts of interest.

Acknowledgments

This study was supported by Shanghai Lixin University of Accounting and Finance.

References

[1] G. Xian and M. Crane, "An analysis of urban thermal characteristics and associated land cover in Tampa Bay and Las Vegas using Landsat satellite data," *Remote Sensing of Environment*, vol. 104, no. 2, pp. 147–156, 2006.

[2] B. C. Hedquist, H. Su, D. Herrera, and J. Byerly, "Remote sensing image-based analysis of the relationship between the urban heat island and recent land use/cover change in San Antonio, Texas," in *Proceedings of the Association of American Geographers Annual Conference*, Chicago, Ill, USA, April 2015.

[3] M. Xie, Y. Wang, Q. Chang, M. Fu, and M. Ye, "Assessment of landscape patterns affecting land surface temperature in different biophysical gradients in Shenzhen, China," *Urban Ecosystems*, vol. 16, no. 4, pp. 871–886, 2013.

[4] R. Lu and Z. Lu, "Research on interactive landscape design of urban commercial complex," *Shanghai Textile Technology*, vol. 47, no. 6, p. 3, 2019.

[5] N. Zhang and J. Lian, "Interactive architectural garden landscape roaming design based on 3DMAX," *Modern Electronic Technology*, vol. 43, no. 3, p. 5, 2020.

[6] F. Fu, Z. Liu, and Q. Huang, "Three-dimensional urban landscape pattern change characteristics in Futian District, Shenzhen," *Acta Ecologica Sinica*, vol. 39, no. 12, p. 10, 2019.

[7] D. A. Quattrochi and M. K. Ridd, "Measurement and analysis of thermal energy responses from discrete urban surfaces using remote sensing data," *International Journal of Remote Sensing*, vol. 15, no. 10, pp. 1991–2022, 1994.

[8] I. Ogashawara and V. Bastos, "A quantitative approach for analyzing the relationship between urban heat islands and land cover," *Remote Sensing*, vol. 4, no. 11, pp. 3596–3618, 2012.

[9] R. Geiger, R. H. Aron, and P. Todhunter, *The Climate Near the Ground*, Rowman & Littlefield, Lanham, Md, USA, 6th edition, 2003.

[10] B. C. Hedquist and A. J. Brazel, "Urban, residential, and rural climate comparisons from mobile transects and fixed stations: phoenix, Arizona," *Journal of the Arizona-Nevada Academy of Science*, vol. 38, no. 2, pp. 77–87, 2006.

[11] D. Morgan, L. Myrup, D. Rogers, and R. Baskett, "Microclimates within an urban area," *Annals of the Association of American Geographers*, vol. 67, no. 1, pp. 55–65, 2010.

[12] Q. Weng, "Remote sensing of impervious surfaces in the urban areas: requirements, methods, and trends," *Remote Sensing of Environment*, vol. 117, pp. 34–49, 2012.

[13] D. A. Roberts, D. A. Quattrochi, G. C. Hulley, S. J. Hook, and R. O. Green, "Synergies between VSWIR and TIR data for the urban environment: an evaluation of the potential for the hyperspectral infrared imager (HyspIRI) decadal survey mission," *Remote Sensing of Environment*, vol. 117, pp. 83–101, 2012.

[14] R. Lu and Z. Lu, "Urban landscape design works. Research on interactive landscape design of urban commercial complexes," *Shanghai Textile Technology*, vol. 6, no. 6, pp. 69–71, 2019.

[15] Y. Zhang, "Research on the application of landscape elements in the interior space of urban commercial complex," *Modern Horticulture*, vol. 18, no. 18, p. 1, 2016.

Hindawi
Computational Intelligence and Neuroscience
Volume 2022, Article ID 9967681, 10 pages
https://doi.org/10.1155/2022/9967681

Research Article

Performance Test of Micro-Slit Antenna Loaded with High Refractive Index Medium Based on Image Recognition

Wang Yibo, Yu Bo, Zhang Jinju, and Tao Zengjie

School of Electronic Science and Engineering, Hunan Institute of Information Technology, Changsha, Hunan 410138, China

Correspondence should be addressed to Wang Yibo; wangyibo_hnuit@stu.cdsj6.edu.mo

Received 5 July 2022; Revised 3 September 2022; Accepted 7 September 2022; Published 22 September 2022

Academic Editor: Gopal Chaudhary

Image recognition is the pattern recognition of images. Simply put, it is the prescribed use of the pattern recognition technology in the image. It creates an image recognition template for the input of image information, analyzes and extracts the shape characteristics of the image, and then creates a classifier, relying on the shape of the image classified. However, since particles with high refractive index media can detect galvanic couples and magnetic dipoles together under the excitation of an external field, the interference of the radiation fields of galvanic couples and magnetic dipoles can be used to adjust the incident field. For the study of nanocubes with high refractive index media, the polarization phase of the nanocube particle environment is obtained by the method of long-distance propagation. The loaded micro-slit antenna is also a kind of aperture antenna, which is formed by opening a hole in the metal surface, and the hole will emit electromagnetic waves from the outside of the unit. Loaded micro-slit antennas have a variety of shapes, and they have many advantages such as sturdy structure, fast handling, convenient feeding, and being simple, compact, concealed, and decorative. Therefore, it is necessary to verify various performance parameters of the system by simulating performance tests and to verify the performance of the system by simulating various normal, high load, and abnormal load conditions. The performance test includes load and stress tests, and they can be used together. The purpose of load testing is to clarify the performance of the system under different tasks and to verify the changes in various system performance parameters as the load gradually increases.

1. Introduction

The main purpose of image recognition is to resolve and recognize information such as images and texts, so as to solve the direct communication process between the computer and the external environment [1]. The process of image recognition is divided into three stages: text, object, and digital image processing and recognition [2]. In fact, this is the recognition process from simple to structured. It improves the speed of computer performance and improves the corresponding algorithm to make it basic and simple. Image recognition is mainly based on the similarity of "classification" [3]. Under certain conditions, items with the same nature are classified into one category, and objects with different properties are classified into another category. For example, numbers have 10 components, letters have 26 components, and Chinese characters have thousands of components. In addition, different classification methods will lead to different classification results, such as the classification of colors and other characteristics [4]. At present, light field control is still the focus of optical research [5]. With the gradual development of nano-processing technology and nano-material science, more and more attention has been paid to the control of the optical area of micro-nano structures. The reason why the micro-nano structure of high refractive index media can become the focus of research in recent years is because its loss is small, and it also supports magnetic response. In order to determine the regulation effect of the high refractive index medium micro-nano structure on light, we start from the simplest part to study the response of the nano square medium structure to the incident field and the influence of its structural parameters on the control of the light field [6]. In this article, we study the response of the collision site to

the isolated nanocube structure, use the internal electromagnetic field mode to carry out the directional scattering of the incident field, and then modify its geometric parameters to obtain the directional scattering. The loaded micro-slit antenna is a kind of antenna that has been gradually developed in the past 30 years. This idea was proposed in 1946, but it was not used in the engineering field. Simple research was carried out from 1950 to 1960, and it was not really developed and used until 1970. The most commonly used type of micro-strip antenna is located on a thin dielectric substrate (such as PTFE laminated fiber), one side is connected to a thin metal layer as a ground plate, and the other side is made by photolithography and etching, using microstrip lines and axis. The probe feeds the patch, and the loaded micro-slit antenna is thus born. If the patch is a single unit, it is called a micro-strip antenna; if the patch is a thin layer, it is called a micro-strip array antenna; performance testing plays an important role in ensuring program quality. In terms of performance testing, we summarized various solutions and test centers in China to evaluate software performance from three aspects: client application testing, network creation, and server creation testing. Various solutions and test centers evaluate the performance of the software in three aspects: client application testing, network creation, and server creation testing. Under normal circumstances, through the combination of three aspects, the system performance can be comprehensively analyzed and predicted.

2. Related Works

The literature introduces the scattering properties of nanodielectrics and proves the resonance of electric and magnetic dipoles [7]. By selecting the appropriate wavelength to form an electric dipole shape and a magnetic dipole shape of the same size and shape, scattering is achieved. By changing the geometric dimensions of the object, the electric and magnetic fields are combined to achieve unidirectional scattering at the resonance position [8]. In addition, by linking the above-mentioned particles into chains, a broad spectrum of unidirectional scattering can be performed. The literature introduces the interaction between nanodimer dielectric and Gaussian beam and proposes a nanometer displacement measurement method. By measuring the scattered field, the position of the nanodimer corresponding to the center of the collision area can be obtained [9]. The measurement accuracy of this method can reach 10 nm, and HG10 can be used to improve the measurement accuracy. The literature introduces the consistent combination of metasurfaces, the organization of metasurfaces in a systematic way, and the association of its unique Jones matrix [10]. Unlike optically active materials that increase the rotation angle by increasing the length of the propagation direction, the metasurface can achieve the rotation angle by changing the size of the rear part of the structure, and the deviation angle ranges from -90° to +90° [11]. The literature introduces a limited range of Boltzmann machines and SVM to build a multi-layer classification model, uses deep learning methods to extract pattern samples, and then uses SVM methods to classify and apply them to visual recognition work [12]. Experiments with fewer samples confirm that the comparison between vector machines and deep trust networks is better, and after comparing the number of samples, layers, nodes, and accuracy, the relationship between the number of nodes in the hidden layer and the number of support vectors is discussed [13]. The literature introduces the research background and significance of dual-frequency micro-strip antennas. It also explains in detail the electrical parameters and basic theories of micro-strip antennas, the basic theories of slit antennas, and the basic theories and features of dual-band antenna design. Next, this article improves the structure of the dual-frequency microstrip antenna and analyzes its various structural parameters in detail in the HFSS simulation program [14].

The literature describes deep learning systems. It is an advanced machine algorithm that is based on learning to represent complex relationships between simulated data. Observation results can be expressed in many ways, such as using a series of rated powers to represent pixels. Unique representation methods can speed up the algorithm to complete learning activities (such as facial recognition). The purpose of characterization learning is to find a better representation method. By simulating the brain structure and nervous system similar to the human brain, and the data are gradually being developed to form a more visible representation (features or parts). Deep learning uses different layers of indirect information processing to enable or manage image capture and conversion, format analysis and classification, and to interpret data such as images, sounds, and text. High-level forms and concepts are defined by subconcepts and sub-characteristics. The same sub-concept can be used to identify multiple high-level concepts. Such a structure is also called a deep-level structure [15]. The literature introduces that the convolutional neural network is composed of related components and combined lines of a complete integrated line. With this system, CNN can use a two-dimensional data input system, but compared with other deep regions, the custom network shows better results in audio applications [16]. The conversion network can also be trained using standard replication algorithms. Due to its small scale, it can be easily trained from other deep models.

3. Design of Performance Test Model for Micro-Slit Antenna Loaded with High Refractive Index Medium Based on Image Recognition

3.1. Image Recognition Technology. Boltzmann's deep machine is a binary pairwise undirected probability graph model (i.e., Markov random field) and has a wide range of anonymous segments and a network of interconnected units. In RBM, there is no connection between hidden layers and between visible layers. The criteria assigned to the visible layer are

$$p(v) = \frac{1}{Z} \sum_{h} e^{\sum_{ij} W_{ij}^{(1)} v_i h_j^{(1)} + \sum_{jl} W_{ij}^{(2)} h_j^{(1)} h_l^{(2)} + \sum_{m} W_m^{(3)} h_l^{(2)} h_m^{(3)}}. \quad (1)$$

Like DBN, a deep Boltzmann machine can use a limited amount of labeled data to improve the characterization of a large amount of unlabeled data, so that it can check complex performance and summary. Different from deep

convolutional neural network and DBN, DBM uses a two-way training method and reasoning, that is, transfer from top to bottom and from bottom to top, so that the system can better display the fuzzy and complicated feature. In DBN, the uppermost RBM is an undirected graph model, and the bottom layer consists of a directed model. As a DBM, it is difficult to obtain the maximum possible probability. We can use the most reasonable estimate or use the mean field inference model to estimate the probability of the data and use it with the Markov chain Monte Carlo model according to the random estimation method. However, because the estimation reasoning is based on the standard site method, it is 25–50 times slower than the following DBN model, which makes its application unsuitable for many types.

In a single RBM, assuming that the pixel corresponds to the visible layer as v, there is n nodes; the obtained shape corresponds to the hidden layer as h, there is m nodes; the visible layer and the hidden layer system (v, h) have energy as follows:

$$E(v,h) = -\sum_{i=1}^{n} a_i v_i - \sum_{j=1}^{m} b_j v_j - \sum_{i=1}^{n}\sum_{j=1}^{m} v_i w_{ij} h_j. \quad (2)$$

It can be seen that by expanding and normalizing the energy performance, the joint probability distribution of the unit vector of the visible layer and the hidden layer in the vector can be obtained:

$$\mathrm{p}(\mathbf{v},\mathbf{h}) = \frac{1}{Z} e^{-\mathrm{E}(\mathrm{v},\mathrm{h})}. \quad (3)$$

In the formula, Z represents the normalization constant, adding all pairs of visible and hidden layers:

$$\mathrm{Z} = \sum_{v,h} e^{-\mathrm{E}(\mathbf{v},\mathbf{h})}. \quad (4)$$

The possibility for the network to provide visible layer vectors is to include all visible layer vectors in the layer:

$$\mathrm{p}(\mathbf{v}) = \frac{1}{Z} \sum_{h} e^{-\mathrm{E}(\mathbf{v},\mathbf{h})}. \quad (5)$$

Because the visible layer vector and the hidden layer vector are independent of each other, there are

$$\mathrm{p}(\mathbf{h} \mid \mathbf{v}) = \prod_{j}^{m} \mathrm{p}\left(\mathrm{h}_j \mid \mathbf{v}\right), \mathrm{p}(\mathbf{v} \mid \mathbf{h}) = \prod_{i}^{n} \mathrm{p}\left(\mathrm{v}_\mathrm{i} \mid \mathbf{h}\right). \quad (6)$$

If the visible layer v is given, the probability that the binary state of v is 1 is

$$\mathrm{p}\left(\mathrm{h}_j = 1 \mathrm{I} \mathbf{v}\right) = \sigma\left(b_j + \sum_{i=1}^{n} v_i w_{ij}\right). \quad (7)$$

If the hidden layer h is given, the probability that the binary state of v is 1 is

$$\mathrm{p}\left(\mathrm{v}_i = 1 \mid \mathbf{h}\right) = \sigma\left(a_i + \sum_{j=1}^{m} w_{ij} h_j\right). \quad (8)$$

Table 1: The prediction accuracy of different methods under a single hidden layer (%) (number of samples: 1000/200).

Method	Number of hidden layer nodes						
	100.00	200.00	300.00	400.00	500.00	600.00	700.00
DBN	91.5	92.5	94	94.5	92.5	93	93
RBM-SVM	92	93.5	93.5	93	93	93	93
SVM	82	82	82	82	82	82	82

Table 2: The prediction accuracy of different methods under a single hidden layer (%) (number of samples: 5000/1000).

Method	Number of hidden layer nodes						
	100.00	200.00	300.00	400.00	500.00	600.00	700.00
DBN	93.5	92.5	93	93	92.5	92	97
RBM-SVM	96	97.5	92.4	90	91	96	91
SVM	88.1	88.1	88.1	88.1	88.1	88.1	88.1

Table 3: The prediction accuracy of each method when there are two hidden layers (%).

Method	Number of hidden layer nodes						
	100.00	200.00	300.00	400.00	500.00	600.00	700.00
DBN	92.4	91.5	92	92	91.5	91	96
RBM-SVM	95	96.5	91.4	91.2	91.4	96	91.7

In the reverse probability vector obtained through this step, the result is used as the weight increment between the input layer and the output layer. In each case, the weight increment and the bias update are the same at about $1w$.

By sorting out and summarizing the algorithms above, different training samples are selected for comparative testing, and the results are shown in Tables 1–3.

Table 1 tests the test accuracy of a single hidden layer, when the number of samples is 1000/200, and when the number of samples is 5000/1000, the test results are shown in Table 2.

Table 3 summarizes the research results in Tables 1 and 2 and analyzes the corresponding prediction accuracy when the design has two hidden layers.

By comprehensive analysis of Tables 1–3, it can be seen that the increase in the number of samples can promote the improvement of accuracy, and the prediction accuracy of multiple hidden layers is higher than that of a single hidden layer. The relationships are shown in Figure 1.

This test has a different C value. In this experiment, the number of training samples is 5000, the number of test samples is 1000, other parameters are unchanged, and the y value is a standard instrument of 0.0033. Take different C values and compare the accuracy of training samples, the number of support directions, and the accuracy of test samples of the C-to-SVM method and the RBM-SVM method, as shown in Table 4.

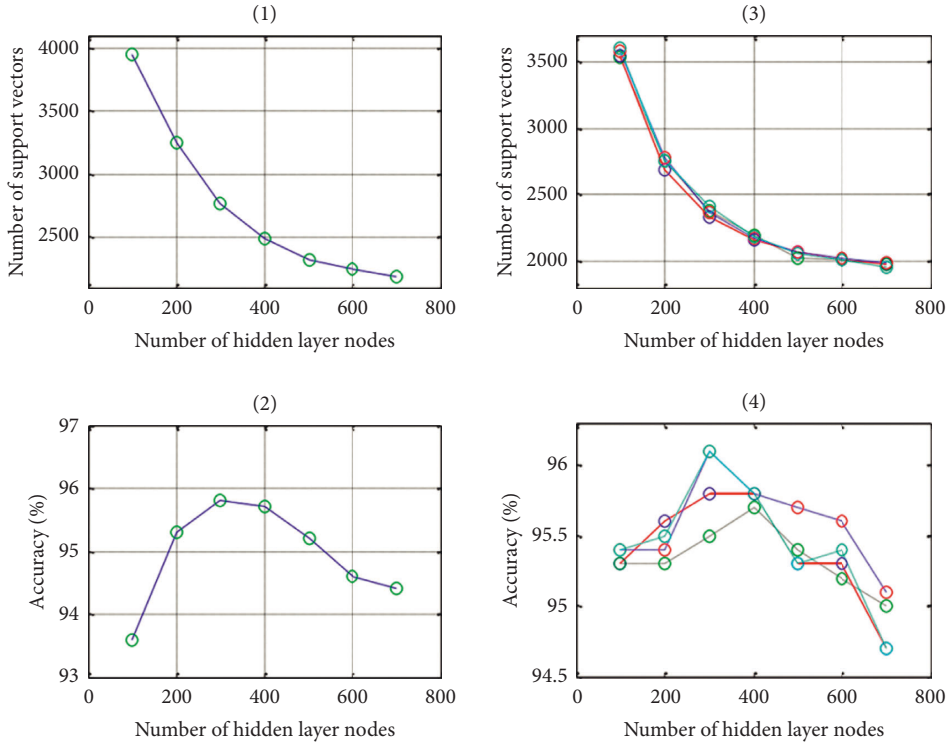

Figure 1: The relationship between the number of hidden layer nodes and the number of support vectors and the accuracy of prediction.

Table 4: Relationship between C value and study accuracy when using support vector machine approach.

C value	1	5	10	15	20	25	30	40	50
Number of support vectors	3110	2155	1908	1806	1740	1712	1712	1715	1725
Test sample prediction accuracy	88.1	91.2	91.4	92.3	92.3	92.3	91	91.5	91.5
Training sample prediction accuracy	92.7	95.76	96.85	97.61	98.25	98.4	98.83	99.21	99.5

Table 5: The influence of method C value on accuracy in this paper.

C value	1	5	10	15	20	25	30	40	50
Number of support vectors	2681	27166	2718	2718	2718	2718	2718	2718	2718
Test sample prediction accuracy	95.9	97	97	97	97	97	97	97	97
Training sample prediction accuracy	99.57	100.00	100.00	100.00	100.00	100.00	100.00	100.00	100.00

The RBM-SVM method is used for a single hidden layer, and the number of hidden layer nodes is 300. The experimental results are shown in Table 5.

As shown in Figure 2, the straight line uses the SVM method, and the dotted line uses the RBM-SVM method. For *C*, the SVM method and RBM-SVM method correspond to the number of support. As shown in the figure, the value of *C* increases. For the RBM-SVM method, the number of support vectors increases slightly, the number of parasites decreases significantly, and then becomes flat. There is almost no change in development. For the SVM method, the number of support vectors accelerates and decreases and then gradually develops with slight changes.

3.2. Mode Analysis of High Refractive Index Medium. Now suppose that the scattering part of the measurement length is placed in an infinite environment of space and is directly illuminated with a combined wavelength.

$$\mathbf{E_s} = \mathbf{E_{MD}} + \mathbf{E_{ED}} + \mathbf{E_{MQ}} + \mathbf{E_{EQ}} + \dots. \tag{9}$$

Quadrupole Power (EQ). If the particle size is smaller than the length, the radiation length of the long-order end is much smaller than the radiation length of the dipole and quadrupole, which can be ignored. Sometimes, we can ignore the four-level mode and consider the dipole mode,

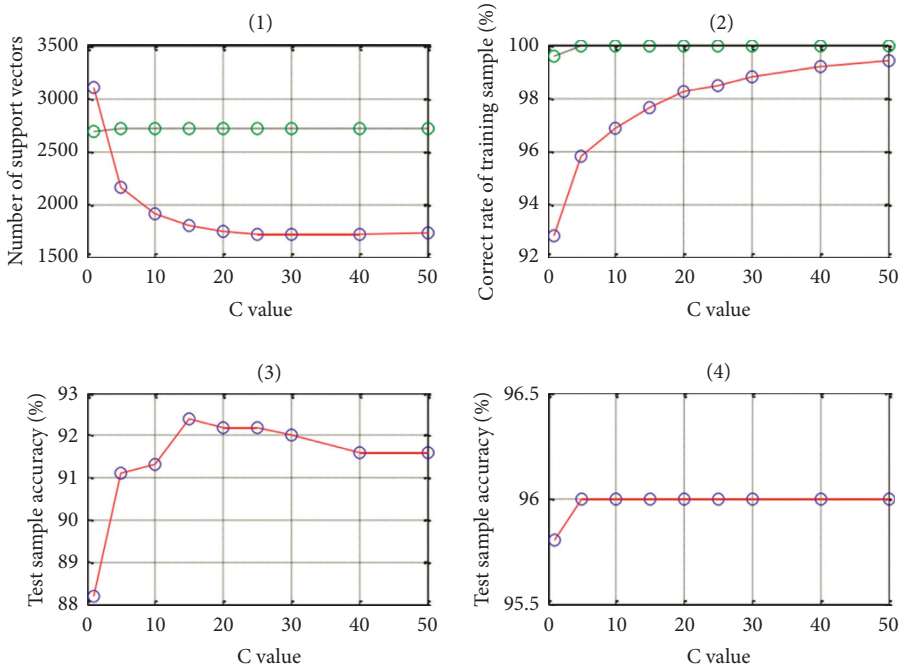

Figure 2: The effect of penalty factor C value on accuracy.

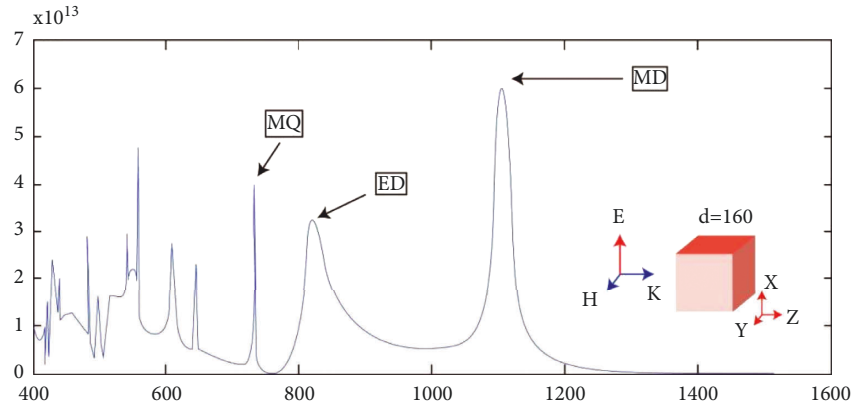

Figure 3: Numerical simulation results of scattering spectra of nanocubes.

which is called dipole approximation. The corresponding vector of the polar radiation plant is expressed as

$$\mathbf{E}_{\mathbf{MD}} = -\eta_0 \frac{k^2}{4\pi} \frac{e^{ikr}}{r} \mathbf{n}_{\mathbf{r}} \times \mathbf{m}, \mathbf{E}_{\mathbf{ED}} = \eta_0 \frac{ck^2}{4\pi} \frac{e^{ikr}}{r} \mathbf{n}_{\mathbf{r}} \times \mathbf{p} \times \mathbf{n}_{\mathbf{r}}, \tag{10}$$

$$\mathbf{E}_{\mathrm{MQ}} = \eta_0 \frac{ik^3}{24\pi} \frac{e^{ikr}}{r} \mathrm{n}_{\mathbf{r}} \times \mathbf{Q}_{\mathrm{MQ}}, \mathbf{E}_{\mathrm{EQ}} = -\eta_0 \frac{ick^3}{24\pi} \frac{e^{ikr}}{r} \mathbf{n}_{\mathbf{r}} \times \mathbf{Q}_{\mathrm{MQ}} \times \mathbf{n}_{\mathbf{r}}. \tag{11}$$

It can be seen from formulas (9–11) that in order to find the scattering area of the incident field, it is necessary to know the magnitude of the internally induced polar moment. The magnitude of the polar moment is determined by its own polar quantization, the Eoc of the local power plant, and the regional magnetic field. Take the dipole moment as an example:

$$\mathbf{p} = \overline{\overline{\alpha}}_{ee} \mathbf{E}_{\mathbf{loc}} + \overline{\overline{\alpha}}_{em} \mathbf{H}_{\mathbf{loc}}, \mathbf{m} = \overline{\overline{\alpha}}_{me} \mathbf{E}_{\mathbf{loc}} + \overline{\overline{\alpha}}_{mm} \mathbf{H}_{\mathbf{loc}}. \tag{12}$$

As shown in Figure 3, the magnetic field distribution in the plane xy refers to the upper and lower films, and the orientation is opposite, forming a circular distribution in the plane yz, so the electric field along the x direction is induced, corresponding to the distribution in A circular spot in the cy plane. The distribution of this form of electromagnetic field is a form of electric dipole radiation polarized along the x direction, which represents the electrode peak corresponding to the corresponding resonant peak.

3.3. Micro-Slit Antenna. As a new type of antenna, microstrip antennas have developed slowly in the past 30 years. This idea was proposed as early as the beginning of 1946, but it did not attract the attention of the engineering field. There was only a small amount of research from 1950 to 1960, and

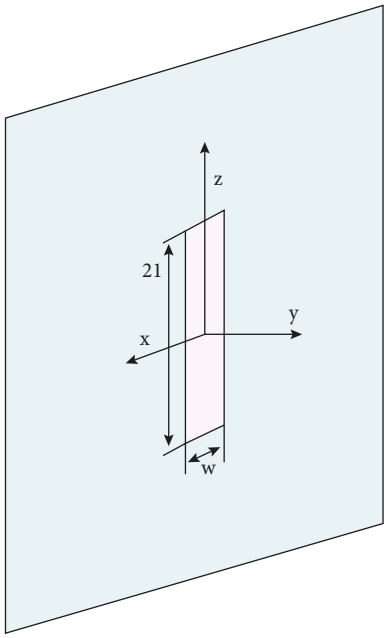

Figure 4: Structure diagram of slot antenna.

the real development and use was in 1970. The common type of micro-strip antenna is suspended on a thin medium (such as Platinla laminated fiber), one side is connected to a thin metal layer as a ground plate, and the other side is made of a specific metal frame. Use the micro-strip line and the axis probe to feed, and this is the composition of the micro-strip antenna. Compared with ordinary micro-strip antennas, micro-strip antennas have many advantages:

(1) Small size, light weight, low profile, and conformal to the carrier.

(2) The electrical properties are diverse, and different components are easily available.

(3) Easy to install. It can be used in combination with active devices and integrated circuit boards.

Due to the inherent advantages of micro-strip antennas, it is now widely used in many high-precision fields such as satellite phone communications, aircraft antennas, Doppler radar, and missile telemetry.

The slit antenna is an antenna aperture antenna that is generated by the open position of the metal surface and the electromagnetic wave emitted from the external position. In 1953, H. G. Booker proposed the concept of slit antenna. Slit antennas have a variety of shapes and have many advantages: solid structure, fast processing, convenient feeding, compactness, low profile, good hiding and good decoration, and many other advantages, making it an important communication field including 3G technology, LAN, wireless network, and other important applications.

Figure 4 shows a diagram of the overall structure of a general slit antenna. In an ideal state, a narrow slit can be opened, which can be regarded as two different dipole antennas; assuming the length is $2L$ and the width is w, $(2L >> w)$.

The electric field is perpendicular to the gap, which can be expressed as

$$E_x = \frac{U_{ms}}{w} \sin\ k_0 (l - |z|). \tag{13}$$

In the formula, U_{ms} is the antinode voltage. At the corresponding height of the electromagnetic zone and the electromagnetic wave, the radiation can be expressed in the same magnetic direction in the z-axis direction where the surface of the gap is located, and the surface density of the magnetic field can be displayed, as shown in the following formula:

$$J_{ms} = \hat{z}^2 \frac{U_{ms}}{w} \sin\ k_0 (l - |z|). \tag{14}$$

Assuming that the slit magnetic current is uniformly distributed on x, the slit magnetic current can also be expressed as

$$I_{ms} = 2U_{ms} \sin\ k_0 (l - |z|). \tag{15}$$

If the principle of equivalence is used, the correct position can only be calculated on one side of the space and zero on the other side. If the magnetic current is used as the hypothetical source, if the gap area is found on one side, the field on the other side of the field is found symmetrically. The local radiation can be obtained directly from the dipole antenna using the principle of the double-sided electromagnetic zone, and the results are as follows:

$$\vec{A}_m (r) \approx \frac{\varepsilon_0}{4\pi r} e^{-jk_0 r} \int \vec{J}_m (z') e^{jk_0 r'} dv'$$

$$= \frac{\varepsilon_0 U_{ms} \vec{z}}{\pi k_0 r} e^{-jk_0 r} \frac{\cos(k_0 l \cos\theta) - \cos k_0 l}{\sin^2 \theta},$$

$$H_\theta = -j\omega A_{ms} = j \frac{U_{ms}}{\eta_0 \pi r} \frac{\cos(k_0 l \cos\theta) - \cos k_0 l}{\sin\theta} e^{-jk_0 r},$$

$$E_\varphi = -H_\theta \eta_0 = -j \frac{U_{ms}}{\pi r} \frac{\cos(k_0 l \cos\theta) - \cos k_0 l}{\sin\theta} e^{-jk_0 r}. \tag{16}$$

According to Maxwell's equation and given conditions, the electric field of the symmetrical dipole antenna can be obtained:

$$E_{\theta t} = j \frac{I_{m\,d}}{2\pi r} \sqrt{\frac{\mu}{\varepsilon}} e^{-jkr} f(\theta). \tag{17}$$

For a half-wave ideal slit antenna, $2l = \lambda/2, kl = \pi/2$; therefore,

$$f(\theta) = \frac{\cos(\pi/2 \cos\ \theta)}{\sin\theta}. \tag{18}$$

Both have the same radiation field, and the radiation power of the symmetrical dipole antenna is

$$P_{rd} = \frac{1}{2} I_{md}^2 R_{rd}. \tag{19}$$

The radiation power of an ideal slit antenna is

$$P_{rs} = \frac{1}{2} U_{ms}^2 G_{rs}. \tag{20}$$

Therefore, the input conductance of an ideal slit antenna can be expressed as

$$G_{as} = \frac{G_{rs}}{\sin^2 (kl)}. \tag{21}$$

The results obtained by the above calculation method show that the antenna shape of the finite plane has the following characteristics: the slit of the slit antenna has no radiation on the slit axis, and the size of the structured plane affects the radiation amount and position of the antenna. The shape of the emission plane has a negative influence on the antenna position in this direction, so the exact position of the plane (i.e., the shape of the H plane) is no different from an ideal antenna.

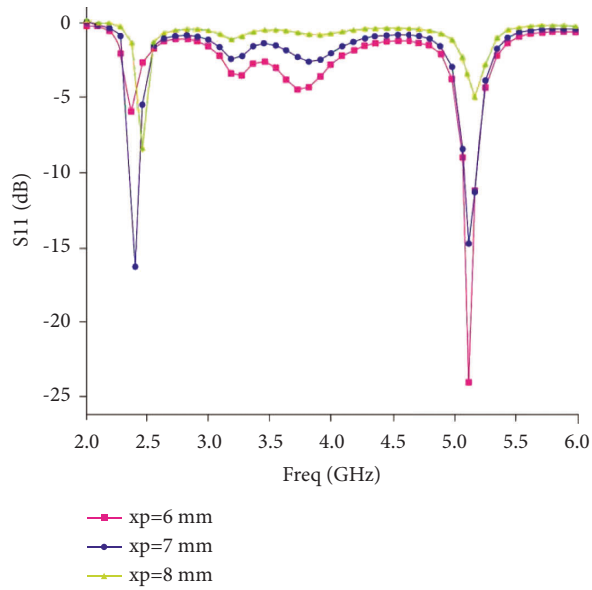

Figure 5: Influence curve of micro-strip line position on S11.

4. Performance Test Practice of Micro-Slit Antenna Loaded with High Refractive Index Medium Based on Image Recognition

4.1. Antenna Structure. The geometric structure of the modified antenna is different from the original antenna in that a structural branch structure is added at the end of the feeding micro-strip, and a metal bottom is added at the bottom. Adding branches to the sector terminal makes it easier and more adjustable to connect the antenna. The metal material improves the efficiency of the original antenna and improves the radiation performance.

The upper part of the dielectric substrate is a ground plane, a radiation gap is drilled on the ground plane, and on the other side is a micro-strip line with multiple terminal branches for power supply. A 40 mm × 40 mm metal substrate was added to the place below 8 mm from the dielectric device to improve the performance of capture and radio antennas.

4.2. Antenna Improvement Analysis. For the antenna area, micro-strip line feed and coaxial feed are used. The antenna in this article is a micro-strip line feeding method. At the end of the micro-strip line, the terminal branch structure of this structure is used to improve antenna reception. The continuous and effective dielectric is a, the width of the micro-strip line is w, the thickness of the dielectric substrate is h, s represents the frequency of the electric field, and u and s represent the permeability and permittivity of the electric field, respectively. Therefore, in a micro-strip line with a dielectric thickness and a constant dielectric, the width becomes the only condition for its characteristic impedance. Because of the existence of the terminal branch, it changes the original part of the antenna radiation. Adjusting the angle and length of the terminal branch can make the overall radiation of the antenna close to zero, while ensuring that the internal power of the antenna is free from oscillation. The use of radiation solves the problem of imbalance between the antenna and the feeding point. In the following, simulation analysis will be carried out on the influence of fine-tuning of the impedance of the fan-shaped terminal stub.

The antenna gain in the article is −10 dB and -2 dB at 2.4 GHz and 5.2 GHz, respectively. This shows that most of the energy transmitted by the wire transmission to the antenna is not well radiated in the form of electromagnetic waves but is consumed in the antenna. In order to solve this problem, the component first uses (0.002) F4B material with very low dielectric loss and then adds a metal substrate larger than the antenna size to the lower part of the antenna to achieve the mirror image effect and make it have good radiation performance.

The use of low dielectric constant devices can effectively reduce the loss of electromagnetic waves in the medium transmission process and improve the radiation efficiency of the antenna. The role of the metal bottom is to change electromagnetic radiation from downward radiation to upward radiation.

4.3. Simulation Analysis. The previous article introduced four kinds of electromagnetic simulation software. This topic uses Ansoft's HFSS electromagnetic simulation tool as the main simulation software. In HFSS, modeling is carried out according to the design structure scheme, and it is used when waiting for the next optimization. It is impossible to design an antenna once, and every change of antenna parameters must undergo several tests to gradually approach the most effective result. In most cases, several parameters need to be tuned together to produce close to ideal results. The simulation results of multiple parameters will be given below. These results have the greatest impact on the results of the antenna simulation process.

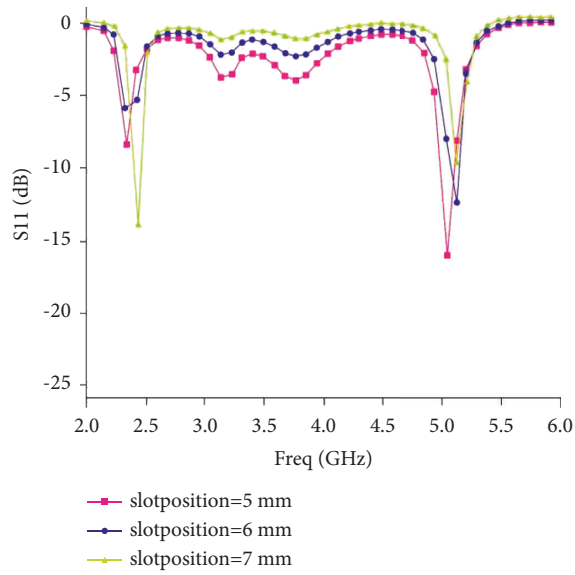

Figure 6: Influence curve of gap position.

Table 6: Optimized parameters.

Parameter	Numerical value	Remarks
ws	35 mm	Media board width (x direction)
Is	24 mm	Media plate length (y direction)
xp	7 mm	Distance from bottom micro-strip line to origin
istrip	8.3 mm	Micro-strip line length (y direction)
wstrip	1.7 mm	Micro-strip line width (X direction)
wl	12.5 mm	Two U-shaped gap distances
slitposition	6 mm	The distance between the bottom of the gap and the origin
ss	1.5 mm	Gap width in Y-axis direction
sh	2 mm	X-axis direction gap width
Theta	70°C	The angle between one side of the fan-shaped terminal branch at the front end of the micro-strip line and the X-axis
w2	3.5 mm	The distance between two U-shaped gaps
Istub	2 mm	The length of the fan-shaped terminal stub at the front end of the micro-strip line
hg	8 mm	The distance between the bottom metal plate and the dielectric plate (Z direction)
wg	66 mm	The width of the bottom metal plate (X direction)

This antenna can successfully perform dual operations because the micro-strip feeder is at a different distance from the two main radiation fields. Since different positions are found in the feed, these two positions adapt electromagnetic waves to different waves. Figure 5 shows the simulation result of xp = 6, xp = 7, and xp = 8 under the condition of observing other boundaries.

From the figure, xp plays an important role in the doubling process. A little change will cause a sudden change in one of the frequency points and lose its dual-frequency characteristics. Taking xp = 7 mm as the midpoint, if xp becomes larger, the upper wave and the lower wave will also move with the change of the upper wave. Two or more changes will not only cause the position of the repeated points to change but also make the combination of two repeated points worse. If xp = 7 mm, you can see the ideal situation.

In the latest analysis, micro-strip line feeding is a one-time feeding method. At the same time, the distance between the feeding micro-strip and the radiating unit must be correct, and repeated attention and caution must be exercised. In slit antennas, the main effect of radiation is the slit, which will naturally have a significant impact on the antenna performance. Figure 6 is a graph showing the result of the difference in x-axis length.

From Figure 6, changing the position of the y-axis will also change the performance of the antenna. However, unlike xp at the xp distance in the micro-strip feeder, the change of sp usually affects the position of the frequency resonance. If sp decreases, the matching degree of the low frequency becomes worse, and the matching degree of the high frequency becomes better; this can be clearly seen in the above figure (sp = 5 mm and sp = 6 mm). Considering the

relevance of repetition and consistency, sp = 6 mm is selected as the standard setting for the following simulations.

4.4. Optimization Results. For each parameter, the method of obtaining the result is adopted, that is, whenever the other parameters are unchanged, a unit will be changed to a specific value. Each value represents a result. If the result is close to the optimal condition, the corresponding result is regarded as the ideal value. According to the above method, each parameter that may lead to the change of the composite distance is studied separately, and finally the best combination of parameters is obtained, as shown in Table 6.

5. Conclusion

In summary, by studying the origin of high refractive index media, this article introduces a new type of optical fiber sensor, which has a very good prospect. The first part of this article introduces the research background and importance of high refractive index media and further understands the application aspects of high refractive index media. Then, we summarized and studied the status quo and progress of liquid level sensing and temperature sensing and understood their progress and differences. It lays a solid foundation for the subsequent high refractive index medium in liquid level and temperature sensing. Next, we studied the basic viewpoints of long-term optical fiber networks and analyzed several characteristics of optical fibers. First, the integrated structure theory of its long-period optical fiber network has been systematically analyzed to fully understand the principle of long-period fiber packaging. Second, in-depth study of the directional patterns, flow patterns, and radiation patterns in the optical fiber will lay a solid foundation for the next simulation analysis; then, this article describes the origin and importance of the micro-strip antenna research and briefly summarizes what the outside world uses (four kinds of simulation software). Third, this article summarizes the electrical parameters of antennas, the basic views of slit antennas and micro-strip antennas, and introduces many methods commonly used to achieve dual frequency. Finally, this article improves the double U-slit antenna and conducts a detailed simulation analysis. This article summarizes the antenna parameters used in antenna production and the structural influence of each component, such as S11 and gain. It also summarizes the steps of visual recognition, highlights common methods and current problems related to image acquisition and image recognition, and deepens the status quo and concepts of deep learning, as well as the benefits of development and research. Also, we carried out the study of Boltzmann's principle and its limitations and the study of Boltzmann machine conversion, expounding many common methods and the basic structure of deep intelligence. Convolution neural network is the research result of neural system. The stimulus signals are transmitted through the nervous system of the brain and rely on their own functions, such as low connectivity, reduced sampling, and so on, and have shown self-learning in various cognitive functions. In particular, if the input is a two-dimensional image, a consistent network structure can widely spread the original information part of the visualization layer (invisible layer) and capture the parallel movement and rotation of a specific layer. We found that the optical architecture is compatible, so the antenna can work in the two frequency bands 2.4 GHz and 5.2 GHz. Finally, based on the simulation analysis, this antenna was designed, and after testing, the simulation combination for the expected purpose was realized.

Data Availability

The data used to support the findings of this study are available from the corresponding author upon request.

Conflicts of Interest

The authors declare that they have no conflicts of interest.

Acknowledgments

This study was supported by the Natural Science Foundation of Hunan Province, China (grant no. 2021JJ30478) (A mechanism study of the generation of a low diffractive pseudo-Bessel beam which is used in remote microwave power supply for long standing ocean surveillance UAV).

References

[1] B. Zoph, V. Vasudevan, J. Shlens, and Q. V Le, "Learning transferable architectures for scalable image recognition," in *Proceedings of the IEEE conference on computer vision and pattern recognition*, pp. 8697–8710, UT, USA, June 2018.

[2] Z. Wu, "Overview of biometric patented technologies based on multi-feature fusion recognition," *Industrial Science and Technology Innovation*, vol. 2, no. 13, pp. 66-67, 2020.

[3] A. Khotanzad and Y. H. Hong, "Invariant image recognition by Zernike moments," *IEEE Transactions on Pattern Analysis and Machine Intelligence*, vol. 12, no. 5, pp. 489–497, 1990.

[4] C. Kanan and G. W. Cottrell, "Color-to-grayscale: does the method matter in image recognition?" *PLoS One*, vol. 7, no. 1, Article ID e29740, 2012.

[5] L. Cai, P. Luo, G. Zhou, and Z. Chen, "Maneuvering target recognition method based on multi-perspective light field reconstruction," *International Journal of Distributed Sensor Networks*, vol. 15, no. 8, 12 pages, Article ID 155014771987065, 2019.

[6] D. E. Lucchetta, A. Di Donato, O. Francescangeli, G. Singh, and R. Castagna, "Light-controlled direction of distributed feedback laser emission by photo-mobile polymer films," *Nanomaterials*, vol. 12, no. 17, p. 2890, 2022.

[7] T. J. Lewis, "Charge transport in polyethylene nano dielectrics," *IEEE Transactions on Dielectrics and Electrical Insulation*, vol. 21, no. 2, pp. 497–502, 2014.

[8] F. Xu, H. Wang, S. Xing, M. Tang, H. Zhang, and Y. Wang, "Seeking optimized transformer oil-based nanofluids by investigation of the modification mechanism of nano-dielectrics," *Journal of Materials Chemistry C*, vol. 8, no. 22, pp. 7336–7343, 2020.

[9] J. J. Burgos-Mármol, A. Patti, and A. Patti, "Molecular dynamics of janus nanodimers dispersed in lamellar phases of a block copolymer," *Polymers*, vol. 13, no. 9, p. 1524, 2021.

[10] D. Penninckx and V. Morénas, "Jones matrix of polarization mode dispersion," *Optics Letters*, vol. 24, no. 13, pp. 875–877, 1999.

[11] K. Sridharan, T. Endo, S. G. Cho, J. Kim, T. J. Park, and R. Philip, "Single step synthesis and optical limiting properties of Ni–Ag and Fe–Ag bimetallic nanoparticles," *Optical Materials*, vol. 35, no. 5, pp. 860–867, 2013.

[12] A. S. Ahmad, M. Y. Hassan, M. P. Abdullah et al., "A review on applications of ANN and SVM for building electrical energy consumption forecasting," *Renewable and Sustainable Energy Reviews*, vol. 33, pp. 102–109, 2014.

[13] U. Chakraborty, A. Kundu, S. K. Chowdhury, and A. K. Bhattacharjee, "Compact dual-band microstrip antenna for IEEE 802.11 a WLAN application," *IEEE Antennas and Wireless Propagation Letters*, vol. 13, pp. 407–410, 2014.

[14] S. Du, Q.-X. Chu, and W. Liao, "Dual-band circularly polarized stacked square microstrip antenna with small frequency ratio," *Journal of Electromagnetic Waves and Applications*, vol. 24, no. 11-12, pp. 1599–1608, 2010.

[15] I. Y. Park, J. Eom, H. Jang et al., "Deep learning-based template matching spike classification for extracellular recordings," *Applied Sciences*, vol. 10, no. 1, p. 301, 2019.

[16] T. Kattenborn, J. Leitloff, F. Schiefer, and S. Hinz, "Review on convolutional neural networks (CNN) in vegetation remote sensing," *ISPRS Journal of Photogrammetry and Remote Sensing*, vol. 173, pp. 24–49, 2021.

Hindawi
Computational Intelligence and Neuroscience
Volume 2022, Article ID 6728784, 8 pages
https://doi.org/10.1155/2022/6728784

Research Article

Intelligent Reading of English Text Based on the Generative Model Constraint Label Fusion

Hua Yang[1] **and Huiliang Wei**[2]

[1]*College of Excellence, Baoding University of Technology, Baoding, Hebei, China*
[2]*Hebei College of Science & Technology, Baoding, Hebei, China*

Correspondence should be addressed to Huiliang Wei; 2007028@muc.edu.cn

Received 2 July 2022; Revised 19 August 2022; Accepted 6 September 2022; Published 21 September 2022

Academic Editor: Gopal Chaudhary

The intelligent reading of English text is affected by complex environmental factors, which will result in low reading accuracy and poor reader experience. Based on the artificial intelligence model, this study constructs the artificial intelligence English text reading model by using the generative model constraint label, which helps to improve the intelligence of the English text reading effect. This study also designs a multigraph label fusion algorithm based on generative model constraints. By making full use of the prior knowledge of multiple graphs, the result of fusion graph segmentation is achieved. Moreover, this study also uses the combination of two algorithms, namely, the combination of GMM and MRF, to express the spatial correlation of local statistical features and image pixels in a comprehensive and all-round way. Another model design also includes a series of joint distributions of the learning data for the construction of the image energy function, and the conditional probability distribution is used as the model for prediction. At the end of the study, another variable control experiment is carried out to analyze the performance of the model and the accuracy of the model in English text recognition and classification is studied and counted. The research results show that the intelligent reading model constructed based on this study can meet the needs of the actual situation.

1. Introduction

As the third wave of artificial intelligence swept across, artificial intelligence technology, which is at the forefront of science and technology, began to penetrate, influence and be applied to all fields of society [1]. This includes the field of mobile reading. In addition to reading newspapers, news, and other content, people usually choose a book reading application software loaded on smart devices (such as mobile phones), such as palm reading, book banners, and novels [2]. In the field of artificial intelligence technology, intelligent computer technologies such as speech recognition technology, big data technology, and human-computer interaction are constantly developing and integrating. Product innovation through the development and application of the abovementioned intelligent technologies is a new channel for mainstream mobile reading applications to seek technological innovation [3]; providing users with multiple experiences that include audiovisual and even interaction in addition to single text reading has become a new focus of mobile reading app product development [4].

After entering the twenty-first century, our life belt is being changed by digital media, and we are in the era of transition from paper media to electronic media. This situation is reflected in reading, and browsing computer web files, reading emails, text messages, news on web pages, and comments have become very common on mobile phones and other electronic devices [5]. These behaviors are all digital reading. In the past ten years, many users have read this way. With the advancement of science and technology, reading behavior has undergone a quiet and dramatic change, and books have gradually developed in the direction of digitization, and e-books were born under this background [6]. Moreover, in order to read electronic books more conveniently, people have begun to use various electronic devices. However, compared with paper books,

the most significant difference between e-books is the form and operation method and e-books should not be a substitute for the former [7]. People's reading carrier has undergone tremendous changes from traditional paper to mobile devices. However, the interface design of e-books has not exerted the maximum value of information technology and cannot provide sufficient support for communication between people. Moreover, with the increasing advancement of information technology, paper media have also embarked on the road of digitization and the interactive design mode of e-books urgently needs to be innovated [8]. At present, most of the reading software on the market basically simulates paper books, which redesigns the electronic reading interface to satisfy people's reading behavior. Because of this, this kind of simple imitation of paper books cannot make today's readers feel a better reading experience, and it often leads to various problems and also it does not allow users to browse data conveniently and comfortably. The root cause of this problem is that it is not people-oriented and it does not combine science and technology with people's reading methods, and blindly copy the results of the paper-based reading mode [9].

2. Related Work

In the past two years, the research on machine reading comprehension tasks has gained unprecedented attention abroad. Many well-known research institutions, such as Stanford University, Carnegie Mellon University, and Allen Research Institute, and industry giants such as IBM, Google, Facebook, and other giants, have also joined the research of this task.

The literature proposed two naive unsupervised baseline methods when publishing the MCTest dataset, which obtained the corresponding 4 paragraphs of text by concatenating the question and the candidate's answer [10]. For each piece of spliced text, this method uses a sliding window with the same length as the spliced text to slide in the reading material. Moreover, it counts the number of words in the window that contain the same words as the text to measure the degree of semantic matching between the question answer text and the reading material and then selects the answer. The literature added linguistic features such as coreferencing rules and negative detection to improve the performance of the system [11]. The literature used the rhetorical structure theory (RST) and the event entity coreferencing method to model multiple pairs of sentences [12]. Moreover, it obtained the part related to the question and made an organic combination to judge the implication relationship between the reading document and the question-answer text, and it also formalized the reading comprehension task into text implication for processing. Although there are differences in the internal structures of the three deep learning models involved in the literature, their overall framework is to carry out intelligent learning of the problem and the representation of each word in the original text through neural networks and to meet various types of reading needs of readers through diverse data accumulation and interaction [13]. According to the representation of the word, the final word with the highest score is the correct answer. Literature mentions that character-level word vectors and character-level dynamics can be combined by the gating mechanism design, which to some extent alleviates the problems caused by unregistered words [14]. Now, it has become a common practice in the field of machine reading comprehension to use both character-level and word-level word vectors to represent words together.

3. Atlas Preprocessing

Figure 1 shows the steps of map preprocessing. In the Atlas preprocessing stage, each Atlas image and the image to be segmented need to be processed as follows: skull removal, extraction of regions of interest, Atlas preselection, and global coarse registration of Atlas images.

This article uses the brain surface extractor (BSE) algorithm to preprocess English text images. The BSE algorithm uses the Laplacian of Gaussian (LoG) edge detection operator for skull edge detection. This method uses a Laplacian sharpening filter and a Gaussian smoothing filter. The two filters are combined. It first performs the Gaussian filtering on the image to reduce noise while smoothing the image and then calculates the Laplacian second derivative. The edge of the skull in the image is obtained by zero crossings, and finally, the background is eliminated without changing the internal structure of the brain according to the knowledge of morphology.

The Gaussian function is as follows:

$$h(r) = -e^{-\frac{r^2}{2\sigma^2}}. \tag{1}$$

Among them,

$$r^2 = x^2 + y^2. \tag{2}$$

σ is the standard deviation. The Laplacian of this function (the second derivative of r) is as follows:

$$\nabla^2 h(r) = -\left[\frac{r^2 - \sigma^2}{\sigma^4}\right] e^{-\frac{r^2}{2\sigma^2}}. \tag{3}$$

The image gradient algorithm takes into account the gray changes in the neighborhood of each pixel. It obtains the change rule by solving the first or second derivative between the pixel values of the neighborhood, that is, when the gray value of a neighborhood in the image changes greatly, the neighborhood must have a larger gradient value, which has edge features. Otherwise, the gray value of the neighborhood changes little and the image is smoother.

Mutual information can describe the correlation between two different systems. The greater the mutual information value, the greater the correlation between the two systems, or the more mutual information between the two systems. In English text image segmentation, since each Atlas image contains the same brain structure anatomy information, when the spatial positions of the two images are the same, the mutual information value of the corresponding

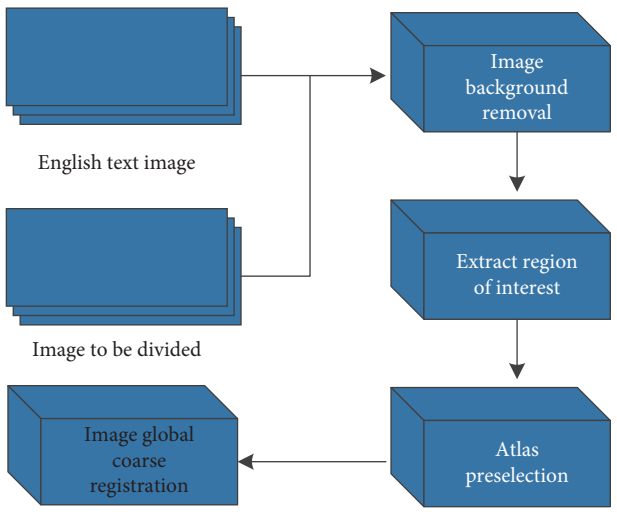

Figure 1: Flowchart of map preprocessing.

pixel grayscale is the largest. The mutual information calculation formula is as follows:

$$I(F,M) = H(F) + H(M) - H(F,M),$$
$$H = \sum_{i=0}^{N} p_{ij} \log p_{ij}. \tag{4}$$

In the formula, $H(F), H(M)$ represents the entropy of fixed image F and floating image M, $H(F,M)$ is the mutual information of F, M.

$$p_{ij} = \frac{f(i,j)}{N^2}. \tag{5}$$

Because the English text images are affected by instrument errors and the surrounding environment during the acquisition process, the differences between different images are large. Therefore, the global rigid coarse registration can be performed before the fine registration. The registration methods of English text images are classified according to the spatial transformation relationship and two categories of rigid registration and nonrigid registration can be obtained. Rigid registration is the overall translation, rotation, and scaling of the English text image, and both affine transformation and rigid body transformation belong to rigid registration. Nonrigid registration is achieved by calculating the position offset (deformation field) of each spatial point. This kind of registration method is computationally expensive and the spatial transformation is relatively complicated, but it can achieve better registration results. Nonrigid registration mainly includes Demons registration and B-spline interpolation transformation.

Due to the large amount of data in magnetic resonance images, rigid registration is not only computationally intensive but also time-consuming. Therefore, this study uses resampling to process the image to achieve the same effect as the coarse registration. The essence of resampling is image registration based on gray values, which can achieve the same effect as coarse registration. It aligns the Atlas grayscale image with the target image, and the sampling size of the image, the pixel spacing of the sampling space, and the direction of the three-dimensional image are all kept consistent. Moreover, resampling does not need to calculate the registration result as accurately as rigid registration, which reduces the calculation time. Therefore, this study uses bilinear interpolation in rough image registration. It maps the sampled image according to the distance, origin, and direction of the reference image to adjust the size and sample point of the two to be consistent. The core idea of bilinear interpolation is to perform linear interpolation in two directions. If it is assumed that A, B, C, and D are the four pixel points in the image; the coordinates are, respectively, marked as (x_1, y_2), (x_2, y_2), (x_1, y_1), and (x_2, y_1), and X is the sampling point; then, the pixel value of the sampling point can be calculated by the following formula:

$$f(X_1) = \frac{x_2 - x}{x_2 - x_1} f(A) + \frac{x - x_1}{x_2 - x_1} f(B),$$
$$f(X_2) = \frac{x_2 - x}{x_2 - x_1} f(C) + \frac{x - x_1}{x_2 - x_1} f(D), \tag{6}$$
$$f(X) = \frac{y_2 - x}{y_2 - y_1} f(X_1) + \frac{y - y_1}{y_2 - y_1} f(X_2).$$

In the formula, $f(X_1)$ and $f(X_2)$ are pixel values linearly interpolated in the x-axis and y-axis directions, respectively, using four pixels around the sampling point. The bilinear interpolation principle diagram is shown in Figure 2.

The target energy function of the differential homeomorphism Demons registration algorithm is as follows:

$$E^{D_i} = \left\| F - M \circ S \circ e^u \right\|^2 + \frac{\sigma_i^2}{\sigma_x^2} dist\left(S, S \circ e^u\right)^2. \tag{7}$$

In the formula, F represents the target image, M represents the floating image, and $\circ$ is the transformation operation. At the same time, S: $p \longrightarrow S(p)$ is a nonparameter geometric transformation, which means that the target image and the floating image are geometrically transformed to achieve a mapping relationship, that is, the point $S(p)$ in the floating image is the mapping value of the point p in the target image. p is the position point in the image, and $dist(\cdot)^2$ is the Euclidean distance. u is the updated deformation field and can also be called the deformation vector. When updating the deformation field, the exponential mapping of the deformation field and the compound operation $c \leftarrow S \circ e^u$ are used to obtain the following updated dense velocity field:

$$u(P) = -F(P) - M \circ S(p) \left\| J^P \right\|^2 + \frac{\sigma_i^2(p)}{\sigma_x^2} J^{P^T}. \tag{8}$$

In the formula, $\sigma_i(p) = |F(P) - M \circ S(P)|$ is the local estimation of image noise and σ_x represents the degree of uncertainty between S and c. The smaller the deformation, the smaller the value of σ_x. The constraint condition of σ_x on the maximum step size $\|u(P)\|$ of the dense velocity field is $\|u(P)\| \le \sigma_x 2$, and adding this constraint can improve the

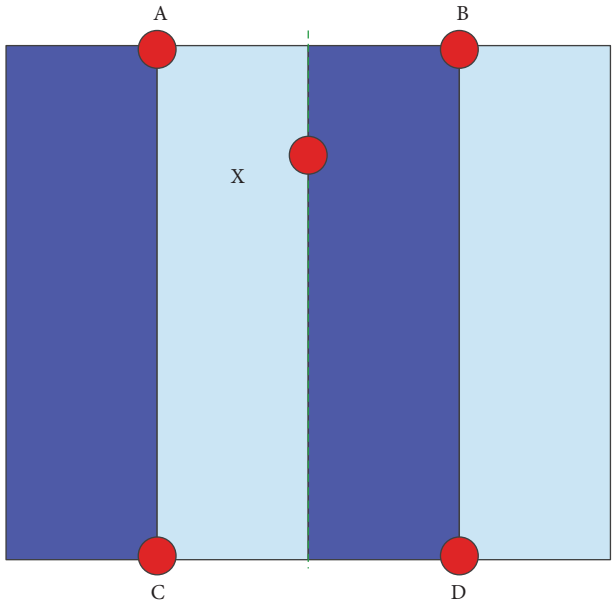

Figure 2: Bilinear interpolation principle diagram.

image registration effect. J^P is the Demons force of diffeomorphism.

$$J^P = -\frac{1}{2}\left(\nabla_P^T F + \nabla_P^T (M \circ S(p))\right). \tag{9}$$

Thus, the calculation efficiency of the algorithm can be improved.

The steps of the Demons algorithm are as follows:

Step1: Demons deformation field wW is calculated and updated;

Step2: u is subjected to fluid regularization, that is, $u \leftarrow K_{fluid} * u$

Step3: e^u obtained by Lie group transformation is calculated and $c \leftarrow S \circ e^u$ is also calculated

Step4: S is regularized by diffusion, $S \leftarrow K_{diff} * S$ Markov characteristics describe the distribution characteristics between random variables, that is, when a random variable sequence is arranged in a time sequence, the value of the random variable at the current moment determines the distribution characteristic at the next moment, and its value is different from other moments. The Markov random field is cited in the image field, which means that the feature of any pixel in the image is only related to the pixel value of a small neighborhood where the pixel is located, and it will not be affected by other neighborhood pixel values. Combining the prior knowledge of the image with the neighborhood correlation of the MRF can effectively segment the MR image.

Image segmentation can be regarded as a label classification problem. The pixel set of the image to be segmented is denoted as $X = \{x_1, x_2, \cdots, x_n\}$, n is the number of pixels of the image, the image pixels belonging to a certain label category is denoted as $L = \{l_1, l_2, \cdots, l_m\}$, and m is the number of label categories. According to Bayesian estimation, the calculation of the image segmentation problem can be expressed as follows:

$$p(L \mid X) = \frac{p(X \mid L) \cdot p(L)}{p(X)}. \tag{10}$$

In the formula, $p(L)$ represents the prior probability of the image and $p(X)$ is the probability density function of the image to be segmented, which is an invariant. Therefore, the maximum posterior probability of the abovementioned formula can be expressed as follows:

$$p(L \mid X) = \text{argmax} p(X \mid L) \cdot p(L). \tag{11}$$

That is, only the maximum value of the numerator in formula (10) needs to be solved.

4. The Gaussian Mixture Model

For English text images, the gray level changes in each area of the image are relatively slow, and the overall gray level statistical histogram of the English text image always presents a multimodal distribution. Therefore, it can be described by a Gaussian mixture model (GMM). The GMM refers to a model formed by a linear combination of multiple Gaussian probability density functions. Generally speaking, GMM can fit most types of data distributions. This model is often used to describe a dataset containing multiple types of distributions or distributions with the same type of distribution but different parameters.

GMM has better results than a single Gaussian model in reducing the misclassification of pixels. Therefore, this article uses GMM to describe the grayscale characteristics of English text images, and its mathematical expression can be expressed by a weighted function of the probability distribution density function of a single Gaussian model as follows:

$$p(x_i) = \sum_{g=1}^{m} \alpha_g N_g\left(x_i; \mu_g, \varepsilon_g\right). \tag{12}$$

4.1. The Graph Cuts Algorithm. The graph cuts algorithm can be used to minimize the energy function. This algorithm can obtain a better segmentation effect while ensuring the segmentation speed. The graph cuts algorithm first maps the image to a weighted undirected graph $G = (V, E)$. G contains source point S (representing target), sink point T (representing background), and node (pixel). V represents the set of image pixel nodes, $x_i \in V$ is a pixel of the image, and adjacent nodes are connected by edges. At the same time, E represents the set of edges between nodes and $B_{i,j}$ represents the connection weight of each edge of adjacent pixels, that is, the cost of cutting the edge. R_i represents the weight of the edge connecting each node with S and T. The weight represents the probability that the current node belongs to the target or background.

We assume that the label of each pixel in the image is $L =$ and Zf is the background or foreground (target), and the

calculation formula for the weight of the connecting edge of adjacent pixels is as follows:

$$B_{i,j}(x,l) = \lambda B_{\langle i,j\rangle}\delta(i,j). \tag{13}$$

In the formula,

$$\begin{aligned} \lambda &= 50 \\ B_{\langle i,j\rangle} &= e^{-\left(\beta\left\|z_i - z_j\right\|^2\right)} \\ \delta(i,j) &= \begin{cases} 1, x_i = x_j \\ 0, x_i \neq x_j \end{cases} \end{aligned}. \tag{14}$$

β is determined by the degree of difference between image pixels as follows:

$$\beta = \left(2\left(z_i - z_j\right)^2\right)^{-1}. \tag{15}$$

The calculation formula for the connection weight between each pixel and the source point and sink point is as follows:

$$R_i(x,l) = -\log p\left(l_i, x_i\right). \tag{16}$$

This formula represents the negative logarithm of the probability that a pixel x_i is divided into a marker l_i.

5. The Graph Cuts Label Fusion Algorithm Based on the Generative Model Constraints

This study uses the Gaussian mixture model to describe the distribution of image pixels. Combined with the neighborhood correlation of MRF, a graph cuts algorithm based on the generative model constraints is proposed, which improves the situation that the traditional label fusion methods cannot effectively describe the real model of the target structure. This algorithm is essentially a segmentation method that minimizes the energy function. The combination of GMM and MRF as generative models can effectively characterize the spatial correlation and local statistical characteristics of image pixels. By learning the joint distribution of the data, the conditional probability distribution is solved as a predictive model and the energy function is constructed. The graph cuts algorithm is used to correspond the energy function to the minimum cut set of the image, that is, the generative model is used to constrain the graph cuts algorithm to achieve the segmentation of the target image, and the energy function can be minimized by obtaining the minimum cut, that is, the segmentation is completed task.

$p(X \mid L) \cdot p(L)$ is $p(X \mid L)$ which represents the joint probability distribution of image and segmentation information, so the formula can be written as follows:

$$p(L \mid X) = \operatorname{argmax} p(X \mid L). \tag{17}$$

According to the Hammersley–Clifford theorem, it is known that the Markov random field and the Gibbs distribution are consistent, that is, the probability distribution of the Markov random field can be represented by the Gibbs energy function (potential energy of the potential group) as shown

$$p(L) = z^{-1}e^{-u_1(L)}. \tag{18}$$

Among them, $z = \sum_L e^{-u_1(L)}$ is the normalization constant and the parameter X can control the shape of $p(L)$. The larger the X value, the smoother the $p(L)$. $u_1(L) = \sum_c v_c(L_c)$ represents the prior energy function, where c is the set of all potential groups. $v_c(L_c)$ represents the potential energy of the potential group, and the potential energy function is as follows:

$$v_c(L_c) = v_{i,j}\left(L_i, L_j\right) = \begin{cases} -\beta & L_i = L_j \\ \beta & L_i \neq L_j \end{cases}. \tag{19}$$

Among them, i and j represent two adjacent pixels and β represents the coupling coefficient, which is used to describe the interaction strength between pixels in the potential cluster.

With the introduction of GMM, it is possible to judge which classification a certain pixel is in according to its value. The energy function of the likelihood function $p(X \mid L)$ can be expressed by the following formula:

$$\begin{aligned} p(X \mid L) &= z^{-1}e^{-u_2(X \mid L)}, \\ u_2(X \mid L) &== \sum_s \left(In\left(\sqrt{2\pi}\,\sigma_i\right) - In\alpha + \frac{\left(X_i - \mu_i\right)^2}{2\sigma_i^2}\right). \end{aligned} \tag{20}$$

Among them, $In\alpha$ is the weighting coefficient of the Gaussian mixture model, and σ_i and μ_i correspond to the variance and mean of the same labeled pixel set in the labeled set L, respectively.

The joint formula obtained is displayed as follows:

$$p(L \mid X) = \operatorname{argmax}\left\{z^{-1}e^{-\left(u_2(X \mid L) + u_1(L)\right)}\right\}. \tag{21}$$

We set the following:

$$R = \operatorname{argmax}\left\{z^{-1}e^{-\left(u_2(X \mid L) + u_1(L)\right)}\right\}. \tag{22}$$

and we obtain the following:

$$InR \propto -\left(u_2(X \mid L) + u_1(L)\right). \tag{23}$$

Thus, we derive as follows:

$$p(L \mid X) = \operatorname{argmax}\left(u_2(X \mid L) + u_1(L)\right). \tag{24}$$

Thus, the problem of maximum posterior probability is transformed into a problem of solving the minimum value of the energy function.

6. Model Building

The reader starts with an English text reading service. The business process runs through reader DRM authentication, MEB e-book content analysis, reading resource content reading, and radiates to other auxiliary functions of each business module, such as bookmarking, book downloading,

and automatic playback. The full-function module of the reader is shown in Figure 3. Due to the numerous business functions of the reader, the content of this study cannot describe all business function modules one by one. Therefore, this article only provides a relevant introduction to the content designed for other key business requirements derived from the core business.

The function of bookmarks is to help users enter the previously reserved reading interface as soon as possible. The bookmark function is added to the bookshelf module, which makes it convenient for users to find the content of the books that need to be read before. The flow of the bookmark function design is that when users log in to the book reading module, if they need to read the relevant content previously read, they enter the interface where the bookmark function is located, and through the bookmark search, they enter the previously read interface. If there is no bookmark function and there is a need to read the previous content, the user must find the corresponding book through search, and find the corresponding chapter content within the scope of the book. The flowchart of the bookmark function is shown in Figure 4.

If the system is often in a reading background, the user will feel visual fatigue, so the background can be set in the black and white sky mode and the color difference can be adjusted in the book reading page. According to the current reading conditions, users can choose a background color that they feel comfortable to read books. This helps users to protect their eyesight, improve reading comfort, and also helps to extend the reading time. There are different groups of people using this system, so everyone has different vision conditions. In the process of reading, some users have blurred and unclear reading of the initial default font. Therefore, the font adjustment function is added to the reading page of the book. The font adjustment function can change the font size of the reading content. Users can choose a font suitable for their own reading for convenient reading.

The book recommendation function allows users to recommend favorite books they have read to users who have installed a smartphone reading system. After receiving the message, the other party will check the recommended books. This not only increases the market share of the smartphone reading system but also improves the stickiness of the system. It also facilitates users to obtain more up-to-date and useful information, which achieves a win-win situation for service providers and users.

Software testing is the guarantee of software quality, so the testing process adopts the V-graph model for testing, as shown in Figure 5. The V-shaped diagram of the development model is accompanied by the entire software development cycle, and the object of testing is not only the program but also the requirements and designs. The V-shaped chart development model is conducive to the early and comprehensive discovery of problems. In the software development stage, the development process needs to be from rough to detailed, and it is necessary to adopt advanced requirements analysis, requirement decomposition, and list all requirements to ensure that the required information is clear and not omitted. Then, we design each requirement.

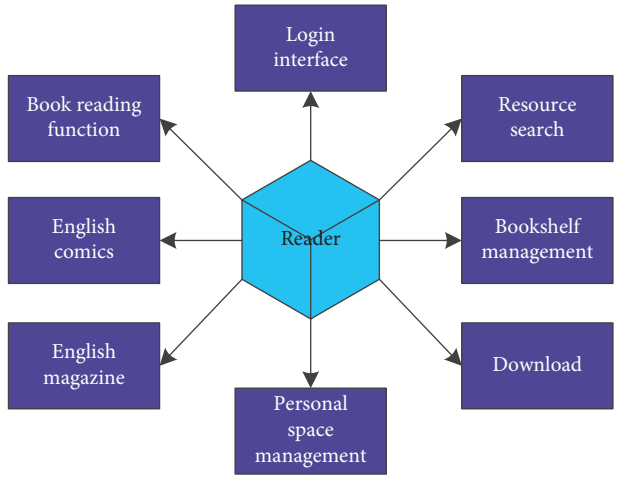

Figure 3: The reader function module diagram.

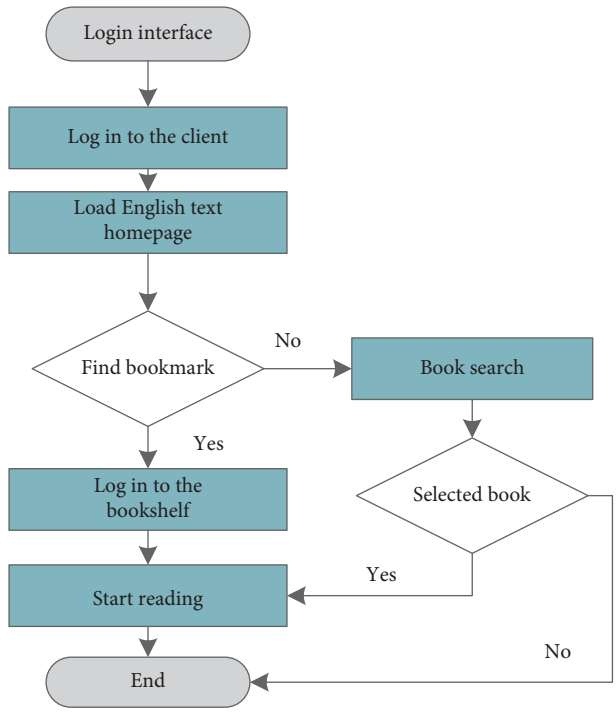

Figure 4: Bookmark function flowchart.

The design includes system design, outline design, and detailed design. It also adheres to the principle of gradual progress from coarse to fine to make the design clearer and simpler. This development model is also a typical waterfall development model but we use agile development, which belongs to the waterfall model applied in the iterative model.

Based on the abovementioned construction model, the model is tested and the reading situation of English text is counted. This article first sets up100 groups of English reading texts to analyze the accuracy of English reading recognition. The results are shown in Figure 6.

The data show that the intelligent reading model constructed in this study has a high reading accuracy for English

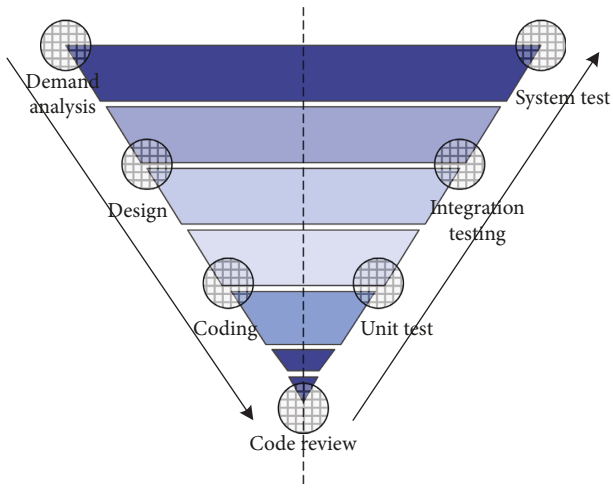

Figure 5: V-type test model diagram.

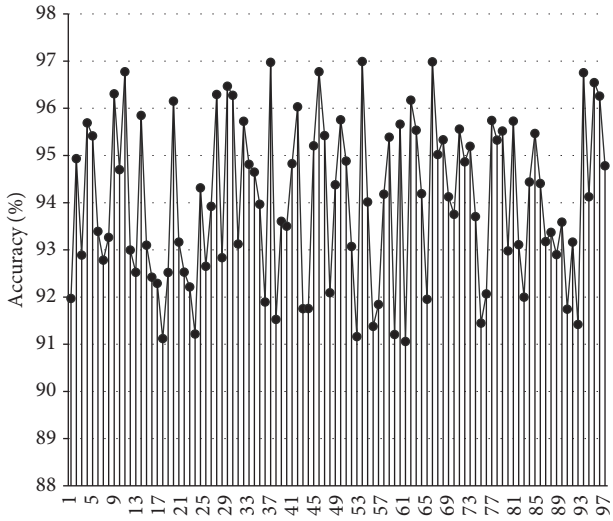

Figure 6: Accuracy of English reading.

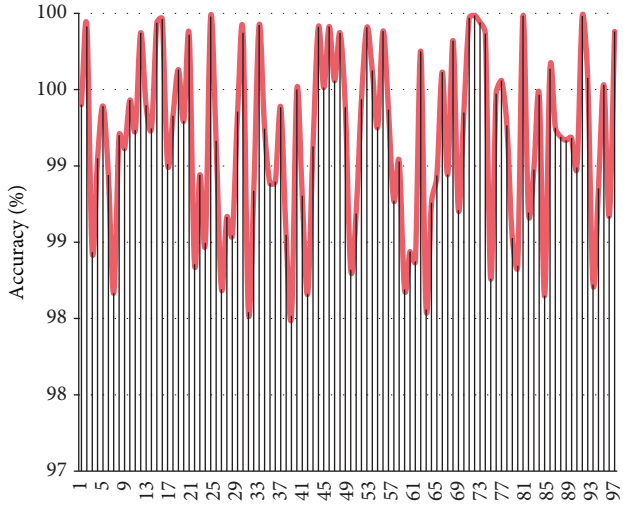

Figure 7: A statistical diagram of the model's recognition accuracy of English text types.

texts. The recognition effect of English text types in the system is shown in Figure 7.

From the results, it can be seen that the model constructed in this study has a very good classification effect on English text.

7. Conclusion

In order to recognize the intelligent reading of English text at the image level, this study proposed a multi-image label fusion algorithm design model of graph cuts based on the generative model constraints. This model can be used for intelligent and automatic pixel segmentation of the image structure of English text, which is the result of unitized segmentation of the fused image by utilizing the prior knowledge data reserve of multiple images. In addition, in order to reduce the complexity of the subsequent calculation, this study uses the open source code library 1 TK and visual studio-integrated development environment to process the image in advance in the image preprocessing module.

This study proposes to use a generative model combining GMM and MRF to express the spatial correlation and local statistical characteristics of image pixels. By learning the joint distribution of the data, the conditional probability distribution is solved as a prediction model and the image energy function is constructed. Moreover, this study uses the graph cuts algorithm to correspond the energy function to the minimum cut set of the image, that is, it uses the generative model to constrain the graph cuts algorithm to obtain the minimum cut to minimize the energy function. In addition, after constructing the model structure, this article sets up a control experiment to analyze the model's performance from two aspects: the accuracy of the model's recognition of English text and the accuracy of text classification. The research results show that the intelligent reading model constructed in this study performs well in meeting the needs of practical applications.

Data Availability

The data supporting the current study are available from the corresponding author upon request.

Conflicts of Interest

The authors declare that they have no conflicts of interest.

Acknowledgments

The authors would like to thank the Baoding University of Technology for supporting this article.

References

[1] X. Yang, H. Li, L. Ni, and T. Li, "Application of artificial intelligence in precision marketing," *Journal of Organizational and End User Computing*, vol. 33, no. 4, pp. 209–219, 2021.

[2] J. D'Ambra, C. S. Wilson, and S. Akter, "Application of the task-technology fit model to structure and evaluate the

adoption of E-books by Academics," *Journal of the American Society for Information Science and Technology*, vol. 64, no. 1, pp. 48–64, 2013.

[3] N. H. Ibrahim, K. N. Chee, and N. Yahaya, "Effectiveness of mobile learning application in improving reading skills in Chinese language and towards post-attitudes," *International Journal of Mobile Learning and Organisation*, vol. 11, no. 3, pp. 210–225, 2017.

[4] K. Holl and F. Elberzhager, "Mobile application quality assurance: reading scenarios as inspection and testing support," in *Proceedings of the 2016 42th Euromicro Conference on Software Engineering and Advanced Applications (SEAA)*, pp. 245–249, IEEE, Limassol, Cyprus, September 2016.

[5] R. Schroeder, "Towards a theory of digital media," *Information, Communication & Society*, vol. 21, no. 3, pp. 323–339, 2018.

[6] W. D. Woody, D. B. Daniel, and C. A. Baker, "E-books or textbooks: students prefer textbooks," *Computers & Education*, vol. 55, no. 3, pp. 945–948, 2010.

[7] J. Staiger, "How E-books are used," *Reference and User Services Quarterly*, vol. 51, no. 4, pp. 355–365, 2012.

[8] M. V. Pabrua Batoon, L. D. Glasserman Morales, and J. A. Yanez Figueroa, "Instructional design to measure the efficacy of interactive e-books in a high school setting," *The Turkish Online Journal of Distance Education*, vol. 19, no. 2, pp. 47–60, 2018.

[9] R. J. Bian, "An empirical study on the influencing factors of customer satisfaction in mobile reading," Nanjing University of Posts and Telecommunications, Nanjing, China, 2018.

[10] M. Imdadullah, M. Aslam, and S. Altaf, "Mctest: an R package for detection of collinearity among regressors," *The RUSI Journal*, vol. 8, no. 2, p. 495, 2016.

[11] T. Vo, "SynSeq4ED: a novel event-aware text representation learning for event detection," *Neural Processing Letters*, vol. 54, no. 1, pp. 227–249, 2022.

[12] X. Liu and X. Liu, "Online suicide identification in the framework of rhetorical structure theory (RST)," *Healthcare*, vol. 9, no. 7, p. 847, 2021.

[13] A. Mosavi, S. Ardabili, and A. R. Varkonyi-Koczy, *List of deep learning models International Conference on Global Research and Education*, pp. 202–214, Springer, Cham, Berlin/Heidelberg, Germany, 2019.

[14] P. Bojanowski, E. Grave, A. Joulin, and T. Mikolov, "Enriching word vectors with subword information," *Transactions of the association for computational linguistics*, vol. 5, pp. 135–146, 2017.

Hindawi
Computational Intelligence and Neuroscience
Volume 2022, Article ID 1608167, 10 pages
https://doi.org/10.1155/2022/1608167

Research Article

IoT Network for International Trade Cold Chain Logistics Tracking Based on Kalman Algorithm

Chao Zhang and Wei Wei

School of Management, Wuhan College, Wuhan, Hubei 430212, China

Correspondence should be addressed to Wei Wei; 8557@whxy.edu.cn

Received 5 July 2022; Revised 2 September 2022; Accepted 6 September 2022; Published 19 September 2022

Academic Editor: Gopal Chaudhary

The application of Internet of Things technology in cold chain transportation can greatly strengthen the monitoring of all aspects of cold chain logistics, so as to promote the progress of cold chain logistics industry. In order to study this aspect, this paper chooses the key link of the Internet of Things as a breakthrough. By analyzing various aspects of the transportation process, an Internet of Things middleware framework serving cold chain transportation tracking is designed. The main products of logistics cold chain transportation are fresh agricultural products, so in order to further make the research fit the actual situation, this paper collects the logistics data and information of agricultural products through investigation and combines the core technology of agricultural products logistics with the Internet and the key technology of cold chain transportation to process the obtained information. The analytic hierarchy process and fuzzy comprehensive evaluation method are used in this process. The processing results prove the validity and rationality of the established index system. The purpose of developing the international trade management system is to enable the company to optimize its international trade management process, reduce some tedious and inconvenient manual operations, make the recording and statistics of international trade information very simple, improve work efficiency, and satisfy the information needs of various departments to enable enterprises to minimize costs, thereby enabling enterprises to obtain better economic benefits.

1. Introduction

The emergence of the Internet of Things platform has greatly facilitated our daily lives and has also greatly improved people's work efficiency [1]. However, it must be noted that only by complying with the rules and standards of the Internet of Things platform at this stage can the corresponding technical equipment be fully connected. Cold chain transportation is the successful application of the Internet of Things technology in the logistics platform [2]. In this link, the widespread use of sensors has greatly promoted the development of cold chain transportation. This article mainly studies how to use various types and functions. The sensors provide better service for cold chain transportation [3]. The Internet of Things middleware in the cold chain transportation link is selected as the research object. By analyzing various aspects of the transportation process, an Internet of Things middleware framework serving cold chain transportation tracking is designed [4]. In addition, in order to better deal with the communication obstacles between different sensors, and, at the same time, to filter the useless and redundant data in the sensors, we adopted D-Bus technology and designed the communication means between different sensors [5]. The focus of this article is to prove that IoT technology can optimize and enhance China's agricultural cold chain logistics. In view of this problem, the literature combined with the actual situation of the operation and development of agricultural cold chain logistics enterprises, in view of the problems existing in the enterprise process, the agricultural cold chain logistics mode starting from the enterprise was constructed [6]. The literature combines the previous research experience, uses the Internet technology, solves the practical problems in the development process of cold chain logistics, and upgrades and improves the existing logistics [7]. The international trade management system enables companies to minimize costs and better select

suppliers, products, and customer information, thereby enabling companies to obtain better economic benefits [8].

2. Related Works

The literature has done in-depth research on cold chain logistics middleware; its purpose is to solve the problem of connection and data interaction between different sensor nodes in the cold chain tracking process in the Internet of Things environment, while ensuring the accuracy of data transmission. In the cold chain transportation link, data errors are not allowed [9]. This article adds a data processing module to the middleware of the Internet of Things, which improves the efficiency and accuracy of data collection by the middleware. The literature designed the cold chain logistics tracking middleware to solve a series of problems when collecting cold chain sensor data. The purpose of developing an international trade management system is to enable a limited company to optimize its international trade management process [10]. The international trade management system can reduce some tedious and inconvenient manual operations, make the recording and statistics of international trade information very simple, and improve work efficiency [11, 12]. The international trade management system can meet the information needs of various departments, so that companies can minimize costs and better select suppliers, products, and customer information, so that companies can obtain better economic benefits [13].

In embedded devices, embedded devices usually have many sensor nodes. It should be noted that, in these sensor nodes, the memory of each sensor node is relatively small [14]. However, according to the current state of technological development, most operating systems on the market are equipped with large-capacity storage devices, and large-capacity storage devices can promote the increase in computing speed to a certain extent. Therefore, when comparing embedded devices with other operating systems on the market, the processing speed of the embedded operating systems is much lower than other large operating systems [15, 16]. In the following description in this article, nonembedded general-purpose computer devices are collectively referred to as general-purpose devices. In daily real-life use, the general-purpose device must support the data transmission function of the near-end network, and the data transmission function enables communication and data exchange between the sensor node and the general-purpose device [17]. D-Bus technology is an end-to-end communication technology, which is used for each sensor and general device in the near-end network to ensure that the communication and data transmission between the sensor node and the general device can be carried out normally [18].

3. Construction of IoT Sensor Network for Cold Chain Logistics Tracking

3.1. Overview of Related Technologies of IoT Middleware. REST refers to the state transfer of the presentation layer, which means that the relevant data of the resource network management center is transferred in a certain way or in a certain state. The main manifestations of the resource representative data are JSON, XML, etc., and the state change is through HTTP verb implementation.

In a period when Internet technology and science and technology were not developed, there was a problem of low penetration rate of mobile device terminals. Therefore, in order to save resources and reduce expenses, the client and server are usually combined together. However, in recent years, science and technology have continued to develop, and the penetration rate of the Internet and the Internet of Things has been rising, and various types of Client service plug-ins have appeared. Therefore, REST can provide services for various types of platforms through related service plug-ins.

In the process of REST providing services for various platforms, REST is always in the stateless constraint stage. Therefore, when the server and the client use the REST framework for interactive communication, the server does not need to know the usage status of the client. Moreover, in the process of interaction, there will be no information loss, and the server and the client can clearly identify and judge the received information.

REST is in the stateless constrained stage. It means that when REST provides services, each web service in REST is in an independent state, and the server does not save the relevant state information of the client.

The REST system conducts standard state interaction through its own resources. Therefore, when REST provides services, it does not require a specific interface as an intermediary.

Four basic HTTP verbs are used in the REST system to interact with resources, as shown in Table 1.

Using the REST architecture can make full use of the various functions brought by the HTTP protocol and make the software architecture design clearer and maintainable.

Hidden Markov model is a kind of probability model, which expresses the sequentiality of a set of random processes through probability description. In the hidden Markov model, the most important component is the Markov chain. In the actual application process of the hidden Markov model, the real state of the location is represented by the hidden Markov chain.

$$P\left(X_n = x \mid X_0, X_1, X_2, \ldots X_{n-1}\right) = P\left(X_n \mid X_{n-1}\right). \tag{1}$$

Assume that Q is the set of all states, and V is the set of all observed states.

$$Q = \{q_1, q_2, \ldots, q_N\}, V = \{v_1, v_2, \ldots, v_M\}. \tag{2}$$

I is the state sequence of length T, and O is the corresponding observation sequence.

$$I = \{i_1, i_2, \ldots, i_T\}, V = \{o_1, o_2, \ldots, o_T\}. \tag{3}$$

The state transition probability matrix is as follows:

$$A = \left[a_{ij}\right]_{N*N}. \tag{4}$$

Among them,

Table 1: HTTP verbs in REST.

Verb	Operating
GET	Retrieve a specific resource or collection of resources
POST	Create a new resource
PUT	Update a specific resource (by id)
DELETE	Delete specific resources by id

$$a_{ij} = P\left(i_{t+1} = q_j \mid i_t = q_i\right), 1 \le i, j \le N. \tag{5}$$

The observation probability matrix is

$$B = \left[b_j(k)\right]_{N*M}. \tag{6}$$

Among them,

$$\pi_i = P\left(i_1 = q_i\right), 1 \le i \le N. \tag{7}$$

The hidden Markov model is represented by a ternary symbol:

$$\lambda = (A, B, \pi). \tag{8}$$

The Kalman algorithm is the most commonly used estimation algorithm. The Kalman algorithm has the characteristics of small calculation requirements and good recursion in the actual application process. Therefore, since the Kalman algorithm was proposed, it has been widely used, and the Kalman algorithm has gradually developed into an optimal estimation algorithm. The typical use of Kalman algorithm is to smooth noisy data. Kalmar filter is an accurate reasoning algorithm, which is similar to Bayesian model, but there are certain differences between the two. The latent variable of Kalman filter is always in a continuous state in the state space.

Kalman filter is mainly used in solving random linear discrete systems and parameter estimation. In the actual application process, the steps of using the Kalman filter are divided into estimation and correction. Estimation refers to constructing a priori estimation of the next state based on the current prior state value and then after a reasonable calculation. Correction refers to the use of parameter update equations to check the previously constructed prior estimates. The correction process is mainly a feedback process.

The time update equation and state update equation of the discrete Kalman filter are as follows:

$$\begin{aligned}
\widehat{X}_k^- &= A\widehat{X}_{k-1} + B\widehat{U}_{k-1} \\
\widehat{P}_k^- &= A\widehat{P}_{k-1}A^T + Q \\
K_k &= P_k^- H^T\left(HP_k^- H^T + R\right)^{-2} \\
\widehat{X}_k &= \widehat{X}_k^- + K_k\left(Z_k - H\widehat{X}_k^-\right) \\
P_k &= (I - K_k H)P_k^-.
\end{aligned} \tag{9}$$

3.2. IoT Middleware Architecture for Cold Chain Logistics Tracking. This article assumes that each node with middleware installed is peer-to-peer; that is, each node can be either a consumer or a producer. Consumers remotely call the near-end network to find the required nodes and obtain services, and the provider nodes have unique IDs to facilitate the calls of consumers. Figure 1 describes how external devices access specific services required in a near-end network.

Based on the design idea of this article, in the cold chain traceability environment, the IoT middleware needs to trace all the data in its environment and also provide services for each node of the sensor. The IoT middleware can schedule the location and location of sensor nodes in real time. The current data transmission method uses the above functions to complete data collection and data error correction. In summary, the detailed system architecture diagram of the IoT middleware is shown in Figure 2.

According to Figure 2, the IoT middleware proposed in this article mainly does the following work:

(1) Access technology abstraction layer: when sensor nodes choose different transmission methods, there is no need to write communication code.

(2) Data processing: including filtering of redundant data and error correction of data with strict requirements.

(3) Remote call node service: the method executed by remote call runs in the remote node. Unlike local call, the remote node service runs in a different process. To communicate with it, the following problems need to be solved:

   (a) ID mapping: because the function pointer cannot be used like a local call, the corresponding method in each node must have a corresponding ID to implement the corresponding method.
   (b) Serialization and deserialization.
   (c) Data transmission.

(4) Different node communication design: introduce D-Bus technology, connect each sensor node to the session bus, connect general equipment to the session bus and system bus, and then use the system bus daemon to communicate with the sensor nodes.

In the process of cold chain traceability, a large number of sensor nodes are used, and these sensors will generate a large amount of real-time data. However, in actual use, due to various problems such as poor network quality, some error data will be generated, resulting in redundancy of data information; due to the existence of error data, the processing efficiency of the system is greatly reduced. Therefore, how to deal with these wrong data has become the focus of the next research. Because the cold chain link requires data to have high accuracy, data error correction is required, and unnecessary network expenses can be reduced through data error correction.

3.2.1. Redundant Data Filtering. In the Bloom Filter-based filtering algorithm, the system adds a timestamp attribute to each data that reaches the data processing layer and sets the time threshold between two data receptions. When the time difference between two adjacent data received exceeds the

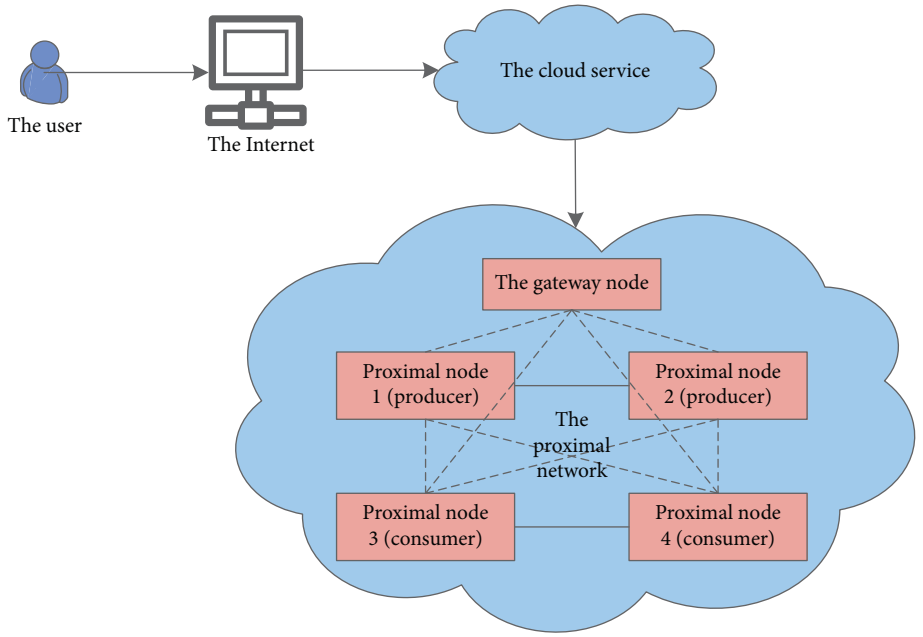

Figure 1: Middleware remote access network architecture.

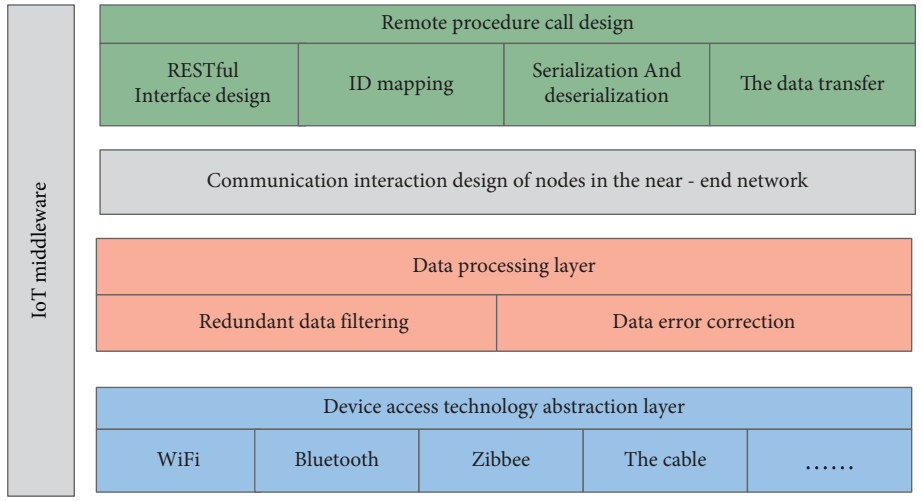

Figure 2: Middleware architecture block diagram.

threshold, or the time difference is less than the threshold, but the data is the same, it is determined as redundant data; otherwise, it is determined that the remaining data is nonredundant data.

Set Terminal ID to represent the ID of the sensing device, which has unique properties, and Send Time represents the timestamp when data is sent to the data processing layer, and the set time interval between adjacent data is the Time Threshold. The specific schematic diagram is shown in Figure 3.

Then, establish the following rules:

(a) Check the parity bit of the data to determine whether the data is distorted.

(b) After receiving the data, the data processing layer determines whether there is a terminal identification code in the sensor device information corresponding to the receiving time point.

(c) Judging whether the new data value of the same terminal identification code in rule (b) is the same: if they are the same, it is judged as duplicate data; if they are different, the original data is updated.

(d) The old data and the same data are judged as redundant data, and the redundant data is directly discarded.

Therefore, when the data processing layer receives data, the system processing steps are as follows:

(a1) Determine whether the data is distorted by the check bit, and discard it if distorted.

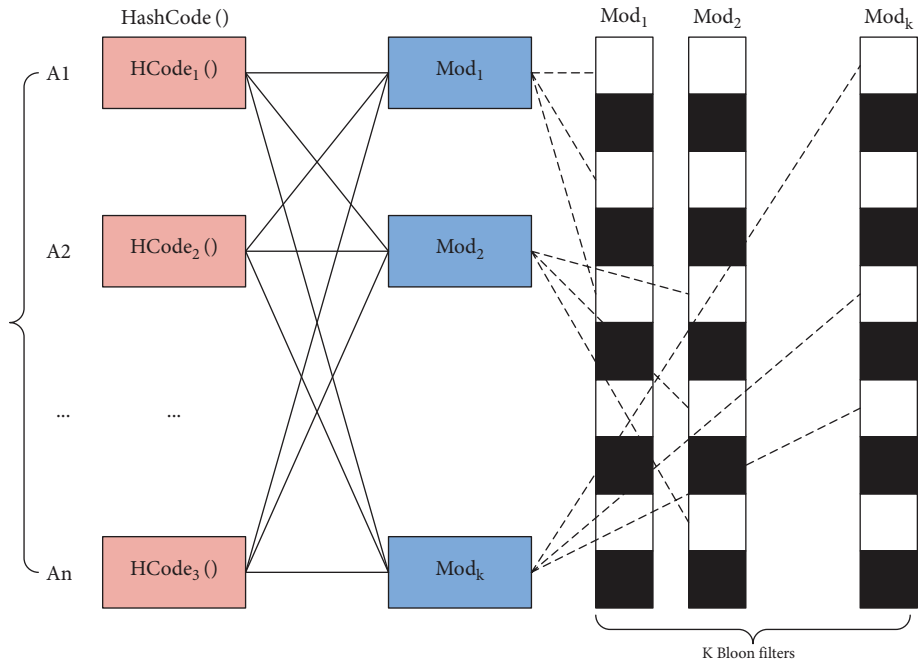

Figure 3: Bloom filter filtration diagram.

(b1) If the received data is not distorted, judge whether there is a device ID in the sensor device information corresponding to the receiving time point. If not, directly add the data to the data structure; if there is, determine whether it is old data. If it is old data, discard it; if it is new data, go to step (c).

(c1) Determine whether the added data is duplicate data; if it is duplicate data, discard it.

Sensor data error correction: after the transmission data is obtained, due to the influence of factors such as environment and equipment, in the process of data display and processing using the obtained data, error data that obviously does not conform to the logic and the scene will be found. Therefore, a corresponding data error correction module needs to be added to the middleware of the Internet of Things. The data error correction is performed through the data error correction module, and the error data is eliminated, thereby improving the accuracy of the collected data.

3.2.2. Design and Implementation of Middleware Remote Procedure Call. In the cold chain traceability link, users of sensor nodes and middleware can call the internal data of the system at any time and can provide users with corresponding service requirements by calling the data.

(1) REST Interface Design. It is extremely important to design a unified style interface, which is also clear for later maintenance. The corresponding verbs and resource operations are shown in Table 2.

According to the above principles, the design of the cold chain link interface is as follows:

(1) GET: get the temperature of a specific node

Table 2: Verb resource operation table.

Verb	Operating
GET	Get resources (by id)
POST	New resource (by id)
PUT	Update resource (by id)
DELETE	Delete resource (by id)

(2) POST: update the temperature of the node (error correction operation, etc.)

When using the local method for data processing, you only need to add the data to be processed to the relevant stack, and the local method can automatically call the relevant parameters to process the relevant data. In the method of using remote calls, the programming language used by the client and the server may be different, and the processing process may not be at the same stage. Therefore, the memory transfer method cannot be used for data processing. Therefore, the client needs to convert the parameters and data it wants to transmit into a binary byte stream and then send it to the server. Finally, the server converts the received binary byte stream into a coded form that it can read. In the above operations, the process of converting parameters and data into a binary byte stream is called serialization, and the process of converting a binary byte stream into a readable encoding form is called deserialization. In the actual application process, whether the client transmits parameters and data to the server, or the server transmits parameters and data to the client, both of them need to undergo the serialization and deserialization processes. The related schematic diagram is shown in Figure 4.

In the actual application process, the programming languages used by different servers and different clients are not the same, and different programming languages will cause

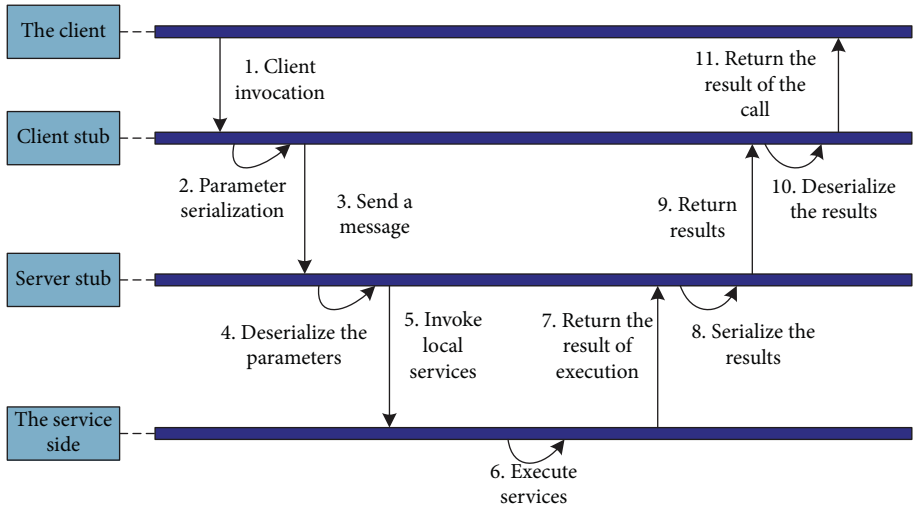

Figure 4: Serialization and deserialization diagram.

differences in data structures, and differences in data structures will lead to differences in the representation of binary structures. If different, the client and server need to specify some transmission protocols when performing serialization and deserialization operations. Currently, common transmission protocols include XML, JSON, and Thrift. However, the XML transfer protocol has certain disadvantages. Since the amount of information transmitted between the sensor node and the client is not large, the resulting byte stream will be lengthy and complicated when the XML protocol is used for serialization. In contrast, the JSON protocol is better in the process of use. Compared with the XML protocol, the JSON protocol uses the data processed by the JSON protocol to have a simpler data format, faster parsing density, and better readability. The most important point is that, after serialization using the JSON protocol, the resulting file size is smaller. Therefore, in actual applications, in order to ensure the conciseness of the obtained data, we often use the JSON protocol as an intermediate protocol when performing serialization and deserialization operations.

In the actual use, you will find that the computing power of embedded devices will be affected by the memory of the sensor node. If the memory of a sensor node is larger, its computing power will be stronger. Similarly, if the memory of a sensor node is smaller, the computing power of the embedded device is smaller. Therefore, when the sensor node is in use, it is only introduced into the session bus to reduce expenses through such measures. General-purpose devices are different from sensor nodes because general-purpose devices need to serve the entire system at all times. Therefore, in the process of use, general-purpose devices are introduced into the system bus and the session bus. The system bus will automatically start when the general-purpose device is running and shut down when the general-purpose device is closed. In the system bus, the bus daemon can communicate with other processes in the system during the running process, and the sensor node is running. In the process, different sensors can use different session buses to access the system bus. Therefore, sensor nodes can send

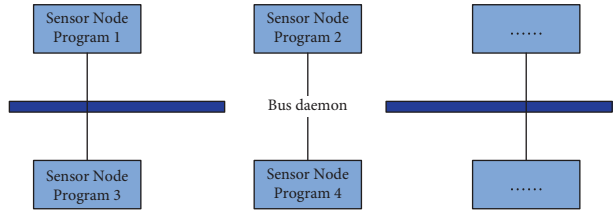

Figure 5: Schematic diagram of communication between near-end nodes.

signals by using the session bus and then connect with each process. The specific steps are divided into the following: (1) the node first sends the target address to the general-purpose device to request access to the system bus. (2) The system bus processes the request information relayed by the general-purpose equipment and forwards the request information to the logo node. (3) The slogan node responds to the received information, and then the daemon sends the response information back to the node.

Through the specific communication steps, it can be seen that the communication between the node and the system needs to pass through the daemon of the system bus, which means that when the sensor node communicates with the system, the daemon of the system can play an intermediary role, and at the same time, it can ensure the security of messages and the schematic diagram of communication between nodes, which are shown in Figure 5.

In summary, sensor nodes can communicate with general-purpose devices. In the process of connection and communication, the daemon acts as an intermediary to ensure the security of information in this way.

3.3. Research on Data Error Correction Technology of Cold Chain Logistics Middleware. The Kalman filter is suitable for the estimation of dynamic data. The optimal state is given by estimating the dynamic data. Because there is noise in the

dynamic data, the data measured by the sensor is not accurate, so the Kalman filter is used to filter out the noise and estimate the true state value of the data.

During data calculation, vector data such as temperature and humidity can be converted into scalar data.

The predicted deviation of temperature type is

$$T_{pe} = \sqrt{T_{oe}^2 + T_{ue}^2}. \tag{10}$$

In a cold chain vehicle, first assume that the temperature at time K and at time $K-1$ are the same. At this time, calculate the Kalman gain:

$$Kg = \frac{T_{pe}^2}{T_{pe}^2 + T_{se}^2}. \tag{11}$$

And estimate the temperature at time K:

$$T_k = T_{k-1} + Kg * (T_s - T_{k-1}). \tag{12}$$

Solve the optimal deviation at time T_k:

$$T_{oe} = \sqrt{(1 - Kg) * T_{pe}^2}. \tag{13}$$

Iteratively process the calculated temperature at T_{k+1} and the measured temperature to obtain more realistic temperature data.

It should be noted that if the monitored data is very far away from the corresponding road section, it can be determined with a high probability that the detected location point is not on the road section. However, if the GPS signal has a large error, the above situation will also occur. Therefore, under this background, this article gives a related optimization plan, through which this kind of situation can be avoided, thereby improving the accuracy of trajectory correction. The relevant calculation formula is as follows:

$$p(y_x \mid p_x = p_i). \tag{14}$$

In the calculation process, taking into account the GPS noise during the transportation process, the value of the element in the observation probability matrix is set as

$$bi = p(y_x \mid p_x = p_i) = \frac{1}{\sqrt{2\pi\sigma}} e^{\left(\frac{\|y_x - p_i\| gc}{\sqrt{2}\,\sigma}\right)^2}. \tag{15}$$

Among them, σ is the standard deviation of GPS measurements. When solving the state transition probability function, there is no need to consider the positioning information relationship between the devices; only the information between the real positions is considered. If the distance between the two candidate real positions is shorter, the probability that the two candidates actually undergo a state transition is also greater. Based on the above situation, it can be seen that the state transition probability is proportional to the distance between candidate points.

The relevant calculation formula is as follows:

$$aij = p(p_{x+1} = p_j \mid p_x = p_i) \propto e^{-\beta d_{ij}}. \tag{16}$$

Table 3: First-level index weight judgment matrix.

First level indicator	U1	U2	U3	U4
Organizational structure of the internet of things U1	1	1/5	1/3	3
IoT benefits u2	5	1	3	7
RFID technology U3	3	1/3	1	9
GPS/GIS technology U4	1/3	1/7	1/9	1

The initial state probability of the vehicle trajectory model can be expressed as

$$p(y_1 \mid p_1 = p_i). \tag{17}$$

The path solved by the Vibit algorithm will correspond to a hidden state sequence. Its iterative principle formula is as follows:

$$\begin{aligned} \delta_{t+1}(i) = &\max_{i_1, i_2, \ldots, i_{t-1}} P(i_{t+1} = i, i_t, \ldots, i_1, o_{t+1}, \ldots, o_1 \mid \lambda) \\ &\max_{1 \le j \le N} \left[\delta_t(j) a_{ji}\right] b_i(o_{t+1}), i = 1, 2, \ldots N; \\ &t = 1, 2, \ldots, T-1. \end{aligned} \tag{18}$$

Then, in time t, the maximum probability node of a single path is

$$\Psi_t(i) = \underset{1 \le j \le N}{\operatorname{argmax}} \left[\delta_{t-1}(j) a_{ji}\right] b_i(o_{t+1}), i = 1, 2, \ldots N. \tag{19}$$

In the actual survey process, the original data was obtained through questionnaire surveys, and the corresponding weight judgment matrix was determined by comparing the importance of indicators. First-level index weight judgment matrix is shown in Table 3. IOT organizational structure U1 weight judgment matrix is shown in Table 4. Secondary index score is shown in Table 5.

(1) Data that requires stable temperature and humidity:
In the process of data processing, the temperature of the cold chain vehicle is set to $T = 5^{\circ}\mathrm{C}$, and then the values of Tpe, Kg, Tk, and Toe are calculated according to the smooth data error correction algorithm of Kalman filtering.

(2) Latitude and longitude:

Choose about 500 anchor points, and the time interval between each anchor point is s to obtain ten trajectory data sets. The time is stored in a unix timestamp format for convenience. Some data are shown in Table 6.

4. Demand Analysis and System Realization of International Trade Management

4.1. International Trade Management Demand Analysis. Through the LAMP trade management system, users can conveniently and quickly query relevant data and information, while also reducing management costs, making enterprise management systematized and accurate. The system management module is composed of many

Table 4: IOT organizational structure U1 weight judgment matrix.

Organizational structure of the internet of things U1	U11	U12	U13	U14
Internet of things U11	1	1/6	1/5	1/3
Internet of things technology U12	6	1	3	2
Talent U13	5	1/3	1	3
System flexibility U14	3	1/2	1/3	1

Table 5: Secondary index score.

Impact level\secondary index standard	Very satisfied	Quite satisfied	General	Not so satisfied	Very dissatisfied
IoT devices	0.2	0.3	0.3	0.1	0.1
Internet of Things technology	0.3	0.4	0.2	0.1	0.0
Talent allocation	0.1	0.2	0.4	0.2	0.1
System flexibility	0.2	0.4	0.2	0.1	0.1
Business operations	0.1	0.4	0.2	0.1	0.2
Total operating cost	0.1	0.5	0.2	0.1	0.1
Service quality	0.2	0.1	0.1	0.3	0.3
Information processing level	0.4	0.3	0.1	0.1	0.1
Information collection	0.2	0.5	0.2	0.1	0.1
Agricultural product traceability	0.3	0.4	0.1	0.1	0.1
Temperature and humidity control	0.4	0.3	0.2	0.1	0.0
Information security	0.2	0.3	0.2	0.2	0.1
Distribution vehicle skeleton	0.4	0.3	0.2	0.1	0.0
Delivery vehicle positioning	0.2	0.5	0.1	0.1	0.1
Warehouse location setting	0.3	0.3	0.2	0.2	0.0
Comprehensive map query	0.0	0.2	0.4	0.2	0.2

Table 6: Partial data of trajectory data set.

Coordinate system	Longitude	Latitude	Positioning time (unix timestamp)	Speed (km/h)
BD09	118.9430657846885	32.117O51885385809	1544569487	32.09
BD09	118.94337778538228	32.1I619665702898	1544369492	32.22
BD09	118.94353585 19896	32.115779705285238	1544569497	32.84
BD09	118.94582966804825	32.115190979212808	1544569502	36.26
BD09	118.9441687O733784	32.11463515998318	1544569507	38.61
BD09	118.94441540247716	32.11411700783336	1544369512	39.21
BD09	118.94471602414238	32.11361997022351	1544569517	40.09
BD09	118.945O6685865O49	32.113045092045648	1544569522	42.07
BD09	118.94533914710071	32.11259178169525	1544369527	41.83

management subsystems, and the administrator manages the whole by manipulating the subsystems. The management system mainly provides managers with the following two aspects of help: first, manage employee information. Second, the system administrator can back up, restore, and manage the information in the database. At the same time, the system also restricts the administrator's authority and functions to a certain extent to ensure the safety of the entire system, thereby providing convenience for international trade management activities.

The purchasing management module of the system is usually controlled by purchasing personnel. The specific business process is as follows: first, the purchasing personnel determine the purchase list according to the actual situation, and the management and modification of the list are controlled by the purchasing personnel. After receiving the purchase list, the purchasing department confirms the content of the purchase order. The system combines the data and information of each supplier in the database to make a comprehensive judgment and gives the most cost-effective supplier information. The purchasing department conducts actual negotiation with the supplier based on the information provided by the system and then confirms the purchase.

The inventory management module provides support for warehouse administrators in the following activities: product storage, product delivery, supplier information management, and product viewing. The data analysis module is solely responsible for the corporate accounting. The accountant can perform the following activities in the system data analysis module: manage loss information, manage financial information, and query out-of-stock information.

4.2. Implementation of an International Trade Management System. System management mainly includes four aspects: data security, administrator, user management, data backup and recovery, and authority management. The system has a

strong ability to protect information. When the computer is running the system, if the user leaves in the middle, the system will automatically lock the computer to protect the important information from being read by others. At the same time, the system gives the administrator an important authority, which is to modify the login restrictions of ordinary users.

The procurement management module is the most critical and core part of the entire system. This module is responsible for purchasing planning, expediting, checking, and receiving warehouse, settlement and payment, etc. At the same time, the procurement management module realizes a global material supply cycle. The main process of procurement management is as follows: the buyer determines the purchase list in the purchase interface according to the actual situation, the system sends the purchase information to the supplier, and then the supplier is responsible for transporting the purchased materials. After the materials arrive, the inspection department will proceed according to the purchase list acceptance. Therefore, the inventory management module must have three functions: inbound acceptance, outbound acceptance, and raw material inventory inquiry.

Sales are inseparable from any commodity, so the sales management module is also an extremely important part of the system. The sales management module provides sales forecasts, sales plans, and sales contracts for corporate sales personnel, as well as a series of information about product sales to improve the core competitiveness of the company in the commercial field. The data analysis module uses a series of high-tech methods such as big data, the Internet, and intelligent algorithms to analyze the current operating conditions and competitive environment, while giving correct judgments. The data analysis module can truly understand the market and can respond to market changes in a timely and effective manner.

5. Conclusion

The rapid development of the Internet of Things technology makes the Internet of Things platform based on the Internet of Things technology spring up like mushrooms. The emergence of the Internet of Things platform has greatly facilitated our daily lives and has also greatly improved people's work efficiency. However, at present, there are multiple communication standards and mechanisms in the Internet of Things platform. How to quickly and conveniently exchange information between different devices is a key issue that we must consider in the research process of Internet of Things middleware. The article selects the Internet of Things middleware in the cold chain transportation link as the research object and designs an Internet of Things middleware framework for cold chain transportation tracking by analyzing various aspects of the transportation process. In addition, in order to better deal with the communication obstacles between different sensors and filter the redundant data in the sensors, we adopted D-Bus technology and designed the communication means between different sensors. The development and utilization of the international trade management system can reduce some tedious and inconvenient manual operations, make the recording and statistics of international trade information very simple, improve work efficiency, and, at the same time, meet the information needs of various departments, so that enterprises can minimize cost and better select suppliers, products, and customer information, so that enterprises can obtain better economic benefits.

Data Availability

The data used to support the findings of this study are available from the corresponding author upon request.

Conflicts of Interest

The authors declare that they have no conflicts of interest.

Acknowledgments

This work was supported by Wuhan College.

References

[1] L. Atzori, A. Iera, and G. Morabito, "The internet of things: a survey," *Computer Networks*, vol. 54, no. 15, pp. 2787–2805, 2010.

[2] V. Adat and B. B. Gupta, "Security in internet of things: issues, challenges, taxonomy, and architecture," *Telecommunication Systems*, vol. 67, no. 3, pp. 423–441, 2018.

[3] X. Wang, X. Li, D. Fu, R. Vidrih, and X. Zhang, "Ethylene sensor-enabled dynamic monitoring and multi-strategies control for quality management of fruit cold chain logistics," *Sensors*, vol. 20, no. 20, p. 5830, 2020.

[4] F. Qiu, G. Zhang, P. K. Chen et al., "A novel multi-objective model for the cold chain logistics considering multiple effects," *Sustainability*, vol. 12, no. 19, p. 8068, 2020.

[5] N. Ahmed, M. Rutten, T. Bessell, S. S. Kanhere, N. Gordon, and S. Jha, "Detection and tracking using particle-filter-based wireless sensor networks," *IEEE Transactions on Mobile Computing*, vol. 9, no. 9, pp. 1332–1345, 2010.

[6] J. W. Han, M. Zuo, W. Y. Zhu, J. H. Zuo, E. L. Lü, and X. T. Yang, "A comprehensive review of cold chain logistics for fresh agricultural products: current status, challenges, and future trends," *Trends in Food Science & Technology*, vol. 109, pp. 536–551, 2021.

[7] F. Wu and J. Ma, "The equilibrium, complexity analysis and control in epiphytic supply chain with product horizontal diversification," *Nonlinear Dynamics*, vol. 93, no. 4, pp. 2145–2158, 2018.

[8] M. J. Smith, H. Benítez-Díaz, M. Á. Clemente-Muñoz et al., "Assessing the impacts of international trade on CITES-listed species: current practices and opportunities for scientific research," *Biological Conservation*, vol. 144, no. 1, pp. 82–91, 2011.

[9] R. Zheng, X. Xu, J. Xing et al., "Quality evaluation and characterization of specific spoilage organisms of Spanish mackerel by high-throughput sequencing during 0 °C cold chain logistics," *Foods*, vol. 9, no. 3, p. 312, 2020, https://doi.org/10.3390/foods9030312.

[10] T. Potts and M. Haward, "International trade, eco-labelling, and sustainable fisheries–recent issues, concepts and practices," *Environment, Development and Sustainability*, vol. 9, no. 1, pp. 91–106, 2007.

[11] E. Brynjolfsson, X. Hui, and M. Liu, "Does machine translation affect international trade? Evidence from a large digital platform," *Management Science*, vol. 65, no. 12, pp. 5449–5460, 2019.

[12] F. R. Seringhaus and P. J. Rosson, "Firm experience and international trade fairs," *Journal of Marketing Management*, vol. 17, no. 7-8, pp. 877–901, 2001.

[13] O. K. Essandoh, M. Islam, and M. Kakinaka, "Linking international trade and foreign direct investment to CO2 emissions: any differences between developed and developing countries?" *Science of the Total Environment*, vol. 712, p. 136437, 2020.

[14] J. E. Laird, C. Lebiere, and P. S. Rosenbloom, "A standard model of the mind: toward a common computational framework across artificial intelligence, cognitive science, neuroscience, and robotics," *AI Magazine*, vol. 38, no. 4, pp. 13–26, 2017.

[15] D. Mendez Mena and B. Yang, "Decentralized actionable cyber threat intelligence for networks and the internet of things," *IoT*, vol. 2, no. 1, pp. 1–16, 2020.

[16] D. H. Castillo-Martínez, A. J. Rodríguez-Rodríguez, A. Soto et al., "Design and on-field validation of an embedded system for monitoring second-life electric vehicle lithium-ion batteries," *Sensors*, vol. 22, no. 17, p. 6376, 2022.

[17] S.-C. Chen, "Is artificial intelligence new to multimedia?" *IEEE MultiMedia*, vol. 26, no. 2, pp. 5–7, 2019.

[18] F. Tang, B. Mao, Y. Kawamoto, and N. Kato, "Survey on machine learning for intelligent end-to-end communication toward 6G: from network access, routing to traffic control and streaming adaption," *IEEE Communications Surveys & Tutorials*, vol. 23, no. 3, pp. 1578–1598, 2021.

Hindawi
Computational Intelligence and Neuroscience
Volume 2023, Article ID 9762702, 1 page
https://doi.org/10.1155/2023/9762702

Retraction

Retracted: Innovation and Reform of Ideological and Political Course Mode in Colleges and Universities Based on Big Data Network Platform

Computational Intelligence and Neuroscience

Received 22 August 2023; Accepted 22 August 2023; Published 23 August 2023

This article has been retracted by Hindawi following an investigation undertaken by the publisher [1]. This investigation has uncovered evidence of one or more of the following indicators of systematic manipulation of the publication process:

(1) Discrepancies in scope

(2) Discrepancies in the description of the research reported

(3) Discrepancies between the availability of data and the research described

(4) Inappropriate citations

(5) Incoherent, meaningless and/or irrelevant content included in the article

(6) Peer-review manipulation

The presence of these indicators undermines our confidence in the integrity of the article's content and we cannot, therefore, vouch for its reliability. Please note that this notice is intended solely to alert readers that the content of this article is unreliable. We have not investigated whether authors were aware of or involved in the systematic manipulation of the publication process.

Wiley and Hindawi regrets that the usual quality checks did not identify these issues before publication and have since put additional measures in place to safeguard research integrity.

We wish to credit our own Research Integrity and Research Publishing teams and anonymous and named external researchers and research integrity experts for contributing to this investigation.

The corresponding author, as the representative of all authors, has been given the opportunity to register their agreement or disagreement to this retraction. We have kept a record of any response received.

References

[1] D. Qiu, "Innovation and Reform of Ideological and Political Course Mode in Colleges and Universities Based on Big Data Network Platform," *Computational Intelligence and Neuroscience*, vol. 2022, Article ID 1036168, 9 pages, 2022.

Hindawi
Computational Intelligence and Neuroscience
Volume 2022, Article ID 1036168, 9 pages
https://doi.org/10.1155/2022/1036168

Research Article

Innovation and Reform of Ideological and Political Course Mode in Colleges and Universities Based on Big Data Network Platform

Dandan Qiu

College of Marxism, Jilin Jianzhu University, Changchun, Jilin 130008, China

Correspondence should be addressed to Dandan Qiu; 19407097@masu.edu.cn

Received 14 June 2022; Accepted 11 August 2022; Published 16 September 2022

Academic Editor: Gopal Chaudhary

With the continuous development of the computer field, the Internet has become the main way of education in today's era. The development of computer technology and big data has brought innovation and opportunities to the teaching mode of ideological and political courses in colleges and universities. Due to the dynamic change of big data, there are many difficulties in the establishment of ideological and political course models in colleges and universities. This paper studies the innovation of ideological and political course modes in colleges and universities on the network platform under the background of big data. This paper mainly compares the traditional teaching mode and explores the formal modeling method of network platform education. The discrete dynamic modeling technology of the complex system is used to model the formal process of online education. Then, it carries out nonlinear prediction modeling for the operation efficiency and traffic change of the network platform under the big data environment and uses dynamic modeling to predict the learning effect of college students' ideological and political course mode. The results show that the formal method of education under dynamic modeling can improve the defects of traditional teaching and give full play to the advantages of network platform teaching. Improving the teaching mode of network platform can improve students' learning efficiency. Finally, in the dynamic model prediction, the problem of big data affecting the model results is improved, and the accuracy of the prediction model is improved.

1. Introduction

According to the statistics of network information platforms, the student group accounts for the largest proportion in the classification of Internet users [1] followed by workers and journalists. Most students have mastered the basic user functions of the Internet and can independently query, obtain information, and communicate [2]. Therefore, the teaching environment in colleges and universities should also be optimized and improved in combination with network technology [3]. Combining the traditional teaching mode and educational concept with new technology to adapt to the development of the times is our focus [4]. The main work of ideological and political courses in colleges and universities is to establish the correct three concepts and improve students' moral quality and political level. The ideological and political theory course undertakes the task of systematic Marxist theory education for college students. It is an important position to consolidate the guiding position of Marxism in the ideological field of colleges and universities and adhere to the direction of socialist school running. It is the main channel and core course to comprehensively implement the party's educational policy and the fundamental task of building morality and cultivating people. It is the soul course to strengthen and improve the ideological and political work in colleges and universities and realize the connotative development of higher education. With the promulgation of national policies, many schools have focused on the content of ideological and political education [5]. However, the traditional teaching mode and concept are relatively single and cannot be better integrated into Internet thought [6]. Due to the limitations of technical means and

analysis methods, the collection of students' various demands and information mainly adopt the form of a manual sampling survey, but this form will make the survey results too general and inaccurate. Using inaccurate information as the basis for carrying out ideological and political theory teaching activities in colleges and universities will obviously directly affect the effectiveness of education. With the introduction of information technology, many schools gradually began to adopt online teaching mode and integrate Internet information to carry out education. With the use of the network platform, the teaching content of ideological and political courses in colleges and universities has been gradually enriched and the teaching environment has been improved [7]. The network platform model under the big data environment cannot only open the school's publicity channels, reduce the school's education cost but also expand the scope of students' communication [8, 9]. Because online education is different from the traditional education model, although it can improve students' participation in the classroom, there are also problems such as face-to-face communication between teachers and students [10]. Based on the abovementioned situation, many educational researchers have proposed to apply big data dynamic modeling technology to college classroom models. Dynamic modeling is a technology for processing dynamic data supported by complex systems [11]. It can filter interference data in massive data information and get accurate results. At present, the formal teaching modeling proposed by combining big data technology with subject theory teaching is the main method to deal with the defects of network platform teaching mode [12]. At present, China's Internet coverage is gradually expanding, and mobile terminals are widely popularized. On the basis of continuing to adhere to the traditional advantages, the ideological and political theory course in colleges and universities should actively realize the integration, mutual assistance, and progress with big data technology, form a new idea of combining traditional advantages with big data technology, and enhance the liveliness and attractiveness of the traditional model. For example, we can use the support of big data information and network technology to conduct preclass research and prediction; in class monitoring and analysis; and after class inspection and feedback are integrated into the whole process of lesson preparation, teaching, and assessment of ideological and political theory courses.

This paper is mainly divided into three parts. The first part briefly describes the main problems and solutions of the network platform mode of ideological and political courses in colleges and universities under the big data environment and analyzes the application status of dynamic modeling technology in various countries. The second part mainly uses big data dynamic modeling technology to study the formal modeling of ideological and political course modes. Finally, it explores the operation efficiency and influencing factors of network platforms under the background of dynamic data, and forecasts the learning effect of students' network platforms through the prediction model of complex systems. The third part analyzes the results of the research on the dynamic modeling of the network platform in the mode of ideological and political courses in colleges and universities under the background of big data.

2. The Related Works

With the advent of the big data era, many schools use computer technology to form a dynamic interactive platform to carry out educational work [13]. Most online education platforms can change the complex process in the traditional teaching mode and simplify students' learning process [14]. The dynamic information of the Internet is used as the current news in the learning content, and the teaching demonstration is carried out by means of video, audio, pictures, and so on. The traditional teaching mode has some problems, such as the teaching content is not direct, while the online environment of the network platform can intuitively show the students' learning content and let the learners form a three-dimensional knowledge impression [15]. However, in the Internet big data environment, students will encounter a lot of bad information when using the network platform. This bad information and useless news will have a bad impact on students' physical and mental content [16]. The emergence of a lot of junk information is easy to make immature, unstable three values and poor judgment students have confused cognition [17]. There are no strict regulations on the use of network platforms. This loose network environment is easy for students to express their own comments and opinions. If students' moral quality is affected, it will have an irreparable impact [18]. Therefore, with the support of big data information, we need to build an ideological and political course network platform education model to improve students' learning environment. In the construction of ideological and political network platform, we should pay attention to updating the concept of ideological and political education; expanding the space and channels of ideological and political education by using modern and advanced network information means; improving the pertinence, effectiveness, attractiveness, and appeal of ideological and political education; actively exploring effective ways to innovate the ideological and political education of college students; and gradually forming a theme website target orientation that conforms to the ideological reality of our students. Let students combine ideology and morality with the use of the Internet. In order to distinguish between bad information and interference data, we use dynamic modeling technology to formally model the teaching mode [19].

The UK combines big data dynamic modeling technology with information network structure to form an intelligent information processing system [20]. Research on multi-source data fusion in complex data information environment. The combined dynamic modeling technology is applied to the power system to solve the problems of poor data test accuracy in power engineering.

The United States focuses on the privacy of Internet information, and they are ahead in the development of big data technology [21]. With the rapid efficiency of data flow, security and privacy have become the focus of people's attention. In order to solve the problem of poor performance

of privacy protection systems, researchers proposed the modeling of complex network security systems. The experimental results show that the security system can effectively protect users' personal information.

French researchers applied dynamic modeling technology to severe weather prediction [22]. With the expansion of global warming trend, bad environment and bad weather occur frequently. Many cities are vulnerable to tornadoes and rainstorms. The establishment of risk early warning and prediction models based on big data complex systems can improve people's ability to judge the environment. This model cannot only predict environmental changes but also carry out a risk assessment and loss assessment [23, 24].

China applies big data dynamic modeling technology to the field of education, including data modeling in mathematics classrooms [25, 26]. Let students intuitively understand the changes and principles of mathematical models. With the continuous improvement of people's living standards through big data technology, ideological, and political education is also an open and complex system. Based on the development status of big data dynamic modeling technology in various countries, this paper puts forward the research on dynamic modeling in the network platform mode of ideological and political courses in colleges and universities under the big data environment.

3. Research on Dynamic Modeling of Ideological and Political Course Mode Innovation in Colleges and Universities Based on Big Data Network Platform

3.1. Research on Formal Dynamic Modeling of Ideological and Political Education in Colleges and Universities Based on Big Data Network Platform. At present, Internet online platform teaching has become the main research direction of the new education model. Compared with the traditional teaching environment, online teaching has many defects, which cannot meet the requirements of face-to-face communication between teachers and students. The interactivity is poor because the teaching process does not require strict synchronization in time and space, resulting in poor interactivity. Students cannot put forward the problems encountered in the process in a timely and effective manner, nor can they give clear and clear answers in real-time. Although the technology of enhancing interactivity is widely used in the teaching process, its effect is much inferior to that of traditional process communication, which is also a disadvantage. In order to overcome the defects of network platform teaching mode, we need to integrate big data technology and education methods. In the process of ideological and political teaching in colleges and universities, teaching activities are an auxiliary coordination way. In order to intuitively analyze the teaching process of ideological and political courses and effectively guide students' learning activities, we need to practice educational principles. The analysis teaching process is divided into two stages. One is to analyze the learning content, the other is to analyze

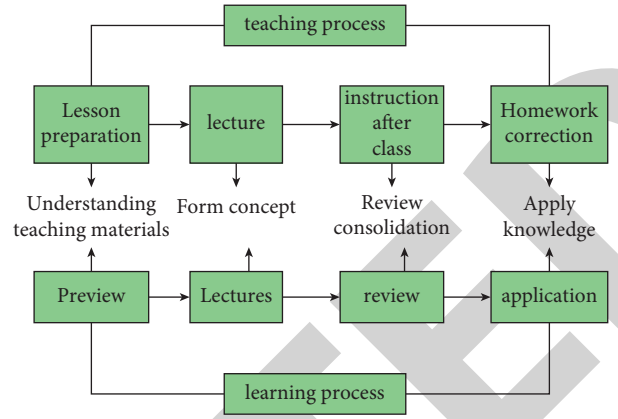

Figure 1: Relationship between professor and learning system.

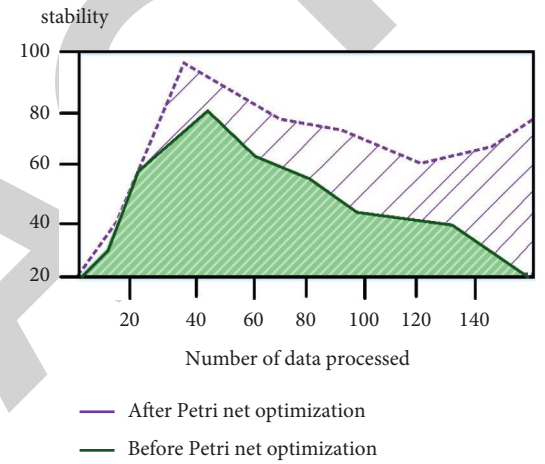

Figure 2: Comparison diagram of system stability before and after Petri net optimization.

the teaching process. Only under the condition of mutual adaptation and integration can a correct teaching method be formed. The teaching process of ideological and political courses mainly includes lesson preparation, lecture, homework after class, homework correction, and so on. The learning process is divided into preview, listening, review, and other stages. In order to explore the innovative content of ideological and political course models in colleges and universities, we need to analyze the relationship between professors and learners, as shown in Figure 1.

It can be seen from Figure 1 that the teaching link and learning link are connected and adapt to each other. They interact and can influence each other. The first stage is the key premise of imparting knowledge, and the second stage is the core content of the teaching process. Through the analysis of the relationship between them, we can know that the teaching mode of ideological and political courses is not only a complex system structure but also a nonprocess and nonlinear link. Network platform system is also a computer system, which needs to be formalized strictly. Therefore, we formally model the teaching mode of ideological and political courses in colleges and universities and build a network platform for ideological and political course teaching

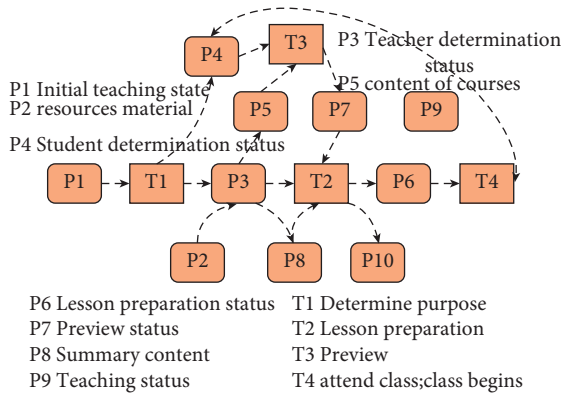

Figure 3: Formal dynamic model of network teaching of ideological and political course under Petri net system.

systems. This formal modeling is dynamic. Through the analysis of asynchrony in the learning process, we know that teaching and learning are interrelated. In addition, the educational process also includes concurrency and uncertainty. The comparison of the distribution of online education on the network platform shows that the traditional teaching mode cannot share resource information. In dealing with this sharing mode, we use discrete dynamic modeling Petri net to analyze it. Petri net is a tool for describing data in large data complex systems. It can effectively deal with concurrent, distributed, and uncertain data information. In the data system, we will use Petri nets to analyze the stability of the system before and after processing big data, as shown in Figure 2.

It can be seen from Figure 2 that with the increase in the amount of data to be processed, the modeling system optimized by Petri net can quickly solve complex data problems and improve the stability of the model. Compared with the traditional system without Petri net optimization, its functionality has been effectively improved. System variables need to be initialized and defined first as:

$$N_1 = B; E; F; c_{\text{in}}. \tag{1}$$

After the initialization definition, we define the modality of the directed variables of the basic network as:

$$c_{\text{in}} = \{s_1, s_2, s_3\} B = \{s_1, s_2, s_3, s_4\} E = \{a, b\}, \tag{2}$$

where $B = \{s_1, s_2, s_3, s_4\}$ is the condition set and $E = \{a, b\}$ is the event set. The whole system is a completely closed structure with connectivity. After the condition content and event content are specially defined, we can simulate the data information of the initial system. When the difficulty of learning content is different, we find that a formal system can be used for teaching description. Because there are many definitions of elements in the teaching link, most of them have their own meanings, so we need to add Petri nets for formal descriptions. Firstly, the elements generated in teaching activities are classified, and then the formal dynamic modeling model of ideological and political course network teaching under Petri net system is constructed, as shown in Figure 3.

As can be seen from Figure 3, the nodes of the system structure include variable parameters, which are mainly composed of teacher status, student status, teaching materials, teaching purpose, etc. According to the formal dynamic modeling model, we can define the modeling formula of the system as:

$$\psi = R, T, F, C, I_-, I_+, M_0. \tag{3}$$

The abovementioned variables are the meanings of nodes in the corresponding system. Due to the teacher's class process, students can ask questions and answer questions independently. Therefore, Petri net is a simplified system of adaptive cyclic rules. It can eliminate the unnecessary process in the teaching link and improve the operation efficiency of the whole model. Compare the operation efficiency of the network platform teaching system before and after Petri net optimization, as shown in Figure 4.

It can be seen from Figure 4 that the teaching system optimized by dynamic modeling Petri net can process a large amount of student information. With the increase of student data, the operation efficiency of the system does not decline. The course of dynamic data modeling includes theory and practice. For the theoretical course of ideological and political courses, we mainly use the modeling method to improve it. Be able to analyze students as the main body of learning. Firstly, take examples as cases in the network platform, and take mastering knowledge and learning ideas as the key content of cultivating students. According to the complex information in the big data environment as the basis for knowledge expansion, students will be brought into the actual problem situation for learning. Finally, for the purpose of correctly expressing their ideas, the learning effect is displayed in the form of dynamic modeling. According to the abovementioned research, Petri net can optimize the performance of the whole network teaching platform and provide effective technical support for the innovation of ideological and political course modes in colleges and universities.

3.2. Research on Dynamic Modeling of Learning Effect Prediction of College Ideological and Political Course Network Platform Based on Big Data Environment. Compared with the traditional teaching mode, teachers on the network teaching platform cannot accurately grasp the current learning state of students. Through the investigation, it is found that most students' learning attitude in the online teaching process is not correct, and their class concentration is not strong. They are often late for the first online class in the morning, and they cannot answer the questions by roll call in class. Some students even use their computers to have classes while playing games on their mobile phones. Some students even sleep while listening to the online live class. According to the background data of superstars, the ratios of submitting homework and completing homework are 46% and 65%, respectively. Students often ask their teachers to hand in their homework after class. With the popularization of network teaching platforms, the resource information of related courses is becoming more and more extensive.

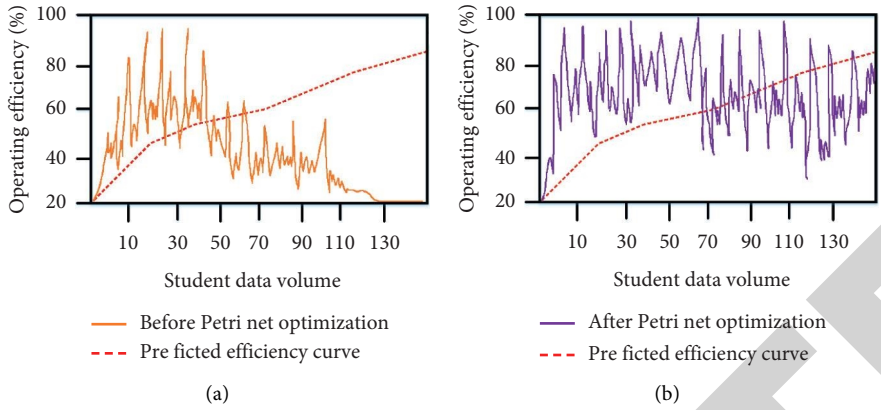

Figure 4: Comparison of operation efficiency of network platform teaching system before and after Petri net optimization.

Online teaching has become an indispensable member of the classroom of primary and secondary schools. In the big data environment, when the network platform uses teaching resources, it is easy to produce a large number of garbage data and browsing records. Some of these browsing records can represent students' learning traces and learning status. Through the analysis and retrieval of historical trace information, we can immediately understand the learning effect of students on the network platform. Before the prediction of students' learning effect, it is necessary to analyze the data flow in the big data system and detect the length and efficiency of students' learning according to the change in data flow. Big data dynamic modeling technology can model and predict the data flow and judge the changing trend and historical trend of the whole network data. Then the prediction results are provided to teaching workers to analyze the use effect of the platform independently. In the use of prediction models, most researchers use periodic modeling to predict and analyze the trend according to the periodic changes in data. However, periodic modeling can only describe the local change characteristics of data flow, not the change of dynamic data. The stability of periodic model is also poor, and the accuracy of model prediction decreases with the increase of users. Therefore, this paper uses big data dynamic discrete modeling to improve the prediction effect of the system. We use the computing model to process massive data, form a distributed state, and define the discrete model. The basic working principle is to divide the data into small sets of tasks and use different nodes to execute the tasks. In order to solve the bottleneck problem of the model, we define input variables, storage variables, and output variables as:

$$\begin{aligned} u(n) &= \left(u_1(n), u_2(n), \ldots, u_K(n)\right)^T, \\ x(n) &= \left(x_1(n), x_2(n), \ldots, x_N(n)\right)^T, \\ y(n) &= \left(y_1(n), y_2(n), \ldots, y_L(n)\right)^T, \end{aligned} \tag{4}$$

$u(n)$, $x(n)$, and $y(n)$ are input, storage, and output variables, respectively. At a certain time, the updated state equation and calculation formula of the network system are as follows:

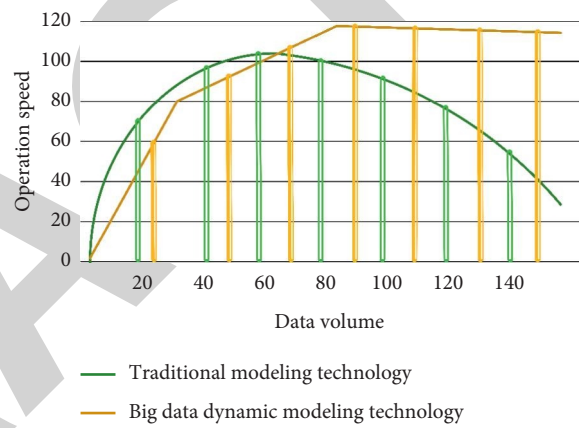

Figure 5: Comparison of operation speed between them in processing a large amount of data.

$$\begin{aligned} x(n+1) &= f_1\left(W^{\text{in}}u(n+1) + Wx(n)\right), \\ y(n+1) f_2\left(W^{\text{out}}u(n+1)\right). \end{aligned} \tag{5}$$

In the formula, W^{in}, W^{out}, f_1, and f_2 represent the parameter connection weight value and activation function of the computer system, respectively. The steps of the whole system structure are as follows: initialize according to the problem, define parameter variables, and establish the expected relationship between parameter samples and prediction samples. In the feedback elimination state, the abovementioned variable parameters are fixed, and the following formula can be obtained by training the subsequent model as:

$$W^{\text{out}}x(n) \approx y_t(n+1). \tag{6}$$

According to the formula, it can be judged that the vector $x(n)$ is represented by $u(n)$, and the relationship between them is:

$$u(n) \longrightarrow y_t(n). \tag{7}$$

We represent the state vector of the participation matrix with the training objective:

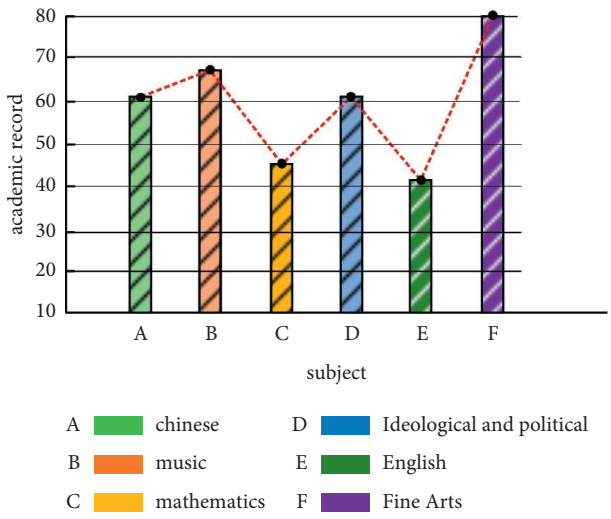

Figure 6: Trend chart of students' scores in various subjects.

$$Y = W^{\text{out}} X$$
$$\min \left| Y - Y_t \right|^2 \tag{8}$$
$$W^{\text{out}} = Y_t \times X^{+}.$$

There is an inverse matrix definition in the above-mentioned formula and the variable X^{+} is the parameter representative of the inverse matrix. Finally, the actual output value is predicted according to the training results as:

$$\hat{y}(n) = W^{\text{out}} x(n). \tag{9}$$

We compare the big data dynamic modeling technology with the traditional modeling technology to explore their operation speed in processing a large amount of data, as shown in Figure 5.

It can be seen from Figure 5 that the big data dynamic modeling technology can handle the calculation of dynamic complex data and improve the running speed of the model. The traditional modeling technology image is a falling curve, and the operation will be slower with the increase in the amount of data. Finally, according to the changing trend of big data information, this paper analyzes the learning effect of students' ideological and political courses on the online platform. In this paper, the decision tree algorithm ID3 in discrete dynamic modeling is used for research. This algorithm has high calculation accuracy and dynamic data processing function. ID3 algorithm takes the data as the variable of node redundancy and uses node splitting for evaluation. The node definition formula is as follows:

$$\text{Entropy}(t) = -\sum_{c=1}^{c} p(c \mid t) \log_2 p(c \mid t). \tag{10}$$

In practice, in order to avoid the over-fitting problem of data, we usually use the data growth rate instead of the evaluation standard. We randomly selected the academic performance of some students in the university database as the prediction data. First, compare the performance trends of students in various subjects, as shown in Figure 6.

As can be seen from Figure 6, there is little difference between the average score for Chinese and ideological and political courses, and the score for mathematics is poor. In contrast to the above, in order to test the effectiveness of the model, we divide the students into two parts. One part adopts the traditional offline teaching mode; the other part adopts the network platform teaching mode. A control group was established to track the ideological and political and Chinese scores of the students in the two parts, as shown in Figure 7.

It can be seen from Figure 7 that the scores of students, who use the network platform to teach ideological and political courses and Chinese courses have been improved, and the rising effect of ideological and political courses is greater than that of Chinese courses. Therefore, it can be proved that the high-efficiency ideological and political course model innovation system based on a big data network platform has a positive impact on students' learning effect. The traditional ideological and political education is mainly based on the simple indoctrination education mode, which is boring and lacks of vividness and flexibility. Network ideological and political education takes advantage of the characteristics of a large amount of network information, fast transmission speed, and strong influence, integrate other media, such as newspapers, radio, and television, enriches the content of ideological and political education, so as to enhance the attraction of network ideological and political education, and also enable the educated students to receive information independently and sublimate their thoughts.

4. Analysis of Dynamic Modeling Research Results of Ideological and Political Course Mode Innovation in Colleges and Universities Based on Big Data Network Platform

4.1. Analysis of Research Results of Formal Dynamic Modeling of Ideological and Political Education in Colleges and Universities Based on Big Data Network Platform. In the process of school education, the level of students' learning ability is not balanced. We divide students' learning ability into low level, intermediate level, and high level. In order to study the impact of big data network platforms on the innovation of ideological and political course modes in colleges and universities, we analyze the characteristics of teaching activities in the school and require teachers to teach only one specified course at the same time. Set the learning process of students as preview and review, and judge the learning situation of students at three levels according to the length of learning time. Students' basic learning knowledge shall be evaluated according to the content of the syllabus, as shown in Figure 8.

It can be seen from Figure 8 that students with advanced learning abilities have the best performance in learning on the network platform. With the increase in review and preview time, the performance changes more and more.

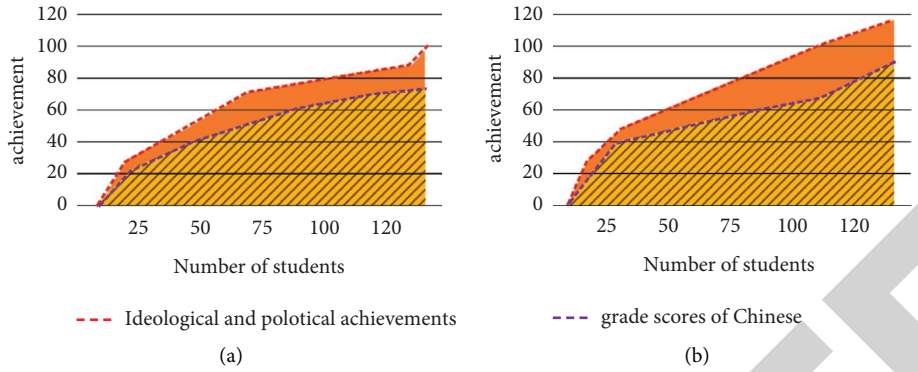

Figure 7: Comparison between network platform teaching and traditional teaching. (a) Traditional teaching mode. (b) Network teaching mode.

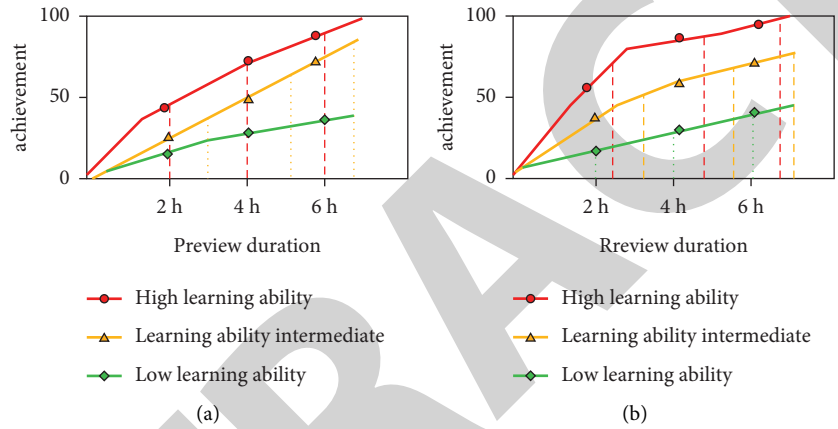

Figure 8: Comparison chart of changes in learning ability.

Therefore, we can judge that students with low learning ability can improve learning efficiency after preview and review. Therefore, the system optimized by Petri net can achieve positive help to students' achievement in dealing with nonlinear formal teaching.

4.2. Dynamic Modeling and Analysis of Learning Effect Prediction of College Ideological and Political Course Network Platform Based on Big Data Environment. To explore the nonlinear prediction principle of data flow in the big data environment, we first need to collect a certain range of data history traces. Finally, the historical traces are divided to obtain multiple subset training samples. Finally, discrete dynamic modeling technology is used to predict the sample data. In database selection, we set one server as the initial node and the other three as auxiliary nodes. In order to analyze the advantages of data modeling, we compare the accuracy coefficient of experimental results between traditional modeling algorithm and big data dynamic modeling algorithm, as shown in Figure 9.

As can be seen from Figure 9, the accuracy of traditional modeling technology is significantly reduced by increasing the amount of data. The accuracy of the dynamic modeling technology studied in this paper remains above the standard

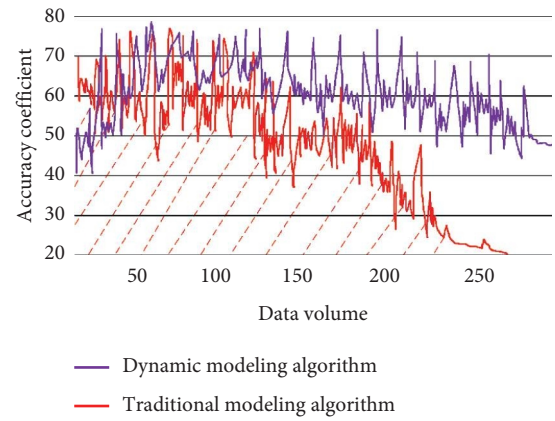

Figure 9: Accuracy comparison between traditional modeling algorithm and big data dynamic modeling algorithm.

coefficient. Therefore, dynamic modeling technology is effective and applicable to the performance of prediction models. In exploring the impact of network platforms on ideological and political courses in colleges and universities, we mainly analyze the learning effect of students. With the increase of the characteristic coefficients of the decision tree model samples, the training time of the model becomes

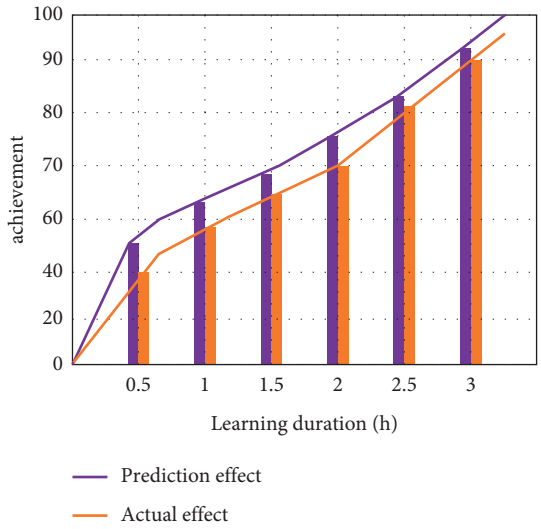

Figure 10: Comparison between prediction effect and actual effect.

longer. The more complex the structure of the model, the higher the degree of calculation, resulting in poor applicability and feedback efficiency of the model. We divide students' midterm test scores, ordinary quiz scores, and final exam scores into data of the same level. In order to improve the efficiency and accuracy of the prediction model, we use the cross-validation method to test. The data are randomly divided into several parts, half of the set is selected as the training data, and the other part is the control data. There are many influencing factors in the learning effect of students' network platforms, among which the effect of after-school homework is the greatest. We compared the time of students' online classes with the prediction rate of achievement change. Explore the gap between the predicted effect and the actual effect, as shown in Figure 10.

As can be seen from Figure 10, with the increase in students' class time on the network platform, the scores show a positive curve change. There is little difference between the prediction coefficient of dynamic data modeling and the actual coefficient, so the dynamic data modeling technology in the big data environment can accurately analyze the influencing factors and change trend of the network platform on students' learning effect.

5. Conclusion

With the Internet big data environment gradually improving people's lifestyles, school education has also established a new model. Most schools have adopted the network platform for teaching. Different from traditional teaching methods, students and teachers cannot communicate face-to-face. Therefore, teachers cannot accurately grasp students' feedback to the classroom, nor can they grasp students' current learning state. Based on the abovementioned situation, this paper studies the innovation of ideological and political course modes in colleges and universities on the big data network platform. Firstly, the big data dynamic modeling technology is used to formally model the ideological and political course on the network platform, and the teaching process and learning process in the formal modeling are analyzed. Due to a large amount of data on the network platform and the sharing of information. In this paper, Petri net is established to model and analyze the shared dynamic data, which improves the problem of data redundancy in the teaching mode and improves the stability of the teaching platform. The results show that big data dynamic modeling technology can effectively improve the system model, optimize the feedback efficiency of the education system, and improve the applicability of the network platform application. Finally, explore the impact of network platforms on students' learning efficiency. Firstly, the data mobility in the education system is analyzed. With the growth of the liquidity index, the data changes nonlinearly. Therefore, we use dynamic modeling technology to analyze the changes in the number of students using network platforms. Compare the traditional teaching mode with the network teaching mode, and compare the ideological and political course with other courses. Through the analysis of discrete dynamic modeling, the experimental results show that the network teaching mode can improve the overall learning efficiency of students. In the learning process, preview and review are also the main factors affecting students' performance changes.

Data Availability

The figures used to support the findings of this study are included in the article.

Conflicts of Interest

The authors declare that they have no conflicts of interest.

Acknowledgments

The authors would like to show sincere thanks to those technicians, who have contributed to this research. This work was supported by The National Social Science Fund of China 2020 annual project "The Research of Revolutionary Culture Identity and Transmission for 'the Generation after 00s' College Students."

References

[1] S. Zhang, "Research on mutual aid teaching mode of "online teaching platform and social platform," *Journal of Hubei Open Vocational College*, vol. 34, no. 16, pp. 137-138, 2021.

[2] J. Zhu, X. Yue, W. Zhang, and X. Tang, "Exploration on network teaching mode of programming courses," *Computer Knowledge and Technology*, vol. 17, no. 24, pp. 248-249, 2021.

[3] B. Sun, "Exploration and construction of "cloud mutual evaluation" mathematics teaching model," *Basic Education Forum*, no. 21, pp. 68-69, 2021.

[4] X. Peng and X. Hu, "Hybrid Teaching Model under the background of intelligent education," *Fujian Computer*, vol. 37, no. 6, pp. 96–99, 2021.

[5] T. Xu, "Research on higher mathematics teaching model based on network sharing platform," *Computer Knowledge and Technology*, vol. 17, no. 17, pp. 156-157, 2021.

Hindawi
Computational Intelligence and Neuroscience
Volume 2022, Article ID 9464785, 9 pages
https://doi.org/10.1155/2022/9464785

Research Article

Sponge City Planning and Information System Development Based on Geographic Information Fuzzy Processing

Mingxin Gan and Tongfang Li

University of Science and Technology Beijing, Beijing 100083, China

Correspondence should be addressed to Tongfang Li; wahahah1126@163.com

Received 6 July 2022; Revised 3 September 2022; Accepted 7 September 2022; Published 15 September 2022

Academic Editor: Gopal Chaudhary

During the development of the urban water system from 1.0 to 3.0, the impervious surface area gradually increased, hindering the natural infiltration and self-purification process of urban rainwater, resulting in serious urban water pollution, urban waterlogging in the rainy season, and groundwater problems. Since water will seep into the ground, serious water pollution will cause damage to the ground. Therefore, in dealing with urban rainwater problems, we want to use the sponge's ability to absorb and store water to build our cities into sponge cities. In this paper, we have constructed a sponge city planning and information system development based on geographic information fuzzy processing. We use differentiated fuzzy processing methods to eliminate classified information to achieve a perfect combination with nearby images and use ordinary fuzzy processing methods to solve the problem of nonconfidential information. This paper discusses the impact of natural topography on the planning and construction of sponge cities, including whether natural topography will affect rainwater, whether it will affect the distribution of different strata, and whether it will affect the utilization of groundwater resources. The basic functions of this platform are provided by a series of functions of GIS, and multiple modules are developed according to management requirements. The initial state of street view data is a lot of fisheye lens photos and corresponding point location information, which are displayed online after data preprocessing, detection information, editing information, and blurring processing.

1. Introduction

The stable development of a city depends on the city's infrastructure, strengthening people's awareness of environmental protection, improving the overall capacity of the city, improving city operation efficiency, and promoting urbanization [1]. In the conference on urban facility construction a few years ago, many people expressed some real opinions in this conference and proposed that my country's urban infrastructure construction should take the path of "green" development and proposed for the future development of my country Reasonable suggestion [2]. It is believed that the construction of sponge cities is an important turning point in the construction of urban infrastructure in my country. The earliest use of the term "sponge city" in my country comes from the method of using sponge soil to store water and fertilizer proposed by Chinese experts in the 20th century [3]. In 2010, some researchers proposed to transform the city into a sponge city, storing rainwater for later reuse during heavy rains, using rainwater for flood control and cooling on hot days, and using nature to give us resources for repeated use [4]. In 2011, researchers proposed that the "ecological sponge" area should be able to store rainwater like a sponge to facilitate subsequent use so that the rainwater can be fully utilized [5]. In 2012, another researcher proposed that the construction of a "sponge city" means that rainwater is directly discharged into a storage tank, the use of soil can seep and other reasons, combined with the recycling of rainwater and presenting it to people for visual enjoyment, to prevent urban construction from affecting the water cycle, etc., [6].

2. Methods of Fuzzy Processing of Geographic Information

2.1. Overall Platform Design. The platform is controlled by a distributed storage computing system, which includes important modules such as data processing, detection information, editing information, and fuzzy processing. The structure design is shown in Figure 1.

The software platform composed of millions of servers handles millions of data every day. The average daily input data is millions, and the total number of images generated is billions. The platform is still running in an orderly manner and the processing results are accurate. The rate is quite high, which shows that the efficiency of this module is relatively good. In addition, the module can be easily expanded horizontally to double the calculation of business data to meet the needs of larger data calculations. The initial state of street view data is a lot of fisheye lens photos and corresponding point position information, which are displayed online after data preprocessing, detection information, editing information, and blur processing. The platform function module and processing procedure are shown as in Figure 2. The first data processing refers to the screening and sorting of relevant data before relevant work is carried out. This module will work day and night and can execute commands issued by different aspects, without interfering with each other. The detection information combines the automatic identification system of the computer software with the human operating system to achieve precise identification and selection of street views with strict security information. The location information provided by it is used to reverse the calculation of the information that is at risk of leakage. This process includes identifying pictures and associated topology. Editing information refers to the identification and screening of the identified security and confidential information based on the information detection results when the information detection results do not meet the requirements. If the judgment is wrong or the screening is unqualified, it can be re-edited through manual intervention Information, to achieve the final result we get is true and reliable and can withstand scrutiny data. Blur processing refers to the use of image blurring and texture transplantation to hide information that should not appear and find its location. There are different ways to process different types of data. For example, for processing private information, the platform uses Gaussian filters to filter the privacy area, and autonomously determines the degree of blurriness of the processed area, making it difficult for people to see the processed area. When processing nonpublic information, the platform perfectly integrates the surrounding information with the processed information, instead of deleting it directly.

NG transplantation coding makes the whole area look more consistent, without any sense of violation, and it is difficult to identify whether it has been processed or not. Editing integration will use two technical means to make work, approval, and online work together to perform high-efficiency work. Offline editing software uses the face to

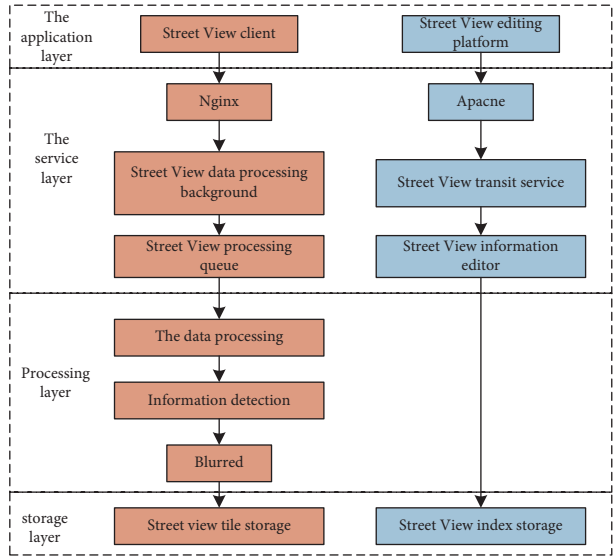

Figure 1: Structure design of street view security and confidential information processing platform.

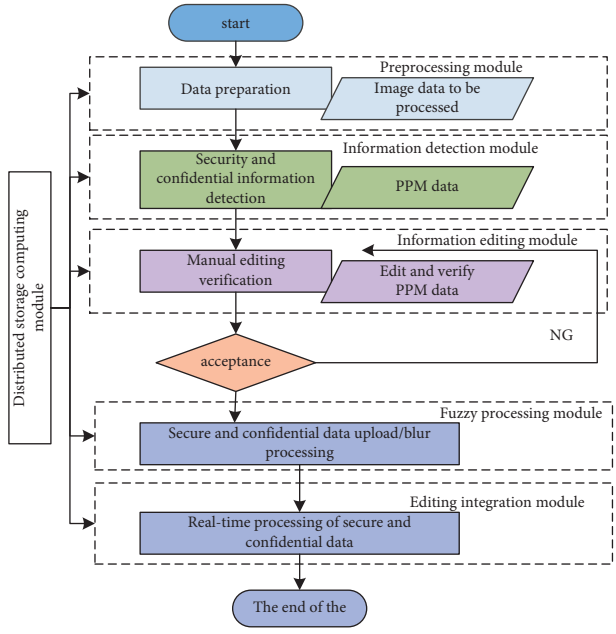

Figure 2: Platform function modules and processing flowchart.

realize the automatic recognition process, assisting the manual more efficient detection and modification to obtain the final result. To achieve the highest editing efficiency. The online editing software can realize the entire process of manually correcting results and updating and processing a series of problems feedback from users within 30 minutes, and can flexibly handle various situations encountered. There is no influence between the data of each operating environment, and the results of editing can be shared at any time and any place, which maximizes the sharing of results and the data is also safe.

2.2. Key Technology Analysis. Internet Street View security and confidential information is widely distributed, has large differences, and does not have certain rules. There are the following difficulties in dealing with these problems: first, some information without obvious characteristics cannot be automatically extracted and identified; second, there are a small amount of information has similarities with nonconfidential security information, so processing with this method may lead to some wrong judgments. After processing, it is particularly easy to cause damage to the overall perception of the image, thereby affecting the product experience; third, although part Information can be distinguished from nonsecure and confidential information, but his algorithm cannot be applied to other types of data, and plays a very small role for a large amount of street view data; fourth, there may be a variety of information types in reality. But we can't build a complete recognition sample library to distinguish effectively; finally, under the condition of not affecting the judgment errors and omissions of classified information, both the integrity of the scene elements and the visual the aesthetics on the Internet has higher requirements for the security and confidential information processing technology of Internet Street View. In order to meet this requirement, we will use different methods to identify classified information and nonconfidential information. The differentiated fuzzy processing method eliminates confidential information and achieves a perfect combination with nearby images. The ordinary fuzzy processing method is used to solve the problem of nonconfidential information and protect personal privacy. Associated topology refers to some important location information provided to us through the information database when processing some undisclosed information data, rechecking and verifying the problems in the data, and finally manually confirming the elements and related secrets. The basis for the realization of the above technology is the establishment of street view data security and a confidential information database. Through nearly two years of collecting and processing street view data, Tencent has street view data for nearly 300 cities in China. In the current related scenes, the accuracy of detecting confidential information is quite high. The implementation of this technology determines the scope of the subsequent inspection data to maximize the efficiency of information inspection.

3. Sponge City Planning Strategy Based on Fuzzy Processing of Geographic Information

3.1. Data Acquisition and Preprocessing. In the past few years, the country proposed that by this year, most cities in the country have basically completed sponge construction. The construction of sponge cities mainly manages and controls urban construction, and systematically deals with the problem of interception of urban rainwater [7]. Through the above-given understanding and analysis, it is easy to know that terrain, climate factors, and rainfall conditions play an important role in the construction of sponge cities [8]. We must balance and coordinate the study of the geomorphic features of the regional climate, and use ArcGIS, SWMM, and other hydrological analysis simulation software to calculate and analyze the data to put forward reasonable suggestions. The important idea of this article is how to conform to nature so that nature can absorb, store and purify rainwater by itself. DLR is the DEM data obtained in the radar mapping method used in previous years [9]. DLR data are relatively high-precision data. Although this type of data has been covered in all aspects, it has not yet covered all areas. The main reason is that during the radar surveying and mapping process in 2000, German surveyors used Endeavour to measure and used X-band coverage, but the coverage area was not large. The Americans used C-band radar for coverage, and the Space Shuttle was based on C-band [10, 11]. The surveying and mapping require flying, resulting in a smaller area covered by the x-band.

The high accuracy of DLR and GDEM-V2 data meets all the requirements for building a sponge city. In China, these two types of data need to be used in many places, but it is relatively difficult to obtain these two types of data from China. If we need these two kinds of data in our work, we can take some measures to obtain them from foreign databases [12]. ASTERGDEM, namely, GDEM-V1 and SRTMC can be downloaded from the Chinese Academy of Sciences. Most of the accuracy obtained here can meet the required requirements. Relatively speaking, the accuracy of the data obtained by GDEM-V1 is higher. It is difficult to obtain data from GMTED, and the accuracy of the obtained data is not high, so we basically do not use this method. Converting TIN to Grid in ArcToolbox will lay the foundation for our next terrain analysis [13]. Run the command TINtoGrid in 3DAnalyst to get the TinGrid data. Execute the surface analysis-slope command in 3DAnalyst, set the parameters to select the input surface as TinGrid and get the slope grid SlopofTinGrid. The slope is then reclassified. If it is the same grade, execute the surface analysis-aspect command in 3DAnalyst. For Qujiang New District of a certain city, the results of calculation from DEM topographic data are shown in Figure 3 for the analysis results of elevation, slope, and aspect of a certain city [14].

3.2. Propose a Water System Construction Method Suitable for the Terrain and Reasonable Overall Indicators. In ArcGIS, the direction of water flow is the basis for analysis using DEM elevation data. Judge the direction of the water flow in the grid we made, and the water flow has the law of flowing from a high place to a low place. In each small grid, the flow direction of water is also a process from high to low [15]. Now, there are two methods of single flow direction algorithm and multiple flow direction algorithm to determine the flow direction of water flow. Compared with the multiflow algorithm, the single-flow algorithm is simpler and more accurate, so we generally choose the simple and convenient single-flow algorithm when judging the water flow [16]. In Hydrology, the hydrology processing module in ArcGIS, the D8 method in the single flow direction algorithm is used to determine the flow direction of the water flow. Now, we use a grid information to illustrate that the flow of water flows in only 8 situations, namely, due east, due

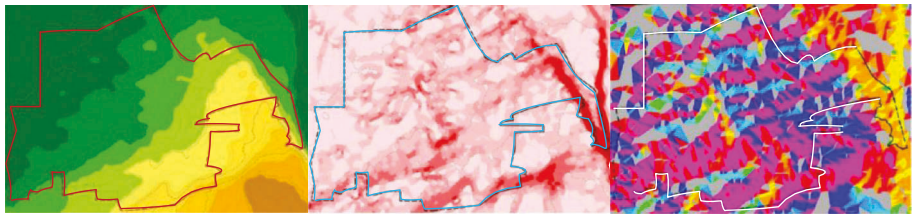

Figure 3: Analysis results of elevation, slope, and aspect of a city.

west, due south, due north, and southeast, southwest, northeast, and northwest; as shown in Figure 4 ArcGIS water flow direction D8 algorithm generalization diagram.

In ArcGIS, the maximum distance weight difference between the center grid and the adjacent grid is calculated to determine the flow direction. The process of determining the direction of water flow in ArcGIS is: open ArcToolbox in ArcMap, start the SpatialAnalysisTools module, find the Hydrology toolset, click on the FlowDirection tool, and the page for calculating the direction of water flow will appear. Provide the data type to the calculation software. The data type we want to discuss is DEM data, so enter the DEM data type, name the file and save it. Select the raster flow direction according to the DEM data provided by us, and it is not selected by default. The output drop raster is the output distance weight drop, expressed as a percentage; here we do not make a choice. In the simulated catchment path, the cumulative result is calculated based on the data of the water flow direction. This principle is based on the regular grid calculation of DEM data without depressions. We assume that each small grid has a unit volume of water flow. And, because the direction of the water flow is from high to low, we can roughly calculate the water flow through each grid, and finally calculate the value of the water flow of these grids.

The water flow direction is judged on the basis of the DEM data without depressions calculated above, the FlowAccumulation tool is used in the Hydrology tool set, and the regional confluence accumulation can be obtained through the relevant data of the water flow direction obtained. A drainage basin refers to a concentrated area formed by the discharge of water or pollutants from a certain area. From the basin data, we can know the size of the catchment area within the scope of our study. Generally speaking, the place where water flows out of the basin is the lowest point in this area. The watershed basin is bounded by watersheds, and the area surrounded by watersheds becomes the catchment area. The watershed divides the entire watershed basin into multiple catchments. In ArcGIS, the water direction data is analyzed to calculate the relevant sinks. Water path, and count the amount of water from the same path. The first thing we need to do is to find the outlets of the catchment area and the small grid where all outlets are located.

Input the DEM elevation data into the algorithm to calculate the direction of water flow, and use the corresponding tool to get the natural catchment area. The use of Tyson polygons divides the natural catchment area into multiple partial catchment zones so that each outlet has a corresponding catchment zone. According to a city's urban planning and the characteristics of water catchment area division, it is judged as three levels. A comprehensive analysis of the characteristics of a certain city's watershed and water system determines the first-level division; on the basis of the first-level division, the second-level division combines the control planning unit and the watershed division; the third-level division proposes methods to determine the control indicators of each district. According to the development index of sponge city shadow, it is also divided into three levels. The first level is the data in the divided first level partition, the second level is the data in the divided second level partition, and the third level should consider the specific conditions and determine the corresponding indicators according to the actual situation. Combined with the classification and structure of the underlying surface construction, land development, etc., the weighted average method is used for calculation. The ability of each area to build sponge cities based on the sponge city construction status, green area ratio, water surface ratio, construction intensity, and other factors in each district are evaluated. First, obtain the total annual runoff control rate of each district and use the weighted average method to calculate and determine the total annual runoff of the city. The volume control rate meets the requirements of urban planning, construction, and management control. If the requirements are not met, the total meridian flow control rate of each district should be adjusted according to the planned land use situation, underlying surface construction intensity and hydrogeological characteristics, and finally reach the control range. In order to evaluate the ability of each district to build a sponge city and whether it has the conditions for building a sponge city, this article first analyzes and counts the status quo of the first-level districts and analyzes the proportion of built-up areas, green area ratios, and water surface ratios of the first-level districts. Quantitative scoring on 1–5 levels. Evaluation factors for the suitability of sponge city construction in the secondary zone is as shown in Table 1.

Then, through the corresponding scores of the green space rate, water surface rate, and built-up area ratio of each district and then assign corresponding weights to them according to their importance in reality and then obtain the total score of each area, comprehensively evaluate the contribution of each district to the construction of sponge cities. The ability and whether it can be built into a sponge city.

$$\begin{aligned}&\text{Comprehensive score}\\&= (\text{Green Space} \times 3 + \text{Surface rate} \times 3\\&\quad + \text{Completion zone ratings} \times 4)/10.\end{aligned} \tag{1}$$

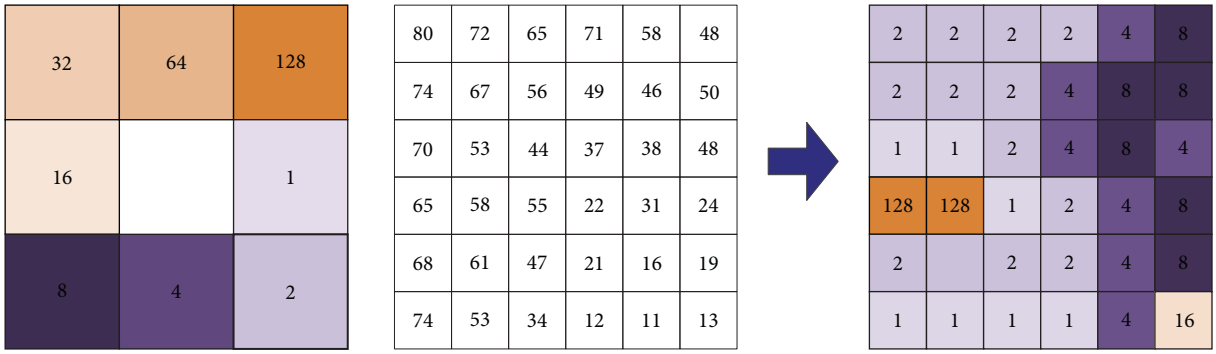

Figure 4: A generalized diagram of ArcGIS water flow direction D8 algorithm.

Table 1: Evaluation factors for the suitability of sponge city construction in the secondary zone.

Factor	Range	Scoring
Green area rate	<20%	1
	20%~30%	2
	30%10%	3
	40%~50%	4
	>50%	5
Surface rate	<3%	1
	3%~6%	2
	6%~9%	3
	9%~12%	4
	>12%	5
Proportion of built-up area	>85%	1
	60%~85%	2
	45%~60%	3
	20%~45%	4
	<20%	5

3.3. Sponge Tissue Method Combined with Natural Topography. This section first explains how to construct a sponge city system based on topographical conditions. It also refers to the domestic and foreign control and operation methods of rainfall runoff and what technical means they use to operate and then compares my country's topographic factors and construction of sponges. For the conditions required by the city, construct a topographic feature index and comparison benchmark model, as shown in Table 2 Applicable Topographic Feature Index Evaluation and Comparison Benchmark for Sponge Facilities.

3.4. Check the Layout of Sponge Facilities. Sponge city planning and construction are often related to newly-built areas and old urban areas. Compared with newly-built areas, the conflicts of interest in old urban areas are relatively complex and the degree of development is relatively large. For this mature area, the layout of sponge facilities is of special significance. Even in low-lying areas with relatively poor soil permeability, it is not suitable to take up too much area for water storage facilities such as ponds. At this time, it is necessary to adjust the selection of sponge facilities according to local conditions and measure the function and scale of various facilities according to the water distribution index and economic value in the area. For example, consider whether it is possible to use sponges to cover all green areas or place some water storage tanks underground to offset some of the indicators, or whether to increase the area of green roofs to purify rainwater and to infuse and store the purified rainwater. Biodiversity is threatened by various road networks, which has attracted the attention of many scholars at home and abroad who design safe passages for wildlife. In the arrangement of sponge facilities, if there is a conflict between wetland parks and urban highways, it should be considered whether motor vehicles pose a threat to the lives of animals. We should make use of reasonable time intervals and take some protective measures for wild animals in appropriate places to provide a guarantee for the living environment and life safety of wild animals.

Combining sponge facilities with other landscape facilities, consider whether there is a connection between landscape facilities and sponge facilities from multiple aspects. When the beach is distributed near the landscape facility, the water system can be introduced into the sponge facility. The introduction of sponge city facilities can not only enhance the ability to store rainwater but also bring people a bright visual enjoyment, enabling them to realize the function of playing a role and enriching the landscape. As shown in Figure 5, the sponge facilities and the activity space are combined to enrich the landscape.

When the development of the city affects the construction of the sponge city, we can make reasonable use of the sponge facilities to achieve the indicator of rainwater control. If the rainwater purification facilities we want to achieve cannot be achieved, we can increase the green area of the roof and rationally design rainwater purification facilities to achieve the purpose of rainwater purification and storage. For another example, if the sunken green space reduces the survival rate of plants due to some objective conditions, it is difficult to use the rainwater that seeps into the ground, we can reprocess the sponge facilities.

We should first fully understand the local terrain and the functions of sponge facilities and make a reasonable plan and then start to implement it. However, we need to know that the

Table 2: Applicable topographic feature index evaluation and comparison criteria for sponge facilities.

Sponge facility		Location characteristics		Soil condition	Natural terrain conditions				
					Groundwater characteristics	Topography	Nature of catchment		Space requirement
		Land use type	Pollution load intensity	Soil type	The highest underground water level is from the bottom of the facility (m)	Confluence gradient (%)	Catchment area (ha)	Impermeability (%)	Area (ha)
Permeable sponge facilities "seepage"	Permeable paving	R/B/G/S	Low	A-B	>0.61	1–3	<1	>0	—
	Sunken green space	R/S/B/G	In	A-B	>0.61	1–5	>4	>0	In
	Biological retention facility	R/S/B/G	In	A-B	>1.22	1–5	<4	>0	In
	Infiltration pond	R/S/B/G	In	A-B	>3	<15	1–4	>0	Big
	Seepage well	R/S/B/G	Low	A-B	>0.61	<10	<1	>0	Small
Adjustment category sponge facilities "stay"	Regulating pond	R/G	Low	A-D	>1	<10	>6	>0	Big
Adjustment category sponge facilities "stay"	Regulation pool	R/S/B/G/M	Low	A-D	>1	—	—	>0	Small
Storage type sponge facilities "fan, use"	Wet pond	R/G	High	A-D	>1.22	<10	>6	0–80	Big
	Rain wetland	R/G	High	B-D	>1.22	4–15	>10	0–80	Big
	Reservoir	R/S/B/G	Low	A-D		—	—	>0	Small
	Rainwater irrigation	R/B	Low	—	—	—	—	—	Small
Purification category sponge facility "clean"	Green roof	R/B/M	In	—	—	<4	—	—	—
	Vegetation buffer zone	R/S/B/G/M	High	A-D	>0.61	2–6	>4	>0	In
	Initial rainwater abandonment facility	R/B/M	High	—	—	—	—	—	Small
	Artificial soil	R/B/M	In	A-D	>0.61	<10	<2	0–50	Small
Transfer type sponge facility "row"	Zhicaogou	R/S/B/G	In	A-D	>0.61	0.5–5	<2	>0	In
	Seepage pipe/drain	R/G	Low	A-B	>1.22	—	<2	>0	In

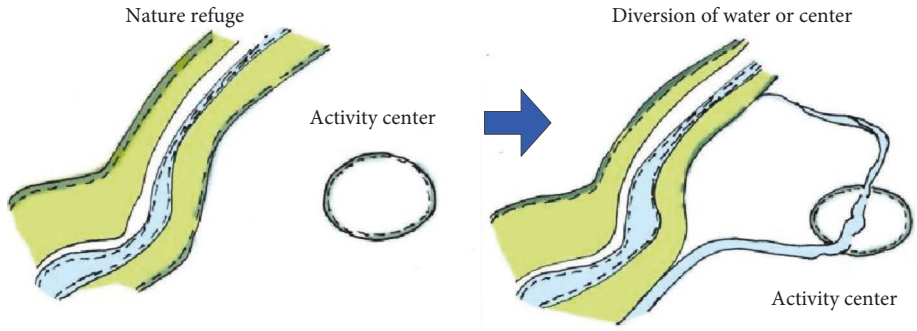

Figure 5: Combining sponge facilities with activity space to enrich the landscape.

Table 3: Key issues and main tasks of each work stage.

Work phase	The key issue	Main mission
Definition and plan	What is the question?	Determine the outline of the system plan; survey tasks for the transportation requirements; make preparations for the survey
Feasibility study	Is there a feasible solution?	Provide expert opinions and suggestions
Demand analysis	What must the system do?	Understand the artificial system model; determine user needs; order current business flow and data flow; collect original business data, analyze demand survey results, and make design preparations
Outline design	How to solve the problem?	Determine system design principles and goals, carry out system control structure design, software function structure design, database design, operating environment design and interface design; determine system implementation plan
Detailed design	How to implement the system concretely?	Familiar with the basic development platform software; determine the module function and the calling relationship between the modules; determine the module interface; give the module control mix diagram 1 gives the software guide and user input and output interface
Program code	How to design the correct program unit?	According to detailed design results and programming guidelines, the functions of each caution block are realized with code
Test inheritance	How to ensure that the software meets the requirements?	Install and develop the application system on-site, and conduct anti-image debugging through simulation operation; meanwhile, conduct system use training for business personnel at all levels of the planning bureau
Operation and maintenance	How to make the system persistently meet the requirements?	The system enters the formal operation stage, during which system identification is completed; operation and maintenance are carried out

terrain is not the only criterion for testing whether the layout of the sponge facilities is reasonable. Need specific analysis. Arranging sponge facilities is not the only way to solve related problems. We can design or even transform the function and scale of sponge facilities to meet the required requirements. When we select the location of sponge facilities, we should comprehensively consider the local natural topography, building conditions, development conditions, etc. In order to reduce the occurrence of disasters, it is also an indispensable step to check whether there are earthquake zones in the layout area. Consider the influence of setting sponge facilities on various factors before layout.

4. GIS-Based Urban Information System Development Method

4.1. System Design Pattern. After more than 30 years of development and practical application of GIS, there has been a fairly mature system including a software cycle model and a rapid prototyping model. In the actual development process, these two models are often combined and applied. The rapid prototyping model is used to sort out the requirements, and the software cycle model is used to carry out the subsequent work to ensure the orderly progress of the work. The rapid prototyping model is mainly a model that enables the software system to run quickly through rough analysis. By solving the problems feedback from users, continuous improvement, and finally achieve the results that are satisfactory to both parties. Compared with the traditional method, the object-oriented method has more advantages. Of course, the object-oriented method is not a method without any defects. The object-oriented method absorbs the essence of structured thinking and supplements the structured thinking.

The urban planning and management information system platform is a large-scale software consisting of data engineering, software engineering, and hardware engineering. What is interesting is that software engineering also includes hardware. Table 3 shows the key issues and main tasks of each work stage.

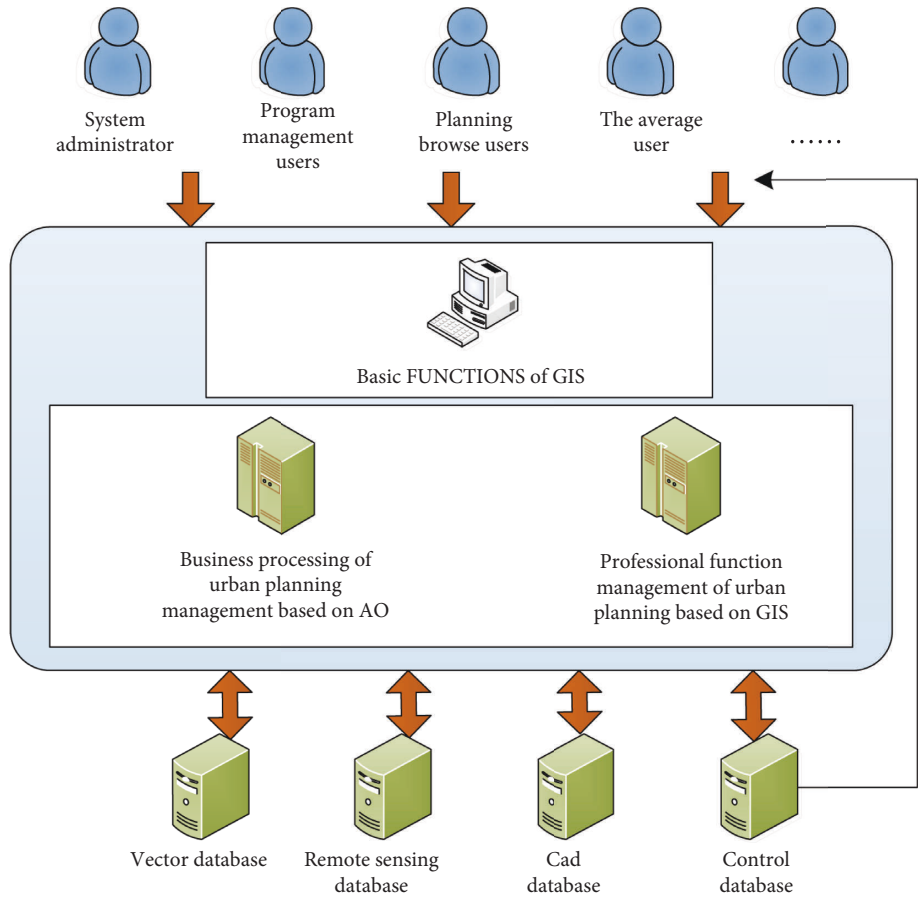

Figure 6: Platform architecture.

For the planning and management of urban construction, the platform software uses geographic information (GIS), office automation (oA), computer networks, and other technical means to achieve comprehensive applications such as homework, data sorting, and image processing. According to consistent information classification standards, a series of data generated during the planning and management of the city are managed in a unified manner to obtain a shareable resource. Relevant staff can check the authenticity of these data anytime and anywhere, and some new approval information and opinions can also be included in the database in a timely manner. According to the work tasks and work processes of the staff of each department, the corresponding registration, inquiry, and statistical processes are proposed and applied to realize the management and supervision process achieved through the computer network.

4.2. System Structure. The basic functions of this platform are provided by a series of GIS functions, and multiple modules are developed according to management requirements. At the same time, the platform has installed an automation module in the platform in order to reduce the work pressure of the staff in the planning department. It can be seen from Figure 6 that after the user logs in to the platform software, he uses the software's functions to call the database to achieve the purpose of database management.

The functions of the software development platform are divided into the following parts: user authority management; basic GIS functions; GIS functions related to urban management and control work; OA functions related to urban management and control work. On top of this, break it down into modules capable of different data encapsulation functions, so that they can further form components. Only the necessary data interfaces are disclosed to the outside world; as long as the required standards are met, the program can be inserted into the platform software, all of which greatly improve the scalability of the platform. In the process of urban management and control, the platform software widely uses component development methods.

5. Conclusion

This article discusses the influence of natural topography on the planning and construction of sponge cities, including whether natural topography can affect rainwater, whether it can affect the distribution of different grounds, whether it can affect the use of groundwater resources, and whether it is because of this topography. In the event of a natural disaster, if you think that changing the topography will have any impact on it, then analyze whether the stability of the natural

topography of the northern cities is affected by rain. At present, the situation of informatization construction is developing rapidly. Most of the relevant personnel in the urban planning work departments have begun to build their own information systems. However, it seems that the established systems are almost only office automation systems. A small number of geographic information systems and office automation systems are combined, and the comprehensive application of G1S, OA, and MIS is rarely achieved. The software platform design process proposed in this article strives to reflect the perfect combination of the three methods, and in the software platform, the idea of workflow is realized in the components of, users can independently view the working status and perform operations, which provides convenient conditions for urban management and control staff. This article combines VB and ArcGISEngine to build platform development software. This software has the characteristics of easy operation, simple page, and convenient and quick user use.

Data Availability

The data used to support the findings of this study are available from the corresponding author upon request.

Conflicts of Interest

The authors declare that they have no conflicts of interest.

References

[1] I. Hryshchenko and S. Lavshchenko, "Impact of local market development on sustainable (stable) city development," *E3S Web of Conferences*, vol. 208, Article ID 04009, 2020.

[2] X. Dong, H. Guo, and S. Zeng, "Enhancing future resilience in urban drainage system: green versus grey infrastructure," *Water Research*, vol. 124, pp. 280–289, 2017.

[3] H. Li, L. Ding, M. Ren, C. Li, and H. Wang, "Sponge city construction in China: a survey of the challenges and opportunities," *Water*, vol. 9, no. 9, p. 594, 2017.

[4] T. T. Nguyen, H. H. Ngo, W. Guo et al., "Implementation of a specific urban water management - sponge City," *Science of the Total Environment*, vol. 652, pp. 147–162, 2019.

[5] J. Li, C. Deng, Y. Li, Y. J. Li, and J. Song, "Comprehensive benefit evaluation system for low-impact development of urban stormwater management measures," *Water Resources Management*, vol. 31, no. 15, pp. 4745–4758, 2017.

[6] J. Xia, Y. Zhang, L. Xiong, S. He, L. Wang, and Z. Yu, "Opportunities and challenges of the Sponge City construction related to urban water issues in China," *Science China Earth Sciences*, vol. 60, no. 4, pp. 652–658, 2017.

[7] H. Jia, Z. Wang, X. Zhen, M. Clar, and S. L. Yu, "China's sponge city construction: a discussion on technical approaches," *Frontiers of Environmental Science & Engineering*, vol. 11, no. 4, pp. 18–11, 2017.

[8] T. T. Nguyen, H. H. Ngo, W. Guo, and X. C. Wang, "A new model framework for sponge city implementation: emerging challenges and future developments," *Journal of Environmental Management*, vol. 253, Article ID 109689, 2020.

[9] K. Alonso, M. Bachmann, K. Burch et al., "Data products, quality and validation of the DLR earth sensing imaging spectrometer (DESIS)," *Sensors*, vol. 19, no. 20, p. 4471, 2019.

[10] M. E. Bouzouraa and U. Hofmann, "Fusion of occupancy grid mapping and model based object tracking for driver assistance systems using laser and radar sensors," in *Proceedings of the 2010 IEEE Intelligent Vehicles Symposium*, pp. 294–300, 2010.

[11] X. Shen, D. Wang, K. Mao, E. Anagnostou, and Y. Hong, "Inundation extent mapping by synthetic aperture radar: a review," *Remote Sensing*, vol. 11, no. 7, p. 879, 2019.

[12] U. G. Sefercik, "Productivity of terraSAR-X 3D data in urban areas: a case study in trento," *European Journal of Remote Sensing*, vol. 46, no. 1, pp. 597–612, 2013.

[13] M. Uysal, A. S. Toprak, and N. Polat, "DEM generation with UAV Photogrammetry and accuracy analysis in Sahitler hill in Sahitler hill," *Measurement*, vol. 73, pp. 539–543, 2015.

[14] S. Wu, J. Li, and G. H. Huang, "A study on DEM-derived primary topographic attributes for hydrologic applications: sensitivity to elevation data resolution," *Applied Geography*, vol. 28, no. 3, pp. 210–223, 2008.

[15] F. Schmidt and A. Persson, "Comparison of DEM data capture and topographic wetness indices," *Precision Agriculture*, vol. 4, no. 2, pp. 179–192, 2003.

[16] A. Md Ali, D. P. Solomatine, and G. Di Baldassarre, "Assessing the impact of different sources of topographic data on 1-D hydraulic modelling of floods," *Hydrology and Earth System Sciences*, vol. 19, no. 1, pp. 631–643, 2015.

Hindawi
Computational Intelligence and Neuroscience
Volume 2022, Article ID 5932554, 8 pages
https://doi.org/10.1155/2022/5932554

Research Article

A Deep Machine Learning-Based Assistive Decision System for Intelligent Load Allocation under Unknown Credit Status

Wenjing Yan,[1] **Hong Wang**,[1] **Min Zuo**,[1] **Haipeng Li**,[2] **Qingchuan Zhang**,[1] **Qiang Lu**,[1] **Chuan Zhao**,[1] **and Shuo Wang**[3]

[1]*National Engineering Research Centre for Agri-product Quality Traceability, Beijing Technology and Business University, Beijing 100048, China*
[2]*Capinfo Company Ltd., Beijing 100010, China*
[3]*School of Mechanical Engineering, Beijing Institute of Technology, Beijing 100081, China*

Correspondence should be addressed to Min Zuo; zuomin1234@163.com

Received 28 June 2022; Revised 12 August 2022; Accepted 16 August 2022; Published 8 September 2022

Academic Editor: Gopal Chaudhary

Nowadays, the banks are facing increasing business pressure in loan allocations, because more and more enterprises are applying for it and financial risk is becoming vaguer. To this end, it is expected to investigate effective autonomous loan allocation decision schemes that can provide guidance for banks. However, in many real-world scenarios, the credit status information of enterprises is unknown and needs to be inferred from business status. To handle such an issue, this paper proposes a two-stage loan allocation decision framework for enterprises with unknown credit status. And the proposal is named as TLAD-UC for short. For the first stage, the idea of deep machine learning is introduced to train a prediction model that can generate credit status prediction results for enterprises with unknown credit status. For the second stage, a dynamic planning model with both optimization objective and constraint conditions is established. Through such model, both the profit and risk of banks can be well described. Solving such a dynamic planning model via computer simulation programs, the optimal allocation schemes can be suggested.

1. Introduction

Since the rise of banks, loans have become the most common way of financing the process of enterprise development. Two main bodies are involved in general loan activities [1]. One is the communities that provide funds, such as financial companies and banks, while the other is the communities that apply for borrowing funds, such as enterprises [2, 3]. With the continuous growth of urbanization and modernization, the business volume of loans shows a gradually increasing trend [4]. This not only brings greater capital pressure to banks but also increases some uncertain financial risk for banks [5, 6]. Because the operation status and qualification of many enterprises are diverse, a great challenge is posed to the later management of banks [7, 8]. Therefore, how to calculate the optimal loan schemes that can maximize profit or minimize risk for banks under limited capital, serves as an important problem [9, 10].

It is never an easy task to determine the optimal loan allocation schemes for banks [11]. Although there are some research works focused on this issue, most of them did not consider the limitation of the total capital amount [12, 13]. They focused more on the scenes that decide whether to provide loans to specific enterprises [14–16]. They did not consider more substantive issues such as amount setting or global risk [17–19]. In addition, in the process of loan review, the most important consideration of enterprises is credit status. In the existing research works, they basically assume that the credit status of enterprises is known [20, 21]. However, in many actual business scenarios, the credit status of enterprises is unknown. The circumstances bring many challenges to the formulation of loan allocation plans. Therefore, how to generate the optimal loan allocation scheme for enterprises with unknown credit status is essentially a more realistic problem.

To deal with such an issue, this paper proposes a two-stage loan allocation decision framework for enterprises with unknown credit status, which is named as TLAD-UC for short. For the first stage, it is expected to tackle with the issue that credit status for enterprises is unknown. As a consequence, a typical machine learning named as K-nearest neighbor (KNN) is utilized here to predict credit status for enterprises. Specifically, a historical dataset that records information of 123 enterprises with credit status is selected to train the machine learning-based prediction models. And the trained models will be used to generate prediction results for enterprises with unknown credit status. For the second stage, a dynamic planning model is formulated to fit the decision process of banks, in which profit and risk are both expressed with quantified expressions. The dynamic planning model is composed of both optimization objective and constraint conditions. By solving the dynamic planning model, the optimal loan allocation decision schemes can be obtained. The main contributions of this paper can be summarized in three aspects.

(1) It is recognized that loan allocation for enterprises with unknown credit status is challenging.

(2) We propose TLAD-UC which is a two-stage loan allocation decision framework for enterprises with unknown credit status.

(3) Simulation is conducted on a real-world dataset to demonstrate the workflow of the proposed TLAD-UC.

2. Preliminaries

Two datasets are involved in this work. Dataset A records some information of 123 enterprises and has credit status information for them. Dataset B only has some basic information of 302 enterprises yet has no credit status information. Inside both datasets, each enterprise has some business records of input invoices and sale invoices as their basic features. Let n denote the index number of enterprises that ranges from 1 to N, and the N equals to the number of enterprises in corresponding datasets. Taking the 123 enterprises with credit information as references, the main goal is to determine loan allocation schemes for the 302 enterprises without credit information. To handle such a problem, the TLAD-UC is implemented via two stages. As is shown in Figure 1, the two stages involved in the architecture of TLAD-UC are the machine learning stage and the optimization decision stage.

For the first stage, initial business data is preprocessed into a format that is suitable for data analysis models. And then, the KNN model is trained on the basis of dataset A. After training, it can directly predict unknown credit information for 302 enterprises in dataset B. For the second stage, the profit and risk of the 302 enterprises are quantified via mathematical expressions. On such a basis, a dynamic planning model with both optimization and constraint conditions is established for the side of banks. Then, the dynamic planning model can be solved by using computer simulation programs to search for optimal solutions for the planning model. Naturally, the optimal loan allocation schemes can be obtained after a solution to the optimization objective.

3. The Proposed Approach

3.1. Data Preprocessing. In the beginning, the initial datasets need some basic procedures to extract features. The following procedures are the basic process of feature engineering:

(1) For each enterprise, the total amount of its input invoices and the total amount of its sale invoices are respectively counted via aggregation of all related records that are labeled as "valid". For the n-th enterprise, its amount of input invoices and amount of sale invoices are denoted as $F_{n,1}$ and $F_{n,2}$, separately.

(2) It is noted that some of the values in $F_{n,1}$ and $F_{n,2}$ are less than 0, which means that the corresponding business record is a chargeback record. Similarly, the total amount of chargeback for each enterprise is counted. For the n-th enterprise, its amount of chargeback amount in input invoices and sale invoices are denoted as $F_{n,3}$ and $F_{n,4}$, respectively.

(3) The ratio of chargeback data can be computed for both input invoices and the sale invoices via the following two formulas:

$$F_{n,5} = \frac{F_{n,3}}{F_{n,1}}, \qquad F_{n,6} = \frac{F_{n,4}}{F_{n,2}}. \tag{1}$$

For the n-th enterprise, its ratio of chargeback data in input invoices and sale invoices are denoted as $F_{n,5}$ and $F_{n,6}$, respectively.

(4) It is noted that values in $F_{n,1}$ and $F_{n,2}$ do not equal to the turnover amount because there exists the tax. The real turnover amount for a business record equals the sum of the invoice amount and tax amount. Thus, the turnover amount of input business and sale business can be calculated and denoted as $F'_{n,7}$ and $F'_{n,8}$, respectively. For the two indicators, their average values of one day can be computed as follows:

$$F_{n,7} = \frac{F'_{n,7}}{365}, \qquad F_{n,7} = \frac{F_{n,8}^{'}}{365}. \tag{2}$$

For the n-th enterprise, its ratio of chargeback data in input invoices and sale invoices are denoted as $F_{n,7}$ and $F_{n,8}$, respectively.

(5) For each enterprise, the number of chargeback records is counted. For the n-th enterprise, such feature is denoted as $F_{n,9}$.

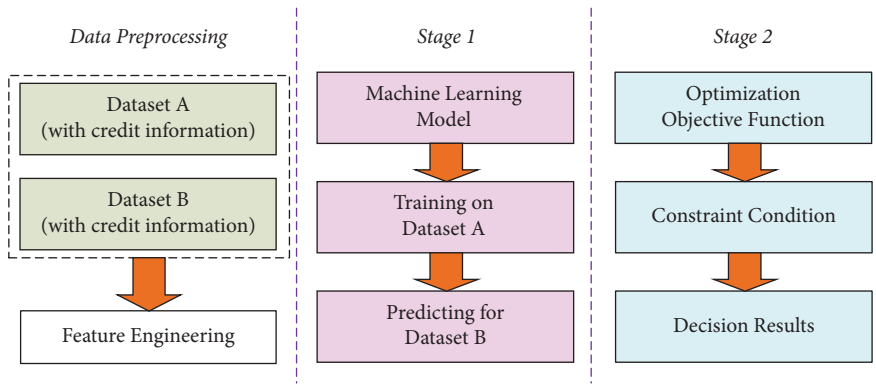

Figure 1: The main architecture of the proposed TLAD-UC.

(6) For each enterprise, its turnover amount needs to be processed by introducing logarithmic operations, which can be calculated as follows:

$$F_{n,10} = \log_2\left(F_{n,1}\right) + \log_2\left(F'_{n,7}\right),$$
$$F_{n,11} = \log_2\left(F_{n,2}\right) + \log_2\left(F'_{n,8}\right). \quad (3)$$

For the n-th enterprise, its two features are denoted as $F_{n,10}$ and $F_{n,11}$, respectively.

(7) For each enterprise, its turnover amount also needs to be processed by introducing logarithmic operations, which can be calculated as follows:

$$F_{n,12} = \left|\log_2\left(F'_{n,7}\right)\right|,$$
$$F_{n,13} = \left|\log_2\left(F'_{n,8}\right)\right|. \quad (4)$$

For the n-th enterprise, its two features are denoted as $F_{n,12}$ and $F_{n,13}$, respectively.

(8) For each enterprise, it has four possible label options which correspond to four credit ratings. The label of n-th enterprise is denoted as y_n.

As shown in Figure 2, the main workflow of machine learning algorithms is composed of four procedures: data preprocessing, model selection, model training, and prediction. Having finished the data preprocessing, it is expected to implement model selection and model training. For the n-th enterprise, its thirteen features can be denoted as $F_{n,m}$, where m ranges from 1 to 13. Given $F_{n,m}$, it is expected to generate prediction results for it. This process can be represented as the following formula:

$$F_{n,m} \longrightarrow y_n. \quad (5)$$

To realize such a goal, the idea of machine learning is then introduced.

3.2. Prediction of Unknown Credit Information. As has been mentioned above, the dataset A has credit information and dataset B has no credit information. Thus, the dataset A is viewed as a golden dataset, from which unknown pattern rules can be discovered. Viewing the dataset A as a training set and the dataset B as the set to be predicted, a typical machine learning model named as KNN is selected here for this purpose.

The full name of KNN is K-nearest neighbors, and the KNN can be used for both classification problems and regression problems. The KNN realizes classification tasks or regression tasks by measuring the distance between different eigenvalues. Naturally, the selection of K-nearest neighbors is upon the basis of distance in sample spaces. The KNN is a quite easy but special machine learning algorithm, as it lacks the general learning process. Its working principle is to divide the feature vector space by using the training data and take the division results as the final algorithm model. After entering the unlabeled data, it is supposed to compare each feature of the unlabeled data with the corresponding feature of the data in the sample set. Then, the classification labels of the data with the closest features (nearest neighbors) in the sample are extracted.

We take Figure 3 as an example to illustrate the basic principles of KNN. Inside the figure, red points and blue points refer to samples that have been labeled. They belong to two different classes. It is expected to generate classification results for the green point. When K equals to 3, the selected neighbors for the green point include two red points and one blue point. According to the majority voting rule, the green point will be annotated as the class of red points. When K equals to 5, the selected neighbors for the green point include two red points and three blue points. According to the majority voting rule, the green point will be annotated as the class of blue points. From this example, it can be deduced that the setting of K is quite important in KNN because the constitution of neighboring samples may be diverse with different settings of K. Then, there is an essential problem in KNN, how to measure the distance in sample spaces?

In this work, the most prevalent distance measurement named as "Euclidean distance" is selected for use. Supposing that there are two sample points denoted as α and β in sample spaces, they are both four-dimensional samples. The Euclidean distance between α and β is calculated as the following formula:

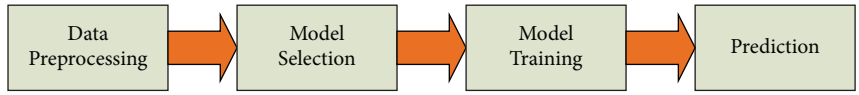

Figure 2: The main workflow of the machine learning algorithms.

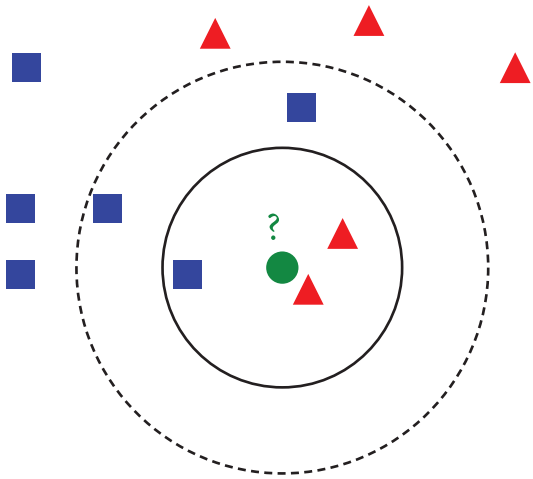

Figure 3: An example to illustrate the KNN algorithm.

$$\text{Dist}(\alpha,\beta) = \sqrt{(\alpha_1-\beta_1)^2+(\alpha_2-\beta_2)^2+(\alpha_3-\beta_3)^2+(\alpha_4-\beta_4)^2}. \tag{6}$$

It can be seen from the formula that the value of $\text{Dist}(\alpha,\beta)$ is sensitive to a diverse value range. For example, if the value range of α_1 and α_2 is larger than other features, the final value of $\text{Dist}(\alpha,\beta)$ will be influenced to some extent. To reduce such an effect, it is supposed to make normalization operations towards all the feature values. Universally, the value range of normalization is fixed as $[0,1]$. Taking α_1 as an example, the normalization procedure can be calculated as follows:

$$\alpha_1^{\text{new}} = \frac{\alpha_1^{\text{old}} - \min(\alpha_1)}{\max(\alpha_1) - \min(\alpha_1)}, \tag{7}$$

where $\min(\alpha_1)$ denotes the minimum value in all the α_1 values in sample spaces, and $\max(\alpha_1)$ denotes the maximum value in all the α_1 values in sample spaces. Naturally, all the features need to be normalized before substituting into models.

Therefore, major procedures of the KNN algorithm can be described as follows:

(1) The distance between the test data and each training data is calculated.

(2) All the possible neighbors are sorted by an increase in distance.

(3) K samples with the nearest distance are selected as the neighbors.

(4) The occurrence frequency of the category to which these k samples belong to is counted.

(5) The category with the highest frequency in the K samples is returned as the prediction classification of the test data.

And the above process can be summarized in Figure 4.

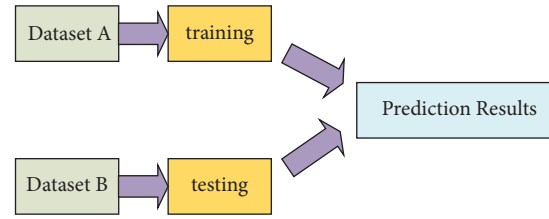

Figure 4: Workflow of the KNN model used in this work.

3.3. Model Evaluation and Prediction. After training a KNN model, the credit status information in dataset B can be calculated accordingly. Before that, we would like to evaluate the performance of the KNN model. For dataset A, it is further divided into two parts the training part and the evaluation part. Of all the 123 samples, the training part has 93 samples, and the evaluation part has 30 samples. The 93 samples are used to train a KNN model and the 30 samples are used to evaluate the performance of the KNN model because the 30 samples have been labeled. Their labels are removed at first and then are compared with predicted labels.

The KNN model outputs prediction results for the 30 results, of which 18 of them are correct and the other 12 of them are incorrect. Thus, we can say that prediction accuracy in the evaluation data is 0.6. Although such accuracy is still not ideal, it can have some guidance for enterprises with unknown credit status information. Because it can predict credit status information for the enterprises with some reliability. After training, the KNN model is implemented on dataset B to predict unknown credit status for them. Then KNN model is implemented on computers with the use of Python language. The running result of the computer program can be demonstrated in Figure 5.

In the next stage, the optimization decision model will be formulated on the basis of such prediction results. To sum up, 27 enterprises are labeled as credit rating A, 149 enterprises are labeled as credit rating B, 74 enterprises are labeled as credit rating C, and 52 enterprises are labeled as credit rating D.

3.4. Optimization Decision. To generate optimal allocation decisions for enterprises, a dynamic planning model is formulated in this section to realize this purpose.

From the side of banks, their total income from loan activities can be represented as the following formula:

$$I = c_1 d_1 s_1 Q_1 + c_2 d_2 s_2 Q_2 + c_3 d_3 s_3 Q_3 + c_4 d_4 s_4 Q_4, \tag{8}$$

c_1, c_2, c_3, and c_4 are the number of enterprises with four different credit ratings. d_1, d_2, d_3, and d_4 are loan amounts for enterprises with four different credit ratings. s_1, s_2, s_3, and s_4 are interest ratios for enterprises with four different

```
model = knn_classifier (x_train, y_train)
y_predict = model, predict (x_test)
y_predict
```

```
array ([4, 4, 4, 4, 3, 3, 3, 3, 4, 3, 3, 4, 4, 4, 3, 4, 4, 4, 3, 3, 3, 4,
        4, 3, 3, 3, 3, 3, 3, 3, 4, 3, 4, 3, 3, 3, 3, 4, 4, 4, 3, 3, 3, 4,
        3, 3, 3, 3, 3, 4, 3, 3, 3, 3, 3, 3, 3, 3, 3, 3, 3, 3, 3, 3, 3, 2,
        3, 3, 2, 4, 3, 3, 3, 4, 3, 2, 3, 3, 3, 3, 3, 3, 3, 3, 3, 3, 3, 2,
        3, 3, 3, 2, 3, 2, 2, 2, 3, 2, 3, 3, 4, 3, 3, 3, 3, 3, 2, 2, 3, 3,
        2, 2, 2, 2, 3, 3, 3, 2, 3, 2, 2, 2, 2, 3, 3, 3, 2, 3, 2, 2, 2, 3,
        2, 3, 3, 2, 2, 3, 2, 3, 3, 2, 2, 3, 2, 2, 2, 2, 3, 2, 2, 3, 3, 3,
        3, 2, 3, 3, 2, 3, 3, 2, 3, 3, 3, 3, 3, 3, 3, 3, 2, 3, 3, 3, 3, 3,
        3, 3, 3, 3, 3, 2, 3, 2, 3, 3, 3, 3, 3, 3, 2, 3, 3, 2, 2, 3, 3, 3,
        3, 3, 3, 3, 3, 2, 2, 2, 2, 2, 4, 2, 3, 3, 2, 2, 2, 2, 2, 2, 2, 3,
        4, 3, 2, 4, 4, 3, 1, 1, 3, 2, 3, 1, 2, 2, 2, 1, 2, 2, 2, 1, 3, 2,
        1, 3, 1, 1, 3, 2, 3, 3, 2, 1, 1, 1, 1, 1, 2, 3, 1, 1, 2, 1, 2, 1,
        1, 1, 1, 2, 1, 1, 1, 3, 1, 1, 1, 1, 1, 1, 1, 2, 1, 1, 1, 1, 1, 1,
        1, 1, 1, 1, 1, 1, 1, 1, 1, 1, 1, 1, 1, 1, 1, 1], dtype=int64)
```

Figure 5: Running result of the KNN algorithm for prediction.

credit ratings. Q_1, Q_2, Q_3, and Q_4 denote the proportion of no default for enterprises with four different credit ratings.

And for the side of banks, their risk in loan activities can be represented as the following formula:

$$\begin{aligned} R = {} & c_1^2 d_1^2 s_1^2 t_1 (1 - t_1) + c_2^2 d_2^2 s_2^2 t_2 (1 - t_2), \\ & + c_3^2 d_3^2 s_3^2 t_3 (1 - t_3) + c_4^2 d_4^2 s_4^2 t_4 (1 - t_4). \end{aligned} \tag{9}$$

Among, t_1, t_2, t_3 and t_4 denote the ratio of enterprises with four different credit ratings.

Besides, there are also some constraint conditions to be satisfied as follows:

(1) $c_1 d_1 + c_2 d_2 + c_3 d_3 + c_4 d_4$;

(2) $0 \le d_1, d_2, d_3, d_4 \le A$;

(3) $0.04 \le s_i \le 0.15$;

(4) $s_1 \le s_2 \le s_3 \le s_4$.

Here, A denotes the total amount that can be used for loan activities in banks.

Further, the total profit for the side of banks can be represented as the following formula:

$$\begin{aligned} TP = {} & c_1 d_1 s_1 t_1 (1 - L_1) + c_2 d_2 s_2 t_2 (1 - L_2), \\ & + c_3 d_3 s_3 t_3 (1 - L_3) + c_4 d_4 s_4 t_4 (1 - L_4), \end{aligned} \tag{10}$$

among, t_1, t_2, t_3 and t_4 denote customer loss ratio of enterprises with four different credit ratings. Then, the optimization objective can be formulated from two aspects: risk minimization and profit maximization.

For risk minimization, the following optimization model can be formulated as follows:

$$\min R \quad s.t. \begin{cases} c_1 d_1 + c_2 d_2 + c_3 d_3 + c_4 d_4 = A \\ 0 \le d_1, d_2, d_3, d_4 \le A \\ 0.04 \le s_i \le 0.15 \\ TP \ge 0.07 \end{cases}. \tag{11}$$

Substituting $c_1, c_2, c_3, c_4, d_1, d_2, d_3, d_4, L_1, L_2$, and L_3 into the model, the total profit and total risk can be written as follows:

$$\begin{aligned} \mathrm{TP} &= 2.92 d_2 s_2 + 2.84 d_3 s_3, \\ R &= 2.92 d_2^2 s_2^2 + 2.84 d_3^2 s_3^2. \end{aligned} \tag{12}$$

Assuming that the total amount for loan activities is set as 1, the optimal allocation scheme is computed as follows:

$$d_1 = 0.72, d_2 = 0.18, d_3 = 0.10. \tag{13}$$

It is noted that enterprises with credit rating D will not be approved for loans here. And the interest ratio is set at 0.08.

For profit maximization, the following optimization model can be formulated as follows:

$$\min TP \quad s.t. \begin{cases} c_1 d_1 + c_2 d_2 + c_3 d_3 + c_4 d_4 = A \\ 0 \le d_1, d_2, d_3, d_4 \le A \\ 0.04 \le s_i \le 0.15 \\ R \le 0.03 \end{cases}. \tag{14}$$

Substituting $c_1, c_2, c_3, c_4, d_1, d_2, d_3, d_4, L_1, L_2$, and L_3 into the model, the optimal decision for allocation schemes can be represented as follows:

$$d_1 = 0.48, d_2 = 0.28, d_3 = 0.24. \tag{15}$$

It is noted that enterprises with credit rating D will not be approved for loans here. And the interest ratio is set at 0.15.

In order to visualize the allocation results more clearly, Figure 6 demonstrates the allocation results of three kinds of enterprises via a stacked bar chart. Inside the figure, the blue bar corresponds to allocation results for enterprises with credit rating A, the green bar corresponds to allocation results for enterprises with credit rating B, and the yellow bar corresponds to allocation results for enterprises with credit rating C, while no allocation is provided for enterprises with credit rating D. And the results under two situations are also

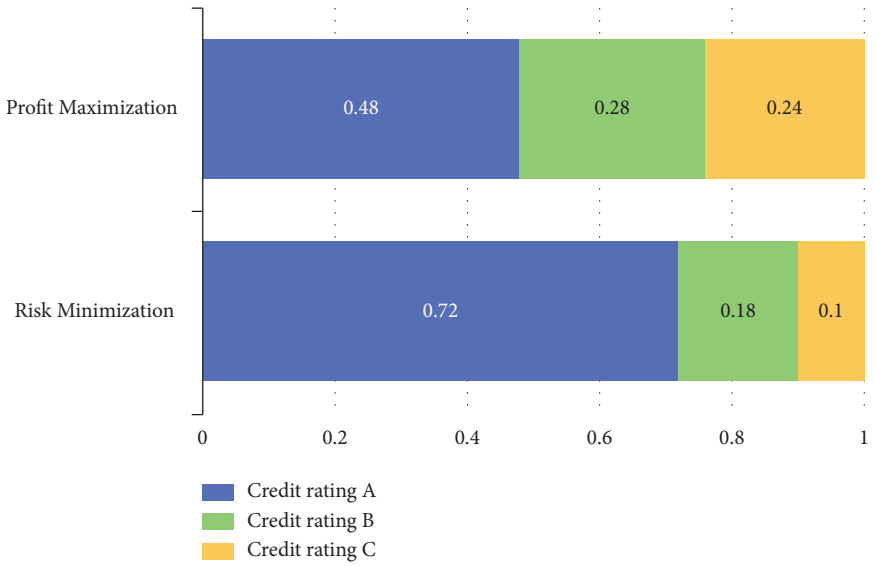

Figure 6: Final allocation results for the two situations.

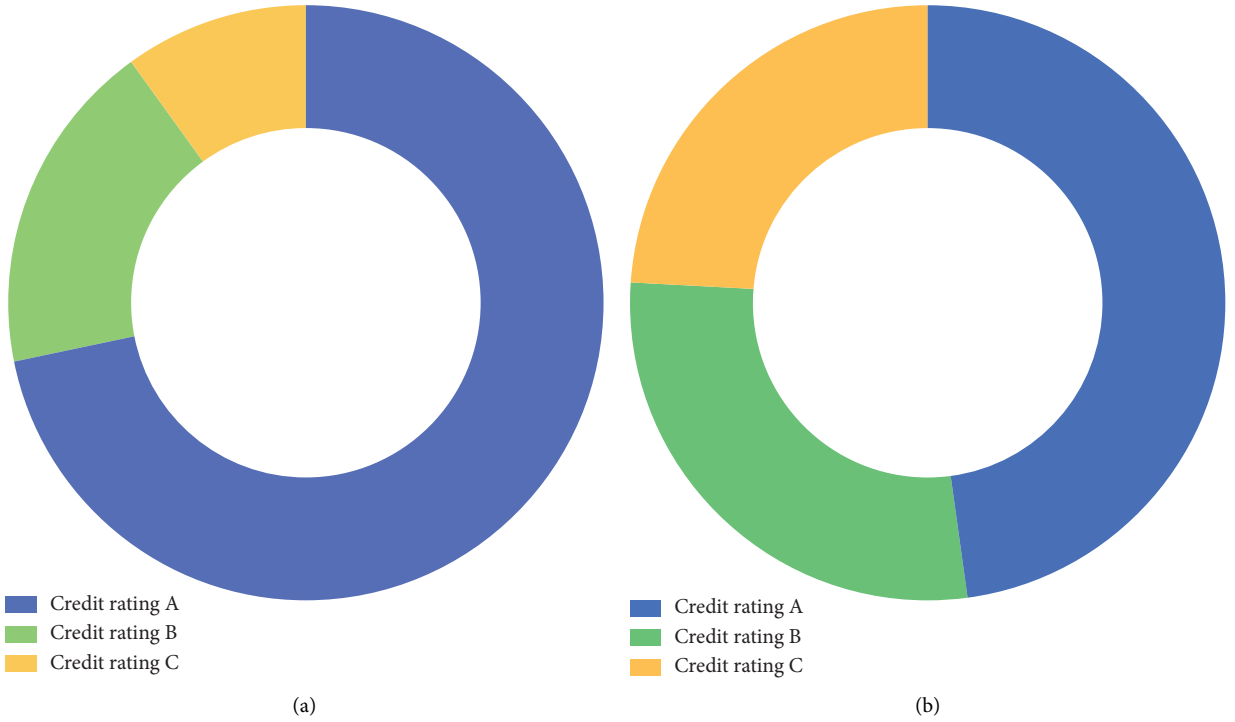

Figure 7: The suggested allocation schemes are under two different situations. (a) A scheme under risk minimization. (b) A scheme under profit maximization.

illustrated respectively in Figure 7, in which two subfigures correspond to situations of risk minimization and profit maximization. We also make a visualization of interest rate under two situations in Figure 8. It is a bar chart with two main bars, in which the blue bar corresponds to the interest rate under risk minimization and the red bar corresponds to the interest rate under profit maximization.

4. Discussion about Machine Learning Application

This work deals with loan allocation decision situations where the credit status information of enterprises is unknown. As a consequence, this work introduces machine learning to predict unknown credit status information. The

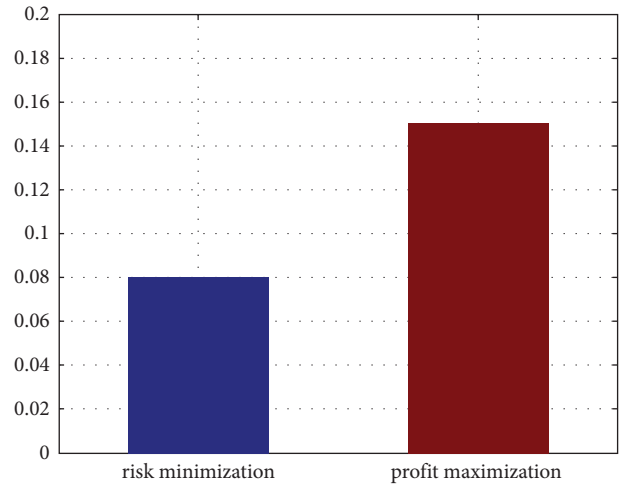

Figure 8: Final interest rate results for the two situations.

machine learning models are with simple principles and are more resilient compared with general mathematical modeling thoughts. Besides, there are many support services for the machine learning models, as many available interfaces can be directly imported. It can really act as an alternative for time-consuming manual decision tasks and can even be comparable to expert experience in some situations.

However, the machine learning models also have some limitations. The most common issue for machine learning models lies in the fact that they are highly reliable on labels and sample amounts, because the machine learning models need to be trained on the basis of gold labels in the training set and are quite sensitive to sample amount. In other words, there needs some cost to train an effective machine learning model. In addition, the selection of features may also have some effect on the fitting efficiency of machine learning models, which is attributed to the explainability problem of general machine learning models. Due to the weak explainability, the establishment of models may lead to many redundant labors. But on the whole, the machine learning models can still work as a feasible solution in many business scenarios.

5. Conclusion

This paper focuses on a smart finance task using machine learning methods. To complete unknown credit status information of users, this work uses the KNN model for this purpose. After that, a dynamic planning model is utilized to realize decision-making processes. The whole technical framework is named as TLAD-UC for short which is composed of two stages. A real-world dataset is selected to evaluate the performance of the proposed TLAD-UC. A case study is presented to display the workflow of the proposal. It is also noted that the current technique is still in the initial exploration of this area, and efficiency needs to be further improved in future works. Therefore, it is expected to improve technical methods and promote decision effect. And the idea of an autonomous decision may be considered in future works.

Data Availability

The research data can be requested from the first author via e-mail.

Conflicts of Interest

The authors declare that they have no conflicts of interest.

Acknowledgments

This work was supported in part by National Natural Science Foundation of China (No. 71902007), in part by the General project of Social Science of Beijing Municipal Education Commission (SM202210011004), and in part by Open Project Program of National Research Centre for Agri-Product Quality Traceability (AQT-2022-YB4).

References

[1] F. Ding, G. Zhu, M. Alazab, X. Li, and K. Yu, "Deep-learning-empowered digital forensics for edge consumer electronics in 5g hetnets," *IEEE Consumer Electron. Mag.*vol. 11, no. 2, pp. 42–50, 2022.

[2] T. Teng and L. Ma, "Deep learning-based risk management of financial market in smart grid," *Computers & Electrical Engineering*, vol. 99, Article ID 107844, 2022.

[3] Z. Zhou, X. Dong, Z. Li, K. Yu, C. Ding, and Y. Yang, "Spatio-temporal feature encoding for traffic accident detection in vanet environment," *IEEE Transactions on Intelligent Transportation Systems*, 2022.

[4] X. Fu, "Research on artificial intelligence classification and statistical methods of financial data in smart cities," *Computational Intelligence and Neuroscience*, vol. 2022, Article ID 9965427, 12 pages, 2022.

[5] M. Lai, "Smart financial management system based on data ming and man-machine management," *Wireless Communications and Mobile Computing*, vol. 2022, Article ID 2717982, 10 pages, 2022.

[6] L. Zhao, H. Chai, Y. Han, K. Yu, and S. Mumtaz, "A collaborative v2x data correction method for road safety," *IEEE Transactions on Reliability*, vol. 71, no. 2, pp. 951–962, 2022.

[7] Y. Chen, "Framework of the smart finance and accounting management model under the artificial intelligence perspective," *Mobile Information Systems*, vol. 2021, Article ID 4295191, 2021.

[8] B. Zhu, K. Chi, J. Liu, K. Yu, and S. Mumtaz, "Efficient offloading for minimizing task computation delay of noma-based multi-access edge computing," *IEEE Transactions on Communications*, vol. 70, no. 5, pp. 3186–3203, 2022.

[9] R. Hamadi, H. Ghazzai, H. Besbes, and Y. Massoud, "Financial advisor recruitment: a smart crowdsourcing-assisted approach," *IEEE Trans. Comput. Soc. Syst.*vol. 8, no. 3, pp. 682–688, 2021.

[10] D. Meng, Y. Xiao, Z. Guo et al., "A data-driven intelligent planning model for uavs routing networks in mobile internet of things," *Computer Communications*, vol. 179, pp. 231–241, 2021.

[11] K. Li, F. Zhou, Z. Li, W. Li, and F. Shen, "A semi-parametric ensemble model for profit evaluation and investment decisions in online consumer loans with prepayments," *Applied Soft Computing*, vol. 107, Article ID 107485, 2021.

[12] E. Fusco and B. Maggi, "Computing nonperforming loan prices in banking efficiency analysis," *Computational Management Science*, vol. 19, no. 1, pp. 1–23, 2022.
[13] S. Wu, X. Gao, and W. Zhou, "COSLE: cost sensitive loan evaluation for P2P lending," *Information Sciences*, vol. 586, pp. 74–98, 2022.
[14] M. Li, C. Yan, and W. Liu, "The network loan risk prediction model based on convolutional neural network and stacking fusion model," *Applied Soft Computing*, vol. 113, Article ID 107961, 2021.
[15] E. Tang, "Research on interest rate risk of housing mortgage loan based on computer simulation," *Computational Intelligence and Neuroscience*, vol. 2021, Article ID 6035022, 2021.
[16] J. Blaszczynski, A. T. de Almeida Filho, A. Matuszyk, M. Szelag, and R. Slowinski, "Auto loan fraud detection using dominance-based rough set approach versus machine learning methods," *Expert Systems with Applications*, vol. 163, Article ID 113740, 2021.
[17] A. Botha, C. Beyers, and P. de Villiers, "Simulation-based optimisation of the timing of loan recovery across different portfolios," *Expert Systems with Applications*, vol. 177, Article ID 114878, 2021.
[18] L. a. Dong, X. Ye, and G. Yang, "Two-stage rule extraction method based on tree ensemble model for interpretable loan evaluation," *Information Sciences*, vol. 573, pp. 46–64, 2021.
[19] W. Zhu, B. Liu, Z. Lu, and Y. Yu, "A DEALG methodology for prediction of effective customers of internet financial loan products," *Journal of the Operational Research Society*, vol. 72, no. 5, pp. 1033–1041, 2021.
[20] F. J. I. A. Azzawi, "Data mining in a credit insurance information system for bank loans risk management in developing countries," *International Journal of Business Intelligence and Data Mining*, vol. 18, no. 3, pp. 291–308, 2021.
[21] K. Zhuang, S. Wu, and X. Gao, "A deep metric learning approach for weakly supervised loan default prediction1," *Journal of Intelligent and Fuzzy Systems*, vol. 41, no. 4, pp. 5007–5019, 2021.

Hindawi
Computational Intelligence and Neuroscience
Volume 2022, Article ID 8409495, 11 pages
https://doi.org/10.1155/2022/8409495

Research Article

A Data-Driven Intelligent System for Assistive Design of Interior Environments

Guoxing Chen

College of Fine Arts, Guangdong Polytechnic Normal University, Guangzhou 510665, Guangdong, China

Correspondence should be addressed to Guoxing Chen; chenguoxing@gpnu.edu.cn

Received 20 June 2022; Revised 30 July 2022; Accepted 2 August 2022; Published 24 August 2022

Academic Editor: Gopal Chaudhary

This paper analyses the design of a healthy interior environment using big data intelligence. The application of big data intelligence in the design of healthy interior environments is necessary because the traditional interior design approaches consume a lot of energy and other problems. Benefited by its strong ability of computation and analytics, artificial intelligence can well improve a series of problems in the field of interior design. The proposal summarizes the sources, classifications, and expressions of behavioral data in interior spaces, carries out analysis and research on behavioral data from two aspects: display space and supermarket space, summarizes the interior methods based on behavioral data, and analyses the visualization application of behavioral data in different interior scenes, to explore the application value of behavioral data in interior design. In contrast to it is the unconscious behavioral response, the biggest characteristic of which is that it is regulated by the behavioral subject's physiological factors or habits of the behavior issuer. In this paper, we convert the layout recommendation problem of a space into a functional classification problem of segmented segments and household segments on a plane. The scene layout features are extracted by binary coding, the abstraction of the cross features between the vector segments is achieved by using a word embedding algorithm, the feature matrix is reduced in dimensionality, and finally, the segmentation network model and the layout network model are constructed, respectively, by using a bidirectional LSTM. The experiments show that the accuracy of the layout recommendation model in this paper is 98%, which can meet the demand for real-time online layouts.

1. Introduction

In today's rapidly developing society and technology, people's life is becoming increasingly fast paced, and those who have been working all day, need a convenient and comfortable interior design to meet their needs under extremely exhausting conditions [1]. The integration of AI intelligence into the interior design will improve some of the shortcomings and deficiencies of current interior design, maximizing the needs of occupants, bringing more convenience and safety to people's daily lives, and minimizing energy consumption. For a long time, the original interior design concept of modern housing was created by the rationalization of room layouts and the convenience of interior lighting. More attention has been paid to the extent to which the objective hardware matches and only a few designers have taken the initiative to focus on the type of environment in which the inhabitants live, but this is the only way in which they can truly experience the comfort and pleasure of everyday life. Home designs that overlap with more interior decoration can accidentally cause damage while requiring more time and more difficult cleaning, which in turn makes residents regret having chosen this type of interior design and often worry about it [2]. The model of the next stage is constructed based on the model of the previous stage, and the construction of the model of the previous stage should be considered for the construction of the next stage. These types of interior furnishings are beautiful from the resident's point of view but certainly, add to the many potential problems from the feeling of the experience. In this way, the interior design has little connection to the inhabitants, and then the existence of the interior design is not important to the inhabitants, which is extremely detrimental to the development of the interior design.

AI intelligence falls under the umbrella of computer science, which aims to create intelligent machines using human intelligence. The scientific revolution is one of the main reasons for the emergence of AI intelligence and is one of the keys to its technological development. Scientific research suggests that AI intelligence has emerged to effectively stimulate people's minds, understand themselves, and change the world. In the field of AI intelligence, attitudes toward AI intelligence research are different, but the overall performance is in favor of creating strong AI intelligence with the same level of thinking and understanding as humans and in favor of creating weak AI intelligence with incomplete information. AI intelligence is based on the combined behavior of systems research, psychology, control technology, computer technology, and sound technology [3, 4]. In addition, various mathematical models and theories are needed to increase the speed of AI intelligence. Today, the development of AI intelligence technology is mainly seen in facial recognition, autonomous driving, and banking data systems. The three main technologies that provide AI intelligence are common programming methods, machine learning methods, and learning methods[5, 6]. In modern society, entertainment and recreation are an important part of people's activities. The advancement of urbanization and the improvement of people's quality of life have led to a tendency for cinema spaces to focus on people's own experiences, promoting design that keeps pace with the times and focuses on the human experience, promoting interaction between people in their activities, mainly the formation of interactions between people, objects, and the environment.

Currently, some people are adding one or more home cleaning robots to their homes to enhance the comfort of rest and living and to regularly clean dead areas that are difficult to clean manually, for overall cleaning. However, for a significant segment of the robots on the market, this cleaning is only superficial, i.e., the quality of the cleaning depends on the exact position of the furniture and appliances. The functional spaces that are related to each other and close to each other are divided into the same model file, which not only meets the design requirements but also realizes the effective use of resources. The cleaning path is created and works according to the installed route, with the disadvantage that it cannot be disturbed by the outside world while working. If a person is in the same room as the cleaning robot, he or she should carefully avoid it so as not to interfere with the robot's normal work, but this can affect people's daily experience. In addition to this, very few indoor appliances are in an intelligent state, which shows that the current application of artificial intelligence in the field of interior design still needs to be improved and popularized. Therefore, the introduction of a new multiorder modulation and demodulation technology in indoor multicolor multiplexed VLC systems, and the integration with commonly used fiber optic communication systems, can effectively improve the system transmission rate and band utilization, and reduce the cost of transceiver consumption. Based on the above considerations, it is of great theoretical and practical significance to research modulation and demodulation techniques for multicolor multiplexed visible light signals for indoor big data access.

2. Related Works

Behavior generates behavioral data, and behavior data are a quantitative representation of behavior. Behavior is diverse, so there are differences in the corresponding behavior data. Based on the above research results, this thesis classifies behavior data into two main categories: location data and experience data [7, 8]. Location data refers to objective data in life, mostly monitored or uploaded by mobile phones, radio frequency identification devices, GPS, and other devices, including the location of the user, the trajectory line data of individual movement, the surface data of group movement, and the related thermal data [9]. Experience data include user evaluation and feedback data, which is highly subjective and is mainly collected from web pages and mobile clients. The research in this paper focuses on the location data of user behavior data. Indoor location data contain rich and complex behavior information, which provides new research ideas for interior design innovation, so that design relies on scientific and rigorous data analysis, rather than relying on previous empirical talk. Serrano et al. address the problems of low electrical energy utilization and waste in library lighting systems by analyzing the data collected from seated readers and designing a zoning lighting system that meets the behavior habits of readers while saving resources and reducing waste [10]. The research results were successfully applied to the secondary planning and renovation of the commercial street by using behavior models and computer simulation methods and based on the virtual visitation data of the online Expo, they obtained the behavior data of the visitors and carried out the temporal and spatial simulation of the multi-individual visitation behavior through the model, achieving the prediction and guidance of the number of visitors, the flow of people and the demand for facilities at the Expo [11]. The average accuracy of a single unit segment of the layout model without the word embedding layer is calculated to be 89.75%, and the average accuracy of the entire sequence of units is 73.48%; the average accuracy of a single unit segment of the layout model with the word embedding layer added is 98.60%. The model is used to predict and guide the number of visitors, and the demand for facilities, and to visualize the spatial and temporal changes in the pavilion.

Rosário et al. proposed an improved Pearson collaborative filtering algorithm, which uses a prediction model calculated from user profiles, item characteristics, and user behavior data instead of the similarity calculation of traditional algorithms, optimizing the traditional recommendation algorithm [12]. Hong et al. proposed an improved CF recommendation algorithm using singular value decomposition to achieve dimensionality reduction, which can alleviate the sparsity problem of the scoring matrix and achieve better recommendation results [13]. Barbar et al. proposed a deep learning-based multi-criteria collaborative filtering model, which takes the characteristics of users and items as inputs to a standard rating deep neural network, and

the prediction results of the first part form the inputs to the second part of the overall rating deep neural network [14]. The study of this model provides a basis for using deep learning and multi-criteria in recommender systems [15].

As mentioned above, content-based recommendation algorithms need to know information about 3D home models, 3D layout scenes, etc. Although there is no project could start problem, the extraction process of its features is difficult and computationally complex; a single collaborative filtering algorithm will have problems such as matrix sparsity and cold start when solving the intelligent design problem studied in this paper; association rules and popularity recommendation algorithms are effective in the cold start problem. However, there are still some shortcomings in achieving fast and accurate recommendation effects. Because of this, to better solve the recommendation problem faced by this paper, inspired by many recommendation algorithms, this paper is based on a hybrid recommendation algorithm, taking the strengths of each, dividing the intelligent design process into two parts: home matching and home layout, designing different recommendation models, respectively, and combining the two recommendation models utilizing transformation, triggering the corresponding recommendation model according to the user's needs.

3. Artificial Intelligence in Interior Environment Design Application under Big Data Environment

3.1. AI Analysis of Big Data for Indoor Environments. The rapid development of the Internet has catalyzed the advent of the era of information data explosion, and the emergence of massive information data has exacerbated the problem of information overload. To effectively alleviate this pain point of information data overload, recommendation algorithms have shown their great charm by analyzing the behavior characteristics of users and the attributes of items to obtain effective recommendation data, and then provide more meaningful recommendation services for users [16]. Grid floor plans are not optimal for retailers who want to create an upscale branded environment, which can cause customers to browse easily and not be impressed with the merchandise. A model-based recommendation algorithm is a typical machine learning problem in which historical data of a research object is used as a training sample, a network model is defined to describe the potential recommendation relationship between the research object, and model parameters are obtained through an optimization process, and an appropriate prediction model is trained to achieve recommendations.

The matching recommendation model in this paper is designed for the matching of 3D home models. Considering the professional nature of interior matching solutions, the aesthetics of ordinary users, and the limited matching data make it difficult to construct a recommendation model with good recommendation results, so user-based recommendation solutions are discarded. In this paper, professional matching schemes are selected as the data set and the matching correlation between items is used to build a basic matching recommendation model:

$$Q = \int_{280nm}^{720nm} 683 \frac{lu}{W} S\left(\kappa^2\right) v(\lambda) \mathrm{d}\lambda. \tag{1}$$

To improve the efficiency of the intelligent design algorithm, this chapter investigates the matching recommendation algorithm for 3D home models in the context of an interior space design software platform. The basic collocation recommendation model is constructed using the item-based collaborative filtering recommendation algorithm [17]. To improve the computational efficiency, the two-dimensional rendered image of the home model is taken as the processing object, the features of the image are extracted by the convolutional neural network, the feature vector library of the image is constructed, and the ideas of the content-based recommendation algorithm are mixed to populate the highly sparse collocation recommendation matrix to realize a new hybrid collocation recommendation model:

$$I(\phi) = \frac{I_0(\phi)}{d}. \tag{2}$$

In this paper, 846-bedroom home matching solutions paired with professional designers were selected for experiments on the interior space design software platform, which contained 5 home item categories with a total of 1240 home items, 190 TV cabinets, 418 beds, 257 bedside tables, and 201 wardrobes. In total, 600 randomly selected matching data were used as the training set to build the matching recommendation model, and 300 randomly selected data were used as the test set from the 712-test data constructed from the remaining 246 data expansions to test the accuracy of the recommendation model. A set of matching solutions can be represented as a five-tuple (TVark_14, bed_149, bedtable_12, dresser_1, wardrobe_1), and each household item can be represented as where "type" is the type name of the item and "num" is the type number of the item. Therefore, each matching scheme can be represented by a five-tuple, where 0 means that the corresponding household item in the scheme does not exist (Table 1).

The correlation of design information in this row refers to the interrelationship between various information and components, e.g., nongeometric information needs to be represented by geometric information as a carrier, and the description of the performance of geometric forms needs to be represented by nongeometric information. In the process of using information models to describe the interior design, the information model is used in the design expression, design and construction, and operation and maintenance phases [18]. Therefore, the user-based recommendation scheme is abandoned. This paper selects the professional collocation scheme as the data set and uses the collocation correlation between items to construct the basic collocation recommendation model. The description of interior components in the information model is based on real building components and has the same building properties and interrelationships between components as reality.

Table 1: Home matching schemes.

Scenario	TV cabinet	Bed	Bedside table	Dresser	Wardrobe
Scenario 1	TV_1	12	10	dresser_1	12
Scenario 2	TV_2	16	19	17	13
Scenario 3	TV_3	15	15	16	wardrobe_1
Scenario 4	TV_4	bed_149	bedtable_12	10	10
Scenario 5	TV_5	14	13	18	16
Scenario 6	TV_6	11	15	20	20

Doors and windows are dependent on walls and cannot be created without the existence of walls, i.e., walls are the subject of the existence of doors and windows; there is a spatial distance between the floor and the ceiling, etc. The logical interconnection between this information forms the spatial use ecosystem of the interior information model.

$$S(\phi) = \begin{cases} \dfrac{m+1}{2\pi}\sin^m(\phi), & \phi \in \left[-\dfrac{\pi}{2}, \dfrac{\pi}{2}\right], \\ 0, & \text{others.} \end{cases} \tag{3}$$

Combining the definition of BIM and the characteristics of interior design itself, I believe that the interior information model is based on the information models of architecture, structure, and electromechanical pipelines and consists of a library of various resources related to interior design, which can assist in design, design collaboration, visual design, parametric design, and other functions, throughout the design stages such as scheme design, deepening design and construction drawing design, and can be a 3D visual information model for drawing output (effect drawings, scheme drawings, effect drawings, etc.), construction management, production and processing of decorative components, etc. The interior information model enables the management of the life cycle of interior spaces [19]. The model is based on design information, and by integrating the information associated with it, it forms a database that can be used to manage and maintain the entire life cycle of interior space (Figure 1).

In simple terms, an interior information model is an overview of the interior design process, an abstract understanding and representation of the form, composition, and materials of the interior space, and the manufacture, construction, and management of the building components. The features of the image are extracted by the convolutional neural network, the feature vector library of the image is constructed, the idea of a content-based recommendation algorithm is mixed, and the highly sparse matching recommendation matrix is filled to realize a new mixed matching recommendation model. An interior information model in its fullest sense should contain two related aspects: a spatial geometry model and design data information. The spatial geometry model reflects the relationship, form, and composition of the interior space and is the carrier of the design data information; the design data model reflects the nongeometric information related to the spatial geometry model, including technical requirements and design parameters.

$$g(\theta) = \begin{cases} \dfrac{m^2}{\sin^m(\theta)}\sin^2(\theta), & \theta \in \left[-\dfrac{\pi}{2}, \dfrac{\pi}{2}\right], \\ 1, & \text{others.} \end{cases} \tag{4}$$

The result of using BIM in interior design should be that all designers apply it to the whole design process. However, at this early stage of application, the conditions for full application are not yet available, and the application of partial stages and partial processes will be a norm for the application of interior information models.

According to the division of specific project design requirements, design process and design stages, different stages of model construction can be selected in the process of interior information model construction. From a macro perspective, the life cycle of an interior space is divided into five stages: requirements analysis, conceptual design, design deepening, design implementation, and maintenance support [20]. The function of the information model is in the stages of design expression, design and construction, operation, and maintenance, etc. According to the divided stages, design demand models, conceptual design models, design deepening models, design construction models, and operation and maintenance service models can be built, respectively, while the conversion, integration, and operation between the models of each stage need to be organically realized.

On the one hand, in terms of specific meaning, the understanding of interior space is very different from the understanding of space in other fields, it is formed according to the modern living space to divide, has the function of enclosing the architectural structure, and is formed by a real substance to form an objective existence. On the other hand, the design of four-dimensional space incorporates the way people live and behave, making it possible to use time as a primary measure in this new spatial system, giving space, which does not have any qualities in the first place, an external substance and time, so that space has its value of existence in this dimension. All these manifestations culminate in a spatial essence with its characteristics, as shown in Figure 2.

Based on the relevant project information, the first step is to carry out a design analysis. Design analysis is the partial reverse operation of design thinking, the purpose of which is to extract as much information as possible about design thinking from local or limited material, and to synthesize, summarize and refine it through the analyst's thinking so

Figure 1: Diagram of the interior information model.

that it becomes an important part of his or her design ideas, techniques, and approaches.

Interior space is variable, and changes to the physical interior, such as changing the location of a home or removing or adding new walls, can actively or passively change the structure and connectivity of the interior space [21]. The description of the interior components by the information model is based on the real building components, and has the construction attributes consistent with reality and the interrelation between components. It is because of this variability that people can personalize the design of interior spaces to meet their individual needs. Indoor spaces are generally private, which is a significant difference from publicly shared outdoor spaces. Private spaces are designed to better protect the privacy of the individual so that the individual can be free from the outside world, and free from the influence of the outside world. Certain public spaces also have a certain degree of privacy, such as warehouses or self-service withdrawal areas in banks, which are open to specific people at specific times.

3.2. Artificial Intelligence in the Design of Interior Environment Applications. Behavior is generated by a variety of physical and psychological needs. There are a variety of behavioral responses to external information, but these can be broadly divided into conscious and unconscious responses. Conscious reactions are widespread in people's daily lives and come from their control, often with a strong sense of purpose [22]. In contrast, there are unconscious reactions, which are characterized by the physiological factors or habits of the subject of the act, which wield the behavior of the emitter.

The geometric information is highly visible and includes both the visual presentation of geometric forms and the two-dimensional planar relationships of drawings. This

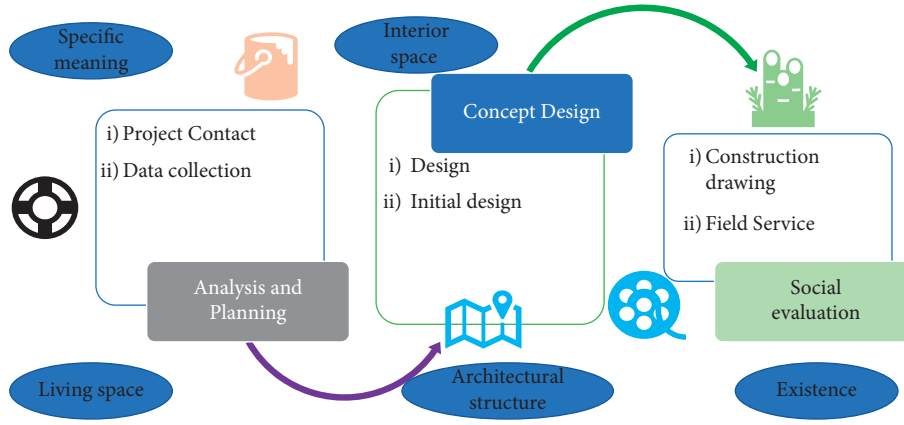

Figure 2: The data realization process.

collaborative working process brings together information from within and outside the various disciplines to synthesize and communicate information in the same information model, i.e., through a single design medium.

As can be seen in Figure 3, the collaboration between team members throughout the process, from design conception to design expression to design implementation, is based on the same information model, through which information is obtained and transferred between team members. In this process, the geometric and nongeometric information of the design is transferred through the visual information model, with a high degree of visibility of the geometric form. The model is based on design information, and at the same time, by integrating the information associated with it, a set of data information bases that can be used to manage and maintain the entire life cycle of indoor space is formed. At the same time, information transfer and communication between design and construction are based on the visual information model, which has both three-dimensional geometry and two-dimensional drawing lines.

Unlike CAD, which is a geometric description of the design object, the information model is a description of the characteristics of the design object, and the geometric modeling and information description of the space for each stage of the different characteristics, resulting in different descriptive models, which are used throughout the life cycle of the space, connecting all aspects of the space from planning to use and even redesign, creating a virtual space that is consistent with the real space.

The phasing principle is based on the model deepening method to construct the model in stages: design requirements stage, conceptual design stage, design deepening stage, construction design stage, and operation and maintenance stage, each of which has a different level of maturity for the design model. In the process of constructing an interior information model, different stages of information models are constructed according to the different levels of information generated at different stages [23]. To provide users with more meaningful recommendation services. Throughout the design process, the design model of the interior information model will include the design requirements model, the conceptual design model, the design deepening model, and so on.

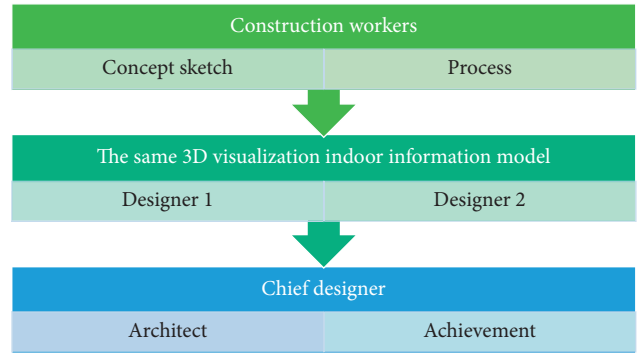

Figure 3: Schematic diagram of interior design collaboration centered on the information model.

The design requirements model is mainly used to model the user's needs, by analyzing and collating the user's design requirements for the interior space, the user's behavior habits, and other factors, the user's needs information is transformed into design information. The conceptual design model is a conceptual arrangement and planning of the design through the analysis and synthesis of the user's demand information, mainly based on the geometric information of the space, including the spatial shape, spatial relationship, environmental analysis, and other content. The design deepening model is based on the conceptual design model, further quantifying the information of various design parameters, verifying the design scheme, forming a clearer design scheme, and preparing for the construction model construction.

The principle of model layering refers to one of the ideas on how to solve the problem of increasing the amount of information in the model, model layering is achieved through the division of the model. It is necessary to divide the model of the whole project into several relatively independent files based on the design task requirements, functional zoning, etc. and to integrate and link the various parts of the files after the model is constructed, as shown in Figure 4.

Since there are relatively few links between floors and the upper and lower floor spaces do not affect each other,

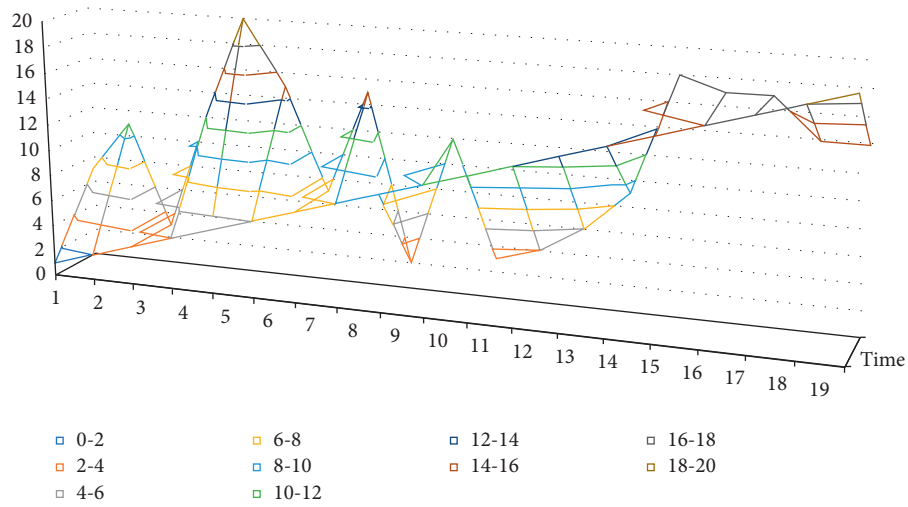

Figure 4: Time-domain waveform of the signal.

dividing the model files according to floors is the commonly used layering approach. According to the divided stages, the design requirement model, conceptual design model, design deepening model, design and construction model, and operation and maintenance service model can be established, respectively. However, if there is an overhead space, which is often the outstanding part of the design, it is no longer appropriate to divide the space according to the floor area, so it is necessary to divide it according to the functional area of the space and divide the functional spaces that are close to each other into the same model file, to meet the design requirements and achieve the effective use of resources.

In interior design, the choice of decorative materials is a fundamental issue, and without the appropriate tailoring support, the best spatial design concepts cannot be fully expressed. Before selecting decorative materials, it is necessary to grasp the characteristics of the different materials and the context in which they are used [24]. Virtually every material in the world can be used as a decorative material, but the range of materials chosen is directly related to the type of material known. The best way to have better creativity is to broaden your knowledge of decorative materials and to have a thorough and systematic understanding of new materials. Again, good materials can sometimes lead to better creativity and ideas. About the understanding of the concept of good materials, many people think that expensive materials are good materials, but they are not. The goodness or badness of materials is usually determined by the designer's design requirements, for different situations, and for individual interior design, material innovation is also important.

4. Analysis of Results

4.1. Performance Results of Artificial Intelligence Algorithms for Interior Environment Big Data. The structure of the layout network model is like that of the segmentation network model, and the parameter adjustment process of the layout network model is used here as an example to analyze the parameter determination method during the experiment in detail. It will actively or passively change the structure of the interior space and the connectivity of the interior. The training process uses the batch method to split the whole dataset into different small subsets, using these small subsets to complete a forward and backward iterative process, making full use of computer resources. Different values of batch size were used for comparison experiments, and the curves of accuracy and loss of the training set with the number of iterations were obtained as shown in Figure 5 below. The following curves were analyzed, and the best accuracy rate could reach 100%, while the size of batch size would affect the training speed, and considering the smoothness of the curve and the training speed, the batch-size size of 128 was chosen for this paper.

This experiment uses 3000 household layout data to test the accuracy of the layout network model. The accuracy of individual household segments refers to the prediction accuracy of a single segment in the sequence describing the household information, and for the whole sequence of household segments, if one of the segments is incorrectly predicted, the prediction result of the sequence of household segments is inaccurate and the value is 0. The scene layout features are extracted in the form of binary coding, and the abstract extraction of cross features between vector segments is realized by a word embedding algorithm. The average accuracy of a single segment of the layout model without the word embedding layer was 89.75% and the average accuracy of the whole sequence of segments was 73.48%; the average accuracy of a single segment of the layout model with the word embedding layer was 98.60% and the average accuracy of the whole sequence of segments was 92.16%. Embedding network model and the Before_Embedding network model are shown in Figure 6, the average test speed of the After_Embedding network model is 17.88 s, and the average test speed of the Before_Embedding network model is 309.43 s.

The layout network model with the word embedding layer learns the features between scene information and layout better, and its performance in the test set is

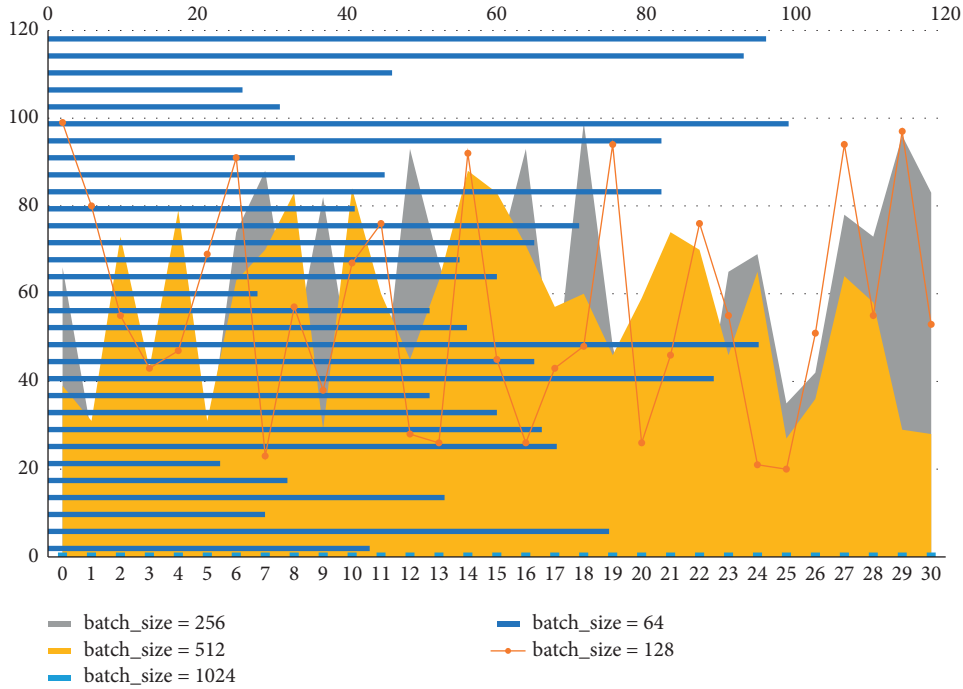

Figure 5: Layout network model comparison experiment.

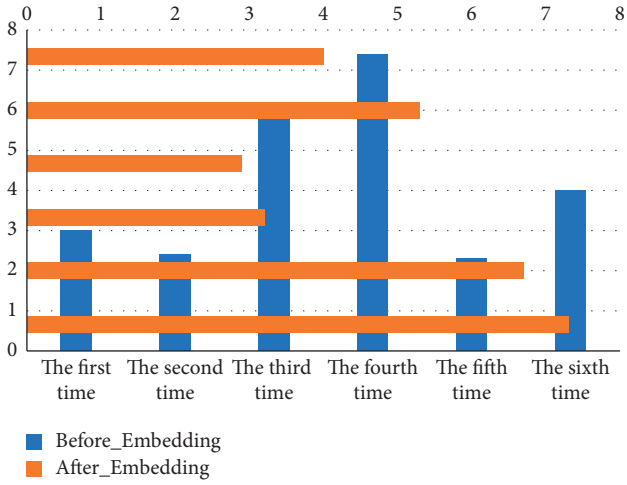

Figure 6: Test set accuracy.

significantly better than that of the Before_Embedding model; comparing the average prediction accuracy of individual household segments and the whole sequence of household segments under the same layout network model, the After_Embedding model has a higher accuracy of the whole sequence of household segments than that of individual household segments. The sequential accuracy of the After_Embedding model decreased by 6.53% compared to that of the individual household segments, while the sequential accuracy of the Before_Embedding model decreased by 18.13% compared to that of the individual household segments.

But only in this way can the occupants truly experience the comfort and joy of daily life. This is because the features characterized by One-hot coding are independent of each other, which ignores the similarity and correlation between coded segments, while the word embedding layer can more reasonably express the relationship between the size and distance of coded segments, which is the abstraction of the extraction between features and the expression of the potential relationship between coded values. In addition, the word embedding layer thickens the One-hot matrix and reduces the dimensionality of the feature matrix, which greatly improves the prediction speed of the model.

Considering that the layout time of the distance field algorithm and the placement field algorithm is densely related to the number of models to be laid out in the scene, here 1000 randomly selected data to be laid out are used to evaluate the algorithm performance in terms of their total layout time. It should be added that the running times of the distance field layout algorithm and the placement field layout algorithm in Figure 6 are estimated based on the experimental results of the algorithm proponents, and the time of the layout algorithm in this paper is the sum of the segmentation and layout times. The comparison leads to the conclusion that the layout algorithm in this paper has better performance in terms of real-time processing.

4.2. Analysis of the Results of the Application of Artificial Intelligence in the Design of Indoor Environments. The artificial intelligence environment can monitor every electrical appliance in the home in real-time, so that not only can the waste of resources be reduced, but also avoid accidents, for example, the power can be cut off in time or when there is a fire can be implemented automatically in the whole room in time to put out the fire, and other dangerous situations can be strongly avoided, so that it brings a higher level of security

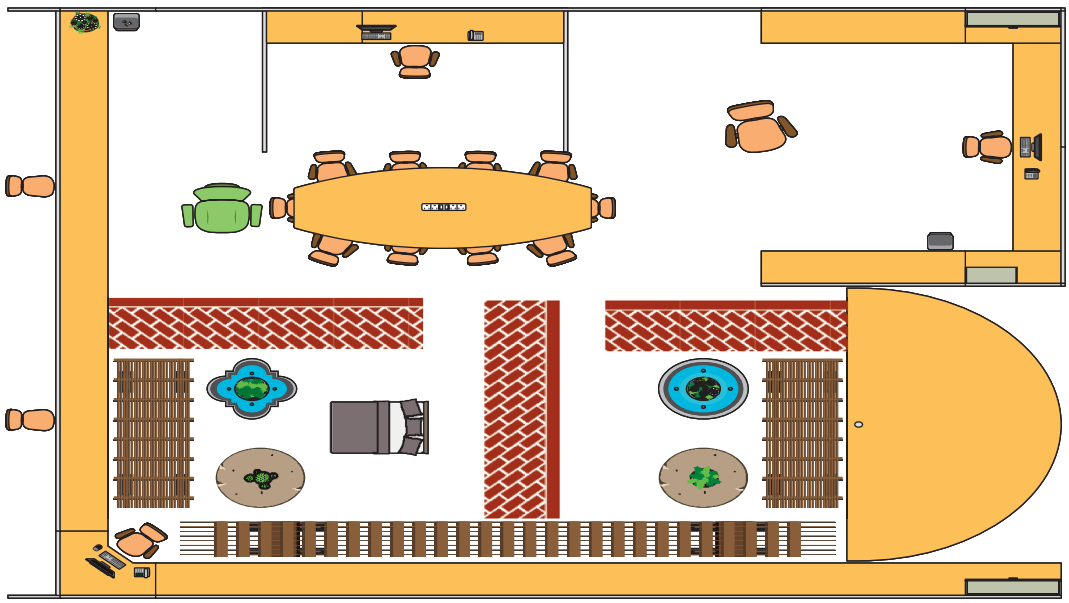

Figure 7: Layout diagram.

to people's living. It also provides a certain level of security for the elderly and children.

The inhabitants of an artificially intelligent environment can turn many electronic devices on and off at any time, depending on when they leave home in the morning and when they return home in the evening. When leaving the house in the morning, appliances such as lamps, microwave ovens, and air conditioners can be switched off automatically, which reduces unnecessary electricity bills; when returning in the evening, essential items such as lighting and air conditioning are automatically set to recognize the occupant and turn on automatically, thus reducing the tedious process of manually setting switches and providing a humane living environment for a weary worker.

In the specific construction process of interior space environment design, and new construction solutions, designers are often excited by their bold ideas, but we cannot try and verify whether they are correct. The traditional implementation plan inevitably has errors in the construction data, then, the design plan draft and the construction of the handover link must have a professional engineer to do guidance, according to the construction site to do size adjustments and modifications. In this way, the interior design has little connection with the occupants, so for the occupants, the existence of the interior design is not important, which is extremely unfavorable to the development of the interior design. The corresponding construction plan is verified in time. The use of digital technology allows for more precise positioning of the design, while the specific construction plan can be demonstrated through three-dimensional technology, simulating the impact of environmental factors on the construction, to develop a feasible construction plan and verify the feasibility of the finalized construction plan. This improves the efficiency of construction and shortens the construction cycle.

As a kind of art closely related to human lifestyle, interior environmental art design, in the era of rapid development of digital technology, new means of design are emerging, and traditional design procedures and methods can no longer adapt to the current needs. All make the cinema space tend to pay attention to people's own experience, promote the design to keep up with the pace of the times, take people's experience as the core, and promote people to interact in activities, mainly the formation of the interaction among people, objects, and the environment. It will inevitably continue to develop and improve itself with the development of science, social progress, and the changes of the times. Therefore, the goal of the digital representation of interior environmental art design is to establish and improve a new design system. The use of digital technology to reflect the state and structure of indoor and outdoor space, the texture of decorative materials, and light and shadow, is shown more realistically in Figure 7.

As grid layouts are used in most grocery and convenience stores, they create a familiar feeling for customers. However, because of this familiarity, it tends to give the customer an on-the-go shopping experience that does not convert traffic into value. Grid layouts are a good option for smaller retailers that have a large inventory, such as toy shops, bookstores, specialty food shops, and home furnishing shops. Support the creation of weak AI intelligence under incomplete information. However, grid floor plans are not optimal for retailers who want to create an upscale branded environment that leads to easy browsing for customers and fails to create a strong impression of the merchandise.

A circular floor plan, sometimes referred to as a runway layout, allows for the best-guided shopping experience. This layout guides the customer through every item on display in the retail shop and is therefore particularly suitable for regional marketing strategies. In a circular plan, the surrounding walls are highly visible and all types of items can be displayed. The loop plan also provides a good basis for a combined layout. With the loop plan, the central part of the

retail shop can be set up as a grid or free-flow layout, or even a mixture of the two. The circular floor plan is suitable for most small retail shops, such as clothing and accessories, toys, home furnishings, kitchenware, personal care, and specialty products.

5. Conclusion

In today's era of rapid economic and technological development, traditional interior design has completely failed to meet people's current needs, and people need a more comfortable, convenient, intelligent, and accessible lifestyle. With people's high demand for quality of life, artificial intelligence can meet a variety of needs and can be a good solution to the problems of traditional interior design as well as make up for its shortcomings in terms of safety. The cleaning path is made and worked according to the installation route, and the disadvantage is that it cannot be disturbed by the outside world. Artificial intelligence provides favorable conditions for the development of the interior design. Therefore, the application of artificial intelligence in the field of interior design in the big data environment is extremely necessary. In the context of the data era, interior designers can use data thinking to design and use data as a support to guide interior design. Based on behavioral data analysis for interior design, it is important to follow the principle of data shareability as well as to pay attention to user privacy issues in the access to data acquisition. This paper is limited by the technical problems of the equipment, the research is mostly based on theoretical knowledge, and the research is not perfect, so I hope to explore it more deeply in future studies.

Data Availability

The data used to support the findings of this study are available from the author upon request.

Conflicts of Interest

The author declares that there are no conflicts of interest or personal relationships that could have appeared to influence the work reported in this paper.

Acknowledgments

This work was supported by Guangdong Province Philosophy and Social Science "Thirteenth Five-Year Plan" 2018 Annual Project (GD18CYS02).

References

[1] L. Yang, K. Yu, S. X. Yang, C. Chakraborty, Y. Lu, and T. Guo, "An intelligent trust cloud management method for secure clustering in 5G enabled internet of medical things," *IEEE Transactions on Industrial Informatics*, vol. 2021, p. 1, 2021.

[2] Z. Guo, Y. Shen, S. Wan, W. Shang, and K. Yu, "Hybrid intelligence-driven medical image recognition for remote patient diagnosis in internet of medical things," *IEEE Journal of Biomedical and Health Informatics*, vol. 2021, p. 1, 2021.

[3] K. Yu, L. Tan, S. Mumtaz et al., "Securing critical infrastructures: deep-learning-based threat detection in IIoT," *IEEE Communications Magazine*, vol. 59, no. 10, pp. 76–82, 2021.

[4] Z. Guo, C. Tang, W. Niu et al., "Fine-grained recommendation mechanism to curb astroturfing in crowdsourcing systems," *IEEE Access*, vol. 5, pp. 15529–15541, 2017.

[5] Q. Zhang, K. Yu, Z. Guo et al., "Graph neural networks-driven traffic forecasting for connected internet of vehicles," *IEEE Transactions on Network Science and Engineering*, vol. 2021, p. 1, 2021.

[6] D. Meng, Y. Xiao, Z. Guo et al., "A data-driven intelligent planning model for UAVs routing networks in mobile internet of things," *Computer Communications*, vol. 179, pp. 231–241, 2021.

[7] F. Ding, K. Yu, Z. Gu, X. Li, and Y. Shi, "Perceptual enhancement for autonomous vehicles: restoring visually degraded images for context prediction via adversarial training," *IEEE Transactions on Intelligent Transportation Systems*, vol. 23, no. 7, pp. 9430–9441, 2022.

[8] Z. Guo, Y. Shen, M. Aloqaily, Y. Jararweh, and K. Yu, "Probabilistic inference-based modeling for sustainable environmental systems under hybrid cloud infrastructure," *Simulation Modelling Practice and Theory*, vol. 107, Article ID 102215, 2021.

[9] J. R. DeLisle, B. Never, and T. V. Grissom, "The big data regime shift in real estate," *Journal of Property Investment & Finance*, vol. 38, no. 4, pp. 363–395, 2020.

[10] W. Serrano, "Digital systems in smart city and infrastructure: digital as a service," *Smart cities*, vol. 1, no. 1, pp. 134–153, 2018.

[11] H. Hua, Z. Wei, Y. Qin, T. Wang, L. Li, and J Cao, "Review of distributed control and optimization in energy internet: from traditional methods to artificial intelligence-based methods," *IET Cyber-Physical Systems: Theory & Applications*, vol. 6, no. 2, pp. 63–79, 2021.

[12] A. Rosário, L. B. Moniz, and R. Cruz, "Data science applied to marketing[J]," *Journal of Information Science and Engineering*, vol. 37, no. 5, pp. 1067–1081, 2021.

[13] L. Hong, M. Luo, R. Wang, P. Lu, W. Lu, and L Lu, "Big data in health care: applications and challenges," *Data and information management*, vol. 2, no. 3, pp. 175–197, 2018.

[14] C. Barbar, P. D. Bass, R. Barbar, J. Bader, and B Wondercheck, "Artificial intelligence-driven automation is how we achieve the next level of efficiency in meat processing," *Animal Frontiers*, vol. 12, no. 2, pp. 56–63, 2022.

[15] M. J. C. van den Homberg, C. M. Gevaert, and Y. Georgiadou, "The changing face of accountability in humanitarianism: using artificial intelligence for anticipatory action," *Politics and Governance*, vol. 8, no. 4, pp. 456–467, 2020.

[16] Q. Zhu, Z. Liu, and J. Yan, "Machine learning for metal additive manufacturing: predicting temperature and melt pool fluid dynamics using physics-informed neural networks," *Computational Mechanics*, vol. 67, no. 2, pp. 619–635, 2021.

[17] S. J. Quan, J. Park, A. Economou, and S. Lee, "Artificial intelligence-aided design: smart design for sustainable city development," *Environment and Planning B: Urban Analytics and City Science*, vol. 46, no. 8, pp. 1581–1599, 2019.

[18] G. Teles, J. J. P. C. Rodrigues, R. A. L. Rabêlo, and S. A. Kozlov, "Comparative study of support vector machines and random forests machine learning algorithms on credit operation," *Software: Practice and Experience*, vol. 51, no. 12, pp. 2492–2500, 2021.

[19] D. Pesce, P. Neirotti, and E. Paolucci, "When culture meets digital platforms: value creation and stakeholders' alignment in big data use," *Current Issues in Tourism*, vol. 22, no. 15, pp. 1883–1903, 2019.

[20] H. Rahmanifard and T. Plaksina, "Application of artificial intelligence techniques in the petroleum industry: a review," *Artificial Intelligence Review*, vol. 52, no. 4, pp. 2295–2318, 2019.

[21] P. Sikora, L. Malina, M. Kiac et al., "Artificial intelligence-based surveillance system for railway crossing traffic," *IEEE Sensors Journal*, vol. 21, no. 14, pp. 15515–15526, 2021.

[22] J. B. Ahn, "A study on advertising future development roadmap in the fourth industrial revolution era," *International Journal of Internet, Broadcasting and Communication*, vol. 12, no. 2, pp. 66–76, 2020.

[23] K. M. Jablonka, D. Ongari, S. M. Moosavi, and B. Smit, "Big-data science in porous materials: materials genomics and machine learning," *Chemical Reviews*, vol. 120, no. 16, pp. 8066–8129, 2020.

[24] H. Zhou, W. Xu, J. Chen, and W. Wang, "Evolutionary V2X technologies toward the internet of vehicles: challenges and opportunities," *Proceedings of the IEEE*, vol. 108, no. 2, pp. 308–323, 2020.